

## Molecular Weight of Poly(vinyl Chloride)

M. FREEMAN and P. P. MANNING, *Imperial Chemical Industries Ltd., Plastics Division, Welwyn Garden City, Herts., England*

### Synopsis

A number of fractionated and unfractionated poly(vinyl chlorides) have been characterized by light scattering, osmometry, and solution viscometry. From the results on fractions it is concluded that the larger molecules contain long branches. For linear fractions the relation between intrinsic viscosity in tetrahydrofuran at 25°C. and weight-average molecular weight measured by light scattering is:  $[\eta] = 1.63 \times 10^{-4} \bar{M}_w^{0.766}$  dl./g.

### INTRODUCTION

A number of workers have measured number-average molecular weights for vinyl chloride polymers and have related these to solution viscosity.<sup>1-9</sup> However, very little has been published on the weight-average molecular weight, which is more directly related to solution viscosity than the number-average molecular weight.<sup>10-13</sup> In this paper an account is given of the relationships between weight-average molecular weight, number-average molecular weight, and solution viscosity for fractionated and unfractionated poly(vinyl chloride). The paper is particularly concerned with the measurement of weight-average molecular weights by the light-scattering technique.

### EXPERIMENTAL

#### Sample Preparation

Vinyl chloride is commonly polymerized in emulsion or suspension and, as a result, the polymers often contain small quantities of water-soluble dispersing agents. These may be insoluble in tetrahydrofuran, which is used as solvent for the polymer, and if they are not removed are liable to form colloidal aggregates which cannot be entirely removed by filtration and so greatly distort the light-scattering results. However, purification can be effected by repeated precipitation from tetrahydrofuran solution into water, filtering the solution through a No. 1 or No. 2 filter paper prior to each precipitation. Four precipitations are usually sufficient. The conditions for precipitation are fairly critical. If too dilute a solution is used, unrecoverable colloidal material is formed, while too concentrated solutions give lumps of solvent-swollen polymer which trap impurities and

are difficult to dry. A suitable concentration for most commercial polymers is 12–15 g./l. A tenfold excess of water over tetrahydrofuran is used. The water should be stirred with a partially immersed paddle so as to splash against the sides of the beaker and so keep the drops of solution falling into it separated. This method produces the precipitated polymer in a good physical form which is easily filtered off on a fine nickel gauze. After the final precipitation the polymer is washed with distilled water and methanol, and dried in a vacuum oven for 24 hr. at 35°C.

To prepare fractions, purified polymer was dissolved at 5 g./l. in tetrahydrofuran and placed in a thermostat at 25°C. Distilled water was then run slowly into the stirred solution until a slight persistent turbidity was noted. The addition of a further small quantity of water then brought the fraction out of solution as small viscous droplets. Stirring was continued for 4–5 hr. to facilitate equilibrium between the phases and the fraction left to settle overnight. Most of the solution was then siphoned off. In the case of the higher molecular weight fractions the precipitated phase was in the form of a gelatinous mass attached to the walls of the flask and the solution remaining after siphoning could be simply poured off. With the lower molecular weight fractions it was necessary to centrifuge the residue after siphoning to effect a complete separation. Subsequent fractions were obtained by adding further water to the residual solution. This relatively crude fractionation procedure gave samples which are thought to be sharp enough to determine the intrinsic viscosity-weight-average molecular weight relation with reasonable accuracy, this not being sensitive to polydispersity.<sup>14</sup> A few high molecular weight samples were prepared in a two-stage fractionation. The precipitated fractions were diluted with tetrahydrofuran, precipitated in water, and dried in the same way as purified polymers.

### Solvent Purification

Tetrahydrofuran as received contained some peroxide and a stabilizer. It was refluxed over potassium hydroxide pellets for 3 hr. and then distilled through a very short column and stored in dark bottles. This solvent was used for polymer purification, viscometry, and osmometry, and was never used after more than three weeks in case fresh peroxide had formed. Solvent for light scattering was further purified by fractionation through a 20-plate column at a reflux ratio of 10:1, the distillation again being over potassium hydroxide pellets. This process produced solvent with a remarkably constant water content of 0.15%.

### Light Scattering

The light-scattering instrument based on the design of Peaker et al.<sup>15,16</sup> and constructed by Polymer Consultants Ltd. was modified in our own workshops to facilitate the accurate adjustment of the periscope device which rotates the light beam, and to reduce the chance of stray light reaching the photomultipliers. The 4358 Å. mercury line was isolated

by using the solution filters given by Bowen.<sup>17</sup> Calibration was by an elaboration of the method used by Ovenall and Peaker<sup>16</sup> which took the nonuniformity of intensity of the beam and polarization at the mirrors in the periscope system into account.<sup>18</sup> This calibration gave the 90° Rayleigh ratio of benzene at 20°C. and 4358 Å. as  $(43.3 \pm 1.8) \times 10^{-6} \text{ cm.}^{-1}$ , and the excess turbidity of 0.5 g. of the Cornell polystyrene in 100 ml. of toluene as  $3.28 \times 10^{-3} \text{ cm.}^{-1}$ . These compared with published values in the ranges  $(44\text{--}50) \times 10^{-6} \text{ cm.}^{-1}$  and  $(3.25\text{--}3.70) \times 10^{-3} \text{ cm.}^{-1}$ , respectively, quoted by Kratochvil et al.<sup>19</sup> the lower half of the range for benzene being favored by more recent work. A cylindrical block of turbid glass the same size as the scattering cell was used as a secondary standard. Polymer solutions were filtered through a No. 5 porosity sintered glass disk directly into the optical cell. Measurements were made at room temperature, which was  $20 \pm 2^\circ\text{C.}$ , over the angular range 30–90° for several concentrations and the molecular weight calculated from extrapolation to zero angle and concentration on a Zimm plot. Standard deviations on the molecular weight were estimated from a least-squares fit to the zero angle line.

The use of dry tetrahydrofuran was not found to be necessary in this work, though Laker<sup>10</sup> found it to be so in his. This may be because we removed water-soluble impurities before preparing solutions for light scattering, these possibly being more liable to form colloidal dispersions which interfere with light scattering when a small quantity of water is present in the solvent.

### Differential Refractometry

The refractive index increment for poly(vinyl chloride) in tetrahydrofuran at 4358 Å. was measured on a Hilger Rayleigh differential refractometer. Measurements were made at room temperature when this was stable to  $20 \pm 0.5^\circ\text{C.}$ , the cell being shielded from drafts and radiation by two layers of metallized plastic film. Tetrahydrofuran is volatile so it was necessary to close the open top of the cell supplied with the instrument. This was done by polishing the top of the cell optically flat and then using a plate of optically polished glass as a lid. There was a very slight tendency for the polymer solution to creep into the solvent side of the cell, but the effects of this could be made quite negligible by changing the solvent whenever the polymer solution was changed. The refractive index increment, measured on several fractions and whole polymers, was found to be  $0.1124 \pm 0.00044 \text{ ml./g. at } 4358 \text{ Å. and } 20^\circ\text{C.}$

### Osmometry

The osmometers were very similar to those used by Zimm and Myerson,<sup>20</sup> the main difference being the application of the clamping pressure through a ball-and-socket joint at the center of one of the side plates to ensure that the pressure was evenly distributed. The membranes were Ultracella feinst grade (Membranfilter Gasellschaft) conditioned from water to

tetrahydrofuran through ethyl alcohol. The osmometers were mounted in a water thermostat controlled to better than  $\pm 0.02^\circ\text{C}$ .

### Viscometry

Intrinsic viscosities were measured in tetrahydrofuran at  $25^\circ\text{C}$ . in a modified Ubbelohde<sup>21</sup> viscometer. For most samples concentrations up to 5 g./l. can be used, but solution of some high molecular weight fractions is incomplete above 1 g./l.

## RESULTS AND DISCUSSION

### Fractions

A number of fractions were characterized by both light scattering and osmometry. The results are shown in Table I, the errors being standard deviations. As would be expected from the simple fractionation procedure there is appreciable polydispersity, especially at higher molecular weights, though the fractions are narrower than the polymers from which they were made, the latter having  $\bar{M}_w/\bar{M}_n$  ratios of about 2.5.

TABLE I  
Molecular Weights of Poly(vinyl Chloride) Fractions

Fraction	Molecular weight $\times 10^{-3}$		$\bar{M}_w/\bar{M}_n$
	Weight-average, $\bar{M}_w$	Number-average, $\bar{M}_n$	
2P/2	$214 \pm 6.6$	$134 \pm 7.6$	$1.60 \pm 0.10$
1P/3	$198 \pm 5.5$	$102 \pm 7.6$	$1.94 \pm 0.16$
2P/3	$149 \pm 4.0$	104	1.43
5P/4	$138 \pm 2.6$	$112 \pm 8.5$	$1.24 \pm 0.10$
1P/4	$102 \pm 1.3$	$90.2 \pm 16.7$	$1.13 \pm 0.21$
2P/4	$79.1 \pm 2.1$	$70.6 \pm 1.8$	$1.12 \pm 0.04$
1P/5	$71.3 \pm 0.5$	50.3	1.42

A double logarithmic plot of weight-average molecular weight against intrinsic viscosity is shown in Figure 1. All fractions with  $\bar{M}_w$  below 170,000, and a few of higher molecular weight, lie about a straight line from which most of the upper fractions deviate substantially in the direction of low viscosity. By making a least-squares fit of a line through the points indicated in Figure 1 the following Mark-Houwink equation is obtained:

$$\log \bar{M}_w = (4.945 \pm 0.038) + (1.306 \pm 0.027) \log [\eta] \quad (1)$$

or

$$[\eta]_{\text{THF}}^{25^\circ\text{C}} = 1.63 \times 10^{-4} \bar{M}_w^{0.766} \text{ dl./g.} \quad (2)$$

Linear polymers usually obey the Mark-Houwink equation over a wide range of molecular weight, and the molecular weight exponent of 0.766



observed here is a typical value for a polymer free of long branching in a good solvent. The deviations from eq. (1) at high molecular weight, and the greater scatter of points in that region require explanation. The

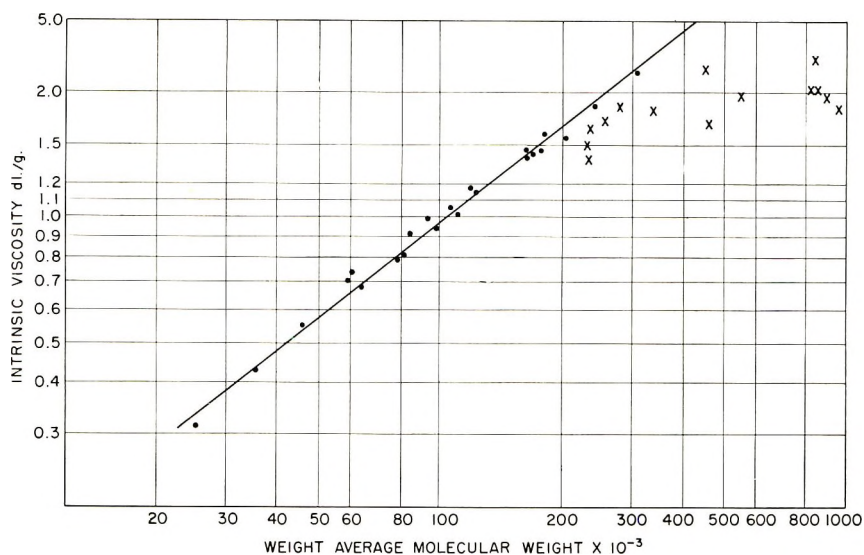


Fig. 1. Weight-average molecular weight vs. intrinsic viscosity for fractions: (—) by eq. (1); (●) points used to determine eq. (1); (×) points deviating from eq. (1).

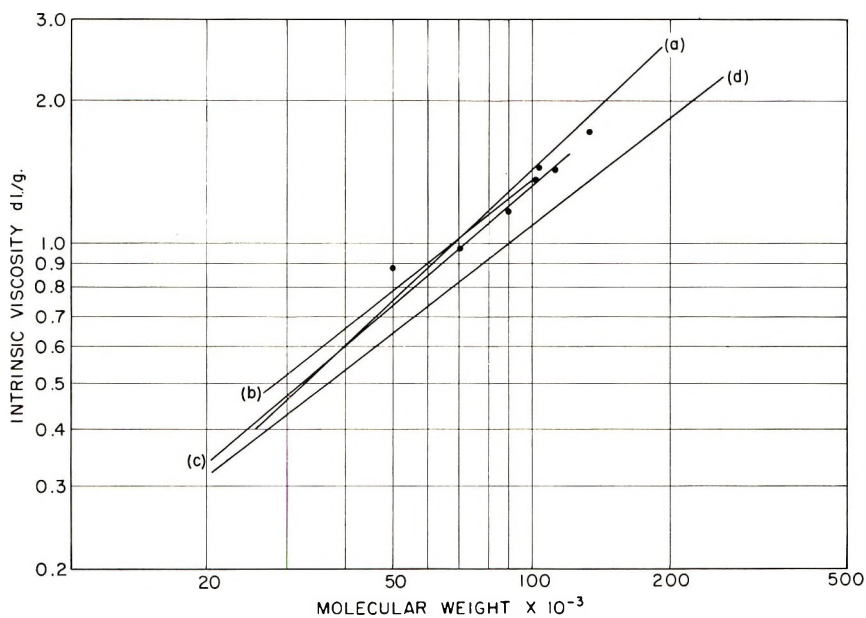


Fig. 2. Molecular weight and intrinsic viscosity relationships for fractions: (a) Batzer and Nisch<sup>2</sup> by osmometry; (b) Guyot and Benevise<sup>8</sup> by osmometry; (c) Krasovec<sup>1</sup> by osmometry, (d) this paper by light scattering; (●) this paper by osmometry.

deviations are much too large to be accounted for by polydispersity,<sup>14</sup> and the most likely explanation is that the upper fractions contain an appreciable number of long-branched molecules, and so have a low solution viscosity for their molecular weight. Krasovec, using number-average molecular weights, also found deviations from his linear correlation at high molecular weights and attributed them to long branching.<sup>1</sup> This interpretation is consistent with the kinetics of free radical polymerization, since long branches would be expected to be due to secondary reaction with preformed polymer and so to occur preferentially in the larger molecules.

There are no data in the literature directly comparable with eq. (1), other work being based on number-average molecular weights. Viscosity-molecular weight relations based on number-average rather than weight-average molecular weights are more sensitive to polydispersity. Figure 2 compares eq. (1) with three equations based on number-average molecular weight measurement on fractions.<sup>1,2,8</sup> Two of these are for solution viscosities measured at 20°C. rather than 25°C., but intrinsic viscosity is not sufficiently sensitive to temperature to invalidate the comparison. Number-average data for the fractions in Table I are also plotted and lie on the other number-average correlations, suggesting that other authors' fractions have been of similar width to ours and that the differences in the correlations is due to the sensitivity of the number-average relation to polydispersity. This being so, eq. (1), being based on weight averages, gives the best estimate of the viscosity-molecular weight relation for linear monodisperse fractions and should, in fact, give a close estimate to the monodisperse line, since even the highest measured polydispersity is unlikely to alter the observed intrinsic viscosity for a given molecular weight by more than 5%.<sup>14</sup>

### Unfractionated Polymers

A number of commercial and experimental polymers covering a wide range of molecular weight were also studied. Figure 3 shows the molecular weights for these plotted against the intrinsic viscosity, together with the linear fraction line for comparison. As expected, the whole polymers have higher weight-average molecular weights than linear fractions of the same solution viscosity. Part of this displacement is due to polydispersity, but most of it is due to long branching. As the molecular weight increases, so the width of the molecular weight distribution as measured by the ratio of weight-average to number-average molecular weight increases. This is for molecular weights of about 40,000 and above; below this the accuracy of the light-scattering technique falls off, and the data are not sufficiently reliable for firm conclusions to be drawn.

Poly(vinyl chloride) polymers are commonly characterized by the Fikentscher  $K$  value derived from a solution viscosity measurement.<sup>22</sup> Figure 4 relates the  $K$  value in ethylene dichloride at 25°C. for 0.5 g. polymer in 100

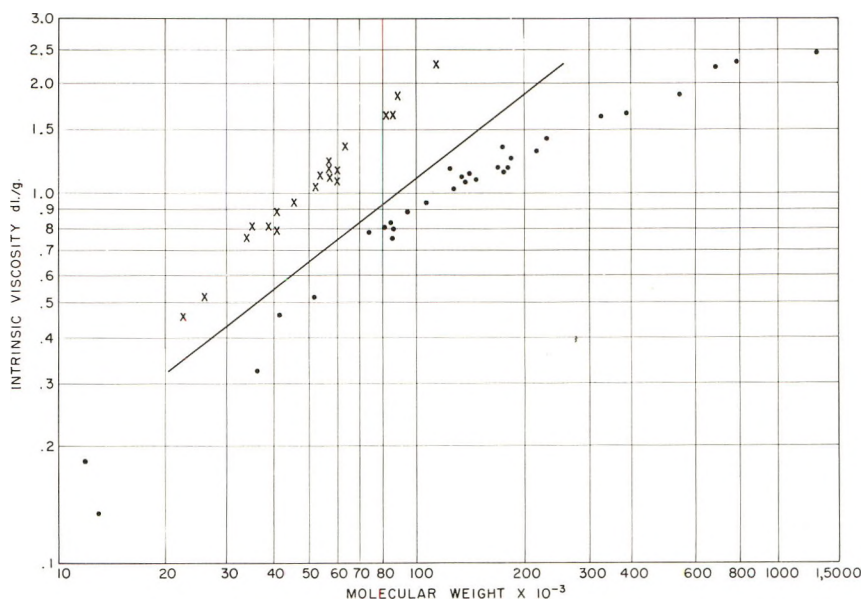


Fig. 3. Intrinsic viscosity vs. molecular weight for unfractionated polymers: (×) number-average molecular weight by osmometry; (●) weight-average molecular weight by light scattering; (—) eq. (1) from this paper.

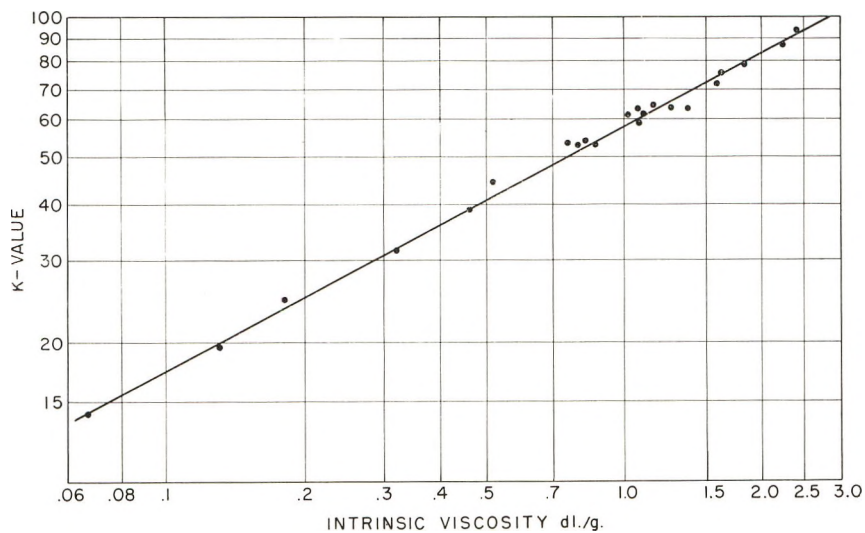


Fig. 4.  $K$  value vs. intrinsic viscosity.

ml. of solvent to the intrinsic viscosity in tetrahydrofuran at 25°C. for the polymers studied here.

The line shown in Figure 4 is:

$$\log [\eta]_{\text{THF}}^{25^\circ\text{C.}} = 1.91 \log (K)_{\text{EDC}}^{25^\circ\text{C.}} - 3.38 \quad (3)$$

We would like to thank Miss D. Timms, Mr. J. Bishop, Mr. K. S. Moors, and Mr. A. Titterton for their help with the experimental work.

### References

1. Krasovec, F., *Repts. J. Stefan Inst.*, **3**, 203 (1956).
2. Batzer, H., and A. Nisch, *Makromol. Chem.*, **22**, 131 (1957).
3. Mencik, Z., *Chem. Abstr.*, **50**, 650i, 1360h (1955).
4. Bier, G., and H. Kramer, *Makromol. Chem.*, **19**, 151 (1956).
5. Endo, R., *Kobunshi Kagaki*, **18**, 143 (1961).
6. Breitenbach, J. W., E. L. Forster, and A. J. Renner, *Kolloid Z.*, **127**, 1 (1952).
7. Danusso, F., G. Moraglio, and A. Gazzera, *Chim. Ind. (Milan)*, **36**, 883 (1954).
8. Guyot, A., and J. P. Benevise, *Ind. Plast. Mod.* **13**, 37 (June 1961).
9. Hengstenberg, *Angew. Chem.*, **62**, 26 (1950).
10. Laker, D., *J. Polymer Sci.*, **25**, 122 (1957).
11. Doty, P., H. Wagner, S. Singer, *J. Phys. & Coll. Chem.* **51**, 32 (1947).
12. Peterlin, A., paper presented at IUPAC Symposium on Macromolecular Chemistry Milan, 1954; *Ricerca Sci. Suppl.*, **25B**, 533 (1955).
13. Guzman, G. M., and J. M. G. Fatou, *Ann. Real. Soc. Espan. Fis. Quim.*, **54**, 601 (1958).
14. Tompa, H., *Polymer Solutions*, Butterworths, London, 1956.
15. Bosworth, P., C. R. Masson, H. W. Melville, and F. W. Peaker, *J. Polymer Sci.*, **9**, 565 (1952).
16. Ovenall, D. W., and F. W. Peaker, *Makromol. Chem.*, **33**, 222 (1959).
17. Bowen, E. J., *Chemical Aspects of Light*, Clarendon Press, London, 1942.
18. Freeman, M., unpublished results.
19. Kratochvil, J. P., G. J. Dezelic, M. Kerker, and E. Matijevic, *J. Polymer Sci.*, **57**, 59 (1962).
20. Zimm, B. H., and I. Myerson, *J. Am. Chem. Soc.*, **68**, 911 (1946).
21. Ubbelohde, L., *Ind. Eng. Chem. Anal. Ed.*, **9**, 85 (1937).
22. Fikentscher, H., *Zellulosechem.*, **13**, 58 (1932).

### Résumé

On a pu caractériser, par diffusion lumineuse, osmométrie et viscosimétrie en solution, des chlorures de polyvinyle fractionnés et non-fractionnés. A partir des résultats obtenus sur ces fractions, on peut conclure que les molécules plus grandes contiennent de longues ramifications. Pour les fractions linéaires la relation entre la viscosité intrinsèque dans le tétrahydrofurane à 25°C et le poids moléculaire moyen en poids mesuré par diffusion lumineuse est donné par:  $(\eta) = 1.63 \times 10^{-4}(M_w)^{0.766}$  dcl/g.

### Zusammenfassung

Eine Anzahl fraktionierter und unfraktionierter Polyvinylchloridproben wurden durch Lichtstreuung, Osmometrie und Lösungsviskosimetrie charakterisiert. Aus den Ergebnissen an Fraktionen wird geschlossen, dass die grösseren Moleküle lange Verzweigungen enthalten. Für lineare Fraktionen lautet die Beziehung zwischen der Viskositätszahl in Tetrahydrofuran bei 25°C und dem aus der Lichtstreuung bestimmten Gewichtsmittelwert des Molekulargewichts:  $[\eta] = 1,63 \times 10^{-4}(M_w)^{0.766}$  dcl/g.

Received June 26, 1963



## The Use of Syton 2X Colloidal Silica as a Calibration Medium for Light-Scattering Photometers

B. R. JENNINGS and H. G. JERRARD, *Department of Physics, The University of Southampton, Southampton, England*

### Synopsis

Details are given of studies made on a colloidal silica suspension known as Syton 2X. The studies were carried out to investigate the possibilities of Syton as a calibration medium for light-scattering photometers. The requisites of a suitable calibration medium are discussed. The same studies were made on another silica suspension, Ludox, which has been much used by others for calibration and the results obtained for the two substances compared. Transmission and angular scattering properties were studied using a spectrophotometer and a light scattering photometer respectively. The calibration constant  $J$  of the latter instrument was determined using Syton and Ludox. The values obtained for  $J$  were almost identical. The instrument was used to determine the Rayleigh ratios  $R_{90}$  of benzene, toluene, and carbon disulfide for two wavelengths (4358 and 5641 Å.). The values compare favorably with those of other workers and are considered very reliable. Weight-average particle sizes were found with the use of an electron microscope, an analytical ultracentrifuge, and the light-scattering and transmission data. The electron micrographs showed Ludox and Syton particles to be almost spherical. The particle diameters of Ludox were found to be 199 Å. by the electron microscope, 174 Å. by the ultracentrifuge, and 195 Å. by light-scattering and transmission measurements. For Syton the corresponding values were 145 Å., 142 Å., and 142 Å., respectively. Depolarization ratios were also determined; in both cases they were small. It is concluded that provided oil-free samples are used, Syton is a good substitute for Ludox. Its particles are smaller and the solutions are less polydisperse. It is thought that the ultracentrifuge gives low values for particle diameters and that this is possibly due to an incorrect assumption for the frictional coefficient of the sedimenting particles.

### INTRODUCTION

The technique of light scattering is a well-established one for the measurement of molecular weight and anisotropy of large molecules.<sup>1</sup> It is required to find the intensity of the light scattered at various angles, and this is expressed in terms of the reduced intensity  $R_{\theta}$  or Rayleigh ratio. In recent years a number of light-scattering photometers have been described in which the scattered intensity is detected by a photon multiplier.<sup>1-13</sup> To obtain the absolute value of the reduced intensity from the photon multiplier current it is necessary to calibrate the apparatus, and the most usual and best method is to make observations on a suitable scattering medium. The medium most frequently used is Ludox HS (supplied by E. I. du Pont

de Nemours, Wilmington, Delaware, U.S.A.; English agents, Brown and Forth, London, England). This is a suspension of colloidal silica of amorphous form with approximately spherical particles<sup>6,14,15</sup> of diameter about 200 Å., and its suitability has been investigated by a number of workers.<sup>6,16-25</sup> Another amorphous silica suspension is Syton 2X. This is easily obtained (Monsanto Chemicals Ltd., London, England) and has been used as well as Ludox to calibrate the light-scattering photometer employed in this laboratory.<sup>13</sup> The suitability of this material has been fully investigated and compared with Ludox by studies with an electron microscope, an ultracentrifuge and by light-scattering and turbidity measurements. The results of these studies, including the determination of the particle sizes of both Syton and Ludox, are presented in this paper.

### REQUIREMENTS OF A CALIBRATION MEDIUM

Calibration may be effected in light-scattering photometers by using the instrument to find the Rayleigh ratio at 90° of a suitable solution and using a spectrophotometer to find the turbidity  $\tau$ . The latter is defined either by the equation  $I = I_0 e^{-\tau L}$ , in which  $I$  is the intensity of light after traversing a distance  $L$  in the medium, or, in terms of the optical density  $D$ , by the equation  $\tau = 2.303 D/L$ . If  $J$  is the calibration constant of the light scattering photometer and  $S$  the reading corresponding to  $R_{90}$ , then

$$\tau = (16\pi/3)R_{90} = (16\pi/3)JS e^{-\tau l} \quad (1)$$

where  $e^{-\tau l}$  is a correction term for the attenuation<sup>20,21</sup> which will arise when there is a difference  $l$  in the paths traversed in the solution by the direct and scattered beams. Evaluation of  $\tau$  thus enables  $J$  to be found. The method is absolute but certain qualities are required of the solution. Thus (1) all the light lost while traversing the solution must be due to scattering and none through absorption, (2) the scattering particles must be small compared to the wavelength of light, (3) the particles must be optically isotropic, (4) the solution must be stable and not prone to aggregation for as long a period as is required to perform the calibration, (5) the particles should be sufficiently dense to give reasonably high turbidity values at the low concentrations necessary for calibration. Low concentrations are necessary to avoid such adverse effects as secondary scattering and particle interaction.

Since the intensity of scattered light is dependent on the inverse of the fourth power of the wavelength *in vacuo*,  $\lambda_0$ , condition (1) will be fulfilled only if  $\tau$  or  $D$  is proportional to  $\lambda_0^{-4}$  over the wavelength region required. If condition (2) is not satisfied, the light scattered in the forward direction exceeds that scattered in the backward direction as a result of interference of the scattered light so that a dissymmetric angular scattering pattern is obtained. Anisotropic particles will give rise to an additional horizontally polarized component in the scattered intensity which leads to an increase

in  $R_{90}$ , so that the isotropic condition is manifest by the requirement that the medium should possess a small depolarization ratio  $\rho_u$ . This, for light scattered horizontally from a horizontal incident unpolarized beam, is the ratio of the intensities of the horizontally and vertically vibrating components. The requirement of stability is not coupled with that of reproducibility, for the solution acts only as a temporary link between the light-scattering photometer and the spectrophotometer so that it is sufficient only for the solution to remain stable for the time required to perform both sets of measurements. The method of suspending the silica in a dilute salt solution to achieve better reproducibility,<sup>22, 24, 26</sup> although to be commended, is not a necessity.

## MATERIALS AND RESULTS

Syton and Ludox are colloidal suspensions of silica in water. The manufacturers suppose the particles to be approximately spherical with a Gaussian distribution of sizes. Each is provided as a stock solution of 30% concentration at pH 9 with negligible amount of free electrolyte. The Ludox used was a technical sample and the Syton an oil-free sample (Batch No. R/V 3733).

The samples were made up for study to the approximate concentration required by adding fresh glass distilled water to the stock solution and were then centrifuged in an MSE preparative centrifuge at 15000 g for 60 min. The supernatant was removed from the centrifuge tube without removing the latter from the centrifuge. This was done with the aid of a hypodermic syringe fitted with a separate inlet and an outlet nozzle on which was fitted a 1.2  $\mu$  Millipore filter unit (Millipore Filter Corporation, Bedford Massachusetts, U.S.A.; English agents V.A. Howe and Co. Ltd., London, England). Centrifugation and filtration were necessary to remove dust and large aggregates. For light-scattering measurements the solution was injected directly into the light-scattering cell through a serum-seal cap in the cell lid so that no dust could enter. Concentrations were determined by evaporating and drying to constant weight.

### Transmission Measurements

Readings of optical density  $D$  over the wavelength range 4200–6000 Å. for different concentrations of Ludox and Syton were taken with a Unicam SP 500 spectrophotometer in which cells of length 4 cm. were used. The reference solution employed was freshly distilled water which had been filtered through a 1.2  $\mu$  Millipore filter. Any possible errors which could occur by the cells not being perfectly matched were eliminated by interchanging the solution and solvent and averaging the two results obtained. Care was taken to place the cells in the same position. Graphs of  $D$  against the reciprocal of the fourth power of the wavelength were drawn (Fig. 1) for different concentrations and were found to be linear except for high

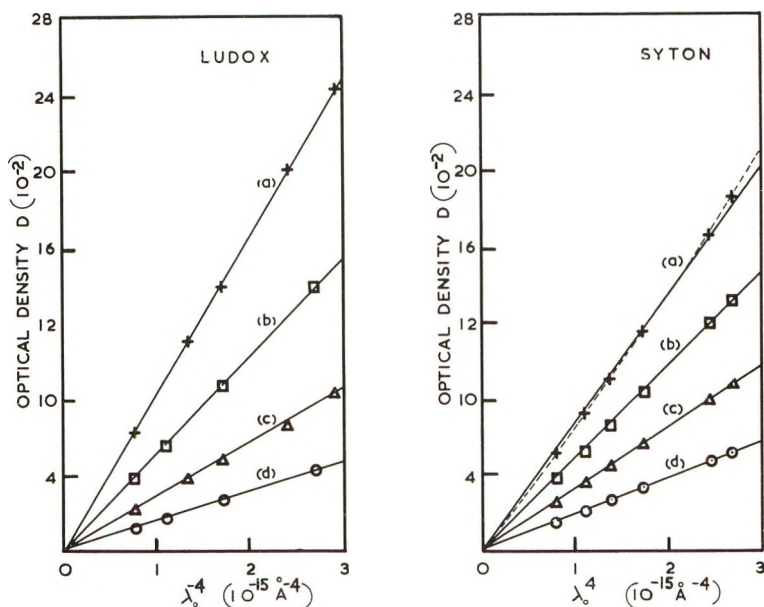


Fig. 1. Variation of optical density with the reciprocal of the fourth power of the wavelength at four concentrations. Ludox: (a) 3.93 g./100 cc.; (b) 1.97 g./100 cc.; (c) 0.984 g./100 cc.; (d) 0.492 g./100 cc. Syton: (a) 14.23 g./100 cc.; (b) 7.12 g./100 cc.; (c) 3.56 g./100 cc.; (d) 1.78 g./100 cc.

concentrations of Syton for which the graph is slightly curved (see dotted line). In general, therefore, the solutions are free from absorption.

### Angular Scattering Measurements

Scattering observations were taken using an apparatus in which a null modulation method was used to measure the ratio of the intensity  $I_\theta$  of the light scattered at an angle  $\theta$  to the direction of the incident light, to that ( $I_0$ ) incident on the scattering volume. This is accomplished by attenuating  $I_0$  until it equals  $I_\theta$ , the condition being found by an electronic detector. The angular distributions of intensity were obtained for both Ludox and Syton over the range  $35^\circ < \theta < 145^\circ$  for two wavelengths. The measured values of intensity  $I_\theta$  were multiplied by  $\sin \theta$  to allow for the volume change seen by the viewing system as  $\theta$  changed and then by  $(1 + \cos^2\theta)^{-1}$  to account for the presence of light with its electric vector horizontal. The latter supplements the light with its electric vector vertical which exists for all values of  $\theta$ . These experiments were carried out for four concentrations and typical results are shown in Figure 2, in which the ordinates are given in terms of  $R_\theta$  which is proportional to  $I_\theta$ . The absence of dissymmetry is clearly shown, and the standard deviations from the constant value of the ordinate are 0.15% and 0.38% for Ludox at 4358 Å. and 5461 Å., respectively, while the corresponding values for Syton are 0.26% and 0.23%.



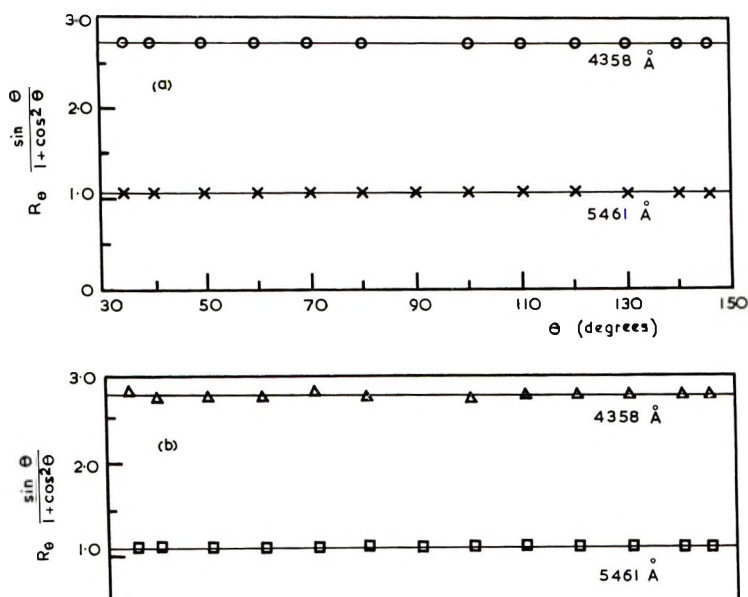


Fig. 2. Typical graphs of  $R_\theta \sin \theta / (1 + \cos^2 \theta)$  as a function of angle of scattering  $\theta$  at two wavelengths for (a) Ludox (concn. = 0.984 g./100 cc.; and (b) Syton (concn. = 3.558 g./100 cc.).

The solutions therefore consist of particles which must be small compared to the wavelength of light.

The optical anisotropy of the particles will be reflected in the depolarization ratio  $\rho_u$ . The intensities of the horizontally and vertically vibrating components were measured at  $\theta = 90^\circ$  for five concentrations at 4358 Å. In all cases the intensities increased with concentration but had zero values when extrapolated to zero concentration which for this value of  $\theta$  indicated the absence of stray light. Graphs of  $\rho_u$  against concentration are shown in Figure 3, from which the values of  $\rho_u$  at zero concentration were found to be 0.0039 and 0.0053 for Ludox and Syton, respectively. These values, which give Cabanne's factors<sup>27</sup>  $(6 - 7 \rho_u) / (6 + 6 \rho_u)$  of almost unity, show that the particles possess negligible anisotropy, since  $\rho_u$  for small isotropic spheres is zero.

#### Determination of Calibration Constant

Thus far it has been shown that Syton, like Ludox, satisfies the first three requirements listed above. Requirements (4) and (5) are also met. The solutions were next used to calibrate the light-scattering photometer used by the authors. Of the two common methods of calibration available, one due to Goring et al.<sup>22</sup> and the other to Maron and Lou,<sup>20</sup> that of the former

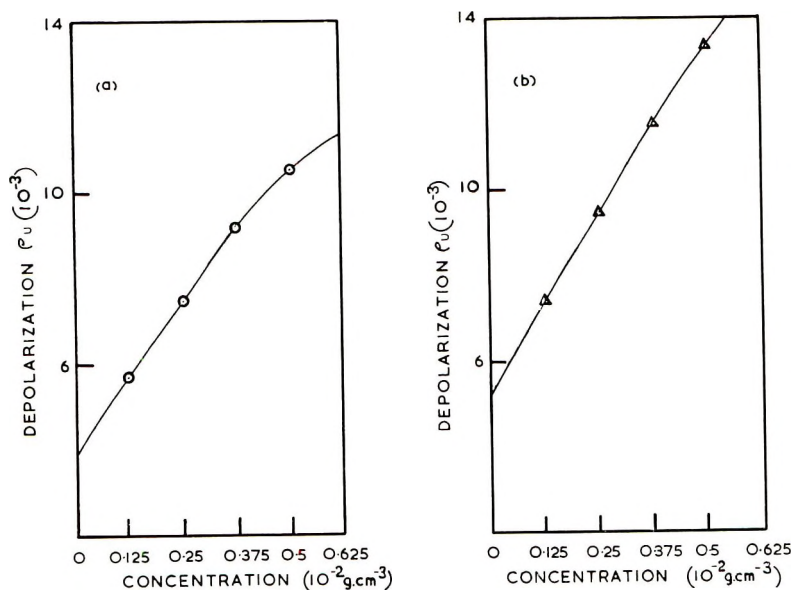


Fig. 3. Variation of depolarization ratio with concentration at 4358 Å. for (a) Ludox and (b) Syton.

was used. This was because the correction term  $e^{-\tau l}$  in eq. (1) was easily applied. An additional advantage is that the method gives data which enable particle sizes to be found. The details are as follows. The attenuation, previously mentioned, of the transmitted intensity  $I_0$  is accomplished by the insertion of a neutral filter to make the resultant transmitted light of the same order as that of the scattered light and then finally letting it pass through two linear polarizing devices  $P_1$  and  $P_2$ . The second of these,  $P_2$ , is rotated to a position  $\phi$  read on a graduated circle so that the final transmitted intensity equals the scattered intensity. The reading  $S$  of eq. (1) is then a function of  $\phi$ , i.e.,  $f(\phi)_{90}$ , so that eq. (1) reads

$$\tau = (16\pi/3) R_{90} = (16\pi/3) Jf(\phi)_{90}e^{-\tau l}$$

If  $f(\phi)_{90} e^{-\tau l}$  be written as  $I'_{90}$   
then

$$J = R_{90}/I'_{90} = (3/16\pi) (\tau/I'_{90})$$

or

$$J = (3/16\pi) [(c/I'_{90})/(c/\tau)]_{c=0} \quad (2)$$

By use of the data obtained with Ludox and Syton from the transmission and angular scattering studies described in the previous sections, graphs of  $c/I'_{90}$  and  $c/\tau$  against  $c$  were drawn (Figs. 4 and 5). (The apparently greater scattering shown at the higher wavelength in Figures 4a and 5a, although corresponding to a smaller turbidity is due to the use of different

neutral filters.) By extrapolation, values for zero concentration were found and  $J$  calculated from eq. (2). The results are tabulated in Table I. The accuracies are about  $\pm 1\%$  so that good agreement exists and there ap-

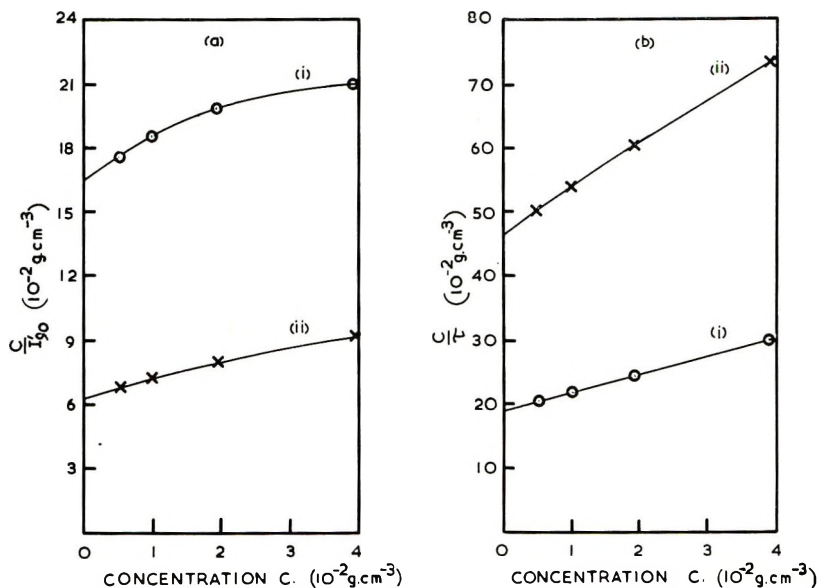


Fig. 4. Graphs of (a)  $c/I'_{90}$  and (b)  $c/\tau$  against concentration  $c$  for Ludox at wavelengths (i) 4358 Å. and (ii) 5461 Å.

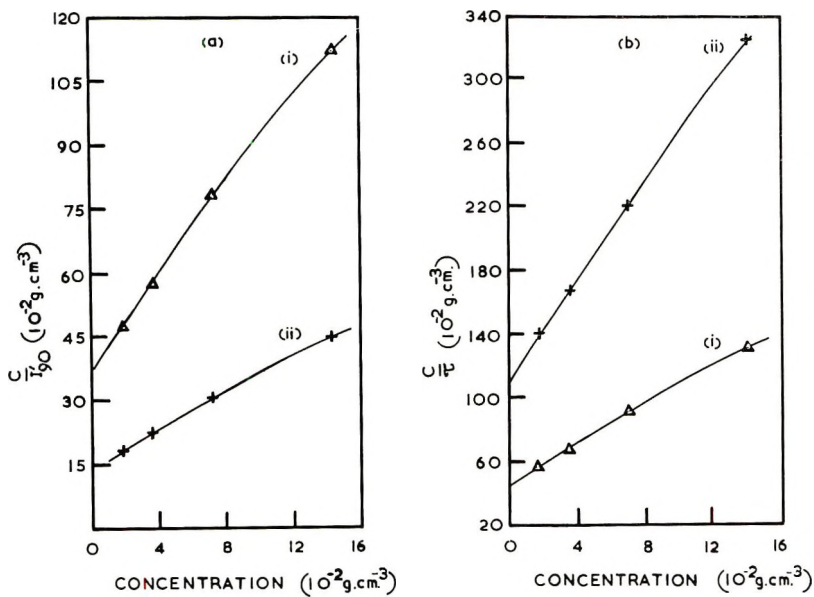


Fig. 5. Graphs of (a)  $c/I'_{90}$  and (b)  $c/\tau$  against concentration  $c$  for Syton at wavelengths (i) 4358 Å. and (ii) 5461 Å.

pears to be no significance in the Syton values being lower than those obtained with Ludox.

TABLE I  
Calibration Constants  $J$  Obtained with Ludox and Syton 2X

	$\lambda_0 = 4358 \text{ \AA.}$			$\lambda_0 = 5461 \text{ \AA.}$		
	$(c/\tau)_{c=0}$	$(c/I'_{90})_{c=0}$	$J \times 10^{-2}$	$(c/\tau)_{c=0}$	$(c/I'_{90})_{c=0}$	$J \times 10^{-3}$
Ludox	0.191	0.163	5.10	0.469	0.063	7.98
Syton	0.455	0.382	5.04	1.117	0.147	7.87

As a check upon the validity of the calibration constants the Rayleigh ratio was determined for benzene, toluene, and carbon disulfide at 21°C. using the mean values for  $J$  given in Table I. Readings were corrected for the refraction effect<sup>28</sup> which arises from the difference in refractive index between the liquid and the calibration solution. Fluorescence was allowed for by placing a filter in the path of the scattered light before it entered the photometer. The Fresnel<sup>19</sup> and volume corrections<sup>29</sup> were negligibly small. The results, given in Table II, compare favorably with those listed by Kratochvil et al.<sup>25</sup>

TABLE II  
Rayleigh Ratios  $R_{90}$  for Some Pure Liquids

	$R_{90} \times 10^{-6}, \text{ cm.}^{-1}$	
	4358 \AA.	5461 \AA.
Benzene	46.8	17.5
Toluene	56.1	20.4
Carbon disulfide	244.6	82.9

## DETERMINATION OF PARTICLE SIZES

Although the suitability of Syton as a calibration medium has been shown by the results described above, for completeness information on particle sizes was found. These were obtained by using an electron microscope, an analytical ultracentrifuge, and the results of the angular scattering and turbidity experiments.

### Electron Microscope

If the diameters of a number  $k$  of particles are measured then the weight-average and number-average diameters  $d_w$  and  $d_n$  may be found. Assuming the particles are spherical, so that their molecular weight is given by  $M = \pi \rho N_A d^3/6$ , then



$$d_w = \left[ \frac{\sum_1^k n_i d_i^6}{\sum_1^k n_i d_i^3} \right]^{1/3} \quad (3)$$

and

$$d_n = \left[ \frac{\sum_1^k n_i d_i^3}{\sum_1^k n_i} \right]^{1/3} \quad (4)$$

where  $n_i$  is the number of particles with diameter  $d_i$ . From these equations the diameters and degree of poly-dispersity  $d_w^3/d_n^3$  ( $\equiv M_w/M_n$ ) may be found.

The electron microscope used was a Philips Model EM 75. After the preparative centrifugation one drop of each of Syton and Ludox at a concentration of about 1.5% was added to 100 ml. of freshly distilled, filtered water. Small droplets of these solutions were transferred to bronze grids covered by a thin Formvar film which had been stripped from glass slides. In Figure 6 are shown typical electron micrographs. Measurements of the particle diameters of some 100 particles were taken directly from the photographs by using a calibrated microscope. From eq. (3) the weight-average diameters were calculated to be 199 Å. and 145 Å., respectively, for Ludox and Syton. From eq. (4) the corresponding number-average diameters were 162 Å. and 130 Å. These figures give poly-dispersity ratios of 1.88 and 1.39.

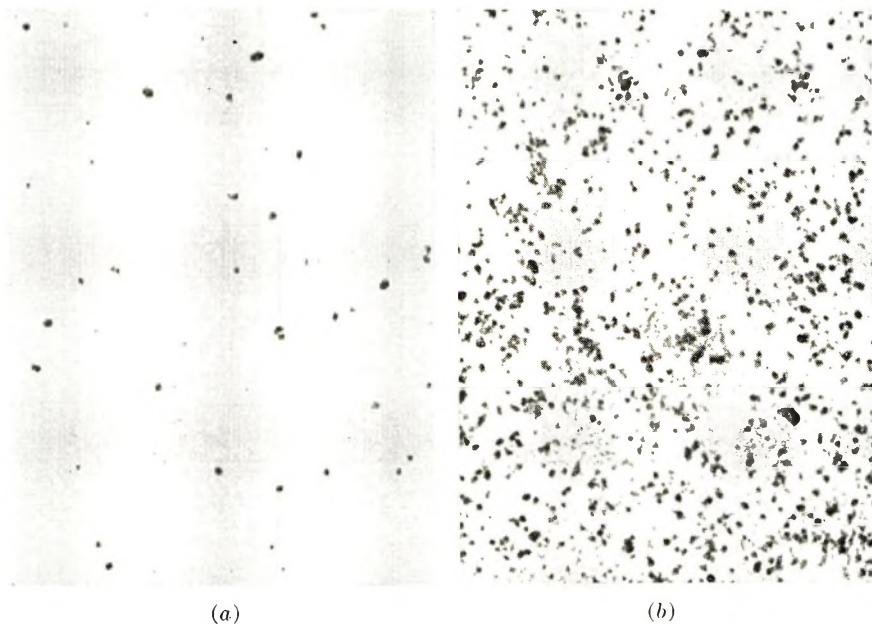


Fig. 6. Electron micrographs of (a) Ludox and (b) Syton at magnification 51,300:1.

### Ultracentrifuge

For the centrifuge studies a Spinco Model E analytical ultracentrifuge was used. Schlieren optics was employed. By this means the passage of the maximum concentration gradient down the cell with time caused by the centrifugal force is seen as the movement of a curve having a pronounced peak. If  $x$  is the distance of the peak at any time  $t$  from the axis of rotation and  $\omega$  is the angular velocity, then the sedimentation constant  $s$  given by

$$s = \dot{x}/\omega^2 x = (2.303/\omega^2) [\partial(\log x)/\partial t] \quad (5)$$

may be found from a graph of  $\log x$  against  $t$ . When the particles are traveling down the cell without acceleration, the mass  $m$  is related to the frictional resistance  $f$  and to  $s$  by the equation

$$sf = m[1 - (\rho_0/\rho)]$$

in which  $\rho_0$  and  $\rho$  are the densities of the solvent and solute respectively. For spherical particles of diameter  $d$  in a liquid of dynamic viscosity coefficient  $\eta_0$ , according to Stokes,  $f = 3\pi\eta_0 d$  so that

$$d^2 = 18 \eta_0 s / (\rho - \rho_0) \quad (6)$$

from which  $d$  may be found.

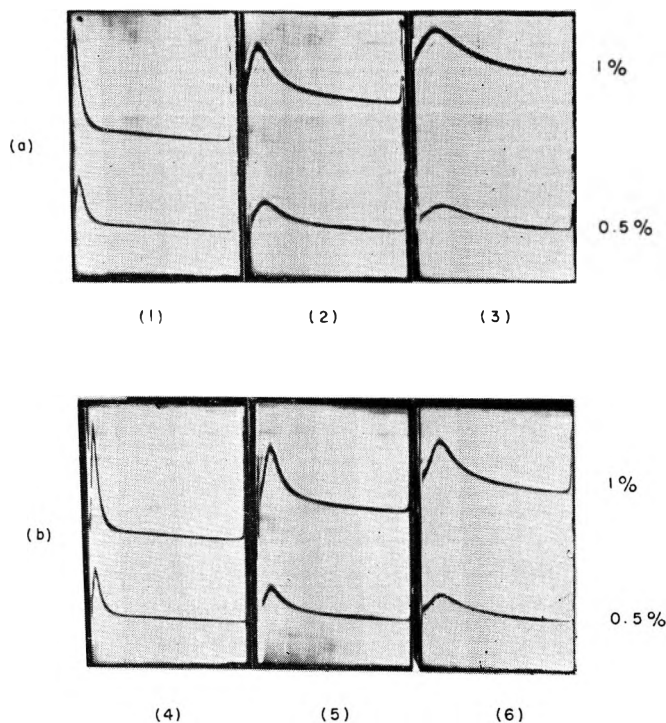


Fig. 7. Schlieren ultracentrifuge patterns for (a) Ludox and (b) Syton at times 0, 8, and 16 min. after attaining an acceleration of 13,060 g at various Schlieren angles: (1) 50°; (2) 40°; (3) 35°; (4) 55°; (5) 45°; (6) 40°. Concentrations 1 and 0.5%; temperature 20°C.

Owing to interaction effects  $s$  changes with concentration and so the value to be used in eq. (6) is that for zero concentration. Measurements were made at a number of concentrations varying from 1% to 0.1%. A centrifugal force of 13,060 g was used. Typical sedimentation-velocity patterns are shown in Figure 7. Graphs of  $s$  against  $c$  are given in Figure 8 from which the values of  $s$  at zero concentration were found. Measurements were taken at a temperature of 20°C. If  $\rho_0$  is taken as 0.9978 g./cm.<sup>3</sup>

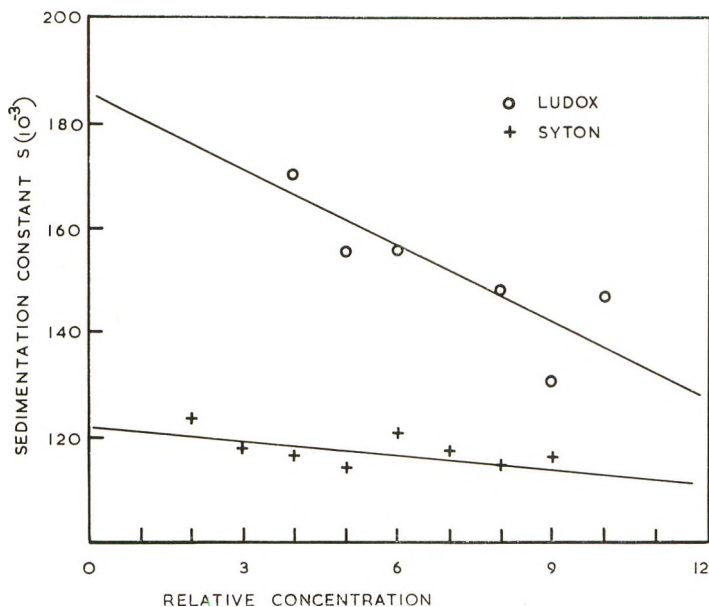


Fig. 8. Variation of sedimentation constant  $s$  with concentration for Ludox and Syton.

and the values of  $\rho$  for Ludox and Syton, respectively, as 2.278 and 2.2 g./cm.<sup>3</sup>, as given by the manufacturers, then with a value of  $1.6019 \times 10^{-2}$  poise for  $\eta_0$ , a particle diameter of 174 Å. was found for Ludox and 142 Å. for Syton. The rate at which the concentration peaks broaden in Figure 7 indicates that the Ludox suspension is more polydisperse than the Syton.

### Light Scattering and Turbidity

From the Rayleigh-Gans theory the Rayleigh ratio at 90° is given by

$$R_{90} = Kc'M_w P(\theta) \quad (7)$$

where  $c'$  is the concentration (in grams per cubic centimeter of solution),  $M_w$  is the weight-average molecular weight,  $K$  is a constant, and  $P(\theta)$  a particle scattering factor.

$$K = \frac{2\pi^2 n_0^2 (\partial n_0 / \partial c)^2}{\lambda_0^4 N_A} \quad (8)$$

where  $N_A$  is Avogadro's number and  $n$  and  $n_0$  the refractive indices of the solute and solvent, respectively. For a sphere of diameter  $d$

$$P(\theta) = \left[ \frac{3}{x^3} (\sin x - x \cos x) \right]^2$$

in which

$$x = (2\pi/\lambda_0) n_0 d \sin (\theta/2)$$

Since

$$M = N_A \rho \pi d^3 / 6$$

and for dilute solutions

$$n = n_0 + (\partial n / \partial c) (\rho / \rho_0)$$

$$\text{by eqs. (7) and (8)} \quad R_{90}/c = (\pi^3 d^3 / 3 \lambda_0^4) n_0^2 (\partial n / \partial c)^2 (\rho / \rho_0) P(\theta) \quad (9)$$

In this equation  $c$  is the concentration in grams of solute per gram of solution i.e.,  $c = \rho_0 c'$ .

Similarly, from the turbidity equation.

$$\tau/c = (16\pi^4 / 9 \lambda_0^4) d^3 n_0^2 (\partial n / \partial c)^2 (\rho / \rho_0) Q \quad (10)$$

in which  $Q$  is the particle dissipation factor.<sup>1,30</sup> The values of  $(\tau/c)$  and  $(R_{90}/c)$  in eqs. (9) and (10) must be those for zero concentration since the theory has not taken particle interaction into consideration. Values of  $P(\theta)$  and of  $Q$  are tabulated in the literature<sup>1,30</sup> in terms of  $n_0 d / \lambda_0$ . To determine  $d$  for both Ludox and Syton the following procedure was adopted. For a series of arbitrary values of  $n_0 d / \lambda_0$  for which the tables gave the corresponding values of  $Q$  and  $P(\theta)$ , eqs. (9) and (10) were used to calculate values of  $(\tau/c)_{c=0}$  and  $(R_{90}/c)_{c=0}$  for Ludox at 20°C. in water and for a wave length  $\lambda_0$  of 5461 Å. From the results (Table III) reference curves of  $(\tau/c)_{c=0}$  and  $(R_{90}/c)_{c=0}$  against  $n_0 d / \lambda_0$  were drawn. The appropriate curve was then used to find the value of  $n_0 d / \lambda_0$  corresponding to the value found experimentally for either  $(R_{90}/c)_{c=0}$  or  $(\tau/c)_{c=0}$  so that  $d$  could be calculated. To find  $d$  from experimental results obtained at a different

TABLE III

Values of Intrinsic Turbidity  $(\tau/c)_{c=0}$  and Scattering Intensities  $(R_{90}/c)_{c=0}$  for values of  $n_0 d / \lambda_0$ , calculated for  $\rho = 2.279$  g./cm.<sup>3</sup>,  $\rho_0 = 0.9978$  g./cm.<sup>3</sup>,  $\lambda_0 = 5461$  Å.,  $(\partial n / \partial c) = 0.06203$  cm.<sup>3</sup>/g., and  $n_0 = 1.3345$ .

$n_0 d / \lambda_0$	$Q$	$P(\theta)$	$(\tau/c)_{c=0}$	$(R_{90}/c)_{c=0}$
0.04			1.50	0.089 <sup>a</sup>
0.05	0.986	0.990	2.57	0.154
0.06			4.25	0.26 <sup>a</sup>
0.08			10.50	0.63 <sup>a</sup>
0.10	0.958	0.961	19.96	1.20
0.12			34.23	2.03 <sup>a</sup>
0.15	0.909	0.917	63.95	3.86

<sup>a</sup> Extrapolated values.



wavelength  $\lambda_0'$  or in a different solvent (density  $\rho_0'$ , refractive index  $n_0'$ ) or for a different solvent (density  $\rho'$ ), the same reference curve was used but with the experimental values corrected to the conditions under which the reference curve data were found. This meant multiplying by the factor  $Z$ , where

$$Z = \left[ \frac{(\partial n / \partial c)}{(\partial n / \partial c)'} \right]^2 \frac{\rho}{\rho'} \frac{\rho_0'}{\rho_0} \frac{n_0'}{n_0} \frac{\lambda_0'}{\lambda_0}$$

in which the primed parameters refer to values when different from the reference curve data.

Values of  $(\partial n / \partial c)$  were found with a Rayleigh interferometer using cells 1 cm. in length. To avoid any shift of the zero-order fringe, solutions of small concentration difference were compared. Five concentrations were used in the range 0.5–4% at a temperature of about 22°C. with the temperature held constant to within  $\pm 0.02^\circ\text{C}$ . The results are shown in Table IV and the particle sizes in Table V.

TABLE IV  
Relative Refractive Indices  $n/n_0$  for Ludox and Syton 2X

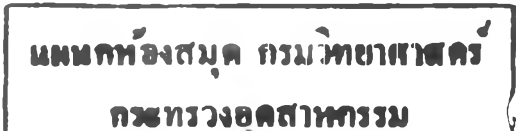
	$\lambda_0 = 4368 \text{ \AA.}$			$\lambda_0 = 5461 \text{ \AA.}$		
	$n_0$	$\partial n / \partial c,$ cm. <sup>3</sup> /g.	$n/n_0$	$n_0$	$\partial n / \partial c,$ cm. <sup>3</sup> /g.	$n/n_0$
Ludox	1.3408	0.0625	1.106	1.3345	0.0620	1.106
Syton	1.3408	0.0643	1.105	1.3345	0.0638	1.106

TABLE V  
Particle Sizes from Rayleigh-Gans Theory

	$\lambda_0$ A.	$(I'_{90}/c)'_{c=0}$	$(R_{90}/c)'_{c=0}$	$(R_{90}/c)_{c=0}$	$(\tau/c)'_{c=0}$	$(\tau/c)_{c=0}$	$d,$ A.
Ludox	5461	15.94	0.127	0.127	2.133	2.133	195
	4358	6.128	0.313	1.577	5.239	4.156	195
Syton	5461	6.789	0.054	0.529	0.896	0.875	141
	4358	2.615	0.133	0.660	2.196	1.701	142

### DISCUSSION

Ludox appears to be the most widely used medium for the calibration of light-scattering photometers. Justification for its use has been amply demonstrated, particularly if a number of precautions are taken.<sup>25</sup> In this paper it has been demonstrated that Ludox serves as a good approximation to a solution of Rayleigh (point) scatterers. The absence of any absorption or dissymmetry combined with a low depolarization ratio all recommend it. It is found that Syton also displays these qualities and is a good substitute for Ludox. The results obtained show Syton particles to be smaller than those of Ludox and the electron microscope and ultracentrifuge data indi-



cate that the Syton system is less polydisperse. Both these facts further commend the use of Syton. The depolarization ratio  $\rho_u$  was slightly higher than the value for Ludox, which suggests a slightly greater optical anisotropy. For both media however  $\rho_u$  is very small and they have Cabanne's correction factors of almost unity, so that for practical purposes their anisotropies can be considered as being negligible. The principal defect of Syton was the slight curvature in the absorption curve at high concentrations due possibly to slight contamination by mineral oil. It is essential therefore to obtain oil free samples.

The values of the Rayleigh ratio for pure liquids (Table II) all come among the so-called "high" values. The benzene results agree particularly well with those of Swenson<sup>31</sup> et al. for both 4358 Å. and 5461 Å. and are in very close agreement with the values of Moacanin,<sup>32</sup> Varadaiah,<sup>33</sup> and Oster.<sup>7</sup>

The accuracy of the values of  $d$  found from light-scattering measurements depend on the accuracy of the values of  $\partial n/\partial c$ . There is wide divergence in the reported values for Ludox—thus for a wavelength 5461 Å., Alexander and Her give a value of 0.076 cm.<sup>3</sup>/g. at 27°C., Trap and Hermans give 0.066 cm.<sup>3</sup>/g. at 25°C., and Dezelic and Kratochvil obtain 0.061 cm.<sup>3</sup>/g. at 23 ± 2°C. The latter claim their value as being the most reliable, and it agrees with the value of 0.062 cm.<sup>3</sup>/g. reported here (Table IV).

The particle sizes found by the different methods are given in Table VI. As is to be expected, the values obtained by scattering and transmission

TABLE VI  
Summary of Particle Sizes for Ludox and Syton as Found by Different Methods

Method	Particle size, Å.	
	Ludox	Syton
Electron microscope	199	145
Ultracentrifuge	174	142
Light scattering	195	142
Turbidity	195	142

measurements are the same because of the method of calibration but they are about 1.3% greater than those which would be obtained from simple Rayleigh theory. The reason for the low value obtained for Ludox by ultracentrifugation is uncertain—it may either be due to the expression assumed for the frictional resistance on the particles being too small because they are unlikely to be smooth spheres or to too low a value for  $s$ . The former would appear to make the major contribution. The same argument could apply to Syton but the particles are smaller and more monodisperse which may account for the effect being less.

The values found for Ludox and Syton are in general agreement with the sizes suggested by the manufacturers, although it is believed that no reliable value for Syton has been given previously.

One of us (B. R. J.) thanks the Department of Scientific and Industrial Research for the award of a postgraduate research studentship and both authors thank the Professors of Physics in whose department this work was carried out. The centrifuge used was purchased by a D.S.I.R. grant for special researches. The authors also wish to thank Dr. G. Kerkut of the Department of Physiology and Biochemistry for allowing them the use of the electron microscope and for his help.

### References

1. Stacey, K. A., *Light-Scattering in Physical Chemistry*, Butterworths, London, 1956.
2. Debye, P., *J. Appl. Phys.*, **17**, 392 (1946).
3. Zimm, B. H., *J. Chem. Phys.*, **16**, 1099 (1948).
4. Brice, B. A., M. Halwer, and R. S. Spieser, *J. Opt. Soc. Am.*, **40**, 768 (1950).
5. Bosworth, P., C. R. Masson, H. W. Melville, and F. W. Peaker, *J. Polymer Sci.*, **9**, 565 (1952).
6. Goring, D. A. I., *Can. J. Chem.*, **31**, 1078 (1953).
7. Oster, G., *Anal. Chem.*, **25**, 1165 (1953).
8. M'Ewen, M. B., and M. I. Pratt, *Nature and Structure of Collagen*, Butterworths, London, 1953, p. 158.
9. Aughey, W. H., and F. J. Baum, *J. Opt. Soc. Am.*, **44**, 833 (1954).
10. Hughes, W. J., and P. Johnson, *J. Sci. Instr.*, **35**, 157 (1958).
11. Baum, F. J., and F. W. Billmeyer, *J. Opt. Soc. Am.*, **51**, 452 (1961).
12. Martinez, A., and A. Massonier, *J. Phys. Radium*, **23**, 135 (1962).
13. Jerrard, H. G., and D. B. Sellen, *Appl. Optics*, **1**, 243 (1962).
14. Iler, R. K., *The Colloidal Chemistry of Silica and Silicates*, Cornell Univ. Press, Ithaca, N. Y., 1955.
15. Deželić, Dj., M. Wrischer, Z. Devide, and J. P. Kratochvil, *Kolloid-Z.*, **171**, 42 (1960).
16. Mommaerts, W. F. H., *J. Colloid Sci.*, **7**, 71 (1952).
17. Tietze, F., and H. Neurath, *J. Biol. Chem.*, **194**, 1 (1952).
18. Oster, G., *J. Polymer Sci.*, **9**, 525 (1952).
19. Oth, A., J. Oth, and V. Desreux, *J. Polymer Sci.*, **10**, 551 (1953).
20. Maron, S. H., and R. L. Lou, *J. Polymer Sci.*, **14**, 29 (1954).
21. Kraut, J., and W. Dandliker, *J. Polymer Sci.*, **18**, 563 (1955).
22. Goring, D. A. I., M. Senez, B. Melanson, and M. M. Huque, *J. Colloid Sci.*, **12**, 412 (1957).
23. Bonnelycke, R., and W. Dandliker, *J. Colloid Sci.*, **14**, 567 (1959).
24. Deželić, Gj., and J. P. Kratochvil, *Kolloid-Z.*, **173**, 38 (1960).
25. Kratochvil, J. P., Gj. Deželić, M. Kerker, and E. Matijević, *J. Polymer Sci.*, **57**, 59 (1962).
26. Deželić, Gj., and J. P. Kratochvil, *J. Phys. Chem.*, **66**, 1377 (1962).
27. Cabannes, J., *La Diffusion Moléculaire de la Lumière*, Presses Universitaires de France, Paris, 1929.
28. Hermans, J. J., and S. Levinson, *J. Opt. Soc. Am.*, **41**, 460 (1957).
29. Carr, C. I., and B. H. Zimm, *J. Chem. Phys.*, **18**, 1616 (1950).
30. Doty, P., and R. F. Steiner, *J. Chem. Phys.*, **18**, 1211 (1950).
31. Swenson, H. A., A. J. Morak, and S. Murath, *J. Polymer Sci.*, **51**, 231 (1961).
32. Moacanin, J., *J. Appl. Polymer Sci.*, **1**, 272 (1959).
33. Varadaiah, V. V., and V. S. R. Rao, *J. Polymer Sci.*, **50**, 31 (1961).

### Résumé

On donne des détails concernant des études effectuées sur une suspension colloïdale de silice connu sous le nom de Syton 2X. Ces études ont été entreprises en vue d'examiner les possibilités du Syton comme substance de calibrage pour les appareils de diffusion lumineuse. On discute des qualités requises d'une substance de calibrage.

Les mêmes études ont été effectuées sur une autre suspension de silice, le Ludox, qui a été beaucoup utilisé pour le calibrage et on compare les résultats obtenus pour les deux substances. On a étudié les propriétés de transmission et de diffusion angulaire au moyen d'un spectrophotomètre et d'un appareil de diffusion lumineuse. La constante de calibrage  $J$  pour ce dernier instrument a été déterminé au moyen de Syton et de Ludox. Les valeurs obtenues pour  $J$  sont tout à fait identiques. L'appareil a été employé pour déterminer le rapport de Rayleigh  $R_{90}$  pour le benzène, le toluène et le sulfure de carbone à deux longueur d'onde (4358 et 5641 Å.). Les valeurs obtenues comparées à celles d'autres auteurs peuvent être considérées comme tout à fait convenables. Le poids moyen des particules a été trouvé au moyen du microscope électronique, et d'une ultracentrifuge analytique et à partir des résultats obtenus par lumière diffusée et transmission. Les clichés obtenus au microscope électronique montrent que les particules de Ludox et de Syton sont presque sphériques. Le diamètre des particules de Ludox est de 199 Å. par microscopie électronique, 174 Å. par ultracentrifuge et 195 Å. par les mesures de lumière diffusée et de transmission. Pour le Syton les valeurs correspondantes sont 145 Å., 142 Å. et 142 Å. Les rapports de dépolarisation ont également été déterminés, dans les deux cas, ils sont très petits. On peut conclure que, pourvu que les échantillons utilisés soient exempts d'huile, le Syton est un bon substitut du Ludox. Ses particules sont plus petits et les solutions sont moins polydispersées. On peut penser que l'ultracentrifuge donne des valeurs faibles pour les diamètres des particules et que cela est probablement dû à une évaluation incorrecte du coefficient de friction des particules subissant la sédimentation.

### Zusammenfassung

Es werden eingehende Untersuchungen an einer unter dem Namen Syton 2X bekannten, kolloiden Kieselsäuresuspension beschrieben; Diese Untersuchungen dienten dem Zweck, die Verwendbarkeit von Syton als Eichsubstanz für Lichtstreuungsphotometer zu prüfen. Es werden die Bedingungen diskutiert, die eine geeignete Eichsubstanz erfüllen muss. Gleichartige Untersuchungen wurden an Ludox, einer zweiten Kieselsäuresuspension, die von anderen Autoren viel zur Eichung verwendet wurde, durchgeführt und die an beiden Substanzen gewonnenen Ergebnisse verglichen. Durchlässigkeits- und Winkelabhängigkeit der Streuung wurden mittels eines Spektrophotometers bzw. eines Lichtstreuungsphotometers untersucht. Die Eichkonstante  $J$  des letzteren Instrumentes wurde mit Syton und Ludox bestimmt. Die ermittelten  $J$ -Werte sind fast identisch. Das Instrument wurde zur Bestimmung des Rayleigh-Verhältnisses  $R_{90}$  von Benzol, Toluol und Schwefelkohlenstoff bei zwei Wellenlängen (4358 und 5641 Å.) verwendet. Die Werte stimmen mit denen anderer Autoren gut überein und werden als sehr zuverlässig betrachtet. Zur Bestimmung des Gewichtsmittels der Teilchengröße wurden ein Elektronenmikroskop, eine analytische Ultrazentrifuge sowie Lichtstreuungs- und Durchlässigkeitsdaten verwendet. Die elektronenmikroskopischen Aufnahmen ergaben, dass die Ludox- und Syton-Teilchen kugelförmig sind. Der Teilchendurchmesser von Ludox wurde mit dem Elektronenmikroskop zu 199 Å. mit der Ultrazentrifuge zu 174 Å. und durch Lichtstreuungs- und Durchlässigkeitsmessungen zu 195 Å. bestimmt. Die entsprechenden Werte für Syton waren 145 Å. bzw. 142 Å. bzw. 142 Å. Das ausserdem bestimmte Depolarisationsverhältnis war in beiden Fällen klein. Die Ergebnisse zeigen, dass bei Benützung ölfreier Proben Syton einer guten Ersatz für Ludox darstellt. Seine Teilchen sind kleiner und die Lösungen weniger polydispers. Die Ultrazentrifuge scheint zu niedrige Werte für den Teilchendurchmesser zu ergeben, was möglicherweise auf eine unkorrekte Annahme für den Reibungskoeffizienten der sedimentierenden Teilchen zurückgeht.

Received March 28, 1963

## Analysis of the Gases Evolved from Irradiated Polyethylene\*

R. SALOVEY and J. V. PASCALE, *Bell Telephone Laboratories,  
Incorporated, Murray Hill, New Jersey*

### Synopsis

Saturated hydrocarbons evolved during electron irradiation of polyethylene are characteristic of short side chains in the polymer. A convenient analysis is effected by programmed temperature gas chromatography. In order to minimize the relative concentrations of extraneous hydrocarbons, i.e., those not arising from selective scission of complete side chains, it is necessary to irradiate at low temperatures and doses. Such analyses of a high pressure polyethylene (DYNK) indicates that the two methyls per 100 carbon atoms detected in infrared absorption are probably equal amounts of ethyl and butyl branches. These arise by intramolecular chain transfer during polymerization. At a dose of 10 Mrad about 1/4% of the alkyl groups are removed. Methane is the only hydrocarbon detected on irradiation of polypropylene, indicating little combination of methyl radicals to form ethane during irradiation.

### INTRODUCTION

The physical properties of solid polyethylene are sensitive to the presence of short branches on the polymer backbone. In polyethylene characterization, the total concentration of such branches is routinely determined by infrared absorption. In fact, from the infrared absorption characteristic of the methyl group ( $1378\text{ cm.}^{-1}$ ), it is possible to conclude that high pressure polyethylene may have three branches per 100 carbon atoms, whereas the physically different low pressure polyethylenes evidence methyl concentrations at least an order of magnitude lower. Aside from the major effects attributable to the number of branches, it is likely that physical properties reflect the lengths of these short side chains. Moreover, the presence of specific side chains is a reflection of the polymerization process and their characterization may elucidate polymerization mechanisms.

Estimates of the nature of short branches in polyethylene may be obtained from an analysis of the gaseous hydrocarbons evolved during electron bombardment. Mass spectrometric studies of such gaseous products have demonstrated irradiation-induced detachment of complete alkyl units.<sup>1</sup> In addition to saturated alkanes characteristic of the branches,

\* Presented at the New York-North Jersey Metropolitan Regional Meeting of the American Chemical Society, Newark, New Jersey, January 28, 1963.



small quantities of methane, other paraffins, and olefins were simultaneously evolved. It was suggested that "extraneous" paraffins result from cleavage of the main chain.<sup>1,2</sup> In this communication, we point out that a convenient analysis of the gaseous products of polymer irradiation may be effected by programmed temperature gas chromatography and indicate the effect of irradiation dose and temperature.

## EXPERIMENTAL

### Samples

The polyethylene samples examined included DYNK, a high pressure polyethylene produced by the Union Carbide Company and Marlex, 6000 series, type 50, a Phillips Petroleum Company low pressure polyethylene. In addition, some preliminary research is reported on an isotactic polypropylene obtained from Avisun and an atactic polypropylene, designated Epolene and a product of the Eastman Company. All samples were molded into 10 mil sheets, sealed in thin-walled ( $1/2$  mm.) Pyrex "breakoff" tubes, evacuated to high vacuum for about 16 hr., and sealed in vacuum prior to irradiation.

### Irradiation

Breakoff tubes containing 0.3 g. polyethylene or 0.1 g. polypropylene were irradiated in a beam of 1 m.e.v. electrons from a Van de Graaff generator at a dose rate of about 2.5 Mrad/min.<sup>3</sup> During bombardment, the sample tubes were supported in the ridges of a hollow copper block cooled by circulating cold water. Subsequent to irradiation all samples were annealed in the original tubes at 100°C. for 1 hr.

### Chromatographic Analysis

Breakoff tubes were then sealed into a gas sampling system consisting of a mechanical pump, a sampling valve and a vacuum gage. The system was evacuated, isolated from the pump, and the breakoff tube was broken. After recording an equilibrium pressure, 25 ml. of the gas was injected into the carrier gas stream (helium) of an F & M Scientific Company Model 500 gas chromatograph. The gases were separated and analyzed in duplicate on 3-ft.-long columns containing either molecular sieve 5A and programmed at 21°C./min. from 35 to 350°C. or activated alumina programmed similarly at 11°C./min. Retention times and ratios of injection pressure to peak area were determined by calibrating the system with known gases.

## RESULTS AND DISCUSSION

In all the chromatographic analyses reported, hydrogen, oxygen, and nitrogen are detected, being well resolved on the molecular sieve column. Hydrogen is the major gas evolved on irradiation of polyethylene<sup>4</sup> and

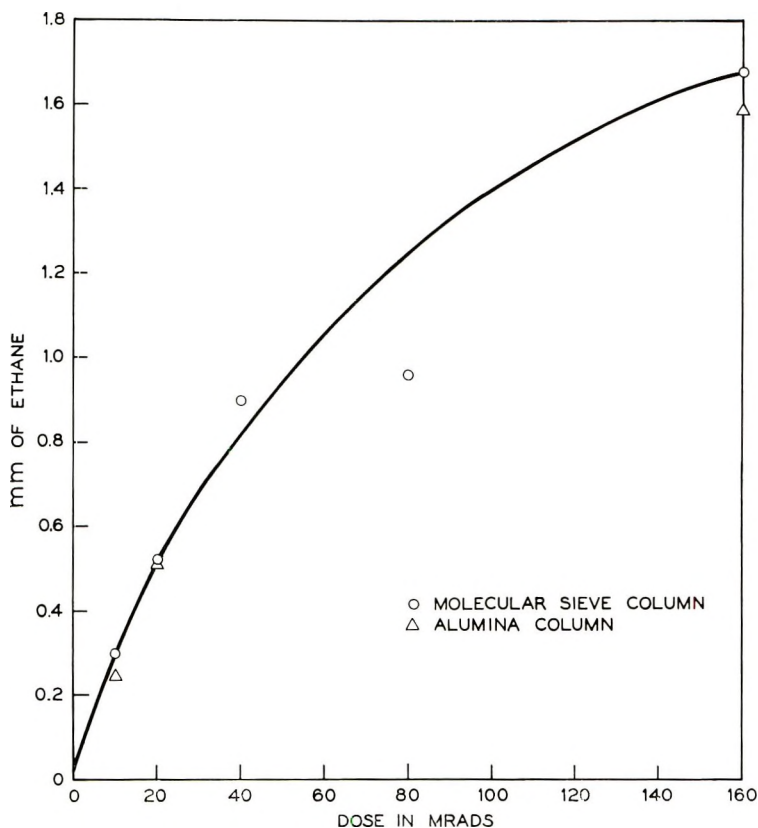


Fig. 1. Evolution of ethane from irradiated DYNK polyethylene.

polypropylene and is not sensitively indicated with helium carrier gas and a thermal conductivity detector. In large amounts the hydrogen is characterized by an alternately positive and negative deflection. Oxygen and nitrogen arise from trace air leakage into the gas sampling valve.

The high and low pressure polyethylenes differ markedly in the evolution of other gases on irradiation. At low doses, the high pressure polyethylene evidences only ethane with the molecular sieve column and ethane, propane, butane, and possibly pentane with the alumina column. At higher doses some methane is also separated on the molecular sieve column. The simultaneously irradiated low pressure polyethylene does not evidence hydrocarbons at 10 Mrad. However, at quite high doses, trace amounts of methane and ethane are observed. Figure 1 shows the evolution of ethane from the irradiated high pressure polyethylene on molecular sieve and alumina columns. Ethane determinations with either column are in good agreement, although better resolution of ethane and air is obtained with the molecular sieve. The pressure of ethane in millimeters (as derived from a previous calibration of peak area as a function of pressure with pure ethane) is given on the ordinate for a sampling system of about 25 ml.

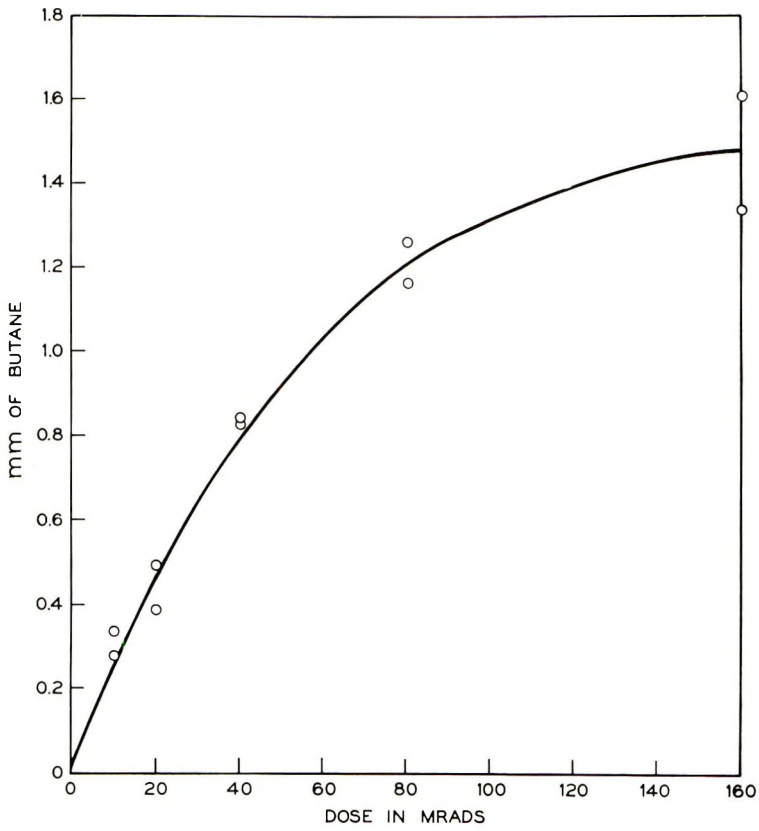


Fig. 2. Evolution of butane from irradiated DYNK polyethylene (alumina column).

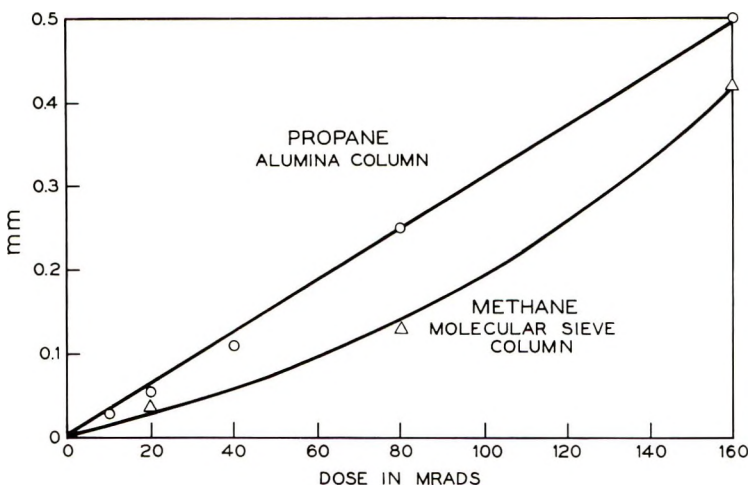


Fig. 3. Evolution of methane and propane from irradiated DYNK polyethylene.

An analogous plot of evolved butane as resolved on the alumina column is given in Figure 2. Besides hydrogen, at low doses ethane and butane are overwhelmingly the main gases evolved from irradiated high pressure polyethylene. From 10 to 160 Mrad approximately equal quantities of ethane and butane are evolved. In Figure 3, we plot pressures of propane and methane from irradiated high pressure polyethylene. The evolution of propane bears a linear relation to irradiation dose and is significant at higher doses. The rate of evolution of methane increases rapidly with dose. In addition, it was found that if the temperature of the irradiated sample was permitted to rise during irradiation, increasing amounts of various gases, including oxygenated products, were formed.

At a dose of 20 Mrad, it may be seen that there is about ten times as much evolved ethane or butane as methane or propane. From infrared absorption it is found that this high pressure polyethylene (DYNK) evidences two methyl branches per 100 carbon atoms whereas the low pressure material (Marlex) has less than 0.2 methyls per 100 carbons. We suggest that the short branches in the high pressure polymer are approximately one ethyl and one butyl per 100 carbon atoms. Based on this assumption and previous calibrations, a calculation of the absolute amounts of ethyl and butyl branches evolved indicate that at a dose of 10 Mrad only about 1/4% of the alkyl groups are detached. At 160 Mrad the corresponding figure is about 1%. Thus, in spite of the fact that relatively slight branch removal occurs, the evolution of ethane and butane is not linear with dose. It is possible that short chain scission involves a mobile free radical intermediate which preferentially produces cleavage at tertiary carbon atoms. Because of radiation-induced crosslinking, the proportion of tertiary carbon atoms associated with branches decreases during irradiation. Then, the rate of detachment of side chains falls also. That is, tertiary carbon atoms resulting from the crosslinking reaction may compete with tertiary carbons at short side chains in energy dissipation. Since hydrogen comprises at least 90% of the evolved gases from irradiated polyethylene, it is likely that at the higher doses in our study crosslinking (a source of hydrogen) becomes comparable with existing branching.

The presence of butyl branches is a natural consequence of the polymerization mechanism and was predicted to arise from intramolecular chain transfer via intermediate transient six-membered rings.<sup>5,6</sup> An extension of this mechanism to include a second intramolecular transfer, following ethylene addition to the secondary radical, accounts for the presence of ethyl branches.<sup>7</sup>

Since the evolution of hydrogen, as well as that of propane, is a linear function of irradiation dose,<sup>8</sup> perhaps both gases are formed at random in the polymer matrix. The propane may arise from the less frequent chain cleavage at secondary carbon atoms in the butyl branches. Methane evolution is probably associated with cleavage at chain ends. As a result of radiation-induced scission, the number of chain ends and the rate of methane evolution increases with increasing dose.

Perhaps some comments are in order concerning the inconvenience of duplicate analyses on molecular sieve and activated alumina columns. In fact, we are presently examining the feasibility of single column analyses. However, it was initially necessary to examine the wide spectrum of gases which may be resolved on the two columns.

Corresponding studies of the gases evolved from irradiated polypropylene with molecular sieve 5A columns indicated that hydrogen ( $\sim 90\%$ ) and methane are the main gases evolved on irradiation. Equal amounts of methane, increasing linearly with dose, are detected with atactic and isotactic polymers. Again, side chain scission is inefficient—at a dose of 150 Mrad less than  $1/4\%$  of the methyl branches are removed by irradiation. In this case, there is no evidence of the combination of methyl radicals to form ethane.

Our contention that the short side chains in the high pressure polyethylene are equal amounts of ethyl and butyl is open to question. Using copolymers containing branches of a given type, evidence was adduced to show that ethyl branches are detected by irradiation scission with about twice the efficiency of butyl groups.<sup>1</sup> In this interpretation, our data would indicate that butyl branches may be about twice as frequent as ethyl. These points should be examined at low doses and temperatures.

## CONCLUSIONS

Saturated hydrocarbons evolved during electron irradiation of polyethylene are characteristic of short side chains in the polymer.<sup>1</sup> A convenient analysis is effected by programmed temperature gas chromatography. In order to minimize the relative concentrations of extraneous hydrocarbons i.e., those not arising from selective scission of complete side chains, it is necessary to irradiate at low temperatures and doses. Such analyses of a high pressure polyethylene (DYNK) indicates that the two methyls per hundred carbon atoms detected in infrared absorption are probably equal amounts of ethyl and butyl branches. These arise by intramolecular chain transfer during polymerization.<sup>5,7</sup> At a dose of 10 Mrad about  $1/4\%$  of the alkyl groups are removed. Methane is the only hydrocarbon detected on irradiation of polypropylene, indicating, little combination of methyl radicals to form ethane during irradiation.

The authors acknowledge helpful comments by D. W. McCall and infrared data by Mrs. I. Jassie.

## References

1. Boyle, D. A., W. Simpson, and J. D. Waldron, *Polymer*, **2**, 323 (1961).
2. Willbourn, A. H., *J. Polymer Sci.*, **34**, 569 (1959).
3. Salovey, R., and W. Rosenzweig, *J. Polymer Sci.*, **A1**, 2145 (1963).
4. Chapiro, A., *Radiation Chemistry of Polymeric Systems*, Interscience, New York, 1962, p. 408.
5. Roedel, M. J., *J. Am. Chem. Soc.*, **75**, 6110 (1953).
6. For other views, see W. T. Wickham, *J. Polymer Sci.*, **60**, S68 (1962).



7. Boyle, D. A., W. Simpson, and J. D. Waldron, *Polymer*, **2**, 335 (1961).
8. Salovey, R., unpublished results.

### Résumé

Des hydrocarbures saturés issus de polyéthylènes irradiés par des électrons sont caractéristiques de courtes chaînes latérales dans le polymère. Une analyse adéquate est effectuée par chromatographie gazeuse avec programmation de températures. En vue de réduire les concentrations relatives d'hydrocarbures étrangers, c.à.d., ceux qui ne résultent pas d'une scission sélective de chaînes latérales complète, il est indispensable d'irradier à faibles température et concentrations. Des analyses semblables de polyéthylène à haute pression (DYNK) indiquent que les deux méthyles par 100 atomes de carbones détectés par absorption infra-rouge, correspondent probablement aux groupes éthyles ou butyles. Ceux-ci se produisent par transfert de chaîne intramoléculaire au cours de la polymérisation. À une concentration de 10 Mrad environ 1/4% de chaînes alcoyles sont déplacées. Le méthane est le seul hydrocarbure détecté par irradiation du polypropylène, ce qui indique une faible combinaison des radicaux méthyles pour former de l'éthane au cours de la polymérisation.

### Zusammenfassung

Die Bildung gesättigter Kohlenwasserstoffe während der Elektronen-bestrahlung von Polyäthylen ist für die im Polymeren enthaltenen kurzen Seitenketten charakteristisch. Eine geeignete Analysenmethode ist die temperatur-programmierte Gaschromatographie. Es ist notwendig, die Bestrahlung bei niedrigen Temperaturen und Dosen durchzuführen, um die relative Konzentration von "fremden" Kohlenwasserstoffen, d.h. solchen, die nicht durch selektive Abspaltung vollständiger Seitenketten entstanden sind, möglichst herabzusetzen. Eine derartige Analyse von Hochdruckpolyäthylen (DYNK) zeigt, dass die im IT-Spektrum gefundenen zwei Methylgruppen pro hundert Kohlenstoff-Atome wahrscheinlich gleichen Mengen von Äthyl- und Butyl-Seitenketten entsprechen. Diese entstehen durch intramolekulare Kettenübertragung während der Polymerisation. Bei einer Dosis von 10 Mrad wird etwa ein Prozent der Äthylgruppen abgespalten. Bei der Bestrahlung von Polypropylen wird Methan als einziger Kohlenwasserstoff gefunden, d.h. es tritt während der Bestrahlung nur geringfügige Kombination von Methylradikalen zu Äthan auf.

Received March 28, 1963

## Absolute Propagation Rate Constants for the Radical Polymerization of Substituted Styrenes\*

K. P. PAOLETTI† and F. W. BILLMEYER, JR., *Department of Chemistry, University of Delaware, Newark, Delaware*

### Synopsis

Absolute propagation rate constants were determined by application of the Smith-Ewart kinetic theory to the emulsion polymerization of styrene, *o*-methylstyrene, *p*-methylstyrene, and "vinyltoluene" (Dow, 60:40 *m*-*p*-methylstyrene). Conversion during polymerization was followed by dilatometry, and weight-average molecular weights of the latex particles were determined by light scattering. The monomer-polymer equilibrium ratio was determined both dynamically as the inflection point of the rate curve and statically by equilibrating monomer with polymer. For styrene, the propagation rate constant (300 l./mole sec. at 50°C.) and its activation energy (17.6 kcal./mole) are in good agreement with literature values. Both rates and activation energies are lower for the other monomers (*o*-methylstyrene, 60 l./mole sec. and 13.9 kcal./mole; *p*-methylstyrene, 140 l./mole sec. and 7.7 kcal./mole; vinyltoluene, 220 l./mole sec. and 13.4 kcal./mole, all at 50°C.). The differences are attributed to increased radical stability from methyl group contributions to resonance structures and to steric hindrance of the *ortho*-methyl group.

### INTRODUCTION

The rate of propagation in the polymerization of a vinyl compound is determined by the reactivity of both the monomer and the radical derived from it. This reactivity is determined by the molecular structure of the monomer. While theoretical studies can be used to predict the effect of structure on reactivity, experimental data are necessary to provide a sound basis for these predictions. Relatively few data of this sort are available, however, since in the analysis of the kinetics of addition polymerization by steady-state assumptions, the rate constant of propagation does not occur independently but as a ratio with the termination rate constant. Before the absolute value of the propagation rate constant can be determined, the rate of termination must be calculated from nonsteady-state experiments.

The purpose of this work was to determine the absolute propagation

\* Presented at the 14th Delaware Science Symposium, Newark, Del., Feb. 23, 1963. This research was performed by K. P. Paoletti in partial fulfillment of the requirements for the degree of Master of Science, University of Delaware.

† Present address: Textile Fibers Department, E. I. du Pont de Nemours & Co., Inc., Martinsville, Virginia.

rate constants of some substituted styrenes and evaluate the effect of *ortho* and *para* methyl substitution on the reactivity of the styrene monomer. A second objective of this work was to develop an experimental technique which would give accurate polymerization rate data using a minimum of sample.

While the absolute propagation rate constant of styrene has been measured by several investigators using a variety of methods,<sup>1-4</sup> the study of the polymerization kinetics of substituted styrenes has been very limited.<sup>5</sup> Difficulties involved in the preparations of the pure compounds and their relatively low industrial importance have been given as the reasons for the lack of previous detailed investigations of such monomers.<sup>6</sup> The increased availability of substituted monomers coupled with the more simple kinetic analysis of emulsion polymerization systems facilitates the use of homopolymerization data to relate structure with reactivity.

Absolute propagation rate constants,  $k_p$ , can be obtained for emulsion polymerization systems by application of the Smith-Ewart theory,<sup>7</sup> the major result of which states that

$$-dM/dt = k_p M(N/2) \quad (1)$$

where  $-dM/dt$  is the polymerization rate,  $M$  is the monomer concentration in the polymerizing particles, and  $N$  is the number of latex particles per ml. of aqueous phase in the emulsion.

While the rate of polymerization in emulsion systems has generally been followed by gravimetric methods,<sup>4,8</sup> these techniques require relatively large amounts of monomer and frequent sampling if the rate curve is to be followed closely. On the other hand, the large volume change accompanying polymerization makes dilatometry a very simple yet efficient means of following conversion.

Starkweather and Taylor<sup>9</sup> used simple bulb dilatometers to follow the kinetics of vinyl acetate polymerization. Dilatometers with magnetic stirring were used by Bartholomé et al.<sup>10</sup> to test the Smith-Ewart theory for the emulsion polymerization of styrene and by Yurzhenko and Puchin<sup>11</sup> to explore polymerization at atmospheric and higher pressures. Corrin<sup>12</sup> used a more elaborate, high volume dilatometer to study the conversion of styrene in emulsion polymerization.

The monomer-polymer ratio, or the monomer concentration in the polymer particles, has been determined both by static equilibration of diluted latex and inhibited monomer<sup>4,8</sup> and by the inflection point in the rate or heat of reaction curve.<sup>10,13</sup> During actual polymerization, however, since the proportion of monomer in the particles is probably controlled by a dynamic balance between the rate of polymerization and the rate of diffusion of monomer from the large droplets acting as reservoirs, the monomer-polymer equilibrium ratio determined from the inflection point of the rate curve is preferred. In emulsion polymerization where the conversion is followed very closely, as by dilatometry, the dynamic monomer-polymer equilibrium ratio can be easily located in the rate curve.

Application of either the dissymmetry<sup>14</sup> or the Zimm extrapolation<sup>15</sup> technique to light-scattering data from the diluted latex gives the number of polymer particles per milliliter of aqueous phase. While both methods have been used, the Zimm technique is more widely accepted, since it involves no assumptions about the shape of the particles.

## EXPERIMENTAL

### Samples

The monomers used in this work were styrene (E. K. reagent grade), vinyltoluene 12T (60:40 *m*:-*p*-methylstyrene, Dow Chemical Co.), *o*-methylstyrene (Dow Chemical Co. and Monomer-Polymer Corp.), and *p*-methylstyrene (Monomer-Polymer Corp.). Inhibitor was removed from the samples by the accepted technique of alkali washing, drying over white Drierite, and vacuum distillation. Freshly distilled monomer samples were stored at  $-20^{\circ}\text{C}$ . until use for periods of time not exceeding five days. No polymerization during storage was apparent when the monomer was checked periodically for refractive index.

### Dilatometry

The rate of polymerization was determined using a specially designed small volume (20–30 ml.) dilatometer (Fig. 1), constructed by sealing a 50 ml. length of 2 mm. i.d. capillary tubing to the bottom of a 20 ml.

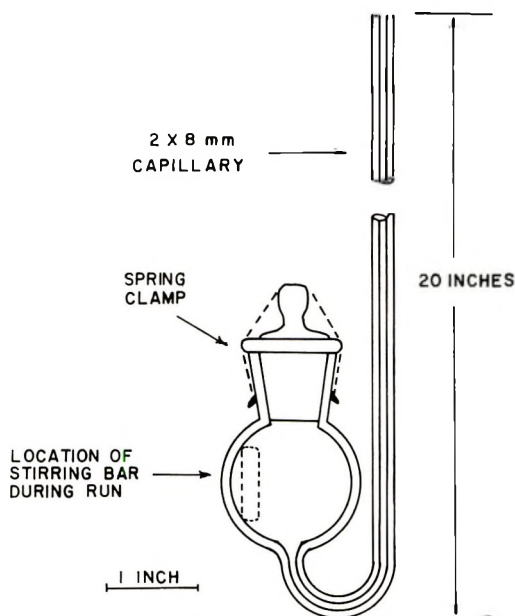


Fig. 1. Small stirred dilatometer for use in emulsion polymerization.

round-bottomed flask. The ground glass stopper was securely held in position by a spring clamp during the run. The dilatometer was placed in a constant temperature bath regulated to within  $\pm 0.01^\circ\text{C}$ . The emulsion was stirred by rotation of a magnetic stirring bar in a vertical plane against the side of the bulb by means of a large magnetic stirrer located outside of the constant temperature bath. An initial dilatometer check was performed by filling the bulb with distilled water at room temperature, immersing it in a  $50^\circ\text{C}$ . bath, and observing the water column height. Satisfactory dilatometer performance was indicated by an initial rapid volume increase during temperature equilibration followed by a constant height.

### Light Scattering

Light-scattering measurements were made with distilled water, filtered through an ultrafine sintered glass filter, as the solvent. The intensity of the scattered light was automatically recorded in a photoelectric turbidimeter<sup>16</sup> as a function of observation angle, the angular range extending from  $30^\circ$  to  $140^\circ$ . Satisfactory alignment of the apparatus was insured by observation of the intensity of fluorescent light from a methanol solution of sodium fluorescein. The intensity of the fluorescent light, when corrected by the sine of the angle of observation, varied less than 1% in the angular range investigated. The calibration constant of the instrument was determined by measuring the scattering from a standard polystyrene sample dissolved in freshly distilled 2-butanone. Plane-polarized light of 5461 Å. wavelength and vertical electric vector was used in all measurements.

The specific refractive increment of the diluted latex was determined on a Brice-Phoenix differential refractometer.<sup>17</sup> The instrument was calibrated with a water solution of sodium chloride.<sup>18</sup>

### Procedure

The compositions of the various polymerization runs are summarized in Table I. The aqueous phase (soap solution) was prepared by adding the tabulated amounts of soap (sodium lauryl sulfate), initiator (potassium persulfate), and buffer (sodium hydrogen phosphate) or other ingredient (sodium sulfite) to filtered, distilled water. This soap solution was stored until use at  $0^\circ\text{C}$ . for periods not exceeding 48 hr. In runs 1-3, 12, and 13, sodium sulfite was added to reduce the induction period. This was shown to be unnecessary, however, and a buffer was used in other runs.

Approximately 7 g. of the monomer and 20 g. of the soap solution were added to the dilatometer bulb. The exact weights were determined by difference from previously weighed samples. The top of the bulb was flushed with nitrogen and the glass stopper inserted and secured. The dilatometer was transferred to the constant temperature bath and the magnetic stirrer started (zero time). If necessary, the height of the water column in the capillary was adjusted with a hypodermic syringe to a level



just below the bath surface. Water heights were recorded to the nearest 0.2 mm. during the polymerization.

After the polymerization had proceeded almost to completion, three weighed latex samples were taken from the bulb, shortstopped with hydroquinone, and evaporated to dryness. These samples were dried for 10 hr. at 35°C. and 25 in. Hg vacuum, then for 6 hr. at 70°C. and 25 in. Hg vacuum. From the weight of these samples, their total conversion was

TABLE I  
Composition of Polymerization Runs

Run	Monomer	Composition of polymerization runs (based on monomer equal to 100 parts)				
		Parts water	Parts soap	Parts initiator	Parts buffer	Parts other <sup>a</sup>
1	Styrene	374	5.7	0.41	—	0.04
2	"	388	6.7	0.49	—	0.09
3	"	331	6.0	0.44	—	0.08
4	"	209	8.5	0.36	0.55	—
5	"	181	7.4	0.32	0.48	—
6	"	218	8.9	0.38	0.40	—
7	Vinyltoluene	194	8.7	0.46	0.52	—
8	"	177	7.9	0.42	0.47	—
9	"	180	8.1	0.43	0.48	—
10	"	194	8.7	0.46	0.52	—
11	"	180	8.1	0.43	0.48	—
12	<i>o</i> -Methylstyrene	324	6.2	0.47	—	0.09
13	"	365	7.7	0.58	—	0.11
14	"	194	8.1	0.36	0.54	—
15	"	202	8.0	0.39	0.51	—
16	"	157	6.6	0.29	0.44	—
17	"	135	5.7	0.25	0.38	—
18	<i>p</i> -Methylstyrene	206	4.3	0.18	0.56	—
19	"	176	3.7	0.15	0.47	—
20	"	171	3.6	0.15	0.46	—
21	"	193	4.1	0.17	0.52	—
22	"	191	2.2	0.10	0.55	—
23	"	179	2.0	0.096	0.51	—
24	"	179	2.0	0.096	0.51	—
25	"	190	2.2	0.10	0.54	—

<sup>a</sup> Sodium sulfite.

determined with respect to the initial monomer-soap solution charge. A per cent polymerization scale was then prepared from the per cent conversion of the latex samples and the corresponding decrease in capillary height.

The latex was diluted 10,000- to 100,000-fold and the turbidity of these solutions measured by light scattering for angles of observation between 30° and 140°. The light-scattering data were plotted graphically as Zimm plots.<sup>15</sup>

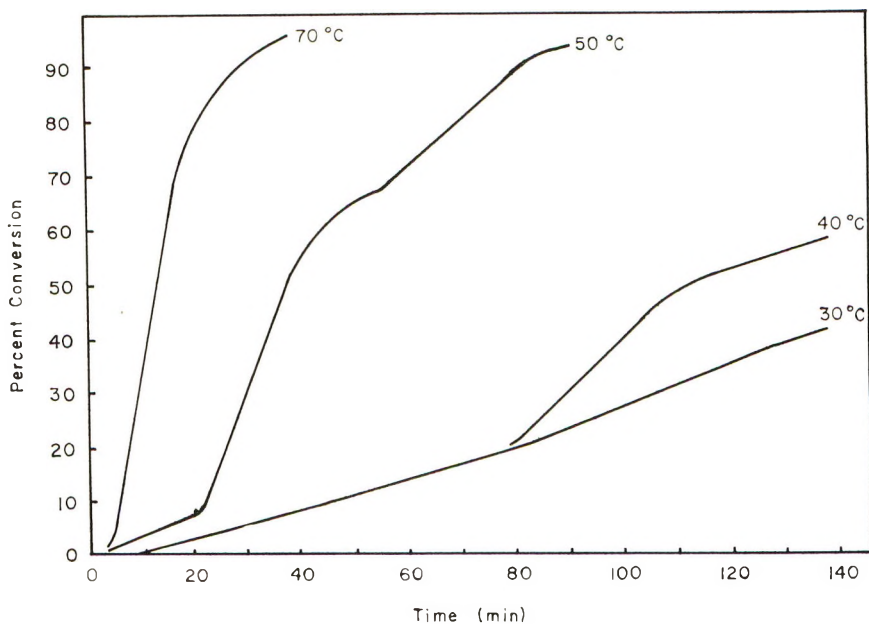


Fig. 2. Typical conversion curves for the emulsion polymerization of styrene. The polymerization of vinyltoluene gave similar results.

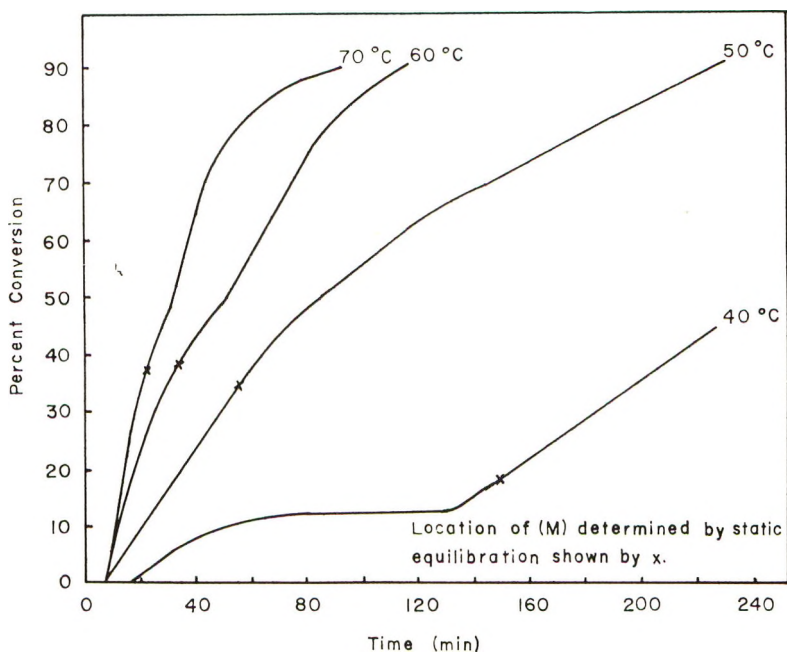


Fig. 3. Typical conversion curves for the emulsion polymerization of *p*-methylstyrene. The polymerization of *o*-methylstyrene gave similar results.

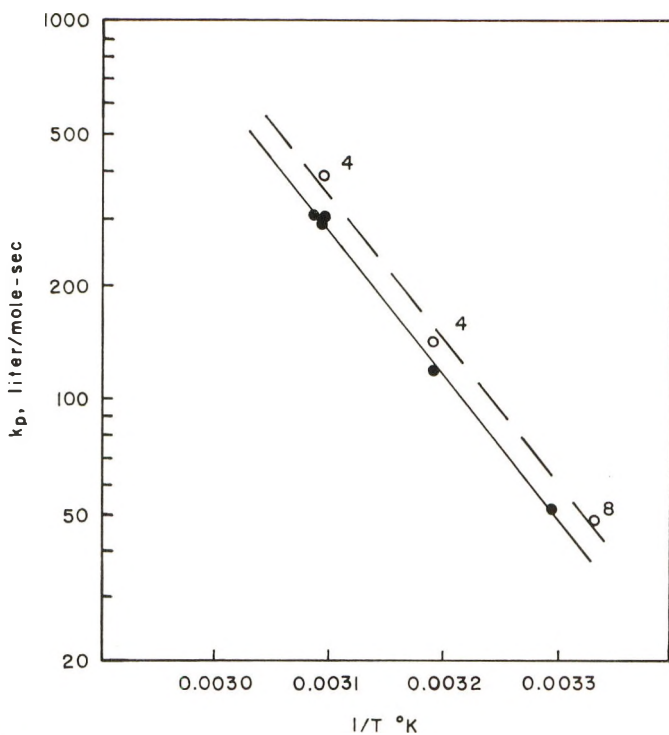


Fig. 4. Arrhenius plot for the absolute propagation rate constant for styrene.

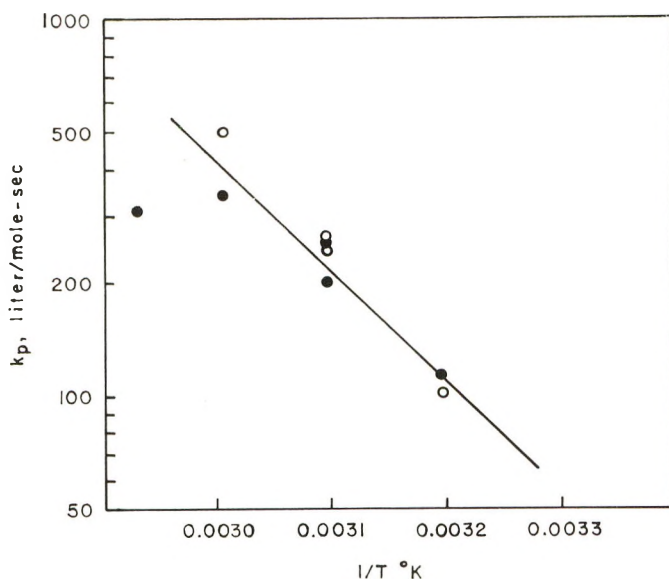


Fig. 5. Arrhenius plot for the absolute propagation rate constant for vinyltoluene.

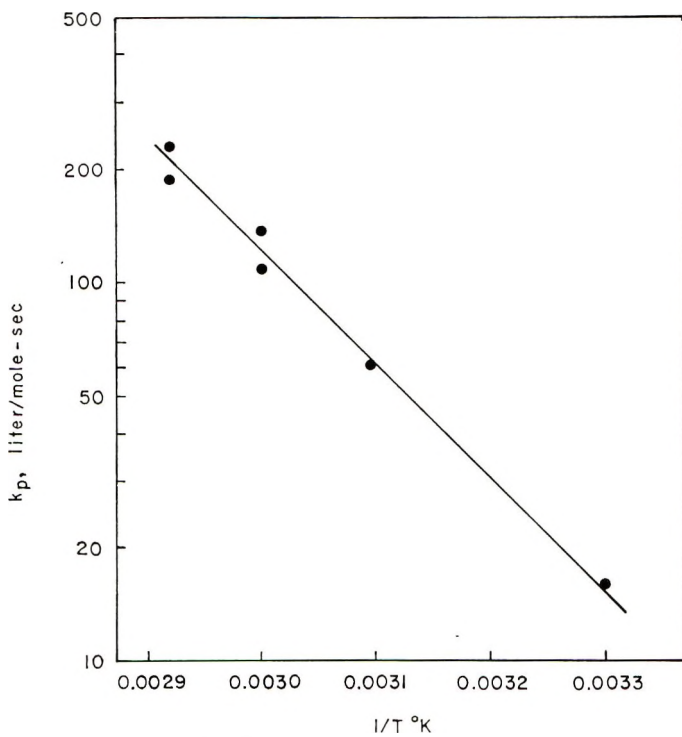


Fig. 6. Arrhenius plot for the absolute propagation rate constant for *o*-methylstyrene

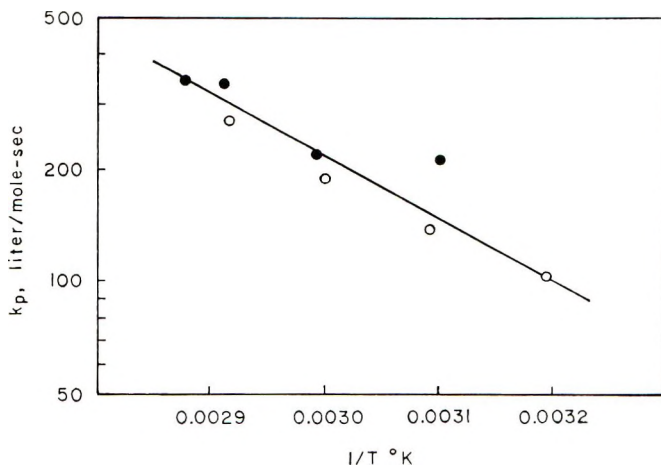


Fig. 7. Arrhenius plot for the absolute propagation rate constant for *p*-methylstyrene.

The monomer-polymer equilibrium ratio was determined both graphically and by static equilibration using the method of Smith<sup>4</sup> and Morton et al.<sup>8</sup> Since dilatometry allowed the conversion to be followed as closely as desired, the monomer-polymer equilibrium ratio could generally be

determined from the per cent conversion at which the rate curve showed an inflection. Such curves of conversion versus time, typical of the results obtained with styrene and vinyltoluene, are shown in Figure 2, while curves typical of the experiments with *o*-methylstyrene and *p*-methylstyrene are shown in Figure 3.

## RESULTS

The experimental results leading to evaluation of the absolute propagation rate constants are listed in Tables II–V for styrene, vinyltoluene, *o*-methylstyrene, and *p*-methylstyrene, respectively. The propagation rate constants for these monomers are plotted as a function of temperature in Figures 4–7, and the activation energies calculated from these Arrhenius plots are summarized in Table VI.

Table III also compares values of the equilibrium monomer–polymer ratio determined from the point of inflection of the rate curve (graphical determination) and by static equilibration. Generally these two methods gave similar results.

TABLE II  
Summary of Styrene Polymerization Data

Run	Temperature, °C.	No. of particles/ ml. of H <sub>2</sub> O × 10 <sup>14</sup>	<i>M</i> , mole/ml. × 10 <sup>-3</sup>	Conversion rate, wt. fraction/ sec. × 10 <sup>-5</sup>	<i>k<sub>p</sub></i> , l./mole sec.	<i>k<sub>p</sub></i> , (literature), l./mole sec.
1	30.5	6.879	4.860	5.55	51.0	48 (25°C.) <sup>a</sup>
2	40.5	7.792	5.154	16.34	120.5	139 (40°C.) <sup>a</sup>
3	51.0	8.917	5.763	46.33	311.1	
4	50.2	13.61	6.491	48.44	300.3	390 (50°C.) <sup>b</sup>
5	50.2	13.39	5.036	31.10	291.0	
6	70.9	40.18	5.683	185.2	357.9	

<sup>a</sup> Data of Morton et al.<sup>8</sup>

<sup>b</sup> Data of Smith.<sup>4</sup>

TABLE III  
Summary of Vinyltoluene Polymerization Data

Run	Temperature, °C.	No. of particles/ ml. of H <sub>2</sub> O × 10 <sup>14</sup>	<i>M</i> , mole/ml. × 10 <sup>-3</sup>		Conversion rate, wt. fraction/sec. × 10 <sup>-5</sup>	<i>k<sub>p</sub></i> , l./mole sec. <sup>a</sup>
			Graphical determina- tion	Static equilibra- tion		
7	40.0	12.34	5.593	5.926	11.91	85.01 (90.07)
8	50.0	18.79	5.035	5.963	40.65	202.0 (239.2)
9	50.0	18.36	5.208	5.426	45.54	255.9 (266.6)
10	59.8	31.42	3.455	5.062	103.7	336.6 (439.1)
11	68.2	44.16	—	4.971	122.5	309.1

<sup>a</sup> Value in parentheses calculated from *M* determined graphically.



TABLE IV  
 Summary of *o*-Methylstyrene Polymerization Data

Run	Temperature, °C.	No. of particles/ml. of H <sub>2</sub> O × 10 <sup>14</sup>	<i>M</i> , mole/ml. × 10 <sup>-3</sup>	Conversion rate, wt. fraction/sec. × 10 <sup>-5</sup>	<i>k<sub>p</sub></i> , l./mole sec.
12	30.0	11.74	7.473	4.467	15.98
13	50.0	17.98	5.501	21.53	60.59
14	60.0	43.38	3.687	32.64	107.2
15	60.0	44.68	4.339	53.08	138.0
16	69.6	57.20	3.887	65.61	187.4
17	69.6	69.14	5.137	122.5	231.4

 TABLE V  
 Summary of *p*-Methylstyrene Polymerization Data

Run	Temperature, °C.	No. of particles/ml. of H <sub>2</sub> O × 10 <sup>14</sup>	<i>M</i> , mole/ml. × 10 <sup>-3</sup>	Conversion rate, wt. fraction/sec. × 10 <sup>-5</sup>	<i>k<sub>p</sub></i> , l./mole sec.
18	40.2	3.712	7.510	5.827	102.7
19	50.5	9.134	5.410	11.96	134.7
20	60.1	17.80	5.816	33.07	187.5
21	69.8	24.76	4.260	53.08	265.4
22	49.8	4.872	6.225	12.15	211.6
23	61.1	9.965	5.521	21.59	219.1
24	69.4	14.45	3.881	33.07	335.6
25	74.6	15.41	3.882	38.76	338.9

 TABLE VI  
 Temperature Dependence of Absolute Propagation Rate Constants  
 for Radical Polymerization of Substituted Styrenes

Monomer	<i>k<sub>p</sub></i> , l./mole sec.	<i>k<sub>p</sub></i> (literature), l./mole sec. <sup>a</sup>
Styrene	$2.24 \times 10^{14} \exp \{-17,570/RT\}$	$2.71 \times 10^{14} \exp \{-17,570/RT\}$
Vinyltoluene	$2.57 \times 10^{11} \exp \{-13,420/RT\}$	
<i>o</i> -Methylstyrene	$1.67 \times 10^{11} \exp \{-13,920/RT\}$	
<i>p</i> -Methylstyrene	$2.27 \times 10^7 \exp \{-7,663/RT\}$	

<sup>a</sup> Calculated from reported values of Smith<sup>4</sup> and Morton et al.<sup>8</sup>

Table II and Figure 4 compare the results of this work to values determined by Smith<sup>4</sup> and Morton et al.<sup>8</sup> for styrene polymerizations.

## DISCUSSION

### Experimental Procedure

The excellent agreement between the values previously reported for styrene<sup>4,8</sup> and the results of this work show that dilatometry is well suited for the kinetic study of emulsion polymerizations. Since dilatometry

lends itself to miniaturization very well, this technique allows intensive investigation of monomers more difficult to prepare. While emulsion volumes in the order of 25 ml. were used in this work, the dilatometer could be reduced further in size to allow volumes of 5–10 ml. to be used without impairing the accuracy of rate measurement. These dilatometers would require only 2–4 ml. of monomer.

Determination of the monomer–polymer equilibrium ratio requires additional investigation in kinetic studies of emulsion polymerization. While the values of the monomer–polymer equilibrium ratio were in general agreement when determined by the equilibration and the graphical technique, some scatter was still observed at the higher temperatures, as may be seen in Table III. If the conversion curves as shown in Figure 3 are examined, it is noted that the per cent conversion corresponding to the monomer–polymer equilibrium ratio is generally higher for the static equilibration than for the departure of the curve from the constant rate. While the experimental error in the static technique may account for the discrepancy, additional investigation into procedure and equipment is necessary to improve the agreement between methods.

The following interpretation of the rate curve as described by Bartholomé et al.<sup>10</sup> has been assumed: a short period of increasing rate followed by a linear portion corresponding to a first-order reaction. This portion is where the Smith-Ewart kinetics are followed. The linear portion ends when the monomer reservoirs are depleted and the reaction rate decreases. Later, however, gel formation may take place, especially at higher temperatures, with a corresponding temporary increase in rate.

## Results

There was good conformance of the kinetic studies of this work to the Smith-Ewart theory<sup>7</sup> for temperatures below 70°C. However, the propagation rate constant for both styrene and vinyltoluene showed atypical behavior in the 70°C. range. Values of  $k_p$  were much lower than expected and did not lie on the  $\log k_p - 1/T$  line established at lower temperatures. The *o*- and *p*-methylstyrene studies, however, gave straight line Arrhenius plots up to a temperature of 70°C. Two possible explanations of this behavior are: (1) the presence of a rate determining step, other than radical formation and propagation, which becomes dominant at approximately 70°C. in emulsion systems where  $k_p$  is excess of 350–400 l./mole sec.; or (2) failure of emulsion systems to follow the Smith-Ewart theory at these higher temperatures. One possible cause of this failure might be that proposed by Smith,<sup>4</sup> that diffusion of monomer cannot keep pace with polymerization. However, Flory<sup>19</sup> concluded from theoretical considerations that monomer can easily be supplied to the polymer.

Another possible explanation of the decrease in rate may involve the larger number of particles per milliliter of water at high temperatures. Van der Hoff<sup>20</sup> deduced that the rate per particle was proportional to the

0.83 power of the number or volume of the particles when in the range of  $5 \times 10^{14}$  to  $5 \times 10^{15}$ /ml.

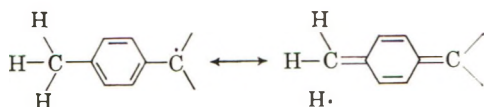
Since the data appear to agree with the Smith-Ewart theory in all cases except the polymerizations at 70°C. for styrene and vinyltoluene, conformance to this theory is assumed in the discussion of results.

### Effect of Molecular Structure on Rate Constants

The absolute propagation rate constants and activation energies of the methyl substituted styrenes are lower than the corresponding quantities for styrene. Reduction of the activation energy may be attributed to the methyl substitution. The reduced rates are assumed due to steric effects of the *ortho* substitution and to increased radical stability.

Vinyltoluene has an activation energy 4.1 kcal./mole below that for styrene. This may be attributed to the increased radical stabilization in vinyltoluene due to resonance. Kennedy and Morton<sup>21</sup> reported a decrease in activation energy of 2–4 kcal./mole on going from *m*-methylstyrene or *p*-methylstyrene to styrene, in good agreement with the results of this work.

Values of  $k_p$  for *o*-methylstyrene and *p*-methylstyrene are lower than that for styrene, as are the activation energies by 3.6 and 9.9 kcal./mole, respectively. *p*-Methylstyrene has a propagation rate constant between those of styrene and *o*-methylstyrene. Reduction of the activation energy of both substituted monomers with respect to that of styrene is attributed to the increased resonance stability of the radicals formed during propagation. The unpaired electron of the newly formed radical is assumed delocalized by hyperconjugation:<sup>22</sup>



This stabilization reduces the potential energy of the transition state with a corresponding lowering of the activation energy.

The increased activation energy and reduced rate constant of the *o*-substituted styrene with respect to the *p*-substituted monomer is attributed to steric factors. Kennedy and Morton explained the difficulty of polymerizing 2,4,6-trimethylstyrene by the steric effect of the *ortho* methyl group, which formed a barrier to the free rotation of the vinyl group. Hence, the attainment of the coplanar configuration necessary for resonance of the vinyl group with the benzene nucleus is hindered. The presence of a similar energy barrier is indicated in this work by the increase of 6.3 kcal./mole in activation energy between the *para*- and *ortho*-substituted monomers.

The authors wish to express their appreciation to the management of the Carothers Research Laboratory, Textile Fibers Department, E. I. du Pont de Nemours and Company, Inc., for the use of the facilities of that Laboratory and to the Dow Chemical Company for the monomers which they supplied.

## References

1. Bamford, C. H., and M. J. S. Dewar, *Proc. Roy. Soc. (London)*, **A192**, 309 (1948).
2. Melville, H. W., and L. Valentine, *Trans. Faraday Soc.*, **46**, 210 (1950).
3. Burnett, G. M., *Trans. Faraday Soc.*, **46**, 772 (1950).
4. Smith, W. V., *J. Am. Chem. Soc.*, **70**, 3695 (1948).
5. Axford, D. W. E., *Proc. Roy. Soc. (London)*, **A197**, 374 (1949).
6. Bamford, C. H., W. G. Barb, A. D. Jenkins, and P. F. Onyon, *The Kinetics of Vinyl Polymerization by Radical Mechanisms*, Academic Press, New York, 1958.
7. Smith, W. V., and R. H. Ewart, *J. Chem. Phys.*, **16**, 592 (1948).
8. Morton, M., P. P. Salatiello, and H. Landfield, *J. Polymer Sci.*, **8**, 279 (1952).
9. Starkweather, H. W., and G. B. Taylor, *J. Am. Chem. Soc.*, **52**, 4708 (1930).
10. Bartholomé, E., H. Gerrens, R. Herbeck, and H. M. Weitz, *Z. Elektrochem.*, **60**, 334 (1956).
11. Yurzhenko, T. I., and V. A. Puchin, *Zavodskaya Lab.*, **21**, 205 (1955).
12. Corrin, M. L., *J. Polymer Sci.*, **2**, 257 (1947).
13. Manyasek, Z., and A. Rezabek, *J. Polymer Sci.*, **56**, 47 (1962).
14. Doty, P., W. A. Affens, and B. H. Zimm, *Trans. Faraday Soc.*, **42B**, 66 (1946).
15. Zimm, B. H., *J. Chem. Phys.*, **16**, 1099 (1948).
16. Baum, F. J., and F. W. Billmeyer, Jr., *J. Opt. Soc. Am.*, **51**, 452 (1961).
17. Brice, B. A., and M. Halwer, *J. Opt. Soc. Am.*, **41**, 1033 (1951).
18. Stamm, R. F., *J. Opt. Soc. Am.*, **40**, 788 (1950).
19. Flory, P. J., *Principles of Polymer Chemistry*, Cornell Univ. Press, Ithaca, N. Y., 1953, p. 210.
20. van der Hoff, B. M. E., *J. Phys. Chem.*, **60**, 1250 (1956).
21. Kennedy, G. T., and F. Morton, *J. Chem. Soc.*, **1949**, 2382.
22. Gould, E. S., *Mechanism and Structure in Organic Chemistry*, Holt, New York, 1960, p. 675.

## Résumé

On a déterminé les constantes absolues de vitesse de propagation en appliquant la théorie cinétique de Smith-Ewart à la polymérisation en émulsion du styrène, de l'*o*-méthylstyrène, du *p*-méthylstyrène et du "vinyl-toluène" (Dow; 60:40 *m*-, *p*-méthylstyrène). Le conversion est suivi en cours de polymérisation par dilatométrie, et le poids moléculaire moyen en poids des particules de latex est déterminé par diffusion lumineuse. Le rapport à l'équilibre monomère-polymère a été établi d'une part dynamiquement grâce au point d'inflexion de la courbe de vitesse et statistiquement en mettant le monomère en équilibre avec le polymère. Dans le cas du styrène, la constante de vitesse de propagation (300 l./mole/sec. à 50°C) et l'énergie d'activation (17.6 kcal/mole) concordent bien avec les valeurs de la littérature. Par contre les vitesses et les énergies d'activation des autres monomères sont inférieures (l'*o*-méthylstyrène 60 l/ms et 13.9 kcal/mole; le *p*-méthylstyrène 140 l/ms et 7.7 kcal/mole; le "vinyl-toluène" 220 l/ms et 13.4 kcal/mole, tout cela à 50°C). Les différences sont attribuées à une augmentation de la stabilité du radical, due à la contribution aux structures de résonance du groupe méthyle et à l'encombrement stérique du groupe méthyle en ortho.

## Zusammenfassung

Durch Anwendung der kinetischen Smith-Ewart-Theorie auf die Emulsionspolymerisation von Styrol, *o*-Methylstyrol, *p*-Methylstyrol und "Vinyltoluol" (Dow; 60:40 *m*:-*p*-Methylstyrol) wurden absolute Wachstumskonstanten bestimmt. Der prozentuelle Umsatz während der Polymerisation wurde dilatometrisch verfolgt und das Gewichtsmittel des Molekulargewichts der Latexteilchen durch Lichtstreuung bestimmt. Das Monomer-Polymer-Gleichgewichtsverhältnis wurde sowohl dynamisch als Wendepunkt der Geschwindigkeitskurve als auch statisch durch Gleichgewichtseinstellung von Mono-

merem mit Polymerem ermittelt. Bei Styrol stimmen Geschwindigkeitskonstante (300 Liter/Mol sec bei 50°C) und Aktivierungsenergie (17,6 kcal/Mol) der Wachstumsreaktion gut mit der in der Literatur angegebenen Werten überein. Bei den anderen Monomeren sind sowohl Geschwindigkeit als auch Aktivierungsenergie niedriger (*o*-Methylstyrol: 60 l/Ms, 13,9 kcal/Mol; *p*-Methylstyrol: 140 l/Ms, 7,7 kcal/Mol; "Vinyltoluol": 220 l/Ms, 13,4 kcal/Mol; alle Werte bei 50°C). Diese Unterschiede werden einer durch den Beitrag der Methylgruppen zu Resonanzstrukturen erhöhten Radikalstabilität sowie einer sterischen Hinderung durch die ortho-Methylgruppen zugeschrieben.

Received March 28, 1963



## Kinetic Study of the Autoxidation of Cellulose Suspended in Sodium Hydroxide Solution

R. I. C. MICHIE,\* *Polymer and Fibre Science Department*, and S. M. NEALE, *Chemistry Department, College of Science and Technology, Manchester, England*

### Synopsis

An apparatus has been designed to measure small extents of gas absorption by a relatively large volume of liquid under conditions of vigorous agitation. With this apparatus a study has been made of the absorption of oxygen by finely divided cotton cellulose suspended in sodium hydroxide solution at 40°C. over a range of alkali concentration, cellulose content, and oxygen pressure. In one series of experiments cellulose depolymerization was also determined and in another experiment the alkaline autoxidation of  $\beta$ -methyl cellobioside was followed. During the early stages the reaction is autocatalytic with alkali concentrations above 8*N*. In the absence of diffusion effects, that is with alkali concentrations below approximately 10*N*, the steady rate of oxygen absorption is given by the equation,

$$-\frac{d[\text{O}_2]}{dt} = K[\text{Cell}]^{1.35} a_{\text{NaOH}} \frac{[\text{O}_2]}{K' + [\text{O}_2]} \phi[M]$$

where [Cell] refers to the weight of cellulose immersed in the solution, [O<sub>2</sub>] the partial pressure of oxygen,  $a_{\text{NaOH}}$  the molal activity of the sodium hydroxide,  $\phi[M]$  a function of the metal ion content and  $K$  and  $K'$  are constants. The known characteristics of the autoxidation are consistent with a modified Gee-Bolland mechanism. Thus a cellulose radical formed as a result of peroxide decomposition reacts with oxygen to form a radical of the type RO<sub>2</sub>. The last named is likely to be unstable and split off the O<sub>2</sub><sup>-</sup> radical ion which is comparatively unreactive but must nevertheless be capable of attacking an ionized cellulose molecule, thus completing one oxidation cycle. In principle a chain reaction could follow but the evidence indicates that a long chain mechanism is not involved, particularly at the stage of attainment of the steady rate.

### INTRODUCTION

The autoxidation which cellulose undergoes in presence of alkali is a process of considerable importance in the rayon industry and has been the subject of widespread investigation during the last three decades.<sup>1</sup> In the main, however, attention has been directed to questions of immediate technical concern and comparatively little information is available with direct bearing on the reaction mechanism. The problem is complicated by the insolubility of the substrate, which precludes a study of the reaction

\* Present address: Columbia Cellulose Ltd., Research and Development Division, Prince Rupert, B.C., Canada.

under strictly homogeneous conditions: previous workers have, with few exceptions, confined their attention to what is termed "alkali-cellulose," that is, cellulose impregnated with an alkaline solution, the excess liquor having been removed by pressing or centrifuging. Recently<sup>2</sup> we described some experiments using a modified system in which cellulose was kept in suspension in a large volume of alkaline solution and exposed to the action of oxygen. It was considered that this technique should afford an approach to homogeneous reaction conditions. The results obtained appeared of sufficient interest to justify a more detailed examination of the system and the present work was undertaken. This is an investigation of the absorption of oxygen by finely divided cellulose dispersed by vigorous agitation in solutions of sodium hydroxide.

## EXPERIMENTAL

### Materials

The cellulose was in the form of scoured bleached cotton yarn cut by hand to an average length of 0.5 mm. The intrinsic viscosity in cuprammonium hydroxide solution was 8.22 dl./g. at 20°C. and the iron content 0.002%, estimated colorimetrically by the addition of thioglycollic acid to an acid solution of an ashed specimen. The moisture content was standardized at 7.5% on the dry weight, as described previously.<sup>2</sup> The  $\beta$ -methyl cellobioside was kindly supplied by Dr. G. F. Davidson of the British Cotton Industry Research Association.

The sodium hydroxide solutions were made up quantitatively from AnalaR pellets and the composition checked by titration, with the exception of the least concentrated which was obtained by dilution of the 8.28*N* solution (thus establishing the iron content). The oxygen was obtained compressed from the British Oxygen Co. The cuprammonium hydroxide solution was of the British Standard composition.<sup>5</sup>

### Apparatus

The apparatus developed to measure small extents of oxygen absorption by a relatively large volume of liquid under conditions of vigorous agitation is shown diagrammatically in Figure 1. The reaction vessel (1) was constructed from a 500 ml. bolt head flask, reshaped as shown to prevent cellulose being deposited on the sides above the level of the solution. The vessel was connected to the socket of a spherical ground glass joint (2) via a B45 standard taper joint (3), and to the manometric system via a B10 joint (4). The stirrer shaft (5) was held firmly inside the ball of the spherical joint by a rubber collar (6) and supported at about midpoint by another collar (7), firmly attached to the shaft and fitting loosely in a glass tube acting as a bearing: lubrication was effected with a drop of the reaction medium. Since the whole apparatus was to be immersed in a water bath, a bell-jar device (8) was fitted over the ball shaft with rubber tubing to

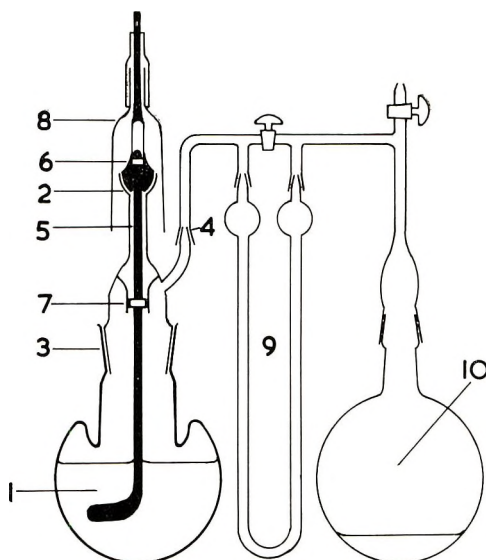


Fig. 1. Absorption apparatus.

keep water away from the spherical joint. The spherical seal was lubricated with three or four drops of Dow Corning silicone high vacuum fluid (DC 703) which gave satisfactory service over the longest period investigated (50 hr.).

A reciprocating motion was found to give optimum stirring efficiency. The motion was transmitted from a cam to an endless belt and from the belt to the stirrer shaft, using a sprocket and chain, the last named forming part of the endless belt. The stirrer described one and a half revolutions for one stroke of the cam-shaft and the same in the opposite direction for the reverse stroke: the speed was normally 100 cycles/min., which gave the most effective mixing.

The spherical seal was entirely free from leakage and functioned smoothly at pressures down to 600 mm. of mercury. Below this figure the joint became stiff and tended to seize up, so that observations at reduced oxygen pressure required to be carried out in presence of nitrogen.

### Procedure

With 100 ml. alkaline solution in the compensating vessel (10) and 400 ml., together with cellulose, in the reaction vessel, the apparatus was charged with oxygen, thermostatted in a water bath at 40°C., and the pressure adjusted to the required value; nitrogen was then added to bring the total pressure to 700 mm. of mercury. Not more than 0.1 ml. oxygen was absorbed per gram of cellulose in this preliminary period. After commencement of stirring, oxygen absorption was measured by following the decrease in pressure in the reaction vessel relative to that in the compensating vessel by means of a dibutyl phthalate manometer (9) read with a

traveling microscope. The overall pressure drop during an experiment was generally in the order of 1% of the total pressure and never more than 2%. In the high pressure region, where accurate measurements are possible, the rate of oxygen absorption is relatively insensitive to oxygen pressure, so that the latter may be taken as effectively constant in any absorption run. The oxygen pressures quoted are mean values over the period of the reaction.

### Calculation of Oxygen Absorption

The relationship between oxygen absorption (in milliliters at S.T.P.) and pressure change has been given by Entwistle, Cole, and Wooding<sup>3</sup> for a manometric system similar to that used here. The following details are relevant: volume of dead space on reaction side, 303 ml.; volume of dead space on compensating side, 606 ml.; cross-sectional area of manometer tube 0.0314 cm.<sup>2</sup>; density of dibutyl phthalate at 40°C., 1.0287 g./cm.<sup>3</sup>.

### Determination of Molecular Weight

After oxidation, specimens for molecular weight determination were acidified with acetic acid, filtered, washed, and dried. The number-average degree of polymerization was then calculated from the solution viscosity (0.5%) in cuprammonium hydroxide solution, as described previously.<sup>2</sup>

### Determination of Iron

The iron content of the alkaline solutions was determined colorimetrically by a method suggested by Davidson,<sup>4</sup> depending on the fact that traces of iron impart a yellow-orange coloration to concentrated solutions of sodium hydroxide in presence of saturated sodium sulfide solution. The optimum alkali concentration was found to be 7*N*; with cobalt blue glass filters in the colorimeter the method was satisfactory for iron contents up to 10 mg./l. The following iron contents were found at the alkali concentrations noted: 1.3 mg./l., 5.79*N*; 1.6 mg./l., 6.44*N*; 1.8 mg./l., 8.28*N*; 3.7 mg./l., 9.58*N*; 4.8 mg./l., 11.80*N*; 4.4 mg./l., 13.44*N*; 3.5 mg./l., 16.55*N*.

## RESULTS

### Oxygen Absorption under Static Conditions

When cellulose is immersed without agitation in sodium hydroxide solution the rate of oxygen uptake is very low and is almost certainly diffusion-controlled. In Table I are given the steady rates of oxygen uptake by 2 g. of cellulose lying approximately 3.6 cm. below the solution surface.

### Effect of Diffuse Daylight

It was found that the laboratory daylight was without detectable effect on the rate of oxygen absorption. Thus, although the majority of the

TABLE I  
Steady Rate of Reaction under Static Conditions

Normality, NaOH	O <sub>2</sub> press., mm.	O <sub>2</sub> absorbed, ml./g. cellulose/hr.
5.17	698	0.0052
5.17	430	0.0036
9.58	698	0.00103

experiments were not carried out in total darkness, it is clear that only a "dark" reaction was involved.

### Effect of Stirring Speed

The solubility and diffusion coefficient of oxygen in sodium hydroxide solutions decrease with increasing alkali concentration,<sup>6</sup> and so it was anticipated that the rate of stirring would be more important at higher alkali concentrations. This proved to be the case: in 18*N* sodium hydroxide the rate of oxygen absorption depended markedly on the rate of stirring, whereas with alkali concentrations of 8*N* and lower the rate was unaffected by a 60% variation in stirring speed about the standard rate of 100 cycles/min., even at the lowest oxygen pressure and highest cellulose content.

### General Features of the Oxygen Absorption

Typical absorption curves at different alkali concentrations are shown in Figures 2 and 3. At the lower concentrations the rate soon attains a constant value, whereas above 8*N* alkali a prolonged period of autocatalysis is evident. This contrasts with the autoxidation of alkali-cellulose prepared from cotton, which is autocatalytic at all alkali concentrations.<sup>4</sup> The curves also show the effect of interrupting the stirring for a period of 12 hr. At lower alkali concentrations the rate soon regains the steady value observed on the first day: at higher concentrations the reaction begins again at the rate observed just before the stirring was stopped at the end of the first day. It seems clear that when stirring is stopped and the cellulose separates out in a layer well below the surface, any further reaction is largely arrested by a barrier of stagnant alkali solution. Medvedev<sup>7</sup> made a similar observation in the autoxidation of tetralin: if the system were purged with nitrogen and allowed to stand for several hours the reaction ceased, but recommenced at the same rate as before the interruption when oxygen was readmitted.

### Dependence of Rate on Cellulose Concentration

The term, Cellulose concentration, is here used to denote the weight of cellulose suspended in the alkaline solution (g./400 ml.). For a given alkali concentration the shape of the absorption-time plot was substantially the same at all cellulose concentrations studied. Thus in 5.79*N* sodium



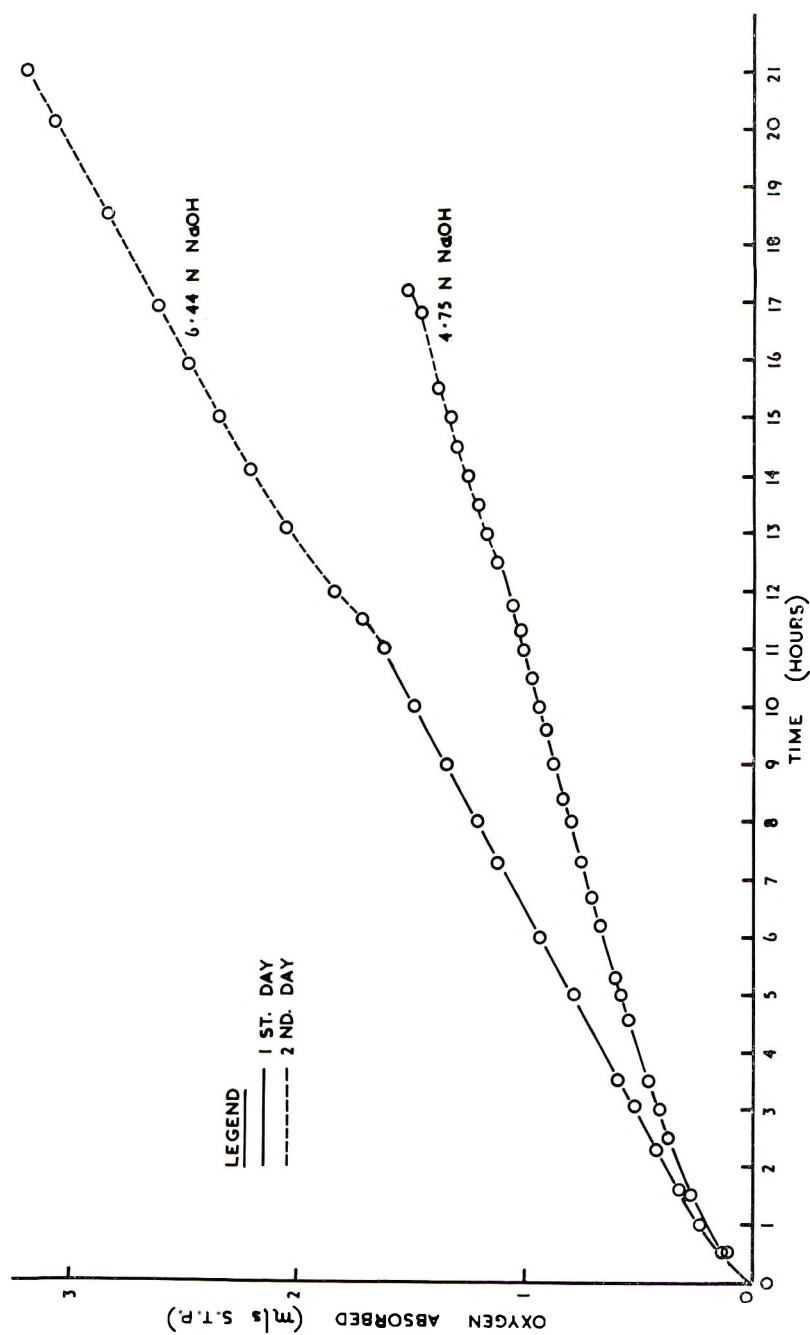


Fig. 2. Oxygen absorption at lower alkali concentrations: 2 g. cellulose, 692 mm. oxygen pressure.

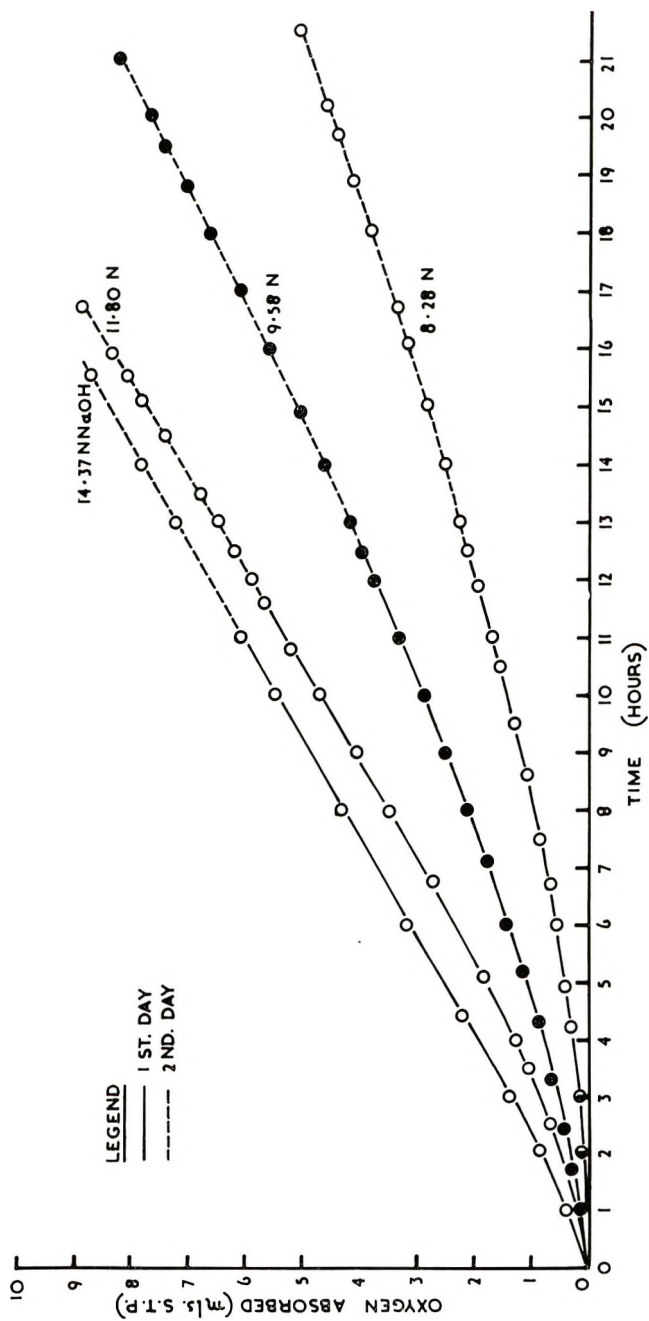


Fig. 3. Oxygen absorption at higher alkali concentrations: 2 g. cellulose, 695 mm. oxygen pressure.

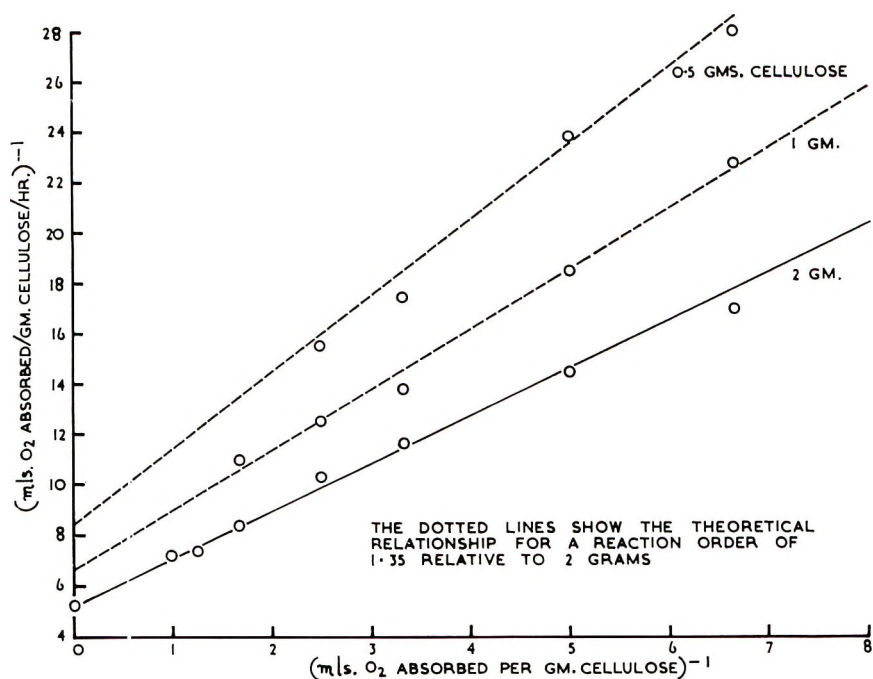


Fig. 4. Variation of reciprocal rate with reciprocal extent of oxidation: 8.28N NaOH, 695 mm. oxygen pressure.

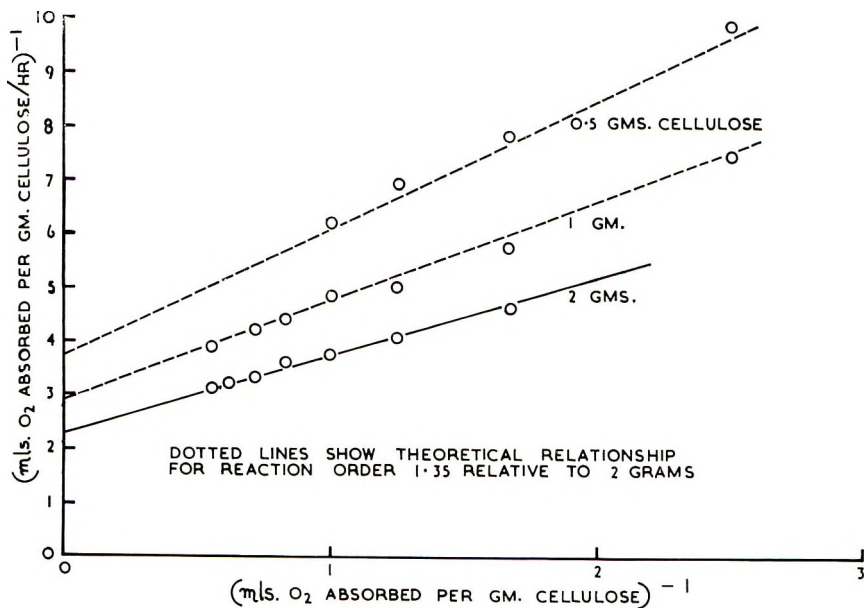


Fig. 5. Variation of reciprocal rate with reciprocal extent of oxidation: 11.80N NaOH, 696 mm. oxygen pressure.

hydroxide the rates soon attained steady values: these were 0.035, 0.042, 0.049, and 0.055 ml. oxygen at S.T.P. per gram of cellulose per hour corresponding to cellulose concentrations of 0.5, 1, 1.5 and 2 g./400 ml. These values are consistent with the following empirical relationships:

$$\text{rate} = K[\text{cellulose}]^{1.35}$$

or

$$\text{rate} = K_1[\text{cellulose}] + K_2[\text{cellulose}]^2$$

At higher alkali concentrations the situation is rather more complicated owing to the protracted autocatalysis. However, it has been found that a linear relationship exists between reciprocal rate and reciprocal oxygen absorption. The plots are shown in Figures 4 (8.28*N*) and 5 (11.8*N*) in which the dashed lines indicate the relationship to be expected if the power

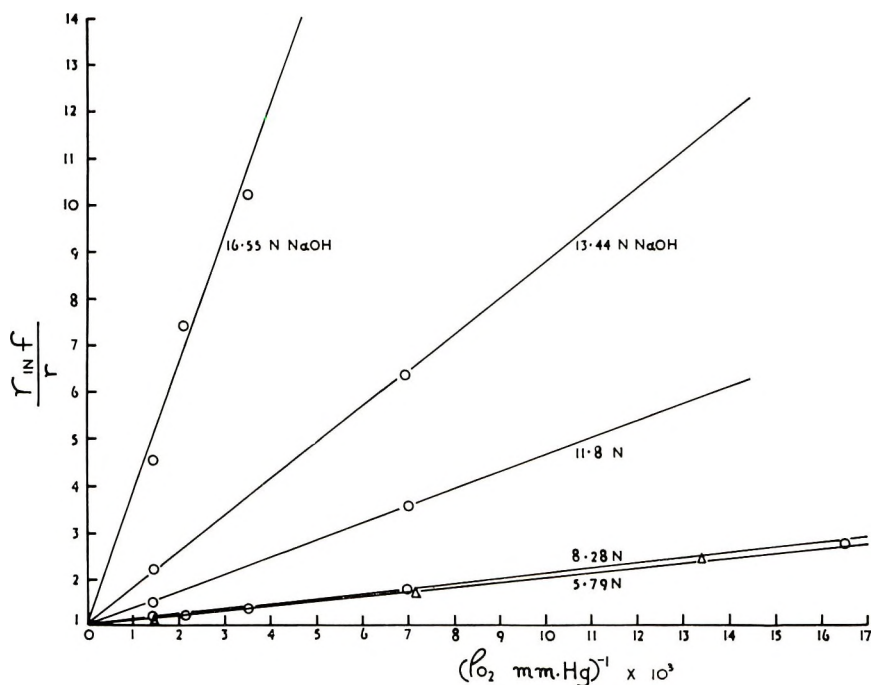


Fig. 6. Variation of reciprocal rate, relative to rate at infinite oxygen pressure, with reciprocal oxygen pressure: 2 g. cellulose.

dependence on cellulose concentration is 1.35 at all extents of oxidation. The agreement between the predicted and the observed rates confirms the above kinetic dependence on cellulose concentration up to 11.8*N* sodium hydroxide. With higher alkali concentration the relationship breaks down, most probably due to interference from diffusion effects; this will be further considered in what follows.

### Dependence of Rate on Oxygen Pressure

The effect of variation in oxygen pressure on the rate of oxygen absorption was studied by carrying out successive absorption measurements on one assemblage of the apparatus. As has been found with certain other autoxidation processes,<sup>10</sup> the plot of reciprocal (steady) rate versus reciprocal oxygen pressure is linear with a positive intercept on the rate axis giving the rate at infinite oxygen pressure  $r_{inf}$ . To facilitate comparison of results at different alkali concentrations the rates have been calculated relative to the values at infinite pressure: the reciprocal plots are shown in Figure 6. The slopes increase quite markedly as the alkali concentration increases above 8*N*, showing the increasing dependence of rate on oxygen pressure. In 16.55*N* sodium hydroxide, an ordinary plot of rate versus oxygen pressure, not given here, reveals a first-order dependence on pressure over the whole pressure range; this is probably a further manifestation of the incidence of diffusion effects at higher alkali concentrations.

### Dependence of Rate on Alkali Concentration

The variation in steady rate of oxygen absorption with alkali concentration at 695 mm. oxygen pressure is shown in Figure 7. Only with the highest cellulose content does the rate pass through a maximum similar to that observed in the autoxidation of alkali-cellulose<sup>3,4</sup> (that is, cellulose in wad form). Again this is most probably due to diffusion effects at high alkali concentration. The condition under which diffusion will become im-

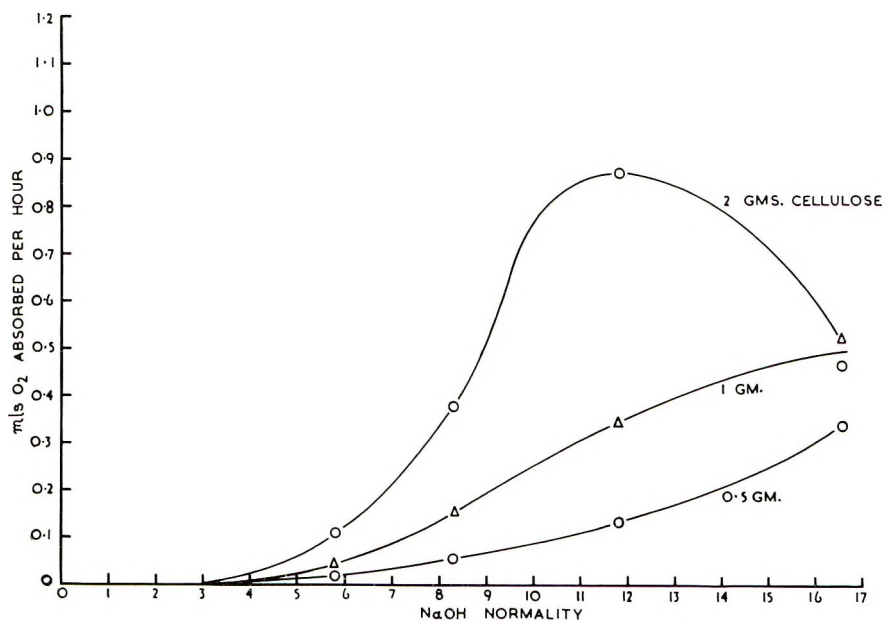


Fig. 7. Effect of alkali concentration on the measured steady rate of oxygen absorption; 695 mm. oxygen pressure.



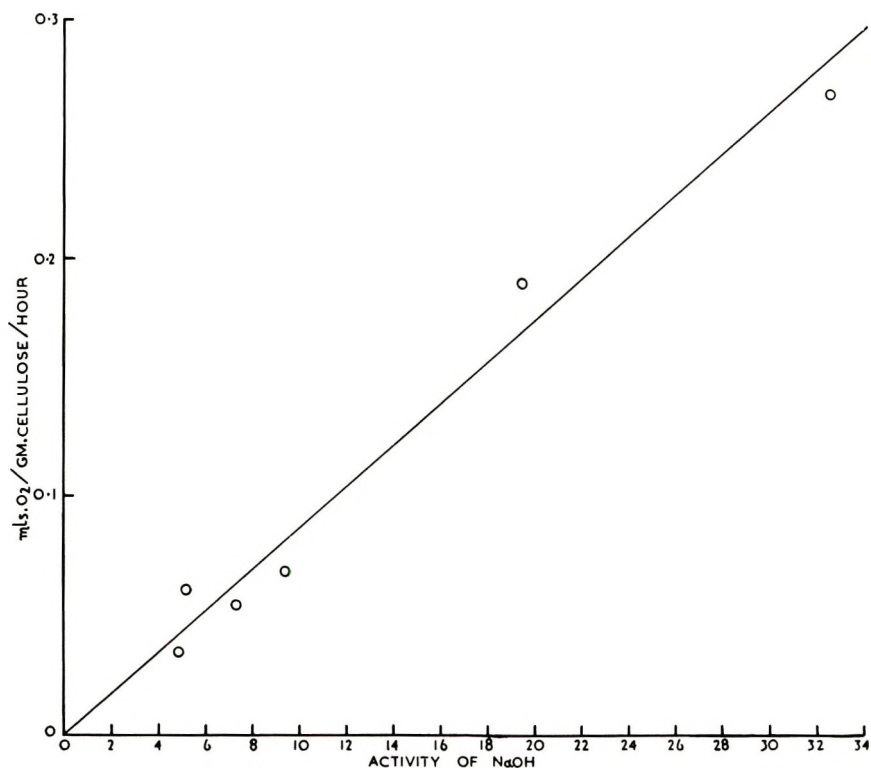


Fig. 8. Variation of steady rate of oxygen absorption per gram of cellulose with NaOH activity: 2 g. cellulose, 695 mm. oxygen pressure.

portant is that the concentration of oxygen in solution should be significantly lower than the solubility. This condition will be fulfilled more readily with higher concentrations of cellulose, corresponding to higher overall rates of oxygen absorption.

In an earlier study<sup>2</sup> it was found that the rate of depolymerization of cellulose immersed in aerated sodium hydroxide solution was proportional to the molal activity of the sodium hydroxide. In Figure 8 the steady rate of oxygen absorption is plotted against the sodium hydroxide activity<sup>8</sup> for the highest cellulose concentration and for alkali concentrations below 10*N*; within this range the plot indicates a direct proportionality. At higher alkali concentrations there is considerable divergence from linearity, but the divergence becomes less pronounced as the cellulose content is decreased (Fig. 9). It does not seem unreasonable to suppose that in the absence of diffusion effects the rate might be proportional to the alkali activity over the whole concentration range.

#### Depolymerization of the Cellulose

A series of reactions was carried out over a range of alkali concentration with 2 g. cellulose and at 145 mm. oxygen pressure for a standard time of 11

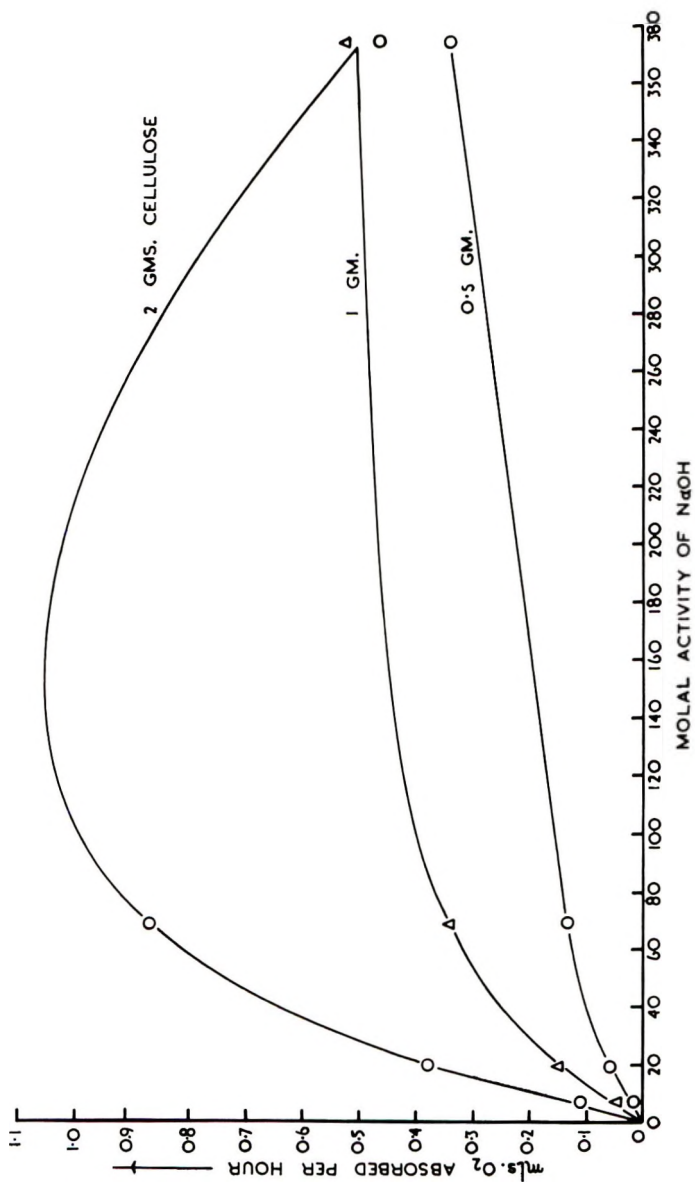


Fig. 9. Variation of measured steady rate of oxygen absorption with NaOH activity: 695 mm. oxygen pressure.

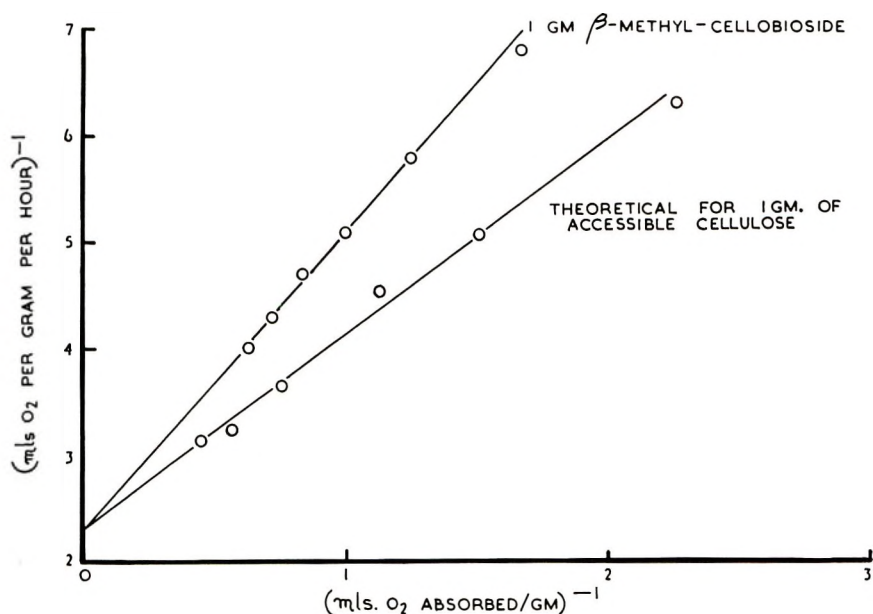


Fig. 10. Comparison of autoxidation characteristics of cellulose and  $\beta$ -methyl cellobioside; variation of reciprocal rate with reciprocal extent of oxidation: 8.28*N* NaOH, 695 mm. oxygen pressure.

hr. Molecular weight determinations were then carried out on the oxidized specimens. The results, summarized in Table II, show that, from the point of view of chain scission,<sup>2</sup> the absorbed oxygen acts most efficiently at high alkali concentration.

TABLE II  
Comparison of Oxygen Absorption with Cellulose Chain Scission (Original Number-Average D.P. of Cellulose-2750)

	4.75 <i>N</i> NaOH	9.58 <i>N</i> NaOH	13.44 <i>N</i> NaOH	16.55 <i>N</i> NaOH
Intrinsic viscosity, dl./g.	5.57	2.78	1.81	2.68
Scissions per original molecule	0.62	2.82	5.49	3.00
O <sub>2</sub> absorbed per gram cellulose				
Steady rate, ml./hr.	0.025	0.065	0.093	0.051
Total in 11 hr., ml.	0.360	0.620	0.985	0.530
Molecules O <sub>2</sub> per chain scission	11.5	4.4	3.6	3.5

### Autoxidation of $\beta$ -Methyl Cellobioside

The autoxidation of  $\beta$ -methyl cellobioside (1 g.) in 8.28*N* sodium hydroxide was followed by the procedure used for cellulose. As with cellulose, reciprocal rate varies linearly with reciprocal oxygen absorption (Fig. 10). The steady rate, obtained by extrapolation, is 0.43 ml. oxygen per gram per hour which compares with the value of 0.19 for cellulose. The dif-

ference would be accounted for on the assumption that the cellulose is 40% accessible, which is a plausible figure, taking into account the nature of the medium in which the reaction is carried out. Assuming the cellulose to be 40% accessible at all degrees of oxidation, a theoretical plot for 1 g. of completely accessible cellulose has been calculated and is shown for comparison in Figure 10. This is not identical with the plot for the simple sugar, but the difference is not such as to suggest any essential difference in the mechanism by which the two materials autoxidize.

## DISCUSSION

### The Role of Diffusion

In deriving a kinetic equation it is clearly necessary to establish that the observed rate of oxygen absorption is a true measure of the reaction rate, free from any influence of diffusion. With alkali concentrations of 8.28*N* and lower, the rate was found to be independent of stirring speed, showing diffusion in the solution phase to be unimportant here. With higher alkali concentrations, particularly in the presence of large amounts of cellulose, diffusion becomes increasingly important and is apparently the rate-determining step in 17*N* sodium hydroxide. Thus the results at higher alkali concentrations have not yielded meaningful kinetic data. However, below approximately 10*N* sodium hydroxide there is good reason to believe that authentic rates have been measured. It is not possible to show directly that diffusion within the cellulose phase is unimportant at low oxygen pressure, where the rate is strongly pressure-dependent. However, indirect evidence stems from the observation that the reaction order with respect to oxygen pressure is practically the same in 8.28*N* alkali as in 5.79*N* (Fig. 6). Since diffusion must have a greater potential influence at the higher alkali concentration the only reasonable conclusion to be drawn is that the influence is negligible in both cases.

### The Rate Equation

The experimentally determined kinetic equation for the steady rate of oxygen absorption by cellulose immersed in alkaline solution is of the form

$$\text{rate} = K[\text{cellulose}]^{1.35} a_{\text{NaOH}} \frac{P}{K' + P} \phi[M]$$

where [cellulose] refers to the quantity of cellulose suspended in sodium hydroxide of molal activity  $a_{\text{NaOH}}$  under a partial pressure  $P$  of oxygen, and  $K$  and  $K'$  are constants.  $\phi[M]$  is a function of the heavy metal content of the solution, studied in the case of copper catalysis in an earlier investigation.<sup>2</sup>

### The Initial Reaction

The autoxidation of alkali cellulose was investigated in some detail by Entwistle, Cole, and Wooding,<sup>3</sup> who put forward a radical chain mechanism analogous to that established for the autoxidation of certain simple olefins.<sup>9,10</sup> The initial rate of oxygen uptake was found to be proportional to the reducing power of the cellulose, and it was suggested that radical chains are initiated by reaction of reducing groups with oxygen. In certain processes such direct attack by oxygen apparently does occur.<sup>11</sup> However, the kinetic evidence indicates that in the present system this mode of initiation is not important, since it would lead to a power dependence of rate on oxygen pressure, whereas the rate is found to become pressure independent at high pressure. The significance of the initial rate in relation to the subsequent steady rate is, furthermore, in some doubt on another count. Bamford and Collins<sup>12</sup> found the rate of alkaline autoxidation of glucose to be unaffected by the presence of free radical generating substances or of radical chain inhibitors, which contrasts with the case of alkali-cellulose autoxidation.<sup>3</sup> Furthermore, the rates are very different for the two substrates: in 6*N* sodium hydroxide and at infinite oxygen pressure, glucose was found to autoxidize nearly 100 times more rapidly at 25°C. than "completely accessible" cellulose does at 40°C. In addition, the rate with glucose was found independent of alkali concentration above about 1*N*, whereas no such independence is observed with cellulose. Obviously, the two processes do not proceed by the same mechanism, and so it is unlikely that direct initiation of cellulose autoxidation takes place at reducing end groups in the cellulose molecule. A similar argument can be leveled against direct initiation at  $\alpha$ -ketol groups in the 2-3 position, based on the known characteristics of  $\alpha$ -ketol autoxidation.<sup>13</sup> Thus reducing groups initially present may be expected to autoxidize rapidly before the main reaction causing cellulose depolymerization is established, although some chain scission would occur with certain types of reducing oxycelluloses.<sup>14</sup> This would reconcile the known dependence of initial rate on reducing power<sup>3</sup> with the manifestly differing mechanisms by which reducing groups and cellulose autoxidize. Also explained would be the observation<sup>3</sup> that while organic autoxidants such as 1,4-naphthaquinone markedly reduced the steady rate of oxygen absorption by alkali cellulose, the initial rate was entirely unaffected in all cases.

Although the presence of reducing groups is probably without direct influence on the main autoxidative reaction, there may well be an important indirect connection. Under alkaline conditions, glucose<sup>12</sup> and  $\alpha$ -ketols<sup>13</sup> react with oxygen with the initial formation of a peroxide, probably hydrogen peroxide; there is evidence that this entity is responsible for initiating cellulose oxidation. Entwistle, Cole, and Wooding observed a peroxide formed during the autoxidation of alkali cellulose and their results show that the peroxide content reached a constant value at approximately the stage of attainment of the steady rate. Furthermore, it is known that

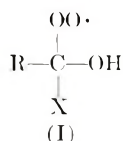


addition of glucose does not affect the initial rate of depolymerization of alkali-cellulose<sup>3</sup> whereas hydrogen peroxide markedly increases the rate.<sup>15</sup>

The decomposition of a hydroperoxide is complex and generally gives some free radicals<sup>16</sup> which would be expected to attack the cellulose. Metal ions are thought to play an important part in the decomposition, possibly through complex formation with the peroxide.<sup>17</sup> Variation in metal content and species might be expected to influence the proportion of radicals formed during peroxide decomposition, which would explain the known dependence of rate on transition metal content.<sup>3,4</sup>

### Subsequent Reactions

Cellulose autoxidation could be effected through hydrogen transfer or electron transfer: in either case the result is essentially the same<sup>16</sup> and for the sake of simplicity it will be arbitrarily taken that hydrogen transfer is involved. Assuming that the successive steps follow the basic pattern common to most other autoxidations, initial formation of a cellulose radical will be followed by uptake of oxygen to give the corresponding peroxy radical. If attack originally takes place on carbons 2, 3, or 6 the structure of the latter will be



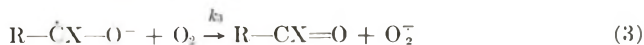
where the identity of R and X depends on the particular position of attack. Structure I is likely to be extremely unstable in view of the known tendency of hydroperoxides to hydrolyze in alkali<sup>18</sup> and in view of the inherent instability of compounds containing a perhydroxyl group and a hydroxyl group on one carbon atom.<sup>19</sup> Rapid scission may therefore be expected with the formation of a carbonyl group and the radical HO<sub>2</sub>. Scission of the cellulose molecule is not directly involved in this sequence, but the introduction of a carbonyl group at positions 2, 3, or 6 may be expected to confer alkali sensitivity to a glycosidic link in the β-position.<sup>20</sup> Under the alkaline conditions of the reaction HO<sub>2</sub> will be almost completely dissociated<sup>21</sup> to the radical ion O<sub>2</sub><sup>-</sup>. Whether or not a chain reaction of the Gee-Bolland type<sup>9</sup> ensues will depend on the reactivity of the mobile O<sub>2</sub><sup>-</sup> radical ion rather than of the relatively immobile cellulose peroxy radical. The redox potentials for electron transfer<sup>22</sup> show that HO<sub>2</sub> is less reactive than the HO· radical: it is apparently incapable of abstracting hydrogen from an unionized alcohol molecule.<sup>23</sup> The ionized form O<sub>2</sub><sup>-</sup> would seem to be an even less powerful oxidizing agent and may itself undergo oxidation under certain circumstances.<sup>24</sup> Normally the radical ion O<sub>2</sub><sup>-</sup> would not be expected to oxidize an organic substrate, but the situation may be different in the strongly alkaline environment of the present system. Indeed, taking into account that bimolecular reaction between cellulose mole-

cules in different fibers would almost certainly be precluded, it has not been found possible to explain how the order of reaction with respect to cellulose can be greater than unity without assuming that  $O_2^-$  does attack the cellulose. It is not, however, necessary to postulate the occurrence of long reaction chains. Tobolsky and co-workers<sup>25</sup> have shown that in the limiting case of a Gee-Bolland mechanism in which the rate of formation of peroxide is equal to the rate of decomposition, the autoxidation rate will attain a constant value proportional to the square of the substrate concentration and that under these conditions the chain length is unity. Certainly the low reactivity of  $O_2^-$  would make the occurrence of long reaction chains unlikely; also the addition of inhibitors to alkali cellulose<sup>3</sup> does not cause the spectacular decrease in rate observed in processes where the uninhibited reaction proceeds by a long chain mechanism.<sup>26</sup>

Some indication of the point of attack in the anhydroglucose unit follows from the relation between rate and alkali activity. The most probable function of the alkali is to promote ionization of hydroxyl groups in the cellulose molecule; in addition, for proportionality with alkali activity the ionization must be small. The first dissociation constant<sup>27,28</sup> is in the region of  $10^{-14}$  so that the first ionization, which presumably takes place at the 2,3  $\alpha$ -glycol,<sup>29</sup> will be more than half complete in 10*N* sodium hydroxide and is thus eliminated. The second ionization will be much smaller and may occur at C<sub>6</sub> or again at the glycol: by analogy with the case of ascorbic acid<sup>13</sup> a double negative charge might be expected to render the glycol particularly susceptible to oxidation.

### Kinetic Analysis

The preceding discussion can be formalized in the simplified reaction scheme of eqs. (1)–(7) relating to the steady rate of oxygen absorption by cellulose in presence of alkali.



Decomposition of (ionized) peroxide by reaction (1) gives one-half equivalent of radicals which subsequently attack the cellulose; these are taken to be  $O_2^-$  for convenience of treatment. In practice less than half may attack the cellulose, but this does not affect the form of the derived rate

equation. Oxidation of ionized cellulose takes place in two stages by reactions (2) and (3), and radicals suffer mutual destruction by reactions (4) and (5). It is assumed that interaction of two cellulose radicals would be precluded because of steric hindrance. For constant peroxide concentration, corresponding to the steady rate, the rate of formation by reactions (2), (4), and (5) is equal to the rate of decomposition by reaction (1). Then by the method of stationary states the following relationships are found for the steady rate of oxygen absorption:

$$\begin{aligned}
 -\frac{d[\text{O}_2]}{dt} &= k_3[\text{R}\dot{\text{C}}\text{XO}^-][\text{O}_2] - \frac{1}{2}k_5[\text{O}_2^-]^2 = \frac{1}{2}k_1[\text{HO}_2] \\
 &= \frac{4k_2^2k_3[\text{RCHXO}^-]^2[\text{O}_2]}{12k_2k_4[\text{RCHXO}^-] + 9k_3k_5[\text{O}_2] + \frac{3k_1k_4k_6[\text{HO}_2]}{4k_2[\text{RCHXO}^-]}}
 \end{aligned}
 \tag{8}$$

Expression (8) cannot be verified as it stands because of the presence of the peroxide-concentration term in the denominator. However, it can be shown that this term is at the most relatively small. At high oxygen pressure, where reaction (4) can be neglected, the rate equation simplifies to

$$-d[\text{O}_2]/dt = (4k_2^2/9k_5)[\text{RCHXO}^-]^2
 \tag{9}$$

while at low oxygen pressure, neglecting reaction (5), the equation becomes

$$-d[\text{O}_2]/dt = (k_2k_3/3k_4)[\text{RCHXO}^-][\text{O}_2]
 \tag{10}$$

so that in these extreme cases the term in peroxide concentration vanishes. At a certain oxygen pressure between these extremes, expression (8) can be simplified by equating the terms  $12k_2k_4[\text{RCHXO}^-]$  and  $9k_3k_5[\text{O}_2]$ . Here it can be shown by successive approximations that effect of the peroxide concentration term is to reduce the calculated rate by 9.9%. This would introduce slight curvature in the plot of reciprocal rate versus reciprocal oxygen pressure, too small to detect in the present experiments. Thus the peroxide concentration term may be disregarded, and the dependence of rate on oxygen pressure becomes of the form found experimentally.

For a given alkali concentration the concentration of ionized cellulose will be proportional to that of the original cellulose, since the alkali is present in large excess. Thus at infinite oxygen pressure the rate should vary with the square of the cellulose concentration, according to eq. (9). Under the oxygen pressure used experimentally the power dependence would be slightly less—approximately 1.9. The observed power dependence of 1.35 is significantly lower than the theoretical value and this probably results from an oversimplification in the reaction scheme. It can be shown that the calculated power dependence of rate on substrate concentration is equal to the order of reaction by which the  $\text{O}_2^-$  radicals are destroyed. Thus for example at low oxygen pressure these radicals are destroyed by reaction (4), which is first order with respect to  $\text{O}_2^-$ ; the over-

all rate is then first order with respect to substrate. It is not difficult to imagine other radical terminating reactions which would give the same kinetic result at high oxygen pressure; electron transfer between a radical and a metal ion is one obvious possibility.

By eq. (6) the concentration of ionized cellulose is given as  $K_a[\text{RCHXOH}][\text{OH}^-]$ , where  $K_a$  is the acidic dissociation constant of the reactive position and  $[\text{OH}^-]$  the hydroxyl ion concentration (or, at high concentration, the activity). For low degrees of dissociation  $[\text{RCHXOH}]$  will be sensibly equal to the total cellulose present and independent of  $[\text{OH}^-]$ . The rate should then show the same power dependence on alkali activity as on cellulose concentration. The results are in fact consistent with a proportionality between rate and alkali activity to the power 1.35, up to 8.3*N* sodium hydroxide. Above this concentration the plot (not shown here) diverges from linearity rather more abruptly than does the first power plot of rate versus activity (Fig. 9). It is not possible to say to what extent this divergence may be due to diffusion effects since if the cellulose dissociation becomes significant at higher alkali concentrations some divergence would be expected anyway. The results up to 10*N* alkali are in fact consistent with a dissociation constant of  $7 \times 10^{-16}$  at 40°C. for the reactive position.

The authors wish to thank Drs. H. R. Cooper and T. P. Nevell for helpful discussions during the preparation of the manuscript. One of us (R. I. C. M.) is indebted to the trustees of the Courtauld Scientific and Educational Trust Fund for the award of a Research Scholarship.

### References

1. Cf. Müller, H. G., *Textil-Rundschau*, **12**, 622, 671 (1957); *ibid.*, **13**, 67 (1958).
2. Michie, R. I. C., and S. M. Neale, *J. Polymer Sci.*, **A2**, 225 (1954).
3. Entwistle, D., E. H. Cole, and N. S. Wooding, *Textile Res. J.*, **19**, 527, 609 (1949).
4. Davidson, G. F., *J. Textile Inst.*, **23**, T95 (1932).
5. British Standard Specification 2610: 1955
6. Geffcken, G., *Z. Physik. Chem.*, **49**, 257 (1904); W. W. Ipatieff, W. P. Teodorovitch, and S. I. Druschina-Artemovitsch, *Z. Anorg. Chem.*, **216**, 66 (1933); M. I. Levina and N. P. Stsibarovskaya, *J. Phys. Chem. (U.S.S.R.)*, **12**, 653 (1939), per *Chem. Abstr.*, **34**, 306 (1940).
7. Medvedev, S., and A. Podyapolskaya, *J. Phys. Chem. (U.S.S.R.)*, **12**, 719 (1939).
8. Åkerlöf, G., and G. Kegeles, *J. Am. Chem. Soc.*, **62**, 620 (1940).
9. Bolland, J. L., *Quart. Rev.*, **3**, 1 (1949).
10. Bateman, L., *Quart. Rev.*, **8**, 147 (1954).
11. Cooper, H. R., and H. W. Melville, *J. Chem. Soc.*, **1951**, 1984.
12. Bamford, C. H., and J. R. Collins, *Proc. Roy. Soc. (London)*, **A204**, 62 (1950).
13. Weissberger, A., J. E. Luvall, and D. S. Thomas, *J. Am. Chem. Soc.*, **65**, 1934 (1943); A. Weissberger and J. E. Luvall, *J. Am. Chem. Soc.*, **69**, 1567 (1947).
14. Corbett, W. M., *J. Soc. Dyers Colourists*, **76**, 265 (1960).
15. Kleinert, T. N., *Textil-Rundschau*, **14**, 249 (1959).
16. Ingold, K. U., *Chem. Rev.*, **61**, 563 (1961).
17. Kremer, M. L., *Trans. Faraday Soc.*, **58**, 702 (1962): see also *Discussions Faraday Soc.*, No. 29 (1960).
18. Waters, W. A., *The Chemistry of Free Radicals*, Clarendon Press, Oxford, 1946, p. 244.



19. Cooper, H. R., private communication.
20. Corbett, W. M., in *Recent Advances in the Chemistry of Cellulose and Starch*, J. Honeyman, Ed., Heywood, London, 1959, p. 106 et seq.
21. Uri, N., *Chem. Revs.*, **50**, 375 (1952).
22. Mead, J. F., in *Autoxidation and Autoxidants*, Vol. I, W. O. Lundberg, Ed., Interscience, (Wiley), New York-London, 1961, p. 302.
23. Bolland, J. L., and H. R. Cooper, *Proc. Roy. Soc. (London)*, **A225**, 405 (1954).
24. Barb, W. G., J. H. Baxendale, P. George, and K. R. Hargreave, *Trans. Faraday Soc.*, **47**, 462 (1951).
25. Tobolsky, A. V., D. J. Metz, and R. B. Mesrobian, *J. Am. Chem. Soc.*, **72**, 1942 (1950): see also ref. 22 p. 115.
26. Bolland, J. L., and P. ten Have, *Trans. Faraday Soc.*, **43**, 201 (1947).
27. Neale, S. M., *J. Textile Inst.*, **21**, T225 (1930).
28. Pennings, A. J., and W. Prins, *J. Polymer Sci.*, **58**, 229 (1962).
29. Cf. Hine, J., and M. Hine, *J. Am. Chem. Soc.*, **74**, 5266 (1952).

### Résumé

On a dessiné un appareil pour mesurer de petites quantités d'absorption de gaz pour un volume relativement grand de liquide dans des conditions d'agitation énergétique. A l'aide de cet appareil, une étude d'absorption d'oxygène a été faite sur du coton cellulosique finement divisé, suspendu dans une solution d'hydroxyde de sodium à 40°C pour une série de concentrations en alcalis, de contenu en cellulose et de pression en oxygène. Dans une série d'expériences, la dépolymérisation de la cellulose a aussi été déterminée et dans une autre expérience on a suivi l'auto-oxydation du  $\beta$ -méthyl cellobioside. Durant les étapes initiales, la réaction est autocatalytique pour des concentrations en alcali au-dessus de 8N. En absence des effets de diffusion, c.a.d., pour des concentrations en alcalis approximativement inférieures à 10N, la vitesse stationnaire d'absorption d'oxygène est donnée par l'équation:

$$- \frac{d[\text{O}_2]}{dt} = K[\text{Cell}]^{1.35} a_{\text{NaOH}} \frac{[\text{O}_2]}{K' + [\text{O}_2]} \phi[M]$$

où [cell] désigne le poids de la cellulose dans la solution,  $[\text{O}_2]$  la pression partielle en oxygène,  $a_{\text{NaOH}}$  l'activité molaire de l'hydroxyde de sodium,  $\phi[M]$  une fonction de la teneur en ion métallique et  $K$  et  $K'$  sont des constantes. Les caractéristiques connues de l'autoxydation sont en accord avec un mécanisme modifié de Gee-Bolland. Ainsi un radical cellulosique formé par décomposition de peroxyde réagit avec l'oxygène pour former un radical du type  $\text{RO}_2^{\cdot}$ . Le dernier nommé est vraisemblablement instable et se sépare en un ion radical  $\text{O}_2^{\cdot -}$  lequel est comparativement non réactionnel mais doit néanmoins être capable d'attaquer une molécule de cellulose ionisée, complétant alors un cycle d'oxydation. En principe un mécanisme en chaîne en suivrait mais l'évidence montre qu'un mécanisme à longue chaîne n'est pas incluí, en particulier lorsqu'on atteint la vitesse stationnaire.

### Zusammenfassung

Es wurde ein Apparat zur Bestimmung kleiner, von einem relativ grossen Flüssigkeitsvolumen unter heftigem Rühren absorbierter Gasmengen entwickelt. Mit Hilfe dieses Apparates wurde die Absorption von Sauerstoff durch fein verteilte, in Natriumhydroxydlösung suspendierte Baumwollcellulose bei 40°C über einen grossen Bereich der Alkalikonzentration, des Cellulosegehaltes und des Sauerstoffdruckes untersucht. In einer Versuchsreihe wurde ausserdem die Cellulose-Depolymerisation, in einem anderen Versuch die alkalische Autoxydation von  $\beta$ -Methyl-Cellobiosid verfolgt. Im Anfangsstadium verläuft die Reaktion bei Alkalikonzentrationen über 8 n autocatalytisch. Treten keine Diffusionseffekte auf, was bei Alkalikonzentrationen unter etwa 10



n der Fall ist, so ist die stationäre Geschwindigkeit der Sauerstoff-absorption durch die Gleichung

$$-\frac{d[\text{O}_2]}{dt} = K [\text{Cell}]^{1.35} a_{\text{NaOH}} \frac{[\text{O}_2]}{K' + [\text{O}_2]} \phi[M]$$

gegeben, wobei [Cell] das Gewicht der in der Lösung enthaltenen Cellulose,  $[\text{O}_2]$  der Sauerstoffpartialdruck,  $a_{\text{NaOH}}$  die molare Aktivität von Natriumhydroxyd,  $\phi[M]$  eine Funktion des Metallionengehaltes (frühere Untersuchungen<sup>2</sup>) und  $K$  und  $K'$  Konstanten sind. Die bekannten Charakteristika der Autoxydation stehen mit einem modifizierten Gee-Bolland-Mechanismus im Einklang. Demnach reagiert ein durch Peroxydzersetzung gebildetes Celluloseradikal mit Sauerstoff unter Bildung eines Radikals vom Typ  $\text{RO}_2$ . Dieses ist wahrscheinlich instabil und spaltet das Radikalion  $\text{O}_2^-$  ab, welches im Vergleich dazu wenig reaktionsfähig ist, aber dennoch fähig sein muss, ein ionisiertes Cellulosemolekül anzugreifen und so einen Oxydationszyklus zu schliessen. Im Prinzip könnte zwar eine Kettenreaktion folgen, doch die Befunde zeigen, dass, besonders bei der Erreichung der stationären Geschwindigkeit, kein Mechanismus mit langer Kette wirksam ist.

Received March 28, 1963

## Photodegradation of Poly(methyl Acrylate)\*

R. B. FOX, L. G. ISAACS, S. STOKES, and R. E. KAGARISE, *U. S. Naval Research Laboratory, Washington, D. C.*

### Synopsis

Thin films of poly(methyl acrylate) at room temperature have been photodegraded in air and in vacuum by radiation from a low-pressure mercury source. Changes in intrinsic viscosities, ultraviolet absorption, and volatile products were followed as a function of the energy absorbed. Crosslinking occurs in both air and vacuum, but at a slower rate in air. The apparent quantum yield for random scission in air was 0.013 scissions per quantum absorbed. In air, carbonyl groups are formed along the backbone chain. Most of the volatile products studied appear to originate from the ester groups in the polymer; formaldehyde, methanol, and methyl formate evolved at a constant rate for doses up to at least  $2 \times 10^{20}$  quanta/g.; quantum yields for each were determined. Carbon dioxide forms in amounts increasing exponentially with dose. Small amounts of carbon monoxide, methane, and hydrogen were detected qualitatively, but monomer was not observed. A mechanism compatible with these findings is suggested.

### INTRODUCTION

Previous reports from this Laboratory on the photodegradation of thin polymer films have been concerned with poly- $\alpha$ -methylstyrene<sup>1</sup> and poly(methyl methacrylate)<sup>2</sup> (PMMA). These studies have allowed us to compare under similar conditions linear polymers having chains containing alternating quaternary carbon atoms but different chromophores. In the solid state, this type of polymer has usually been found to undergo degradation without significant crosslinking. On the other hand, polymers having tertiary hydrogen atoms along the carbon chain are notable for their tendency to crosslink under the influence of radiant energy.<sup>3,4</sup> It is of interest, therefore, to compare the photodegradation of polymers having the same chromophores but differing backbone structures. For example, films of poly(methyl vinyl ketone) and poly(methyl isopropenyl ketone) have been photolyzed in vacuum, but the temperatures for the photolyses of the two materials were quite different.<sup>5</sup> Wide variations in experimental conditions for the photodegradation of other polymers<sup>6</sup> makes further comparisons difficult.

As a companion to our investigation of PMMA, we have undertaken a study of the photodegradation of films of poly(methyl acrylate) (PMA) in air and in vacuum at room temperatures under irradiation by a low-

\* Presented in part at the 142nd meeting of the American Chemical Society, Atlantic City, N. J., September 1962.

pressure mercury source. PMA has been observed to crosslink during both radiolysis<sup>7</sup> and thermolysis,<sup>8</sup> whereas in PMMA crosslinking is usually absent during degradation except under special conditions such as photolysis in the presence of specific sensitizers.<sup>9</sup> An analog of PMA, poly(ethyl acrylate), has been found to undergo extensive crosslinking during photolysis.<sup>10</sup>

## EXPERIMENTAL

### Materials and Apparatus

PMA was prepared under helium by adding, over a period of 90 min., a solution of 0.166 g. of azobisisobutyronitrile in 132 g. of a freshly distilled and degassed heart cut of methyl acrylate to 320 g. of refluxing ethyl acetate. Refluxing was continued an additional hour. The polymer was isolated by pouring the mixture into methanol. After two reprecipitations from tetrahydrofuran solution with methanol, the material was dried in vacuum at room temperature. The yield of PMA was 68 g. The polymer had an intrinsic viscosity of 1.036 dl./g. in benzene at 30°C.

All solvents were spectroscopic or redistilled reagent grade materials. Tetrahydrofuran was treated with lithium aluminum hydride before distillation under nitrogen.

Ultraviolet spectra were measured with a Perkin-Elmer Spectracord Model 4000 recording spectrometer. Mass spectrometric analyses were carried out with a Consolidated Electrodynamics Model 21-620 mass spectrometer.

### Irradiation Cell, Source, and Actinometry

Films were exposed in a quartz irradiation cell similar to that described previously.<sup>1,2</sup> The radiation source was a Hanovia 93A-1 low-pressure mercury lamp which emits 88% of its energy at 2537 Å. Since longer wavelength radiation is not significantly absorbed by the PMA films used here, and energy emitted at shorter wavelengths (principally 1849 Å.) is absorbed by the quartz cell, the 2537 Å. radiation has been assumed to be the only photolytically active energy in this work. Wire screens were used to vary the incident intensity of the radiation. Actinometry was carried out by the ferrioxalate method<sup>11</sup> before each exposure.

### Viscosity Measurements

Intrinsic viscosities of the polymer samples before and after irradiation were determined in benzene solution at  $30 \pm 0.01^\circ\text{C}$ . by extrapolation of  $\eta_{sp}/c$  versus  $c$  plots to zero concentration. Huggins constants for both degraded and undegraded samples were the same within experimental error. Ubbelohde-type dilution viscometers having running times of about 170 sec. for benzene were used, and kinetic energy and shear cor-

reactions were not made. Number-average molecular weights were related to intrinsic viscosities by the equation of Sen and co-workers:<sup>12</sup>

$$[\eta] = 3.09 \times 10^{-5} \bar{M}_n^{0.72} \quad (1)$$

### Procedure

Approximately 50 cm.<sup>2</sup> films were prepared in flat rectangular quartz or Pyrex dishes by slow evaporation over a 24 hr. or longer period of a methylene chloride solution containing 200 mg. of PMA. After evaporation, most of the remaining solvent was removed at room temperature at 1 mm. pressure. For air exposures, the dish containing the film was irradiated in the cell with the top removed. The cell was evacuated (mercury diffusion pump) continuously for 24 hr. at room temperature and sealed off at  $10^{-5}$  mm. pressure in the vacuum runs. All runs were made at room temperatures,  $22 \pm 2^\circ\text{C}$ .

After irradiation, spectra of the degraded films were measured in air; in vacuum runs, the films were re-evacuated after each such measurement. Degraded films were dissolved in benzene for viscosity determinations. Insoluble material was removed by filtration and weight losses thus incurred were always less than 1% of the total sample. Volatile products condensable by liquid nitrogen were collected in a series of traps during successive periods of irradiation by the following procedure. The evacuated cell containing the film was heated for 6 hr. at  $80\text{--}85^\circ\text{C}$ . prior to irradiation to remove traces of volatiles. Products were trapped during a given irradiation period and a subsequent 3-hr. heating period, the trap was sealed off, and the process repeated with the same film. Longer heating periods or higher temperatures did not yield additional products.

Films having thicknesses within 10% of  $30 \mu$  were used. Over a thickness range of  $15\text{--}40 \mu$ , a constant absorbed dose per gram of polymer produced the same number of scissions per polymer molecule within experimental error. In both air and in vacuum, an absorbed dose of  $2 \times 10^{19}$  quanta/g. of polymer resulted in the same number of scissions whether the dose was absorbed in one interval or over a series of intervals interrupted by six 10-min. periods of darkness; to this extent, dark reactions were absent.

### RESULTS AND DISCUSSION

The apparent molecular weight changes based on a random scission process taking place in PMA films during photodegradation by 2537 Å. radiation in air and in vacuum are shown in Figures 1 and 2, respectively. In vacuum runs in which more than  $3 \times 10^{19}$  quanta/g. had been absorbed by the sample, crosslinking was indicated by the formation of benzene-insoluble material. In air exposures, no visible insoluble material was formed. However, a qualitative comparison of the sedimentation patterns of undegraded and degraded samples of PMA showed that crosslinking was occurring under either set of exposure conditions. This is in

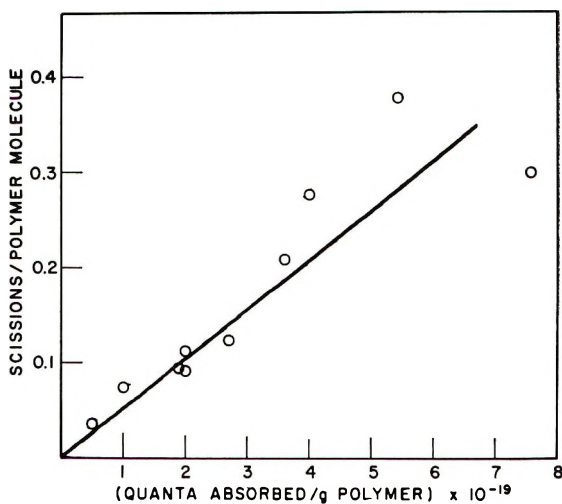


Fig. 1. Photodegradation of PMA in air.

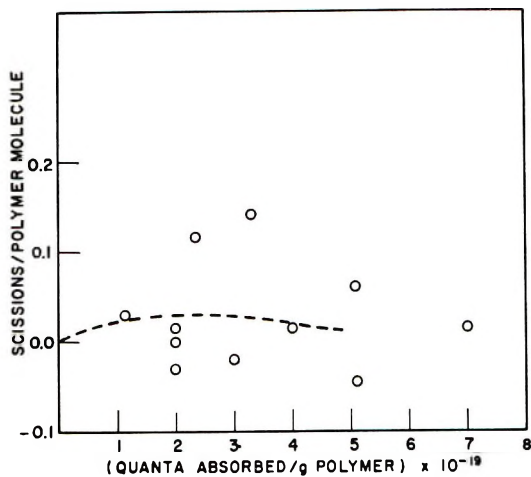


Fig. 2. Photodegradation of PMA in vacuum.

marked contrast to a similar comparison with PMMA, in which no crosslinking could be detected. Since PMMA and PMA possess the same ester groups and give rise to similar volatile products, it may be inferred that crosslinking in PMA occurs through radicals formed by abstraction of the tertiary hydrogen atoms along the polymer chain. This assumes similar molecular configurations for both polymers and the absence of any form of steric hindrance to crosslinking in PMMA. It is likely that in PMA gelation during air exposures is retarded by oxygen acting as a radical scavenger, the effect of which would be to inhibit crosslinking without affecting scission.



In contrast to the results with PMMA, molecular weight changes in photodegraded PMA cannot be assessed quantitatively on the basis of viscosity measurements. If no crosslinking occurred, apparent quantum yields for random chain scission,  $\Phi_s$ , could in principle be evaluated from Figures 1 and 2 by the equation

$$\Phi_s = (A/\bar{M}_{n_0}) [([\eta_0]/[\eta])^{1/\alpha} - 1]/I_{at} \quad (2)$$

where  $A$  is Avogadro's number and  $I_{at}$  is the number of quanta absorbed per gram of polymer. It has been assumed that the number of scissions per polymer molecule,  $(\bar{M}_{n_0}/\bar{M}_n) - 1$ , is equivalent to  $([\eta_0]/[\eta])^{1/\alpha} - 1$ , where the subscript zero refers to undegraded polymer and  $\alpha$  is the Mark-Houwink equation exponent, 0.72, in eq. (1). With an average value of 6.5% for the proportion of incident radiation absorbed by the film, the results for air exposures lead to  $\Phi_s = 0.013$  scissions per quantum absorbed. This should be regarded as a minimum value in view of the probable scavenging role played by oxygen. No evaluation of  $\Phi_s$  in vacuum can be made on the basis of the data plotted in Figure 2.

As in the case of PMMA,<sup>2</sup> the apparent number of scissions per PMA molecule in air was independent of the intensity of the incident radiation, as shown in Table I.

TABLE I  
Effect of Intensity on the Photolysis of PMA in Air

Rate of energy absorption $\times 10^{-16}$ , quanta/g./sec.	Absorbed energy $\times 10^{-19}$ , quanta/g.	Scissions/molecule
1.20	1.10	0.068
4.29	1.10	0.065
8.7	1.10	0.063

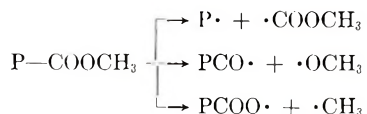
This is taken as evidence that the termination of polymer radicals is primarily through combination with small, relatively mobile, radicals in the vicinity of the chain break rather than through recombination of polymer radicals.

Spectral changes in PMA during photodegradation in both air and vacuum are shown in Figure 3 and are similar to those found in PMMA. The increased absorption in the region usually associated with the carbonyl chromophore again indicates the possible formation of aldehyde groups along the polymer chain, at least in the air exposures.

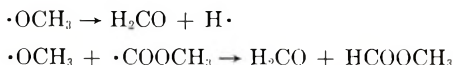
Since only liquid nitrogen-condensable volatile products were collected during the photolysis of PMA in vacuum, a complete analysis could not be made. The major products evolved and studied were formaldehyde, methanol, methyl formate, and carbon dioxide; carbon monoxide, methane, and hydrogen were also observed, but no quantitative collection was attempted. At no time was methyl acrylate detected. Depolymerization

absorbed by the sample. The results for carbon dioxide are entirely different. As seen in Figure 4, the amount of carbon dioxide formed increased exponentially with the number of quanta absorbed, indicating a first-order dependence on a species being formed in, but not removed from, the polymer film.

All of these products can be visualized as originating from the ester groups in the polymer. The possible major homolytic pathways are

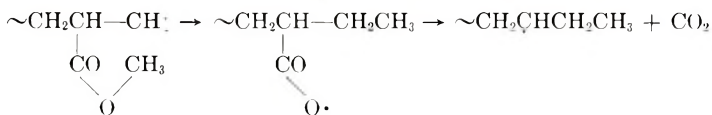


where P represents the polymer molecule. Combination of hydrogen atoms with the carbomethoxy and methoxy radicals would yield methyl formate and methanol, respectively. Formaldehyde may be a major product through one of the following reactions:



Although a quantitative analysis for methane was not carried out, the absence of dimethyl ether among the products is notable in view of the presence of methoxy radical-derived products.

Both carbon dioxide and carbon monoxide have been observed in the photolysis of methyl formate,<sup>13</sup> and carbon dioxide was a major product in the methyl radical-sensitized decomposition of this ester.<sup>14</sup> These types of reactions are insufficient to account for the observed rate of formation of carbon dioxide during the photolysis of PMA, however. It is suggested that most of the carbon dioxide is associated with the formation of chain ends through random scission, since the cumulative number of chain ends is increasing rapidly with time. An example of such a decomposition is



A similar six-membered ring "back-biting" reaction might also be envisioned. Such reactions, it will be noted, would not give rise to small molecules derived from methyl radicals. On the other hand, the decomposition of the acyloxy radical to carbon dioxide should be efficient<sup>15</sup> and relatively uncomplicated in such a viscous environment.<sup>16</sup>

The authors are indebted to Dr. T. F. Ford and Mr. Owen Nichols for the sedimentation pattern determinations.

## References

1. Stokes, S., and R. B. Fox, *J. Polymer Sci.*, **56**, 507 (1962).
2. Fox, R. B., L. G. Isaacs, and S. Stokes, *J. Polymer Sci.*, **A1**, 1079 (1963).
3. Jellinek, H. H. G., *Degradation of Vinyl Polymers*, Academic Press, New York, 1955.

4. Grassie, N., *Chemistry of High Polymer Degradation Processes*, Interscience, New York, 1956.
5. Wissbrun, K. F., *J. Am. Chem. Soc.*, **81**, 58 (1959).
6. Jellinek, H. H. G., *Pure Appl. Chem.*, **4**, 419 (1962).
7. Shultz, A. R., *J. Polymer Sci.*, **35**, 369 (1959).
8. Madorsky, S. L., and S. Straus, *J. Res. Natl. Bur. Std.*, **50**, 165 (1953).
9. Oster, G., G. K. Oster, and H. Moroson, *J. Polymer Sci.*, **34**, 671 (1959).
10. Jacobs, H., and R. Steele, *J. Appl. Polymer Sci.*, **3**, 239, 245 (1960).
11. Hatchard, C. G., and C. A. Parker, *Proc. Roy. Soc. (London)*, **A235**, 518 (1956).
12. Sen, J. N., S. R. Chatterjee, and S. R. Palit, *J. Sci. Ind. Res. (India)*, **11B**, 90 (1952).
13. Ausloos, P., *Can. J. Chem.*, **36**, 383 (1958); *J. Am. Chem. Soc.*, **80**, 1310 (1958).
14. Thynne, J. C. J., *Trans. Faraday Soc.*, **58**, 676 (1962).
15. Kharasch, M. S., J. L. Rowe, and W. H. Urry, *J. Org. Chem.*, **16**, 905 (1951).
16. Braun, W., L. Rajbenbach, and F. R. Eirich, *J. Phys. Chem.*, **66**, 1591 (1962).

### Résumé

On a dégradé à la lumière en présence d'air et sous vide par irradiation au moyen d'une source de mercure à faible pression des films minces de polyacrylate de méthyle à température de chambre. On a suivi des changements de viscosité intrinsèque, l'absorption ultraviolette et les produits volatils en fonction de l'énergie absorbée. Le pontage se produit aussi bien à l'air et sous vide, mais plus lentement à l'air. Le rendement quantique apparent de la rupture statistique à l'air est de 0.013 scissions par quantum absorbé. Dans l'air, les groupements carbonyles sont formés le long de la chaîne principale. La plupart des produits volatils semblent provenir des groupes esters du polymère; les formaldéhyde, méthanol et formiate de méthyle sont formés à une vitesse constante pour des doses atteignant au moins  $2 \times 10^{20}$  quantum par g. Le rendement quantique de chacun de ceux-ci est déterminé. L'anhydride carbonique est formé en quantités augmentant exponentiellement avec le dosage. On constate qualitativement des faibles quantités d'oxyde de carbone, de méthane et d'hydrogène, mais on n'observe pas de monomère. Un mécanisme compatible avec ces résultats est proposé.

### Zusammenfassung

Dünne Polymethylacrylatfilme wurden bei Raumtemperatur in Luft und im Vakuum durch Bestrahlung mit einer Niederdruck-Quecksilberlampe photochemisch abgebaut. Die Veränderung der Grundviskosität, der UV-Absorption und der flüchtigen Produkte wurden in Abhängigkeit von der absorbierten Energie untersucht. Sowohl in Luft als auch im Vakuum tritt Vernetzung auf, in Luft jedoch mit kleinerer Geschwindigkeit. Die scheinbare Quantenausbeute für die statistische Spaltung war in Luft 0,013 Spaltungen pro absorbiertes Quant. In Luft werden längs der Hauptkette Carbonylgruppen gebildet. Die meisten der untersuchten flüchtigen Produkte scheinen aus den Estergruppen des Polymeren zu entstehen. Bis hinauf zu Dosen von wenigstens  $2 \cdot 10^{20}$  Quanten pro Gramm war die Bildungsgeschwindigkeit von Formaldehyd, Methanol und Methylformiat konstant; für jede dieser Substanzen wurde die Quantenausbeute bestimmt. Die gebildete Kohlendioxidmenge nahm exponentiell mit der Dosis zu. Kleine Mengen von Kohlenmonoxid, Methan und Wasserstoff wurden qualitativ nachgewiesen, dagegen wurde kein Monomeres gefunden. Ein mit diesen Befunden übereinstimmender Mechanismus wird vorgeschlagen.

Received March 11, 1963

## Intramolecular Hydride Shift Polymerization by Cationic Mechanism. II. Spectroscopic Analysis of Poly-3-methylbutene-1

J. P. KENNEDY, L. S. MINCKLER, JR., G. WANLESS,  
and R. M. THOMAS, *Chemicals Research Division, Esso Research  
and Engineering Company, Linden, New Jersey*

### Synopsis

The structures of cationically obtained poly-3-methylbutene-1, isotactic poly-3-methylbutene-1, and hydrogenated 3,4-polyisoprene have been investigated by nuclear magnetic resonance and infrared spectroscopy. These studies corroborate the previously proposed structure of an  $\alpha, \alpha'$ -dimethylpropane repeating unit for the cationic polymer and they confirm the conventional 1,2 head-to-tail enchainment for the isotactic polymer and for the hydrogenated 3,4-polyisoprene. The NMR spectra of cationic poly-3-methylbutene-1 and polyisoprene are very similar and show only two peaks. They are quite different from the spectra of isotactic poly-3-methylbutene-1 and hydrogenated 3,4-polyisoprene. The isotactic product was solubilized by careful pyrolysis to render it amenable to spectroscopic studies. Unfortunately, present-day NMR spectroscopy does not possess high enough resolution to be useful in the quantitative investigation of mixtures of 1,3 and 1,2 enchainments. The NMR spectrum of polyisobutylene oxide can be used to distinguish cationic poly-3-methylbutene-1 from the isotactic modification and from the hydrogenated 3,4-polyisoprene. The more important bands have been analyzed and assigned. Isotactic poly-3-methylbutene-1 and hydrogenated 3,4-polyisoprene both have a conventional 1,2 structure, and their infrared spectra are essentially identical.

### I. INTRODUCTION

In the first paper of this series we discussed a thoroughly documented case of an intramolecular hydride shift polymerization.<sup>1</sup> This resulted when 3-methylbutene-1 was polymerized cationically at low temperatures. Structure analysis of the product revealed an unusual repeat unit, viz.,  $\alpha, \alpha'$ -dimethylpropane, which was explained by postulating the intramolecular hydride migration polymerization. Our conclusions were based on results obtained by careful pyrolysis combined with fragment analysis using gas chromatography, infrared spectroscopy, and mass spectroscopic studies.

At this time we report further results from nuclear magnetic resonance, infrared, and x-ray diffraction studies. These findings are in agreement with earlier conclusions. They substantiate the proposed unusual struc-

ture of cationically obtained poly-3-methylbutene-1 and the concept of intramolecular hydride shift polymerization.

## II. EXPERIMENTAL

### A. Polymerizations

The source and purity of materials used has been reported.<sup>1</sup> 3-Methylbutene-1 was polymerized at  $-96^{\circ}\text{C}$ . in methyl chloride diluent with aluminum chloride catalyst dissolved in methyl chloride. Amorphous, rubbery poly-3-methylbutene-1 was thereby obtained. Isotactic polymer was prepared by using an alkyl metal transition halide catalyst system (Ziegler-Natta type). The synthesis of hydrogenated 3,4-polyisoprene has been described.<sup>1</sup> Polyisobutylene oxide was obtained by polymerizing isobutylene oxide monomer with titanium tetrachloride.<sup>2</sup> Isobutylene oxide was obtained from Farchen Research Laboratories. Gas chromatographic analysis indicated that the material was 96.4% pure; nine impurities were present; the nature of impurities was not defined except that every one of them were isomers of isobutylene oxide (mol. wt. 72).

### B. Analytical Techniques

The NMR spectra were obtained with a 60 A Varian NMR spectrometer at 60 Mcycles. Tetrachloroethylene was used as solvent.

The infrared spectra were obtained on a Baird Model 4-55 instrument. With one exception, all scans were made on film cast on a NaCl window from  $\text{CS}_2$  solution, followed by solvent evaporation. The isotactic poly-3-methylbutene-1 sample, being insoluble, was prepared as a hot pressed film.

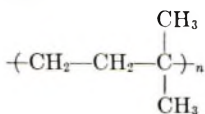
## III. RESULTS AND DISCUSSION

### A. NMR Spectroscopic Studies

The NMR spectra of polyisobutene and various poly-3-methylbutene-1 samples have been compared. Figures 1 and 2 show results for polyisobutene and poly-3-methylbutene-1, respectively. Both samples were obtained by low temperature cationic polymerization technique (e.g.,  $\text{AlCl}_3$  catalyst in methyl chloride at  $-96^{\circ}\text{C}$ .).

Qualitatively these spectra are quite similar. Both show only two sharp peaks, one at higher field representing *gem*-dimethyl hydrogens, and another at lower field due to methylene hydrogens.

Based on this similarity and other qualitative considerations, Edwards and Chamberlain<sup>3</sup> concluded that cationic poly-3-methylbutene-1 consists exclusively of 1,3 structure, e.g.,





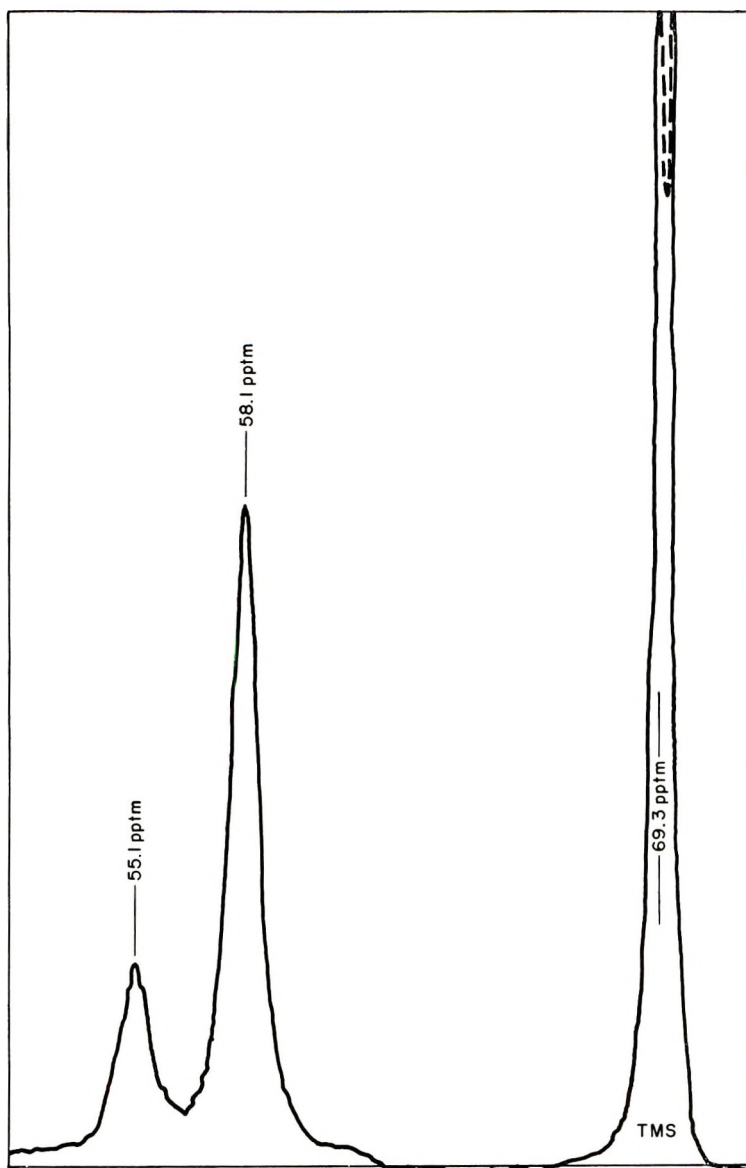
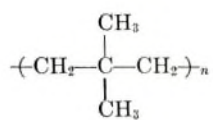


Fig. 1. Polyisobutylene: 60 Mcycle NMR spectrum. TMS denotes the tetramethylsilane reference spike.

Another view is to regard the polymer as a succession of "neopentyl" groups, e.g.,



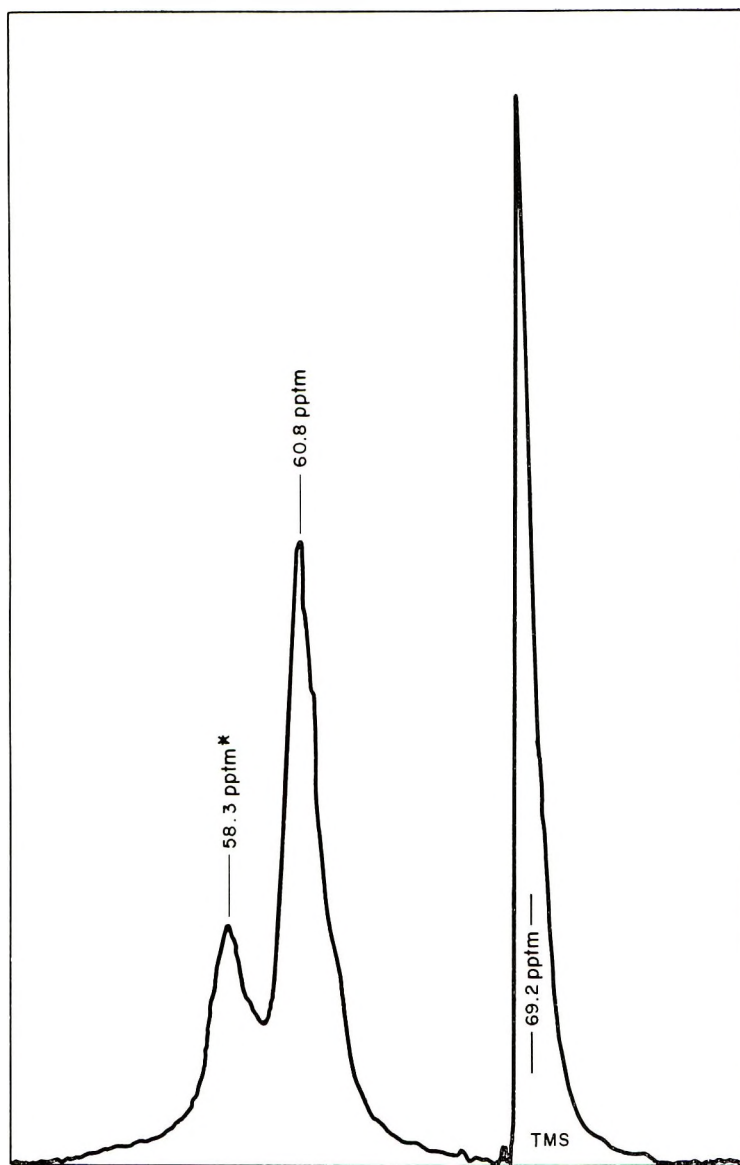
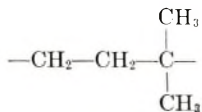
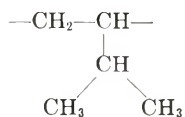


Fig. 2. Cationic poly-3-methylbutene-1: 60 Mcycle NMR spectrum; pptm\* denotes parts per 10 million measured from benzene.

A detailed quantitative analysis of these spectra has indicated that the situation is far from being simple, and that present-day NMR spectra are not well enough resolved to be used to decide whether cationic poly-3-methylbutene-1 represents exclusively a 1,3 structure,



or mixtures of 1,3 and 1,2 structures,



Study of these mixtures is impeded by the fact that the tertiary hydrogens are not clearly resolved. At best one can consider only the ratio of  $\text{CH}_3/\text{CH}_2 + \text{CH}$  protons. This makes it impossible to distinguish at present between mixtures of the unusual 1,3 and the conventional 1,2 structures by NMR spectroscopy.

If cationic poly-3-methylbutene-1 were, in fact, exclusively of the 1,3 type, the NMR spectrum would consist of two peaks corresponding to 6-methyl and 4-methylene hydrogens. Consequently, the area ratio of these peaks should then correspond to 1.5. On the other hand, if the true structure were of the conventional 1,2 type, a more complicated spectrum would be expected due to the presence of three kinds of protons.

Several samples of cationic poly(3-methyl butene-1) prepared at  $-96^\circ\text{C}$ . have been examined by NMR spectroscopy, and the ratio  $\text{CH}_3/(\text{CH}_2 + \text{CH})$  was determined. It was found that the area ratio varied between 1.78 and 2.09 (average 2.0). No completely satisfactory explanation of this can be given at present, but it may be due to difficulty in making the "split" between the methyl hydrogen peak area and that of the (methylene + methine) hydrogens.

Notwithstanding this difficulty, it is of significance that it has been possible to shift this ratio of  $\text{CH}_3/(\text{CH}_2 + \text{CH})$  by employing more extreme polymerization conditions (e.g., working at  $-130^\circ\text{C}$ ). Such products have given the expected NMR area ratio of 1.5. Also these low temperature products are crystalline as judged by their x-ray diffraction patterns in contrast to polymers obtained at  $-96^\circ\text{C}$ .<sup>4</sup> We believe that crystalline cationically obtained poly-3-methylbutene-1 represents the closest approach so far to pure 1,3 structure.

As for the other samples made at  $-96^\circ\text{C}$ ., we regard them as mixtures of about 70% 1,3 and 30% 1,2 structure based on independent analytical studies reported earlier.<sup>1</sup>

It has been pointed out already<sup>1</sup> that no authentic polymer structure exists with a *bona fide* 1,3 enchainment which would correspond to the structure of cationic poly-3-methylbutene-1. Consequently the NMR spectra in Figure 2 cannot be corroborated directly. However, for comparison, the NMR spectra of two polymers having authentic 1,2 structures can be examined.

Thus a crystalline isotactic polymer having a conventional *bona fide* 1,2 enchainment was obtained with an alkyl metal coordination catalyst of the Ziegler-Natta type. The isotactic polymer is insoluble in solvents suitable for NMR examination, but it has been solubilized by conversion to a heavy oil through vacuum pyrolysis.<sup>1</sup> This is reasonably satisfactory

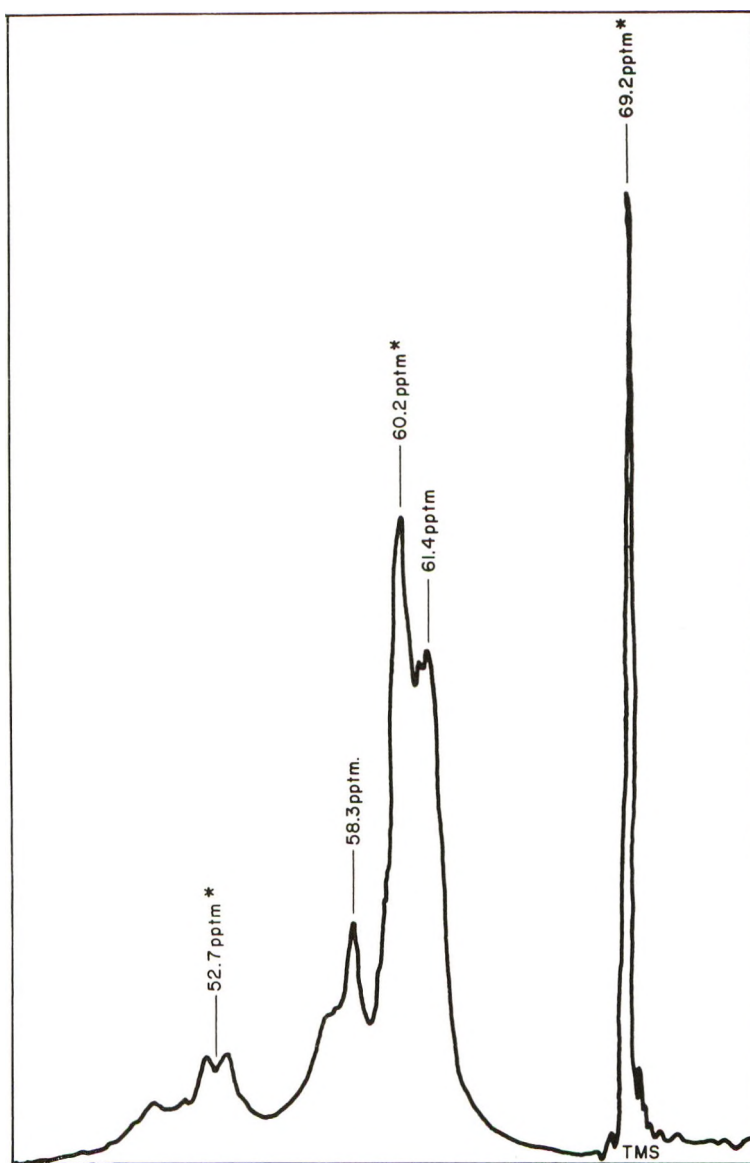


Fig. 3. Ziegler-Natta poly-3-methylbutene-1 (polymer converted to a heavy oil by vacuum pyrolysis): 60 Mcycle NMR spectrum.

from an NMR standpoint, since the amount of double-bond hydrogens introduced into the spectra is not more than 6% of the total hydrogens. Figure 3 shows the NMR spectrum of pyrolyzed, soluble Ziegler-Natta type poly-3-methylbutene-1.

Another approach is to obtain a conventional 1,2 structure by first polymerizing isoprene selectively through the 3-4 double bond and subsequently hydrogenating the pendant isopropenyl groups.<sup>1</sup> (The inter-

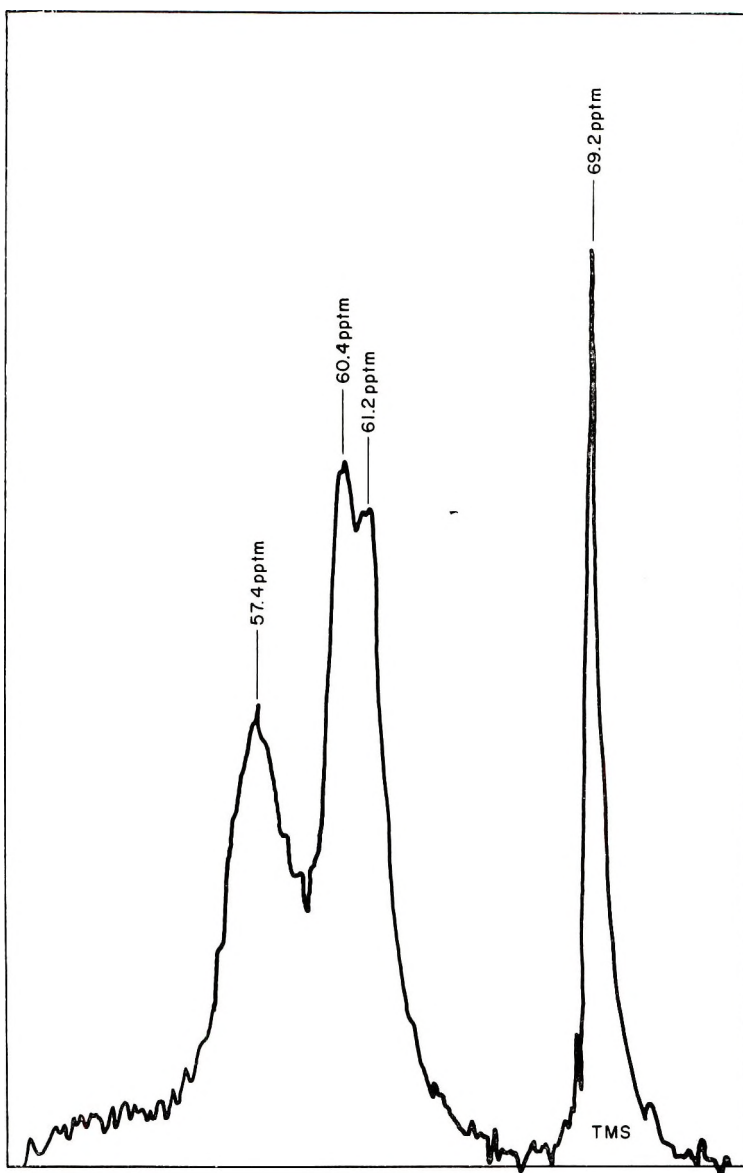


Fig. 4. Hydrogenated 3,4-polyisoprene (Wilke-type catalyst) (not depolymerized): 60 Mcycle NMR spectrum.

mediary 3,4-polyisoprene showed a predominant infrared band for an isopropenyl group at  $11.29 \mu$ , indicating better than 95% of 3,4 enchainment.) Figure 4 shows the NMR spectrum of this amorphous, soluble (tetrachloroethylene) polymer.

The NMR spectra of Figures 3 and 4 are significantly different than those of Figures 1 and 2 for polyisobutylene and cationic poly-3-methylbutene-1.



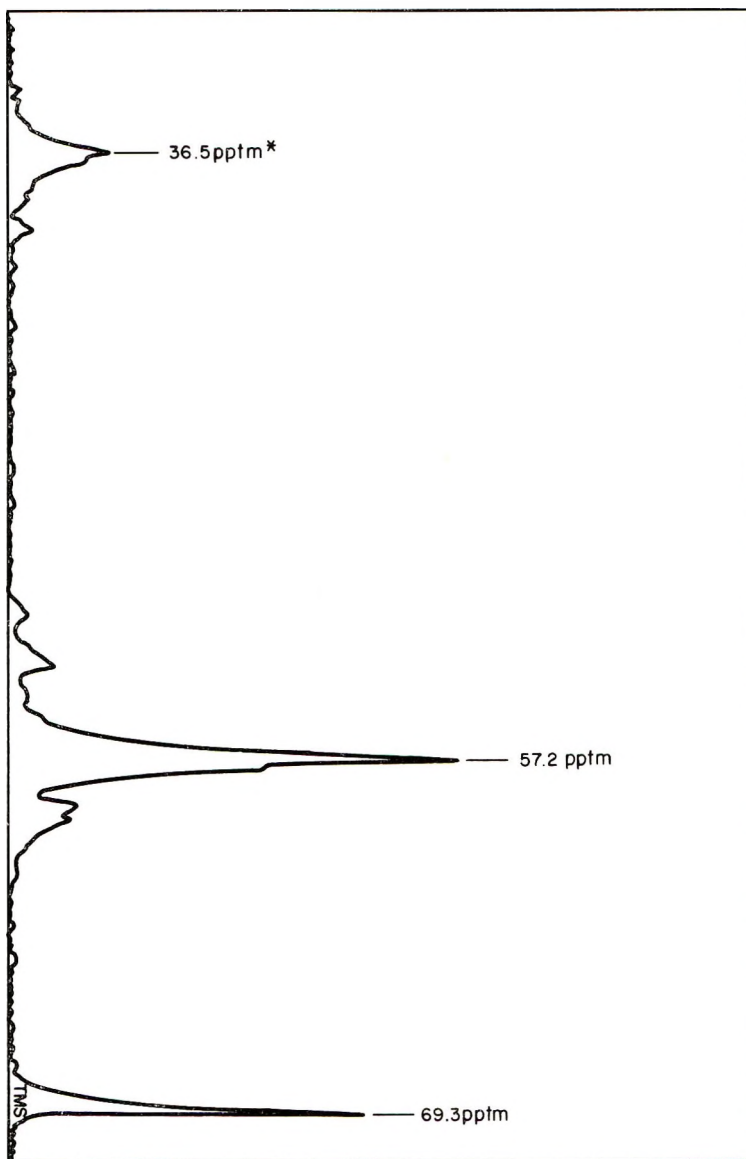


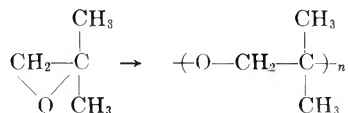
Fig. 5. Poly(isobutylene oxide): 60 Mcycle spectrum NMR.

The 1,2 structures possess a doublet which is characteristic of an isopropyl group, and which is due to the interaction of methyl and methine hydrogens ( $60.3 \pm 0.1$  and  $61.3 \pm 0.1$  pptm. measured from benzene). The 1,3 structure (Fig. 2) and polyisobutylene (Fig. 1) possess a singlet methyl peak which is consistent with a *gem*-dimethyl structure.

There may be some unexplained differences in fine structure between the polymers represented by Figures 3 and 4, but based on studies of vacuum

pyrolysis gas data and infrared studies,<sup>1</sup> these possible differences do not seem to be associated with the isopropyl group in hydrogenated-3,4-polyisoprene.

One further effort was made to provide a reference polymer which should possess some of the structural features of the 1,3 type cationic poly-3-methylbutene-1. Thus the oxygen homolog of this macromolecule was obtained by polymerizing isobutylene oxide:<sup>2</sup>



The NMR spectrum of this product (Fig. 5) resembles Figures 1 or 2 for polyisobutylene and poly-3-methylbutene-1. All three polymers contain the singlet methyl peak. In Figure 5 the bands are found at 57.2 and 36.5 pptm., and are assigned to *gem*-dimethyl hydrogens and methylene hydrogens, respectively. In this case the well resolved peaks approach the expected area ratios of 3.0 corresponding to 6-methyl and 2-methylene hydrogens. (As judged from the spectrum about 5% of an unidentified structure is present also.)

### B. Infrared Spectroscopic Studies

The infrared spectra of cationically obtained and isotactic poly-3-methylbutene-1 samples as well as hydrogenated 3,4-polyisoprene specimens have been analyzed (Figs. 6-8). In addition Figures 9 and 10 show the spectrum of polyisobutylene and polyisobutylene oxide, respectively, which will also be discussed.

All the polymers examined showed the characteristic carbon-hydrogen stretching vibration in the region between 3000 and 2700  $\text{cm}^{-1}$ ; but, without high resolution, this region did not reveal features useful for distinguishing between structures. Neither was the region from 2700 to 1500  $\text{cm}^{-1}$  revealing, since it is relatively transparent in saturated hydrocarbons. The only significant absorption was noted at 1718  $\text{cm}^{-1}$  in hydrogenated 3,4-polyisoprene. Similarly, a weak band appeared at 1681  $\text{cm}^{-1}$  in isotactic poly-3-methylbutene-1. No assignment is made; however, it may be the result of a combination of frequencies. A similar band is observed in a number of related hydrocarbon molecules.

For each polymer the  $\text{CH}_2$  and  $\text{CH}_3$  hydrogen bending vibrations were found at their assigned frequencies<sup>5</sup> at about 1470 and 1455  $\text{cm}^{-1}$ , respectively. The asymmetrical  $\text{CH}_3$  bending vibration appeared as a shoulder on the  $\text{CH}_2$  bending band. No distinguishing features were expected in this region.

The region of significant qualitative differences begins with the symmetrical  $\text{CH}_3$  hydrogen deformation frequencies. The characteristic splitting of the symmetrical  $\text{CH}_3$  deformation band, which occurs whenever two or more methyl groups are attached to the same carbon atom,<sup>5-11</sup> was

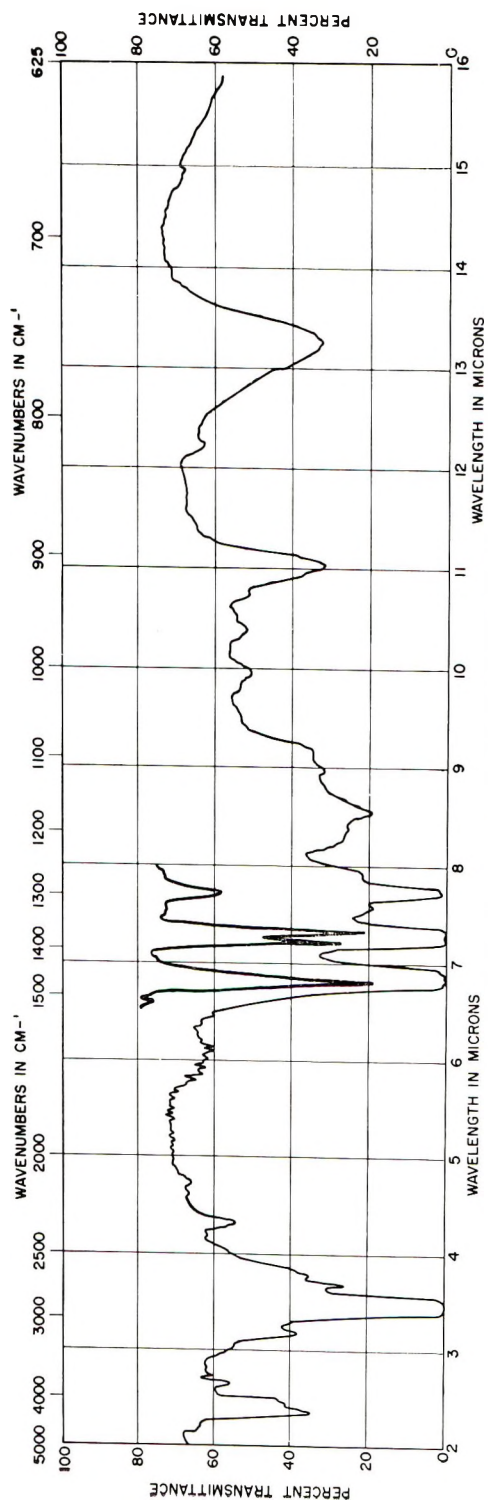


Fig. 6. Infrared spectrum of cationic poly-3-methylbutene-1.

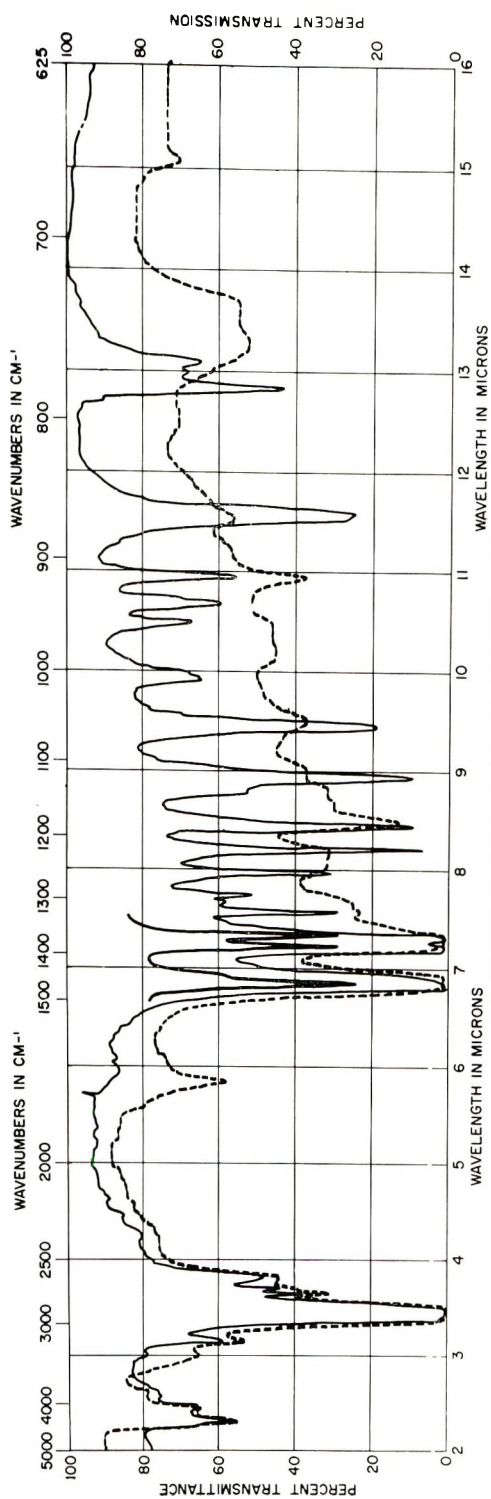


Fig. 7. Infrared spectrum of isotactic poly-3-methylbutene-1.

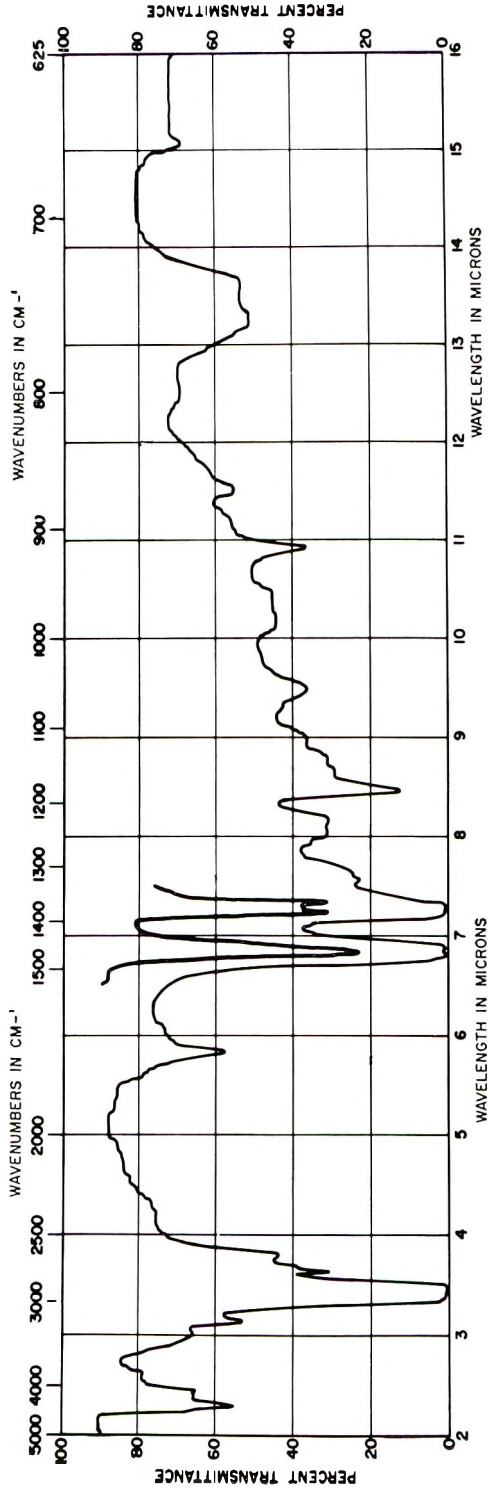


Fig. 8. Infrared spectrum of hydrogenated 3,4-polyisoprene.



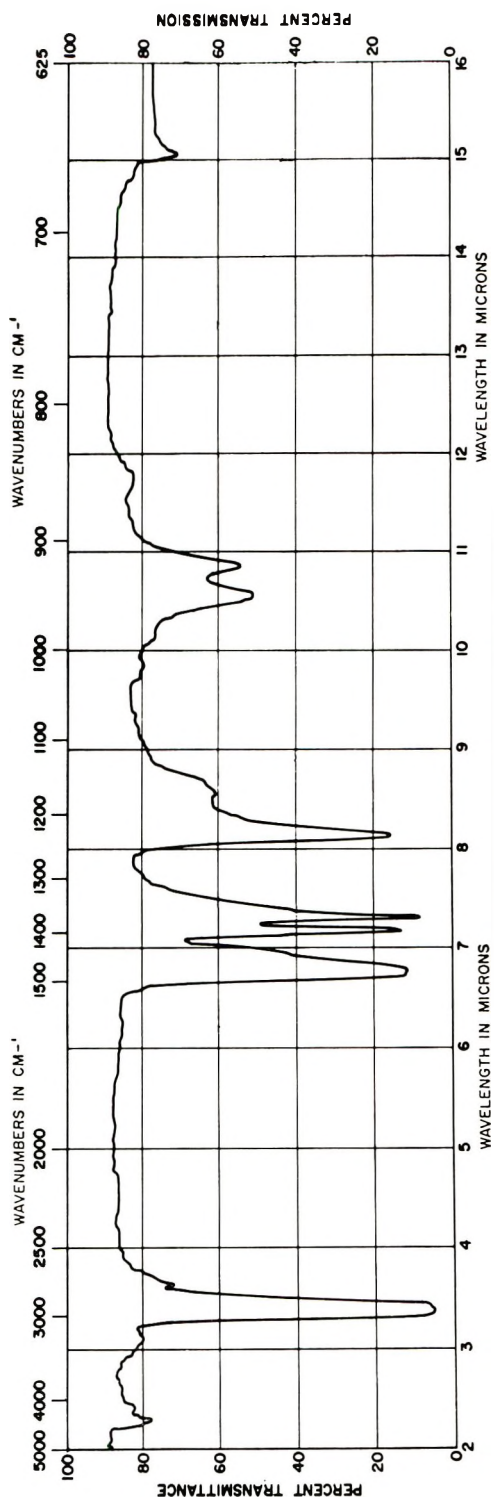


Fig. 9. Infrared spectrum of polyisobutene.

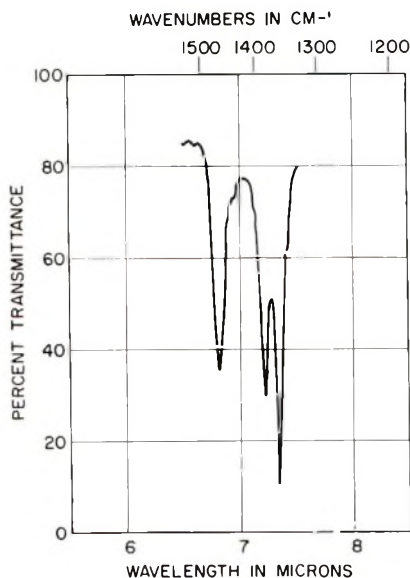


Fig. 10. Infrared spectrum of poly(isobutene oxide).

easily recognized. The spectra of isotactic poly-3-methylbutene-1 and hydrogenated 3,4-polyisoprene showed approximately equal intensities at 1388 and 1370  $\text{cm.}^{-1}$ , indicating the presence of isopropyl groups. In contrast, the intensity of the first band (1379  $\text{cm.}^{-1}$ ) in cationic poly-3-methylbutene-1 was found to be less than the second (1359  $\text{cm.}^{-1}$ ), possibly a feature of the *gem*-dimethyl structure. This may be partially supported by the fact that the first  $\text{CH}_3$  vibration of a tertiary butyl group is about half the intensity of the second. The latter correlation has been reported,<sup>5</sup> together with a statement that the split  $(\text{CH}_3)_2\text{CH}-$  and  $(\text{CH}_3)_2\text{CR}-$  bands are of about equal intensity. Our observations indicate that an imbalance of intensities may also be characteristic of a *gem*-dimethyl group. The spectra of at least two other such polymers, polyisobutylene and polyisobutylene oxide,<sup>2</sup> as well as 1,1-dimethylcyclohexane, support this conclusion. In these examples interference from other  $\text{CH}_3$  vibrations is excluded. On the other hand, the split methyl bands of polyisobutylene and polyisobutylene oxide showed a greater difference in intensity than did those of cationic poly-3-methylbutene-1. This may be attributed to isopropyl groups which result from a small amount of 1,2 polymerization in a predominantly 1,3-system. Alternately, it may be associated with interactions due to the relative proximity of the *gem*-dimethyl groups or oxygen functionality.

The CH (tertiary) bending vibration for isotactic poly-3-methylbutene-1 and hydrogenated 3,4-polyisoprene should be close to 1340  $\text{cm.}^{-1}$ ; however, this band is not sufficiently intense to be easily located. In the presence of intense  $\text{CH}_3$  deformation vibrations the CH vibration is obscured.<sup>11</sup>

The prominent band at  $1297\text{ cm.}^{-1}$  in the cationic polymer is an important distinguishing feature which is not matched in intensity by any similar band in the isotactic product and in hydrogenated polyisoprene. We have assigned this frequency to the  $-\text{CH}_2\text{CH}_2-$  group which can occur only in the proposed  $\alpha,\alpha'$ -dimethylpropane type structure. This is consistent with numerous examples of multiple methylene group absorption in this area. The assignments for the  $\text{CH}_2$  wagging and twisting modes have been made in this region,<sup>8,9,11-17</sup> which suggest a similar assignment here. Specifically, the  $1299\text{ cm.}^{-1}$  frequency of *n*-butane has been assigned to the  $\text{CH}_2$  twisting mode,<sup>8,12,15</sup> although Tschamler<sup>17</sup> prefers the wagging mode. Others<sup>16</sup> suggest mixing of the two modes in this region. Additional support for the  $1297\text{ cm.}^{-1}$  assignment is evidenced by the presence of corresponding bands in 2,2,5,5-tetramethylhexane and 2,5-dimethylhexane, the former being most prominent. This may suggest that adjacent quaternary structures enhance the  $-\text{CH}_2\text{CH}_2-$  absorption. Finally, there are no comparable bands in 2,2,4,4-tetramethylpentane, 2,4-dimethylpentane, and polyisobutylene.

Sheppard and Simpson<sup>11</sup> have reported that the *gem*-dimethyl group and, in general, the internal quaternary carbon structure give a skeletal vibration at  $1195\text{ cm.}^{-1}$ . They also indicate that a second frequency near  $1210\text{ cm.}^{-1}$  may be active in some cases. This correlation may not be flexible enough in its application to polymers, in view of polyisobutylene's absorption at  $1168$  and  $1230\text{ cm.}^{-1}$ , respectively. The second band is quite strong. The band corresponding to the  $1168\text{ cm.}^{-1}$  polyisobutylene frequency appears at  $1166\text{ cm.}^{-1}$  in cationic poly-3-methylbutene-1, but only a shoulder is indicated in the  $1200\text{ cm.}^{-1}$  region.

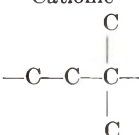
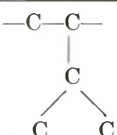
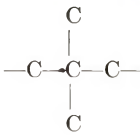
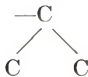
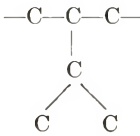
Relative to this discussion, we have found that polymers of the type  $-\text{[CH}_2\text{C(CH}_3\text{)R]}_n-$  also have bands (shoulders) at  $1168\text{ cm.}^{-1}$ . The way in which R influences the higher frequency is shown in Table I. It seems reasonable that the  $1230\text{ cm.}^{-1}$  frequency of polyisobutylene results from a shift in the reported  $1195\text{ cm.}^{-1}$  frequency. It should therefore correspond to the characteristic internal quaternary carbon frequency. It may be significant that this shift is toward a region assigned to the tertiary butyl group.

The fact that the  $1195\text{ cm.}^{-1}$  band is missing (or weak) in the cationic polymer may be related to the degree of separation, or the nature of the separating units between quaternary carbon atoms. It may be relevant that this band is either missing or has shifted considerably in polyisobutylene oxide.

TABLE I

R	Frequency, $\text{cm.}^{-1}$
$\text{CH}_3-$	1230
$\text{CH}_3\text{CH}_2-$	1198
$\text{CH}_3\text{CH}_2\text{CH}_2-$	1195

TABLE II  
 Summary of Infrared Findings<sup>a</sup>

Frequency, cm. <sup>-1</sup>	Group assignment	Cationic 	Hydrogenated polyisoprene	
			Isotactic 	
1297, 752	—CH <sub>2</sub> —CH <sub>2</sub> —	m, s	—	—
1199, 1087 931, 905		w, vw, vw, m	—	—
1185, 956		—	m, w	m, w
1112, 1057 916		—	m, m, w	vw, w, w

<sup>a</sup> vw = very weak; w = weak; m = medium; s = strong.

It now appears that the 1168 cm.<sup>-1</sup> absorption is associated with the quaternary carbon structure. However, this frequency is generally assigned to an isopropyl skeletal vibration. Inasmuch as some 1,2 polymerization may have occurred in the cationic product, this band may also have an isopropyl component, although it is not resolved. Both isotactic poly-3-methylbutene-1 and hydrogenated polyisoprene exhibit a frequency at 1185 cm.<sup>-1</sup>, which must be assigned to the isopropyl group. This, too, is abnormal, since 1175–1165 cm.<sup>-1</sup> is the reported isopropyl assignment.<sup>5,11</sup>

The infrared region between 1170 and 900 cm.<sup>-1</sup> is complex, but the observed frequencies are generally in agreement with assigned structures.<sup>5,10,11</sup> The band at 906 cm.<sup>-1</sup> in the cationic polymer, for example, is characteristic of the *gem*-dimethyl structure, while bands at 915 cm.<sup>-1</sup> in the isotactic modification and in the hydrogenated polyisoprene result from two adjacent tertiary carbon atoms. Polyisobutylene again deviates from assigned frequencies by absorbing at 925 cm.<sup>-1</sup>, which is more characteristic of a tertiary butyl group.

The methylene rocking frequency of the cationic polymer occurs as a strong band at 754 cm.<sup>-1</sup> which is characteristic of the —CH<sub>2</sub>CH<sub>2</sub>— group.<sup>5,9,10,14</sup> Related compounds with similar groups and frequencies are 2,2,5,5-tetramethylhexane (755 cm.<sup>-1</sup>) and 2,5-dimethylhexane (753

TABLE III  
Infrared Frequency Assignments for Cationic Poly-3-methylbutene-1

$\lambda$	Frequency, cm. <sup>-1</sup>	Intensity <sup>a</sup>	Structural assignments
2.35	4255	w	
3.17	3155	w	
3.37-3.46	2965-2890	vs	C-H hydrogen stretching —CH, —CH <sub>2</sub> , CH <sub>3</sub>
3.71	2695	w	
3.81	2625	vw	
6.81	1468	s	CH <sub>2</sub> hydrogen bending modes
6.88	1453	s (sh)	CH <sub>3</sub> Asym. hydrogen bending modes
7.25	1379	s	CH <sub>3</sub> Sym. hydrogen bending modes
7.36	1359	s	CH <sub>3</sub> Sym. hydrogen bending modes
7.57	1321	vw (sh)	
7.71	1297	m	—CH <sub>2</sub> CH <sub>2</sub> — twisting (or wagging) vibration
7.94	1259	vw (sh)	
8.34	1199	w (sh)	Internal quaternary carbon atom
8.58	1166	mw	Internal quaternary carbon atom and/or isopropyl
8.96	1116	vw	
9.20	1087	vw	Internal quaternary carbon atom
9.97	1003	w	(appears in 2,2,5,5-tetramethylhexane)
10.39	963	vw	(an isopropyl region)
10.74	931	vw	Internal quaternary carbon atom
11.06	905	m	Internal quaternary carbon atom
12.25	817	vw	(an isopropyl region)
13.30	752	s	—CH <sub>2</sub> CH <sub>2</sub> — skeletal rocking mode
15.00	667	vw	

<sup>a</sup> vw = very weak; w = weak; m = medium; ms = medium strong; s = strong; (sh) = shoulder.

cm.<sup>-1</sup>). Where more than two methylene groups appear in series, the frequency shifts to about 725 cm.<sup>-1</sup>, while a single methylene group generally absorbs at about 770 cm.<sup>-1</sup>. Consistent with this assignment, bands appear at 771 and 766 cm.<sup>-1</sup> in the isotactic product. The spectra of hydrogenated polyisoprene is more complicated in this region, which is not surprising in view of its structure and physical state. It has weak bands at 771 and 765 cm.<sup>-1</sup>, but also absorbs at 755 and 735 cm.<sup>-1</sup>.

The salient results of the infrared studies are summarized in Table II. Although it is not presently possible to completely assign all the infrared bands of the three polymeric samples investigated, they are listed and partially assigned in Tables III and IV. This qualitative treatment seems adequate to distinguish the structure of cationically obtained poly-3-methylbutene-1 from that of the isotactic modification or from the hydrogenated 3,4-polyisoprene. It is also apparent that by infrared spectroscopy the structures of isotactic poly-3-methylbutene-1 and hydrogenated 3,4-polyisoprene are essentially identical. The differences in sharpness and in several of the frequency locations was expected in view of the highly crystal-



TABLE IV  
Infrared Frequency Assignments for Isotactic Poly-3-methylbutene-1 and Hydrogenated 3,4-Polyisoprene

Isotactic poly-3-methylbutene-1			Hydrogenated 3,4-polyisoprene			Structural assignments
$\lambda$	Frequency, cm. <sup>-1</sup>	Intensity <sup>a</sup>	$\lambda$	Frequency, cm. <sup>-1</sup>	Intensity <sup>a</sup>	
2.30	4350	w	2.30	4350	w	
2.45	4080	w	2.45	4080	w	
2.61	3830	vw	2.61	3830	vw	
3.00	3330	vw	3.00	3330	vw	
3.16	3165	w	3.16	3165	w	
3.35-3.48	2985-2875	vs	3.35-3.48	2985-2875	vs	CH hydrogen stretching —CH, CH <sub>2</sub> & CH <sub>3</sub>
3.63	2755	w	3.63	2755	w	
3.68	2715	w (sh)	3.68	2715	vw	
3.81	2625	w	3.81	2625	w	
5.95	1681	vw	5.82	1718	w	
6.80	1470	s	6.80	1470	s	CH <sub>2</sub> Hydrogen bending mode
6.87	1455	s (sh)	6.87	1455	s (sh)	CH <sub>3</sub> Asym. hydrogen bending mode
7.20	1388	s	7.20	1388	s	CH <sub>3</sub> Sym. hydrogen bending mode
—	—	—	7.25	1379	w	CH <sub>3</sub> sym. hydrogen bending mode
7.30	1370	s	7.30	1370	s	CH <sub>3</sub> Sym. hydrogen bending mode
7.56	1323	w	7.56	1323	vw	
7.65	1307	vw	7.65	1307	vw (sh)	

7.73	1294	vw	7.73	1294	vw (sh)	
7.88	1269	vw (sh)	7.90	1266	vw (sh)	
7.95	1258	w	7.97	1255	w	
8.20	1220	ms	8.19	1221	w	
8.44	1185	ms	8.44	1185	ms	Isopropyl
8.76	1142	w (sh)	8.65	1155	vw (sh)	Isopropyl or tertiary carbon atoms
—	—	—	8.81	1135	vw (sh)	Isopropyl or tertiary carbon atoms
8.93	1120	ms	8.99	1112	vw	Adjacent tertiary carbon atoms
9.44	1059	m	9.46	1057	w	Adjacent tertiary carbon atoms
9.91	1009	w	10.15	985	w	
10.46	956	w	10.46	956	w	Isopropyl
10.65	939	w	—	—	—	
10.93	915	w	10.92	916	w	Adjacent tertiary carbon atoms
11.54	866	ms	11.50	870	w	Internal tertiary carbon atoms
12.81	781	w	—	—	—	Isopropyl
12.97	771	w	12.97	771	vw (sh)	Single methylene rocking mode and adjacent tertiary carbon atom
13.06	766	vw	13.07	765	vw (sh)	Single methylene rocking mode and adjacent tertiary carbon atom
—	—	—	13.24	755	w	
—	—	—	13.61	735	w	
14.96	669	vw	15.02	666	vw	

<sup>a</sup> vw = very weak; w = weak; m = medium; ms = medium strong; s = strong; (sh) = shoulder.

line state of the isotactic polymer relative to amorphous hydrogenated 3,4-polyisoprene.

### References

1. Kennedy, J. P., L. S. Minckler, Jr., G. G. Wanless, and R. M. Thomas, *J. Polymer Sci.*, **A2**, 1441 (1964).
2. Ishida, S., *Bull. Chem. Soc. Japan*, **33**, 924 (1960).
3. Edwards, W. R., and N. F. Chamberlain, paper presented at the 142nd Meeting of the American Chemical Society, Atlantic City, September 1962.
4. Kennedy, J. P., and R. M. Thomas, *Makromol. Chem.*, **53**, 28 (1962).
5. Bellamy, L. J., *The Infrared Spectra of Complex Molecules*, Wiley, New York 1958, Chap. 2.
6. Barnes, R. B., R. C. Gore, U. Liddel, and V. Z. Williams, *Infrared Spectroscopy*, Reinhold, New York, 1944.
7. Thompson, H. W., and P. Torkington, *Proc. Roy. Soc. (London)*, **A184**, 3 (1945).
8. Rasmussen, R. S., *J. Chem. Phys.*, **16**, 712 (1948).
9. Sheppard, N., *J. Inst. Petrol.*, **37**, 95 (1951).
10. McMurry, H. L., and V. Thornton, *Anal. Chem.*, **24**, 318 (1952).
11. Sheppard, N., and D. M. Simpson, *Quart. Rev.*, **7**, 19 (1953).
12. Stepanov, B. I., *Acta Physicochim.*, **22**, 238 (1947).
13. Axford, D. W. E., and D. H. Rank, *J. Chem. Phys.*, **17**, 430 (1949).
14. Axford, D. W. E., and D. H. Rank, *J. Chem. Phys.*, **18**, 51 (1950).
15. Brown, J. K., N. Sheppard, and D. M. Simpson, *Discussions Faraday Soc.*, **9**, 261 (1950).
16. Liang, C. Y., M. R. Lytton, and C. J. Boone, *J. Polymer Sci.*, **54**, 523 (1961).
17. Tschamler, H., *J. Chem. Phys.*, **22**, 1845 (1954).

### Résumé

On a examiné les structures de poly(3-méthylbutène-1), de poly(3-méthylbutène-1) isotactique et de 3,4-polyisoprène hydrogéné, obtenus cationiquement, au moyen de la résonance magnétique nucléaire et de la spectroscopie infra-rouge. Ces études corroborent la structure précédemment proposée d'unités  $\alpha, \alpha'$ -diméthylpropane se répétant dans le polymère cationique et confirmant l'enchaînement 1,2 tête à queue pour le polymère isotactique et pour le polyisoprène-3,4. Les spectres NMR du poly(3-méthyl-butène-1) et du polyisoprène-3,4 hydrogéné sont très similaires et ne montrent que deux pics. Ils sont complètement différents des spectres du poly(3-méthylbutène-1) et du 3,4-polyisoprène. Le produit isotactique fut solubilisé par pyrolyse prudente pour le rendre accessible aux études spectroscopiques. Malheureusement à ce jour, la spectroscopie de RMN ne possède pas de résolution suffisamment haute que pour être d'utilité dans l'étude quantitative des mélanges d'enchaînements 1,3 et 1,2. Les spectres de RMN de l'oxyde de polyisobutylène a été pris et interprété. On peut utiliser la spectroscopie infra-rouge pour distinguer le poly(3-méthylbutène-1) cationique de la modification isotactique et du polyisoprène-3,4 hydrogéné. On a analysé et assigné les bandes les plus importantes. Le poly(3-méthylbutène-1) et le polyisoprène-3,4-hydrogéné ont tous deux une structure conventionnelle "1,2" et leurs spectres infra-rouges sont essentiellement identiques.

### Zusammenfassung

Die Struktur von kationisch hergestellten Poly-3-methylbuten-1, isotaktischem Poly-3-methylbuten-1 und hydriertem 3,4-Polyisopren wurde mittels magnetischer Kernresonanz und IR-Spektroskopie untersucht. Die Ergebnisse bestätigen die früher angenommene Struktur einer sich wiederholenden  $\alpha, \alpha'$ -Dimethylpropan-Einheit für das kationische Produkt und die konventionelle 1,2-Kopf-Schwanz-Anordnung für das iso-

taktische Polymere und das hydrierte 3,4-Polyisopren. Die NMR-Spektren von kationischem Poly-3-methylbuten-1 und Polyisobuten sind einander sehr ähnlich und weisen zwei Maxima auf. Sie unterscheiden sich deutlich von den Spektren von isotaktischem Poly-3-methylbuten-1 und hydriertem 3,4-Polyisopren. Um das isotaktische Produkt der spektroskopischen Untersuchung zugänglich zu machen, wurde es durch sorgfältige Pyrolyse solubilisiert. Leider ist die Auflösung der NMR-Spektroskopie derzeit noch nicht so hoch, dass eine quantitative Untersuchung von Mischungen von "1,3"- und "1,2"-Anordnungen möglich wäre. Das NMR-Spektrum von Polyisobutylenoxyd wurde aufgenommen und interpretiert. Die IR-Spektroskopie kann zur Unterscheidung von kationischen Poly-3-methylbuten-1 von der isotaktischen Modifikation und dem hydriertem 3,4-Polyisopren dienen. Die wichtigeren Banden wurden analysiert und zugeordnet. Sowohl isotaktisches Poly-3-methylbuten-1 als auch hydriertes 3,4-Polyisopren besitzen die konventionelle "1,2"-Struktur und liefern im wesentlichen identische Infrarotspektren.

Received March 21, 1963

## Polyesters of 1,4-Cyclohexanedimethanol<sup>1</sup>

CHARLES J. KIBLER, ALAN BELL, and JAMES G. SMITH,  
*Research Laboratories, Tennessee Eastman Company, Division of  
Eastman Kodak Company, Kingsport, Tennessee*

### Synopsis

A series of polyesters of *trans*-1,4-cyclohexanedimethanol was prepared and the melting points compared with those of the analogous series of polyesters prepared from *p*-xylylene glycol. Only slight differences in melting points were noted between the corresponding pairs of polyesters prepared from a single aliphatic dicarboxylic acid and from the two glycols. However, polyesters derived from aromatic dibasic acids and *trans*-1,4-cyclohexanedimethanol melt at a higher temperature than the corresponding polymer from *p*-xylylene glycol. The probable molecular configuration of polyesters based on *trans*-1,4-cyclohexanedimethanol is discussed. It is suggested that the diol moiety in the polyester can adopt a slightly contracted conformation so that the oxygen-oxygen distance is less than in polyesters derived from *p*-xylylene glycol. This, together with the similar degree of rigidity and symmetry of the *trans*-1,4-cyclohexylene and *p*-phenylene ring systems, is employed to explain the observed melting points. Polyesters prepared from *cis*-1,4-cyclohexanedimethanol are also described. As expected from the lower degree of symmetry of the diol, these polyesters have lower melting points than the analogous compositions prepared from *trans*-1,4-cyclohexanedimethanol. Polyesters of *cis*-1,4-cyclohexanedimethanol and trimethylene glycol have similar melting points. It is suggested that a *cis*-1,4-cyclohexylene ring and a methylene group have a similar effect on the melting point of a polyester. Copolyesters of *cis*- and *trans*-1,4-cyclohexanedimethanol with terephthalic acid do not form a minimum melting composition. Instead, they show a continuous change of melting point from that of the polyester prepared from one stereoisomer to that of the polymer prepared from the other isomer.

There are frequent references in the literature which imply that the presence of aromatic rings in a polyester molecule raises the melting point of the polymer<sup>2-4</sup> in comparison with the analogous polyester containing the cyclohexane ring. The evidence cited in support of this is that the melting point of poly(ethylene terephthalate) is 265°C.<sup>5,6</sup> and that of poly(ethylene *trans*-1,4-cyclohexanedicarboxylate) is 120°C.<sup>3</sup>

This evidence is not considered reliable for two reasons. Firstly, the melting points of polyesters derived from 1,4-cyclohexanedicarboxylic acids may well be lowered by isomerization of the acids during preparation of the polyester.<sup>7</sup> Such an isomerization would explain the discrepancies in melting points which have been reported by several investigators.<sup>3,8,9</sup> Recently, evidence has been published<sup>10</sup> establishing such an isomerization during the preparation of poly(ethylene 1,4-cyclohexanedicarboxylate).

Secondly, the reduction in melting point caused by "replacing" the ben-



zene ring of terephthalic acid by the cyclohexane ring of 1,4-cyclohexanedicarboxylic acid may be caused not only by the substitution of a nonplanar cyclohexane ring for a planar, rigid, aromatic ring, but also by the elimination of the resonance interaction of the carboxylate group with the aromatic ring.<sup>8,11,12</sup>

To isolate these two effects, that of the aromatic ring itself and that of the resonance interaction between an aromatic ring and the carboxylate groups, a comparison of the melting points of polyesters prepared from *p*-xylylene glycol and *trans*-1,4-cyclohexanedimethanol was made. Both of these diols possess cyclic, centrosymmetrical structures and differ only in the presence of an aromatic system in the former and a hydrogenated aromatic system in the latter. Such a comparison should demonstrate the effect on a polyester's melting point of an aromatic *p*-phenylene ring versus a *trans*-1,4-cyclohexylene ring.

TABLE I  
Polyesters of *p*-Xylylene Glycol and *trans*-1,4-Cyclohexanedimethanol

Acid	<i>p</i> -Xylylene glycol			<i>trans</i> -1,4-Cyclohexanedimethanol	
	Reported m.p., °C.	Observed m.p., °C.	{ $\eta$ }	m.p., °C.	{ $\eta$ }
Oxalic	210-214	—	—	210-215	0.77
Succinic	103-108	108-115	0.61	145-147	0.64
Glutaric	54-58	—	—	45-50	0.78
Adipic	78-81	75-80	0.46	122-124	0.49
Pimehic	63-66	64-67	0.46	38-42	0.56
Suberic	76-79	79-82	0.44	94-96	0.61
Azelaic	74-79	72-74	0.41	45-50	0.66
Sebacic	86-88	88-93	0.82	72-78	0.82
Dodecanedioic	—	90-94	0.61	80-85	0.87
<i>trans</i> -1,4-Cyclohexanedicarboxylic	50-60	85-106	0.25	244-246	0.86
Isophthalic	94-100	—	—	190-197	0.26
Terephthalic	238-242	263-272	0.59	312-318	0.58
2,6-Naphthalenedicarboxylic	—	275-280	0.56	335-341 <sup>a</sup>	0.55

<sup>a</sup> Prepared from a *cis/trans* mixture containing 68% *trans* isomer.

The melting points of these polyesters are listed in Table I. The compositions synthesized from *p*-xylylene glycol have been reported previously,<sup>13</sup> but, for comparison, were resynthesized here by using a titanium alkoxide<sup>14</sup> catalyst. In general, the reported melting points agree well with those determined in this work. The discrepancy in the melting point of the *trans*-1,4-cyclohexanedicarboxylate is probably due to different degrees of isomerization of the acid during the polymer preparation. Korshak<sup>13</sup> used lithium hydroxide as a catalyst, and the basic nature of this catalyst would cause more isomerization than the neutral catalyst, titanium tetraisopropoxide, used in this work.

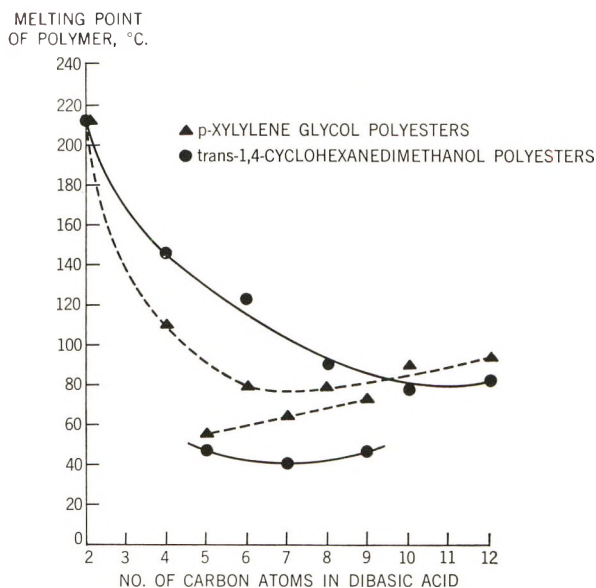


Fig. 1. Melting points of polyesters of aliphatic dibasic acids with *p*-xylylene glycol and with *trans*-1,4-cyclohexanedimethanol.

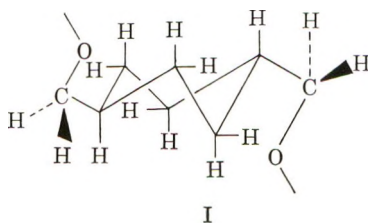
A comparison of the melting points of the polyesters from the two glycols shows that the polyesters of the *trans*-1,4-cyclohexanedimethanol and the aliphatic dibasic acids with an even number of carbon atoms melt at a slightly higher temperature than the analogous polyesters from *p*-xylylene glycol. In the case of polyesters from aliphatic dibasic acids with an odd number of carbon atoms, the situation is reversed and the polyesters of *trans*-1,4-cyclohexanedimethanol melt at a slightly lower temperature (see Fig. 1).

Insofar as polyesters from aliphatic dibasic acids are concerned, it must be concluded that the *trans*-1,4-cyclohexylene and the *p*-phenylene rings are about equal in their ability to confer high melting points upon polyester molecules containing them. Furthermore, this ability must be due to the rigidity and symmetry of the rings, properties which are not uniquely characteristic of aromatic rings.

Polyesters prepared from aromatic dibasic acids and *trans*-1,4-cyclohexanedimethanol or *p*-xylylene glycol contain a combination of rigidity and/or symmetry in the acid component with rigidity and symmetry in the diol component. In such cases *trans*-1,4-cyclohexanedimethanol appears to be superior to *p*-xylylene glycol insofar as the melting points of the polyesters are concerned. With *trans*-1,4-cyclohexanedimethanol, polyesters of exceptionally high melting points are formed.

Molecular models of the repeat units of these polyesters were constructed from Fisher-Taylor-Hirschfelder molecular models on the following assumptions. (1) That the carbonyl group of the ester linkage bisects the angle H-C-H of the methylene group of the diol which is attached to the

ether oxygen in the ester group. Such an arrangement is found in poly(ethylene terephthalate).<sup>7b</sup> (2) That the cyclohexane ring is in the chair form and that the methanol groups are attached by equatorial bonds to the ring. Such a conformation is suggested by Boye in his examination of poly(*trans*-1,4-cyclohexylenedimethylene terephthalate) by infrared spectroscopy<sup>15</sup> and x-ray diffraction.<sup>16</sup> (3) That *trans*-1,4-cyclohexanedimethanol is in that conformation (I) which minimizes steric interaction of the substituent hydroxymethyl groups with the ring hydrogen atoms.



An examination of the molecular models reveals that the repeat unit of the polyesters from *trans*-1,4-cyclohexanedimethanol and from *p*-xylylene glycol are very similar in overall shape. However, the repeat distance, as measured on the molecular models, for a polyester from *trans*-1,4-cyclohexanedimethanol is smaller than the repeat distance of the analogous polyester from *p*-xylylene glycol. This shorter repeat distance is due to the smaller distance that exists between the oxygen atoms of the *trans*-1,4-cyclohexanedimethanol than between the oxygen atoms of *p*-xylylene glycol. Consequently, a polyester of *trans*-1,4-cyclohexanedimethanol has a higher "concentration" of rigidity and symmetry per unit distance along the polymer chain than the analogous polyester of *p*-xylylene glycol. It would be expected, then, that the former polyester would melt at a higher temperature than the latter.

A molecular model of poly(*trans*-1,4-cyclohexylenedimethylene terephthalate) was constructed on the basis of the above assumptions as well as on the assumption that the terephthalate moiety was planar.<sup>12</sup> The model so produced was found to have the benzene ring rotated about the axis of the polymer chain and set at 90° relative to the plane of the cyclohexane ring. The repeat distance measured on the model was found to be approximately 14.3 Å., a remarkably good agreement with that determined by Boye (14.2 Å.).<sup>16</sup>

The expected higher melting point of *trans*-1,4-cyclohexanedimethanol polyesters is realized to some extent in those polyesters derived from aliphatic dibasic acids containing 4, 6, and 8 carbon atoms. With a larger number of carbon atoms, the polyester chain becomes largely aliphatic in nature, and differences between the *trans*-1,4-cyclohexanedimethanol and *p*-xylylene glycol polyesters are diluted. This dilution is probably caused by the flexibility of the aliphatic acid moiety in the polymer chain, which allows a slight expansion of the repeat unit and so nullifies the effect of the

TABLE II  
Polyesters of *cis*-1,4-Cyclohexanedimethanol and Trimethylene Glycol

Acid	m.p. of polyester from <i>cis</i> -1,4- cyclohexane- dimethanol, °C.	$[\eta]$	m.p. of polyester from trimethylene glycol, °C.
Succinic	58–62	0.48	52 <sup>a</sup>
Adipic	50–55	0.53	46 <sup>a</sup>
Pimelic	Liquid at 20°C.	0.52	51 <sup>a</sup>
Suberic	45–50	0.44	52 <sup>a</sup>
Azelaic	37–41	0.52	60 <sup>a</sup>
Sebacic	47–50	0.74	58 <sup>a</sup>
Dodecanedioic	43–46	0.27	—
<i>trans</i> -1,4-Cyclohexanedicarboxylic	203–205	0.82	ca. 110 <sup>b</sup>
Terephthalic	251–256	0.85	220 <sup>c</sup>
1,4-Benzenediacetic	40–55	0.62	54–58 <sup>b</sup>
2,6-Naphthalenedicarboxylic	281–287	0.86	—

<sup>a</sup> Data of Doak and Campbell.<sup>18</sup>

<sup>b</sup> Data of Korshak et al.<sup>8</sup>

<sup>c</sup> Data of Hill and Walker.<sup>17</sup>

slightly smaller oxygen–oxygen distance in *trans*-1,4-cyclohexanedimethanol.

In the case of the rigid aromatic dicarboxylic acids, however, there is little possibility for this type of flexibility to exist in the repeat unit. Consequently, the slightly smaller oxygen–oxygen distance of *trans*-1,4-cyclohexanedimethanol over that of *p*-xylylene glycol exerts its fullest effect and manifests itself in the appreciably higher melting points of the former polyester compositions.

The polyesters derived from aliphatic dibasic acids containing an odd number of carbon atoms melt lower than polyesters containing one more or one less methylene group. Such a behavior has been reported previously<sup>7c,17</sup> for other series of polymers. Indeed, this behavior appears to be characteristic for most series of polyesters and is often termed the odd-even effect.

The surprising feature of these polyesters derived from the “odd” aliphatic dibasic acids is the lower melting points of the *trans*-1,4-cyclohexanedimethanol polyesters compared to the *p*-xylylene glycol polymers. The opposite would be expected in view of the shorter repeat distances estimated for the former compositions. Probably an explanation of this difference in behavior must await a satisfactory explanation of the odd-even effect.

A series of polyesters was also prepared using various dibasic acids and the *cis* isomer of 1,4-cyclohexanedimethanol. The melting points of these polyesters are given in Table II. As might be expected from the reduced symmetry of the repeat unit, these polyesters in general melt at a lower temperature than their analogous *trans* derivatives. A comparison of these

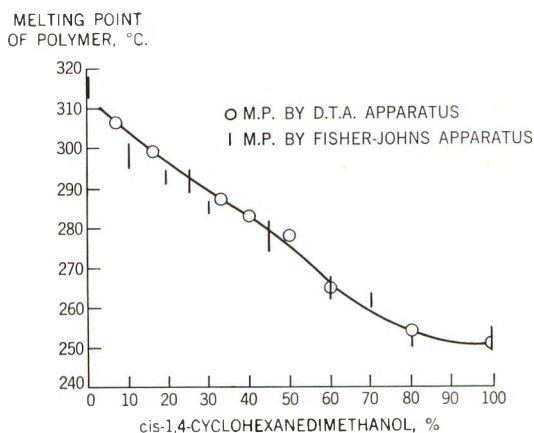


Fig. 2. Melting points of poly(1,4-cyclohexylenedimethylene terephthalates).

polyesters with similar compositions prepared from trimethylene glycol shows a rather close similarity in melting point. It is suggested that the *cis*-1,4-cyclohexylene ring may be regarded as equivalent to a methylene group insofar as its effect on the melting point of polyesters derived from aliphatic dibasic acids is concerned.

It is of interest to examine the melting points of the series of polyesters prepared from terephthalic acid and mixtures of the *cis*- and *trans*-1,4-cyclohexanedimethanol. The melting points obtained are summarized in Table III and presented graphically in Figure 2. In addition, some melting points determined by differential thermal analysis<sup>19</sup> have been made availa-

TABLE III  
Melting Points of Poly(1,4-Cyclohexylenedimethylene terephthalates)

<i>cis</i> -Isomer, %	Polyester	
	m.p., °C.	$[\eta]$
0	312-318	0.58
7	306 <sup>a</sup>	0.74
10	295-302	0.73
16	299 <sup>a</sup>	0.72
19	291-295	0.88
25	289-295	1.16
30	284-287	0.79
33	287 <sup>a</sup>	0.84
40	283 <sup>a</sup>	0.70
45	274-282	0.83
50	278 <sup>a</sup>	0.73
60	262-267, (265) <sup>a</sup>	0.75
70	260-264	0.97
80	250-254, (254) <sup>a</sup>	0.74
100	251-256, (251) <sup>a</sup>	0.85

<sup>a</sup> Melting point was determined by differential thermal analysis.



ble to us.<sup>20</sup> These are included in Table III and Figure 2 to provide an independent substantiation of the melting points determined here.

It can be seen that no minimum melting polyester composition is formed by the mixtures of isomers. Instead, a continuous increase in melting point occurs from the 100% *cis* to the 100% *trans* polyester. Apparently, the polyester molecules containing the *cis* diol can fit readily into the crystalline lattice of the polyester containing the *trans* diol (and vice versa). Boye has reported a continuous transformation of the x-ray diffraction pattern from that characteristic of the polyester containing the *cis* isomer to that characteristic of the polyester containing the *trans* isomer.<sup>16</sup> Such a facile substitution of one isomeric polyester into the crystalline lattice of the other is unusual in view of the measured difference in repeat unit of the two isomeric polyesters.<sup>16</sup>

## EXPERIMENTAL

### Reagents

***trans*-1,4-Cyclohexanedimethanol.** The *trans*-1,4-cyclohexanedimethanol can be isolated in the crude state by filtration of the semisolid commercially available mixture supplied by Tennessee Eastman Co.<sup>21</sup> Recrystallization from ethyl acetate gave material which was shown by gas chromatographic analysis on a Celite column containing 20% Carbowax 20M at 195°C. to be 95% or better *trans* isomer. This material had a boiling point of 283°C. at 735 mm.

***cis*-1,4-Cyclohexanedimethanol.** The mixture of isomers, available from Tennessee Eastman Co., was converted to the diacetate with acetic anhydride. The diacetate was distilled (b.p. 137–139°C. at 3.5 mm.) and dissolved in five volumes of pentane. The solution was cooled with Dry Ice–acetone mixture to –50°C. to effect crystallization of a gummy solid which contained a high proportion of *trans*-1,4-cyclohexanedimethanol diacetate. The supernatant liquid was decanted and the solvent removed; the residue was treated a second time with five volumes of pentane and cooled to –50°C. The supernatant solution was again decanted from the gummy solid which separated and was concentrated. The residue was hydrolyzed with aqueous sodium hydroxide, and the *cis*-1,4-cyclohexanedimethanol was isolated by extraction of the aqueous solution with butyl alcohol. The butyl alcohol solution was washed with a small volume of water, dried over magnesium sulfate, and distilled. The material, b.p. 118–120°C. at 1 mm. (286°C. at 735 mm.), was shown to be 92–95% *cis*-1,4-cyclohexanedimethanol by gas chromatographic analysis.

**Other Reagents.** *p*-Xylylene glycol was obtained from Diamond Alkali Co. and was recrystallized twice from 1,1,2-trichloroethane, m.p. 117–120°C.

Diethyl oxalate and diethyl succinate were obtained from Eastman Kodak Co.

Dibutyl glutarate was prepared from butyl alcohol and the glutaric acid-anhydride mixture available from Union Carbide and Carbon Co. Distillation gave the ester, b.p. 146°C. at 3 mm.,  $n_D^{20}$  1.4315.

Diisobutyl adipate was obtained from Eastman Chemical Products, Inc.

Pimelic acid was obtained from the American Cyanamid Co., m.p. 105–106.5°C.

Suberic acid was obtained from the Harchem Division of Wallace and Tiernan Co., m.p. 143–145°C.

Azelaic acid was obtained as a purified grade from Emery Industries, Inc., m.p. 100–105°C.

Dimethyl sebacate was Eastman Kodak Co., practical grade, redistilled, b.p. 160–162°C. at 0.2 mm.

Dodecanedioic acid was obtained from the Harchem Division of Wallace and Tiernan Co., m.p. 128–130°C.

Dimethyl terephthalate was obtained from Hercules Powder Co., Inc., m.p. 143–144°C.

Dimethyl isophthalate was obtained from Amoco Chemicals Corp., m.p. 68–69°C.

Dimethyl 2,6-naphthalenedicarboxylate was obtained from the Sun Oil Co., m.p. 194–195°C.

Diethyl 1,4-benzenediacetate (m.p. 55–56°C.) was prepared by the method described by Reynolds and Van der Beighe.<sup>22</sup>

### Melting Point Determinations

The melting points were determined on a Fisher-Johns melting point apparatus. Near the melting point, the sample was repeatedly pressed gently with a pencil point, and the temperature at which the sample flowed freely under this pressure is reported as the melting point. Usually, there is a preliminary softening of the polymer sample approximately 5°C. below the melting point, but this softening is not accompanied by any liquefaction.

### Preparation of Polyesters

**Melt-Phase Polymerization.** Polyesters which melted below 200°C. were prepared by a melt-phase polymerization at 270–280°C. of the reaction product prepared from the diol and a dialkyl ester of the dibasic acid, or from the diol and the dibasic acid itself. A typical procedure is described in detail below.

**Preparation of Poly(*trans*-1,4-cyclohexylenedimethylene sebacate).** The reaction vessel was a test tube constructed from a  $\frac{3}{4}$ /<sub>45</sub> joint. This test tube was capped with a head provided with a nitrogen inlet, an  $\frac{18}{9}$  socket joint for the stirrer shaft, and an outlet, connected with a condensing system, for condensation of the volatile compounds and for the application of a vacuum. Agitation was provided by a motor-driven paddle stirrer which entered the reaction vessel through the socket joint and was equipped with a matching ball joint.

The test tube was charged with 4.60 g. (0.02 mole) of dimethyl sebacate, 3.60 g. (0.025 mole) of *trans*-1,4-cyclohexanedimethanol, and 4 drops of a 28.4 wt.-% solution of titanium tetraisopropoxide in butyl alcohol. After the test tube was swept with nitrogen, the contents of the flask were stirred and heated to 200°C. by means of a Wood's metal bath. A slow stream of nitrogen was permitted to flow through the reaction flask to remove the methanol as it formed.

The mixture was heated with stirring at 200°C. for 1 hr. (a reaction time of 90 min. to 2 hr. was adopted if the free dibasic acid was used). The temperature of the metal bath was then raised over a 30–45 min. period to 275°C. When this temperature was reached, the nitrogen stream was stopped, and a vacuum was applied at such a rate that a pressure of at least 1 mm. of mercury was attained within 5 min. The molten reaction product was stirred at 275°C. and approximately 0.5 mm. for 1 hr. At the end of this polymerization period, the material was cooled *in vacuo* and removed from the tube. The plug of polymer was usually removed easily by rewarming the exterior of the glass tube until the outer layers of polymer softened. The remainder of the plug could then be lifted out with a spatula or forceps. The polymer had an inherent viscosity of 0.62 in 60/40 phenol/tetrachloroethane solution at 25°C. ( $C = 0.25$ ).

**Solid-Phase Polymerization.** Polyesters which melted above 200°C. were more conveniently prepared by polymerizing a low molecular weight polyester in the solid phase. The procedure described above was followed, except that the vacuum was applied for only 5–10 min. A low molecular weight polyester, termed a prepolymer, was obtained. For very high melting polyesters, such as the terephthalates or 2,6-naphthalenedicarboxylates, bath temperatures as high as 300–310°C. were necessary to keep the polyester molten. The procedure for polymerizing the prepolymer is described in detail below.

**Preparation of Poly(*trans*-1,4-cyclohexylenedimethylene oxalate).** The prepolymer obtained was a brittle, clear solid having an inherent viscosity of 0.20 and a melting point range of 190–197°C. This material was ground to pass a 40-mesh screen, and 0.5 g. of this material was placed in the bottom of a 19-mm. diameter test tube. The test tube was evacuated to a pressure of less than 0.1 mm. of mercury, and the tube was placed in a heated (thermostatically controlled) aluminum block whose temperature was 190°C. The prepolymer was heated at 190°C. for 2 hr. The temperature of the block was then raised to 210°C. and heating was continued for an additional 2 hr. The final polymer was cooled *in vacuo*, then removed from the tube. The polymer had an inherent viscosity of 0.77 and a melting point range of 210–215°C.

For high-melting polymers, the temperature of solid-phase polymerization was 240°C. or 260°C.

The authors are indebted to Miss S. Joelle Rush and W. A. Arnold, who have prepared many of the polymers described in this work.

## References

1. Kibler, C. J., A. Bell, and J. G. Smith, U. S. Pat. 2,901,466; Brit. Pat. 818,157; Can. Pat. 603,847; to Eastman Kodak Co., 1959.
2. Wilfong, R. E., *J. Polymer Sci.*, **54**, 385 (1961).
3. Carpenter, A. S., *J. Soc. Dyers Colourists*, **65**, 469 (1949).
4. Bannerman, D. G., and E. E. Magat, in *Polymer Processes*, Vol. X, C. E. Schildknecht, Ed., Interscience, New York, 1956, p. 280.
5. Whinfield, J. R., *Nature*, **158**, 930 (1946).
6. Whinfield, J. R., and J. T. Dickson, U. S. Pat. 2,465,319; to E. I. du Pont de Nemours and Co., Inc., 1949.
7. Reynolds, R. J. W., *Fibers From Synthetic Polymers*, R. Hill, Ed., Elsevier, 1953, (a) pp. 151-152; (b) p. 295; (c) pp. 310, 311.
8. Korshak, V. V., S. V. Vinogradova, and V. M. Belyakov, *Bull. Acad. Sci. U. S. S. R., Div. Chem. Sci.*, **1957**, 1029 (in English); **1957**, 1000 (in Russian).
9. Batzer, H., and G. Fritz, *Makromol. Chem.*, **14**, 179 (1954).
10. Chien, J. C. W., and J. F. Walker, *J. Polymer Sci.*, **45**, 239 (1960).
11. Izard, E. F., *J. Polymer Sci.*, **9**, 35 (1952).
12. Bunn, C. W., *J. Polymer Sci.*, **16**, 323 (1955); Ref. 5, pp. 316, 327.
13. Korshak, V. V., and S. V. Vinogradova, *Bull. Acad. Sci. U. S. S. R., Div. Chem. Sci.*, **1959**, 138 (in English); **1959**, 154 (in Russian).
14. Haslam, John H., U. S. Pat. 2,822,348; to E. I. du Pont de Nemours and Co., Inc., 1958.
15. Boye, C. A., *J. Polymer Sci.*, **55**, 263 (1961).
16. Boye, C. A., *J. Polymer Sci.*, **55**, 275 (1961).
17. Hill, R., and E. E. Walker, *J. Polymer Sci.*, **3**, 609 (1948).
18. Doak, K. W., and H. N. Campbell, *J. Polymer Sci.*, **18**, 215 (1955).
19. Boy, R. E., Jr., "Differential Thermal Analysis of Crystallizable Polymers," paper presented at the Southeastern Regional Meeting of the American Chemical Society, Gainesville, Florida, December 1958.
20. Schulken, R. M., and R. E. Boy, private communication.
21. Hasek, R. H., and M. B. Knowles, U. S. Pat. 2,917,549; to Eastman Kodak Co., 1959.
22. Reynolds, D. D., and J. Van der Beighe, U. S. Pat. 2,789,970, to Eastman Kodak Co., 1957.

## Résumé

On a préparé une série de polyesters de *trans*-1,4-cyclohexanediméthanol et les points de fusion ont été comparés à ceux des séries analogues des polyesters préparés à partir de *p*-xylylène glycol. On a seulement noté de légères différences dans les points de fusion entre les paires correspondantes de polyesters préparés à partir d'un simple acide aliphatique dicarboxylique et de deux glycols. Cependant, les polyesters dérivés des acides aromatiques dibasiques et du *trans*-1,4-cyclohexanediméthanol fondent à une température plus élevée que le polymère correspondant provenant du *p*-xylylène glycol. On discute la configuration moléculaire probable des polyesters basés sur le *trans*-1,4-cyclohexane-diméthanol. On suggère que la fraction diol dans le polyester peut adopter une conformation légèrement contractée de sorte que la distance oxygène-oxygène est moindre que dans les polyesters dérivés du *p*-xylylène glycol. Cela, ainsi que le degré de rigidité et de symétrie des systèmes cycliques *trans*-1,4-cyclohexylène et *p*-phénylène est employé pour expliquer les points de fusion observés. Les polyesters préparés à partir du *cis*-1,4-cyclohexane diméthanol sont également décrits. Comme on peut s'y attendre à partir du degré plus faible de symétrie du diol, ces polyesters ont des points de fusion plus bas que les compositions analogues préparées à partir de *trans*-1,4-cyclohexane-diméthanol. Les polyesters de *cis*-1,4-cyclohexanediméthanol et de triméthylène

glycol ont des points de fusion semblables. On suggère qu'un cycle *cis*-1,4-cyclohexylène et un groupe méthylène ont un effet semblable sur le point de fusion d'un polyester. Les copolyesters de *cis*- et *trans*-1,4-cyclohexanediméthanol avec l'acide téréphtalique ne forment pas une composition à point de fusion minimum. Au lieu de cela, ils présentent un changement continu du point de fusion depuis celui du polyester préparé à partir d'un stéréoisomère jusqu'à celui du polymère préparé à partir de l'autre isomère.

### Zusammenfassung

Es wurde eine Reihe von Polyestern aus *trans*-1,4-Cyclohexandimethanol hergestellt und deren Schmelzpunkte mit denjenigen der aus *p*-Xylylenglykol hergestellten analogen Polyester verglichen. Die Schmelzpunkte der aus derselben aliphatischen Dicarbonsäure und den beiden Glykolen hergestellten Polyester unterscheiden sich nur wenig. Dagegen schmelzen die aus aromatischen zweibasischen Säuren und *trans*-1,4-Cyclohexandimethanol hergestellten Polyester höher als die entsprechenden, von *p*-Xylylenglykol abgeleiteten Polymeren. Es wird die wahrscheinlichste molekulare Konfiguration der aus *trans*-1,4-Cyclohexandimethanol hergestellten Polyester diskutiert. Man nimmt an, dass der Diol-Teil des Polyesters eine leicht kontrahierte Konformation annehmen kann, so dass der Sauerstoff-Sauerstoff-Abstand kleiner ist als in den von *p*-Xylylenglykol abgeleiteten Polyestern. Auf Grund dieses Umstandes und des ähnlichen Starrheits- und Symmetrie-grades des *trans*-1,4-Cyclohexylen- und des *p*-Phenylen-Ringsystems können die beobachteten Schmelzpunkte erklärt werden. Die aus *cis*-1,4-Cyclohexandimethanol hergestellten Polyester werden ebenfalls beschrieben. Wie auf Grund der niedrigeren Symmetrie des Diols zu erwarten ist, haben diese Polyester niedrigere Schmelzpunkte als die aus *trans*-1,4-Cyclohexandimethanol hergestellten analoger Zusammensetzung. Die Polyester von *cis*-1,4-Cyclohexandimethanol und Trimethylenglykol haben ähnliche Schmelzpunkte. Man nimmt an, dass ein *cis*-1,4-Cyclohexylenring und eine Methylengruppe den Schmelzpunkt eines Polyesters in ähnlicher Weise beeinflussen. Copolyester von *cis*- und *trans*-1,4-Cyclohexandimethanol mit Terephthalsäure bilden keine Zusammensetzung mit Schmelzpunktminimum. Der Schmelzpunkt ändert sich vielmehr kontinuierlich von demjenigen des aus dem einen Stereoisomeren bis zu demjenigen aus dem anderen Isomeren hergestellten Polyesters.

Received April 5, 1963



## The Reaction between Dicumyl Peroxide and Butyl Rubbers

L. D. LOAN, *Rubber and Plastics Research Association of Great Britain,  
Shawbury, Shrewsbury, England*

### Synopsis

The reaction between dicumyl peroxide and butyl rubbers has been followed by means of molecular weight measurements. In all cases except that of the rubber with highest unsaturation the molecular weight falls, and the scission efficiency of the peroxide is found to depend quite markedly upon the unsaturation. For the rubber of highest unsaturation a small overall crosslinking reaction was observed. The results are interpreted as showing that cumyloxy radicals react with isoprene units in the chain about 300 times as fast as with isobutylene units. The molecular weight dependence upon time during the reaction has been investigated but has not been satisfactorily explained.

### INTRODUCTION

Previous work in these laboratories has shown that the reaction between dicumyl peroxide and rubbers varies widely depending on the rubber used. The observed behavior varies from that observed with polyisobutylene (PIB),<sup>1</sup> where the peroxide is found to give one carbon-carbon scission reaction for each molecule decomposed, to that observed with styrene-butadiene rubber,<sup>2</sup> where the peroxide shows a crosslinking efficiency of about 12. Between these two extremes lies natural rubber<sup>3</sup> and some other synthetic rubbers<sup>2</sup> where the crosslinking efficiency is in the region of unity.

With this wide range of observed behavior it is of interest to investigate the reaction between dicumyl peroxide and butyl rubbers where a behavior between that of natural rubber and PIB would be expected. Such a polymer, where the amount of isoprene units copolymerized into the PIB may be varied, should enable some measure to be made of the relative reactivity of the two types of monomeric unit toward the radicals formed from the peroxide.

### EXPERIMENTAL

#### Materials

The butyl rubbers used were obtained from Polymer Corporation and had unsaturations in the range 0.6-3 mole-%. The PIB used was Oppanol B



200. In each case the polymers were thoroughly extracted with acetone and dried *in vacuo* before use.

Squalene was purified by passing through an alumina column immediately before use. Infrared analysis showed that this procedure removed all carbonyl absorption initially present.

Dicumyl peroxide was obtained from Hercules Powder Company and was recrystallized from methanol and water.

### Methods

The peroxide was milled into the rubber on a 6 × 2 in. two-roll mill at room temperature, and the reaction was normally carried out by heating in a press for 70 min. at 153°C. to give virtually complete decomposition of peroxide. Experiments to determine the rate of scission were carried out by heating the compound in a sealed tube *in vacuo*.

The PIB compounds containing squalene were prepared by allowing the required amount of squalene to swell into the rubber and then refining the mixture on a mill.

Molecular weights were determined viscometrically in diisobutylene at 20°C. from the equation:<sup>4</sup>

$$[\eta] = 3.60 \times 10^{-4} M^{0.64}$$

This equation was obtained with PIB and its use here assumes that the small amount of unsaturation present has no effect on the intrinsic viscosity of the polymer.

The peroxide content was normally checked by an ultraviolet analysis of the uncured compound.

Product analyses were carried out by dissolving the degraded polymer in carbon tetrachloride immediately after heating and measuring the optical density in the infrared region at 3520  $\text{cm}^{-1}$  and 1730  $\text{cm}^{-1}$ . The extinction coefficient of cumyl alcohol at 3520  $\text{cm}^{-1}$  is unfortunately rather low, and since the polymer gives bands interfering in this region, no accurate measurements have been possible.

## RESULTS AND DISCUSSION

### a. Scission Efficiency

With only one exception the peroxide was found to produce a more or less marked decrease in molecular weight similar to but less than that previously observed with PIB. The results obtained are shown in Figure 1 as a graph of  $1/M$  versus peroxide content. In each case the point at zero peroxide concentration was obtained from the milled rubber. The dotted line shows the line for unit scission efficiency. The points shown for the rubber of highest unsaturation indicate a line of negative slope; points at higher peroxide concentrations could not be obtained since the polymer became insoluble as further crosslinks were introduced.

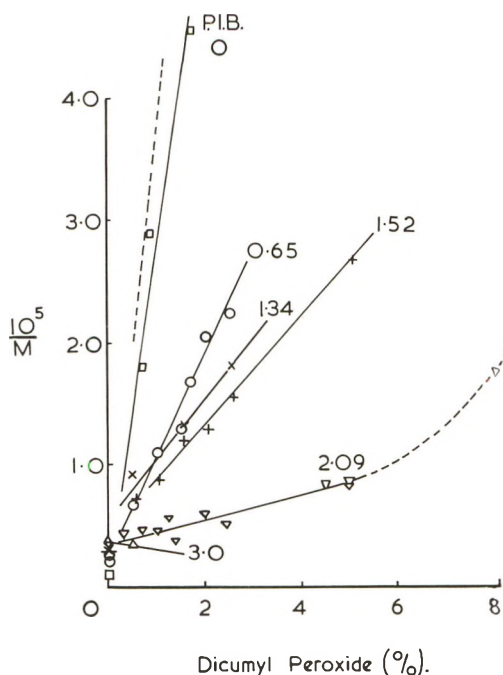


Fig. 1. Reciprocal molecular weight vs. initial peroxide concentration for butyl rubbers of different unsaturations. The mole per cent unsaturation is shown on each line.

It is a little surprising that straight lines result from these plots since the unsaturation in the rubbers is quite low and in some cases could have been markedly reduced by reaction with peroxide. With 5% peroxide in a rubber having 2.09 mole-% unsaturation the peroxide concentration is 1.4 mole-%, and thus a noticeable increase in the scission efficiency over that observed at, say, 1% peroxide might have been expected. That this does not occur suggests that there are around each unsaturated bond more than one labile hydrogen atom which can react. A single experiment at 8% peroxide (corresponding to 2.24 mole-%) shows that an increase in scission efficiency does occur at these much higher concentrations.

The slopes of the lines in Figure 1 are proportional to the scission efficiency of the peroxide in the reaction, that is, to the average number of main chain cuts produced by each molecule of peroxide decomposed. This efficiency has been calculated and is shown plotted against unsaturation in Figure 2. The scission efficiency falls very quickly as the unsaturation is increased. Such an effect will result if the radicals from the peroxide react with the isoprene units without giving chain scission. Such a reaction between radicals and isoprene units may conceivably cause no change in the size of the polymer molecule concerned or it may lead to crosslinking. To try and separate these two possibilities a set of experiments, similar to that above, using mixtures of PIB and squalene were carried out. The results are again shown in Figure 2. In this case the effect of any cross-

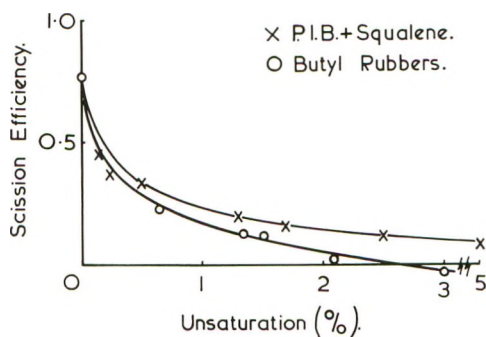


Fig. 2. Scission efficiency of butyl rubbers of various unsaturations and PIB containing various concentrations of squalene as a function of unsaturation.

linking is removed since it would occur only between small molecules and therefore have no effect on the viscometrically measured polymeric molecular weight. The close similarity of the two curves in Figure 2 shows that the crosslinking reaction occurs only to a minor extent, the main drop in scission efficiency being caused by some reaction between radicals and isoprene units which causes no direct change in polymeric molecular weight.

Small amounts of crosslinking do occur, however, as is shown in Figure 2, and would be expected to change the constants of the intrinsic viscosity-molecular weight equation. In our present work, however, we have assumed that such changes would be slight, and the same constants have been used for all the polymers examined.

The full kinetic scheme including all the reactions which probably occur in the system under discussion is very complex and incapable, at this stage, of simple solution. It is however of interest to consider a greatly simplified scheme such as



where  $\text{RO}\cdot$  is a peroxy radical, B and P are isobutylene and isoprene units, and  $\text{B}'\cdot$  and  $\text{P}'\cdot$  are the radicals derived from them. From such a system, assuming  $k_5^2 = k_3k_4$ , we find that the scission efficiency when P is a small molecule is

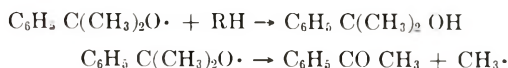
$$E_s \simeq k_1[\text{B}]/(k_1[\text{B}] + k_2[\text{P}])$$

or

$$1/E_s \simeq 1 + (k_2[\text{P}]/k_1[\text{B}])$$

Plotting the present results for PIB and squalene according to this relationship leads to a value for  $k_2/k_1$  of 300, this being the ratio of the reactivities of isoprene and isobutylene units towards cumyloxy radicals.

It is difficult to obtain other estimates for this ratio but previous work here<sup>5</sup> in which ketone and alcohol produced during the reaction between dicumyl peroxide and several hydrocarbons was measured shows that a ratio of the order quoted is reasonable. For example in the reaction of 2,2-dimethyl-butane the low molecular weight products are cumyl alcohol 0%, acetophenone 85%; with natural rubber<sup>3</sup> they are alcohol 90%, acetophenone 10%. These products arise from the cumyloxy radicals by the reactions,



where RH is the hydrocarbon, and it may be seen therefore that the ratio of alcohol to ketone gives a measure of the ease of hydrogen abstraction. Thus treating the butane as a model for an isobutylene unit the reaction of cumyloxy radicals with isoprene units (natural rubber) would be expected to be much faster than with isobutylene units.

Evidence for the relative inertness toward peroxy radicals of the hydrogen atoms in substances such as PIB is also given by Wibaut and Strang,<sup>6</sup> who show that the rate of oxidation of isooctane is negligible when compared with that of the isomeric straight chain hydrocarbon.

### b. Rate of Scission

The linear dependence of the number of scissions upon the initial peroxide concentration shown in Figure 1 suggests that the elementary scission reaction is of the first order with respect to radical concentration. To check that this is so, the molecular weights of butyl rubber–dicumyl peroxide, and PIB–squalene–dicumyl peroxide mixtures were measured after various times of heating. The results are shown in Figures 3 and 4. In

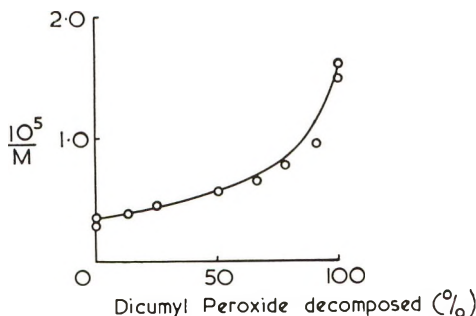


Fig. 3. Reciprocal molecular weight as a function of the fraction of peroxide decomposed during the reaction of 1.5 % peroxide with butyl rubber of 0.65 mole-% unsaturation at 140°C.

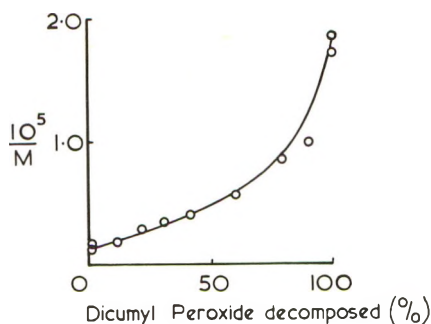


Fig. 4. Reciprocal molecular weight as a function of the fraction of peroxide decomposed during the reaction of 2% peroxide with PIB containing 1.5% squalene at 140°C.

calculating these results, decomposition half lifetimes of 48 min. and 117 min. at 140°C. and 130°C., respectively, were used.

These results show that the scission efficiency rises very rapidly toward the end of the reaction. On each of the two figures the lower point at full decomposition is derived from the experimental data shown in Figures 1 and 2 and is therefore well substantiated. The shape of this curve is somewhat unexpected and rather difficult to explain. It cannot be due to a retarder in the rubber since with a given rubber the same scission efficiency is observed over a range of peroxide concentrations. Likewise, it cannot be explained as due to the decay of unsaturation during the reaction as such a decay would have been shown by the earlier experiments plotted in Figure 1. One further possibility is the presence of an interfering impurity in the peroxide; this can however be discounted on several grounds, the material is supplied in high purity and is carefully recrystallized before use. Its estimation by ultraviolet spectroscopy shows a purity of 100% within experimental error, its melting point is sharp, and it shows a unit crosslinking efficiency when used to cure purified natural rubber.

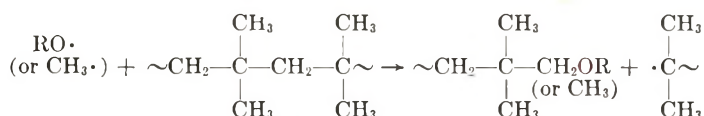
To explain the observed dependence it therefore seems necessary to postulate the existence of an intermediate compound which is formed during the reaction and is capable of producing a chain scission by a further reaction some time after the initial radical attack. There is at present no evidence upon the nature of this intermediate and further work, preferably using low molecular weight model compounds, is required to identify it.

The ratio of  $k_2/k_1 = 300$ , which is of course only a rough value based on an incomplete kinetic scheme, indicates that the cumyloxy radical reacts with the isoprene units (by hydrogen abstraction) much faster than with the isobutylene residues. It is now well known that the reaction of dicumyl peroxide with natural rubber leads predominantly to the production of cumyl alcohol by a hydrogen abstraction by the cumyloxy radical, but



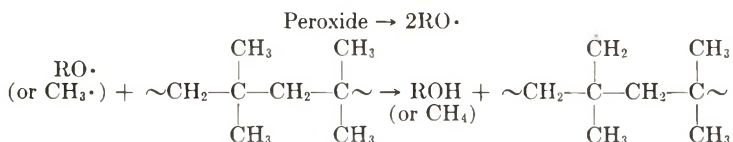
some acetophenone resulting from decomposition of the cumyloxy radical is also formed. Where the primary reaction of the cumyloxy radicals is slower than that with natural rubber an increase in the amount of acetophenone produced would be expected. This increase is shown in Thomas's work with hydrocarbons,<sup>5</sup> but in his study of the PIB-dicumyl peroxide reaction no acetophenone or cumyl alcohol were found within the limits of experimental accuracy.<sup>1</sup>

The mechanism suggested by him for this reaction involves immediate scission of the polymer chain

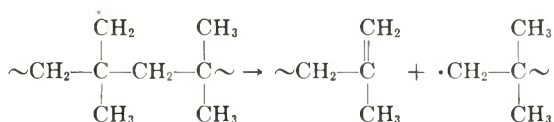


and allows for no unstable intermediate such as appears necessary to explain the scission-time dependence. This mechanism rests mainly upon a failure to find appreciable amounts of cumyl alcohol and or acetophenone among the products. Further work here on this point has indicated yields of up to 50% acetophenone with uncertain amounts of cumylalcohol while yields of 46% acetophenone and 27% cumyl alcohol have been found elsewhere.<sup>7</sup> It is also relevant that the reaction between peroxide and 2,2-dimethylbutane yields around 90% acetophenone.<sup>5</sup> Thus it seems that Thomas's mechanism is open to some doubt.

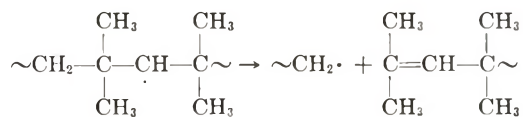
An alternative mechanism, in accord with the presently reported product analyses would be



followed by



together with the usual inter-radical termination steps and or depolymerization steps. A further alternative to this involves a primary abstraction of a secondary hydrogen when the radical rearrangement would be



The secondary hydrogen atoms are, however, heavily shielded by the adjacent methyl groups which are packed very closely together and must



make the chain very rigid. The abstraction of a primary hydrogen atom is therefore considered to be more probable, and although such an abstraction has not often been reported, it has been found that the relative reactivity of secondary to primary hydrogen atoms toward alkoxy radicals is only 3 or 4.<sup>8</sup> This mechanism does not, however, explain the way in which the amount of scission depends upon the time of heating (Figs. 3 and 4) as none of the radicals involved would be expected to have a lifetime long enough to lead to this type of scission dependence. Thus at the moment no kinetic scheme can be confidently suggested for the reaction studied in this paper and further work would seem to be necessary before a full understanding of it appears.

The author wishes to thank Hercules Powder Company for their support of this work which forms part of the Research Association's general program.

### References

1. Thomas, D. K., *Trans. Faraday Soc.*, **57**, 511 (1961).
2. Loan, L. D., *J. Appl. Polymer Sci.*, **7**, 2259 (1963).
3. Thomas, D. K., *J. Appl. Polymer Sci.*, **6**, 613 (1962).
4. Flory, P. J., *J. Am. Chem. Soc.*, **65**, 376 (1943).
5. Thomas, D. K., *Trans. Faraday Soc.*, in press.
6. Wibaut, J. P., and A. Strang., *Proc. Koninkl. Ned. Akad. Wetenschap.* **B54**, 229 (1951).
7. Edwards, D. C., private communication.
8. Walling, C., and B. B. Jacknow, *J. Am. Chem. Soc.*, **82**, 6108 (1960).

### Résumé

La réaction entre le peroxyde de dicumyle et les caoutchoucs butyliques a été suivie au moyen de mesures du poids moléculaire. Dans tous les cas excepté celui du caoutchouc possédant l'insaturation la plus élevée, le poids moléculaire tombe, et l'efficacité de scission du peroxyde dépend fortement de l'insaturation. Pour le caoutchouc possédant l'insaturation la plus élevée on a observé une petite réaction de pontage. On interprète les résultats en montrant que les radicaux cumyloxy réagissent avec les unités isoprène dans la chaîne environ 300 fois aussi vite qu'avec les unités isobutylène. On a étudié la dépendance du poids moléculaire vis-à-vis de la durée de la réaction mais on n'a pas pu trouver d'explication satisfaisante.

### Zusammenfassung

Die Reaktion zwischen Dicumylperoxyd und Butylkautschuk wurde durch Molekulargewichtsmessungen verfolgt. Das Molekulargewicht sinkt in allen Fällen mit Ausnahme des am stärksten ungesättigten Kautschuks und die Spaltungswirksamkeit des Peroxyds hängt deutlich von der Zahl der Doppelbindungen ab. Im Falle des am stärksten ungesättigten Kautschuks wurde eine geringe Brutto-Vernetzungsreaktion beobachtet. Die Interpretation der experimentellen Befunde zeigt, dass das Cumyloxyradikal mit den Isopreneinheiten der Kette etwa dreihundertmal so schnell reagiert wie mit den Isobutyleneinheiten. Die Zeitabhängigkeit des Molekulargewichts während der Reaktion wurde zwar untersucht, konnte jedoch nicht befriedigend erklärt werden.

Received January 15, 1963

Revised March 1, 1963

## Radiation-Initiated Copolymerization of Styrene with Unsaturated Esters

W. BURLANT and J. HINSCH, *Scientific Laboratory, Ford Motor Company,  
Dearborn, Michigan*

### Synopsis

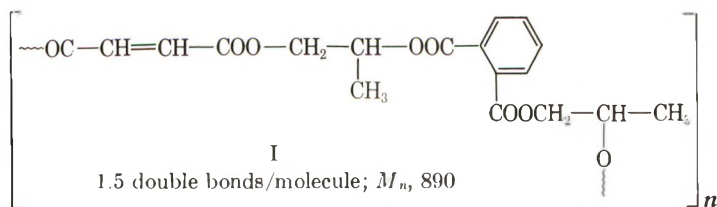
The kinetics of the  $\gamma$ -ray-initiated, gel-forming copolymerization of styrene with the unsaturated ester containing 1.5 double bonds per molecule of number-average molecular weight of 890 (derived from maleic anhydride, phthalic anhydride, and propylene glycol) have been studied with initial ester concentrations ranging from 65% to 2.4%. From experimentally determined gel fractions, rates of disappearance of styrene and ester unsaturation (measured up to complete conversion of ester unsaturation), and the degree of polymerization of the growing chains, a model is suggested based on a free radical copolymerization, assuming a single effective propagation and termination rate constant ( $k_p$  and  $k_t$ , respectively), and bimolecular chain termination except between a pair of immobile gel radicals. Three ester concentration ranges were considered. At high ester concentrations ( $\geq 50\%$ ), styrene and ester enter the gel at a constant rate (molar ratio of styrene:ester double bond of 2:1), precluding application of conventional copolymer composition theory. The rate at which overall unsaturation,  $\alpha$ , disappears, is given by  $d\alpha/dt = (k_p^2/k_t)M_2^\circ$ , where  $M_2^\circ$  is the initial molar concentration of ester unsaturation. The rate at which styrene,  $\alpha_1$ , disappears is given by  $d\alpha_1/dt = 2/3(k_p^2/k_t)M_2^\circ(M_1^\circ + M_2^\circ)/M_1^\circ$ . The rate at which styrene is consumed in the dilute ester-styrene solutions ( $\leq 4.6\%$ ), where  $M_2^\circ$  is negligibly small, is given by  $d\alpha_1/dt = k_p(k_1/2k_t)^{1/2}$ . Polymerization rates of the intermediate ester concentration ranges (10% to 30%) are higher than predicted from the simple model. An empirical rate expression is presented which describes these systems to 40% conversion of styrene:  $d\alpha_1/dt = (k_p^2/k_t)M_2^\circ \{[(1+M)(r_1+M)]/(r_1+2M)\}$ , where  $M$  is the ratio of ester unsaturation to styrene in the starting mixture and  $r_1$  is the reactivity ratio for styrene, defined in the usual manner. For initial conversions of ester unsaturation (to 10%)  $d\alpha/dt = (k_p^2/k_t)M_2^\circ$ .

### INTRODUCTION

Most data on vinyl-divinyl copolymerizations, in which gel formation accompanies chain growth, describe either the kinetics of the reaction in the pregel region, or emphasize the role of conversion at which gelation occurs. Kinetics of the polymerization in the gelling region have been studied only briefly: For a range of polyethylene fumarate-methyl methacrylate mixtures (molar ratios of fumarate unsaturation to methyl methacrylate of 1.8 to 0.1; peroxide-initiated), Gordon and McMillan report<sup>1</sup> that the conventional radical scheme obtains up to the gel point, which occurs at less than 4% conversion. Beyond this stage there is noted an increase in rate, attributed to the well-known gel effect on the

termination step; and at higher degrees of crosslinking even the propagation step, therefore the overall rate, also slows down. The conclusions are based on overall conversions measured dilatometrically in the pregel region, densitometrically after gelation, and assuming applicability of the copolymer composition equation throughout the concentration range.

The present paper describes in greater detail the kinetics at 33°C. of the  $\gamma$ -ray-induced gel-forming copolymerization of styrene with the unsaturated ester (I) derived from maleic anhydride, phthalic anhydride



and propylene glycol. Starting ester concentrations employed ranged from 65% to 2.4%; molar ratios of ester unsaturation to styrene from 0.327 to 0.004. Gelation occurs at a few per cent conversion of unsaturation, which is the point at which kinetic runs were begun; monomer consumption and gel fractions then were measured up to complete reaction of ester double bonds.

This system is amenable to analysis because: (1) disappearance of ester and styrene unsaturation can be followed separately in most cases by high resolution infrared spectrometry; (2) the isolated gel is hydrolyzable to a tractable styrene-maleic acid copolymer, so that the average degree of polymerization of the growing chains is estimable; (3) initiation by  $\gamma$ -rays at 33°C. obviates experimental difficulties inherent in the use of conventional chemical initiators requiring somewhat higher polymerization temperatures; (4) the observed absence of dark or autoaccelerative reactions simplifies the kinetic treatment.

### APPROACH

Based on gel fractions, rates of disappearance of monomers, and the applicability of the steady state treatment, a simple kinetic scheme is proposed. Free radicals are produced by the  $\gamma$ -radiation and are assumed to initiate network copolymerization independently at each ester double bond. Gelation occurs at about 1% unsaturation conversion; at this stage the system is comprised of a gel, highly swollen with the mixture of monomers, in which are incorporated pendant vinyl groups. Growing copolymer radicals attain only short chain lengths before adding to gel, as propagation and gel formation continue. If chain termination is bimolecular, but cannot occur between two gel radicals because of their large size, and employing a single effective propagation and termination rate constant to

describe the copolymerization, the concentration of radicals separately in the sol and gel is approximated by:

$$\frac{d[S\cdot]}{dt} = k_1(1 - g) - k_t[S\cdot](2[S\cdot] + [G\cdot]) - k_p[S\cdot]M_2 = 0 \quad (1)$$

and

$$\frac{d[G\cdot]}{dt} = k_1g - k_t[S\cdot][G\cdot] + k_p[S\cdot]M_2 = 0 \quad (2)$$

where  $[S\cdot]$  = concentration of soluble radicals at time  $t$  (in mole/liter);  $k_1$  = initiation rate constant (in mole/liter-minute);  $g$  = gel fraction;  $(1 - g)$  = sol fraction =  $S$ ;  $k_t$  = termination rate constant (in liter/mole-minute);  $[G\cdot]$  = concentration of radicals in the gel phase (in mole/liter);  $k_p$  = propagation rate constant (in liter/mole-minute);  $M_2$  = overall concentration of ester double bonds at time  $t$  (in mole/liter).

The term  $k_1(1 - g)$  in eq. (1) describes the rate at which radicals are formed in the sol phase. The last two terms in this equation represent the several rates at which radicals are removed from the sol phase: by combination with another sol or gel radical, or by incorporation into the gel via a propagation step.

The rate at which overall unsaturation disappears is

$$d\alpha/dt = k_p(1 - \alpha)([S\cdot] + [G\cdot]) \quad (3)$$

where  $\alpha$  is the fraction of initial unsaturation that has reacted.

When eqs. (1) and (2) are solved for  $1/[S\cdot]$  and  $([S\cdot] + [G\cdot])$ , there is obtained:

$$\frac{1}{[S\cdot]} = \frac{k_pM_2}{k_1(1 - 2g)} + \left\{ \left[ \frac{k_pM_2}{k_1(1 - 2g)} \right]^2 + \frac{2k_t}{k_1(1 - 2g)} \right\}^{1/2} \quad (4)$$

and

$$([S\cdot] + [G\cdot]) = \frac{k_pM_2}{2k_t(1 - 2g)} + \left\{ \left[ \frac{k_pM_2}{2k_t(1 - 2g)} \right]^2 + \frac{k_1}{2k_t(1 - 2g)} \right\}^{1/2} \quad (5)$$

When radical concentrations in eq. (3) are eliminated by using equation (5), the rate at which overall unsaturation disappears in the copolymerization of the styrene-ester mixture is given by the general expression:

$$\frac{d\alpha}{dt} = \frac{k_p^2}{2k_t} \left\{ \frac{M_2(1 - \alpha)}{(1 - 2g)} + \sqrt{\left[ \frac{M_2(1 - \alpha)}{(1 - 2g)} \right]^2 + \frac{2k_1k_t(1 - \alpha)^2}{k_p^2(1 - 2g)}} \right\} \quad (6)$$

## RESULTS AND DISCUSSION

It is convenient to divide applications of the rate equation, eq. (6), and discussion of results into three sections, depending on the ester concentration of the solutions.

### I. Concentrated ( $\geq 50\%$ ) Ester Solutions

Figure 1 represents the measured rates at which styrene and ester unsaturation disappear in the irradiated mixtures. It is seen that each component enters the gel at a constant rate, and at a molar ratio of styrene to ester double bond of 2:1. Not only is such linearity not predicted from copolymer reactivity ratios determined from the more dilute ester solutions (see below), but established theory predicts a ratio of about 1.5 at these conversions. Molecular models indicate that while both configurations are attainable, the one with only a single styrene unit between ester

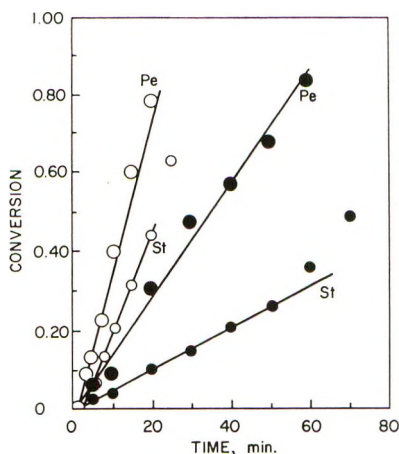


Fig. 1. Conversion of styrene and ester unsaturation with time for initial mixtures containing (O) 65% ester and (●) 50% ester.

molecules is sterically hindered. Since the glass transition temperature of the gel is about<sup>2</sup> 100°C., it is suggested that the 2:1 ratio results from the fact that the  $\gamma$ -initiated reaction occurs in the glassy state, where limited segmental mobility of the gel prohibits incorporation of only one styrene molecule between chains. In any case, these experimental data preclude use of the conventional copolymerization composition scheme to obtain the required relation between  $M_2$  and  $\alpha$ . This information, however, can be calculated from Figure 1: for each system,  $M_2 = M_2^0 - \alpha/3 (M_1^0 + M_2^0)$ , and  $M_1 = M_1^0 - 2\alpha/3 (M_1^0 + M_2^0)$ , where  $M_1^0$  and  $M_2^0$  are the initial molar concentrations of styrene and ester, respectively.

If we let  $A_3 = (k_p^2/2k_t)M_2^0$  and  $A_6 = (M_1^0 + M_2^0)/3M_2^0$ , eq. (6) can be rewritten in terms of the initial concentrations of components:

$$\frac{d\alpha}{dt} = A_3 \left\{ \frac{(1 - A_6\alpha)(1 - \alpha)}{(1 - 2g)} + \sqrt{\left[ \frac{(1 - A_6\alpha)(1 - \alpha)}{(1 - 2g)} \right]^2 + \frac{2k_1k_t(1 - \alpha)^2}{k_p^2(M_2^0)^2(1 - 2g)}} \right\} \quad (7)$$



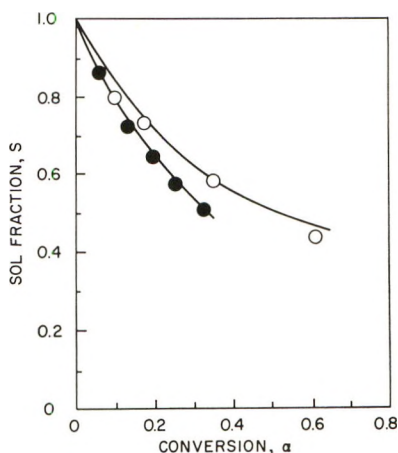


Fig. 2. Dependence of sol fraction on conversion of unsaturation for (O) 65% and (●) 50% ester solutions.

where

$$\frac{2k_1k_t}{k_p^2(M_2^0)^2} \cong \frac{1}{DP^2} \cong \frac{1}{1000}$$

From experimentally determined gel fraction-conversion data (Fig. 2), the first term under the square root sign is approximately 1 and according to the measured degree of polymerization, DP, of the reaction (about 30), the last term under the square root sign in eq. (7) is much smaller than 1; eq. (7), therefore, can be simplified:

$$\frac{d\alpha}{dt} = 2A_2 \left[ \frac{(1 - A_6\alpha)(1 - \alpha)}{(1 - 2g)} \right] \quad (8)$$

This can be integrated analytically if  $(1 - 2g)$  can be expressed in terms of  $\alpha$ . Curve fitting of gel fraction-conversion data (Fig. 2) indicates that

$$(1 - 2g) = 1 - 2A_1\alpha + 2A_2\alpha^2 \quad (9)$$

where  $A_1 = 1.48$  and  $2.10$  and  $A_2 = 0.85$  and  $1.85$  for the 65% and 50% ester solutions, respectively.

If eq. (9) is substituted into eq. (8) and the resulting expression integrated:

$$\frac{2A_2\alpha}{A_6} + \left[ \frac{2A_1 - 2A_2 - 1}{A_6 - 1} \right] \ln \left( \frac{1}{1 - \alpha} \right) + \left\{ \frac{[1 + (2A_2/A_6^2) - (2A_1/A_6)]}{A_6 - 1} \right\} \ln \left( \frac{1}{1 - A_6\alpha} \right) = 2A_3t \quad (10)$$

Equation (10) can be evaluated for different values of  $\alpha$ , using values of  $A_1$ ,  $A_2$ , and  $A_6$  measured for both the 65% and 50% ester solutions (Fig. 3).

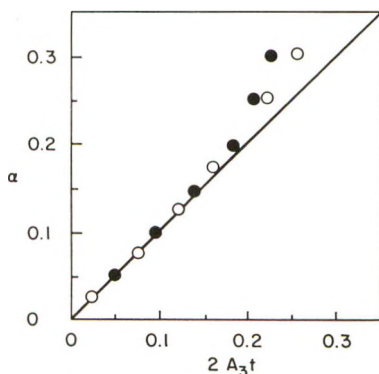


Fig. 3. Plot of overall conversion vs.  $2A_3t$ , according to eq. (10) for (O) 65% and (●) 50% ester solutions.

For conversions up to about 30%, eq. (10) is approximately  $\alpha = 2A_3t$ . The rate at which overall unsaturation disappears, therefore, is given by:

$$d\alpha/dt = 2A_3 \quad (11)$$

an expression consistent with the experimental observation (Fig. 1) that  $d\alpha/dt$  is constant.

If the relation between  $M_1$  and  $M_1^\circ$ ,  $\alpha$ , and  $M_2^\circ$  derived from Figure 1 together with eq. (11) is used, the rate at which styrene disappears is given by  $d\alpha_1/dt = 4/3 A_3 [(M_1^\circ + M_2^\circ)/M_1^\circ]$ .

## II. Dilute (2.4%, 4.6%) Ester Solutions

The consumption of styrene with time for the dilute ester systems is shown in Figure 4. For these cases, since  $M_2$ , which is less than 0.008 mole/l., is small, eq. (6) reduces to:

$$d\alpha/dt = k_p(k_1/2k_t)^{1/2}[(1 - \alpha)/(1 - 2g)^{1/2}] \quad (12)$$

The rate of disappearance of the already low initial concentration of ester cannot be estimated from infrared absorption spectra, i.e.,  $\alpha_2$  is not directly available. However,

$$d\alpha = \frac{M_1^\circ d\alpha_1 + M_2^\circ d\alpha_2}{M_1^\circ + M_2^\circ} \quad (13)$$

and

$$(1 - \alpha) = \frac{[(1 - \alpha_1)M_1^\circ + (1 - \alpha_2)M_2^\circ]}{M_1^\circ + M_2^\circ} \quad (14)$$

Furthermore, reactivity ratios  $r_1$  and  $r_2$ , for styrene and ester, respectively, can be obtained since the dilute solution copolymerizations appear to

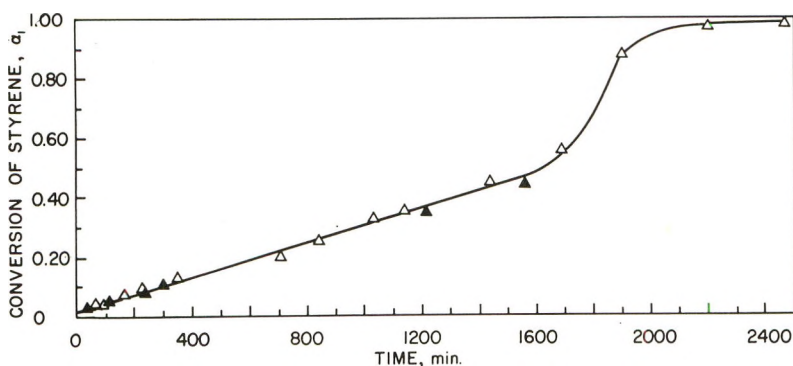


Fig. 4. Conversion of styrene with time for ( $\blacktriangle$ ) 2.4% and ( $\triangle$ ) 4.6% ester solutions; change in slope occurs about the time at which ester unsaturation disappears.

follow the conventional copolymer composition equation.<sup>3</sup> For  $r_2 = 0$ , the latter equation becomes:

$$M_2^\circ d\alpha_2 = \frac{(M_1^\circ d\alpha_1)M_2^\circ(1 - \alpha_2)}{[r_1(M_1^\circ)(1 - \alpha_1) + M_2^\circ(1 - \alpha_2)]} \quad (15)$$

where  $r$  is defined in terms of propagation rate constants for styrene radicals,  $M_1^\circ$ , and ester radicals,  $M_2^\circ$ , toward  $M_1$  or  $M_2$  monomer molecules;  $r_1 = k_{M_1^\circ M_1} / k_{M_1^\circ M_2}$  and  $r_2 = k_{M_2^\circ M_2} / k_{M_2^\circ M_1}$ . If eqs. (13), (14), and (15) are substituted into eq. (12), there is obtained:

$$\frac{d\alpha_1}{dt} = k_p \left( \frac{k_1}{2k_t} \right)^{1/2} \left[ \frac{(1 - \alpha_1)}{(1 - 2g)^{1/2}} \right] \left[ \frac{(1 + M\theta)(r_1 + M\theta)}{(r_1 + 2M\theta)} \right] \quad (16)$$

where

$$M = M_2^\circ / M_1^\circ$$

and

$$\theta = (1 - \alpha_2) / (1 - \alpha_1)$$

For small values of  $M$ , and if  $r_1$  is between 0.1 and 0.9 ( $r_1 = 0.16$  for the present copolymerization) eq. (16) reduces to:

$$\frac{d\alpha_1}{dt} = k_p \left( \frac{k_1}{2k_t} \right)^{1/2} \frac{(1 - \alpha_1)}{(1 - 2g)^{1/2}} \quad (17)$$

Since it was found experimentally that  $d\alpha_1/dt$  is constant,  $(1 - 2g)^{1/2} = B(1 - \alpha_1)$ , where  $B$  is a constant. A plot of gel fraction versus styrene conversion, of the form  $(1 - 2g)^{1/2}$  versus  $(1 - \alpha_1)$  in fact is linear with  $B = 1$  (Fig. 5). It is concluded consequently that for these dilute cases the rate at which styrene disappears, up to 40% conversion is given by:

$$d\alpha_1/dt = k_p(k_1/2k_t)^{1/2} \quad (18)$$

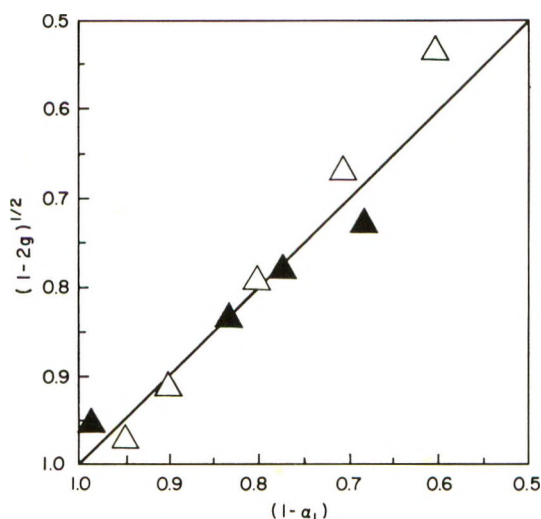


Fig. 5. Plot of  $(1-2g)^{1/2}$  vs.  $(1-\alpha_1)$  according to eq. (17) for (▲) 2.4% and (△) 4.6% ester solutions.

### III. Intermediate Ester Concentrations (9.8%, 20%, 30%)

The simplification of rate equation, eq. (6), so convenient in treating the dilute solution copolymerizations (i.e.,  $M_2^0$  is negligible), cannot be effected for the intermediate ranges. Consequently, if eqs. (13), (14), (15) are substituted in eq. (6), there is obtained:

$$\frac{d\alpha_1}{dt} = A_3 \left\{ \frac{(1-\alpha_1)^2}{(1-2g)} \theta \left[ \frac{(1+M\theta)(r_1+M\theta)}{(r_1+2M\theta)} \right] \times \left[ 1 + \sqrt{1 + \frac{2k_1k_t(1-2g)}{k_p^2(M_2^0)^2(1-\alpha_2)^2}} \right] \right\} \quad (19)$$

Since  $2k_1k_t/k_p^2(M_2^0)^2 \cong 1/DP^2$ , and the latter is very small, eq. (19) becomes:

$$\frac{d\alpha_1}{dt} = 2A_3 \left\{ \frac{(1-\alpha_1)^2}{(1-2g)} \theta \left[ \frac{(1+M\theta)(r_1+M\theta)}{r_1+2M\theta} \right] \right\} \quad (20)$$

From the measured linearity of  $\alpha_1$  with respect to time, to about 40% conversion of styrene (Fig. 6), eq. (20) should reduce to  $d\alpha_1/dt = \text{constant}$ . In fact, eq. (20) is not in accord with experimental data and predicts rates up to threefold slower than observed. The discrepancy is attributed to processes neglected in the present kinetic treatment. Thus, disappearance into the gel phase of branched sol copolymer containing several radical sites, propagation via addition of monomer or soluble copolymer to gel radicals and the increase with conversion of unreacted double bonds in the gel—all difficultly obtainable quantities—perhaps are responsible for the rate increase. For present purposes, the kinetics of this concentration range

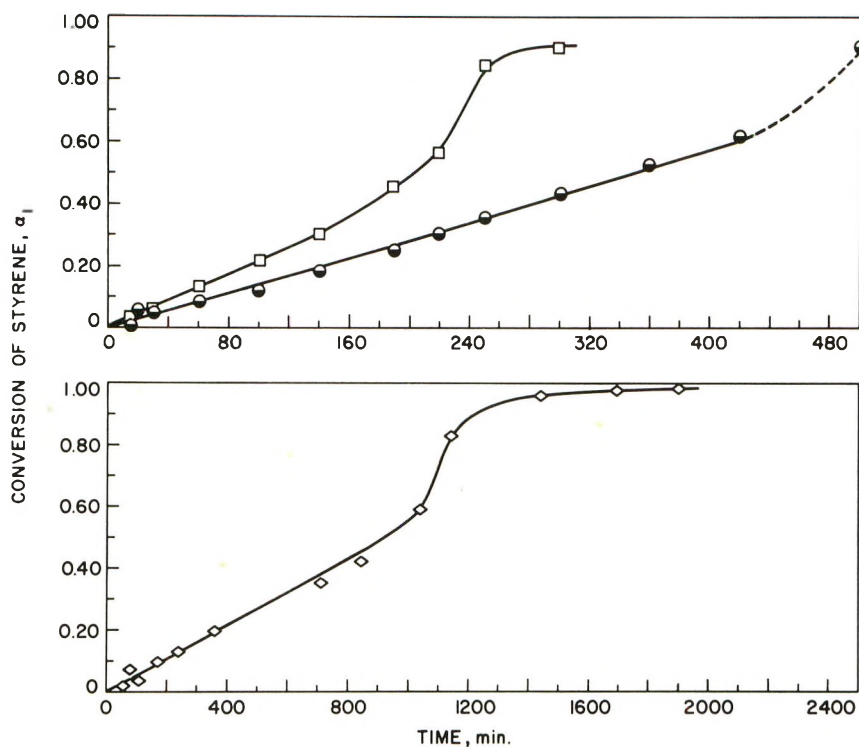


Fig. 6. Styrene consumption vs. time for ( $\diamond$ ) 9.8% ( $\bullet$ ) 20% and ( $\square$ ) 30% ester solutions; change in slope occurs about the time at which ester unsaturation disappears.

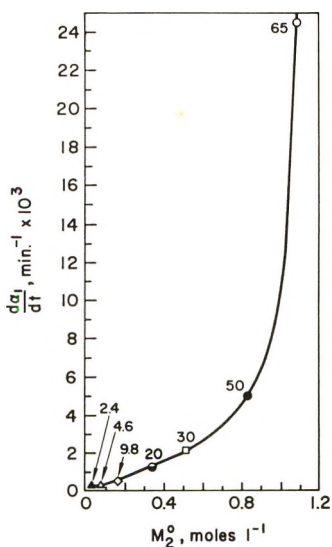


Fig. 7. Effect of initial ester concentration on rate of disappearance of styrene; concentrations in weight-% are given near symbols.



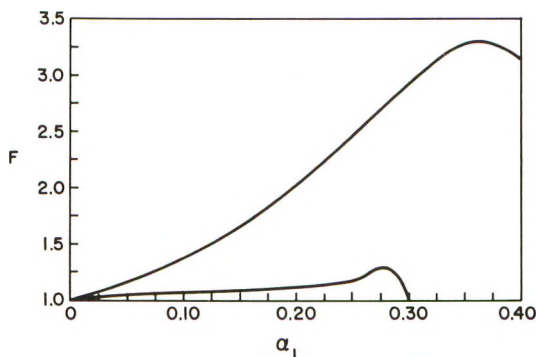


Fig. 8. Plot of  $F$  [eq. (21)] vs.  $\alpha_1$ ; lower curve is the correction factor for the 30% ester-styrene copolymerization; upper curve describes the 9.8% and 20% solutions.

are treated empirically. Multiplication of the right side of eq. (20) by  $F$ , where

$$F = \left[ \frac{(1+M)(r_1+M)}{r_1+2M} \right] \left[ \frac{(1-2g)(r_1+2M\theta)}{(1-\alpha_1)^2\theta(1+M\theta)(r_1+M\theta)} \right] \quad (21)$$

affords an expression [eq. (22)] which completely describes the kinetics of the copolymerization of the 9.8% to 30% ester solutions up to 40% conversion of styrene. Thus:

$$\frac{d\alpha_1}{dt} = 2A_3 \left[ \frac{(1+M)(r_1+M)}{(r_1+2M)} \right] \quad (22)$$

A plot of  $d\alpha_1/dt$  versus  $M_2^0$  is linear in this concentration range (Fig. 7);  $k_p^2/k_t$  is calculable from the slope of this line. Equation (22) is independent of  $r_1$  if  $0 < r_1 < 0.9$  and states that  $\alpha_1$  is linear with time for a given initial feed mixture.

A plot of  $\alpha_2$  versus  $t$  is not linear; from initial conversions of ester unsaturation (to 10%), the rate at which overall unsaturation disappears is given by  $d\alpha/dt = 2A_3$ .

Figure 8 describes the variation in the correction factor  $F$  with conversion; while no significance is attached to numerical values, the shape of the curve suggests that the copolymerization rate increase is related to an inordinate increase in the number of free radicals and/or unreacted double bonds in the gel phase as reaction proceeds.

### Kinetic Parameters

No information about copolymerization rates of similar systems is available. Estimated value for  $k_p^2/k_t$  for the different concentration ranges are summarized in Table I. Diffusion control of any of the rate processes is not noted, presumably because of the high diffusivity of the primary chains formed in this particular system, relative to the long ones in the reported<sup>1</sup> methyl methacrylate copolymerization. Steric control of

the kinetics of the concentrated ester solutions is reflected in the changing  $k_p^2/k_t$  for the 65% and 50% cases. The presently derived  $k_p^2/k_t$  for the most dilute ester-styrene solutions,  $0.43 \times 10^{-2}$  l./mole-min., might be compared with the reported one of  $0.27 \times 10^{-2}$  l./mole-min. for the radiation-initiated bulk polymerization of styrene under roughly similar experimental conditions of dose rate and temperature.<sup>4</sup>

TABLE I  
Kinetic Parameters for Styrene-Ester Copolymerizations

Initial [ester]/[styrene]	$k_p^2/k_t$ , l./mole-min. $\times 10^2$	How calculated
0.327	2.52	eq. (11)
0.175	0.79	eq. (11)
0.075	0.49	
0.044	0.47	eq. (22)
0.019	0.43	
0.008		Assuming values same as
0.004	0.43	that for the 9.8% polyester solution ( $M = 0.019$ )

The initiation rate constant for the dilute systems, approximated from the above value of  $k_p^2/k_t$  together with eq. (18), is  $3.6 \times 10^{-5}$  mole/l.-min.  $G_{\text{radical}}$  (the number of initiating radicals formed by  $\gamma$ -irradiation per 100 e.v. absorbed) calculated from this  $k_i$  is 4.2;  $G_{\text{radical}}$  of 0.9 is reported for bulk styrene.<sup>4</sup>

## EXPERIMENTAL

### Materials

Starting ester was synthesized from reagent grade maleic anhydride, phthalic anhydride, and propylene glycol according to reported procedures.<sup>5</sup>

ANAL. Calculated for two ester molecules comprised of a total of 3 maleic units, 6 phthalic units and 9 propylene glycol units, less 7 water molecules and containing 2 free hydroxyl and 2 free carboxyl groups: C, 60.0%; H, 5.1%;  $\bar{M}_n$ , 870. Found: C, 60.1%; H, 4.8%;  $\bar{M}_n$  (cryoscopic in benzene), 890.

Double bond concentration of 1.5 per molecule was estimated from stoichiometric material balance; monomer was distilled *in vacuo* before use.

### Irradiations and Kinetics

Solutions of the required concentrations of ester in styrene were degassed and sealed *in vacuo* in small ampules the contents of which were transferred to fixed thickness (0.020–0.040 mm.) liquid infrared cells; the latter step was effected in a nitrogen atmosphere (<0.03% oxygen). Irradiations were with  $\gamma$ -rays from  $\text{Co}^{60}$  with dose rates ranging from  $8.33 \times 10^3$  to  $7.10 \times 10^3$  rad/min. at 33°C. It was assumed that a dose of 1 Mrad corresponds to the absorption of  $62.5 \times 10^{18}$  e.v./g. of polymer.

Analyses on a Perkin-Elmer Model 237 spectrophotometer were performed in the infrared cells within 1-2 min. after irradiation, using the  $6.10\ \mu$  and the  $6.15\ \mu$  peak to estimate ester and styrene unsaturation, respectively, by means of the standard base line technique. Previously calibrated styrene-ester solutions were found to obey Beer's law over the ester concentration range from 0% to 65%. Below initial ester concentrations of 30%, the absorption peak for this component was too weak for kinetic analyses. Reproducibility of styrene and ester concentration measurements is estimated to be 1.0% and 5.0%, respectively.

### Gel Fractions

About 0.5 g. degassed samples were irradiated *in vacuo*, then placed in thimbles consisting of a 100-mesh copper screen within a second 200-mesh Monel screen. Soluble polymer was removed quantitatively by hot benzene in 170 hr. in a Soxhlet extractor and the gel dried to constant weight *in vacuo* at 75°C. Gel fractions were reproducible to  $\pm 5\%$ ; most to  $\pm 3\%$ .

That no dark or post-irradiation reaction occurred was confirmed by noting that: (1) transmittances of both unsaturated peaks in the infrared and gel fractions were independent of time elapsed after irradiation and before analyses and (2) use of extraction solvents also containing the radical inhibitor *tert*-butyl catechol did not alter the measured gel fractions.

### Soluble Copolymer

The absence of soluble copolymer (from which it is concluded that copolymer entering the gel phase is of short chain lengths) in the concentrated ester solutions (65-50%) was confirmed from elemental analysis of the nonvolatile residue remaining after removal of the gel fraction; only starting ester was isolated at a total conversion of unsaturation of 16%. Additionally, the molar ratio of styrene:ester in the gel, estimated from elemental analysis of the gel, was identical with the ratio calculated from the fraction of styrene polymerized (measured from infrared), provided all the styrene disappearing enters the gel phase.

### Hydrolysis of Gel

About 60 g. of the rigid gel isolated from low conversion polymerizations (16%) of the 65% ester-styrene solution was hydrolyzed according to a modification of a described procedure.<sup>6</sup> Refluxing in 500 ml. of a 10% potassium hydroxide-benzyl alcohol mixture was continued for 20 days in a stainless steel flask, after which several hundred milliliters of benzene was added and the whole extracted with water. Acidification of the aqueous layer resulted in the white styrene-maleic acid copolymer which was purified by another reprecipitation by aqueous hydrochloric acid from methyl alcohol solution; total yield, 4.0 g. Since about half of the starting gel was attacked, this corresponds to 32% of the theoretical yield. If

bimolecular termination is assumed for the  $\gamma$ -initiated copolymerization, the kinetic chain length contains 15 monomer units (where the monomer units are styrene and ester molecules). Its  $\bar{M}_n$ , measured cyroscopically

TABLE II  
Experimental Data for Styrene-Ester Copolymerizations

Initial [ester] [styrene], $M$	Conversion of		Time $t$ , min.	Dose, Mrad	Rate of conversion of styrene $d\alpha_1/dt$ , min. <sup>-1</sup>	Gel fraction $g$
	Styrene, $\alpha_1$	Ester unsaturation, $\alpha_2$				
0.327(65) <sup>a</sup>	0.094	0.14	3.8	0.030	0.0245	0.21
	0.156	0.24	6.4	0.050		0.26
	0.312	0.48	12.8	0.100		0.41
	0.548	0.85	22.3	0.175		0.57
0.175(50)	0.052	0.09	10.0	0.071	0.0052	0.14
	0.104	0.31	20.0	0.142		0.28
	0.156	0.47	30.0	0.212		0.36
	0.208	0.58	40.0	0.283		0.43
0.075(30)	0.260	0.68	50.0	0.354	0.0021	0.49
	0.043	0.17 <sup>b</sup>	20.0	0.142		0.09
	0.086	0.32	40.0	0.283		0.16
	0.172	0.57	80.0	0.567		0.30
0.044(20)	0.258	0.75	120.0	0.850	0.0014	0.36
	0.344	0.87	160.0	1.133		0.48
	0.027	0.12 <sup>b</sup>	20.0	0.142		0.04
	0.083	0.35	60.0	0.425		0.12
0.019(9.8)	0.166	0.60	120.0	0.850	0.00056	0.21
	0.221	0.73	160.0	1.133		0.27
	0.304	0.85	220.0	1.558		0.35
	0.386	0.93	280.0	1.983		0.41
0.008(4.6)	0.056	0.27 <sup>b</sup>	100.0	0.710	0.00028	0.06
	0.112	0.48	200.0	1.420		0.14
	0.224	0.76	400.0	2.830		0.27
	0.336	0.90	600.0	4.250		0.37
0.004(2.4)	0.448	0.97	800.0	5.670	0.00028	0.50
	0.560	0.99	1000.0	7.100		0.62
	0.045		160.0	1.133		0.02
	0.056		200.0	1.420		0.04
0.004(2.4)	0.112		400.0	2.830	0.00028	0.12
	0.168		600.0	4.250		0.18
	0.224		800.0	5.670		0.24
	0.280		1000.0	7.100		0.28
0.004(2.4)	0.350		1250.0	8.854	0.00028	0.34
	0.420		1500.0	10.625		0.40
	0.009 <sup>c</sup>		330.0	2.337		0.02
	0.028		400.0	2.830		0.04
0.004(2.4)	0.190		1000.0	7.100	0.00028	0.15
	0.244		1200.0	8.500		0.20
	0.336		1540.0	10.907		0.24

<sup>a</sup> Per cent ester given in parentheses.

<sup>b</sup> For these ester concentrations,  $\alpha_2$  was calculated from eq. (23).

<sup>c</sup> The gel point, at which 8% of the styrene had disappeared, was taken as zero conversion.

in dioxane, was 3000;  $DP \cong 30$ . Elemental analysis was in reasonable accord with the 2:1 molar ratio of styrene: starting ester in the gel derived from infrared kinetic data. Calculated for  $(C_{20}H_{20}O_4)_{10}$ : C, 74.0%; H, 6.2%. Found: C, 73.6%; H, 7.2%.

Table II summarizes the experimentally measured parameters on which the kinetic scheme is based. In the figures given in this paper, reproducibility of the measurement is indicated by the size of the symbols used.

### Reactivity Ratios

For the dilute ( $\leq 30\%$ ) ester solutions, the product compositions of which are explainable in terms of normal copolymerization composition theory, approximate reactivity ratios  $r_1$  and  $r_2$  for styrene and ester, respectively, were measured. Based on initial feed mixtures of 30%, 20%, and 9.8% ester solutions polymerized to 10% styrene conversion, and from concentrations of each component in the gel (calculated from infrared and gel fraction data), Fineman and Ross plots<sup>7</sup> indicated  $r_2 = 0$  and  $r_1 = 0.29$ . A better value of  $r_1$  then was obtained from the integrated form of the copolymer composition eq. (15), letting  $r_2 = 0$ :

$$(1 - \alpha_1) = \left( \frac{1 - \alpha_2}{1 - \alpha_1} \right)^{r_1/1-r_1} \left[ \frac{(1 - r_1) - M}{(1 - r_1) - M \left( \frac{1 - \alpha_2}{1 - \alpha_1} \right)} \right]^{1/1-r_1} \quad (23)$$

For the 30% ester solution, at a sol fraction of 0.70 when  $\alpha_1 = 0.17$ ,  $\alpha_2 = 0.59$ ,  $M_2^0 = 0.05$ , and  $M_1^0 = 0.67$ ,  $r_1$  was found to be  $0.16 \pm 0.10$ . This value, used in the present work, is to be compared with reported values<sup>8</sup> for styrene with diethyl fumarate ( $r_1 = 0.30 \pm 0.02$ ,  $r_2 = 0.07 \pm 0.007$ ) and diethyl maleate ( $r_1 = 6.5 \pm 0.5$ ,  $r_2 = 0.05 \pm 0.01$ ).

It is a pleasure to acknowledge the contributions of Dr. Serge Gratch, who suggested the kinetic scheme and offered valuable assistance throughout the course of this work.

### References

1. Gordon, M., and I. McMillan, *Makromol. Chem.*, **23**, 188 (1957).
2. Barrett, R., and M. Gordon, *The Physical Properties of Polymers*, S.C.I. Monograph No. 5, Macmillan, New York, 1959, p. 183.
3. Alfrey, T., J. Bohrer, and H. Mark, *Copolymerization*, Interscience, New York, 1952, p. 10.
4. Chapiro, A., *J. Chim. Phys.*, **47**, 764 (1950).
5. Parker, E., and E. Moffett, *Ind. Eng. Chem.*, **46**, 1615 (1954).
6. Funke, W., W. Gebhardt, H. Roth, and K. Hamann, *Makromol. Chem.*, **28**, 17 (1958).
7. Fineman, M., and S. Ross, *J. Polymer Sci.*, **5**, 269 (1950).
8. Lewis, F., C. Walling, W. Cummings, E. Briggs, and F. Mayo, *J. Am. Chem. Soc.*, **70**, 1519 (1948).

### Résumé

On a étudié les cinétiques de copolymérisation initiée par les rayons gamma, avec formation de gel, du styrène avec l'ester non-saturé contenant 1,5 double liaison par molé-



cule de poids moléculaire moyen en nombre de 890 (dérivé de l'anhydride maléique, de l'anhydride phtalique et du propylène glycol). Les concentrations initiales en ester varient de 65% à 2.4%. A partir des fractions de gel déterminées expérimentalement, des vitesses de disparition du styrène et de l'ester insaturé (mesurées jusqu'à conversion complète de l'insaturation en ester) et du degré de polymérisation des chaînes en croissance, on a proposé un modèle basé sur une copolymérisation par radical libre, en admettant une propagation effective simple, une vitesse de terminaison constante ( $k_p$  et  $k_t$ , respectivement) et une terminaison de chaîne bimoléculaire excepté entre une paire de radicaux de gel immobile. On a considéré trois domaines de concentration en ester. A des concentrations élevées en ester ( $\geq 50\%$ ) le styrène et l'ester pénètrent dans le gel à une vitesse constante (rapport molaire de styrène: double liaison ester 2:1), ce qui exclut l'application de la théorie conventionnelle de la composition du copolymère. La vitesse à laquelle l'insaturation globale,  $\alpha$ , disparaît, est donnée par  $d\alpha/dt = (k_p^2/kt)M_2^0$  où  $M_2^0$  est la concentration molaire initiale de l'insaturation de l'ester. La vitesse à laquelle le styrène,  $\alpha_1$ , disparaît est donnée par  $d\alpha_1/dt = \frac{2}{3}(k_p^2/kt)M_2^0(M_1^0 + M_2^0)/M_1^0$ . La vitesse à laquelle le styrène est consommé dans les solutions diluées ester-styrène ( $\geq 4.6\%$ ), où  $M_2^0$  est petit et négligeable, est donnée par  $d\alpha_1/dt = k_p(k_1/2kt)^{1/2}$ . Les vitesses de polymérisation pour les domaines de concentration intermédiaire en ester (10% à 30%) sont plus élevées que celles prévues à partir du modèle simple. Une expression empirique de la vitesse est présentée et décrit ces systèmes à 40% de conversion du styrène;  $d\alpha/dt = (k_p^2/kt)M \left\{ \frac{(1+M)(r_1+M)}{(r_1+2M)} \right\}$ , où  $M$  est le rapport de l'insaturation de l'ester au styrène dans le mélange de départ et où  $r_1$  est le rapport de réactivité pour le styrène, défini de la manière habituelle. Pour les conversions initiales de l'insaturation de l'ester (jusqu'à 10%)  $d\alpha/dt = (k_p^2/kt)M_2^0$ .

### Zusammenfassung

Es wurde die Kinetik der durch  $\gamma$ -Strahlen gestarteten, unter Gelbildung verlaufenden Copolymerisation von Styrol mit von Maleinsäureanhydrid bzw. Phthalsäureanhydrid abgeleiteten ungesättigten Estern (1,5-Doppelbindungen pro Molekül, Zahlenmittel des Molekulargewichts 890) bei Ester-Anfangskonzentrationen von 65 bis 2,4% untersucht. Aus experimentell untersuchten Gelfraktionen, der Geschwindigkeit des Verbrauches von Styrol- und Esterdoppelbindungen (Messungen bis zum vollständigen Umsatz der Esterdoppelbindungen) und dem Polymerisationsgrad der wachsenden Ketten wird unter der Annahme einer einzigen effektiven Wachstums- und Geschwindigkeitskonstante ( $k_p$  bzw.  $k_t$ ) und eines bimolekularen Kettenabbruches (ausgenommen zwischen einem Paar unbeweglicher Gelradikale) ein Modell auf der Basis einer radikalischen Copolymerisation vorgeschlagen. Es werden drei Bereiche der Esterkonzentration getrennt betrachtet: I. Bei hohen Esterkonzentrationen ( $\geq 50\%$ ) treten Styrol und Ester mit einer konstanten Geschwindigkeit in das Gel ein (molares Verhältnis Styrol: Esterdoppelbindungen von 2:1) und die konventionelle Theorie über die Copolymerzusammensetzung kann nicht angewandt werden. Die Geschwindigkeit, mit der die Bruttoanzahl  $\alpha$  der Doppelbindungen abnimmt, ist gegeben durch  $d\alpha/dt = (k_p^2/kt)M_2^0$ , wobei  $M_2^0$  die molare Anfangskonzentration der Esterdoppelbindungen ist. Die Geschwindigkeit mit der Styrol ( $\alpha_1$ ) verbraucht wird, ist durch  $d\alpha_1/dt = \frac{2}{3}(k_p^2/kt)M_2^0(M_1^0 + M_2^0)/M_1^0$  gegeben. II. In verdünnten Ester-Styrollösungen ( $\geq 4,6\%$ ) mit vernachlässigbar kleinem  $M_2^0$  ist die Geschwindigkeit des Styrolverbrauches  $d\alpha_1/dt = k_p(k_1/2kt)^{1/2}$ . III. Bei dazwischen liegenden Esterkonzentrationen (10% bis 30%) ist die Polymerisationsgeschwindigkeit höher als der Erwartung auf Grund des einfachen Modells entspricht. Es wird eine empirische, für diese Systeme bis zu einem Styrolumsatz von 40% gültige Beziehung für die Geschwindigkeit angegeben,  $d\alpha/dt = (k_p^2/kt)M \left\{ \frac{(1+M)(r_1+M)}{(r_1+2M)} \right\}$ , wobei  $M$  das Verhältnis der Anzahl der Doppelbindungen von Ester und Styrol in der Ausgangsmischung und  $r_1$  das in üblicher Weise definierte Reaktivitätsverhältnis für Styrol ist. Für niedrige Umsätze der Esterdoppelbindungen (bis 10%) gilt  $d\alpha/dt = (k_p^2/kt)M_2^0$ .

Received April 8, 1963



# On the Relation between Long Spacings, Molecular Length, and Orientation in Long Chain Compounds with Reference to the Possibility of Chain Folding.

## Part I. Oligomeric Amides

F. J. BALTA CALLEJA\* and A. KELLER, *H. H. Wills Physics Laboratory, University of Bristol, Royal Fort, Bristol, England*

### Synopsis

In this set of two papers the possibility of chain folding occurring in chain molecules not much longer than the presumed fold length was examined. The present paper deals with oligomeric amides. Following up the preceding work on the relation between long spacing and chain length by Zahn and Pieper on the same compounds, the relation between long spacings and chain orientation was examined in order to assess how far oblique structures could present alternatives to chain folding. It could be concluded that they cannot, the chains remaining straight up to a certain length only (80 Å.), beyond which chain folding offers the most probable explanation. The preparation and examination of oriented aggregates required for this conclusion to be reached are discussed. In addition the dependence of the long spacings on the crystallization temperature, and relation between melting point and long spacing are demonstrated, and examples of annealing behavior are given all of which have their corresponding counterpart in the chain-folded high polymers.

### 1. INTRODUCTION

Long chain polymeric molecules crystallize in a regularly folded configuration from solution, and there are indications that they may well do the same at least to some extent from the melt.<sup>1</sup> The fold period makes itself apparent morphologically through the familiar lamellar type crystallization—the thickness of the lamellae being related to the fold period—and by diffraction effects giving rise to reflections at low angles. Long chain compounds, not yet classified as high polymers, as e.g., paraffinoid substances, are known to form lamellar crystals and give rise to reflections at low angles. In these cases, however, the features in question are related to the length of the extended molecule. Clearly the transition from the straight chain crystallization of oligomers to the folded crystallization of polymers is of central interest.

It has been suggested<sup>2</sup> that oligomers may fold back on themselves once

\* Present address: Instituto de Fisica "Alonso de Sta Cruz," C.S.I.C. Serrano 119, Madrid 6, Spain.

the chain length exceeds a critical value, a point which would have important structural and theoretical implications.<sup>1</sup> A straight attack on this problem has been handicapped by the scarcity of materials of the relevant chain length. An early attempt was made by Keller and O'Connor<sup>3</sup> by using degradation products and the lowest fractions of commercial low pressure polyethylene and the characteristic symptoms of chain folding (long periods shorter than the average chain length, and dependence of these long periods on crystallization temperature) was confirmed for all except the lowest fraction where the chain length (undoubtedly an average) coincided with the long periods measured. Since then oligomeric amides of uniform and well defined lengths were prepared by Zahn and co-workers,<sup>4</sup> and more recently the analogous urethane compounds by Kern and co-workers.<sup>6</sup> It was found that<sup>5, 6</sup> the long periods increase with the chain length up to a point only and remain constant thereafter (affected somewhat by physical treatments,<sup>7</sup> where this approximately constant value falls in the range of the long periods observed in the corresponding polymer. This seems to indicate that at a certain length a sharp transition between straight chain and chain-folded crystallization is reached in accordance with the aforementioned suggestion.\*

However, this conclusion is not yet unambiguous on the evidence presented. The crucial long spacings were derived from powder photographs, the relation between molecular orientation and the planes giving rise to the long spacings being unknown. It is known that paraffinoid substances can crystallize with structures of different obliquities (the chains having different inclinations to the basal planes) while retaining the same subcell (e.g., Keller<sup>8</sup>). This can give rise to different long spacings for the same chain length. Similar effects were noticed also in chain folded polymers<sup>9</sup> This means that not the long period itself but only the value obtained by its division with the sine of the chain, or segment, inclination to the basal plane is equal to the length of the molecule in the former case and to that of the fold length in the latter (the comparatively small end-to-end gap or a part). Where significant conclusions depend on the accurate identification of these quantities clearly the chain inclination has to be assessed independently.

In the present two papers such assessments were carried out within limits which permit conclusions to be reached on the issue in question. In addition some further analogies between oligomers and polymers were found and those reported by Zahn and Pieper previously<sup>7</sup> further extended and elaborated. The material is divided in two papers according to the substances used.

The first (present) paper deals with oligomeric amides. These were available with well-defined uniform chain lengths increasing by small increments up to relatively moderate chain lengths not much in excess of

\* Zahn and Gleitsman (GDCh meeting, Bad Nauheim, 1962, now in press) proposed the name "pleinamer" for oligomers which show long spacings unaffected by the molecular weight.

the long periods normally recorded. The second paper<sup>10</sup> which follows will be concerned with a series of poly(ethylene oxide)s covering a large range of molecular weights, including some very low ones which could be classed as oligomers. Here the chain lengths are not uniform and their mean values differ by much larger steps from one member of the series to the next.

## 2. MATERIALS AND TECHNIQUES

The samples for the amide work were received from Professor Zahn of the Technische Hochschule, Aachen, Germany. They were poly- $\epsilon$ -caproamides of the type Z-(Cap)<sub>*n*</sub>OH, where Cap stands for NH(CH<sub>2</sub>)<sub>5</sub>-CO, and Z for -COOCH<sub>2</sub>C<sub>6</sub>H<sub>5</sub>, *n* ranging from 1 to 12. Owing to the very small quantity of *n* = 12 available, mostly compounds only up to *n* = 11 were used. The compounds were received in powder form as obtained by recrystallization. The higher members were available as recrystallized from two solvents: ethyl alcohol and dimethylformamide (DMF). The compounds were examined by us as received, or were recrystallized again. Examinations were also carried out after annealing and fusion and subsequent recrystallization.

The samples were examined mainly by diffraction methods, primarily x-rays, at low and wide angles, and to some extent also by electron diffraction under the electron microscope. For the first and major part of the work a Kratky-type collimator (slit collimation) was used, but later a focusing Franks<sup>11</sup> camera giving point collimation became available.

## 3. THE DIFFRACTION PATTERN

As reported by Zahn and Pieper<sup>7</sup> all except the two lowest members gave the two characteristic strong polyamide reflections at 4.5 and 3.7 Å. These correspond to planes parallel to the molecules. In nylon 6 (the polymeric analog of our oligomers) they are indexed as 200 and the composite 002 and 202, respectively, where the 002 contains the hydrogen-bonded planes.<sup>12</sup> Both reflections are equatorial in the drawn fiber (*b* being the fiber direction). These two reflections suffice for defining the molecular direction in our oligomers even if the crystal structure is not known. In addition a third reflection of variable intensity at 4.1–4.2 Å. can become occasionally visible. This again has its counterpart in the polymer<sup>13</sup> where it has been attributed to a lateral spacing arising from a less perfect form of chain packing. Further, there are the long spacings in the low angle region already referred to as the main object of our studies. Several reflections in the wide angle region have been identified as due to planes perpendicular to the chain direction (4.4, 5.5, 6.5, 7.8, and 8.5 Å. in the different compounds). These have no counterparts in the polymer. While some of them could be the higher orders of the long spacings, (e.g., 4.4 could be the seventh order of *n* = 4 or ninth order of *n* = 5), others could not. No further reference to these will be made.

Reference will be made to three kinds of repeat unit. Firstly the true unit cell, comprising the whole molecule or straight part thereof, secondly the subcell, comprising the monomer repeat, and thirdly a smaller subcell defined by the repetition of the chain zigzag, ignoring the distinction between  $\text{CH}_2$ ,  $\text{CO}$ , and  $\text{NH}$  groups. This zigzag is essentially the paraffin subcell repetition along the chain and will be denoted by subscript  $s$  all through.

#### 4. EXPERIMENTAL RESULTS AND THEIR INTERPRETATION

##### 4.1. Chain Length-Long Spacing Relation in Samples as Received

The relation between chain length and long spacing of the different samples is shown in Figure 1. Apart from some details, the main trend is identical to that in the curves by Zahn and Pieper.<sup>7</sup> Thus it rises

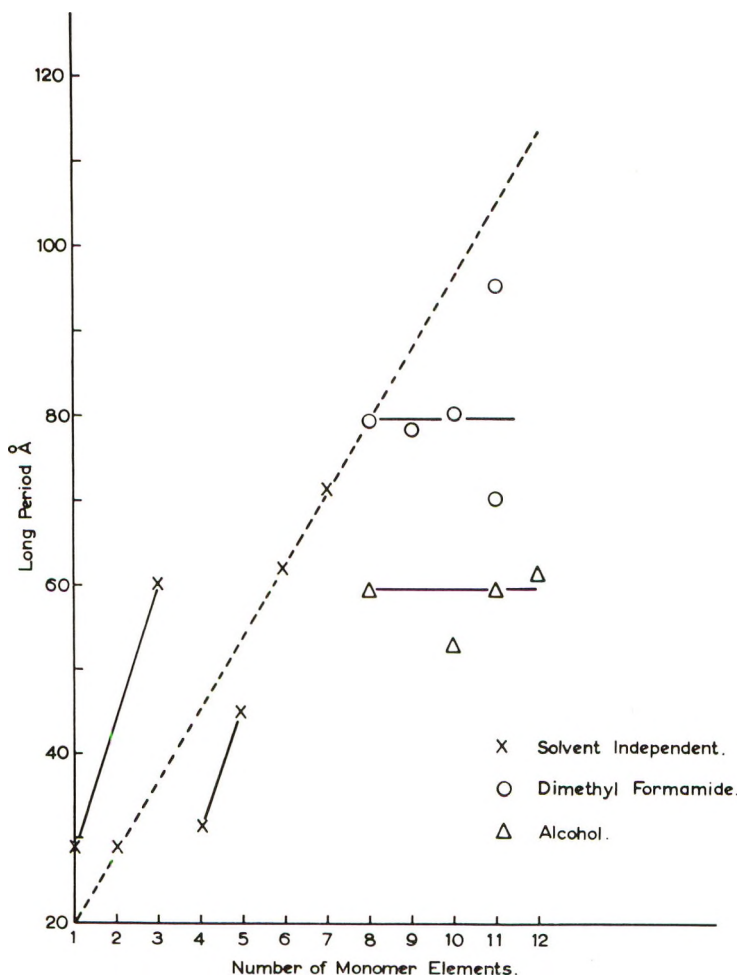


Fig. 1. X-ray long periods as a function of monomer units (see text).



steadily till  $n = 8$ , beyond which it stays approximately constant. For brevity we shall call oligomers with  $n < 8$  "low" and those with  $n > 8$  "high." Figure 1 also gives the spacings expected from extended chains in a vertical structure (molecules perpendicular to basal plane) shown by the interrupted straight line. Its ordinates ( $L$ ) are given by  $L = 8.5n + 11.5$  in Angstroms, where 8.5 A. is the length of the monomer repeat,  $n$  is the number of monomer units, 11.5 is the length of the endgroups (8.5 A.) plus the end-to-end gap between molecules (3 A.).<sup>7</sup>

Among the low members only those with  $n = 2, 6,$  and  $7$  show long spacings corresponding to the fully extended length of the molecule. The values for those with  $n = 1$  and  $3$  are higher, those with  $n = 4$  and  $5$  are lower. Beyond  $n = 8$  all points are below the straight interrupted line but follow the approximately horizontal branches, recrystallization from alcohol giving the lower, that from DMF the higher, with considerable scatter about the horizontal in the latter. ( $n = 11$  from DMF gave no clear reflection as received; the two points in Figure 1 resulted from subsequent recrystallization by ourselves under different conditions to be described in section 4.5.1.)

Spacings shorter than expected from the extended molecule could be due to oblique structures of appropriate obliquities. Where they are longer they could be the first-order reflections of a unit cell two molecules long, spacings shorter than the extended double molecule but longer than the extended single molecule being due again to oblique structures. These considerations could in principle be applied to all points in Figure 1; nevertheless the approximate constancy beyond  $n = 8$  raises the possibility of chain folding.<sup>7</sup>

The obliquities required to account for points in Figure 1 are listed in Table I, where the tilt angles  $\phi$  (angle between the chain direction and the normal to the basal plane) are given by  $\cos\phi = d/L$  ( $d \equiv$  long spacing). It will now be examined whether the tilt values in Table I are feasible or not.

It will be assumed that the adjacent chain atoms, irrespective of their chemical identity, stay in their original register, i.e., the smallest of the subcells defined above is maintained. As done previously in paraffins and polyethylene<sup>8,14</sup> the obliquity will be expressed by defining the  $0k0$  planes (basal planes) of the true unit cell in terms of the indices of the subcell with  $a_s = 9.5$  A.,  $b_s = 2.5$  A.,  $c_s = 8.0$  A.,  $\beta_s = 65^\circ$ ,  $a_s$ ,  $c_s$ , and  $\beta_s$  being the cell parameters of nylon 6 normal to the chain direction (nylon 6 is monoclinic). The obliquity could be achieved by shear on any  $h0l$  plane. In polyamides, however, the shear plane (001) suggests itself as this maintains the hydrogen bonds, the different obliquities arising from the different displacements between the hydrogen bonded sheets. This lead to terminal planes of  $\{0kl\}_s$  type. The preservation of the subcell requires displacements of  $(m/2)b_s$  between adjacent sheets, where  $m$  is an integer and  $b_s$  the zigzag repeat. (With odd  $m$ -s, an additional rotation through  $180^\circ$  is required in alternate sheets (see Keller<sup>8</sup>.) \* This restricts  $k$  and  $l$  to values which make  $l/k$  integer provided that shear is uniform.



The last column in Table I denotes the  $(01l)_s$  planes with inclination ( $\phi'$ , penultimate column) nearest to that observed and consistent with the preservation of the subcell,  $\phi'$ , the angle between chain direction and basal plane normal, being given by  $\tan \phi' = mb_s/d_{002}$  (where  $d_{002} = 002$  interplanar spacing). It is seen that for all low members a satisfactory fit can be achieved where  $\phi$  and  $\phi'$  agree within 1%. For the high members the fit is in general worse, only two tilts that of  $n = 12$  from alcohol and  $n = 10$  from DMF can be accounted for on the basis of (001) as shear plane. While some improvement could be achieved by other physically less realistic shear planes, the tilted structure explanation for long spacings

TABLE I  
Interpretation of Long Spacings in Terms of Chain Inclination from Disoriented Specimens

Number of monomer elements $n$	Exp. tilt angle ( $\phi$ )	Filt angle ( $\phi'$ ) for nearest $(01l)_s$ terminal plane (next column)	Terminal plane
Lower Oligomers			
1	46°30'	46°	$\{013\}_s$
2	No tilt	No tilt	$\{010\}_s$
3	34°	34°20'	$\{012\}_s$
4	45°	46°	$\{013\}_s$
5	45°	46°	$\{013\}_s$
6	No tilt	No tilt	$\{010\}_s$
7	No tilt	No tilt	$\{010\}_s$
Higher Oligomers: Crystallized from Alcohol			
8	42°30'	46°	$\{013\}_s$
10	57°	53°50'	$\{014\}_s$
11	56°30'	53°50'	$\{014\}_s$
12	54°30'	53°50'	$\{014\}_s$
Higher Oligomers: Crystallized from Dimethylformamide			
8	No tilt	No tilt	$\{010\}_s$
9	26°30'	18°50'	$\{011\}_s$
10	33°30'	34°20'	$\{012\}_s$
11	47°50'	46°	$\{013\}_s$
11	26°30'	18°50'	$\{011\}_s$

does not appear to be as satisfying as for the low members. By relaxing the condition of uniform shear terminal planes other than  $01l$  could be admitted. No doubt with a suitable choice of  $k$  and  $l$  indices, where  $l/k$  need not be an integer, the observed obliquities could be closely matched. This possibility, while more complicated, cannot be ruled out based on data from disoriented system alone. To clarify this point some information on the molecular orientation with respect to the terminal planes is required, which only oriented systems can furnish.

In the following we shall concern ourselves with oriented systems. The ideal sample would be the macroscopic single crystal.

#### 4.2. Attempts to Grow Macroscopic Single Crystals

While attempts were only partially successful, they may nevertheless be of some interest. Polar solvents were used: water, ethyl, and methyl alcohol for the low members; ethyl alcohol, DMF, and formic acid for the high ones. The solutions were prepared by heating. Crystallization occurred partly on cooling and partly on evaporation of the solvent over days or weeks. The lowest members ( $n = 1,2,3$ ) gave flat parallelepiped crystals suitable for taking x-ray rotation photographs. The higher members usually gave only spherulite type aggregates and polyhedral



Fig. 2. Single crystals of  $Z-(\text{Cap})_{10}-\text{OH}$  grown from formic acid. Photomicrograph,  $1000\times$ .

nearly uniformly extinguishing objects resembling some objects obtainable in polymers ("hedrites").<sup>15</sup> In one instance, however, the decamer gave clearly defined prismatic crystals from formic acid (Fig. 2). The melting point was near  $200^{\circ}\text{C}$ . which is the one expected.<sup>4</sup> The interface angle  $65^{\circ}$  is equal to  $\beta$  in the nylon 6 structure, implying that the molecules are perpendicular to the basal planes. Spotty x-ray patterns and in one case recognizable layer lines were obtained. In principle, such crystals should permit a complete analysis; however, they were both too small and too clustered for this to be carried out with out x-ray facilities.

### 4.3. Submicroscopic Single Crystals and Their Examination with Electron Diffraction

Crystalline suspensions were prepared by cooling solutions partly in ethyl alcohol and DMF and sometimes in formic acid. The low members from DMF gave flat needles. Higher members both from alcohol and DMF and occasionally from formic acid gave thicker, sheaflike aggregates, often forming star-shaped objects (Fig. 3). (Similar observations were made recently by Pieper.<sup>16</sup>) An underlying lamellar structure could always be recognized, which, as in Figure 4, could closely resemble features encountered in polymers.



Fig. 3. Star-shaped aggregates of Z-(Cap)<sub>11</sub>-OH crystals from alcohol. Electron micrograph, 3000 $\times$ .

The representative objects were, as a whole, too thick for electron diffraction, except for the thinner edges which produced patterns. With a large area being selected (containing sufficient number of thin edges) the two strong polyamide rings at 4.5 and 3.7 Å. and occasionally the third ring at 4.1–4.2 Å., mentioned earlier, could be observed. The spacings were identified by internal calibration with TICl. By reducing the area selected, the rings became spotty, and occasionally single crystal patterns as in Figure 5 were obtained, revealing the 200, 002, and 202 reflections of nylon 6 with the correct spacings and monoclinic angle ( $\beta = 65^\circ$ ). This identifies the polyamide subcell, implying also that the molecules are perpendicular to the substrate.

Even when single crystal patterns were not distinguished, the molecular



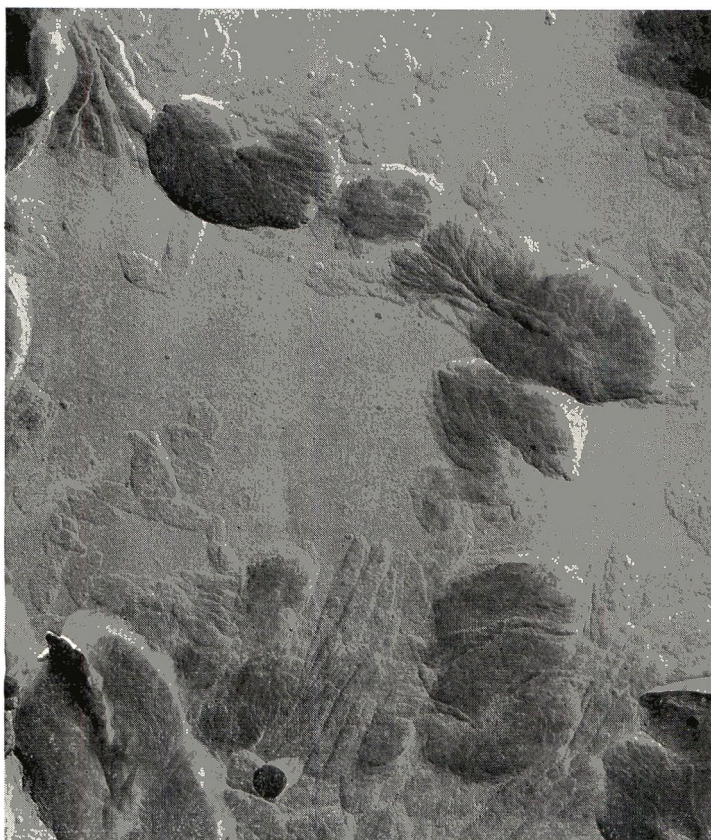


Fig. 4. Layer crystals and aggregates thereof of  $Z-(\text{Cap})_{10}-\text{OH}$  from formic acid. Electron micrograph, 7000 $\times$ .



Fig. 5. Single crystal electron diffraction pattern given by  $Z-(\text{Cap})_{11}-\text{OH}$  from alcohol.

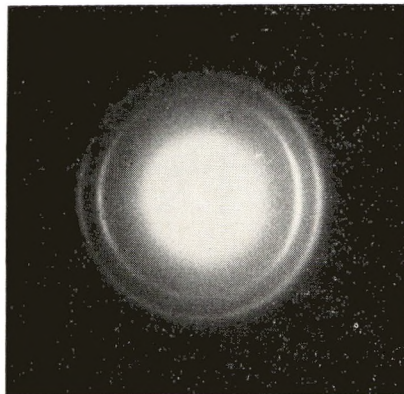
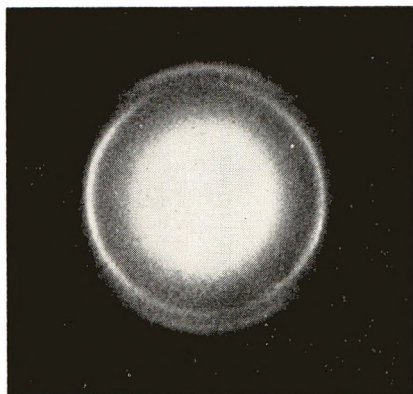


Fig. 6. Electron diffraction patterns given by crystal aggregates of  $Z-(\text{Cap})_5\text{-OH}$  from dimethylformamide. The substrate plane tilted through  $30^\circ$ . Tilt axis horizontal.

Fig. 7. Electron diffraction patterns given by crystal aggregates of  $Z-(\text{Cap})_{11}\text{-OH}$  from alcohol. The substrate plane tilted through  $30^\circ$ . Tilt axis horizontal.

orientation could be assessed by tilting the specimen plane. This leads to arcing in the Debye-Scherrer rings. The inner 200 ring contracted to the tilt axis in all samples while the outer 002 and 202 composite ring behaved differently for the low and high members. In the case of the low members ( $n = 3$  and  $5$  were studied) from alcohol and DMF, the outer ring intensified along the meridian up to tilts of  $30\text{--}40^\circ$  permitted by our tilting stage (Fig. 6). In the case of the high members ( $n = 10$  from DMF and  $n = 11$  from alcohol were studied), also the outer ring intensified on the tilt axis (Fig. 7), but to a lesser extent than the inner 200. The arcs were more spread out, particularly in the case of  $n = 11$  from alcohol where the outer arc was specially broad and could even become a uniform ring, the amount of spread varying from one locality to the other for the same specimen tilt.

Interpretation of these effects is as follows. Arcing of the rings on tilting means that the specimen has "fiber" symmetry around the specimen plane normal. The fiber axis cannot be determined from the presence of reflections alone, owing to large inherent disorientations. On tilting, reflections which are equatorial with respect to the fiber axis will develop arcs centered on the tilt axis for all tilts. The rings from nonequatorial reflections will intensify gradually normal to the tilt axis until the tilt is sufficiently large to bring the maximum of the intensity distribution in reflecting position. Beyond this, the arc will split with the two maxima moving gradually towards the tilt axis (for details and quantitative treatment see Keller and Engelman<sup>17</sup>).

Accordingly, in the above experiments the 200 planes are always parallel or nearly so to the fiber axis. In addition, in the low members the 002 and 202 planes and thus necessarily the molecules are inclined to the fiber axis, in qualitative agreement with Table I. The fact that intensifica-



tion only but not splitting is observed perpendicular to the tilt direction for tilt angles up to  $\sim 40^\circ$ , means that this inclination is appreciable. Bearing in mind that owing to disorientations the tilt must be considerably in excess of the theoretical value for splitting to become noticeable, the permissible lower limit of the inclination is consistent with values in Table I.

For high members all three  $h0l$  reflections intensify on the tilt axis, implying a molecular orientation perpendicular to the substrate. Even if small inclinations may be concealed by the disorientations present the large values required by Table I are certainly excluded. The lower degree of orientation in the outer ring implies additional randomization around the 200 normal. The fact that the amount of this disorientation varies from one locality to another suggests that crystal lamellae which themselves possess perpendicular orientation of the molecules are more or less randomly disposed around the 200 normal (e.g., by curling up around this direction or by growing together in a paddle wheel fashion with the 200 normal as common axis). This situation has its counterpart in the sheaf formation of nylons;<sup>17</sup> further evidence for it is quoted below.

#### 4.4. X-Ray Examination of Sedimented Crystal Mats

Crystals from solution in alcohol and DMF appeared in the form of suspended particles which could be sedimented to give oriented crystal mats in analogy to the well-established procedure in polyethylene.<sup>18, 19</sup> Even if the spread of orientations in such mats is inherently broad, it permits a distinction to be made between structures of largely different obliquities.

In all cases the low angle reflections appeared on the meridian (along the mat normal), except for some high member preparations from alcohol

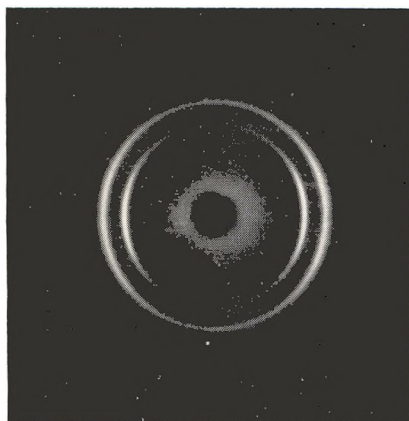
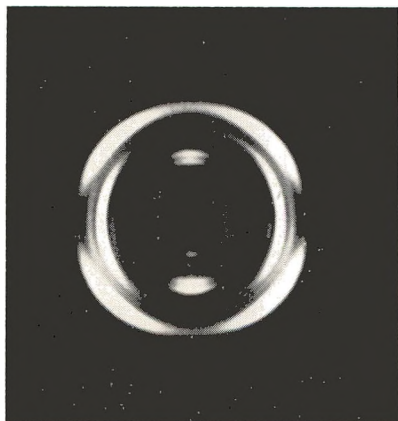


Fig. 8. Wide angle x-ray photograph of sedimented mats of crystals of  $Z-(\text{Cap})_5-\text{OH}$  from dimethylformamide. X-ray beam parallel to the mat plane, which in the present mounting corresponds to the horizontal.

Fig. 9. Wide angle x-ray photograph of sedimented mats of crystals of  $Z-(\text{Cap})_{11}-\text{OH}$  from alcohol. X-ray beam parallel to the mat plane, which in the present mounting corresponds to the horizontal.

where they could be completely disoriented. In the case of the low members they were present in many orders. Of the strong wide angle polyamide reflections, the 200 was invariably broadly arced about the equator; consequently these planes were parallel or at a small angle to the mat normal. In samples with  $n = 4$  and 5 (the lowest ones used for these experiments) the outer 002, 202, ring was highly split (e.g., Fig. 8). In the other samples examined which were  $n = 6, 9, 10,$  and 11 also this ring was equatorial (Fig. 9), even if a slight splitting for  $n = 9$  and 10, both from DMF, was just detectable (Fig. 10). For  $n = 10$  and 11 from alcohol, the outer ring was usually very broadly arced (Fig. 9), (more than the inner 200) and often formed a uniform ring (Fig. 11). These data are given in

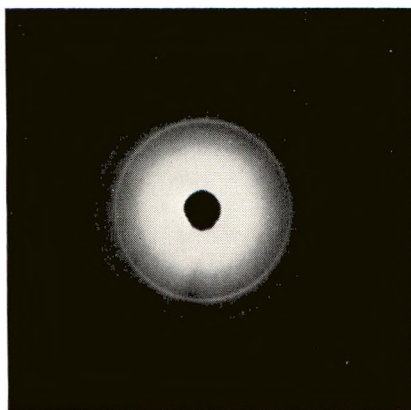
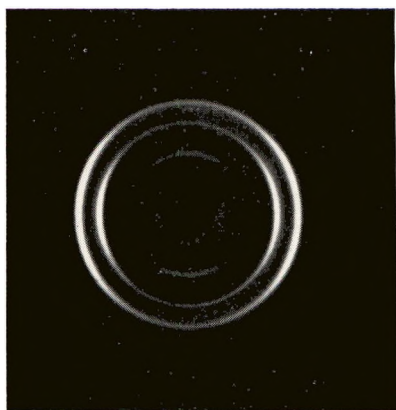


Fig. 10. Wide angle x-ray photograph of sedimented mats of crystals of  $Z-(\text{Cap})_{10}-\text{OH}$  from dimethylformamide. X-ray beam parallel to the mat plane, which in the present mounting corresponds to the horizontal.

Fig. 11. Wide angle x-ray photograph of sedimented mats of crystals of  $Z-(\text{Cap})_{11}-\text{OH}$  from alcohol. X-ray beams parallel to the mat plane, which in the present mounting corresponds to the horizontal.

column five of Table II. The equatorial arcing of the outer ring in the  $n = 10$  and 11 samples from alcohol was sometimes obtained by light pressure of the still moist sediment; without this pressure this would produce a uniform outer ring.

The interpretation is straightforward: the obliquity (a negligible correction apart) is given directly by the outer arc splittings observed, if tilt around an axis in the  $00l$  planes is assumed. This is consistent with the observation of the broad single 200 arc as the small split expected therein (a fraction of  $25^\circ$ , the angle between the 200 plane normal and the postulated tilt axis) would remain unresolved. In case the components of the split were too broad to be resolved they would have to be within that region of the arc where the intensity is high. In view of this, the observations are in agreement with the previous deductions. The low members are in a highly oblique form produced by shear on the hydrogen-bonded

TABLE II  
Wide and Low Angle Results from Oriented Mats and Attempts to Fit These to Oblique Structures

Number of monomer elements $n$	Solvent	Experimental long period $d$ , Å.	Fully extended length of the molecule plus end-to-end gap $L$ , Å.	Observed splitting and spread of wide angle reflections measured from equation		Calculated possible tilt from the ratio $d/L$	Associated terminal planes <sup>a</sup>
				002,020	200		
4	DMF	31.5	45	40-50°	No splitting spread: 30-35°	45°	{013}
5	DMF	38	54	40-50°	No splitting spread: 30-40°	45°	{013}
6	DMF	62	62.5	No splitting	No splitting spread: 30-40°	0°	{010}
9	DMF	75	88	20-25°	No splitting spread: 30-40°	32°	
10	DMF	82	96.5	15-20°	No splitting spread: 30-40°	31°	
10	Alcohol	52	96.5	No splitting	No splitting spread: 30-40°	57°	
11	DMF	70	105	Presence of split uncertain	No splitting spread: 35-45°	48°	
11	Alcohol	60	105	spread: $\leq 35^\circ$	No splitting spread: 30-40°	57°	

<sup>a</sup> Quoted for low members only where they could be clearly assigned.

planes, while in the high members the obliquity is absent or slight. It is seen from Table II that for  $n = 4, 5,$  and  $6,$  the fold surface assignment agrees with that postulated from the long spacings above (Table I). It is of interest that the terminal planes for  $n = 4$  and  $5$  correspond to a stagger of  $3/2b_s$  between adjacent hydrogen-bonded sheets. This stagger is basic to all polyamide structures. In the nylon 66 and 610 structures, adjacent sheets are displaced by this amount always in the same direction, while in nylon 6 they are displaced alternately up and down by this amount<sup>12</sup> (hence the lateral doubling of the cell). Accordingly, the obliquities observed in the above short oligomers correspond to a nylon 66 type layer stacking, and it is very likely that the vertical structure in  $n = 6$  is a nylon 6 type structure, both having the same  $3/2b_s$  stagger between sheets but a different next nearest neighbor relation. (These alternative possibilities have in fact been suggested for the nylon 6 polymer itself, where a second structure, termed  $\beta$ , having all sheet displacements in the same direction has been proposed.<sup>12</sup> It has been pointed out,<sup>19</sup> however, that the diffraction evidence on which this structure is based could also be accounted for by a less ordered arrangement of the sheets which is more in line with the general experience that in the high polymer the diffraction effects in question are associated with a lower degree of crystalline development.)

In contrast to the low oligomers, the obliquity in  $n = 9$  and  $10$  and if present at all in  $11$  from DMF cannot account for the observed long spacings in case of extended molecules, and the same holds even more conspicuously for  $n = 10$  and  $11$  from alcohol. In these latter, the spread of the arcs is large, yet the split required in order to account for the long spacings in column 3 of Table II should be clearly distinguishable, which it is not. If the spread of the outer arcs were due to a range of obliquities present simultaneously, this should be apparent from the corresponding multiplicity or broadening of the low angle reflections, which is not the case. On the other hand, the fact that the spread can be reduced on slight pressure lends strong support to the assumption—made already in connection with the electron diffraction patterns—that the lamellae which have a vertical structure are themselves disoriented when forming aggregates in a fashion which keeps the 200 plane normal in the plane of the mat. Accordingly, slight pressure would make these lamellae lie flat, with their internal structure unaltered. On any other picture, pressure is expected to bring the chains parallel to the substrate and not perpendicular to it (alignment of the chains with the substrate can in fact be achieved by increasing the pressure).

In summation, while in the low members the long spacings could be related to physically reasonable inclined structures, the existence of which was confirmed from patterns showing orientation effects, in the high members it was not possible to account for the long periods by means of the extended chains; these periods remained unaccounted for by inclinations which could still be accommodated by our diffraction patterns.

#### 4.5. Variability of Long Spacings within the Same Oligomer

**4.5.1. Temperature of Crystallization and Long Spacing.** Zahn and Pieper<sup>7</sup> proposed that the long spacing differences between the higher members crystallized from DMF and those from alcohol could be due to differences in crystallization temperature, crystallization of the former occurring at the higher temperatures when the solution is cooled from the solvent of higher boiling point. This behavior would be analogous to the long spacing-temperature of crystallization dependence in high polymers.

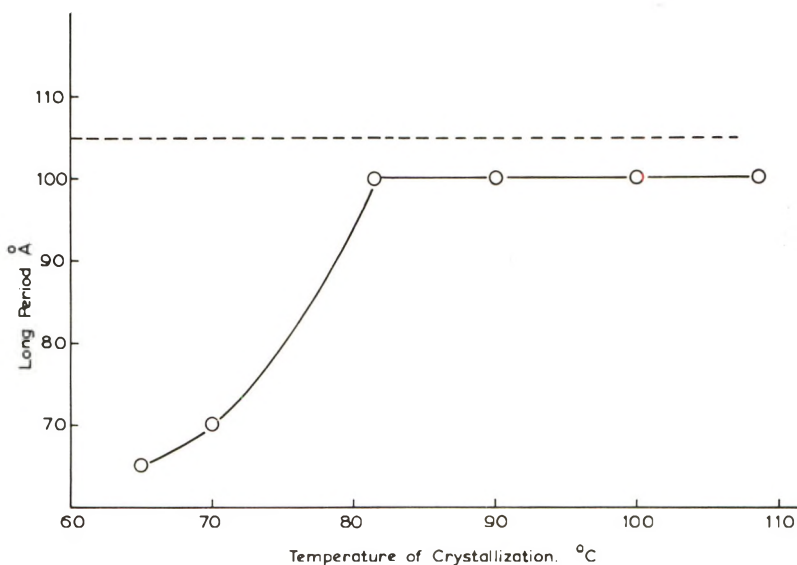


Fig. 12. Variation of long period in  $Z-(\text{Cap})_{11}-\text{OH}$  from dimethylformamide with the temperature of crystallization.

This suggests the same experiment which was used in high polymers, namely, isothermal crystallization at different temperatures from the same solvent. The compound  $n = 11$  was chosen and crystallized from DMF (the low boiling alcohol offered too small a range of supercooling). The long spacing-temperature of crystallization curve obtained is given by Figure 12. It shows that the long period increases with crystallization temperature until  $80^\circ\text{C}$ ., staying constant beyond. This constant value is close to the one expected from the fully extended chain in a vertical structure (straight dotted line). The left part of the curve is similar in shape to that found in polyethylene by Keller and O'Connor.<sup>2</sup>

The wide angle patterns all showed equatorial arcing. General disorientation was rather high in the sample crystallized at  $60^\circ\text{C}$ .. The one crystallized at  $70^\circ\text{C}$ ., however, is that listed in Table II for  $n = 11$  from DMF. Those crystallized at the higher temperatures were essentially similar to this in respect of orientation. Thus oblique structures with varying obliquities could not account for the curve in Figure 12.



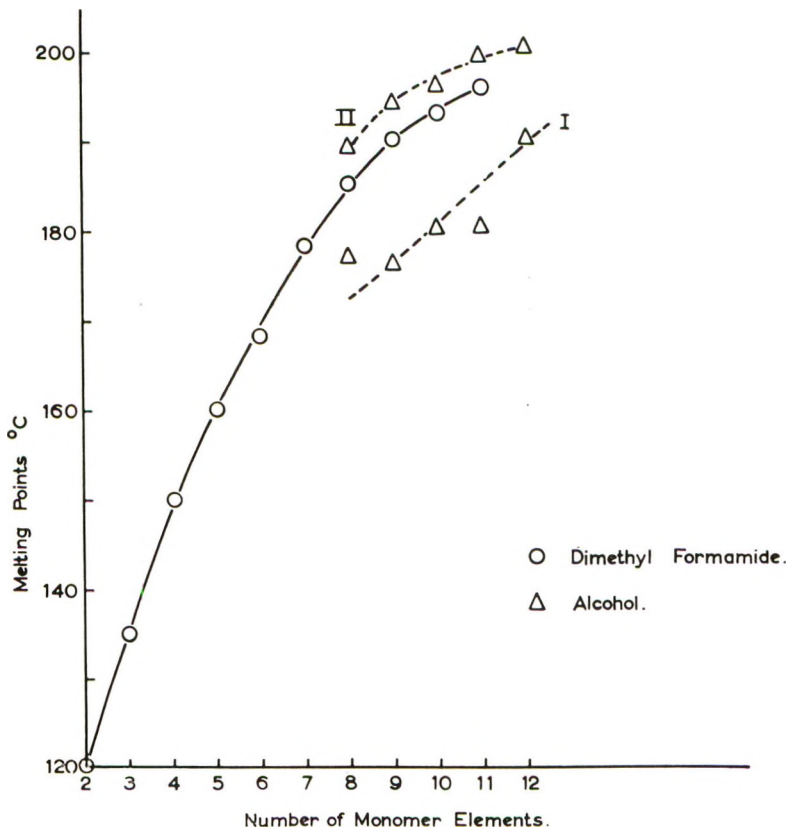


Fig. 13. Melting points as a function monomer units (see text).

**4.5.2. Annealing Behavior.** Zahn and Pieper<sup>7</sup> reported an increase of long spacing on heat annealing in the case of the high members. We carried out a few experiments along these lines. Samples were heated in an inert atmosphere of argon about 10°C. below their melting points and were examined after cooling. The low members showed no change in long spacing. The three higher members examined ( $n = 10$  from alcohol and

TABLE III

Number of monomer elements $n$	Solvent	Crystals sedimented from the solvent		Crystals after annealing 10°C. below M.P.	
		Long period, A.	Melting point, °C.	Long period, A.	Melting point, °C.
10	Alcohol	60	180	90	193-194
11	Alcohol	58	180	96	200
10	Dimethyl-formamide	80	191	91	194

DMF and  $n = 11$  from alcohol), however, showed a significant irreversible increase (Table III, columns 3 and 5), accompanied by an increasing spread in the equatorial reflections.

**4.5.3. Relation between Melting Points and Long Periods.** The melting points were determined on a temperature gradient bar. The results are shown by Figure 13. This figure has some resemblance to Figure 1. There is only one curve till  $n = 8$ . Beyond this there are two branches, one at lower temperatures for samples from alcohol and another at higher temperatures for samples from DMF and alcohol. The duplication of the points for the alcohol arises in the following way. When heated, the samples from alcohol melt first at temperatures along the lower branch (curve 1), but when they resolidify and melt again only at the higher temperature somewhat above those for the corresponding compounds from DMF (curve 2). Thus the melting points correlate with the long spacings, higher melting points belonging to higher spacings and vice versa. This is also borne out by Table III, where the appropriate melting points are also listed. The melting points quoted by Zahn and co-workers are always the highest ones, as only these were observed in the course of their slow heating during which the samples had a chance to anneal.\*

## 5. DISCUSSION AND CONCLUSION

The present work substantiates the contentions of Zahn and Pieper;<sup>7</sup> we have examined and excluded those factors which left alternative interpretations open. Firstly the long spacings of the shorter oligomers have been quantitatively correlated with various inclined crystal forms containing the molecules in an extended configuration. Significantly, the paraffinoid type subcell is maintained in a way such as to leave the hydrogen bonds unaffected in the various inclined forms deduced from experiments.

For the high members the above interpretation fails. The possibility of molecular inclination accounting for the long spacing has been eliminated. While further work on individual crystals would still be desirable, our effects are clear enough for this conclusion to be reached. Accordingly, we are faced with the situation that a periodicity exists along the chain

\* The lower melting of the high oligomers crystallized from alcohol, followed by subsequent resolidification may suggest that the oligomers could have co-crystallized with alcohol, this alcohol being given off at the first melting point. This possibility was checked. A sample of undecamer was first kept in high vacuum at room temperature for many hours in order to remove any unbound alcohol in case such remained after the original crystallization. The original two-stage melting behavior was unaffected by this treatment. Then the sample was heated to 187°C. in a closed container. As found subsequently, the sample exhibited only the higher melting point at 200°C. after this treatment. Consequently the alcohol should have been given off if the co-crystallization explanation had been valid. However, a gas-chromatographic analysis failed to detect any alcohol in the gas filling the container in which the heat treatment had taken place. Under the given experimental circumstances this meant that the alcohol/oligomer molar ratio was less than 1:1000. Thus the possibility of the original solvent having any effect on the melting behavior can be discarded.

direction which beyond the octamer is independent of the molecular length and cannot be accounted for by the extended molecule. Thus, in analogy with polymers, the idea of chain folding suggests itself as already proposed on evidence which was still assailable.<sup>5,6,7</sup> (Kern and co-workers<sup>6</sup> in their urethane oligomers confirmed the constancy of the long spacing up to  $n = 16$ , which makes tilted arrangements less likely than Zahn and Pieper's results going to  $n = 12$ . According to private communication by Pieper, an oligomer with  $n = 16$  has been obtained lately also for the amide used in the present work, and this when recrystallized from alcohol gave the same long spacing as  $n = 8-12$ , i.e., 50-60 Å.) The large periods thus attributable to the folded over molecule can be affected by physical treatments in the same manner as in the case of polymers. The effect of annealing has already been noted previously;<sup>7</sup> to this we now add the confirmation of dependence of the long spacing on the crystallization temperature and that of the melting point. At this juncture the observation of the reversible increase of the long spacing on swelling reported by Zahn and Pieper<sup>7</sup> also needs mentioning.

The remarkable fact is that the folded-over part of the molecule would only be a fraction of the chain length on the present picture. The details of the folding mechanism and of the resulting structure are open to speculation. In the first place, if the hydrogen-bonded structure is to be maintained, the folds must either be limited to certain discrete values or else folding must be restricted to that of the hydrogen bonded planes themselves, which would uniquely define the fold plane. These alternatives are not specific to our oligomers but to all polyamides in general. In addition, our oligomers present the specific problem of accommodating the rather bulky endgroups. In one way, the inertness of the ring would not promote end-to-end association and thus would favor chain folding. However, when folded over it must cause a considerable disturbance in the polyamide structure. Perhaps the observation that beyond the octamer the low angle reflections lose their higher orders and become more poorly defined is a consequence of this fact. Even if the visualization of the details presents many difficulties, there seems to be no alternative proposition to the chain folding idea which could be expressed in any definite structural terms at present.

In the first place we would like to thank Professor H. Zahn (Aachen), for kindly giving us the specimens which made this work possible, and for advanced information of results obtained by him and collaborators. We are obliged to Dr. E. W. Pieper (Aachen), for imparting valuable experience concerning the handling of these materials to us personally, to Mr. P. C. Uden (Chemistry Department, Bristol), for the gas-chromatographic analysis, and to Professor F. C. Frank for many helpful comments. F. J. B. C. wishes to acknowledge the tenure of a Ramsey Memorial Fellowship and that of a C.S.I.C. Fellowship (Spain) during this work.

## References

1. Keller, A., *Polymer*, **3**, 393 (1962).
2. Keller, A., and A. O'Connor, *Discussions Faraday Soc.*, **25**, 114 (1958).
3. Keller, A., and A. O'Connor, *Polymer*, **1**, 163 (1960).
4. Zahn, H., and D. Hildebrand, *Chem. Ber.*, **90**, 320 (1957); *ibid.*, **92**, 1963 (1959).
5. Zahn, H., *IUPAC Symposium on Macromolecules, Wiesbaden, 1959*, Verlag Chemie, Weinheim, Lecture 1B 8.
6. Kern, W., J. Davidovits, K. J. Rautekus, G. F. Schmidt, *Makromol. Chem.*, **43**, 1061 (1961).
7. Zahn, H., and E. W. Pieper, *Kolloid-Z.*, **180**, 97 (1962).
8. Keller, A., *Phil. Mag.*, **6**, 329 (1961).
9. Baltá Calleja, F. J., D. C. Bassett, and A. Keller, *Polymer*, in press.
10. Baltá Calleja, F. J., and A. Keller, *J. Polymer Sci.*, **A2**, 2171 (1964).
11. Franks, A., *Brit. J. Appl. Phys.*, **9**, 349 (1958).
12. Holmes, D. R., C. W. Bunn, and D. T. Smith, *J. Polymer Sci.*, **19**, 401 (1956).
13. Sandeman, I., and A. Keller, *J. Polymer Sci.*, **19**, 401 (1956).
14. Bassett, D. C., and A. Keller, *Phil. Mag.*, **6**, 345 (1961).
15. Geil, P. H., *Growth and Perfection of Crystals*, Wiley, New York, 1958, p. 584.
16. Pieper, E. W., *Kolloid-Z.*, **184**, 18 (1962).
17. Keller, A., and R. Engelman, *J. Polymer Sci.*, **36**, 361 (1959).
18. Keller, A., and A. O'Connor, *Nature*, **180**, 1289 (1957).
19. Keller, A., and A. Maradudin, *J. Phys. Chem. Solids*, **2**, 301 (1957).

## Résumé

Dans cette série de deux articles, on examiné la possibilité de repliement de la chaîne dans les molécules en chaîne qui ne sont pas plus longues que la longueur de repliement présumée. Le présent article envisage les amides oligomères. Faisant suite au travail précédent sur la relation entre l'ordre à grande distance et la longueur de la chaîne par Zahn et Pieper sur les mêmes composés, la relation entre les ordres à grande distance et l'orientation de la chaîne a été examinée en vue d'évaluer comment des structures fort obliques pourraient présenter des alternatives au repliement de la chaîne. On a pu conclure que cela n'était pas possible, les chaînes demeurant droites jusqu'à une certaine longueur seulement (80 Å), au-delà de laquelle le repliement de la chaîne offre l'explication la plus probable. On discute de la préparation et de l'examen des agrégats orientés nécessaires pour arriver à cette conclusion. De plus l'influence de l'ordre à grande distance sur la température de cristallisation et la relation entre le point de fusion et l'ordre à grande distance sont démontrés et des exemples de comportement au recuit sont donnés, exemples qui ont tous leur correspondant dans le chaîne repliée des hauts polymères.

## Zusammenfassung

In den beiden vorliegenden Arbeiten wurde die Möglichkeit einer Kettenfaltung in Kettenmolekülen untersucht, die nicht viel länger als die mutmassliche Faltungslänge sind. Die erste Arbeit befasst sich mit oligomeren Amiden. Im Anschluss an frühere, von Zahn und Pieper an denselben Verbindungen ausgeführte Untersuchungen über die Beziehung zwischen Langperiode und Kettenlänge wurde die Beziehung zwischen Langperiode und Kettenorientierung untersucht, um zu ermitteln, ob schräggestellte Strukturen eine Alternative zur Kettenfaltung darstellen können. Es wurde gefunden, dass dies nicht der Fall ist. Die Ketten liegen nur bis zu einer bestimmten Länge (80 Å) gestreckt vor, von der ab das Auftreten einer Kettenfaltung als wahrscheinlichste Erklärung für die experimentellen Befunde anzunehmen ist. Es wird die Herstellung und Untersuchung der zu diesem Ergebnis führenden orientierten Aggregate diskutiert. Ausserdem wird die Abhängigkeit der Langperiode von der Kristallisationstemperatur

sowie die Beziehung zwischen Schmelzpunkt und Langperiode nachgewiesen und es werden Beispiele für das Temperungsverhalten gegeben, von denen alle ihr entsprechendes Gegenstück in den gefalteten Hochpolymeren haben.

Received April 15, 1963



# On the Relation between Long Spacings, Molecular Length, and Orientation in Long Chain Compounds with Reference to the Possibility of Chain Folding.

## Part II. Poly(ethylene Oxide)s

F. J. BALTA CALLEJA\* and A. KELLER, *H. H. Wills Physics Laboratory, University of Bristol, Royal Fort, Bristol, England*

### Synopsis

Poly(ethylene oxide)s, including low molecular weight Carbowaxes and high molecular weight Polyox resins were examined as regards their long period chain length relationship with reference also to chain inclination with respect to the long spacings. The results show that the chains can only be straight up to a certain length (100-150 Å.), beyond which chain folding needs to be invoked. Reference is made to single crystals required for these experiments. The long spacings (fold length) depend on the solvents, presumably by their effect on the crystallization temperature and on the heat treatment (annealing) of the samples, this providing the continuity between the behavior of the waxy low molecular weight compounds and that of typical high polymers. The general conclusion (based on Part I and II) is reached that in the light of present concepts there seems to be no acceptable alternative to chain folding beyond a certain critical length (dependent on physical factors) to account for the observations.

### 1. INTRODUCTION

Poly(ethylene oxide)s are available in a range of molecular weights. The lower ones (by trade name Carbowaxes, those used by us), range from liquids to waxy solids, while the high molecular weight ones (by trade name, Polyox resins), have the consistency of typical high polymeric substances. Recently Kiessig<sup>1</sup> examined Carbowaxes 1000, 1500, and 4000 (the figures, while trade names, claim to denote the molecular weight), and reported discrete low angle reflections corresponding to spacings increasing with molecular weight. Kiessig claims agreement between spacings and molecular length in the crystal, the latter being based on a chain configuration proposed by Sauter in 1932.<sup>2</sup> While the agreement is by no means good there is no doubt about the trend. The reflections are sharp, which Kiessig considers remarkable in view of the fact that the molecular weight in a given sample is not uniform. In analogy to his earlier work on mixtures of fatty acids,<sup>3</sup> he suggests that the molecules of different lengths fold up (not neces-

\* Present address: Instituto de Física "Alonso de Sta Cruz," C.S.I.C. Serrano 119, Madrid 6, Spain.

sarily regularly) so as to yield molecular layers of uniform thickness. This possibility coincides with our present interest. In Kiessig's case the spacings were in the range of the average chain lengths. In the present work we extended these studies to chain lengths beyond the range where Kiessig's correlation could possibly pertain.

### On the Crystallography of Poly(ethylene Oxide)s

The crystal structure of poly(ethylene oxide)s has not yet been determined. Closely similar unit cells have been assigned by Walter and Reding<sup>4</sup> with  $a = 8.02$  A.,  $b = 13.4$  A.,  $c = 19.25$  A.,  $\beta = 126^\circ 52'$  and Price and Kilb<sup>5</sup> with  $a = 8.35$  A.,  $b = 13.11$  A.,  $c = 19.39$  A.,  $\beta = 126^\circ$ .

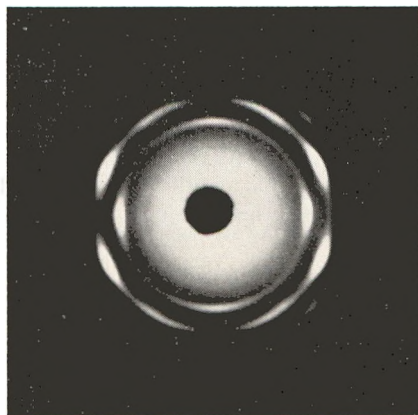


Fig. 1. X-ray diffraction pattern from a drawn fiber of poly(ethylene oxide) (high molecular weight Polyox resin). Fiber axis vertical.

Our own redetermination from single crystal electron diffraction patterns leads to  $a^* = 2b^* = 0.230$ , which, by taking  $\beta = 126^\circ$  would give  $a = 8.39$  A. and  $b = 13.40$  A. A  $c$  (molecular) axis fiber photograph on which the first two determinations<sup>4,5</sup> are based is shown by Figure 1. This diffraction pattern and the above crystallographic data suffice to identify the orientation of the crystal axes, and this only is required for the purpose of the present paper. Additional crystallographic information which has emerged from this work will be published separately later.

The only further information we need here is the relation between the number of monomer units and the length of the chain in the crystal. Price and Kilb<sup>5</sup> propose a  $7_2$  helix (seven monomer repetitions per two turns), where the monomer repeats at every 2.8 A.; this seems to be in accord with some of the data to be presented here. Two alternative proposals will also be referred to: the much flatter helix by Walter and Reding<sup>4</sup> with 1.27 A. for monomer repeat and the meander form by Sauter<sup>2</sup> (2.17 A. per monomer) utilized by Kiessig.<sup>1</sup>

## 2. EXPERIMENTAL

### 2.1. Materials and Techniques

The materials studied were Carbowax 1000, 4000, and 6000 and Polyox resins of 301 and coagulant grade. The latter two have molecular weights of hundred thousands and millions, respectively. The molecular weights of the Carbowaxes are as denoted by the numbers attached (Union Carbide specification, type of average not explicitly stated) although Price and Kilb claim viscosity-average molecular weights of 5500 for Carbowax 4000 and 12,000 for Carbowax 6000. We shall refer to both assignments.

Sample preparation and examination techniques were similar to those listed in Part I.<sup>6</sup> Results on the morphological examinations, however, will be reported separately in a later paper.

### 2.2. Experimental Results and Their Interpretation

**2.2.1. Materials as Received.** The flaky materials of the Carbowaxes possessed characteristic texture patterns. The flake normals were axes of rotational ("fiber") symmetry which usually coincided with  $c$  (molecules) but occasionally with  $b$  (details to be published). They gave rise to low

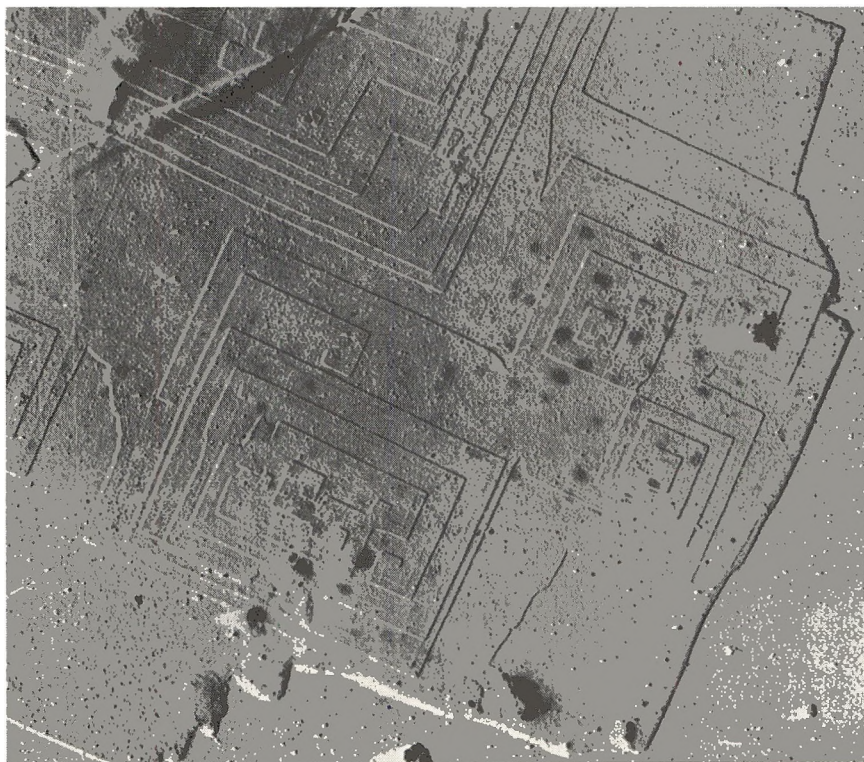


Fig. 2. Single crystal of poly(ethylene oxide) (Carbowax 6000) from amyl acetate solution. Electron micrograph. 14,000 $\times$ .



Fig. 3. X-ray diffraction pattern from sedimented mat of solution crystallized poly-(ethylene oxide) single crystals (high molecular weight Polyox resin). Mat normal, vertical in the present mounting, is perpendicular to the x-ray beam.

angle patterns up to 4-5 orders, the maxima being along the fiber axis where this was parallel to  $c$  or perpendicular to the fiber axis where this was parallel to  $b$ . Consequently they are along the directions of the molecules in the former case; results in the latter are at least consistent with this conclusion. The magnitude of the spacing was 76 Å. for Carbowax 1000, 180 Å. for Carbowax 4000 and 6000. For the powdery high molecular weight compounds there might have been a suggestion of a discrete reflection at around 180 Å. but if present strongly masked by continuous scatter.

**2.2.2. Single Crystal Mats Formed from Solution.** Single crystals were formed by dissolution and subsequent cooling. In general these were square tabular crystals thickening by way of the screw dislocation mechanism. While these will be described in a later publication we show here one example in Figure 2, as this will be referred to in the present paper. By sedimenting these crystals in the form of a mat oriented aggregates were obtained as shown by the wide angle x-ray patterns with the beam parallel to the mat plane (Fig. 3). Such orientations can be identified with a poorly oriented  $c$  axis fiber photograph (Fig. 1) with the molecules perpendicular to the mat plane, which was the case in all the mats examined. Low angle x-ray reflexions from such mats were then recorded in the usual way.

Crystallization could not be readily conducted under controlled conditions, at least with the experimental procedure normally adopted for polyethylene. Precipitation of crystals occurred to a significant extent at or near room temperature over a period of days dependent on concentration and molecular weight. Consequently temperature of crystallization was not as readily controllable as in the case of polyethylene. Two solvents were used in preparations for low angle x-ray work; methyl ethyl ketone (MEK) and xylene. The former being the poorer solvent precipitation of



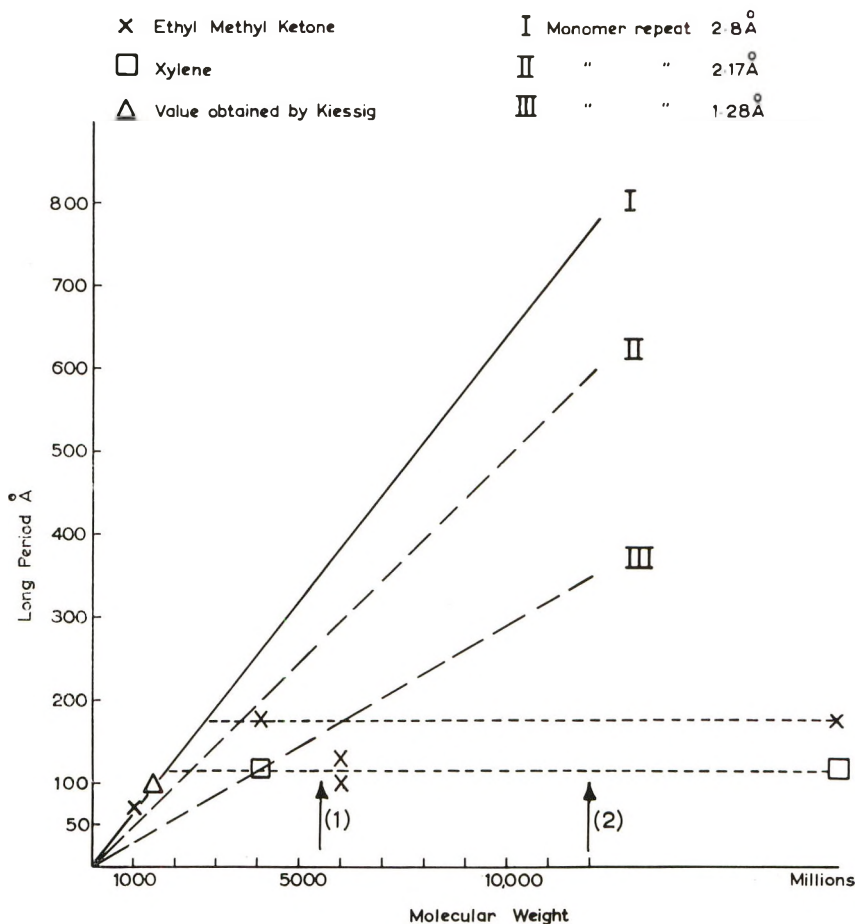


Fig. 4. Experimental long periods vs. molecular weight in poly(ethylene oxides). Lines I, II, and III represent the chain length according to the three different chain configurations.<sup>2,4,5</sup> The two arrows indicate the molecular weights of Carbowax 4000 and 6000, arrows 1 and 2, respectively, according to the assignment of Price and Kilb.<sup>6</sup>

crystals occurred from it sooner to a larger extent during cooling than on subsequent storage, while most of the crystallization from xylene occurred while standing at ambient temperature.

It was found that in the case of Carbowax 1000 the spacing was 70 Å., independent of the solvent, just as in the case of the original flake. For the higher molecular weight compounds the spacings from the MEK preparation was higher (170–180 Å.) than those from xylene (near 100 Å.) whenever spacings from both preparations were obtainable. The figures from MEK coincide with values given by the samples as received already quoted. Unaccountedly Carbowax 4000 gave no distinguishable discrete low angle reflexion from xylene even after several attempts, but gave two different spacings simultaneously from MEK, one at 95 Å., another at



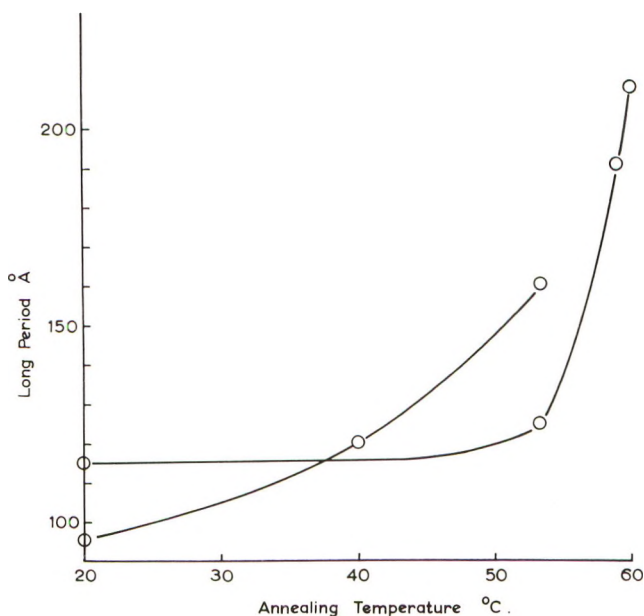


Fig. 5. Long periods of high molecular weight poly(ethylene oxide) (Polyox resin) vs. temperature of annealing.

125 Å. On heating to 50°C. these were replaced by a single spacing at 170 Å. The high molecular weight polymer was also crystallized from ethyl alcohol, giving a spacing of 95 Å. These results are represented in Figure 4 showing also Kiessig's<sup>1</sup> value for Carbowax 1500 not available to us.

Figure 4 also gives the molecular length as a function of molecular weight based on the  $7_2$  model.<sup>5</sup> Those corresponding to the other two alternatives<sup>2,4</sup> featured in the literature are also shown for completeness. The alternative positions of Carbowax 4000 and 6000 along the abscissa based on the data by Price and Kilb<sup>5</sup> are also indicated by arrows. The  $7_2$  helix model accounts for the long spacings in Carbowax 1000 and 1500 in case the helical chains ( $7_2$  helix) were straight and formed vertical structures, but neither this nor the other alternative chain configurations can account for the long spacings in the higher members. Here the spacings are all in the same range unaffected by molecular length dependent somewhat on the solvent, better solvent giving lower spacings. As already stated, the molecules were always perpendicular to the mats on the basis of the wide angle x-ray pattern.

**2.2.3. Annealing Experiments.** Single crystal preparations of high molecular weight were annealed at temperatures 10°C. below the melting point in an inert gas. The long spacings were observed to increase. The increase was found to depend on the initial long spacings. Thus crystals of 95 Å. initial fold length (grown from alcohol) increased their spacing to

160°C. those with initial long periods of 115 Å. (from xylene) to 125 Å. after annealing at 53°C. for 30 min. Further annealing at 60°C. for 30 min. led to a spacing of 210 Å. for both specimens. These effects are shown by Figure 5. The x-ray wide angle patterns showed no change on annealing.

### 3. DISCUSSION

The present results are in line with those in Part I<sup>6</sup> and in some earlier works quoted there. The long spacings are accounted for by the extended molecule only up to a certain molecular length. Beyond that the long spacing becomes independent of molecular length. In the case of poly(ethylene oxide), this limit is reached just above the molecular weight of 1500. The conclusions are unaffected by the alternatives of Union Carbide's or Price and Kilb's molecular weight assignment for Carbowax 4000 and 6000. In the case of both assignments the next highest member beyond 1500 should contain 2-3 fold segments. Our results demonstrate that the long spacings are along the molecular length; obliquities in the structure such as might be accommodated by the spread of the arcs must be small, if present at all. Beyond the molecular length where the correlation between long spacings and chain length ceases to hold the long spacings are affected by the solvents from which the crystallization has occurred (presumably through their effect on the crystallization temperature during cooling) and by heat treatments subsequent to crystallization. The small substeps parallel to the crystal faces in Figure 2 are analogous to those familiar from high molecular weight crystals,<sup>7</sup> where they represent discontinuities in the fold period due to a change in temperature during crystallization. In Figure 2 also incipient thickening effects near the crystal edge are noticeable leading to rounding of the outlines. Such effects were frequently observed also in more pronounced forms, in fact they were difficult to avoid (details to be published). Again this behavior has its counterpart among polymers where it corresponds to a refolding of the molecule to greater layer thickness.<sup>8,9</sup>

All the above effects are consistent with the picture of the chains staying straight in the crystal up to a certain chain length only, beyond which they start to fold. Inclined structures with straight molecules would require very large obliquities which are definitely excluded by the experimental facts, and thus offer no alternative to chain folding. The nonuniformity of the molecular length would in itself require chain folding, already proposed by Kiessig<sup>1</sup> even if in a different context, unless improbably large number of vacancies are to be admitted. In contrast to the preceding work on oligomers (Part I<sup>6</sup>), the step between the last extended and first chain folded state (the nonuniformity problem apart), is here rather large, owing to the lack of available compounds in this range. In any case, in Carbowaxes small chain length differences could not be interpreted in the same clear-cut way in view of the distribution in molecular

weight. The first folded compound Carbowax 4000 would contain 1–2 fairly complete hairpin folds. Again, beyond the molecular length where chain folding becomes a necessity, the material behaves as high polymers do as regards long spacing changes due to variation in crystallization temperature and heat treatment.

#### 4. GENERAL CONCLUSION

The present two studies provide further evidence and substantiate indications already in existence from previous work, that chain folding can occur with fold periods comparable to the chain length once a certain apparently critical molecular length is exceeded. This value is in the range of 80 Å. for the oligomeric amides and of 100–180 Å. for poly(ethylene oxide)s. The folded molecule need only be fractionally longer than the fold length. This fact should have important implications as regards the detailed structure of the crystals and theories on chain folded crystallization (see review by Keller<sup>10</sup>).

Evidence available so far is based on exclusion of alternatives. Direct confirmatory evidence would no doubt be preferable. Nevertheless the material in support of the present conclusion is quite extensive, embraces different compounds, preparations and different kinds of physical effects. It is fair to say that all the numerous observations recorded are in agreement with the point being made and none so far is against it, while no alternative explanation is in sight.

We wish to thank Dr. F. E. Bailey, Union Carbide Chemicals Co., South Charleston, for the supply of specimens and information concerning these, and Professor F. C. Frank for many discussions during the work. F. J. B. C. wishes to acknowledge the tenure of a Ramsey Memorial Fellowship and that of a C.S.I.C. Fellowship (Spain) during this work.

#### References

1. Kiessig, H., *Kolloid Z.*, **181**, 1 (1962).
2. Sauter, E., *Z. Physik. Chem.*, **B21**, 11 (1933).
3. Hess, K., and H. Kiessig, *Chem. Ber.*, **81**, 327 (1948).
4. Walter, E. R., and F. P. Reding, paper presented at 133rd National Meeting of the American Chemical Society, San Francisco, April 1958; *Abstracts*, p. 14R.
5. Price, F. P., and R. W. Kilb, *J. Polymer Sci.*, **57**, 395 (1962).
6. Baltá Calleja, F. J., and A. Keller, *J. Polymer Sci.*, **A2**, 2151 (1964).
7. Bassett, D. C., and A. Keller, *Phil. Mag.*, **7**, 1553 (1962).
8. Statton, W. O., and P. H. Geil, *J. Appl. Polymer Sci.*, **40**, 565 (1959).
9. Keller, A., and A. O'Connor, *Discussions Faraday Soc.*, **25**, 114 (1958).
10. Keller, A., *Polymer*, **3**, 393 (1962).

#### Résumé

Des polyoxydes d'éthylène comprenant des Carbowaxes de faible poids moléculaire et des résines Polyox de poids moléculaire élevé, ont été examinés du point de vue de leur grande longueur de chaîne périodique en se référant également à l'inclinaison de la chaîne par rapport aux ordres à grande distance. Les résultats montrent que les chaînes

peuvent seulement être droites jusqu'à une certaine longueur (100–150 Å) au-delà de laquelle le repliement de la chaîne doit être invoqué. On se réfère aux cristaux simples utilisés pour ces expériences. Les ordres à grande distance (longueur de repliement) dépendent des solvants, probablement par leur effet sur la température de cristallisation et dépendent du traitement thermique des échantillons (recuit), celui-ci fournissant la continuité entre le comportement des composés à faible poids moléculaire et celui des hauts polymères typiques. A la lumière des présents concepts, il semble que l'on puisse tirer comme conclusion générale (basée sur les parties I et II) qu'il n'y a pas d'alternative concevable au repliement de la chaîne au-delà d'une certaine longueur critique (qui dépend de facteurs physiques) si on veut tenir compte des observations.

### Zusammenfassung

Polyäthylenoxyde einschliesslich niedrigmolekularer "Carbowachse" und hochmolekularer Polyox-Harze wurden hinsichtlich ihrer Langperiode-Kettenlänge-Beziehung unter Berücksichtigung der Neigung der Ketten bezüglich der Langperiode untersucht. Wie die Ergebnisse zeigen, können die Ketten nur bis zu einer bestimmten Länge (100–150 Å), von der ab eine Kettenfaltung angenommen werden muss, gestreckt vorliegen. Es wird über die zu diesen Versuchen verwendeten Einkristalle berichtet. Die Langperiode (Faltungsabstand) hängt sowohl vom Lösungsmittel, vermutlich wegen dessen Wirkung auf die Kristallisationstemperatur, als auch von der Hitzebehandlung (Temperung) der Proben ab, was auf die Kontinuität zwischen dem Verhalten der wachsartigen niedrigmolekularen Verbindungen und demjenigen typischer Hochpolymerer hinweist. Aus den beiden Arbeiten (Teil I und II) wird geschlossen, dass derzeit keine andere Möglichkeit als die Annahme einer beim Überschreiten einer bestimmten, von physikalischen Faktoren abhängigen kritischen Länge auftretenden Kettenfaltung zur Deutung der Beobachtungen herangezogen werden kann.

Received April 15, 1963

## Topochemical Control of Solid-State Polymerization

F. L. HIRSHFELD and G. M. J. SCHMIDT, *Department of X-ray Crystallography, Weizman Institute of Science, Rehovoth, Israel*

### Synopsis

A survey of compounds that undergo polymerization in the solid state supports the topochemical postulate that such a reaction is possible only if the monomer crystal structure affords close contact between the reactive centers of neighboring molecules. Even when this condition is fulfilled, chain propagation may be diffusion-limited because of the contraction of the chain on polymerization. When the crystal structure makes such contraction unnecessary, polymerization can proceed without diffusion and the crystal can exert a direct control over the geometric course of the reaction. Several kinds of structures are known in which such behavior has been demonstrated or can be expected.

Recent studies of photochemical and radiochemical polymerization in the solid state<sup>1</sup> have led to discussion of the role played in these reactions by the crystal structures of the monomers. Evidence bearing on this question has been indirect and largely inconclusive, mainly because in only very few instances is crystallographic information available on the materials reported to undergo solid-state polymerization.

Our topochemical studies on the ultraviolet-induced dimerization of *trans*-cinnamic acids in the solid state<sup>2</sup> have disclosed a direct correlation between crystal structure and photochemical behavior. In all crystals of this series that were studied, the environment of the  $>C=C<$  bonds was found to conform to one of three principal types: the  $\alpha$  type, in which the double bonds of neighboring molecules make contact, at a distance of about 3.7 Å., across a center of symmetry; the  $\beta$  type, characterized by a lattice having one axial length of  $4.0 \pm 0.1$  Å., implying contact, at this distance, between translation-related molecules; and the  $\gamma$  type, in which the double bonds of neighboring molecules are nowhere less than 4.7 Å. apart. On ultraviolet irradiation,  $\alpha$ -type crystals give centrosymmetric dimers related to  $\alpha$ -truxillic acid (I),  $\beta$ -type crystals give dimers of mirror symmetry, related to  $\beta$ -truxinic acid (II), while  $\gamma$ -type crystals show no reaction.

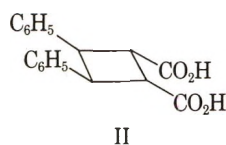
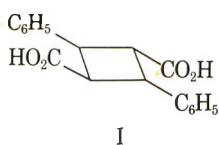
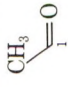
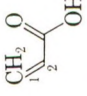
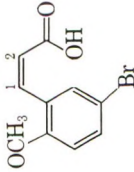
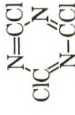


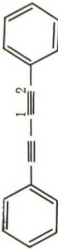
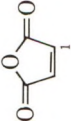
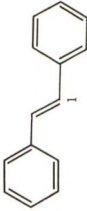



TABLE I  
 Crystallographic Data for Compounds Reported To Polymerize in Solid State

Compound	Formula	Space group	<i>a</i> , A.	<i>b</i> , A.	<i>c</i> , A.	$\beta$	<i>Z</i>	Intermolecular contacts	Radiation	References	
										Polymerization	Structure
Acetaldehyde		<i>Pna21</i>	5.25	7.05	7.05		4	C(1)...O 3.15	$\gamma$	9b	9a
Acrylic acid		<i>Ibam</i>	11.68	10.06	6.38		8	C(1)...C(1) 3.53, 3.66 C(2)...C(2) 3.82 C(1)...C(2) 4.05	$\gamma$ UV	18, 19 20	18
5-Bromo-2-methoxy- <i>cis</i> -cinnamic acid		<i>P21/a</i>	18.01	4.0	15.71	117.9°	4	C(1)...C(2) 3.9 C(1)...C(1) 4.0 C(2)...C(2) 4.0	UV	6	6
Cyanuric chloride		<i>Cc</i> or <i>C2/c</i>	12.92	7.46	7.57	60°9'	4	C...N 4.0	$\gamma$	21	22

Diacetylene dicarboxylic acid		11.15	3.75	20.18	107.0°	4	C <sub>(1)</sub> ...C <sub>(1)</sub> 3.75 C <sub>(2)</sub> ...C <sub>(2)</sub> 3.75	X, UV	10	10
Diketene		4.00	20.67	5.11	101.8°	4	C <sub>(2)</sub> ...C <sub>(2)</sub> 3.73 C <sub>(3)</sub> ...O <sub>(1)</sub> 3.75 C <sub>(1)</sub> ...O <sub>(2)</sub> 3.44	γ	14	23
Methyl <i>m</i> -bromo- <i>trans</i> -cinnamate		7.830	5.976	21.208	99.5°	4	C <sub>(1)</sub> ...C <sub>(2)</sub> 3.53	UV	2b	2b
Phosphonitric chloride trimer		14.15	12.99	6.19		4	P...N 3.95	X	24	25
Thiophene acrylic acid		11.43	5.04	13.02	98.2°	4	C <sub>(1)</sub> ...C <sub>(2)</sub> 3.80	UV	2b	26
Trioxane		Rhomb, 6.07 hex. 9.26		8.60	99.5°	2	C...O 3.7	γ	12, 17	11

TABLE II  
 Crystallographic Data for Compounds Believed Not Polymerizable in Solid State

Compound	Formula	Space group	<i>a</i> , Å.	<i>b</i> , Å.	<i>c</i> , Å.	$\beta$	<i>Z</i>	Intermolecular distances	References	
									Stability	Structure
Diphenyl diacetylene		<i>P</i> <sub>2</sub> <sub>1</sub> / <i>c</i>	6.62	6.05	14.95	105°	2	C <sup>(2)</sup> ...C <sup>(2)</sup> 4.71 C <sup>(1)</sup> ...C <sup>(2)</sup> 4.87	27	28
Maleic anhydride		<i>P</i> <sub>2</sub> <sub>1</sub> <sub>2</sub> <sub>1</sub>	7.180	11.231	5.39		4	C <sub>7</sub> ...C <sub>11</sub> 4.28, 4.59	19	29
Stilbene		<i>P</i> <sub>2</sub> <sub>1</sub> / <i>a</i>	12.35	5.70	15.92	114.0°	4	C <sub>0</sub> ...C <sub>0</sub> 4.66, 4.95	19	30
Tolane		<i>P</i> <sub>2</sub> <sub>1</sub> / <i>a</i>	12.75	5.73	15.67	115.2°	4	C <sub>0</sub> ...C <sub>0</sub> 5.55, 5.73	26,31	32

This correlation supports the general postulate that dimerization in these systems occurs, if at all, via the linking of neighboring molecules whose reactive sites are no further apart, in the monomer crystal, than about 4 Å. A tentative generalization of this postulate leads to the hypothesis that, in polymerizing systems too, suitable contact between the reactive centers of neighboring molecules in the crystal is a necessary condition for the initial dimerization step that must precede chain propagation. It is recognized that what constitutes suitable contact will depend on the type of system considered and may, in particular, vary with the chemical nature of the reacting species and with the choice of initiating radiation. Furthermore, the postulate implies that absorption of the activating radiation leaves the molecular shape essentially unchanged. If the activation process, in itself, were to alter drastically the dimensions of the monomer molecule, the crystallographically determined contact distances might not be relevant to the activated species.

In an attempt at a preliminary verification of the above hypothesis, we have surveyed the available crystal-structure data on compounds known to polymerize in the solid. The results of this survey are collected in the all too brief Table I. Columns 9 and 10 of the table list the contact distances between atoms that, on the chemical evidence, may be the sites of reaction. It must be admitted that for several of these compounds, notably diketene and thiophene acrylic acid, the actual sites of reaction have not been established on chemical grounds so that one has appreciable latitude in seeking crystal contacts of the proper type. At least, we may say that the data presented are consistent with the topochemical hypothesis proposed above.

To complete the argument it is necessary to consider the converse situation of compounds reported not to polymerize in the solid. A selection of the relevant data appears in Table II. For the compounds listed, absence of reaction may be plausibly, though not conclusively, attributed to the isolation of the potentially reactive regions from one another. As against these, there are, of course, numerous examples of unsaturated or cyclic compounds that display apparently favorable intermolecular contacts in the crystal and yet fail to polymerize on irradiation. In many cases, it is probable that this failure is one of propagation rather than of initiation. (We here understand initiation to include the primary dimerization step.) Again, geometric restraints may be a major factor.

Imagine a stack of monomer molecules so aligned in the crystal that the reactive site of each molecule is less than 4 Å. from those of each of its two neighbors in the stack. Suppose that, on absorption of the activating radiation, the reactive monomer  $A^*$  (which may, for the present argument, be a neutral excited molecule, a free radical, an ion, or a radical ion) reacts with its neighbor B to form the reactive dimer  $AB^*$ . The covalent link formed between A and B pulls these two monomer units together and, in so doing, increases the separation between B and its other neighbor C. If this separation is still not too great to permit further reaction, formation of the

trimer ABC\* will open a still wider gap between C and D, so that eventually the orderly propagation of the polymer chain along the stack will be arrested. When this happens the reactive oligomer may be considered trapped. In this state it may be subject to a variety of deactivating processes, depending on the chemical nature of the species involved, which may terminate the chain before it has any opportunity for further growth. The compound will then be classified as incapable of solid-state polymerization or as yielding only low molecular weight oligomers. Alternatively, the reactive chain end may remain indefinitely trapped until released by the melting or dissolution of the crystal. In such a case, the manner of handling the material after irradiation may be crucial because of the possibility of a post-irradiation polymerization, such as has been reported for several monomers.<sup>1,3</sup>

As possible examples of the kind of arrested polymerization we have been considering, we cite the dimerizing cinnamic acids, referred to above, in which termination may be regarded as occurring by ring closure to a saturated cyclobutane derivative; dimethyl fumarate, which likewise dimerizes in the solid state,<sup>4</sup> in contrast to the polymerizable diethyl fumarate<sup>5</sup>; and 5-bromo-2-methoxy-*cis*-cinnamic acid (see Table I), which yields two dimers along with some insoluble material of unknown but probably low molecular weight. In this last example, the C=C bonds make, besides a translation contact of 4.0 Å. between identically oriented molecules, a second contact, of 3.9 Å., between molecules related by screw-axis symmetry.<sup>6</sup> One of us has postulated elsewhere<sup>2b</sup> that the first type of contact leads via the *trans* isomer to a dimer of mirror symmetry while the second affords a mixture of centrosymmetric dimer and polymer. Maleic anhydride may also properly belong in this list; if the dimerization reported by Griffin et al.<sup>4</sup> does not involve a solid-solid phase transition in the monomer, it may mean that the intermolecular separation of 4.28 Å. (see Table II) is not too great for reaction, at least in this system.

Usually, however, we can expect some freeing of the trapped chains by diffusion of monomer toward the reactive sites at temperatures below the melting point. The rate of chain propagation will then depend on the mobility of the monomer molecules in the vicinity of the crystal defect associated with the incipient polymer chain. This process requires a favorable molecular alignment combined with high mobility. Such a combination is evidently realized in the canal complexes of various monomers in urea<sup>7</sup> or thiourea.<sup>8</sup> Here, the monomer molecules are lined up in long rows inside the channels provided by the host crystal, while seemingly retaining appreciable freedom of motion along the channels. It is not surprising that 2,3-dimethyl-butadiene complexed with thiourea polymerizes with zero activation energy to yield a high melting, stereoregular, crystalline polymer.<sup>8</sup> An extreme case of favorable geometry, provided by the crystal, combined with the mobility of the liquid is displayed at the surface of a melting crystal of acetaldehyde, where acid-catalyzed polymerization is exceptionally rapid and occurs far more readily than in either solid or liquid alone.<sup>9</sup>



In the more usual kind of solid-state polymerization, the overall reaction rate is governed by the competition between propagation and termination. Each of these processes is likely to be more or less diffusion-controlled and consequently more or less sensitive to the structure of the crystal. Furthermore, each may vary in a somewhat irregular manner with such experimental parameters as temperature, dose rate, extent of reaction, and impurity concentrations, leading to a kinetic behavior that is not simply interpretable. Thus it is difficult to obtain reliable data on rate constants and activation energies for the individual processes involved. Not only is it often impossible to decide whether a particular reaction proceeds by an ionic or a free-radical mechanism, or both; the role of the crystal structure is equally difficult to ascertain. This role is compounded of geometric factors as well as rigidity, number, and depth of trapping sites, etc. Consequently, the kinetics of diffusion-limited polymerization are not a promising source of information on the topochemical aspects of solid-state polymerization. It is far more useful to seek conditions under which diffusion does not play a crucial role in chain propagation so that one can expect the crystal structure to remain essentially intact in the neighborhood of the growing chain end.

A necessary condition for diffusionless polymerization is the presence in the crystal of a stack of suitably oriented monomer molecules so spaced that no linear contraction of the stack is needed for polymer formation. For example, a molecule with two unsaturated centers may be so oriented in a stack of identical molecules that it can rotate in place to link up with both its neighbors without any linear displacement of the monomer units so joined. Such a process can be readily visualized for a compound like diacetylene dicarboxylic acid, which turns black and insoluble on exposure to x-rays.<sup>10</sup> The crystal structure of this material<sup>10</sup> shows stacks of parallel molecules at a linear separation of 3.75 Å, the length of the molecules being perpendicular to the stacking direction. While the chemistry of the reaction is not known, there is no great difficulty, from a geometric viewpoint, in imagining the molecules to turn so as to line up more nearly parallel with the stacking axis and thus link together to form a polymer chain having the same linear separation of monomer units as that present in the crystal.

A second possibility is exemplified by the cyclic monomer trioxane. Here, the molecules are spaced 4.3 Å apart along the trigonal axis of a rhombohedral crystal, alternate molecules differing by nearly 60° in orientation.<sup>11</sup> Polymerization occurs via the opening of the six-membered rings<sup>12</sup> which then readily expand to span the gap that would otherwise result when the van der Waals separation of 3.7 Å between carbon and oxygen atoms of neighboring molecules contracts to the length of a covalent C—O bond. The result is a crystalline polymer composed of polyoxymethylene chains aligned in the direction of the trigonal axis of the monomer crystal.<sup>13</sup> A similar process probably occurs in diketene,<sup>14</sup> β-propiolactone,<sup>15</sup> and bischloromethyl oxacyclobutane,<sup>16</sup> which likewise polymerize by a ring-

opening mechanism to yield oriented crystalline polymers.<sup>17</sup> In these systems, the role of the crystal structure in providing a suitable alignment of the monomer molecules is evidenced by an abrupt drop in polymer yields on melting, by a negative effect on yields and on intrinsic viscosities of crystal defects produced by sudden chilling, and by a saturation effect, especially near the melting points, attributable to the disruption of the crystal structure attendant on polymerization. The high positive temperature coefficients displayed by some of these polymerizations suggest, nevertheless, that appreciable energy may be required to free the monomer molecule from its position in the rigid structure before it can attach itself to the polymer chain. Any attempt at generalization from the kinetic data must, however, contend with the fact that the overall activation energy is positive for trioxane, negative for diketene, and either positive or negative for propiolactone and for bischloromethyloxetane depending, for the former, on the temperature range considered, and, for the latter, on the extent of reaction.

With vinyl monomers the conditions for diffusionless polymerization are less readily fulfilled. Nevertheless it is quite simple to construct hypothetical models of crystal structures in which each molecule makes contact with at least two neighbors, in different directions, so as to form a zigzag chain in which the movement of each molecule on bonding to its neighbors may be perpendicular to the axis of the chain. Such a chain can then link up by contracting radially rather than longitudinally, leading to no accumulation of strain and no severe disruption of the crystal structure at the growing end. That such a model may be capable of realization in practice is suggested by the crystal structure of acrylic acid.<sup>18</sup> Each molecule makes two different kinds of contact, to neighbors to which it is related by parallel but nonequivalent glide planes. The crystallography appears nicely suited to the formation of an oriented polymer chain, parallel to the *b* axis of the crystal and having alternate head-to-head and tail-to-tail linkages. Nitta<sup>18</sup> reports the production of unoriented polymer on exposure to Co<sup>60</sup>  $\gamma$ -rays at 0°C. Experiments to check the chemical structure and possible crystallinity of polymer obtained by ultraviolet irradiation of solid acrylic acid at various temperatures are currently in progress.

We are grateful to Professor Judith Bregman for an extensive literature survey and to Dr. M. D. Cohen for several illuminating discussions and much useful criticism.

### References

1. See, e.g., M. Magat, *Polymer*, **3**, 449 (1962).
2. (a) M. D. Cohen and G. M. J. Schmidt, in *Reactivity of Solids*, de Boer, Ed., Elsevier, Amsterdam, 1961, p. 556; (b) G. M. J. Schmidt, et al., to be published.
3. Chapiro, A., paper presented at Symposium of Radiation Chemistry, Balatonszöd, Hungary, 1962.
4. Griffin, G. W., J. E. Basinski, and A. F. Velturo, *Tetrahedron Letters*, **2**, 13 (1960).
5. Wiley, R. H., and D. J. Parish, *J. Polymer Sci.*, **45**, 503 (1960).
6. Bregman, J., K. Osaki, G. M. J. Schmidt, and F. Sonntag, to be published.

7. White, D. M., *J. Am. Chem. Soc.*, **82**, 5678 (1960).
8. Brown, J. F., and D. M. White, *J. Am. Chem. Soc.*, **82**, 5671 (1960).
9. (a) M. Letort, and A. J. Richard, *J. Chim. Phys.*, **56**, 752 (1960); (b) C. Chachaty, *ibid.*, **59**, 427 (1962).
10. Dunitz, J. D., and J. M. Robertson, *J. Chem. Soc.*, **1947**, 1145.
11. Moerman, N. F., *Rec. Trav. Chim.*, **56**, 161 (1937).
12. Okamura, S., K. Hayashi, and Y. Nakamura, *Doitai To Hoshasen*, **3**, 416 (1960).
13. Lando, J., N. Morosoff, H. Morawetz, and B. Post, *J. Polymer Sci.*, **60**, S24 (1962).
14. Kitanishi, Y., K. Hayashi, and S. Okamura, *Doitai To Hoshasen*, **3**, 346 (1960).
15. Okamura, S., K. Hayashi, Y. Kitanishi, and M. Nishii, *Doitai To Hoshasen*, **3**, 510 (1960).
16. Okamura, S., K. Hayashi, and H. Watanabe, *Doitai To Hoshasen*, **4**, 73 (1961).
17. Okamura, S., K. Hayashi, and Y. Kitanishi, *J. Polymer Sci.*, **58**, 925 (1962).
18. Nitta, I., paper presented at International Union of Crystallography, Fifth International Congress, Cambridge, England, 1960; Y. Chatani, Y. Sakata, and I. Nitta, *J. Polymer Sci.*, **B1**, 419 (1963).
19. Restaino, A. J., R. B. Mesrobian, H. Morawetz, D. S. Ballantine, G. J. Dienes, and D. J. Metz, *J. Am. Chem. Soc.*, **78**, 2939 (1956).
20. Bamford, C. H., G. C. Eastmond, and J. C. Ward, *Nature*, **192**, 1036 (1961); *Proc. Roy. Soc. (London)*, **A271**, 357 (1963).
21. Okumara, S., K. Hayashi, M. Nishii, and Y. Nakamura, *Doitai To Hoshasen*, **4**, 69 (1961).
22. Hoppe, W., H. U. Lenné, and G. Morandi, *Z. Krist.*, **108**, 321 (1957).
23. Katz, L., and W. N. Lipscomb, *Acta Cryst.*, **5**, 313 (1952).
24. Spindler, M. W., and R. L. Vale, *Makromol. Chem.*, **43**, 231 (1961); V. Caglioti, D. Cordischi, and A. Mele, *Nature*, **195**, 491 (1962).
25. Wilson, A., and D. F. Carroll, *J. Chem. Soc.*, **1960**, 2548.
26. Block, S., and G. M. J. Schmidt, to be published.
27. Koski, W. S., and C. O. Thomas, *J. Chem. Phys.*, **19**, 1286 (1951).
28. Wiebenga, E. H., *Z. Krist.*, **102**, 193 (1940).
29. Marsh, R. E., E. Ubell, and H. E. Wilcox, *Acta Cryst.*, **15**, 35 (1962).
30. Robertson, J. M., and I. Woodward, *Proc. Roy. Soc. (London)*, **A162**, 568 (1937).
31. Sangster, R. C., and J. W. Irvine, *J. Chem. Phys.*, **24**, 670 (1956).
32. Robertson, J. M., and I. Woodward, *Proc. Roy. Soc. (London)*, **A164**, 436 (1938).

### Résumé

Un examen des composés qui conduisent à la polymérisation à l'état solide conduit au postulat qu'une telle réaction n'est possible que si la structure du cristal de monomère offre un contact étroit entre les centres réactifs des molécules voisines. Même lorsque cette condition est remplie, la propagation de la chaîne peut être limitée par diffusion à cause de la concentration de la chaîne par polymérisation. Lorsque la structure du cristal rend une telle contraction non nécessaire, la polymérisation peut avoir lieu sans diffusion et le cristal peut exercer un contrôle direct sur la géométrie de la réaction. Plusieurs sortes de structures sont connues pour lesquelles un tel comportement a été démontré ou bien peut être attendu.

### Zusammenfassung

Eine Betrachtung der zur Polymerisation im festen Zustand fähigen Verbindungen bestätigt das topochemische Postulat, dass eine derartige Reaktion nur dann möglich ist, wenn die reaktiven Zentren benachbarter Moleküle auf Grund der Kristallstruktur des Monomeren in nahem Kontakt miteinander stehen. Allerdings kann auch in Fällen, in denen diese Bedingung erfüllt ist, das Kettenwachstum wegen der Kontraktion der

Kette bei der Polymerisation diffusionskontrolliert sein. Wenn eine derartige Kontraktion auf Grund der Kristallstruktur nicht notwendig ist, kann die Polymerisation ohne Diffusion vor sich gehen und der Kristall eine direkte Kontrolle über den geometrischen Verlauf der Reaktion ausüben. Es sind mehrere Strukturtypen bekannt, an denen ein derartiges Verhalten nachgewiesen wurde oder erwartet werden kann.

Received April 15, 1963

## Poly(1,2-dimethyl-5-vinylpyridinium Methyl Sulfate). Part I. Polymerization Studies

W. P. SHYLUK, *Hercules Research Center, Hercules Powder Company, Wilmington, Delaware*

### Synopsis

1,2-Dimethyl-5-vinylpyridinium methyl sulfate is readily polymerizable in aqueous solution under mild free radical conditions to a high molecular weight, cationic poly-electrolyte. A three-halves order dependence of the rate of polymerization on monomer concentration is indicated for about 75% of the polymerization of 1,2-dimethyl-5-vinylpyridinium methyl sulfate in aqueous solution with potassium persulfate as initiator. A normal dependence of the polymerization rate on the square root of the initiator concentration is also indicated by these data. The overall activation energy is estimated to be about 17 kcal./mole. Preliminary experiments related to the effect of changing the ionic strength of the reaction medium by addition of sodium chloride led to a change in the kinetics with a dramatic slowing-down of the polymerization. Copolymerization studies indicate that the reactivity of this cationic monomer is higher than that of acrylamide, methacrylamide, and methyl methacrylate, but close to that of methacrylic acid.

### INTRODUCTION

Much attention has been given during the last eight years in the patent literature to the preparation of polycationics by free radical polymerization of monomers containing quaternary ammonium groups. One class of easily polymerizable cationic vinyl monomers that has received a great deal of attention includes quaternary ammonium salts derived from dialkyl-aminoalkyl acrylates and methacrylates.<sup>1-8</sup> A similar class of monomers is obtained by the quaternization of *N*-dialkylaminoalkyl acrylamides and methacrylamides.<sup>7,9,10</sup> Other classes of cationic monomers which have been polymerized are vinyloxyalkyltrialkylammonium,<sup>5,11,12</sup> carbovinyl-oxyalkyltrialkylammonium,<sup>13</sup> carboallyloxyalkyltrialkylammonium,<sup>14</sup> *p*-vinylbenzyltrialkylammonium,<sup>15,16</sup> *N*-allylammonium,<sup>17,18</sup> and vinylpyridinium.<sup>5,19-23</sup>

Generally, very little basic information has been reported on the polymerization of cationic monomers. The simplest cationic monomer, a vinyl-trimethylammonium salt, did not copolymerize, presumably because of the charge so near to the double bond.<sup>24</sup> Hart and Timmerman<sup>25</sup> described the synthesis and polymerization of 4-vinylpyridine *N*-butyl sulfobetaine. Jones<sup>26</sup> reported the synthesis and polymerization of some *p*-vinylbenzyl-trialkylammonium salts. The important discovery that linear polymers



are formed by a cyclic polymerization mechanism from diallyl quaternary ammonium salts was reported by Butler and Angelo.<sup>27</sup> Copolymerization studies by Overberger and co-workers<sup>28</sup> with 2-(methacryloyloxy)ethyltrimethylammonium chloride and 4-vinylpyridine indicated that there is a tendency for alternation. Price and Duling<sup>29</sup> have reported some of the polymerization characteristics of *N*-vinylpyridinium salts. This type of monomer apparently receives sufficient activation from the pyridine ring to overcome the effect of the charge next to the double bond.

This paper gives some of the polymerization characteristics of another cationic monomer, 1,2-dimethyl-5-vinylpyridinium methyl sulfate or DMVPMS.<sup>23</sup>

## RESULTS AND DISCUSSION

### Spontaneous Polymerization

Concentrated aqueous solutions of DMVPMS (above 25%) tend to polymerize spontaneously. Reaction temperatures below 25°C. give complete polymerization; above this temperature, the polymerizations appear to stop at about 70% conversion (Table I).

TABLE I  
Spontaneous Polymerization of 1,2-Dimethyl-5-vinylpyridinium Methyl Sulfate in Aqueous Solution

Monomer concentration, %	Temperature, °C.	Reaction time, days	Conversion to polymer, %	Intrinsic viscosity
75	5	1.0	97	10.5
75	25	1.0	93	7.3
75	30	1.0	74	6.6
75	35	1.0	69	6.1
75	40	1.0	73	5.2
75	45	1.0	73	4.9
75	50	1.0	65	4.2
75	65	1.0	70	3.0
65	25	0.030	9.2	5.2
45	25	0.046	7.1	4.0
35	25	0.11	13	3.9
25	25	0.18	11	3.0

Preliminary data indicate a first-order dependence of the rate of polymerization on monomer concentration (Fig. 1). Table II shows that there is no significant change in the intrinsic viscosity with per cent conversion to polymer in these polymerizations.

Peroxides formed by the reaction of the monomer and oxygen are probably involved in the initiation of these polymerizations.<sup>30,31</sup> A very low initiation rate would maintain such a polymerization because of the decreased termination rate in the viscous reaction mixture. That this

TABLE II  
Intrinsic Viscosities Versus Conversion for the Spontaneous Polymerization of a 3.1*M* Solution of 1,2-Dimethyl-5-vinylpyridinium Methyl Sulfate in Water (pH = 2, H<sub>2</sub>SO<sub>4</sub>) at 25°C.

Conversion to polymer, %	Intrinsic viscosity
25	7.3
44	7.3
53	8.0
68	7.3
78	6.6
87	7.1
92	6.6
100	6.8

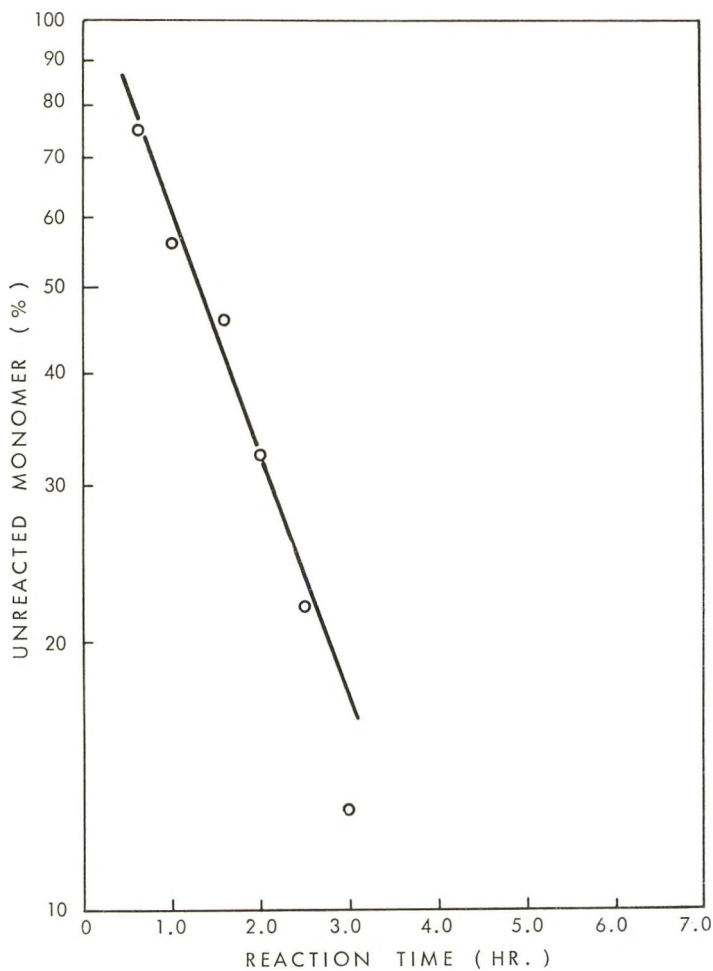


Fig. 1. Spontaneous polymerization of a 3.1*M* solution of 1,2-dimethyl-5-vinylpyridinium methyl sulfate in water at 25°C.

Trommsdorf effect<sup>32</sup> appears to be operating is suggested by the small decrease in the intrinsic viscosity with conversion (Table II) for the polymerizations in Figure 1.

Spontaneous polymerization have also been reported with *p*-vinylbenzyl-trimethylammonium bromide<sup>26</sup> and with an anionic vinyl monomer, sodium ethylenesulfonate.<sup>33</sup>

### Polymerization in the Presence of Initiators

The expected trends for free radical polymerizations occur when DMVPMS is polymerized in aqueous solution in the presence of various initiators (Table III). Unlike the spontaneous polymerizations, these polymerizations go to completion at higher temperatures and at very low monomer concentrations.

TABLE III  
Polymerization of 1,2-Dimethyl-5-vinylpyridinium  
Methyl Sulfate in Aqueous Solution

Monomer concentration, %	Initiator, % <sup>a</sup>	Reaction temperature, °C.	Reaction time, days	Conversion to polymer, %	Intrinsic viscosity
75	0.010% K <sub>2</sub> S <sub>2</sub> O <sub>8</sub>	25	3.8	100	8.4
75	0.10% K <sub>2</sub> S <sub>2</sub> O <sub>8</sub>	25	3.8	100	5.5
75	1.00% K <sub>2</sub> S <sub>2</sub> O <sub>8</sub>	25	3.8	100	3.2
75	0.50% K <sub>2</sub> S <sub>2</sub> O <sub>8</sub> 0.50% Na <sub>2</sub> S <sub>2</sub> O <sub>3</sub>	25-58	1.1	100	0.5
55	0.50% AIBN <sup>b</sup>	60	1.7	100	1.8
50	0.50% AIBN	45	2	93	2.8
24	2.2% K <sub>2</sub> S <sub>2</sub> O <sub>8</sub>	55	1	100	1.4
12	4.4% K <sub>2</sub> S <sub>2</sub> O <sub>8</sub>	55	1	100	0.6
3.1	17.6% K <sub>2</sub> S <sub>2</sub> O <sub>8</sub>	55	1	100	0.1

<sup>a</sup> Based on monomer.

<sup>b</sup>  $\alpha, \alpha'$ -Azobisisobutyronitrile.

According to the well-known kinetic scheme for radical chain polymerization of vinyl monomers,<sup>34</sup> a first-order dependence of the rate of polymerization on monomer concentration would be expected:

$$R_p = \frac{-d[M]}{dt} = K_1[I]^{1/2}[M]$$

where

$$K_1 = k_p (k_d f / k_t)^{1/2} \quad (1)$$

and I = initiator, M = monomer, R<sub>p</sub> = rate of polymerization k<sub>p</sub> = propagation rate constant, k<sub>d</sub> = initiator decomposition constant, k<sub>t</sub> = termination constant.

This, however, was not the kinetic result in the polymerization of DMVPMS in aqueous solution at 55°C. and at two concentrations of potas-

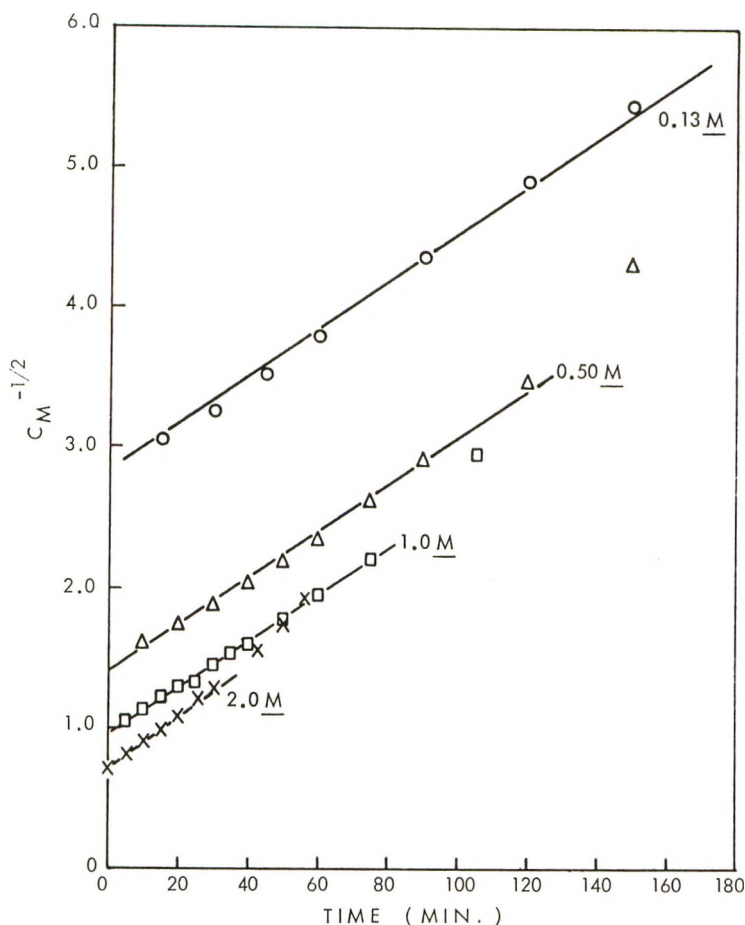


Fig. 2. Three-halves-order plot of the effect of monomer concentration in the polymerization of 1,2-dimethyl-5-vinylpyridinium methyl sulfate at 55°C. in water containing 0.020*M* potassium persulfate.

sium persulfate. Although the data will give a linear relationship when plotted in the usual way for first-order kinetics, the slopes are not constant for each concentration of initiator as required in the equation above.

It appears instead that there is a three-halves dependence of the rate of polymerization on monomer concentration for about 75% of the polymerization and the data are plotted accordingly in Figures 2 and 3. These results are similar to those reported for the benzoyl peroxide-initiated polymerizations of styrene<sup>35,36</sup> and vinyl acetate.<sup>37</sup>

To explain this higher-order dependence on monomer concentration, it was postulated that the monomer is involved in the initiation step.<sup>35-38</sup> Although the mechanism for this more complex initiation step has as yet not been established,<sup>39</sup> it can be written as:



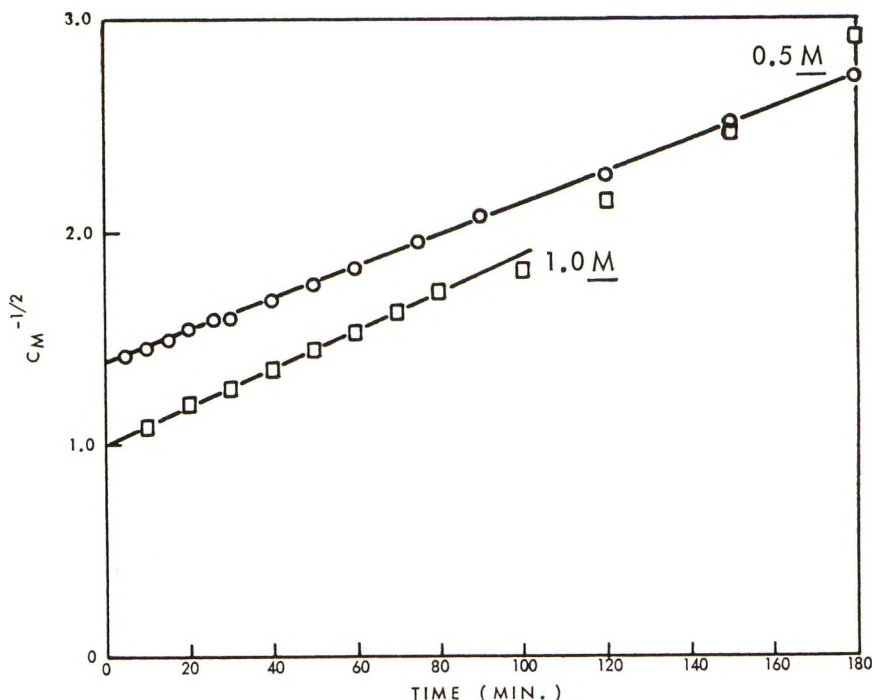


Fig. 3. Three-halves-order plot of the effect of monomer concentration in the polymerization of 1,2-dimethyl-5-vinylpyridinium methyl sulfate at 55°C. in water containing 0.0050*M* potassium persulfate.

This leads to the following expression for the rate of polymerization according to the scheme for the derivation of eq. (1):

$$R_p = -d[M]/dt = K_1 [I]^{1/2}[M]^{3/2} \quad (3)$$

Assuming that the initiator concentration remains constant in these polymerizations, integration of eq. (3) gives:

$$[M]^{-1/2} = -1/2 K_2 t + \text{a constant} \quad (4)$$

where

$$K_2 = K_1 [I]^{1/2}$$

The kinetic data in Figures 2 and 3 meet the two requirements of eq. (4). There is a linear relationship between the reciprocal of the square root of the concentration of the unreacted monomer ( $C_M^{-1/2}$ ) and the reaction time. Also, for each initiator concentration the slopes are essentially equal (given as  $K_2$  in Table IV).

Since the values of  $K_1$  ( $K_2/[I]^{1/2}$ ) in Table IV are nearly constant, the predicted proportionality between the rate of polymerization and the square root of the initiator concentration in eq. (4) is indicated. This result implies that the initiator concentration did not change appreciably during the experiments above, as might be expected because the first-order rate



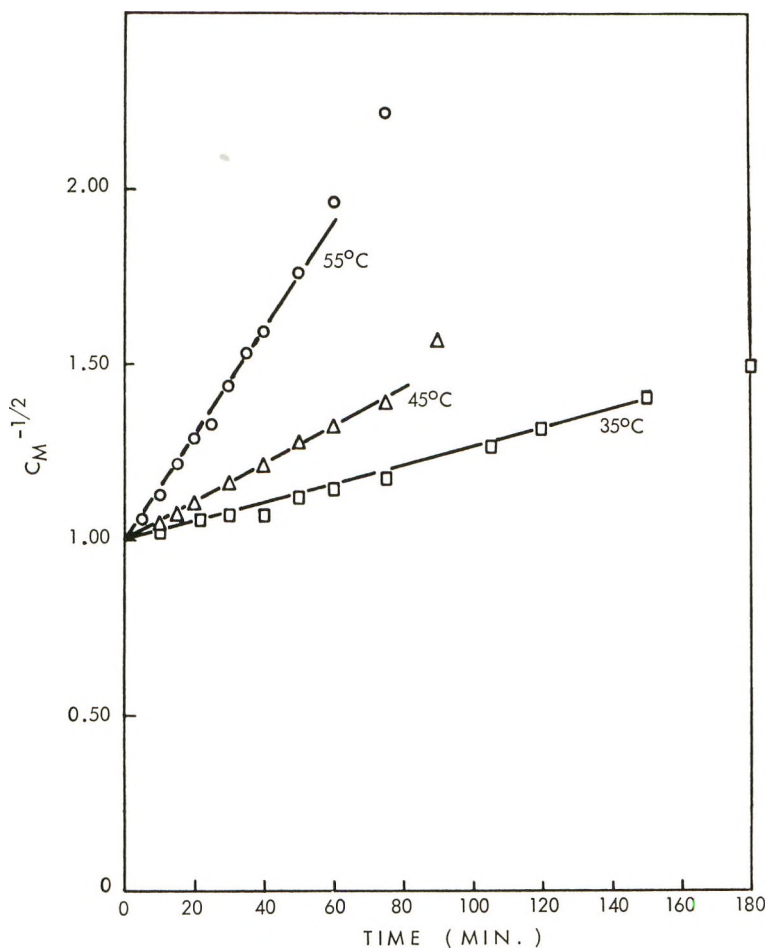


Fig. 4. Three-halves-order plot of the effect of temperature in the polymerization of 1,2-dimethyl-5-vinylpyridinium methyl sulfate in water containing 0.020M potassium persulfate.

TABLE IV  
Effect of Monomer and Initiator Concentrations on the Polymerization of 1,2-Dimethyl-5-vinylpyridinium Methyl Sulfate in Aqueous Solution at 55°C.

Initial monomer concentration, <i>M</i>	Potassium persulfate concentration, <i>M</i>	$K_2$	$K_1$	Conversion to polymer in 19 hr., %	Specific viscosity <sup>a</sup>
0.125	0.0200	0.034	0.24	99	0.017
0.500	0.0200	0.034	0.24	100	0.057
1.00	0.0200	0.032	0.23	100	0.16
2.00	0.0200	0.036	0.25	100	6.5
0.500	0.00500	0.015	0.21	98	0.086
1.00	0.00500	0.018	0.25	100	0.19

<sup>a</sup> 0.50% Polymer in 0.31M NaCl and 0.033M  $K_2S_2O_8$  at 25°C.

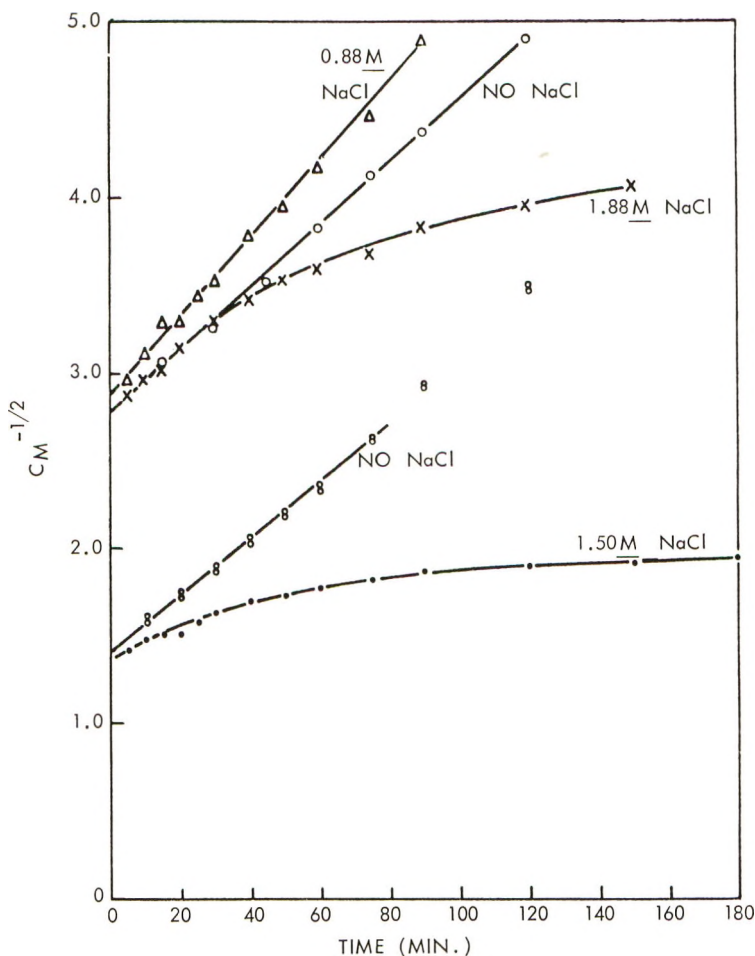


Fig. 5. Three-halves-order plot of the effect of sodium chloride on the polymerization of 1,2-dimethyl-5-vinylpyridinium methyl sulfate in water containing 0.020M potassium persulfate.

constant for the decomposition of potassium persulfate in the absence of any substrates in water at 50°C. is  $0.0036 \text{ hr.}^{-1}$ .<sup>40</sup> Thus, even if the participation of monomer in the initiation step leads to a several-fold increase in the rate of polymerization, there would not be a significant decrease in initiator concentration for the reaction times which were used for the kinetic measurements.

The effect of temperature on the rate of polymerization is given in Figure 4. From the slope of an Arrhenius plot of these data, the overall activation energy was estimated to be about 17 kcal./mole.

In the propagation step of the polymerization, a positively charged monomer molecule must approach a positively charged growing polymer radical. As the ionic strength of the reaction medium increases, these

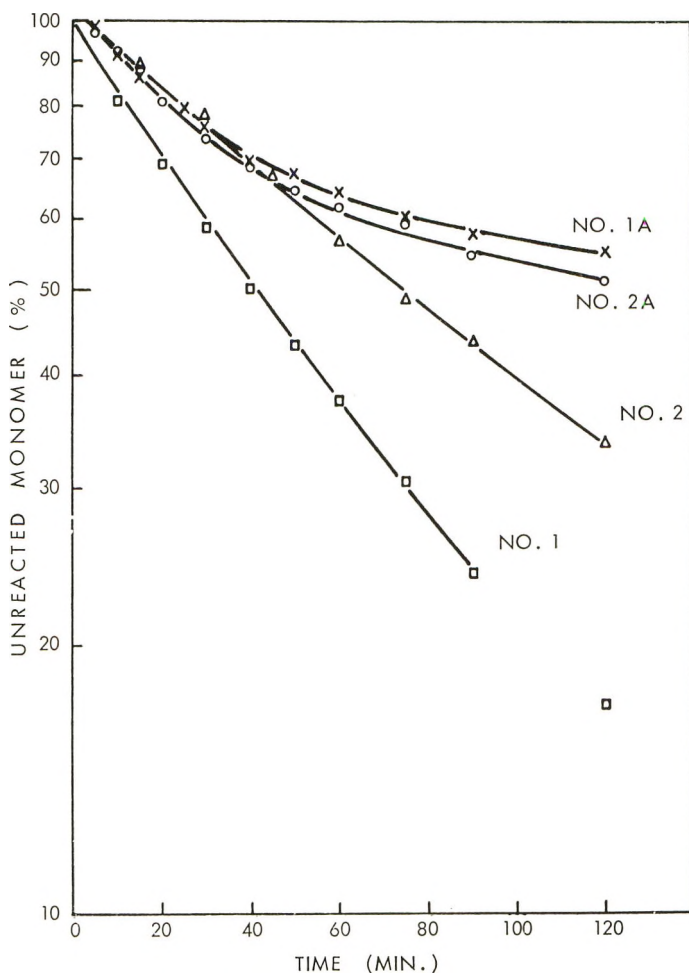


Fig. 6. First-order plot of the effect of sodium chloride on the polymerization of 1,2-dimethyl-5-vinylpyridinium methyl sulfate in water containing 0.020M potassium persulfate: (1) monomer = 0.50M; (1A) monomer = 0.50M, NaCl = 1.5M; (2) monomer = 0.12M; (2A) monomer = 0.12M, NaCl = 1.88M.

charge effects would be expected to decrease. Since the 17-fold increase in the concentration of this ionic monomer in Figure 2 also corresponds to an equivalent increase in ionic strength, it is surprising that there was no apparent effect on the kinetics.

Preliminary results on the effect of changing the ionic strength of the polymerization medium by addition of sodium chloride show some complicated effects (Figs. 5 and 6). Below a certain concentration of sodium chloride, there appears to be an increase in the rate of polymerization. Above this concentration of sodium chloride, the dependence of the rate of polymerization changes to first order with respect to monomer concentration for about the first 25% of the polymerization. After this, the poly-

merization slows down dramatically. This latter result might be explained by a removal of the anionic initiator from the solution during a salting out of the cationic polymer in a predominantly chloride form.<sup>41</sup> No precipitation was observed, but highly ionic polymers are known to separate in a colloidal state.<sup>26</sup>

The viscosity data in Table IV suggest that the viscosity of the polymerization medium may have had an effect on the chain length for the highest monomer concentration (2.0*M*).<sup>32</sup> As would be expected, there appeared to be a slightly higher rate constant ( $K_2$ ) for this experiment. Different experimental techniques will be needed for determining the effects of higher monomer concentrations because of the difficulty of controlling temperature and sampling from a viscous reaction mixture.

### Copolymerization Studies

The reactivity ratios given in Table V<sup>42,43</sup> suggest a high reactivity of DMVPMS with acrylamide, methacrylamide, and methyl methacrylate. Methacrylic acid, however, appears to be closer in its reactivity to that of the cationic monomer.

TABLE V  
Copolymerization Characteristics of 1,2-Dimethyl-5-vinylpyridinium  
Methyl Sulfate ( $M_1$ )

Comonomer ( $M_2$ )	$r_1$	$r_2$	$e_1$	$e_2$	$Q_1$	$Q_2$	Ref- erence
Acrylamide	2.7	0.19	1.6	0.78 <sup>a</sup>	9.6	0.95 <sup>a</sup>	48, 49, 50
Methacrylamide	1.2	0.14	—	—	—	—	—
Methacrylic acid	0.60	0.58	2.0	0.97	12	2.62	48
Methyl methacrylate	1.8	0.12	1.6	0.4	9.0	0.74	41

<sup>a</sup> Average of 3 reported values.

These differences in reactivity are reflected in the solubility of the copolymers at the different stages of the copolymerizations. With methacrylamide, for example, the copolymers are initially soluble, but they become insoluble when the availability of the cationic monomer decreases at the later stages of the polymerization.

An average  $e$  value of +1.7 is indicated for this monomer by these data.<sup>44</sup> A high positive polarity of the vinyl group would be expected because of the adjacent pyridinium ring. The average  $Q$  value of 10 is higher than those which are generally found. It might be expected that the  $Q$  value might be higher than that for styrene ( $Q = 1.0$ ), but not that much higher. The  $Q$  and  $e$  values for unquaternized 2-methyl-5-vinylpyridine are reported to average about 0.8 and  $-0.6$ , respectively.<sup>45</sup>

## EXPERIMENTAL

### Preparation of Monomer

Distilled dimethyl sulfate was added to an acetone solution of an equimolar quantity of distilled 2-methyl-5-vinylpyridine (Phillips Chemical

Co., 1 g./5 ml. of acetone). The reaction temperature was maintained at 25–35°C. by the rate of addition of the dimethyl sulfate, by stirring, and by cooling. Fresh portions of acetone were used for several washes of the crystalline monomer which was then dried under vacuum at 35°C. Generally, the product was obtained in about 90% yield after about a 3-hr. reaction time.

The monomer was recrystallized by dissolving it in boiling absolute ethanol (4 ml./g.) and immediately stirring the solution in an ice water bath. Absolute ether was used to wash the crystals. When the dry crystals were placed in a preheated bath, melting occurred at 137°C. With slow heating, polymerization took place before the melting point was reached.

ANAL. Calculated for  $C_{10}H_{15}O_4NS$ : C, 49.0%; H, 6.16%; O, 26.1%; N, 5.71%; S, 13.1%;  $OCH_3$ , 12.7%. Found: C, 49.2%; H, 6.19%; O, 26.5%; N, 6.03%; S, 12.9%;  $OCH_3$ , 12.4%.

At 25°C., the monomer is soluble to about 75% in water, 50% in methanol, 20% in dimethyl sulfoxide, and 10% in dimethylformamide. It is also soluble in other polar solvents such as glycerol, glacial acetic acid, and nitromethane; it is insoluble in ketones, esters, alcohols higher than ethanol, and nonpolar solvents. The presence of small amounts of water in the polar solvents increases the monomer solubility markedly. Unlike many quaternary salts, this monomer is nonhygroscopic except at very high humidities.

### Solution Polymerization

An aqueous monomer solution containing initiator was sealed in a pressure bottle with a Buna N-lined, two-holed, crimped cap. Generally, 10 cycles of evacuation and repressurization to 10 psig of nitrogen (through hypodermic needles) were used to displace the air. The bottle was placed in a constant temperature bath until the desired amount of polymerization occurred.

The volume of each monomer solution was adjusted to the size of the bottle, so that it was possible for the heat of polymerization to be removed by diffusion through the reaction mixture. This was necessary because firm, rubberlike gels were generally obtained and therefore stirring could not be used in the control of the reaction temperature.

Because the polymer tended to be self-dispersible<sup>26</sup> and the monomer tended to be insoluble, it was not possible to use quantitative reprecipitations for the purification of the polymer. When dry polymer was desired, it was obtained by the addition of about a 5% polymer solution to enough acetone in order to finally give about 5% water in the final mixture.

Generally, the reaction product was swollen and diluted with water to about 1.0% polymer solution. The extent of the polymerization was determined by ultraviolet analysis.

Most of the polymer solutions remained crystal clear, while others showed



TABLE VI  
 Copolymerization of 1,2-Dimethyl-5-vinylpyridinium Methyl Sulfate with Various Comonomers

Comonomer		Monomer concentration, %		Solvent	AIBN, %	Temperature, °C.	Reaction time, hr.	Conversion, %	Comonomer in copolymer	
Name	Mole-%	Mole-%	%						Mole-%	Analyses for estimation
Acrylamide	80	50	50	Water	0.30	48	1.0	12	57	S
Acrylamide	60	51	50	Water	0.30	48	0.8	14	29	S
Acrylamide	40	50	50	Water	0.30	48	0.4	14	15	S
Methacrylamide	80	52	50	Water	0.30	48	1.0	28	61	S
Methacrylamide	60	50	50	Water	0.30	48	0.5	22	35	S
Methacrylamide	40	50	50	Water	0.30	48	0.5	20	23	S
Methyl methacrylate	10	53	50	70% Methanol	0.10	50	0.3	8.4	8	S, N
Methyl methacrylate	30	53	50	70% Methanol	0.10	50	0.3	9.6	18	S, N
Methyl methacrylate	50	53	50	70% Methanol	0.10	50	0.4	8.3	35	S, N
Methyl methacrylate	58	53	50	70% Methanol	0.10	50	0.4	8.4	41	S, N
Methacrylic acid	90	50	50	Water	0.02	50	0.67	3.9	82	C, H, N
Methacrylic acid	70	50	50	Water	0.02	50	0.63	6.4	67	C, H, N
Methacrylic acid	50	50	50	Water	0.02	50	0.50	4.7	49	C, H, N
Methacrylic acid	10	50	50	Water	0.02	50	0.42	4.9	27	C, H, N

mold growth after a few weeks.<sup>46</sup> There were usually significant changes in the solution viscosities during storage at room temperature.

### Rate Studies

The monomer was weighed into a pressure bottle which was sealed with a Buna N-lined, two-holed, crimp cap and evacuated for about 1 hr. A solution containing appropriate amounts of the other constituents to give a 50-ml. reaction mixture was weighed into another pressure bottle and cooled to 0°C. Both bottles were evacuated and repressured with nitrogen (10 cycles). The two bottles were placed for 1 hr. in a bath at the reaction temperature. At zero time, the aqueous initiator solution was transferred under nitrogen through a hypodermic needle into the pressure bottle. The reaction mixture was magnetically stirred under 10 psig of nitrogen. Appropriate volumes of the reaction mixture were removed with a hypodermic syringe and immediately diluted to about 0.006% for ultraviolet analysis.

### Copolymerization

Each copolymerization was accomplished by a solution polymerization similar to that described above. Recrystallized or distilled comonomers were used. When the viscosity of the reaction mixture indicated about 10% polymerization, the copolymer was immediately precipitated by the addition of nonsolvent (acetone, isopropyl alcohol, or *tert*-butyl alcohol). At least one reprecipitation was made before analysis.

It was very difficult to devise precipitation conditions for the complete precipitation of the copolymer. At too high ratios of the nonsolvent, the cationic monomer tended to be insoluble. At all ratios of the nonsolvent, the copolymers tended to a self-dispersible,<sup>26</sup> and it was necessary to add an inert electrolyte in order to overcome their tendency to peptize. The use of 1-methyl-2-bromopyridinium methyl sulfate for this purpose provided a common anion. Bromine analysis established that negligible amounts of this electrolyte were retained in the dry polymers.

Table VI gives the experimental details for the copolymerizations.

### Ultraviolet Analysis

Analyses were made on aqueous solutions containing about 0.005% monomer and polymer. The following expressions were used to calculate the concentrations of monomer ( $x$ ) and polymer ( $y$ ) in grams per liter:

$$x = 0.0308\Delta_{310}^{274} - 0.0344\Delta_{246}^{274}$$
$$y = 0.0537 \Delta_{310}^{274} - 0.00463 \Delta_{246}^{274}$$

where  $\Delta_{310}^{274}$  = difference in absorbance between 274 m $\mu$  and 310 m $\mu$ , and  $\Delta_{246}^{274}$  = difference in absorbance between 274 m $\mu$  and 246 m $\mu$ .

### Viscosity Measurements

Intrinsic viscosity measurements were determined from measurements of reduced specific viscosities at 25°C. in dilution type No. 1 Ubbelohde viscometers and extrapolation of the data to infinite dilution by the method of Martin.<sup>47</sup> To overcome the problems of viscosity measurements on a polyelectrolyte in aqueous solution,<sup>34</sup> 0.200*M* sodium chloride was selected as solvent.

The author is very grateful to Professor C. C. Price for his valuable suggestions in this work. The valuable assistance of many people at the Hercules Research Center is also acknowledged, with special mention of Drs. H. M. Spurlin, D. C. Lincoln, and D. S. Breslow.

### References

1. Barney, A. L., U. S. Pat. 2,677,679 (May 4, 1954), to E. I. du Pont de Nemours & Co., Inc.
2. Hughes, L. E., U. S. Pat. 2,694,688 (November 16, 1954), to E. I. du Pont de Nemours & Co., Inc.
3. Hayek, M., U. S. Pat. 2,723,256 (November 8, 1958), to E. I. du Pont de Nemours & Co., Inc.
4. Hayek, M., U. S. Pat. 2,741,568 (April 10, 1956), to E. I. du Pont de Nemours & Co., Inc.
5. Winberg, H. E., U. S. Pat. 2,744,130 (May 1, 1956), to E. I. du Pont de Nemours & Co., Inc.
6. Barney, A. L., U. S. Pat. RE. 24,164 (June 12, 1956), to E. I. du Pont de Nemours & Co., Inc.
7. Brit. Pat. 796,543 (June 11, 1958), to Ciba Co., Inc.
8. Batty, J. W., and G. T. Jones, Canadian Pat. 584,048 (August 29, 1959), to Imperial Chemical Industries Ltd.
9. Shacklett, C. D., U. S. Pat. 2,777,872 (January 15, 1957), to E. I. du Pont de Nemours & Co., Inc.
10. Jones, G. T., Can. Pat. 583,352 (September 15, 1959), to Imperial Chemical Industries Ltd.
11. Barney, A. L., U. S. Pat. 2,764,578 (September 25, 1956), to E. I. du Pont de Nemours & Co., Inc.
12. Brit. Pat. 815,745 (July 1, 1959), to Rohm and Haas Co.
13. Ham, G. E., U. S. Pat. 2,572,560 (October 23, 1951), to Monsanto Chemical Co.
14. Ham, G. E., U. S. Pat. 2,572,561 (October 23, 1951), to Monsanto Chemical Co.
15. Morris, L. R., U. S. Pat. 2,772,310 (November 27, 1956), to Dow Chemical Co.
16. Clarke, J. T., U. S. Pat. 2,780,604 (February 5, 1957), to Ionics, Inc.
17. Price, J. A., U. S. Pat. 2,654,729 (October 6, 1953), to American Cyanamid Co.
18. Butler, G. B., and R. L. Bunch, U. S. Pat. 2,687,382 (August 24, 1954) to State of Florida.
19. Sprague, R. H., and G. S. Brooker, U. S. Pat. 2,548,564 (April 10, 1951), to Eastman Kodak Co.
20. Forshey, W. O., Jr., and J. E. Kirby, U. S. Pat. 2,680,112 (June 1, 1954), to E. I. du Pont de Nemours & Co., Inc.
21. Clarke, J. T., U. S. Pat. 2,732,350 (January 24, 1956), to Ionics, Inc.
22. Shen, K.-T., U. S. Pat. 2,771,462 (November 20, 1956), to Petrolite Corp.
23. Leubner, G. W., J. L. R. Williams, and C. C. Unrah, U. S. Pat. 2,811,510 (October 29, 1957), to Eastman Kodak Co.
24. Gillis, R. G., Ph.D. Thesis, University of Notre Dame, 1952.
25. Hart, R., and D. Timmerman, *J. Polymer Sci.*, **28**, 638 (1958).

26. Jones, G. D., and S. J. Goetz, *J. Polymer Sci.*, **25**, 201 (1957).
27. Butler, G. B., and R. J. Angelo, *J. Am. Chem. Soc.*, **79**, 3128 (1957).
28. Overberger, C. G., H. Bilech, and R. G. Nickerson, *J. Polymer Sci.*, **27**, 381 (1958).
29. Duling, I. N., Ph.D. Thesis, University of Pennsylvania, 1961.
30. Barnes, C. E., *J. Am. Chem. Soc.*, **67**, 217 (1945).
31. Barnes, C. E., R. M. Eloffson, and G. D. Jones, *J. Am. Chem. Soc.*, **72**, 210 (1950).
32. Trommsdorf, E., H. Kohle, and P. Lagally, *Makromol. Chem.*, **1**, 169 (1948).
33. Breslow, D. S., and A. Kutner, *J. Polymer Sci.*, **27**, 295 (1958).
34. Flory, P. J., *Principles of Polymer Chemistry*, Cornell Univ. Press, Ithaca, N. Y., 1953.
35. Schulz, G. V., and E. Huseman, *Z. Physik. Chem.*, **B39**, 246 (1938).
36. Josefowitz, D., and H. Mark, *Polymer Bull.* **1**, 140 (1945).
37. Kamenskaja, S., and S. Medwedew, *Acta Physicochim, URSS*, **13**, 565 (1940).
38. Matheson, M. S., *J. Chem. Phys.*, **13**, 584 (1945).
39. Walling, C., *Free Radicals in Solution*, Wiley, New York, 1957, p. 77.
40. Kolthoff, I. M., and I. K. Miller, *J. Am. Chem. Soc.*, **73**, 3055 (1951).
41. Marshall, C. A., and R. A. Mock, *J. Polymer Sci.*, **17**, 591 (1955).
42. Fineman, M., and S. D. Ross, *J. Polymer Sci.*, **5**, 259 (1950).
43. Alfrey, T., Jr., J. J. Bohrer, and H. Mark, *Copolymerization*, Interscience, New York, 1952.
44. Alfrey, T., and C. C. Price, *J. Polymer Sci.*, **2**, 101 (1947).
45. Tamikado, T., *Makromol. Chem.*, **38**, 85 (1960).
46. Goldberg, P., and R. M. Fuoss, *J. Phys. Chem.*, **58**, 648 (1954).
47. Martin, A. F., *Tappi*, **34**, 363 (1951).
48. Bourdais, J., *Bull. Soc. Chim. France*, **1955**, 485.
49. Gabriel, C. E., and D. L. Decker, paper presented at the New York Meeting, American Chemical Society of Polymer Chemistry, **1**, No. 2, 213 (1960).
50. Smets, G., and A. M. Hesbain, *J. Polymer Sci.*, **40**, 217 (1959).

### Résumé

Le 1,2-diméthyl-5-vinylpyridinium méthyle sulfate peut être rapidement polymérisé en solution aqueuse par un radical libre dans des conditions douces en un polyélectrolyte cationique de poids moléculaire élevé. Un ordre trois-demi pour la vitesse de polymérisation par rapport à la concentration en monomère est indiqué pour environ 75% de la polymérisation du 1,2-diméthyl-5-vinylpyridinium méthyle sulfate en solution aqueuse avec du persulfate de potassium comme initiateur. Une dépendance normale de la vitesse de polymérisation, racine carrée de la concentration en initiateur est également montrée par des résultats. L'énergie d'activation globale est estimée à environ 17 kcal/mole. Des expériences préliminaires portant sur l'effet du changement de la force ionique du milieu réactionnel par addition de chlorure de sodium, ont montré qu'il y avait un changement dans les cinétiques, ainsi qu'un ralentissement dramatique de la polymérisation. Des études de copolymérisation montrent que la réactivité de ce monomère cationique est plus élevée que celle de l'acrylamide, du méthacrylamide et du méthacrylate de méthyle, mais égale à celle de l'acide acrylique.

### Zusammenfassung

1,2-Dimethyl-5-vinylpyridiniummethylsulfat polymerisiert in wässriger Lösung leicht unter milden radikalischen Bedingungen zu einem kationischen Polyelektrolyten hohen Molekulargewichts. Für etwa 75% der mit Kaliumpersulfat gestarteten Polymerisation von 1,2-Dimethyl-5-vinylpyridiniummethylsulfat in wässriger Lösung wurde eine Reaktionsordnung von  $3/2$  bezüglich der Monomerkonzentration bestimmt. Ausserdem wurde eine normale Abhängigkeit der Polymerisationsgeschwindigkeit von der Quadrat-

wurzel der Starterkonzentration gefunden. Die Bruttoaktivierungsenergie wurde zu etwa 17 kcal/Mol. bestimmt. Bei vorläufigen Versuchen über den Einfluss einer Veränderung der Ionenstärke des Reaktionsmediums auf die Kinetik wurde gefunden, dass ein Zusatz von Natriumchlorid die Polymerisation stark verlangsamt. Wie Copolymerisationsuntersuchungen ergaben, ist die Reaktionsfähigkeit dieses kationischen Monomeren zwar höher als diejenige von Acrylamid, Methacrylamid und Methylmethacrylat, jedoch ähnlich derjenigen von Acrylsäure.

Received April 10, 1963

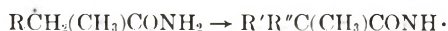


## Electron Spin Resonance Studies of Irradiated Single Crystals of Methacrylamide\*

HISASHI UEDA,† *Department of Physics, Duke University, Durham North Carolina, and Department of Chemistry, The University of British Columbia, Vancouver, British Columbia, Canada*

### Synopsis

Irradiated single crystals of methacrylamide were studied by electron spin resonance. Irradiations were made at 77 and 288°K. and measurements were made at 77, 193, and 293°K. Only chemical changes explain these spectra. The original scission is C—C breakage between (CONH<sub>2</sub>) and CH<sub>2</sub>=C(CH<sub>3</sub>)—, and C—H breakage between CH<sub>2</sub>=C—(CONH<sub>2</sub>)CH<sub>2</sub>— and H; these small fragments react with methacrylamide and finally produce two free radicals at room temperature. These two free radicals are the ones which propagate or terminate the polymerization. The free radical transformation at the last period of polymerization is concluded to be:



### INTRODUCTION

It is extremely difficult to obtain a single crystal of a high polymer which is sufficiently large to permit observation of the electron spin resonance (ESR) after irradiation. Therefore, the only way to determine the exact nature of free radicals trapped in a vinyl polymer by polymerization or radiation damage seems to be to study an irradiated single crystal of its monomer. However, there are very few examples of ESR studies of irradiated single crystals of vinyl monomers. It is also difficult to prepare a single crystal of a vinyl monomer. This is partly because a monomer is readily polymerized during the evaporation of the solvent from its solution to make single crystals. The other difficulty is that most of vinyl monomers are liquid at room temperature. In this respect, acrylamide and methacrylamide have their advantages, as both of them are solid at room temperature.

### EXPERIMENTAL

It was difficult to grow a good single crystal from an alcoholic solution of methacrylamide, as it readily gave very thin and fragile plates. A mixed

\* This work was partly supported by the U. S. Air Force, Scientific Research Development Command, AF-AFOSR-62-327.

† Nishina Memorial Fellow.

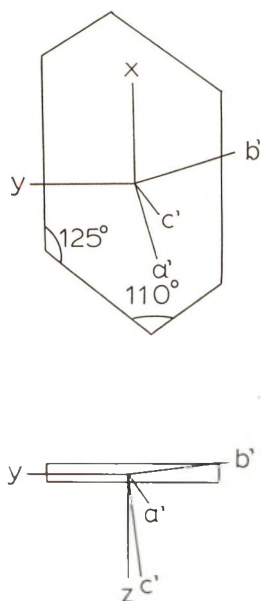


Fig. 1. A single crystal of methacrylamide.  $x$ ,  $y$ , and  $z$  are conventional axes selected for the measurements.  $a'$ ,  $b'$ , and  $c'$  are the directions of the principal values of the hyperfine tensors.

solvent of concentrated HCl and ethanol gave, when the solution was warmed to  $40^{\circ}\text{C}$ . and then cooled and evaporated, several satisfying crystals whose shape is shown in Figure 1. The result of an elementary analysis showed that no acid is bonded in the form of hydrochloride.

Crystals were irradiated at 77 and  $288^{\circ}\text{K}$ ., the ESR measurements were made at 77, 193, and  $293^{\circ}\text{K}$ ., all at a frequency of about 9,400 Mcycles/sec.

The crystal structure and symmetry of this crystal is not known, but a conventional coordinate system was selected as shown in Figure 1. Measurements were made with the magnetic field perpendicular to one of these axes, at  $15^{\circ}$  intervals, or for  $7.5^{\circ}$  if necessary, of rotation about this axis.

## RESULTS

### 1. Irradiation at $288^{\circ}\text{K}$ .

The crystal irradiated with a dose of  $3 \times 10^6$  r at  $288^{\circ}\text{K}$ . was measured at 293 and  $77^{\circ}\text{K}$ .

**A. Spectrum Observed at  $293^{\circ}\text{K}$ .** This spectrum is composed of two groups of lines: a quintet and a sextet, as shown in Figure 2. The quintet is isotropic with an equal spacing of 23 gauss and the same nature as already found in irradiated polymethyl-methacrylate.<sup>1-3</sup> The sextet is anisotropic. From the angular dependence of the splitting, it is concluded that there are one nitrogen and one proton coupling with the unpaired electron. The proton interacts isotropically and its splitting factor,  $A_1$ , is 28.2 gauss.

TABLE I  
Anisotropic Splitting Factors from the Nitrogen Nucleus

I Experimental values			II Principal values			III Direction cosines		
$x$	$y$	$z$	$a'$	$b'$	$c'$	$a'$	$b'$	$c'$
$x + 14.0$	-2.6	-0.3	$a' + 12.8$	0	0	$x - 0.92$	+0.28	-0.25
$y - 2.6$	+21.0	+1.4	$b' 0$	+22.1	0	$y - 0.23$	-0.94	-0.23
$z - 0.3$	+1.4	+12.6	$c' 0$	0	+12.8	$z - 0.29$	-0.14	+0.94

The nitrogen interacts anisotropically and its splitting factor,  $A_a$ , is shown in Table I.

The term  $x-x$  in I denotes the  $A_{xx}$  element of the hyperfine tensor, term  $x-y$ , the  $A_{xy}$  element, etc. In the same way, in II, term  $a'-a'$  denotes

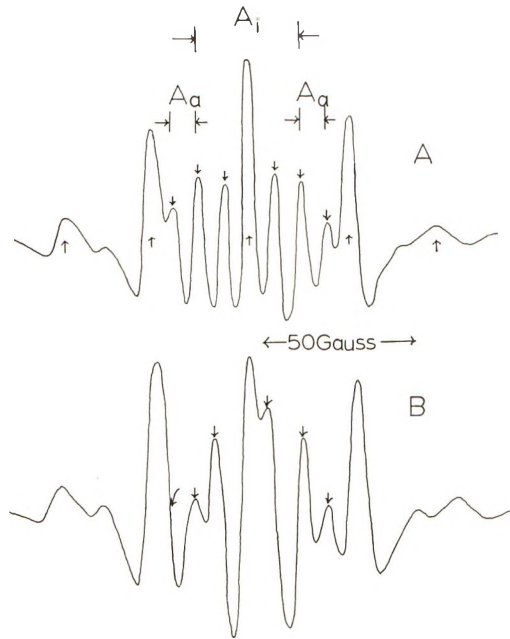


Fig. 2. ESR spectra for the measurements at 293°K.: (A)  $\angle xH = 90^\circ$ ,  $\angle yH = 0^\circ$ ; (B)  $\angle xH = 90^\circ$ ,  $\angle yH = 45^\circ$ .  $A_i$  indicates the isotropic splitting and  $A_a$  indicates the anisotropic splittings.

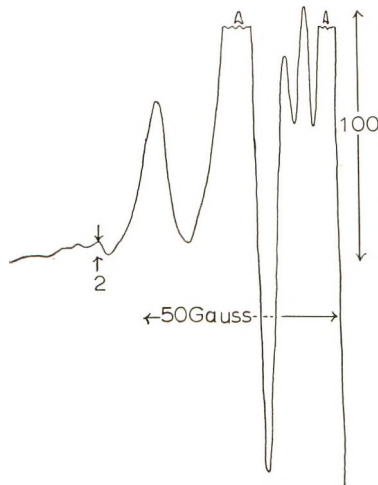


Fig. 3. Carbon-13 lines of the spectrum obtained from an irradiated single crystal of methacrylamide.  $\angle xH = 90^\circ$ ,  $\angle yH = 30^\circ$ . Only the left half of the spectrum is shown. The  $^{13}\text{C}$  splitting constant has been reported as 35 gauss.<sup>4</sup>

one of the principal values  $A_{a'a'}$ . III shows the direction cosines for the transformation of I into II. These principal values can be divided into two terms, the isotropic and anisotropic terms. The isotropic part is 15.9 gauss while the anisotropic principal values are  $-3.1$ ,  $6.2$ , and  $-3.1$  gauss for  $a'a'$ ,  $b'b'$ , and  $c'c'$  elements, respectively.

**B. Spectra Observed at 77 and 193°K.** These are identical with those at 293°K.

**C. Spectra from the Crystal with High Dosage.** The spectra obtained after irradiation with a dose of  $10^8$  r at 288°K. showed no anisotropy. This is because the methacrylamide had polymerized completely and was no longer a single crystal. Actually the spectrum was identical with that of polycrystalline material, and the hardness and brittleness of this crystal was different from that of sample irradiated with  $3 \times 10^6$  r.

**D. Carbon-13 Lines.** Some anisotropic carbon-13 lines are observed when a strong signal is recorded, as shown in Figure 3.

## 2. Irradiation at 77°K.

The crystal irradiated with a dose of  $3 \times 10^6$  r at 77°K. was colored green, while the color of the crystal irradiated at 288°K. is yellow. This crystal was first measured at 77°K., then warmed up to 193°K. and measured,

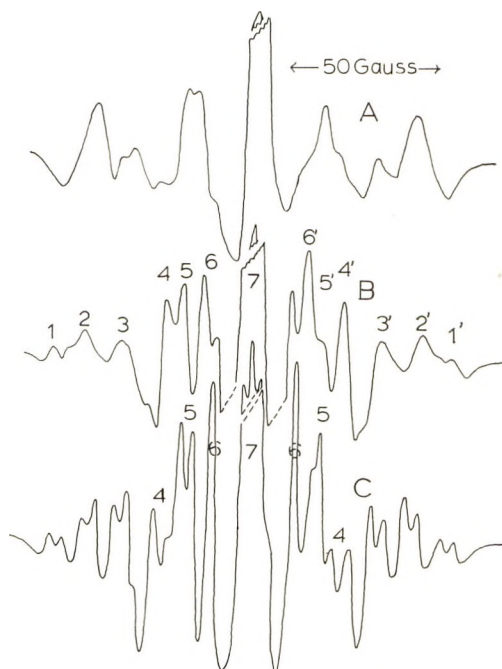


Fig. 4. ESR spectra for the measurements at 77°K. of a crystal irradiated at 77°K.,  $\angle xH = 90^\circ$  for all spectra: (A)  $\angle yH = 75^\circ$  with the incident power of 20 mw.; (B)  $\angle yH = 165^\circ$ , the incident power is 1 mw.; (C)  $\angle yH = 75^\circ$ , with the incident power of 1 mw.



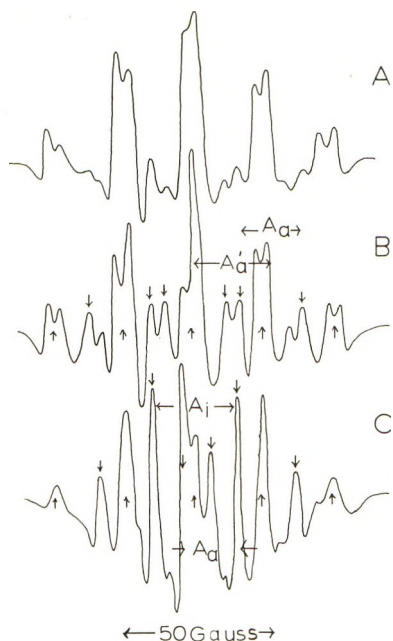


Fig. 5. ESR spectra of the crystal irradiated at  $77^\circ\text{K.}$  and then warmed to  $193^\circ\text{K.}$ ,  $\angle xH = 90^\circ$  for all spectra: (A) measured at  $77^\circ\text{K.}$ ,  $\angle yH = 67.5^\circ$ , the incident power is 20 mw.; (B) at the same orientation and with the same power as in A, but measured at  $193^\circ\text{K.}$ ; (C)  $\angle yH = 30^\circ$ , the incident power is 20 mw., measured at  $193^\circ\text{K.}$   $A_i$  indicates the isotropic splitting, and  $A_a$  and  $A_a'$  indicate the anisotropic splittings, respectively.

then again cooled to  $77^\circ\text{K.}$  and measured, and finally rewarmed to  $293^\circ\text{K.}$  and measured.

**A. Spectra at  $77^\circ\text{K.}$**  The pattern of the spectra at  $77^\circ\text{K.}$  is strongly power-dependent. The spectra at a microwave incident power of about 20 mw. is broadened by power saturation at any orientation in the magnetic field, as shown in Figure 4A. However, when the power is reduced to a few milliwatts, the spectra can be split into about 16 lines, as shown in Figure 4B. When the conventional  $y$ -axis is near  $90^\circ$  to the magnetic field, the lines can further be split twice in its number, as shown in Figure 4C. It seems there are too many lines to be interpreted. However, the following analysis seems the most plausible one. There are three components; a sextet (1,3,5,7,5',3',1'), a quintet (2,4,7,4',2'), and a triplet (6,7,6'). If the total intensities of these different components are put as  $x$ ,  $x + y$ ,  $y$  respectively, the intensity of the central line, i.e., the line marked by 7, should be four times as strong as that of the nearest neighbor, 6 or 6'.

**B. Spectra After Warming to  $193^\circ\text{K.}$**  The shape of the spectrum when the crystal irradiated at  $77^\circ\text{K.}$  was warmed up to  $193^\circ\text{K.}$  and then measured shows far smaller power saturation than that of the crystal before warming.

The spectrum, however, fairly shows power saturation when the crystal is cooled to 77°K. again, as shown in Figure 5A. The spectra has a quintet with the equal splittings of 21.5 gauss, as is clearly seen in the power-saturated spectrum in Figure 5A. The other component is an anisotropic double quartet (sometimes double triplet) with an isotropic splitting of 28 gauss,  $A_t$ , and with two anisotropic splittings,  $A_a$  and  $A_a'$ .

**C. Spectrum After Warming to 293°K.** The spectrum thus obtained is identical with that obtained by irradiation at 293°K.

## DISCUSSION

The number and the spacings of the spectral lines change according to the temperature of irradiation, not of measurement. The spectrum at any condition of measurement has more than two components.

The significant difference of this present compound from other already studied single crystals lies in that it has a C=C double bond, which easily reacts with small fragments produced by the irradiation, e.g., the addition reaction of free radicals.

Abraham and co-workers<sup>2</sup> explained the two species in irradiated PMMA on the basis of configurational isomerism. If the two components of a spectrum are to be explained in that way in this case, they must have at least one common spacing in each of the spectra. In the present case no such common splitting was found.

The quintet of lines is found only in irradiated methyl-substituted vinyl

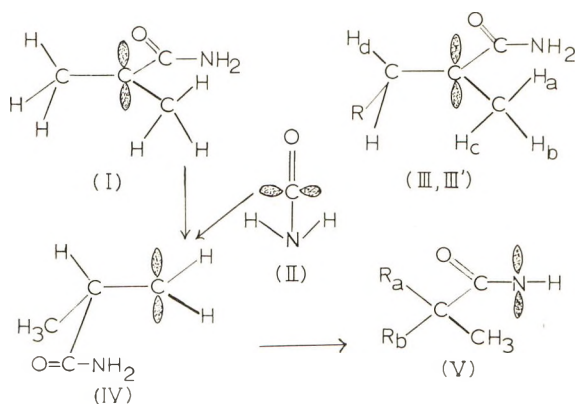
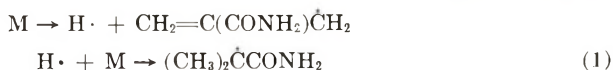


Fig. 6. The scheme of radiation decomposition of methacrylamide. At 77°K., (I), (II), and (III) are observed after irradiation, (I) and (II) change to (IV) between 77 and 193°K. Then at 193°K., both (III) and (IV) are observed. Between 193 and 293°K., (IV) changes to (V). Then at 293°K., both (III) and (V) are observed. From (V), a spectrum which is strongly anisotropic is expected. However, if there is a large contribution of the resonance structures  $\text{RC}(=\text{NH})-\text{O}$  and  $\text{RC}(=\text{NH})\text{O}$ , the anisotropy will be substantially reduced. R is either  $[\text{CH}_2=\text{C}(\text{CONH}_2)\text{CH}_2-]$  in (III) or  $[\text{CH}_2=\text{C}(\text{CH}_3)-]$  in (III') groups. In (V),  $R_a$  and  $R_b$  are H,  $(-\text{CONH}_2)$ , and/or several monomer units. The figure (IV) shows only the species which is formed from (II); (IV') referred to in the text is formed from (I).

monomers and polymers. Therefore, it is clear that two or three of the coupling protons for the quintet of lines are from this methyl group. If the methyl group is rotating at 293°K. and not rotating at 77°K., the spectrum of the crystal irradiated at 288°K. and measured at 77°K. must show great difference from that measured at 293°K. In the present case they are the same.

From these facts, the difference in the present spectra at different conditions is to be interpreted by chemical changes in the structures of the free radicals. The fact that the crystal irradiated at 77°K. gives the same spectrum as that of the crystal irradiated at 293°K. when the former is measured also at 293°K. shows that the radiation damage caused at 77°K. is the more original process. As a matter of possibility several different bond scissions are expected at 77°K. However, only two types of bond scissions were observed in this study.

As the sextet of lines has equal spacings and an approximate intensity ratios of 1:6:15:20:15:6:1, there should be six equally coupling protons. Such spectrum can only be explained by the species I in Figure 6. It should be assumed that two methyl groups are rotating. The species I is formed by an addition of an emitted hydrogen atom from methacrylamide (M).



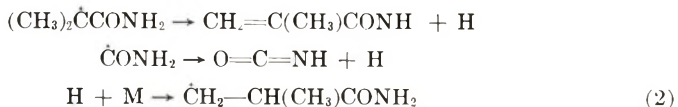
This species  $CH_2=C(\text{CONH}_2)\dot{C}H_2$  was not observed in this experiment. This is interpreted in the way that this species adds to M and forms a free radical, III. The species III gives a quintet by an equal interaction of the unpaired electron with the four protons  $H_a$ ,  $H_b$ ,  $H_c$ , and  $H_d$ , assuming the methyl protons and the proton  $H_d$  are identical. On the other hand, the triplet is to be explained by a species as shown in II. The ESR spectra of species II might show anisotropy; however, a tumbling motion of this species in the crystal lattice will cancel it. Actually, the width of the triplet is smaller than the other lines, as shown in Figure 4. The species II is formed by a C—C scission of M, and the expected counter fragment is  $CH_2=\dot{C}(\text{CH}_3)$ . This latter species was not observed in this experiment, either. This is interpreted as follows: this species is too reactive to exist, and adds to M, forming III', which also gives a quintet. Therefore, the primary radiation damage of M is formulated as:



The ratio of C—H scissions to C—C scissions is  $x:y$  and equals to the intensity ratio of the lines from the species I and II, and is 3:2.

One component of the spectra observed at 193°K. (Fig. 5) is a quintet. This is to be assigned to the species III and III', because these two fragments gave a quintet at 77°K. The spacings have changed from 27 gauss to 21.5 gauss. There will be some difference in the configuration of the free radical between 77°K. and 193°K. The other component is an anisotropic octet. This latter spectrum shows that there is one proton in-

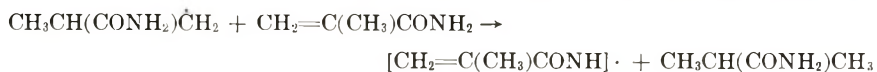
teracting isotropically and two protons equally and anisotropically. The expected structure for this fragment is IV. The species I and II have disappeared on raising of the temperature of the crystal from 77°K. to 193°K., and the species V has appeared instead. The reactions;



are expected between 77°K. and 193°K. The reaction (H + M) was like reaction (1) when it proceeded under irradiation at 77°K., but at 193°K. it is like reaction (2). This difference in the adding sides of the carbon atoms of a double bond, when a hydrogen atom adds to it, will be explained as a thermal effect.

The angle between the direction of the unpaired electron and the direction of the C—H bond interacting isotropically with this electron is calculated from the isotropic splitting of 28 gauss and is about 36°.

After the crystal was warmed to room temperature, the free radical giving rise to the quintet was still present, with four equal spacings of 23 gauss. However, the free radical which gave the octet at 193°K. decayed somewhere below room temperature and instead the double triplet appeared. This double triplet indicates that there is one nitrogen nucleus and one isotropically interacting proton. The free radical as shown in V of Figure 6 will give the double triplet lines. Because the isotropic 28.2 gauss splitting seems a reasonable value for the N—H proton if a contribution of the structures R—C(=NH)—O· and R— $\dot{\text{C}}$ (=NH)—O to the species V is not small. The isotropic splitting of 15.9 gauss of the each triplet is also very probable as a nitrogen splitting. Then, the free radical change is:



This indicates that the RCH<sub>2</sub>· type free radical is not stable at room temperature, perhaps because of its larger mobility than that of R—CH—R' type radical, in which both sides of the free radical carbon atom is more or less fixed. Methacrylamide polymerizes with two different mechanisms.<sup>5</sup> The one is thermal polymerization occurring above 150°C. and the other is free radical polymerization occurring near 100°C. In the spectrum obtained from polycrystalline methacrylamide the double triplet component disappears after the free radical polymerization has started. This indicates that the free radical V has started another polymerization chain. This alternatively can be described that the free radical V has been transformed into a polymerization end type radical RCH<sub>2</sub> $\dot{\text{C}}$ (CONH<sub>2</sub>)CH<sub>3</sub>. However, when the crystal is further heated, all the polymerization end is terminated by a chain transfer process to the amino group, leaving the free radical V, which cannot be further transformed because there is no monomer at this stage of the polymerization. Thus, the resulting spectrum is structureless when observed in the polycrystalline state on account of its anisotropy.<sup>5</sup>



From the polycrystalline study, it was shown that the free radicals stable at room temperatures begin to change their configuration near the melting point. However, the structures of the free radicals change very drastically at a far lower temperature.

Many experimental results have shown that polymethyl methacrylate undergoes C—C scission when irradiated. By a C—C scission, two different fragments can be formed; however, only one of the fragments,  $\text{R}\dot{\text{C}}(\text{CH}_3)\text{COCH}_3$  has been observed.<sup>1-3</sup> Considering that the free radical IV is not stable at room temperature, the unobserved free radical  $\text{RCH}_2\cdot$  will exist in the transient state and will decompose immediately after its formation at room temperature.

### References

1. Ingram, D. J. E., M. C. R. Symons, and M. G. Townsend, *Trans. Faraday Soc.*, **54**, 409 (1958).
2. Abraham, R. J., H. W. Melville, D. W. Ovenall, and D. H. Whiffen, *Trans. Faraday Soc.*, **54**, 1133 (1958).
3. Unger, I. S., W. B. Gager, and R. I. Leiniger, *J. Polymer Sci.*, **44**, 295 (1960).
4. Cole, T., and C. Heller, *J. Chem. Phys.*, **34**, 1085 (1961).
5. Ueda, H., Z. Kuri, and S. Shida, *J. Polymer Sci.*, **61**, 333 (1962).

### Résumé

On a étudié par résonance de spin électronique des cristaux simples de méthacrylamide irradiés. Les irradiations ont été effectuées à 77 et 288° K et les mesures effectuées à 77, 193 et 293°K. Ces spectres s'expliquent uniquement par des changements chimiques. La scission originale est la rupture C—C entre  $(\text{CONH}_2)$  et  $\text{CH}_2=\text{C}(\text{CH}_3)-$ , et la rupture C—H entre  $\text{CH}_2=\text{C}-(\text{CONH}_2)\text{CH}_2-$  et H; ces petits fragments réagissent avec le méthacrylamide et finalement produisent deux radicaux libres à température de chambre. Ces deux radicaux libres sont ceux qui propagent ou terminent la polymérisation. La transformation du radical libre à la période finale de la polymérisation est:



### Zusammenfassung

Es wurden Elektronenspinresonanzuntersuchungen an bestrahlten Methacrylamid-Einkristallen durchgeführt. Die Bestrahlung erfolgte bei 77°K und 288°K, die Messungen bei 77°K, 193°K und 293°K. Eine Deutung der Spektren ist nur unter der Annahme chemischer Veränderungen möglich. Die ursprüngliche Spaltung besteht in einer C—C—Spaltung zwischen  $(\text{CONH}_2)$  und  $\text{CH}_2=\text{C}(\text{CH}_3)-$  und einer C—H—Spaltung zwischen  $\text{CH}_2=\text{C}(\text{CONH}_2)\text{CH}_2-$  und H. Die dabei gebildeten kleinen Bruchstücke reagieren bei Raumtemperatur mit Methacrylamid unter Bildung zweier Radikale. Diese beiden Radikale sind von der Art der am Wachstum oder Abbruch der Polymerisation beteiligten Radikale. Man nimmt an, dass im letzten Schritt der Polymerisation folgende Radikalumwandlung vor sich geht:



Received April 22, 1963



## Thermal Degradation of Poly(*m*-diethynylene Benzene)

A. E. NEWKIRK, A. S. HAY, and R. S. McDONALD,  
*General Electric Research Laboratory, General Electric Company,  
Schenectady, New York*

### Synopsis

Powdered poly(*m*-diethynylene benzene) can be dissolved in hot nitrobenzene, and thin clear sheets having a yellow color and a tensile strength approaching 9000 psi can be cast from this solution. When the polymer powder is heated rapidly *in vacuo*, it explodes gently at about 180°C. to yield carbon, but it can be annealed at 150°C. and then heated to form carbon without the explosive reaction. The major gaseous decomposition products of the explosive reaction are methane and hydrogen. The polymer film can be crystallized in tetrahydrofuran and shows excellent spherulitic growth. The crystalline film as well as aged noncrystalline film degrades when heated rapidly, but without explosive decomposition. Some indication of the mechanism of decomposition is provided by infrared studies of the film pyrolyzed at 100°C. intervals to 600°C. X-ray diffraction studies show that the polymer may exist in amorphous and crystalline forms. In the amorphous form, the diffraction maximum indicates an average interchain separation of 4.28 Å., substantially less than for other polymers. Chars prepared by heating the polymer give diffraction patterns similar to those for amorphous carbon blacks. A related substance, poly(*p*-diethynylene benzene), is an intractable crystalline powder having a hexagonal unit cell,  $a_0 = 7.74$  Å.,  $c_0 = 8.97$  Å., containing three monomer units.

### INTRODUCTION

We became interested in the study of the thermal degradation of the polymeric diethynyl benzenes because their unusually high carbon content, 96.75%, should permit the preparation of carbon with a small weight loss and perhaps an unusual structure. The polymers are readily prepared by the application of the oxidative coupling reaction to *m*- and *p*-diethynylbenzene.<sup>1-3</sup> Poly(*m*-diethynylene benzene) can be dissolved in hot nitrobenzene and cast into thin clear sheets having a yellow color. The *para* isomer is insoluble in all common solvents. Both polymers have the monomer unit  $\text{-(C}_6\text{H}_4\text{-C}\equiv\text{C-C}\equiv\text{C)-}$ .

In the present study, degradation of the polymer was studied by thermogravimetric, x-ray diffraction, and infrared spectroscopic techniques in order to obtain information about the general features of the decomposition.

## EXPERIMENTAL

## Preparation and Analysis

The general method of preparation has been described.<sup>3</sup> The samples were analyzed for C and H by conventional microcombustion techniques with the results shown in Table I.

TABLE I  
Composition of Samples of Poly(*m*-diethynylene Benzene)

Sample	C, % <sup>a</sup>	H, % <sup>a</sup>	Sum	Infrared
Theory	96.75	3.25	100	
1	94.9	2.8	97.7	weak C <sub>6</sub> H <sub>5</sub> NO <sub>2</sub> , ~5% <i>p</i> -isomer, —C≡CH, weak aliphatic CH
2	—	—	—	C <sub>6</sub> H <sub>5</sub> NO <sub>2</sub> , ~5% <i>p</i> -isomer, —C≡CH, aliphatic CH
3	96.0	3.5	99.5	~10% <i>p</i> -isomer, —C≡CH
4	94.6	3.1	97.7 <sup>b</sup>	no —C≡CH

<sup>a</sup> Limits ±0.4%.

<sup>b</sup> Slate grey residue in analysis.

Sample 1 was polymer powder obtained by reprecipitation of the crude polymer from hot nitrobenzene followed by drying under house vacuum at room temperature. Sample 2 was a film cast at 170°C. from a nitrobenzene solution of a portion of sample 1 dried at 100°C. under 10 microns pressure. Sample 3 was a powder prepared at temperatures not exceeding 40°C., and without using nitrobenzene as a solvent. Sample 4 was polymer powder as prepared. The infrared spectra were measured with a Beckman IR-7 spectrophotometer. The KBr disk technique was not satisfactory for the powdered polymers. Specimens were prepared by direct pressing of the powder in an 0.5 in. diameter evacuated die at 3500 psi for 3 min. This caused a color change from yellow to brown and a reduction in intensity (sample 1 versus sample 2) of bands due to nitrobenzene and aliphatic C—H. When a portion of the powder was pressed 1 min. at 200,000 psi, the sample became almost black and about half the acetylenic CH groups disappeared. X-ray emission analysis gave the following results: Sample 1: Cu, 0.0007%; Br, present; Ni and Fe, trace. Sample 4: Cu, 0.007%; Br, present; Ni and Fe, trace.

## Instrumental Methods

Thermogravimetric studies were made with a Chevenard pen-recording thermobalance whose operation and performance have been described elsewhere.<sup>4</sup> X-ray diffraction patterns were made with a GE-XRD-5 spectrometer. The infrared studies of film degradation were carried out on a film sample between two cleaved rock salt plates. This sample was then heated in a stream of dry nitrogen (nominal dew point -40°C., H<sub>2</sub> content <1%), cooled in the nitrogen stream, and removed for infrared

examination. This process was repeated at a series of increasingly higher temperatures. Ultraviolet and visible spectra were also measured on this film with a Cary model 14MS recording spectrometer. Tensile strengths were measured with an Instron tensile tester. Mass spectra were measured on a General Electric mass spectrometer.

## RESULTS AND DISCUSSION

The thermal decomposition behavior of the polymer depends on whether it is crystalline or amorphous. We therefore describe first our observations on the crystallization and crystallinity of the polymers.

### Crystallization of Poly(*m*-diethynylene Benzene)

Clear transparent freshly prepared film (sample 2), 0.02 mm. thick, crystallized rapidly when submerged in tetrahydrofuran as indicated by a change from transparent to a frosted or milky translucent appearance. Dimethyl acetamide acted more slowly, and ethyl acetate still more slowly. Many solvents had no effect on the polymer in 24 hr. among them benzene, chlorobenzene, *o*-dichlorobenzene, toluene, dimethylformamide, tetrahydropyran, 1,4-dioxane, methyl isobutyl ketone, and dibutyl cellosolve. In nitrobenzene, a large number of small spherulites covering about 5% of the area of the sheet formed in 24 hr.

The specificity of tetrahydrofuran as a crystallizing solvent for the polymer seems quite surprising and further microscopic studies of its action were therefore carried out. The films used were several years old.

The untreated polymer film appeared quite rough at 25 $\times$  magnification and contained a number of dark, roughly spherical areas. When placed between crossed nicols, it appeared to contain many bright fine needles (fibrils) on a dark background. At 105 $\times$ , the roughly spherical areas were seen to consist of collections of fine bubbles or particles which, between crossed nicols, showed as hazy areas. At 210 $\times$ , the fibrils appeared curved and branched. Between crossed nicols, they were bright yellow on a dark background and showed a crude parallel extinction. When a 550  $m\mu$  retardation plate was inserted in the optical path, half the fibrils appeared roughly parallel and green; the other half of the fibrils were roughly parallel to each other, yellow in color, and at right angles to the first set, all on a bright red background. Due to the parallel extinction, this general appearance was retained, regardless of the rotation of the stage, although any particular fibril went through a cyclic change yellow-dark green, etc. One spherulite was observed in the original polymer sheet.

When the sheet was placed in tetrahydrofuran, there was no change in the microscopic appearance for the first few minutes. Shortly thereafter, spherulites began to form. After 1 $\frac{1}{2}$  hr., about half the film consisted of spherulites, and after 5 hr., the film was more than 90% crystalline. Periodic rings in the spherulites were visible with difficulty at first, but very clear and definite in the later spherulites. The spherulites also showed the typical Maltese cross appearance between crossed nicols.

The rate of crystallization of the sheet polymer varied from sample to sample. Thus, a piece of film 0.013 mm. thick made from sample 4 appeared faintly frosted in a few minutes, and more strongly frosted and quite wrinkled in 15 min. A piece of sample 1 film, 0.02 mm. thick, exposed simultaneously appeared unchanged after 15 min. exposure and showed only slight crystallization at one corner and along several cracks after 45 min. exposure. Both films decreased slightly in area after treatment for 24 hr. followed by air drying.

### Structure

The x-ray diffraction patterns varied from one of a polymer film which contained no lines or bands thereby indicating completely amorphous polymer, to those containing a few narrow sharp lines indicating that highly crystalline regions are present in the polymer sample. The one sample of poly(*p*-diethynylene benzene) which was examined as prepared was the most crystalline of all the samples examined. This is not too surprising, since the *para* polymer can exist only as a rigid rod, whereas the *meta* polymer chain can bend and assume a variety of configurations.

In addition to the sharp lines, all samples of the *meta* polymer powder contained a strong broad band in the region of 3.5 Å. This band may be taken as indicative of amorphous polymer, but the shortness of the spacing is surprising. Klug and Alexander<sup>6</sup> list a range of 4.0–6.6 Å. for the strong amorphous band in fourteen polymers, and a typical polymer containing a benzene ring, polystyrene, has this band at 4.6 Å. In the diethynylene benzene polymers, the spacing ranged from 3.6 Å. in a sample of *meta* polymer as made to 3.48 Å. in a sample of crystallized *meta* polymer film.

It is generally considered that the noncrystalline x-ray diffraction maxima in polymers denotes the frequent occurrence of some average interatomic distance, and in vinyl polymers, it is thus attributed to the interchain carbon-carbon separation. This separation is not the *d* value calculated from the Bragg equation, but is somewhat longer, being approximately 1.25 *d*.<sup>5</sup> In the diethynylene benzene polymers, therefore, the average interchain distance ranges from 4.50 to 4.28 Å. and is substantially less than for other known polymers.

These facts lead to the speculation that in these polymers there is a considerable amount of ordering so that the plane of different benzene rings are roughly parallel. In going from amorphous to crystallized polymer, the ordering would be expected to increase and the average interchain distance shorten. This is observed experimentally, the crystallized film having a shorter spacing and more lines than the other *meta* polymer samples. Also, in accord with these speculations, the *para* polymer has the shortest spacing. These distances are still considerably larger than those in related simple crystals. For example, the interplanar distance in graphite is 3.35 Å.; and the distance of closest approach of carbon atoms in naphthalene is 3.60 Å.

The x-ray diffraction pattern from a sample of crystallized film of poly(*m*-diethynylene benzene) is given in Table II. The film as made showed no measurable lines or bands. For comparison, sample 4 as made gave a pattern of three lines, 6.8 Å, weak and broad, 4.55 Å, medium and broad, and 3.56 Å, strong and broad.

TABLE II  
X-Ray Diffraction Data for Poly(*m*-diethynylene Benzene), Crystallized Film,  
CuK $\alpha$  Radiation

Observed interplanar spacing, Å.	Intensity
7.52	weak
6.50	v. weak
5.10	strong
4.35	medium
3.48	strong, broad
2.85	v. weak
1.82	v. weak

A sample of poly(*p*-diethynylene benzene) gave a good diffractometer pattern with nine lines (Table III). Attempts to obtain more lines with this sample by using photographic techniques and CrK $\alpha$  or CuK $\alpha$  radiation were unsuccessful. Several attempts to prepare a more crystalline polymer were unsuccessful.

TABLE III  
X-Ray Diffraction Data for Poly(*p*-diethynylene Benzene), Hexagonal Unit Cell,  
 $a_0 = 7.74$  Å.,  $c_0 = 8.97$  Å.<sup>a</sup>

<i>hkl</i>	<i>d</i> , Å.		Intensity
	Obs.	Calc.	
10.0	6.71	6.70	ms
00.2	4.51	4.49	vs
11.0	3.87	3.87	vw
11.1	3.5	3.55	vvs
20.0	3.35	3.35	vvs
11.2	2.93	2.93	vw
30.0/00.4	2.25	2.23/2.24	w
22.0	1.94	1.93	vw
31.0	1.84	1.86	w

<sup>a</sup> Volume per unit cell =  $46.52 \times 10^{-23}$  cc.; calculated density = 0.430 g./cc./monomer unit (C<sub>10</sub>H<sub>4</sub>); measured density = 1.21 g./cc.; monomer unit per unit cell = 2.8.

The regularities observed in the original diffractometer tracing suggested that the sample might be hexagonal, and it was possible to index all the observed lines as shown in Table III. The value of  $a_0$  is averaged from all *hk0* reflections and the value of  $c_0$  the average calculated from this value of  $a_0$  and the observed spacings for 00.2 and 11.2. Although the 11.1 reflection was strong, it was not used for calculation of  $c_0$  because it

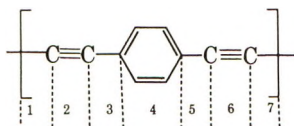


was difficult to locate on the diffractometer tracing used, and results from other samples consistently gave larger spacings for this reflection.

The density of the sample combined with the molecular weight and size of the unit cell gives three monomer units per unit cell as the nearest whole number.

It is interesting to compare the *c* axis spacing with the calculated monomer unit chain length. Table IV gives the calculated data, and it can be seen that even when the effects of neighboring bonds are allowed for, the calculated length expected is 9.4–9.5 Å. versus 8.97 Å. for the *c* axis. From this information and the number of molecules per unit cell we may speculate that the polymer chains are at an angle to the cell axes and are located one at the origin and one each in the center of the two triangles formed by the diagonal of the cell base.

TABLE IV  
Calculated Monomer Unit Chain Length for Poly(*p*-diethynylene Benzene)



Bond	Bond distance, Å. <sup>a</sup>		Bond distance from diphenyl diacetylene, Å. <sup>b</sup>
	Simple	Special	
1 + 7 C—C	1.541	1.373 <sup>c</sup>	1.39
2 + 6 2(C≡C)	2.408	2.412 <sup>d</sup>	2.36
3 + 5 2(C—C)	3.082	2.920 <sup>e</sup>	2.88
4 2 × 1.395 <sup>f</sup>	2.790	2.790	2.78
Chain length, calcd.	9.821	9.495	9.41

<sup>a</sup> Data of Sutton.<sup>6</sup>

<sup>b</sup> Data of Wyckoff.<sup>7</sup>

<sup>c</sup> In C=C—C≡C.

<sup>d</sup> Conjugated.

<sup>e</sup> In C—C≡C.

<sup>f</sup> 1.395 Å. = edge of benzene ring.

### Thermal Decomposition

When a small portion of sample 1 was torched in an evacuated Pyrex tube attached to a mass spectrometer, hydrogen and methane were evolved in the ratio 9/1 by volume along with traces of acetylene and ethylene. It was observed that small glowing particles were ejected from the sample by the decomposition. The amount of methane formed was equivalent to 2% of the carbon in the sample. A test on sample 3 gave similar results, but with slightly more acetylene, about 2% of the total gas evolved. Since this sample was quite a bit purer than sample 1, the observed behavior

TABLE V. Behavior of Poly(*m*-diethynylene Benzene) Heated in Nitrogen

Experiment	Sample	Weight, mg.	Approximate rate of heating, °C./min.	Explosive decomposition temperature, °C.	Weight loss, %	Notes
Tube furnace experiments						
1	4	50-60	25	160	—	
2	5	50-60	25	223	—	
3	5	50-60	25	201	—	
4	4	100	1	None to 200	—	Gained weight on exposure to air
5	4	900	1	None to 835	7.1	Overnight at 160°C.
6	5	50-60	2	None to 1000	—	Held 1.5 hr. at 230°C.
7	4	Small film	30	165	—	Sample "bumped", but remained coherent
Thermogravimetric experiments						
1	505	2.5	182		9.8	
4	200	1	None to 1000		<sup>a</sup>	Held 40 min. at 160°C. then heated to 325°C. and cooled to room temperature
10	4	Previous sample	5	None to 1000	6.3	
11	4	900	1	160	—	Held at 160°C. and exploded after 20 min.
12	6	16	2.5	None to 1000	17, 13 <sup>b</sup>	Crystalline film
13	1 film	12.5	2.5	None to 1000	10, 6 <sup>b</sup>	Aged film
14	1 film	14.8	2.5	None to 1000	10, 5 <sup>b</sup>	Aged and crystalline film

<sup>a</sup> This sample showed a gain of 1.6% at room temperature.<sup>b</sup> Total loss and loss corrected for weight change to 200°C. assumed to be solvent, respectively.

in both cases is characteristic of the polymer and not due to the impurities present in sample 1.

When a small piece of the polymer film was touched with a flame, it burned in less than a second, leaving a wrinkled sheet of carbon. A portion of sample 2 (Table I) thus treated showed a weight loss of 4.7% and a residue composition C = 96.2%, H = 0.8%.

A number of experiments were performed by heating the polymer in flowing nitrogen as summarized in Table V. Freshly prepared samples heated rapidly, decomposed abruptly at temperatures ranging from 160 to 223°C. This abrupt decomposition could be circumvented by slow heating and by two-stage rapid heating, the first stage being stopped at 160°C. for 40 min. or more. In one case, (expt. 11), this annealing did not work with a 900 mg. sample, although it had been successful with samples of 200 mg. or less. Crystallized or aged film did not show the explosive decomposition when small samples were heated at 2.5°C./min. Color changes in the film were noted as follows for experiment 4: Room temperature, dull yellow; 150°C., medium tan; 162°C., light chocolate; 165°C., medium-dark chocolate; 173°C., blackish-brown; 200°C., sooty black.

Thermogravimetric experiments at a heating rate of 150°C./hr. showed the following general behavior with some minor variations from sample to sample. The main weight losses occurred in two stages. The weight loss of the first stage, from room temperature to 200°C., is probably due to loss of solvent from the polymer, and some first stage decomposition (see infrared studies). In nitrogen, the second stage loss was from 300 to 800°C. In air, the sample burned in the range 300 to 500°C.

The observed weight losses in nitrogen of 5–13% are consistent with the mass spectrometric results. Decomposition solely to carbon and hydrogen would cause a weight loss of 3.25%; decomposition to carbon and methane would cause a weight loss of 12.9%. Formation of higher hydrocarbons would cause a greater loss, but they are found in only small amounts and the weight loss is offset in part by the hydrogen remaining in the polymer as is known from analysis and infrared data.

A piece of sample 2 was exposed to the ultraviolet light from a 4-w. germicidal lamp at a distance of 1 cm. The sample and its infrared spectrum were unchanged after exposure for 2 hr., but the infrared spectrum after 18 hr., exposure showed increased absorption in the region 1650–1750  $\text{cm.}^{-1}$  (carbonyl?) and 1150–1350  $\text{cm.}^{-1}$  (ether oxygen). Aged films of samples 2 and 4 were exposed, partially masked with aluminum foil, for 20 days. At the start, the former film was uniform in thickness and orange in color; and the latter film was thinner, irregular in thickness and yellow in color. After exposure, the films were darker. In sample 4, the thinnest areas had completely disintegrated and become holes. In both samples, there appeared dark lines and bundles of dark lines not present in the original sample. No other changes were visible microscopically at magnifications to 210 $\times$ .

## Optical Studies of Thermal Decomposition

Chemical changes which occur as the polymer is converted to carbon were studied by measuring the absorption spectrum of a thin film after each of seven heat treatments at progressively higher temperatures up to 600°C. in "line" nitrogen.

**Vibrational Spectra.** Concentrations of various groups from infrared absorption spectra are summarized in Figure 1. The presence of groups containing oxygen is due to reaction of the specimen with the atmosphere during transfer from oven to spectrometer. The spectrum of the original sample is given in Figure 2, together with spectra after heating to 300 and 600°C.

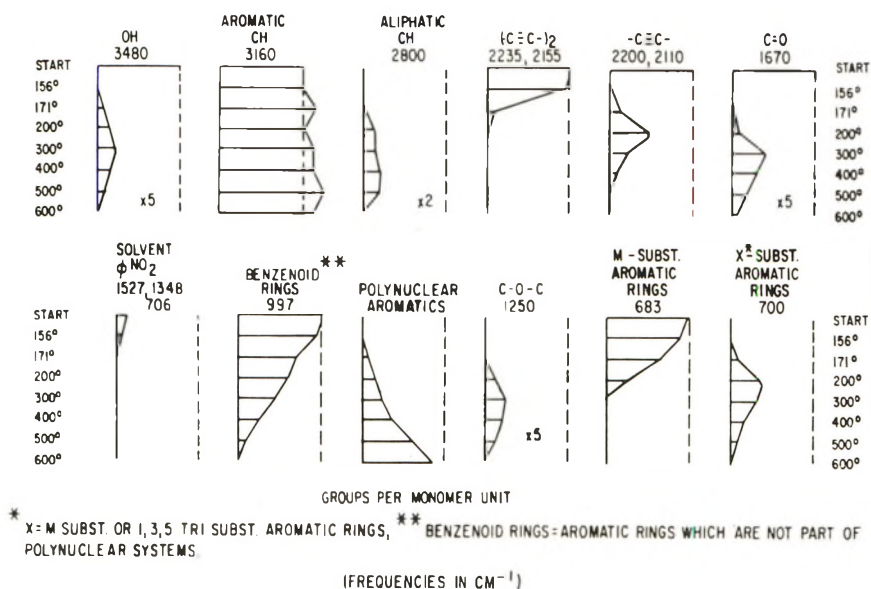
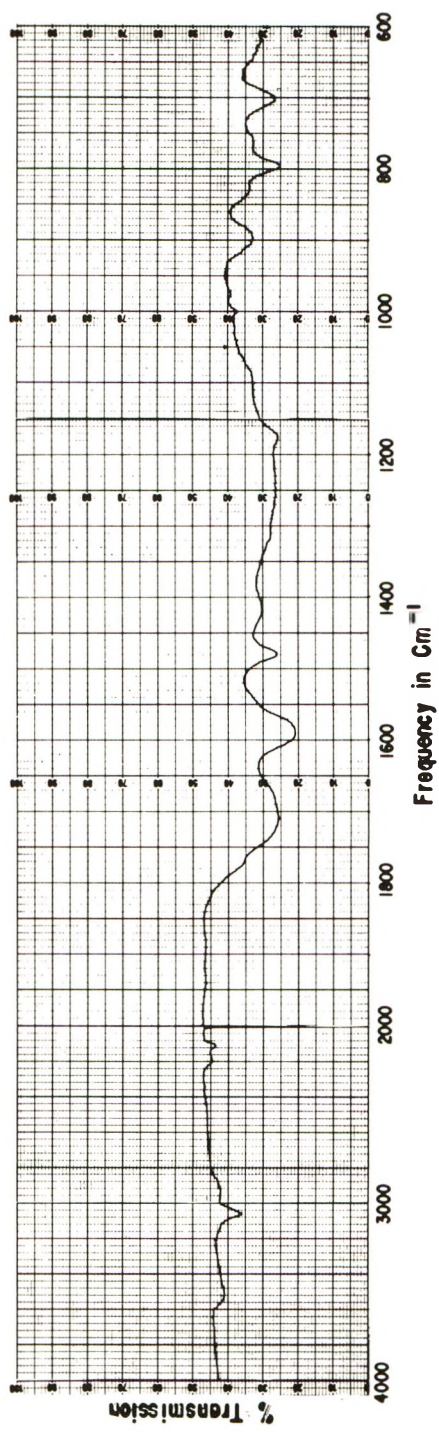
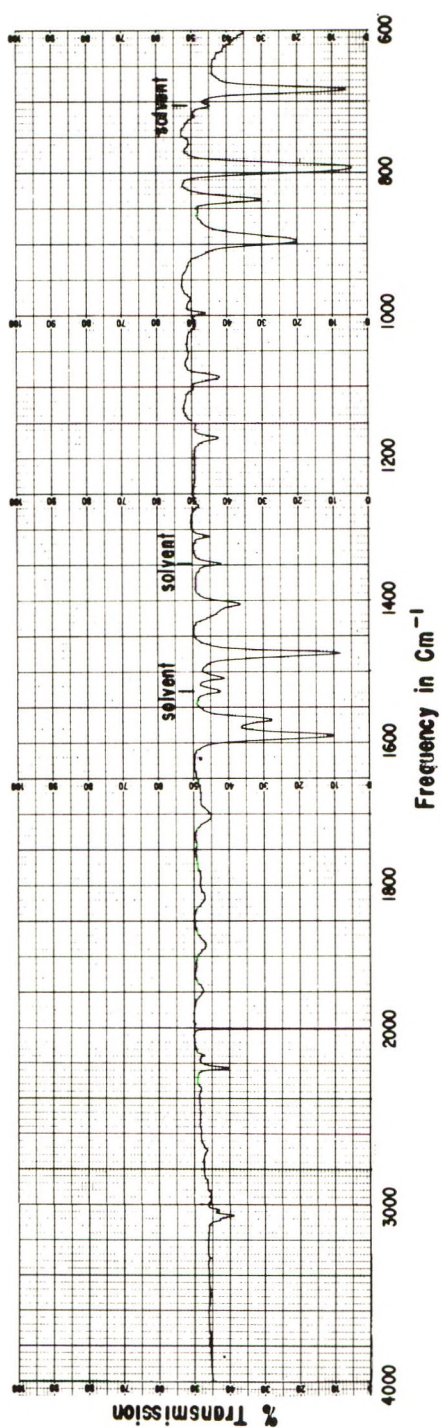


Fig. 1. Relative concentrations of functional groups in poly(*m*-diethynylene benzene) as a function of heat treatment.

The overall rearrangement up to and including 600°C. consisted of reaction of diethynylene groups and aromatic rings to form fused aromatic ring systems (for the moment disregarding the oxygen containing groups). The following steps in the rearrangement can be distinguished: (1) elimination of solvent, (2) elimination of diethynylene groups and *m*-substituted rings, and (3) production of polycondensed aromatic ring structures. From the reduction of intensity of absorption bands during heat treatment, we estimate that 1% of the monomer units were involved in chemical reactions on heating at 156°C. (note that this is below the film casting temperature), 5% at 171°C., 20–40% at 200°C., and progressively more at higher temperatures. After heating at 600°C., all monomer units had reacted in some way.







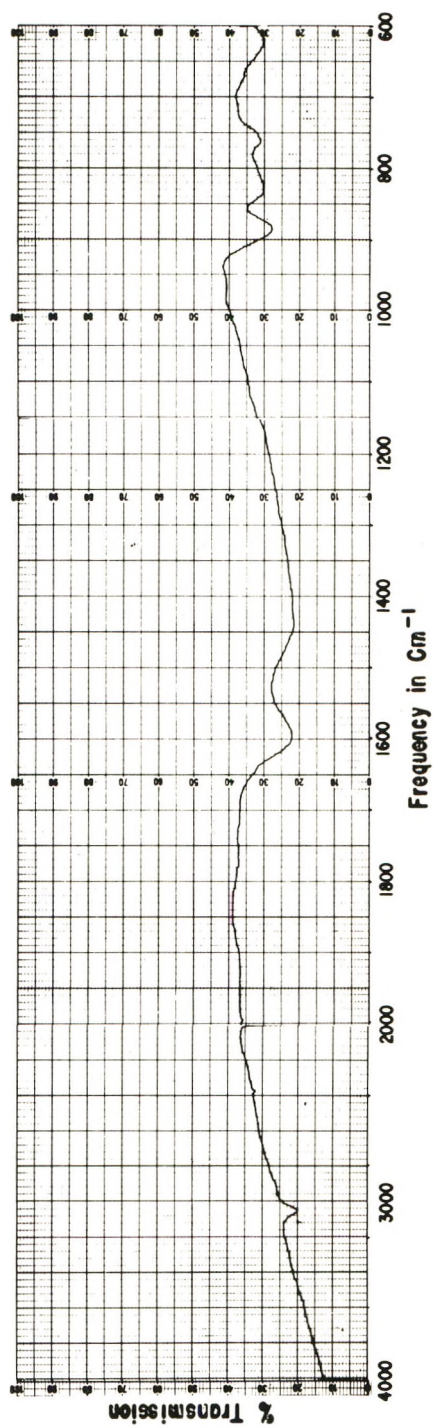


Fig. 2. Spectra of poly(*m*-diethynylene benzene): (a) before heating, (b) after heating 1 hr. at 300°C.; (c) after heating 1 hr. at 600°C.

Both diethynylene groups and *m*-substituted aromatic rings react in at least two steps.

The first reaction of the diethynylene groups occurred at a relatively low temperature: all absorption by these groups at 2215 and 2155  $\text{cm.}^{-1}$  disappeared after heating at 200°C. Simultaneously, two new broader bands appeared at 2200 and 2110  $\text{cm.}^{-1}$ . These bands disappeared on heating at 400°C. On the basis of spectral frequency, these bands could be due to a cumulene type structure ( $\text{C}=\text{C}=\text{C}=\text{C}$ ), but such a structure would not be expected to exist in appreciable amounts after heating at 300°C. It seems more likely that the bands are associated with triple bond stretching frequencies of two different kinds of groups. The great breadth of the 2200  $\text{cm.}^{-1}$  band is probably due to strain. Thus, it appears that one triple bond of the diethynylene groups reacted at relatively low temperature, leaving at least two kinds of isolated triple bonds which were stable to relatively high temperature.

The absorption band at 683  $\text{cm.}^{-1}$  decreased progressively on heating, and disappeared after heating at 300°C. This band is due to an out-of-plane CH bending vibration of the original *m*-substituted aromatic rings. Simultaneously, a sharp band at 700  $\text{cm.}^{-1}$  increased in intensity. This band is probably a similar vibration of a new species of aromatic ring. The type of substitution is somewhat uncertain, but 1,3,5-trisubstituted is most likely. It seems significant that one type of substitution predominates in this reaction between *m*-substituted rings and diethynylene groups. The 700  $\text{cm.}^{-1}$  band, in turn, decreased in intensity at higher temperature and disappeared entirely after heating at 600°C.

Condensation of a diethynylene group with an adjacent aromatic ring probably occurred to only a minor extent, since this would involve simultaneous loss of both triple bonds; thus, the initial reaction must form crosslinks between chains. Crosslinking was extensive after heating at 156°C. This is probably responsible for the inhibition of the explosive decomposition by heat aging below 180°C. The crosslinks cannot be detected directly by spectroscopic means. However, the extensive crosslinking which occurs on heating at the higher temperatures is probably responsible for the progressive broadening of the absorption bands.

There is indirect but clear evidence that 10–20% of the chemical events which occurred below 500°C. produced chemically active groups. These groups were probably prevented from reacting with each other by the three-dimensional crosslinked polymer network which holds them rigidly in position. The groups reacted with atmospheric  $\text{H}_2\text{O}$ ,  $\text{O}_2$ , or both, at room temperature to form OH and C—O—C groups, several kinds of carbonyl groups, and aliphatic CH groups. There is a possibility that the aliphatic CH groups were formed by reaction with the hydrogen in the line nitrogen. Since we have not observed the spectra of the active groups directly, their identity is open to speculation.

It is well known that free radicals are formed copiously when other polymers are degraded at high temperature, and this polymer is probably

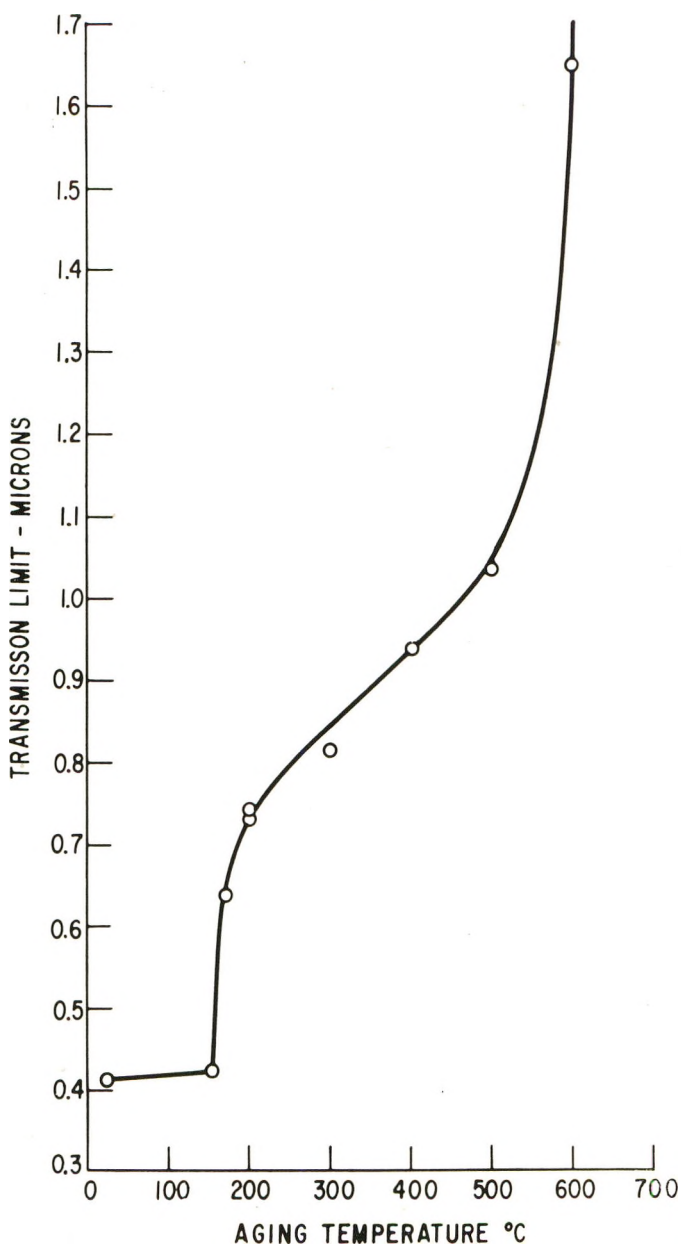


Fig. 3. Short wavelength transmission limit of poly(*m*-diethynylene benzene) as a function of heat treatment.

no exception. Some of the oxygen-containing groups are probably produced by reaction with radicals.

From the number of different kinds of oxygen-containing groups which are formed, it seems that more than one kind of active site must be involved.

It is unlikely that the diethynylene groups could react without formation of any double bonds, but the spectra show no evidence for C=C groups at any stage of the reaction. Thus, any such bonds which may have been formed at high temperature must have reacted with atmospheric gases at room temperature. This indicates that any such bonds are under considerable strain.

The spectra indicate that all OH groups are hydrogen-bonded to electron-donating groups such as C=O and C—O—C groups or to other OH groups; thus, the donor oxygen is within 2.8–3.0 Å. of the oxygen of the OH group. This is unlikely unless there is a strong correlation between the location of the OH group and the donor. For example, both may originate in a reaction between atmospheric gases and one site such as a strained double bond.

The structure of the polymer after heat treatment at intermediate temperatures is probably dependent on whether heating below 180°C. is restricted to that barely necessary to prevent explosive decomposition, or whether heating is prolonged well beyond this point. The structure at intermediate temperatures is also dependent on the exposure to the atmosphere. However, all of the groups which originated by reaction of active groups with atmospheric gases disappeared after heat treatment at 600°C.

**Electronic Spectra.** The limit for 1% short wavelength transmission as a function of heat treatment temperature is shown in Figure 3. There is little change in the limit after heating at 156°C., but above this temperature changes occur rapidly at 156–200°C. and above 500°C. The simplest explanation for this result is to postulate two main degradation processes which overlap in the range 200–500°C. While it is obvious that the degradation cannot be this simple, it is, nevertheless, interesting that the gravimetric and optical data agree in revealing two temperature regions of rapid degradation.

The shift of the electronic absorption to longer wavelength is indicative of growth of conjugated systems. These are probably fused ring systems rather than polyphenyl systems. The length of the longest dimension of these systems after heating at 600°C. is of the order of 25–50 Å.

### Aging

There were several other indications besides its thermal behavior that the polymer changes on aging. It had been noted on several occasions that the surface layer of the polymer powder darkened on standing. An attempt to dissolve sample 4 powder aged for several years, in order to prepare film showed that only a small amount of the polymer was soluble in hot nitrobenzene. A brief comparison was therefore made of the infrared spectra of fresh and aged films.

A film of sample 4, aged several years, showed increased C=O, OH, H<sub>2</sub>O, and aliphatic CH, the latter perhaps from surface contamination. The spectrum of the aged powder was very similar to that of the fresh

powder, and film made from the soluble portion of the gaed powder gave spectrum resembling that of film prepared from the fresh polymer. From these latter observations, we might speculate that the aging reaction of the powder was mainly crosslinking. Solvent treatment would then extract the noncrosslinked portion. What is puzzling is that the film apparently reacted with the atmosphere on aging, but the powder did not. Is it possible that the film is under more strain and therefore more reactive? If so, the partial reaction with the atmosphere would certainly be consistent with its change from explosive to nonexplosive behavior on rapid heating.

Aging also affects the combustion behavior of the film; aged film, either amorphous or crystalline, burns much more slowly than fresh film.

The physical properties of the film varied from sample to sample and on aging. The tensile strength of fresh sample 2 films was found to be 4400 psi. Three samples of film were used ranging in thickness from 0.6 to 1 mil. The films showed very small relaxation, about 1.5% elongation, and a very sharp break normal to the direction of pull. A different preparation tested at the thicknesses of 1.1–1.4 mils gave tensile strengths of 7320–8880 psi., and elongations of 17–31%. The fresh film was strong, easy to handle, and did not crack on folding. The aged film was much more brittle and cracked fairly easily when folded.

### Properties of the Carbon Residue

The carbon residue or char from experiment 9, formed by explosive decomposition at 182°C., was analyzed; C = 96.5%, H = 0.9%, sum = 97.4%. It is assumed that the difference is oxygen and water vapor sorbed from the air. The electrical resistivity of the residue from experiment 5 was 42.3 ohm-cm. This may be compared with ~0.5 ohm-cm. for an acetylene channel black and 0.005 ohm-cm. for a baked carbon.<sup>8</sup> A number of experiments were performed in an attempt to measure the resistance of the free pyrolyzed crystalline polymer film. In one experiment, a piece 10 × 2 × 0.02 mm. was held between two small springs and its resistance monitored with a simple ohmmeter while heating in nitrogen. After a few hours heating at 510–525°C., the indicated resistance changed from infinity to 1,000 megohms at 515°C. On further heating overnight, the resistance dropped to 82 megohms at 511°C.; and during the next day, it

TABLE VI  
Comparison of X-Ray Diffraction Data for Chars with That for a Carbon Black and Graphite

<i>hkl</i>	Spacing, A.		
	Char	Carbon black	Graphite
	Long spacing 9–14	—	—
002	4.1–4.2	3.56	3.35
100	2.1	1.97	2.13
110	1.1	1.20	1.23



dropped to 41 megohms at 514°C. On further heating overnight, the sample broke. Although films carbonized at 1000°C. were coherent and "rang" when struck, they were too fragile for easy handling. Their density was 1.4-1.6 g./cc.

The x-ray diffraction pattern for the chars consisted of a few very broad and weak rings. These are compared in Table VI with diffraction data for carbon black and graphite. The (002) peak of the chars had a shoulder on the side towards a smaller spacing that is absent in published data for carbon blacks. The patterns for the chars indicate a more disordered and slightly different structure from that in carbon blacks.

**Note Added in Proof.** The synthesis of "poly(*p*-diethynylbenzene)" and the changes in its electrical, magnetic, and crystallographic properties on heating from 200-600°C. have been reported by I. L. Kotlyarevskii, L. B. Fisher, A. A. Dulov, A. A. Slinkin, and A. M. Rubenstein, *Vysokomolekul. Soedin.*, **4** (2), 174 (1962).

Mr. L. M. Osika provided us with x-ray diffraction patterns, and both he and Dr. J. S. Kasper gave helpful advice about their interpretation.

### References

1. Hay, A. S., *J. Org. Chem.*, **25**, 1275 (1960).
2. Hay, A. S., *J. Org. Chem.*, **27**, 3320 (1962).
3. Hay, A. S., in preparation.
4. Simons, E. L., A. E. Newkirk, and I. Aliferis, *Anal. Chem.*, **29**, 48 (1957).
5. Klug, H. P., and L. E. Alexander, *X-Ray Diffraction Procedures*, Wiley, New York, 1954, p. 631.
6. Sutton, L. E., Ed., *Interatomic Distances*, Chemical Society Special Publication No. 11, London, 1958.
7. Wyckoff, R. W. G., *Crystal Structures*, Vol. 5, Interscience, New York, 1948, pp. 18-19.
8. Kirk, R. E., and D. F. Othmer, Eds., *Encyclopedia of Chemical Technology*, Vol. III, Interscience, New York, 1949, pp. 19, 67.

### Résumé

Le poly(*m*-diéthynylène benzène) en poudre peut être dissous dans le nitrobenzène à chaud et on peut couler à partir de cette solution des films minces et transparents possédant une couleur jaune et une force de traction approchant de 9000 psi. Lorsque le polymère en poudre est chauffé rapidement sous vide, il explose gentiment à environ 180°C pour fournir du carbone, mais il peut être recuit à 150°C et alors chauffé pour produire du carbone sans réaction explosive. Les produits principaux de la décomposition sous forme gazeuse de la réaction explosive sont le méthane et l'hydrogène. Le film de polymère peut être cristallisé dans le tétrahydrofurane et montre une excellente croissance sphérolitique. Le film cristallin aussi bien que le film non cristallin se dégradent lorsqu'on les chauffe rapidement, mais sans décomposition explosive. Certaines indications sur le mécanisme de décompositions sont obtenues par des études infra-rouges du film pyrolysé à des températures entre 100° et 600°C. Des études de diffraction des rayons-X montrent que le polymère peut exister sous les formes amorphe et cristalline. Dans la forme amorphe, le maximum de diffraction indique une séparation moyenne entre chaînes de 4.28 Å nettement inférieure à celle des autres polymères. Les produits de pyrolyse préparés en chauffant le polymère fournissent des images de diffraction semblables à celles obtenues pour les noirs de carbone amorphes. Une substance voisine, le poly(*p*-diéthynylène benzène), est une poudre cristalline intraitable possédant une cellule unitaire hexagonale,  $a_0 = 7.74 \text{ \AA}$ ,  $c_0 = 8.97 \text{ \AA}$ , contenant trois unités monomériques.

### Zusammenfassung

Aus einer durch Auflösen von pulverisiertem Poly(*m*-diäthynylbenzol) in heissem Nitrobenzol hergestellten Lösung können dünne Platten von gelber Farbe und einer Zugfestigkeit von annähernd 9000 Psi gegossen werden. Wird das Polymerpulver rasch im Vakuum erhitzt, so verpufft es bei etwa 180° unter Bildung von Kohlenstoff. Wird es jedoch bei 150° getempert und dann erhitzt, so erfolgt die Bildung von Kohlenstoff ohne Explosion. Die bei der Explosionsreaktion gebildeten gasförmigen Produkte bestehen in der Hauptsache aus Methan und Wasserstoff. Der Polymerfilm kann in Tetrahydrofuran kristallisiert werden und zeigt ein ausgezeichnetes Sphärolithwachstum. Sowohl der kristalline als auch der gealterte nichtkristalline Film wird beim raschen Erhitzen abgebaut, jedoch tritt keine explosive Zersetzung auf. Durch IR-Untersuchungen des in 100°-Intervallen (bis 600°C) pyrolysierten Filmes wurden gewisse Hinweise auf den Mechanismus der Zersetzung gewonnen. Wie aus Röntgenbeugungsuntersuchungen hervorgeht, kann das Polymere in amorpher und kristalliner Form vorliegen. Aus dem Beugungsmaximum der amorphen Form wurde ein mittlerer Zwischenkettenabstand von 4,28 Å bestimmt, der wesentlich kleiner als bei anderen Polymeren ist. Das Röntgenbeugungsdiagramm der durch Erhitzen des Polymeren hergestellten Verkohlungsprodukte ist demjenigen von amorphem Kohlenstoff ähnlich. Eine verwandte Substanz, Poly(*p*-diäthynylbenzol), ist ein reaktionsträges kristallines Pulver mit einer drei Monomereinheiten enthaltenden hexagonalen Elementarzelle ( $a_0 = 7,74 \text{ \AA}$ ,  $c_0 = 8,97 \text{ \AA}$ ).

Received April 25, 1963

## Radiation-Induced Copolymerization of Tetrafluoroethylene with Propylene at Low Temperature

YONEHO TABATA, *Department of Nuclear Engineering*, and KENKICHI ISHIGURE and HIROSHI SOBUE, *Department of Industrial Chemistry, University of Tokyo, Tokyo, Japan*

### Synopsis

Radiation-induced copolymerization of tetrafluoroethylene with propylene was carried out at low temperature in the liquid phase. The resulting copolymers were found to range from viscous oils to rubberlike materials, depending on the polymerization conditions. It was observed that there are induction periods in these copolymerizations, and that the rate of copolymerization is proportional to the square root of the dose rate. Fluorine contents of the copolymers were determined, and the monomer reactivity ratios in the copolymerization were found to be  $r_{C_3H_6} = 1.0$  and  $r_{C_2F_4} = 0.06$ . The viscosity of the copolymer was measured in tetrahydrofuran at 30°C. Infrared spectra of the copolymers were also measured. It was concluded from these experimental results that the copolymerization proceeds by a radical mechanism.

### INTRODUCTION

Radiation-induced copolymerization of tetrafluoroethylene with ethylene was reported in a previous paper.<sup>1</sup> In this paper, the copolymerization of tetrafluoroethylene with propylene by ionizing radiation is reported.

It was found from this investigation that the copolymerization could take place homogeneously in a wide range of monomer ratios to yield copolymers with a statistical distribution of the monomer units as in the case of copolymerization of tetrafluoroethylene with ethylene.

The copolymer is amorphous over the entire monomer composition range.

### EXPERIMENTAL

The tetrafluoroethylene used was a Nitto Kagaku product. Propylene containing 24.4 vol.-% of propane was used as the other monomer. These monomers were condensed into an ampule at liquid nitrogen temperature. The ampule containing solid monomers was evacuated to  $10^{-2}$ – $10^{-3}$  mm. Hg. Irradiation was carried out by  $\gamma$ -rays from a  $Co^{60}$  source and electrons from a Van de Graaff generator at low temperature.

Fluorine content in the copolymers obtained was determined by a

colorimetric method.<sup>2</sup> Viscosity and infrared spectra of the copolymer were determined.

## RESULTS AND DISCUSSION

### Temperature Dependence of the Copolymerization Rate

The effects of temperature on the copolymerization are summarized in Table I.

TABLE I  
Temperature Dependence of Copolymerization in the  
Tetrafluoroethylene-Propylene System<sup>a</sup>

Polymerization temperature, °C.	Phase	Radiation	Dose rate, r/hr.	Product
-196	Solid	$\gamma$ -ray	$2 \times 10^5$	Homopolymer of $C_2F_4$
-126	Liquid	Electron	$7 \times 10^{7b}$	Homopolymer of $C_2F_4$
-78	Liquid	$\gamma$ -ray	$1 \times 10^5$	Copolymer
-78	Liquid	Electron	$7 \times 10^{7b}$	Copolymer

<sup>a</sup> The mole fraction of tetrafluoroethylene in the monomer mixture was 0.66.

<sup>b</sup> Rad/hr.

It is apparent from the table that the copolymerization could not take place in solid state and liquid state at very low temperature. Therefore, the copolymerization was carried out mainly at  $-78^\circ\text{C}$ .

### Polymerization Rate

The relations between per cent conversion and irradiation time at various dose rates are shown in Figures 1 and 2.

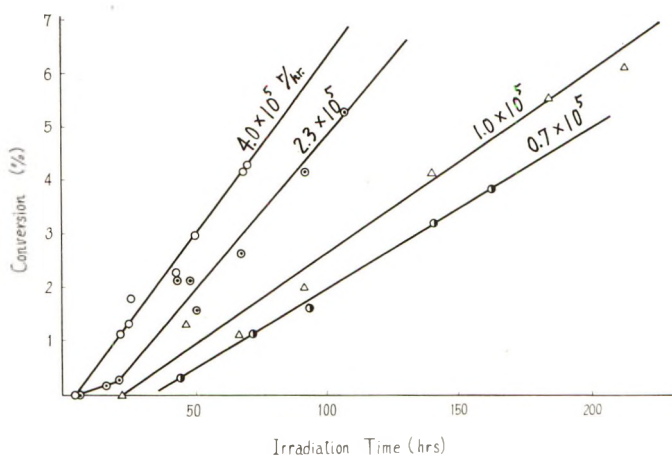


Fig. 1. Relation between conversion and irradiation time ( $\gamma$ -ray irradiation) at various dose rates at  $-78^\circ\text{C}$ . Tetrafluoroethylene content of the monomer mixture was 66.4 mole-%.

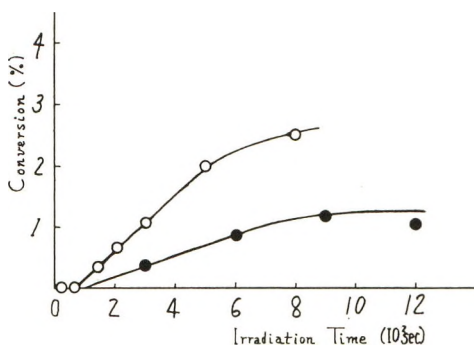


Fig. 2. Relation between conversion and irradiation time (electron irradiation) at various dose rates: (●)  $2.0 \times 10^6$ ; (○)  $0.8 \times 10^6$  r/sec. Tetrafluoroethylene content of the monomer mixture was 66.4 mole-%.

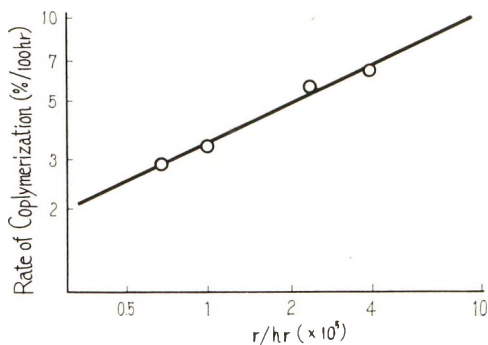


Fig. 3. Dose rate dependence of the rate of copolymerization.

The copolymerization is preceded by an induction period. The conversion increases linearly with the irradiation time.

The dose rate dependence of the copolymerization rate is given in Figure 3.

It is obvious from these results that the rate of copolymerization is proportional to the square root of the dose rate. It suggests that the termination is a bimolecular reaction.

#### Relation of Conversion to Monomer Composition

The relations between the conversion and the mole fraction of tetrafluoroethylene in the monomer mixture are shown in Figure 4.

It is apparent from the figure that the rate of copolymerization increased rapidly with the molar concentration of tetrafluoroethylene in the monomer mixture.

A marked gel effect was observed above a concentration of tetrafluoroethylene of 70 mole-%.

It was observed that the homopolymerization of tetrafluoroethylene takes place at extremely high concentration of the monomer. The critical



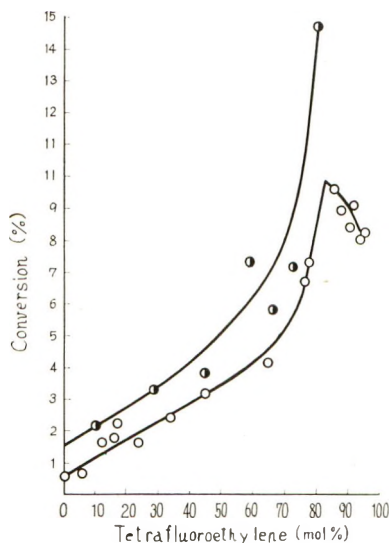


Fig. 4. Relation between conversion and tetrafluoroethylene content of the monomer mixture at various dose rates: (○)  $1.0 \times 10^4$  r/hr.; (●)  $2.3 \times 10^5$  r/hr. Total dose:  $2.1 \times 10^7$  r.

molar concentrations of tetrafluoroethylene monomer were 90.8 at dose rate of  $1.0 \times 10^5$  . . . . . and 95.3 at  $2.3 \times 10^5$  r/hr., respectively.

### Effects of Additives on the Copolymerization

1,1'-Diphenylpicrylhydrazyl(DPPH) and *p*-benzoquinone are hardly soluble in the monomer mixture, but soluble in methylene chloride. On the other hand, the monomer mixture and the solvent are also hardly soluble in each other.

The effects of radical scavengers on the copolymerization in such heterogeneous systems were examined. The results are shown in Table II.

TABLE II  
Effect of Radical Inhibitors on the Copolymerization at an Irradiation Dose of  $10^7$  r

Concentration of tetrafluoroethylene in monomer mixture, mole-%	Added compounds	Amounts of added compounds, wt.-%	Relative yield <sup>a</sup>
46.3	{ <i>p</i> -Benzoquinone Methylene chloride	1.4 12	0.20
66.4	<i>p</i> -Benzoquinone	4.6	0.67
68.8	{ DPPH Methylene chloride	2.2 17.5	0.85

<sup>a</sup> Relative to yield in absence of additives.

It is apparent from the table that the radical scavengers inhibit markedly the copolymerization, in spite of the extremely small solubility of the scavengers in the system. This suggests that the copolymerization may proceed by a radical mechanism, as in the case of the copolymerization of ethylene with tetrafluoroethylene.

The effect of propane on the copolymerization was also examined. The results are presented in Table III.

TABLE III  
Effect of Propane on the Copolymerization

Concentration of tetrafluoroethylene in monomer mixture, mole-%	Amounts of added propane, wt.-%	Relative yield
51.3	24.7	1.45
64.5	27.8	1.33
62.4	29.2	1.30
46.6	33.6	1.42

It is evident from the table that the propane accelerates remarkably the rate of the copolymerization. This may be due to energy transfer among the monomers and the solvent.

### Viscosity of the Copolymer

The copolymer obtained is swelled to some extent by several solvents such as acetone, carbon tetrachloride, and benzene but is not completely soluble. On the other hand, the copolymer is completely soluble in tetrahydrofuran at room temperature. The viscosity of the copolymer is determined in tetrahydrofuran at 30°C. The results are shown in Table IV.

TABLE IV  
Intrinsic Viscosity of the Copolymer Obtained in Various Conditions

Concentration of tetrafluoroethylene in monomer mixture, mole-%	Dose rate $\times 10^{-6}$ , hr.	Dose $\times 10^{-7}$ , r	Intrinsic viscosity $[\eta]$ , dl./g.
85.2	2.3	2.1	0.18
95.2	2.3	2.1	0.095
66.4	1.0	2.3	0.19
66.4	0.7	1.3	0.21

The degree of polymerization of the copolymers is relatively small.

### Infrared Spectra of the Copolymer

The infrared spectra of one of the copolymers in the regions of NaCl and KBr prism are shown in Figure 5.

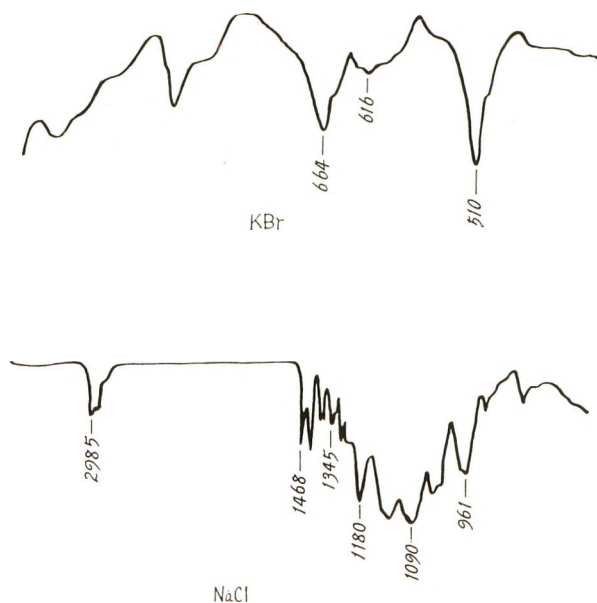


Fig. 5. Infrared spectrum of one of the copolymers.



Fig. 6. The effect of composition in the monomer mixture on the infrared spectra of the copolymers in the region of  $1400\text{--}3000\text{ cm}^{-1}$ . Numbers to the right of the figure indicate tetrafluoroethylene content of the monomer mixture (mole-%).

It is evident from the figure that the spectrum of the copolymer is quite different from those of the two homopolymers.

The intensities of the absorption bands at  $2948$ ,  $1468$ , and  $1393\text{ cm}^{-1}$  increase with the content of propylene in the copolymer, as shown in Figure 6.

Tentative assignments of the absorption bands of the copolymer are shown in Table V.

TABLE V  
Tentative Assignment of Propylene-Tetrafluoroethylene Copolymer

Wavelength, cm. <sup>-1</sup>	Intensity	Assignment
3050	vw	
2985	m	$\nu(\text{CH}_3)$
2948	m	$\nu(\text{CH}_2)$
2890	w	$\nu(\text{CH}_3)$
2870	w	$\nu(\text{CF}_2)$
1468	w	$\delta(\text{CH}_2)$
1441	m	$\delta(\text{CH}_3)$
1403	m	$\delta(\text{CH}_3)$
1393	m	$\delta(\text{CH}_3)$
1345	m	$\delta(\text{CH}_2)$
1321	m	
1275	m	
1237	m	
1180	s	$\nu(\text{CF}_2)$
1126	vs	$\nu(\text{CF}_2)$
1090	vs	$\delta(\text{CH}_2)$
1030	s	
1015		
961	s	$\delta(\text{CH}_3)$
912	m	
810	m	$\delta(\text{CH}_2)$
674	m(sh)	
664	s	$\delta(\text{CF}_2)$
648	m(sh)	
630	w(sh)	
616	w	$\delta(\text{CF}_2)$
604	w(sh)	
541	w(sh)	
510	vs	$\delta(\text{CF}_2)$

### Monomer Reactivity Ratio

The Composition curve of the tetrafluoroethylene-propylene copolymer is shown in Figure 7.

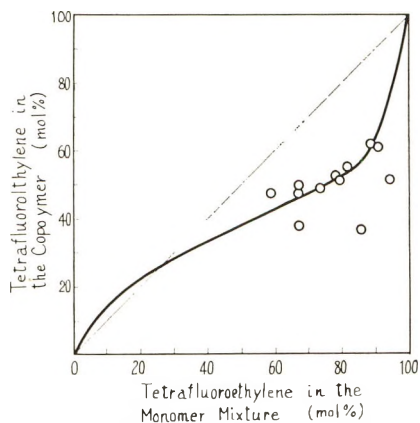


Fig. 7. Composition curves of tetrafluoroethylene-propylene copolymers at  $-78^{\circ}\text{C}$ .

It is well known that the propagation steps of the copolymerization can be represented as follows:



where

$$r_1 = k_{11}/k_{12} \quad (5)$$

$$r_2 = k_{22}/k_{21}$$

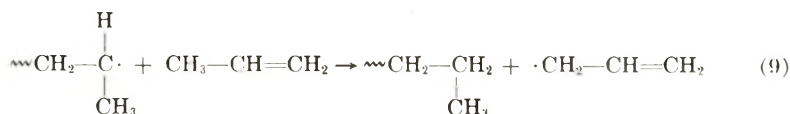
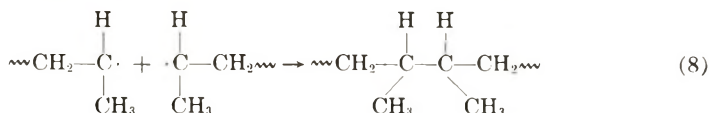
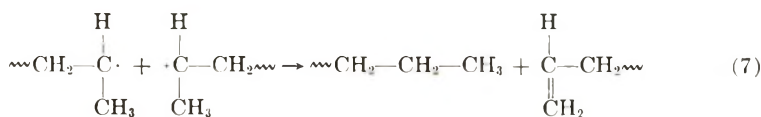
$$\frac{m_1}{m_2} = \left( \frac{M_1}{M_2} \right) \frac{r_1 M_1 + M_2}{r_2 M_2 + M_1} \quad (6)$$

where  $k$  represents the rate constant,  $m_1$ ,  $m_2$  are contents of propylene and tetrafluoroethylene in the copolymer (mole per cent), respectively;  $M_1$ ,  $M_2$  are contents of propylene and tetrafluoroethylene in the monomer mixture (mole per cent).

The reactivity ratios were determined by eq. (6) from the results as  $r_1 = 1$ ,  $r_2 = 0.06$ , respectively.

It is well known that the rate of reaction (1) is very small. Therefore, the rate of reaction (2) is also very small from the results obtained above ( $r_1 = r_{11}/r_{12}$ ). On the other hand, it is also well known that the rate of reaction (4) is extremely high.<sup>3</sup> Then the rate of reaction (3) is much higher than that of reaction (4).

These facts indicate that the propagating propylene radical would be further more stable than the propagating tetrafluoroethylene radical. One can easily postulate from these results that the termination reactions would be the following process:



Reactions (7) (8), and (9) are disproportionation, recombination, and chain transfer processes, respectively. Since the allyl radical  $\cdot\text{CH}_2\text{CH}=\text{CH}_2$



$\text{CH}_2$  is very stable, process (9) would be an unimolecular termination (degradative chain transfer). If the termination is an unimolecular process, the rate of copolymerization must be proportional to the dose rate, under our experimental conditions. In this system, the rate of copolymerization was proportional to the square root of the dose rate, as described in the previous section. Therefore, the contribution of process (9) to the termination would be very small. The  $\text{C}=\text{C}$  absorption band was observed in the copolymer obtained in a dilute range of molar concentrations of tetrafluoroethylene. It is concluded from these experimental results that in the copolymerization of tetrafluoroethylene-propylene, the copolymerization would be mainly initiated by tetrafluoroethylene radical, and be terminated by the disproportionation and recombination of the propagating propylene radical.

### References

1. Tabata, Y., H. Shibano, and H. Sobue, *Kogyo Kagaku Zasshi*, **65**, 737 (1962); *J. Polymer Sci.*, **A2**, 1981 (1964).
2. Kojima and Ueno, *Nagoya Gijutsu Kogyo Shikenjo Hokoku*, **7**, 117 (1958).
3. Tabata, Y., H. Shibano, and H. Sobue, Reports of 4th Conference of Radioisotopes in Japan, October 1961.

### Résumé

On a effectué la copolymérisation à basse température et en phase liquide, du tétrafluoroéthylène avec le propylène sous l'action des radiations. Suivant les conditions de polymérisation, les copolymères obtenus se présentent tantôt sous l'aspect d'huiles visqueuses, tantôt sous l'aspect de substances caoutchouteuses. Dans ces copolymérisations, on a observé l'existence de périodes d'induction. On a également observé que la vitesse de copolymérisation est proportionnelle à la racine carrée de la dose. On a analysé le quantité du fluor contenu dans le copolymère et on a déterminé des rapports de réactivité  $r_{\text{C}_3\text{H}_6} = 1.0$  et  $r_{\text{C}_2\text{F}_4} = 0.06$ . La viscosité du copolymère a été mesurée dans le tétrahydrofurane à  $30^\circ\text{C}$ ; les spectres infra-rouges des copolymères ont également été mesurés. Partant de ces résultats expérimentaux, on a pu conclure que le mécanisme de la copolymérisation était radicalaire.

### Zusammenfassung

Die Strahlungscopolymerisation von Tetrafluoräthylen mit Propylen wurde bei tiefer Temperatur in flüssiger Phase durchgeführt. Die Eigenschaften der gebildeten Copolymeren variieren je nach den Polymerisationsbedingungen zwischen denjenigen viskoser Öle und denjenigen kautschukartiger Stoffe. Bei diesen Copolymerisationen wurden Induktionsperioden beobachtet. Die Geschwindigkeit der Copolymerisation ist der Quadratwurzel der Dosisleistung proportional. Es wurde der Fluorgehalt der Copolymeren durch Analyse ermittelt und die Monomerreaktivitätsverhältnisse bei der Copolymerisation zu  $r_{\text{C}_3\text{H}_6} = 1,0$  und  $r_{\text{C}_2\text{F}_4} = 0,06$  bestimmt. Die Viskosität der Copolymeren wurde in Tetrahydrofuran bei  $30^\circ\text{C}$  gemessen. Ausserdem wurden die IR-Spektren der Copolymeren aufgenommen. Auf Grund dieser experimentellen Ergebnisse nimmt man an, dass die Copolymerisation über einen radikalischen Mechanismus verläuft.

Received April 26, 1963

## Heterophase Polymerization of 4-Vinylpyridine with Butyllithium

P. P. SPIEGELMAN\*† and G. PARRAVANO *Department of Chemical and Metallurgical Engineering, University of Michigan, Ann Arbor, Michigan*

### Synopsis

The butyllithium-initiated polymerization of 4-vinylpyridine in hydrocarbon media proceeded by an anionic addition mechanism. The colorless, soluble reactants rapidly formed a granular, intensely colored, polymer precipitate at temperatures below  $-30^{\circ}\text{C}$ . in heptane and toluene diluents. When the reaction was carried out in an impurity-free environment, the highly colored reaction mixture remained unchanged for indefinite periods of time, and further addition of monomer produced continued growth of polymer chains. A dilatometric technique was employed to follow the rate of polymerization in toluene media. The experimental methods that were used for manipulation of solutions *in vacuo* resulted in polymerization (30–50% conversion) during an initial unsteady temperature period followed by a constant temperature interval during which rate measurements were obtained. Initial monomer and initiator concentrations were varied over a fourfold range. Rate measurements were made in the temperature interval  $-30^{\circ}\text{C}$ . to  $+30^{\circ}\text{C}$ . The dilatometric kinetic experiments together with additional, independent observations established that the rate was proportional to monomer concentration, and to the one half power of the initiator concentration, suggesting an equilibrium complex formation of growing polymeric anions. Rate constants were computed from the values of the rates obtained from the dilatometric kinetic experiments and the square root of the effective initiator concentration. A calculation of the temperature dependence of the rate constants produced an activation energy of 12.7 kcal./mole. As predicted by anionic polymerization theory, the polymer formed in these reactions had a number-average molecular weight equal to the ratio, (weight of polymer)/(equivalents of initiator). The polymer was fractionated by elution chromatography with *tert*-butyl alcohol and benzene solvent–nonsolvent mixtures. The molecular weight distributions of the polymer, constructed from fractionation data, showed a bimodal distribution in two fairly narrow molecular weight ranges. This uncommon molecular weight distribution is due to occlusion of a portion of the active growing chain ends in the polymer precipitate. These trapped reaction sites (which in these experiments amounted to 95% and up of the total initiator concentration) no longer produced chain growth due to the absence of available monomer. The remaining “effective” reaction sites thus grow to high molecular weight and are responsible for the observed kinetics.

### INTRODUCTION

Upon the addition of butyllithium to a solution of 4-vinylpyridine in toluene or heptane an intensely colored granular precipitate of polymer is

\* National Science Foundation Predoctoral Fellow, 1959–60.

† Present Address: E. I. du Pont de Nemours, Elastomer Chemical Dept., Experimental Station, Wilmington, Delaware.

formed. There is at present a relatively large amount of experimental observations on the kinetics and molecular weight distributions of homogeneous anionic polymerizations. There is not a corresponding body of evidence on anionic heterophase polymerization. In this instance it is pertinent to inquire whether or not the presence of a precipitation step during the polymerization reaction influences the overall rate of reaction, molecular weight and molecular weight distribution. Since the polymerization of 4-vinylpyridine initiated by butyllithium in hydrocarbon media involved such a precipitation step during polymerization, it seemed worthwhile to determine by quantitative information whether this heterophase reaction possessed features different from the better known homogeneous anionic systems.

Previous work on the polymerization of 4-vinylpyridine includes bulk, bead, and emulsion polymerization,<sup>1</sup> the study of the hydrodynamic properties,<sup>2</sup> and quaternization reactions<sup>3</sup> of the polymer, and light-scattering and viscometric properties of polymer solutions.<sup>4</sup>

## EXPERIMENTAL

### Materials

**Solvents.** Toluene (Baker, reagent grade) and heptane (Phillips, 99%) were stirred with concentrated sulfuric acid, washed with dilute sodium hydroxide solution, and distilled water and then dried by filtering through Drierite onto Drierite. For final preparation the solvents were dried over phosphorus pentoxide, frozen with liquid nitrogen, degassed on a high vacuum manifold and distilled *in vacuo* into a preweighed solvent ampule fitted with a breakseal side arm and containing a freshly prepared sodium mirror. Upon subsequent freezing and evacuation ( $10^{-5}$ – $10^{-6}$  mm. Hg) the ampule was closed by flame. The solvent ampules along with the Pyrex vacuum connection were weighed to determine the contents by difference in weight. Solvent weights were of the order of 60–80 g., accurate to  $\pm 0.03$  g. The solvents, stored over sodium mirrors under their own vapor pressure, were kept at  $-20^{\circ}\text{C}$ .

**Monomer.** 4-Vinylpyridine (Reilly Coal Tar and Chemical, 95% minimum purity) was dried over calcium hydride and fractionally distilled under dry nitrogen (Matheson prepurified grade, dried over Drierite) in an all-glass wetted-wall, vacuum-jacketed, concentric tube, fractional distillation column into a distribution flask connected to about five calibrated breakseal ampules of known volume. The flask contained calcium hydride and was previously dried by brush heating. The distribution flask was transferred to the high vacuum manifold; the content was frozen with liquid nitrogen and degassed. After repeated melting and degassing, the monomer was refrozen and the distribution flask sealed off at a vacuum of  $10^{-5}$ – $10^{-6}$  mm. Hg. The monomer was allowed to warm to room temperature and was then distilled from the vacuum distribution flask into the

attached ampules, which were then detached by flame sealing. The monomer ampules were stored in the dark at  $-20^{\circ}\text{C}$ . and were used within a period of two to three weeks.

The monomer prepared on the fractional distillation column represented approximately the middle third of the initial charge with a boiling point range of no greater than  $1/2^{\circ}\text{C}$ . At 14 mm. Hg pressure the boiling point was  $68^{\circ}\text{C}$ . The refractive index measured at  $25.5^{\circ}\text{C}$ . on an Abbé refractometer was 1.5489, with a range between 1.5482 and 1.5492.

**Butyllithium.** Butyl chloride (Baker spectro grade) was dried over phosphorus pentoxide, degassed, and distilled on the high vacuum system into weighed breakseal ampules. Amounts of butyl chloride were determined by weight.

Butyllithium was prepared by reacting butyl chloride with excess lithium metal in heptane solvent in an all-glass reaction vessel, flame-dried, and sealed off under high vacuum ( $10^{-6}$  mm. Hg). Mixing of reagents and solvent and subsequent manipulations were carried out through the use of breakseal ampules. The reaction was allowed to proceed in an ice bath for 24 hr. The contents were filtered through a side arm into a receiving vessel attached to the main reaction vessel. The receiving vessel was then sealed off at a constriction.

The contents of the receiving flask were transferred to a second vacuum distribution flask, via breakseal, and from the latter into seven volumetrically calibrated ampules attached to it. The butyllithium solution was distributed into the ampules which were sealed off individually. Three of the samples were broken open in water and titrated with 0.04346*N* hydrochloric acid with phenolphthalein as indicator. The concentration of butyllithium was  $0.470 \pm 0.003N$  (81.1% yield based on butyl chloride).

One of the remaining butyllithium solution ampules was sealed onto another vacuum distribution flask for further dilution with purified heptane. After the usual evacuation and sealing off procedure, heptane and butyllithium ampules were broken open and mixed in the distribution flask. Seven side arm calibrated ampules were filled with the diluted butyllithium solution and sealed off. Three were broken open and hydrolyzed with water and titrated as before. The dilute solution was found to be  $0.0271 \pm 0.0003N$  in butyllithium which compares with a theoretical value of 0.0277-*N*. The remaining four ampules were stored at  $-20^{\circ}\text{C}$ . for use in kinetic experiments. The balance of the dilute solution was stored in the vacuum distribution flask for a repeat of the procedure. No further titrations were performed on the solution. The one batch of dilute solution of butyllithium was sufficient for the entire set of kinetic experiments and it remained clear and colorless.

### Equipment

The kinetic experiments were performed in glass dilatometers (50 cc. volume) containing a Teflon-covered magnetic stirring bar. The reaction dilatometer with auxiliary mixing vessel assembly is pictured in Figure 1.



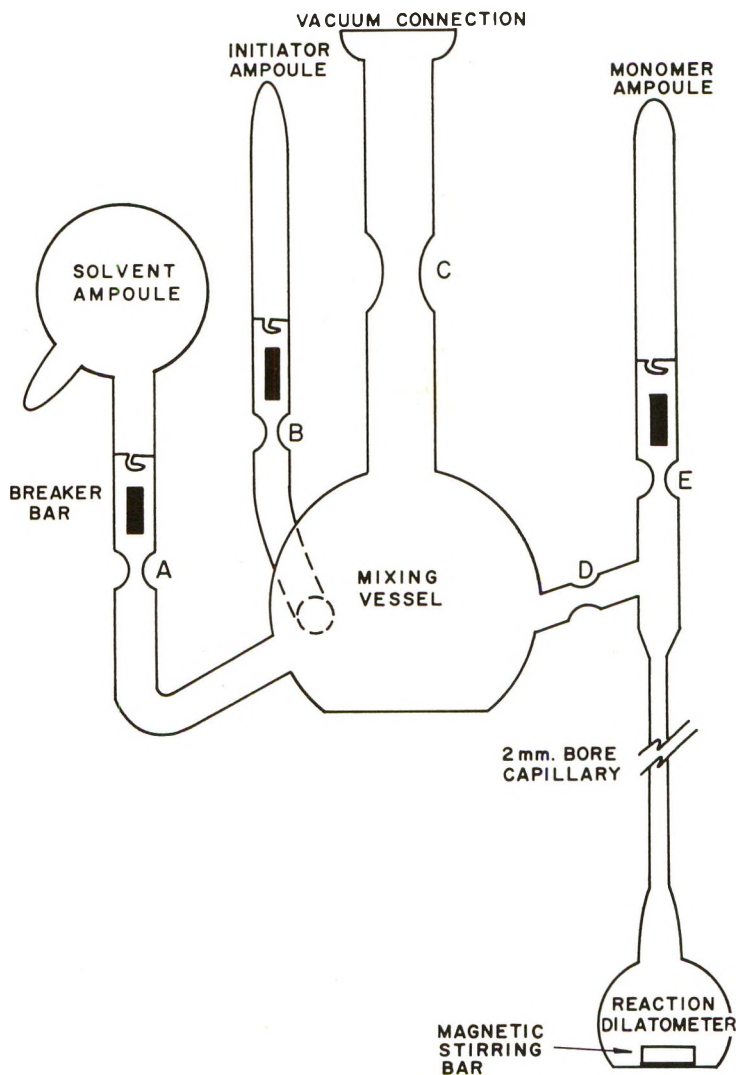


Fig. 1. Vacuum mixing vessel and reaction dilatometer assembly.

The temperature bath for the dilatometric experiments was filled with water for reaction condition above  $0^{\circ}\text{C}$ . or isopropanol for the low temperature runs. Temperature variations were  $\pm 0.15^{\circ}\text{C}$ . at  $-30^{\circ}\text{C}$ .  $\pm 0.10^{\circ}\text{C}$ . between  $-15$  and  $2^{\circ}\text{C}$ ., and  $0.01^{\circ}\text{C}$ . at  $31.4^{\circ}\text{C}$ .

### Procedures

**Polymerization.** The reaction assembly system was flamed and evacuated ( $10^{-6}$  mm. Hg) for 2 hr. and then sealed off at C. The contents of the solvent and initiator ampoules were emptied into the mixing vessel and the ampoules removed. The dilatometer bulb was filled to a predetermined



filling level mark and the dilatometer with attached monomer ampule was sealed off at D.

The assembly was chilled at  $-78^{\circ}\text{C}.$  for 15 min. The monomer ampule was broken open and the monomer allowed to drain into the dilatometer bulb which was kept at  $-78^{\circ}\text{C}.$ , and thoroughly stirred for 25–60 min. The empty monomer ampule was removed at E, and the dilatometer completely submerged in the constant temperature bath and allowed to warm to bath temperature. The reaction mixture was colored a dull red and appeared turbid upon removal from the  $-78^{\circ}\text{C}.$  bath. An orange-red fine particle precipitate formed rapidly during the warmup period. As the reaction mixture approached bath temperature, liquid expanded into the capillary stem. Since the density of the precipitate was greater than that of the solution, little or no polymer rose in the capillary. After the liquid in the capillary stem had reached a maximum height, measurements of the height of the liquid in the stem as a function of time were begun. Measurements were made by means of a Gaertner precision cathetometer (Central Scientific Company) with an accuracy of  $\pm 0.005$  cm.

At the end of the rate measurements, the dilatometer was chilled in a Dry Ice–alcohol slush and broken open, and the contents carefully transferred into a beaker containing 100 ml. toluene and 1 ml. butyl alcohol (Baker reagent grade). The orange-red precipitate turned white immediately, although faint traces of color remained for 1–2 hr. The precipitate was washed in successive portions of toluene and then filtered and placed in a tared vacuum flask, which was attached to the vacuum manifold for drying. The residual solvent and monomer were removed at room temperature. Evaporation of the toluene washings left no residue in those instances where conversion was high, and left an oily liquid (monomer) for runs stopped at low conversion. A check on the effective recovery of the polymer was done by placing 1.672 g. of dried polymer in a 5 vol.-% solution of 4-vinylpyridine in toluene. After following the procedure used in recovering polymer from a typical reaction, 1.646 g. of polymer was recovered, or 98.4% of theoretical.

In one alternate procedure monomer and solvent were premixed in the vacuum mixing and reaction assembly. No trace of polymer was formed. When finally the initiator ampule was broken open, polymer formed rapidly and plugged the capillary stem of the dilatometer.

**Polymer Fractionation and Molecular Weight.** Polyvinylpyridine was fractionated by elution in an all-glass column, packed with a sand bed coated with polymer. Elutriants were mixtures of a solvent (*tert*-butyl alcohol, Eastman reagent grade) and a nonsolvent (benzene).

Eight fractions were usually taken which accounted for 95% and up of the total polymer. The solutions taken off at the bottom were poured into tared vacuum flasks and frozen. The solvent was removed by freeze drying on the high vacuum manifold. The molecular weights of the fractionated samples and of the gross polymer were obtained by dilute solution viscometry in an Ubbelohde viscometer. An intrinsic viscosity–

molecular weight correlation for dilute solutions of poly-4-vinylpyridine in absolute ethanol is:<sup>4</sup>

$$[\eta]_e = 2.5 \times 10^{-4} \bar{M}_v^{0.68}$$

Since the available methanol reagent was of much better quality than the available absolute ethanol, and since the flow times of the pure methanol were much more suitable for measurements, the viscosity measurements were carried out in methanol solution. The value of the exponent of  $\bar{M}_v$  in methanol solutions was found by means of the following equation:

$$\log [\eta]_m = (a_m/a_e) \log [\eta]_e + (a_m/a_e) (\log c_m - \log c_e)$$

which permits the computation of  $a_m$  and  $c_m$  from a knowledge of the intrinsic viscosities of the given polymer fractions in both methanol and ethanol. From five polymer samples whose intrinsic viscosity in methanol ranged from 0.40 to 7.45, the following relation

$$[\eta]_m = 2.4 \times 10^{-4} \bar{M}_v^{0.69} \quad (1)$$

was obtained by a least-squares evaluation of the results. Equation (1) was used to calculate the viscosity-average molecular weights of polymer and polymer fractions.

Specific viscosities were measured for three different concentrations of polymer in solvent for each polymer sample. Values of the intrinsic viscosity,  $[\eta]$ , were obtained in the usual manner by extrapolation of dual linear plots of  $\eta_{sp}/c$  versus  $c$  and  $\ln(\eta_{sp} + 1)/c$  versus  $c$ , according to the well known empirical equations, to zero concentration:

$$\eta_{sp}/c = [\eta] + k' [\eta]^2 c \quad (2)$$

$$\ln(\eta_{sp} + 1)/c = \ln \eta_{rel}/c = [\eta] - k'' [\eta]^2 c$$

Values for  $k'$  were calculated from the slopes of the upper plot and are reported elsewhere<sup>5</sup> along with  $[\eta]$  for the various samples.

Osmotic pressure measurements were made on two polydisperse polymers and one fractionated sample by means of a Zimm-Myerson osmometer (J. V. Stabin Company, model M1) fitted with grade number 450 regenerated cellulose membranes

The results of the measurements on the two polydisperse polymers were similar to results previously published.<sup>6</sup> It is conceivable that lithium butoxide and butyl chloride remnants of the initiator could form quaternary compounds with the nitrogen atom in the pyridine ring, and therefore contribute to the observable osmotic pressure. As a result the osmotic pressure could not be used to determine the number-average molecular weights of the polydisperse samples. The osmotic pressure measurements on the fractionated sample exhibited behavior more characteristic of uncharged macromolecular solutions. For a typical fraction (2-28-3),  $\bar{M}_n = 44,400$ ,  $\bar{M}_v = 47,000$ , and  $\bar{M}_v/\bar{M}_n = 1.06$ .

**Molecular Weight and Frequency Distribution.** The cumulative weight distribution function was constructed by means of the viscosity-average

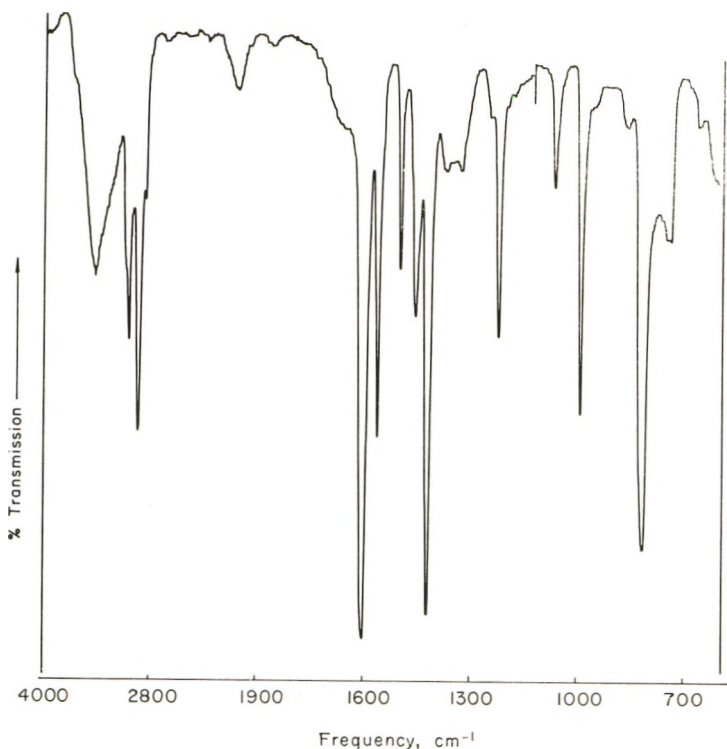


Fig. 2. Infrared absorption spectrum of polyvinylpyridine.

molecular weights, since for a fraction having a very narrow distribution,  $\bar{M}_w = \bar{M}_n = \bar{M}_v$ . This approximation may not hold true for the higher molecular weight fractions, since the resolution of higher molecular weight materials by elution chromatography may become increasingly more difficult.<sup>8</sup> The construction of the distribution curve was performed according to the method proposed earlier.<sup>7</sup> It is possible to show that the application of this procedure to a polydisperse fraction is legitimate.<sup>5</sup>

The unusual molecular weight distribution results that were obtained required an arbitrary cutoff point between the low and high molecular weight materials. These cutoff limits on molecular weight were arbitrarily set approximately 100,000 above the last low molecular weight fraction and 200,000 below the next high molecular weight fraction.

In order to minimize the numerical error in the differentiation of the experimental data, the differentiation of the cumulative weight distribution was accomplished by applying the law of the mean:

$$\frac{f(b) - f(a)}{(b - a)} = f'(x_1) \quad a < x_1 < b$$

to various pairs of values of adjusted cumulative weight per cent. The values of  $f(b)$  and  $f(a)$  refer to the adjusted cumulative weight per cent at

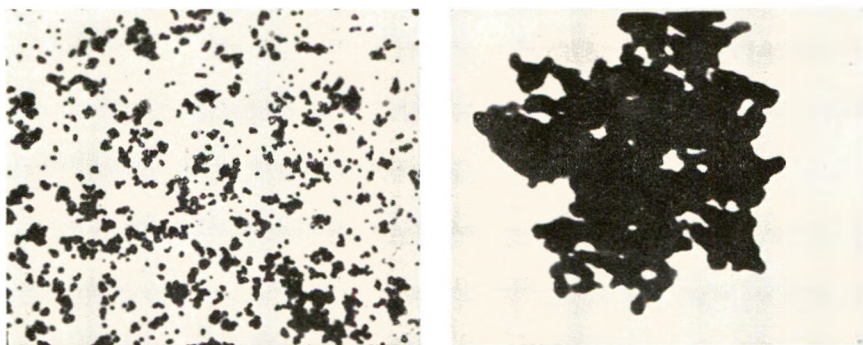


Fig. 3. Transmitted light photographs of polyvinylpyridine particles: (a) 660 $\times$ ; (b) 16,000 $\times$ .

molecular weights  $b$  and  $a$ , respectively. To the extent that the data are correct, the value of  $f'(x_1)$  is an exact value.

**Infrared Absorption Spectra.** Infrared absorption spectra of monomer and polymer were made from films of the polymer with a Perkin-Elmer Model 21 linear wave number infrared spectrometer or on a Baird Model B linear wavelength infrared spectrometer using a sodium chloride prism. The absorption pattern of polymer appears in Figure 2. The spectrum shows the complete absence of the band of the monomer at 923  $\text{cm}^{-1}$ , related to the vinyl group in vinylpyridines,<sup>9</sup> thus excluding amounts of ring linkages in the backbone of the polymer. It should be noted that chain branching cannot be easily ruled out. However, the values of the constant  $k'$  in eq. (2) did not show any apparent trend.<sup>10</sup> On the basis of previous evidence,<sup>11</sup> the side reaction of butyllithium with the nitrogen-carbon bond of 4-vinylpyridine can be neglected under the reaction conditions used in this specific set of experiments.

**Particle Size and Shape.** In order to determine particle size distribution of the polymer produced, photographs were taken of magnified random samples of the polymer. Magnification up to 660 $\times$  (Fig. 3a) was obtained with an optical microscope, while an electron microscope was used for magnifications 1500 $\times$  to 16,000 $\times$  (Fig. 3b). From these photographs, the particle size of the polymer was found to lie in the range 0.2–5  $\mu$ . More complete details on the preparation of materials and experimental procedures, including the determination of the specific volumes of monomer and polymer, the elution fractionation column and elution procedure, the results of the osmotic pressure measurements, the construction of the frequency distribution curves, and the errors involved in setting the arbitrary cutoff of the molecular weight distributions are found elsewhere.<sup>5</sup>

## KINETIC STUDIES

### Anionic Polymerization Mechanism

A summary of the significant experiments is presented in Table I. The polymer produced had a highly intense, orange-red color which remained



TABLE I  
 Polymerization of 4-Vinylpyridine with Butyllithium in Toluene Solution

Expt.	Temp., °C.	$[I_0] \times 10^3$ , mole/l.	$[M_0]$ , mole/l.	Conversion at initial measurement, %	Wt. of polymer, g.	Yield, %	$[\eta]$	$\bar{M}_n \times 10^{-3}$	$[M_0]/[I_0] \times \text{yield} \times 10^{-3}$	$\bar{M}_n \times 10^{-3}$	$k_p \Sigma A_i \times 10^4$ , sec. <sup>-1</sup>	$f_0 \times 10^4$ , mole/l.	$\sqrt{f_0} \times 10^3$ , mole <sup>1/2</sup> /l.	$k_p^{1/2} / \bar{M}_n$ , mole <sup>1/2</sup> /l. sec.
3-14	-29.8	0.941	0.980	6.3	4.45	74.6 <sup>a</sup>	5.20	1930	81.5	105	0.0433	1.76	4.3	0.00103
2-15	31.4	0.396	0.652	23.5	2.53	65.4	3.68	1170	113.					
2-17	31.4	1.11	0.621	40.5	3.56	92.4	3.12	915	54.5	50.6	9.34	0.798	2.82	0.331
2-18	31.4	1.13	1.30	55.2	6.63	78.5	4.34	1500	103.	108.5	15.62	5.16	7.19	0.217
2-19	31.4	1.12	0.32	41.3	1.81	93.3	1.84	427	26.6		7.66			
2-20 <sup>b</sup>	31.4	1.94	0.94		3.60	92.9	2.92	835						
2-21	31.4	1.10	0.635	53.9	3.76	96.0	2.79	783	56.6		7.71			
2-22 <sup>c</sup>	31.4	1.10	0.326	48.0 <sup>d</sup>			3.66	1160	58.3					
2-23	31.4	2.23	0.622	82.1	3.67	94.4	1.36	276	27.7					
2-24	31.4	1.13	1.19	48.4	6.28	80.5	3.02	878	88.5	97.5	6.82	2.49	4.99	0.192
2-25 <sup>e</sup>	-78	1.05	0.630		0.0675	1.7	0.27	26	1.10					
2-26	31.4	1.12	0.635	3.95	3.62	92.8	3.16	940	55		6.49			
2-27	31.4	1.04	1.21		4.62	59.2	2.86	811	72.8	81.5				
2-28 <sup>c</sup>	31.4	1.09	0.293	48.9	2.83	75.7	3.21	959	42.7	43.3	0.67	(0.381)	(1.95)	(0.0344)
2-29	2.0	0.977	1.16	16.8	3.37	45.5	2.52	675	56.7	71.0	1.48	1.98	4.46	0.0332
2-30	-15.3	1.00	1.17	24.4 <sup>f</sup>	2.96	41.4	1.76	400	49.4	53.0	0.549	2.23	4.73	0.0116

<sup>a</sup> Two weeks at room temperature.

<sup>b</sup> Reverse addition.

<sup>c</sup> Two-stage monomer addition.

<sup>d</sup> Estimated.

<sup>e</sup> Initiation reaction.

<sup>f</sup> Reaction run at -30°C. for 1/2 hr.



visibly unchanged for long periods of time (up to two months in vacuum). The results of experiments 2-17, 2-19, 2-22, and 2-28, when considered together, indicate the characteristics of an anionic polymerization. Experiments 2-22 and 2-28 were approximately the same as those of experiments 2-19 in which a 93.3% yield of polymer was obtained in a period of less than 2 hr. Furthermore, the number of chains per unit volume, calculated from the formula:  $105 M_0 \times \% \text{ yield} / 100 \bar{M}_n$ , agrees within experimental error with the initial concentration of initiator in the experiments 2-17 and 2-28 (Table II).

TABLE II

Expt.	$[I_0]$ , moles/l. $\times 10^3$	[Chains], moles/l. $\times 10^3$
2-17	1.11	1.19
2-28	1.09	1.07

These results imply that all of the initiator has been consumed in the formation of polymeric anions from the monomer available (Experiment 2-17), and that the polymerization which follows the addition of more monomer to a system of polymeric anions does not take place via generation of new chains (experiment 2-28), rather by addition to existing active chains. Hence, one can conclude that the butyllithium initiator generates one active chain end for each initiator molecule and that no chain transfer mechanism exists in this polymerization. Thus, the number-average molecular weight may be calculated by:

$$\bar{M}_n = \frac{\text{polymer yield (grams)}}{\text{total initiator (equivalents)}} = \frac{[M_0]}{[I_0]} \times \text{yield}$$

It should be noted, however, that these results do not preclude a partial termination of the active chain ends by any of several mechanisms. Evidence of such termination of active chain ends can be found in the molecular weight distribution of the polymer produced.

### Monomer Concentration Dependence

The following relationship is known to be valid for the special case of rapid initiation:  $\ln [M]/[M_0] = -k_p[I_0]t$ , or in terms of the conversion:

$$\ln (1 - \text{fraction of conversion}) = -k_p[I_0]t \quad (3)$$

As a typical example, the results of experiment 2-26 are plotted according to eq. (3) in Figure 4. The first nonlinear portion of the plot is due to the attainment of thermal equilibrium in the system and it has no significance for the interpretation of the kinetic results. The second nonlinear portion of the plot, which constitutes a decrease in rate from the expected overall first-order reaction, is attributed to a decrease in the number of available active ends. This slowing down of the rate of reaction usually takes place above 85% conversion. In the present instance such a result could

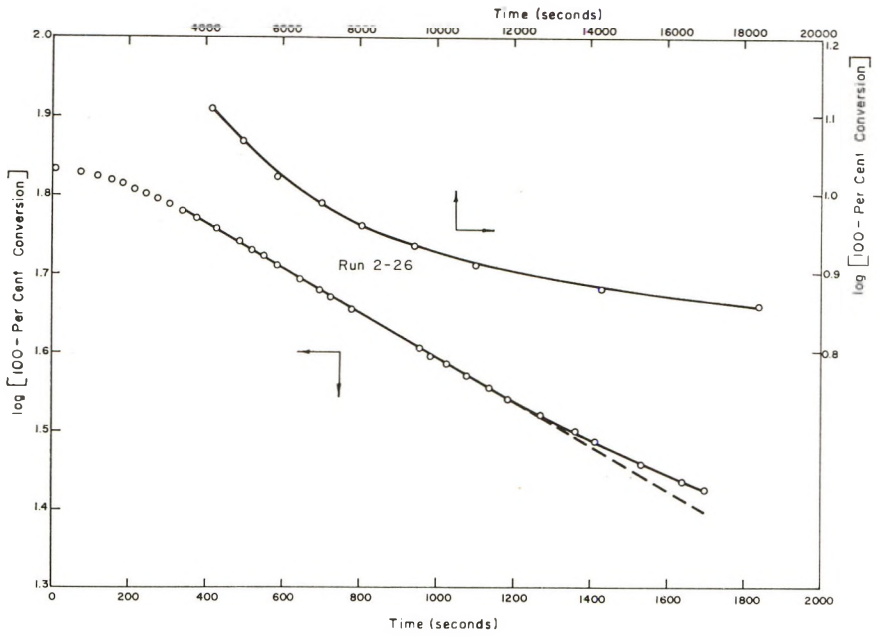


Fig. 4. Polymerization kinetic experimental data, runs 2-26.

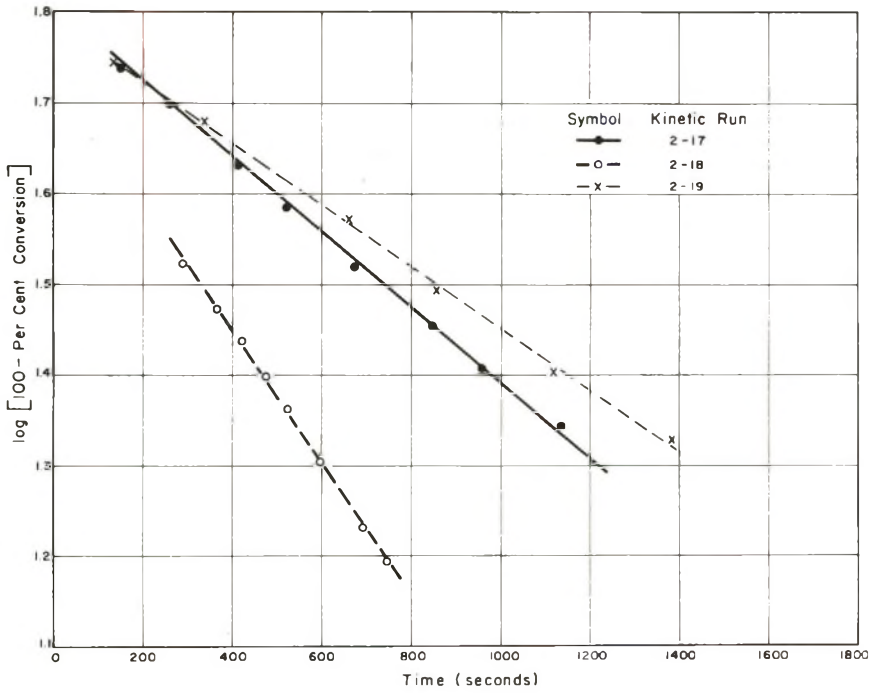


Fig. 5. Comparison of kinetic experimental data, runs 2-17, 2-18, and 2-19.

conceivably be produced by several conditions: nonhomogeneous distribution of the monomer at high conversions, occlusion of active chain ends inside the polymer matrix, or deactivation of chain ends by side reactions (branching on the nitrogen atom in the pyridine ring or termination with impurities). Further results, to be discussed in the subsequent section, suggest one of the first two mechanisms rather than the latter. Other investigators<sup>12</sup> have reported a similar decrease in the expected overall first-order rate of anionic polymerization at high conversion. The complete summary of the rate results is collected elsewhere.<sup>5</sup>

### Initiator Concentration Dependence

Kinetic runs performed at the same temperature and initiator concentration did not produce the same value of  $d\ln[M]/dt$  as predicted by the theory (Fig. 5). A plausible interpretation of the discrepancy will be discussed in the light of the results of the molecular weight distribution (see below).

## EFFECT OF REACTION CONDITIONS ON POLYMER PROPERTIES

### Analysis of the Distribution Functions

As a typical example, the cumulative weight distribution functions for polymers 2-27 and 2-28 are plotted in Figures 6 and 7. The complete experimental data are summarized elsewhere.<sup>5</sup> Examination of the fractionation results points out the existence of two distinct types of polymer in any given sample, one in the molecular weight range of 10,000–300,000

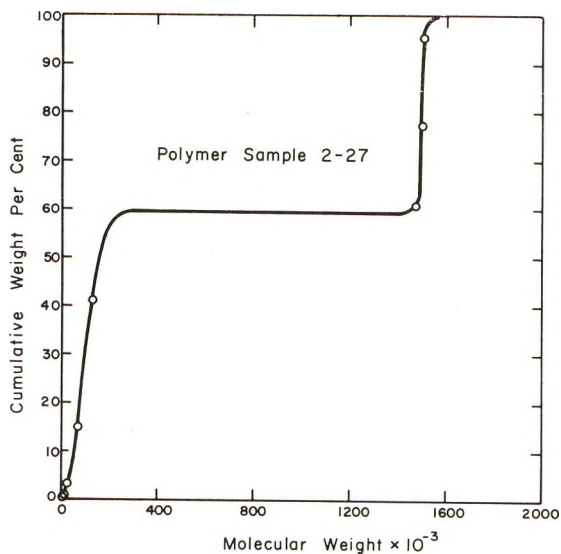


Fig. 6. Cumulative weight distribution for polymer 2-27.

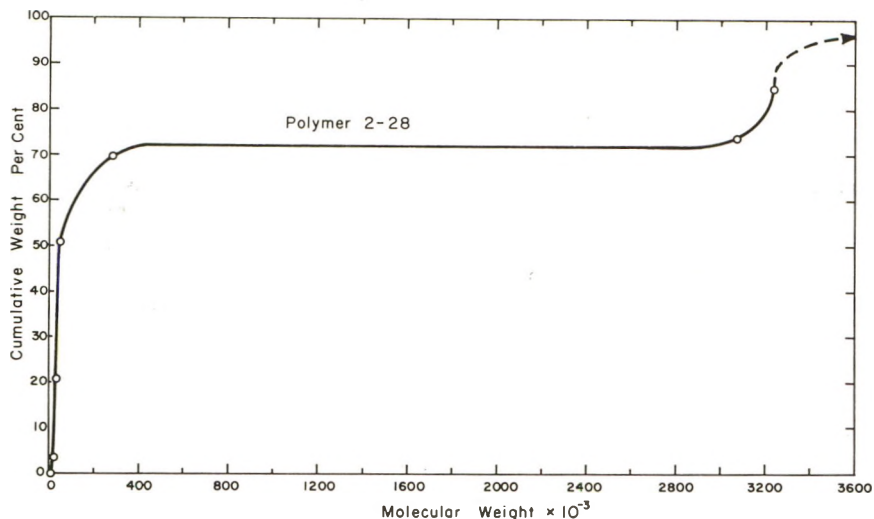


Fig. 7. Cumulative weight distribution for polymer 2-28.

and the second, covering a spread of 300,000, in the range from one to four million, depending on the experiment. No polymer fraction was ever obtained with a molecular weight between 300,000 and 900,000. This bimodal distribution suggests the following model. Polymer particle formation at some critical chain length of the growing polymeric anion traps out varying amounts of the active ends, which can only grow with the amount of monomer trapped in the polymer particle. Furthermore, the diffusion of monomer through the particles or particle agglomerates is slow and only the reactive chain ends at the surface of the precipitate are available for further growth. Since the rate measurements were made after the formation of large solids (30–50% conversion), it is reasonable to expect that the rates observed were preponderantly due to the participation of these “surface” anions only. The observed, overall rates of polymerization of the various experiments can thus be interrelated on the basis of the fraction  $f$  of the original chains that in each experiment have contributed to the observed polymerization. The computation is performed with the help of the frequency distribution curves. In fact, the areas under these curves are equivalent to the number of chains present in each sample.

The frequency distributions of polymer samples 2-17, 2-18, and 2-24 are presented for comparison in Figure 8. From the value of the low molecular weight area, it can be calculated that the percentage of chains in the low end of the distribution represented 95% and up of the total chains in any one experiment. In other words, less than 5% of the initiator is responsible for the observed kinetic. This is consistent with the calculated ratios,  $\bar{M}_v/\bar{M}_{nt}$ , where  $\bar{M}_{nt}$  is the molecular weight average obtained by dividing the weight of polymer by the total initiator concentration (column

10, Table I). The smallest ratio  $\bar{M}_v/\bar{M}_{nt}$  is 8:1 and the ratio ranges as high as 23:1. These large ratios are indicative of broad molecular weight distributions which could only be produced by a process in which a small percentage of the chains could grow to extremely large molecular weights.

The number-average molecular weight of each fractionated polymer was calculated from the values of the areas under the frequency distribution curve of each polymer. These values are reported in column 11 of Table I.

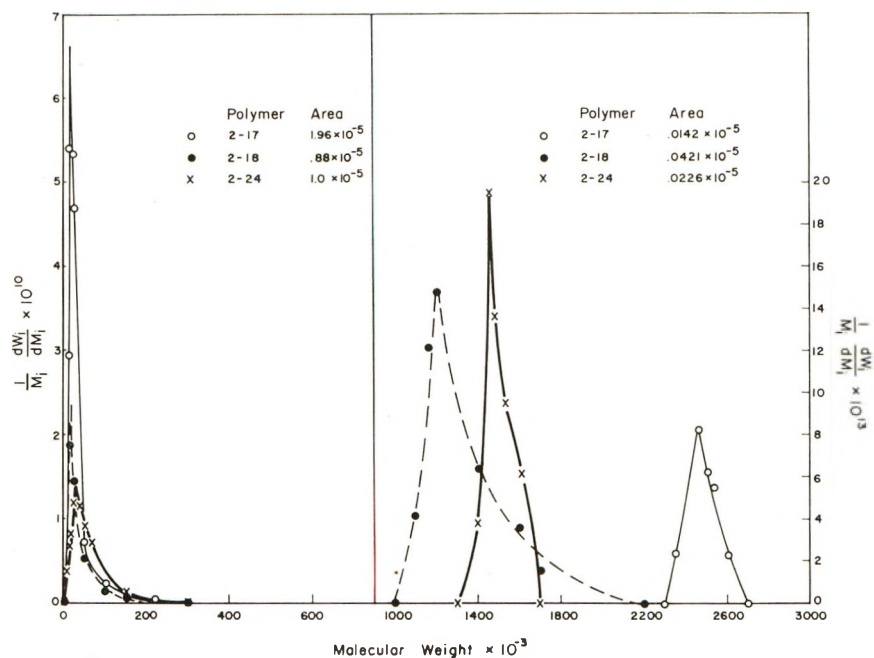


Fig. 8. Comparison of number frequency molecular weight distributions of polymers 2-17, 2-18, and 2-24.

Considering the error involved in the fractionation procedure and in the construction of cumulative and frequency distribution functions, the agreement between theoretical and measured values is considered satisfactory.

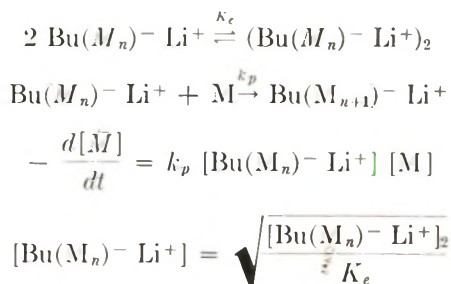
### Rate Dependence on Available Sites

The values for the percentage of chains included in the high molecular weight portions of the fractionated samples can be used to calculate the concentration of the effective active ends,  $fI_0$ , and the value of  $k_p$  [eq. (3)]. The values,  $fI_0$ , are reported in column 13 of Table I. The values of  $k_p$  at 31.4°C. are not constant.

Previous kinetic studies of the polymerization of styrene,<sup>13</sup> butadiene,<sup>14</sup> and isoprene,<sup>14,15</sup> have shown that the rate of polymerization is dependent on the  $1/2$  order of the total organolithium concentration. To explain this result, it has been suggested that the growing polymeric chains are partly



associated in dimeric chains in equilibrium with single chains and that only the single chains add monomer:



Thus for large  $K_e$

$$-d[\bar{M}]/dt = k_p ([I_0]/K_e)^{1/2} [M] \quad (4)$$

Furthermore, it was shown<sup>14,16</sup> by measurements of the bulk viscosity of growing polymeric anion solutions that polystyryl lithium, polyisopropenyl lithium, and polybutadienyl lithium exist as paired chains in hydrocarbon solution.

In view of the correlations obtained in these systems, a rate constant,  $k_2$ , was calculated from the slopes of the plots of kinetic data and the corresponding concentration values of the available reactive chain ends by the equation

$$k_2 = -d \ln [M]/dt / f^{1/2} [I_0]^{1/2} \quad (5)$$

Comparison with eq. (4) gives:

$$k_2 = k_p / K_e^{1/2} \quad (6)$$

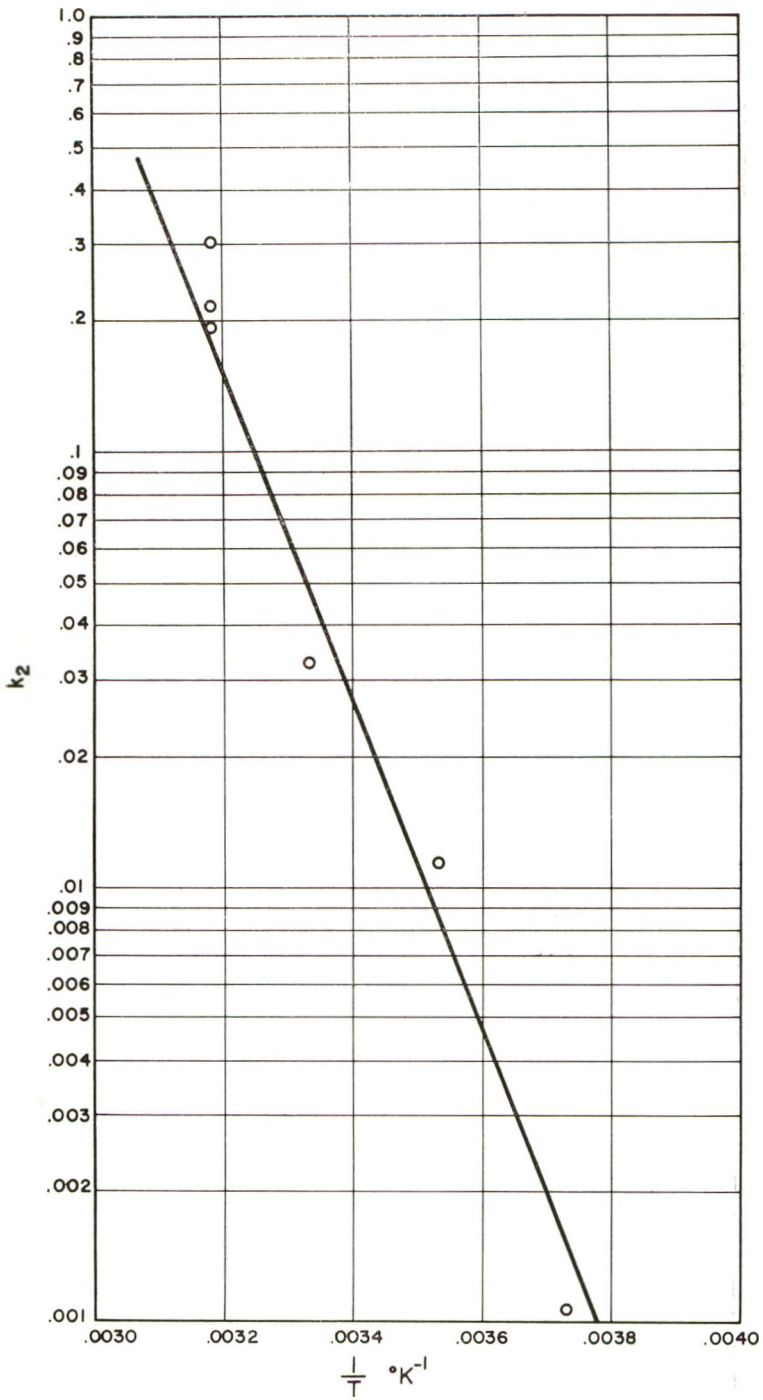
The values of  $k_2$ , calculated from eq. (5) are collected in column 15 of Table I.

The activation energy and frequency factor, calculated from the slope and intercept of an Arrhenius plot of  $k_2$  versus  $\log 1/T$  (Fig. 9), were found to be 12.7 kcal./mole and  $3.65 \times 10^8$ , respectively. These values compare favorably with the values reported<sup>13</sup> for the polymerization of styrene in hydrocarbon solvents, 14.3 kcal./mole and  $2.93 \times 10^8$ . Values of the activation energy for the polymerization of isoprene and butadiene have been computed<sup>14</sup> as 22 kcal./mole and 21.3 kcal./mole, respectively, in hydrocarbon solvents, and 7 kcal./mole and 7.2 kcal./mole, respectively, in tetrahydrofuran.

From eq. (6) one has:

$$E_{a_2} = E_{a_p} - 1/2 E_{a_e}$$

In ether solvents, chain association is small or nonexistent and  $E_{a_2} \cong E_{a_p}$ . The intermediate value of 12.7 kcal./mole found in the present case can be taken as supporting evidence for the presence of chain association during the polymerization of 4-vinylpyridine in hydrocarbon media.

Fig. 9. Arrhenius plot of rate constant  $k_2$ .

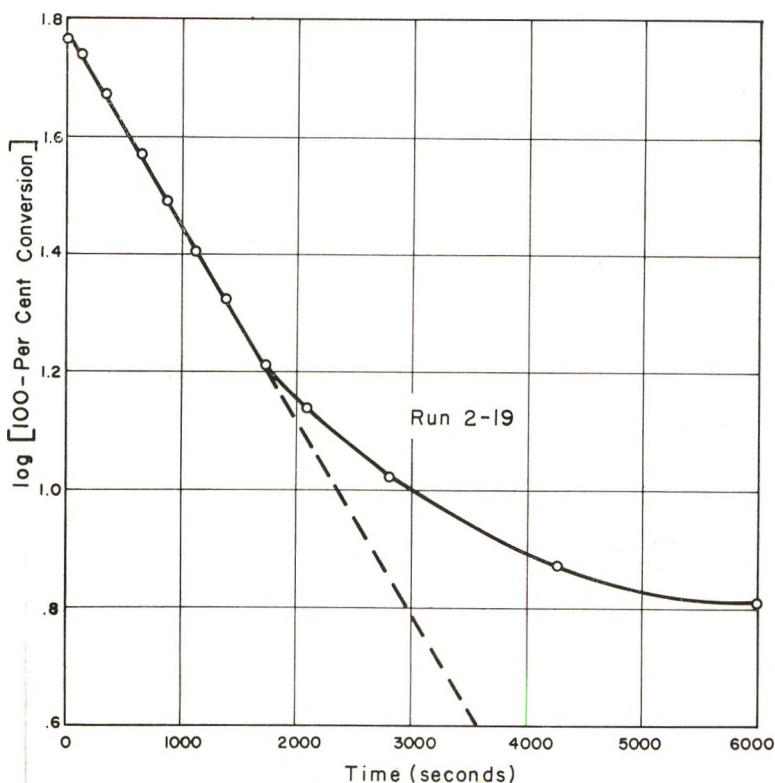


Fig. 10. Polymerization kinetic experimental data, Run 2-19.

The cumulative errors produced as a result of the fractionation experiments, the subsequent determination of a suitable cumulative weight distribution, the differentiation of the cumulative distribution data, and the graphical integration of the function  $(1/M_i)(dW_i/dM_i)dM_i$  account for the scatter of  $k_2$  values at 31.4°C. in experiments 2-17, 2-18, and 2-24, but not the extremely low value obtained for this constant in experiment 2-28, which was also carried out at 31.4°C.

Experiment 2-28 differed from the other experiments at 31.4°C. in that the monomer was added in two stages. The rate constant,  $k_2$ , was obtained from the kinetic measurements during the polymerization of the second monomer portion and from a determination of the value,  $fI_c$ , from the frequency distribution of the high molecular weight portion of polymer 2-28 [see eq. (5)]. The error in the calculation of  $k_2$  results from the assumption that all of the active chain ends in the high end of the molecular weight distribution were contributing to the observed rate of polymerization during the second stage of the experiment. The cumulative weight distribution of polymer 2-28 (Fig. 7) suggests a trimodal distribution rather than the usual bimodal one. This distribution was not completely characterized due to the presence of gellike polymer with molecular

weight ca. 7,000,000. The value of  $fI_0$  in this experiment was obtained by the difference between the total initiator and the chain ends represented by the low molecular weight species, and therefore includes all of the high molecular weight chains from 3,000,000 on. Actually only a portion of these chain ends contributed to the polymerization.

Additional substantiation of this assumption can be found in a comparison of the observed rate measurements of experiments 2-28 and 2-19. The conditions for the first half of experiment 2-28 were equivalent to those in experiment 2-19. The value of the product  $k_2 f^{1/2} [I_0]^{1/2}$  obtained from the slope at the tail end of the kinetic data for experiment 2-19 (Fig. 10) equals  $0.815 \times 10^{-4} \text{ sec.}^{-1}$ . The value compares quite well with the value obtained for the logarithmic linear portion of the second half of experiment 2-28, which is  $0.67 \times 10^{-4} \text{ sec.}^{-1}$ .

### REACTION MECHANISM

Previous kinetic studies on the polymerization of vinyl and diene monomers by organolithium compounds have shown that in general a reaction scheme which includes initiation and propagation steps is adequate for the interpretation of the experimental results.

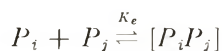
Based on the general set of equations:



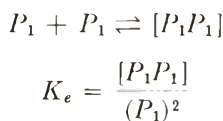
the theoretical molecular weight distribution for the case of rapid initiation is:<sup>17</sup>

$$P_i(\tau) = \frac{I_0 (K_p \tau)^{i-1}}{(i-1)!} e^{-k_p \tau}$$

where  $P_i$  refers to the reactive nonassociated chains and  $\tau = \int_0^t M dt$ . The association of chains can be represented by:



At time  $0^+$  (for rapid initiation)



For  $K_e \gg 1$ :

$$2 [P_1 P_1] \approx I_0$$

$$P_1(0^+) = (I_0 / K_e)^{1/2}$$

The corresponding rate expression for the  $i$ th species is

$$d[P_i]/dt = k_p [P_{i-1}][M] = k_p [P_i][M]$$

The solution for the initial conditions:

$$\begin{aligned} P_1(0) &= (I_0/K_e)^{1/2} \\ P_i(0) &= 0 \\ i &\neq 1 \end{aligned}$$

is:

$$P_i(\tau) = \left(\frac{I_0}{K_e}\right)^{1/2} \frac{(k_p \tau)^{i-1}}{(i-1)!} \exp\{-k_p \tau\} \quad (7)$$

where  $\tau = \int_0^t M dt$ . The total number of active ends remains constant with time since

$$\sum_{i=1}^{\infty} P_i = (I_0/k_e)^{1/2}$$

Equation (7) represents the distribution of nonassociated chains. The distribution of the total chains of length  $i$  is:

$$Q_i = \sum_{j=1}^{\infty} [P_i P_j] + P_i \quad (8)$$

The second term on the right of eq. (8) is negligible in the case of large  $K_e$ . Since:

$$\begin{aligned} [P_i P_j] &= K_e [P_i][P_j] \\ Q_i &\cong \sum_{j=1}^{\infty} K_e [P_i][P_j] \\ Q_i &\cong \sum_{j=1}^{\infty} K_e \left(\frac{I_0}{K_e}\right)^{1/2} \exp\{-k_p \tau\} \frac{(k_p \tau)^{i-1}}{(i-1)!} \left(\frac{I_0}{K_e}\right)^{1/2} \exp\{-k_p \tau\} \frac{(k_p \tau)^{j-1}}{(j-1)!} \\ Q_i &\cong I_0 \exp\{-k_p \tau\} \frac{(k_p \tau)^{i-1}}{(i-1)!} \quad (8a) \end{aligned}$$

The distribution of chain lengths obtained taking into account the equilibrium complex formation is still of the Poisson type with mean  $k_p \tau$ .

#### Evaluation of the Absolute Rate Constant, $k_p$ , and Association Equilibrium Constant, $K_e$

For a simple experimental scheme in which initiation is rapid or performed by polymer anion "seeds,"<sup>15</sup> one can easily obtain separate values for the rate constant,  $k_p$ , and the association equilibrium constant,  $K_e$ . The number-average molecular weight of the polymer in such an experiment has the value  $k_p \tau$  according to eq. (8a). The value,  $\tau$ , can be obtained by a graphical or analytical integration of the monomer concentration with respect to time (obtained from dilatometric measurements) and, therefore, the value of  $k_p$  can be calculated. As shown previously, the slope of the rate of polymerization is equal to  $(k_p/K_e^{-1/2})[I_0]^{1/2}$ . One can,



therefore, determine the value of the association equilibrium constant,  $K_e$ , from the value of this slope and the value of  $k_p$ .

### Interpretation of Actual Experiments

An actual kinetic experiment is schematically represented in Figure 11. The unsteady temperature interval included a "homogeneous" polymerization period,  $t_1'$ , during which all of the chains were growing, and a subsequent heterophase period,  $t_2'$ , in which only a fraction,  $f$ , of the initial

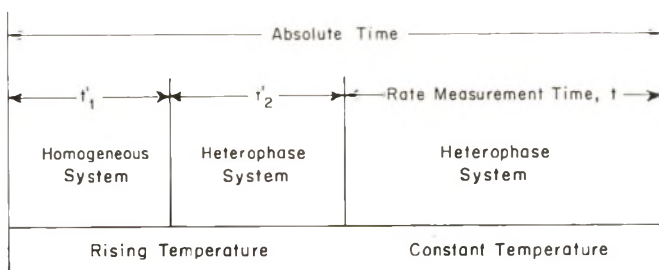


Fig. 11. Actual kinetic experiment.

chains continued growth. For the initial interval of rising temperature, it is possible to set

$$\tau' = \int_0^{t'} k_p(x)M(x)dx$$

From eq. (7)

$$P_i(\tau') = \left(\frac{I_0}{K_e}\right)^{1/2} \frac{(\tau')^{i-1}}{(i-1)!} \exp\{-\tau'\}$$

and the distribution for the total chains becomes:

$$Q_i(\tau) = I_0 \frac{(\tau)^{i-1}}{(i-1)!} \exp\{-\tau\}$$

According to the model previously suggested, at the end of  $t_1'$ , a fraction,  $1-f$ , of the total chains,  $\sum Q_i$ , becomes "unavailable," and only the remaining  $fI_0$  chains are capable of polymerization. Therefore, a portion of the total chains will have the final fixed distribution:

$$(1-f)I_0 \frac{(\tau_1')^{i-1}}{(i-1)!} \exp\{-\tau_1'\}$$

where  $\tau_1'$  is the fixed dimensionless time period for the homogeneous portion of the reaction:

$$\tau_1' = \int_0^{t_1'} k_p(x)M(x)dx$$

Denoting the remaining available associated chain ends by

$$\sum_{i=1}^{\infty} R_i = f \sum_{i=1}^{\infty} Q_i = fI_0$$

the remaining nonassociated active chain ends are:

$$\sum_{i=1}^{\infty} A_i = (fI_0/K_e)^{1/2}$$

At the end of time  $t_1' + t_2'$  the distribution of chains is:

$$R_i = fI_0 \frac{(\tau_2')^{i-1}}{(i-1)!} \exp\{-\tau_2'\}$$

and

$$A_i = \left(\frac{fI_0}{K_e}\right)^{1/2} \frac{(\tau_2')^{i-1}}{(i-1)!} \exp\{-\tau_1'\} \quad (9)$$

where

$$\tau_2' = \int_0^{t_1'} k_p(x)M(x)dx + \int_{t_1'}^{t_1'+t_2'} k_p(y)M(y)dy$$

During the constant temperature interval the rate expression is:

$$\frac{d[A_i]}{dt} = k_p [A_{i-1}][M] - k_p [A_i][M]$$

Using eq. (9) to describe the initial conditions, the solution of the above rate expression is:

$$A_i(\tau) = \left(\frac{fI_0}{K_e}\right)^{1/2} \exp\{-\tau_2'\} \exp\{-k_p\tau\} \frac{(k_p\tau)^{i-1}}{(i-1)!} \left(1 + \frac{\tau_2'}{k_p\tau}\right)^{i-1}$$

and:

$$\sum_{i=1}^{\infty} A_i(\tau) = (fI_0/K_e)^{1/2}$$

Furthermore

$$\begin{aligned} R_i &= \sum_{j=1}^{\infty} K_e [A_i A_j] \\ &= fI_0 \exp\{-\tau_2'\} \exp\{-k_p\tau\} \frac{(k_p\tau)^{i-1}}{(i-1)!} \left(1 + \frac{\tau_2'}{k_p\tau}\right)^{i-1} \end{aligned}$$

Let us now define  $\alpha_i$  as the mole fraction of the  $i$ th species:

$$\begin{aligned} \alpha_i &= \frac{A_i}{\sum_{i=1}^{\infty} A_i} = \frac{R_i}{\sum_{i=1}^{\infty} R_i} \\ \alpha_i &= \exp\{-\tau_2'\} \exp\{-k_p\tau\} \frac{(k_p\tau)^{i-1}}{(i-1)!} \left(1 + \frac{\tau_2'}{k_p\tau}\right)^{i-1} \end{aligned}$$

Then the number-average degree of polymerization,  $\bar{i}$ , is:

$$\bar{i} = \sum_{i=1}^{\infty} i\alpha_i = k_p\tau \left(1 + \frac{\tau_2'}{k_p\tau}\right) \quad (10)$$

Solution of eq. (10) for  $k_p$  yields:

$$k_p \tau = \bar{i} - \tau_2' \quad (10a)$$

The monomer concentration during the constant temperature period can be calculated from the differential equation:

$$-\frac{d[M]}{dt} = k_p[M] \left[ \sum_i A_i \right] = k_p[M](fI_0/K_e)^{1/2}$$

The solution is:

$$M = M_{t=0} \exp\{-k_p(fI_0/K_e)^{1/2}t\} \quad (11)$$

and

$$\tau = \frac{M_{t=0}}{k_p(fI_0/K_e)^{1/2}} [1 - \exp\{-k_p(fI_0/K_e)^{1/2}t\}] \quad (12)$$

Thus, a plot of eq. (11) as  $\ln(M/M_{t=0})$  versus time should produce a straight line with slope,  $(k_p/K_e^{1/2})(fI_0)^{1/2} = k_2(fI_0)^{1/2}$  (Figs. 4 and 5). The only difficulty in applying eqs. (12) and (10a) in determining the absolute rate constant,  $k_p$ , for this system, however, is the determination of the intermediate value  $\tau_2'$ .

The preceding molecular weight distribution derivation points out that even in the presence of equilibrium complex formation and partial inactivation of chain ends the theoretical frequency distributions for the low and high molecular weight polymer fractions are of the Poisson type. The mean and variance of the Poisson distribution are equal, by using a normal approximation to the Poisson distribution, one can determine the theoretical range of molecular weight that each of the two frequency curves should cover. The number-average molecular weight of the low molecular weight material is almost uniformly 32,000, ( $\bar{i} = 300$ ). The number-average molecular weights of the long chain fractions are between 1,000,000 and 3,000,000 ( $\bar{i} = 10,000$  to  $\bar{i} = 30,000$ ). Since 99.7% of the chain lengths should be included in the range of  $-3\sqrt{\bar{i}}$  to  $+3\sqrt{\bar{i}}$  for the normal distribution approximation, it is possible to compute that the range of molecular weights should ideally be 10,000 molecular weight units for low weight species and 60,000 to 180,000 molecular weight units for the high end species. In no case does the range of the low molecular weight material fit the theoretical range. On the other hand, there is fair to good agreement with the expected values for the distributions of high molecular weight material in experiments 2-17, 2-24, 2-27, 2-29, and 2-30. Experiments 3-14 and 2-28 should not be expected to fit this correlation because of different experimental conditions. On the basis of this correlation, as well as the constant slope of the rate data, we can conclude that all of the chain ends represented by the high molecular weight species contributed to the observed rate.

The lack of a correlation with theory in regard to the range of the low molecular weight distribution suggests a continued slow growth of a por-

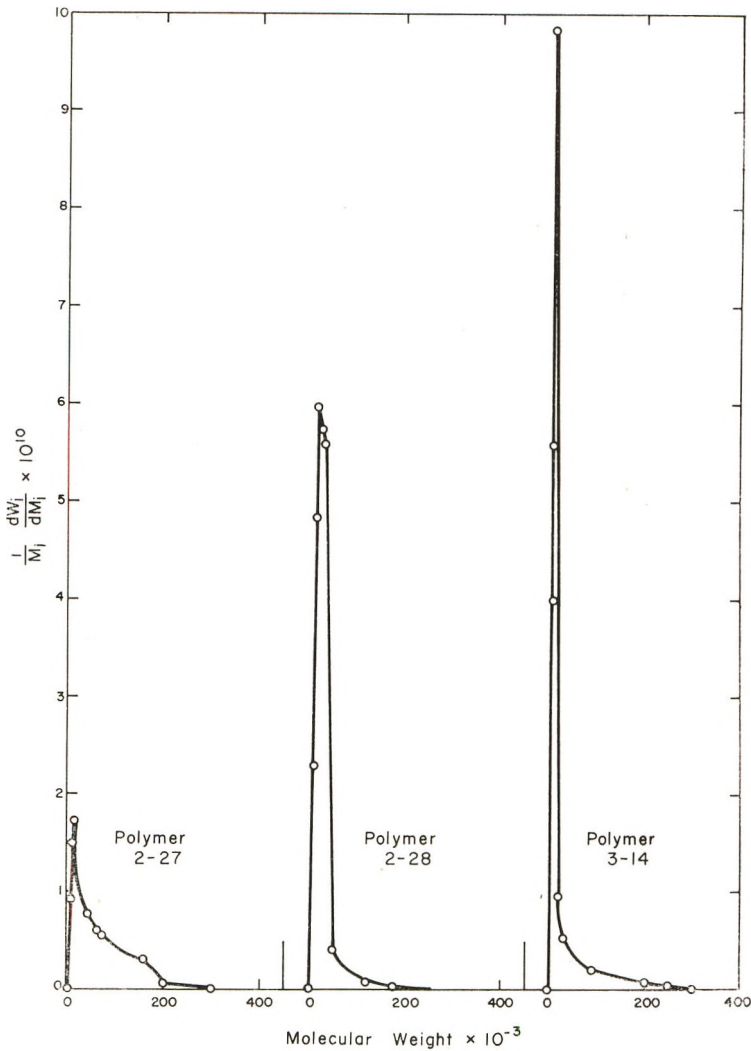


Fig. 12. Comparison of number frequency molecular weight distributions of low molecular weight fractions of polymers 2-27, 2-28, and 3-14.

tion of the low molecular weight material after precipitation. A comparison of the low molecular weight distribution from experiments 2-27, 2-28, and 3-14 (Fig. 12) indicates negligible contribution of this slow growth to the observed rates of polymerization. Experiment 2-27 was terminated at approximately the end of the interval of unsteady temperature (12 min.) before the time of rate measurement. Yet the frequency distribution for the low molecular weight material in this experiment is broad and comparable to that in experiments 2-28 and 3-14, which were allowed to run for periods of three days to two weeks. Thus, it is reasonable to consider that the spread of the low molecular weight distribution may be due to the

finite time required to trap out active chain ends, as well as continued growth of the trapped chain ends with occluded monomer. In either case, the fractionation data indicate that these chain ends do not contribute to the observable rate.

## APPENDIX I

### Solution of Consecutive First-Order Differential Equations for the Initial Condition of a Poisson Distribution

$$\text{Given: } \frac{dA_i}{dt} = k_p A_{i-1} M = k_p A_i M$$

with initial condition:

$$[A_i]_0 = \left( \frac{fI_0}{K_e} \right)^{1/2} \frac{(\tau_2')^{i-1}}{(i-1)!} \exp\{-\tau_2'\}$$

Then:

$$dA_i/dt = -k_p A_i M$$

We define:

$$d\tau = M dt \quad (dA_i/d\tau) = -k_p A_i$$

The solution is:

$$A_1 = [A_1]_0 \exp\{-k_p \tau\}$$

$$dA_2/d\tau = k_p A_1 - k_p A_2$$

The solution is:

$$A_2 = [A_1]_0 k_p \tau \exp\{-k_p \tau\} + [A_2]_0 \exp\{-k_p \tau\}$$

$$\frac{dA_3}{d\tau} = k_p A_2 - k_p A_3$$

The solution is:

$$A_3 = [A_1]_0 \frac{(k_p \tau)^2}{2!} \exp\{-k_p \tau\}$$

$$+ [A_2]_0 k_p \tau \exp\{-k_p \tau\} + [A_3]_0 \exp\{-k_p \tau\}$$

By induction:

$$A_i = \exp\{-k_p \tau\} \sum_{j=1}^{i-1} \frac{(k_p \tau)^{i-j}}{(i-j)!} [A_j]_0$$

$$A_i = \exp\{-k_p \tau\} \sum_{j=1}^i \frac{(k_p \tau)^{i-j}}{(i-j)!} \left( \frac{fI_0}{K_e} \right)^{1/2} \frac{(\tau_2')^{j-1}}{(j-1)!} \exp\{-\tau_2'\}$$



Shift index  $j/j + 1$

$$\begin{aligned}
 A_i &= (fI_0/K_e)^{1/2} \exp\{-\tau_2'\} \exp\{-k_p\tau\} \sum_{j=0}^{i-1} \frac{(k_p\tau)^{i-j}}{(i-j-1)!} \cdot \frac{\tau_2'^j}{j!} \\
 &= \left(\frac{fI_0}{K_e}\right)^{1/2} \exp\{-\tau_2'\} \exp\{-k_p\tau\} (k_p\tau)^{i-1} \sum_{j=0}^{i-1} \frac{(-1)^j(1-i)_j}{(i-1)!j!} \left(\frac{\tau_2'}{k_p\tau}\right)^j \\
 &= \left(\frac{fI_0}{K_e}\right)^{1/2} \exp\{-\tau_2'\} \exp\{-k_p\tau\} \frac{(k_p\tau)^{i-1}}{(i-1)!} \sum_{j=0}^{\infty} \frac{(-1)^j(1-i)_j}{j!} \left(\frac{\tau_2'}{k_p\tau}\right)^j \\
 &= \left(\frac{fI_0}{K_e}\right)^{1/2} \exp\{-\tau_2'\} \exp\{-k_p\tau\} \frac{(k_p\tau)^{i-1}}{(i-1)!} {}_1F_0 \left[ 1-i, - \frac{\tau_2'}{k_p\tau} \right]
 \end{aligned}$$

For notation see Rainville.<sup>18</sup>

$$\begin{aligned}
 A_i &= \left(\frac{fI_0}{K_e}\right)^{1/2} \exp\{-\tau_2'\} \exp\{-k_p\tau\} \frac{(k_p\tau)^{i-1}}{(i-1)!} \left(1 + \frac{\tau_2'}{k_p\tau}\right)^{i-1} \\
 \sum_{i=1}^{\infty} A_i &= \left(\frac{fI_0}{K_e}\right)^{1/2} \exp\{-\tau_2'\} \exp\{-k_p\tau\} \sum_{i=1}^{\infty} \frac{(k_p\tau)^{i-1}}{(i-1)!} \left(1 + \frac{\tau_2'}{k_p\tau}\right)^{i-1} \\
 &= \left(\frac{fI_0}{K_e}\right)^{1/2} \exp\{-\tau_2'\} \exp\{-k_p\tau\} \sum_{i=0}^{\infty} \sum_{j=0}^{\infty} \frac{k_p\tau^i}{i!} \frac{(-1)^j}{j!} \left(\frac{\tau_2'}{k_p\tau}\right)^j (-i)_j \\
 &= \left(\frac{fI_0}{K_e}\right)^{1/2} \exp\{-\tau_2'\} \exp\{-k_p\tau\} \sum_{i=0}^{\infty} \sum_{j=0}^i \frac{(k_p\tau)^i}{j!} \left(\frac{\tau_2'}{k_p\tau}\right)^j \frac{(-1)^j(-i)_j}{i!} \\
 &= \left(\frac{fI_0}{K_e}\right)^{1/2} \exp\{-\tau_2'\} \exp\{-k_p\tau\} \sum_{i=0}^{\infty} \sum_{j=0}^i \frac{(k_p\tau)^{i-j}}{(i-j)!} \frac{(\tau_2')^j}{j!} \\
 &= \left(\frac{fI_0}{K_e}\right)^{1/2} \exp\{-\tau_2'\} \exp\{-k_p\tau\} \sum_{i=0}^{\infty} \frac{(k_p\tau)^i}{i!} \sum_{j=0}^{\infty} \frac{(\tau_2')^j}{j!} \\
 &= \left(\frac{fI_0}{K_e}\right)^{1/2} \exp\{-\tau_2'\} \exp\{-k_p\tau\} \exp\{\tau_2'\} \exp\{k_p\tau\}
 \end{aligned}$$

$$\sum_{i=2}^{\infty} A_i = \left(\frac{fI_0}{K_e}\right)^{1/2}$$

$$\alpha_i = \frac{A_i}{\sum A_i} = \exp\{-k_p\tau\} \exp\{-\tau_2'\} \frac{(k_p\tau)^{i-1}}{(i-1)!} \left(1 + \frac{\tau_2'}{k_p\tau}\right)^{i-1}$$

$$\bar{i} = \sum_{i=1}^{\infty} i\alpha_i$$

$$= \exp\{-k_p\tau\} \exp\{-\tau_2'\} \sum_{i=1}^{\infty} \frac{i(k_p\tau)^{i-1}}{(i-1)!} \left(1 + \frac{\tau_2'}{k_p\tau}\right)^{i-1}$$

$$\begin{aligned}
 &= \exp\{-k_p\tau\} \exp\{-\tau_2'\} \left[ \sum_{i=1}^{\infty} \frac{(i-1)(k_p\tau)^{i-1}}{(i-1)!} \left(1 + \frac{\tau_2'}{k_p\tau}\right)^{i-1} \right. \\
 &\quad \left. + \sum_{i=1}^{\infty} \frac{(k_p\tau)^{i-1}}{(i-1)!} \left(1 + \frac{\tau_2'}{k_p\tau}\right)^{i-1} \right]
 \end{aligned}$$

$$\begin{aligned}
= \exp\{-k_p\tau\} \exp\{-\tau_2'\} k_p\tau \left(1 + \frac{\tau_2'}{k_p\tau}\right) \sum_{i=2}^{\infty} \frac{(k_p\tau)^{i-2}}{(i=2)!} \left(1 + \frac{\tau_2'}{k_p\tau}\right)^{i-2} \\
+ \exp\{-k_p\tau\} \exp\{-\tau_2'\} \sum_{i=1}^{\infty} \frac{(k_p\tau)^{i-1}}{(i=1)!} \left(1 + \frac{\tau_2'}{k_p\tau}\right)^{i-1}
\end{aligned}$$

Shift index on the first sum  $i/i + 2$ .

Shift index on the second sum  $i/i + 1$ .

As shown

$$\begin{aligned}
\sum_{i=0}^{\infty} \frac{(k_p\tau)^i}{i!} \left(1 + \frac{\tau_2'}{k_p\tau}\right)^i = \exp\{k_p\tau\} \exp\{\tau_2'\} \\
i = k_2\tau \left(1 + \frac{\tau_2'}{k_2\tau}\right) + 1
\end{aligned}$$

## APPENDIX II

### Nomenclature

- $a, a_e, a_m$  = constant, subscript e and m refer to ethanol and methanol, respectively
- $A_i$  = molar concentration of the  $i$ th species, (ml.<sup>-1</sup>)
- $c, c_e, c_m$  = constant, subscript e and m refer to ethanol and methanol, respectively
- $E_a$  = activation energy
- $f$  = fractional number
- $f_{(n)}$  = frequency number, function of ( $n$ )
- $\bar{i}$  = number-average degree of polymerization
- $[I], [I_0]$  = initiator concentration (ml.<sup>-1</sup>), subscript zero refers to initial value
- $k_1, k_p$  = rate constants of initiation and propagation, respectively
- $K_e$  = equilibrium constant for association of polymeric chains
- $[M], [M_0]$  = monomer concentration (ml.<sup>-1</sup>), subscript zero refers to initial value
- $M_n$  = growing chain containing only monomer
- $M_i$  = molecular weight of a polymer chain containing  $i$  units
- $\bar{M}_n, \bar{M}_v, \bar{M}_w$  = average molecular weights, subscript  $n, v$ , and  $w$  refer to number, viscosity, and weight averages, respectively
- $N_i$  = number or mole fraction of species  $i$
- $P_i, P_{i0}$  = molar concentration of polymer containing  $i$  units, subscript zero refers to initial value
- $Q_i$  = molar concentration of polymer containing  $i$  units
- $R_i$  = molar concentration of polymer containing  $i$  units
- $t$  = time
- $T$  = temperature

- $W_i$  = cumulative weight fraction including all species less than or equal to  $i$   
 $w_i$  = weight fraction of the  $i$ th specie  
 $x$  = degree of polymerization  
 $\bar{X}_n, \bar{X}_v, \bar{X}_w$  = average degree of polymerization, subscripts  $n, v, w$  refer to number, viscosity, and weight averages, respectively  
 $\Delta$  = difference  
 $\eta_{sp}$  = specific viscosity  
 $[\eta][\eta]_e, [\eta]_m$  = intrinsic viscosity, subscripts  $e$  and  $m$  refer to ethanol and methanol, respectively  
 $\tau, \tau_1', \tau_2'$  = "dimensionless" time, equal to  $\int_0^t g(t)dt$

### References

1. Fitzgerald, E. B., and R. M. Fuoss, *Ind. Eng. Chem.*, **42**, 1603 (1950); P. F. Onyon, *Trans. Faraday Soc.*, **51**, 400 (1955).
2. Jordan, D. O., A. R. Mathieson, and M. R. Porter, *J. Polymer Sci.*, **21**, 473 (1956).
3. Fuoss, R. M., M. Watanabe, and B. D. Coleman, *J. Polymer Sci.*, **48**, 5 (1960).
4. Berkowitz, J. B., M. Yamin, and R. M. Fuoss, *J. Polymer Sci.*, **28**, 69 (1958); A. G. Boyes and J. P. Strauss, *J. Polymer Sci.*, **22**, 462 (1956).
5. Spiegelman, P. P., Ph.D. Thesis, University of Michigan, Ann Arbor, Michigan, 1962.
6. Strauss, U. P., and R. M. Fuoss, *J. Polymer Sci.*, **4**, 457 (1949).
7. Mark, H., and R. Raff, *High Polymeric Reactions*, Interscience, New York, 1941.
8. Hulme, J. M., and L. A. McLeod, *Polymer*, **3**, 153 (1962).
9. Gechele, G. B., and S. Pietra, *J. Org. Chem.*, **26**, 4412 (1961).
10. Berry, G. C., Ph.D. Thesis, University of Michigan, Ann Arbor, Michigan, 1960; V. C. Long, Ph.D. Thesis, University of Michigan, Ann Arbor, Michigan, 1958.
11. Ziegler, K., and H. Zeisser, *Ber.*, **63**, 1847 (1930).
12. Glusker, D. L., I. Lysloff, and E. Stiles, *J. Polymer Sci.*, **49**, 297 (1961); I. Kuntz, *J. Polymer Sci.*, **54**, 569 (1961).
13. Worsfold, D. J., and S. Bywater, *Can. J. Chem.*, **38**, 1891 (1960).
14. Morton, M., E. E. Bostick, and R. Livigni, *Rubber Plastics Age*, **42**, 397 (1961).
15. Livigni, R., Ph.D. Thesis, University of Akron, Akron, Ohio, 1960.
16. Morton, M., N. Calderon, L. N. Fetter, and J. F. Meier, paper presented to Division of Polymer Chemistry, 140th Meeting, American Chemical Society, Chicago, Ill., Sept. 1961; *Preprints*, p. 310.
17. Bresler, S. E., A. A. Korotov, M. I. Mosevitskii, and I. Ya. Poddubny, *Zhur. Tekh. Fiz.*, **28**, 114 (1958); in translation in *Rubber Chem. Technol.*, **33**, 669 (1960).
18. Rainville, E. D., *Special Functions*, Macmillan, New York, 1960.

### Résumé

La polymérisation de la 4-vinylpyridine initiée par le butyllithium dans un milieu hydrocarboné se déroule suivant un mécanisme d'addition anionique. Dans l'heptane et le toluène les réactifs solubles et incolores forment rapidement un précipité de polymère granuleux et intensément coloré à une température inférieure à  $-30^{\circ}\text{C}$ . Lorsque la réaction est faite dans un milieu exempt d'impuretés le mélange réactionnel intensément coloré reste inchangé indéfiniment et une addition ultérieure de monomères continue la croissance des chaînes polymériques. On utilise la technique de la dilatométrie pour suivre la vitesse de polymérisation dans le toluène. Les méthodes expérimentales qui ont été utilisées pour la manipulation des solutions sous vide conduisent à une période

de température initialement instable suivie par une période de température constante pendant laquelle se font les mesures de vitesses. On a fait varier les concentrations initiales en monomère et en initiateur dans quatre domaines. Les mesures de vitesse ont été faites dans un intervalle de température de  $-30^{\circ}$  à  $+30^{\circ}\text{C}$ . Les expériences de cinétique par dilatométrie combinées avec des observations indépendantes permettent d'établir que la vitesse est proportionnelle à la concentration en monomère et avec une puissance un demi pour la concentration en initiateur, suggérant la formation d'un complexe d'équilibre des anions polymériques en croissance. On détermine les valeurs des constantes de vitesse à partir des vitesses obtenues par les expériences cinétiques de dilatométrie et à partir de la racine carrée de la concentration effective en initiateur. Le calcul de la dépendance de la constante de vitesse en fonction de la température permet de déterminer l'énergie d'activation de  $12.7$  kcal/mole. Comme prévu dans la théorie de la polymérisation anionique le polymère formé dans ces réactions a un poids moléculaire en nombre calculé égal au rapport (poids du polymère/équivalent en initiateur). Le polymère est fractionné par élution chromatographique utilisant l'alcool butylique tertiaire et des mélanges de benzène et de non-solvants. La distribution du poids moléculaire des polymères, construit sur la base des valeurs de fractionnement montre une distribution bimodale dans deux régions très étroites de poids moléculaire. Cette distribution de poids moléculaires inhabituelle est due à l'isolement d'une partie de chaînes actives en croissance dans le polymère précipité. Ces sites réactionnels isolés (qui dans ces expériences atteignent 95% et plus de la concentration totale en initiateur) ne produisent plus de chaînes polymériques en croissance ce qui est dû à l'absence de monomère disponible. Les sites réactionnels restant effectifs croissent donc en polymère à haut poids moléculaire et sont responsables des cinétiques observées.

### Zusammenfassung

Die durch Butyllithium gestartete Polymerisation von 4-Vinylpyridin verläuft in Kohlenwasserstoffmedien über einen anionischen Additionsmechanismus. Bei Temperaturen unter  $-30^{\circ}\text{C}$  bildet sich in Heptan und Toluol als Lösungsmittel aus den farblosen, löslichen Ausgangsstoffen rasch ein körniger, tiefgefärbter Polymerniederschlag. Bei Ausführung der Reaktion in einem von Verunreinigungen freien Medium blieb das tiefgefärbte Reaktionsgemisch beliebig lange Zeit unverändert und bei weiterer Zugabe von Monomerem wurde das Wachstum der Polymerketten fortgesetzt. Die Geschwindigkeit der Polymerisation in Toluol als Lösungsmittel wurde dilatometrisch gemessen. Unter Anwendung der für die Handhabung von Lösungen im Vakuum üblichen Methoden erfolgte die Polymerisation (30–50% Umsatz) während einer anfänglichen Periode nichtstationärer Temperatur, gefolgt von einem Bereich konstanter Temperatur, in dem die Geschwindigkeitsmessungen durchgeführt wurden. Die Anfangskonzentrationen von Monomerem und Starter wurden um das Vierfache variiert. Die Geschwindigkeitsmessungen wurden im Temperaturbereich von  $-30^{\circ}\text{C}$  bis  $+30^{\circ}\text{C}$  durchgeführt. Aus den dilatometrischen kinetischen Versuchen und aus anderen, unabhängigen Beobachtungen geht hervor, dass die Geschwindigkeit der Monomerkonzentration und der Quadratwurzel aus der Starterkonzentration proportional ist. Dies weist auf eine Gleichgewichts-Komplexbildung der wachsenden Polymeranionen hin. Aus den bei den dilatometrischen Versuchen erhaltenen Geschwindigkeitsdaten und der Quadratwurzel der effektiven Starterkonzentrationen wurden die Geschwindigkeitskonstanten berechnet. Aus der Temperaturabhängigkeit der Geschwindigkeitskonstanten wurde eine Aktivierungsenergie von  $12,7$  kcal/Mol berechnet. Das Zahlenmittel des Molekulargewichts des gebildeten Polymeren war gleich dem Verhältnis (Gewicht des Polymeren)/(Starteräquivalente). Dies stimmt mit der auf Grund der Theorie der anionischen Polymerisation gemachten Voraussage überein. Das Polymere wurde elutionschromatographisch unter Verwendung von Lösungsmittel-Fällungsmittelgemischen aus tert-Butylalkohol und Benzol fraktioniert. Die aus den Fraktionierungsdaten ermittelte Molekulargewichtsverteilung ist eine bimodale Verteilung in zwei

ziemlich engen Molekulargewichtsbereichen. Diese ungewöhnliche Molekulargewichtsverteilung geht auf eine Okklusion eines Teiles der aktiven Enden der wachsenden Ketten im Polymerniederschlag zurück. Diese "eingeschlossenen" Reaktionsstellen (die in den vorliegenden Versuchen bis zu 95% und mehr der gesamten Starterkonzentration ausmachten) führen wegen des Fehlens an verfügbarem Monomerem zu keiner weiteren Polymerisation. Die restlichen "effektiven" Reaktionsstellen wachsen bis zu einem hohen Molekulargewicht weiter und sind für die beobachtete Kinetik verantwortlich.

Received April 26, 1963



## Theoretical Consideration of Linear Condensation Polymerization in a Dispersed Medium\*

V. S. NANDA, †‡ *Institute of Theoretical Science, University of Oregon, Eugene, Oregon*

### Synopsis

The combinatorial approach to the problem of linear polymers, developed earlier, is applied in the present paper in order to study the statistical nature of condensation polymers obtained from a large number of very small systems. The results of the customary theory become inapplicable in such cases for sufficiently high degrees of polymerization which should be attainable experimentally. The possibility of realizing homogeneous samples by direct polymerization is discussed from a theoretical standpoint.

1. It is not often noted that the customary theory of linear condensation polymerization becomes invalid at extremely high degrees of polymerization. It fails, for example, to predict the decrease in inhomogeneity which must inevitably occur when polymerization is carried beyond a certain stage. On the other hand, the combinatorial approach to the problem of polymers, employed earlier by us,<sup>1,2</sup> gives results which are valid for all stages of the reaction. Taking the clue from exact results, we suggest in the present paper a procedure for obtaining linear condensation polymers with a high degree of homogeneity. Theoretical results are also given for the various statistical quantities when the actual conditions for the preparation do not conform to the ideal requirements.

2. Consider a polymer system with  $n$  monomers. If  $k$  denotes the number of independent entities (molecules) at any stage of reaction, the number fraction of  $i$ -mers in the polymerized material is given by<sup>2</sup>

$$F_i = \binom{n-i-1}{k-2} / \binom{n-1}{k-1} \quad (1)$$

This gives for  $n$  and  $k$  very large

$$F_i = (1-p) p^{i-1} \quad (2)$$

\* Supported in part by the National Science Foundation (G 19518) and the Division of General Medical Sciences, Public Health Service (09153).

† On leave of absence from Physics Department, University of Delhi, Delhi, India.

‡ Mailing address: Chemistry Department, University of Southern California, Los Angeles, California.

where

$$p = 1 - k/n$$

This is the well-known expression for number fraction obtained from the probability considerations. Using eq. (2), one readily finds for the number-average chain length  $i_n$  and the weight-average chain length  $i_w$  the expressions

$$i_n = 1/(1 - p) \quad (3)$$

$$i_w = (1 + p)/(1 - p) \quad (4)$$

Thus

$$i_w/i_n = (1 + p) \quad (5)$$

Since for high degrees of polymerization  $p \rightarrow 1$ , it is clear that the theory predicts progressive increase in inhomogeneity with increasing polymerization. Intuitively, however, one expects this trend to reverse itself after a certain stage of the reaction assuming that it can be carried forward to any desired extent.

The expression (1) for the size distribution is applicable for all stages of reaction, both when the system is undergoing polymerization or degradation. One also has exact expressions for the moments through appropriate generating functions.<sup>1</sup> For example, instead of eq. (5), we get

$$i_w/i_n = 1 + [1 - (k/n)][(k - 1)/(k + 1)] \quad (5a)$$

a result which is exact right up to  $k = 1$ . This predicts a maximum in inhomogeneity for  $k = (2n)^{1/2}$  and a rapid return to the homogeneous state when  $k$  is no longer very large as compared to unity. The size distribution expression itself can be simplified for large  $n$  to

$$F_i = [(k - 1)/n][1 - (i/n)]^{k-2} \quad (1a)$$

a form which is suitable for numerical purposes and is applicable for all  $k \geq 2$  but  $\ll n^{1/2}$ .

3. The failure of the usual results,\* pointed out in the last section, has no impact on ordinary bulk polymerization. This is because in such systems it is not possible, because of thermodynamic reasons,<sup>3,4</sup> to achieve the stages of polymerizations where the two sets of expressions will give significantly different results. Nevertheless, the exact treatment suggests the possibility of obtaining highly homogeneous polymers. The conditions under which the usual formulas no longer apply should be more easily obtainable.

When polymerization is carried out in small isolated systems, such as

\* This is apparently one of the examples where the commonly made assumption in statistical mechanics, that the *mean* state of the assembly is the same as the *most probable* state, is not applicable. For another instance of this type, see C. B. Haselgrove, and H. N. V. Temperley, *Proc. Camb. Phil. Soc.*, **50**, 225 (1954).

globules of the polymerizing material suspended in a suitable medium, it should be possible to have situations corresponding to small  $k$  for realizable values of average chain lengths. It may be noted here that it is primarily the ratio  $k/n$  which is determined by thermodynamics. For small suspensions, since  $n$  can be quite small, the value of  $k$  can be lowered appreciably, which should help in increasing the homogeneity of the resulting polymer [c.f. eq. (5a)]. The feasibility of this procedure is discussed in the last section.

4. We now find the polymer size distribution for the overall system made up of subsystems in the form of suspensions of monomer particles in a suitable medium. For the sake of simplicity, we consider first the case in which all the suspensions,  $\nu$  in number, have the same size. Let  $\kappa (\geq \nu)$  to the number of polymers in the overall system. For the maximum possible polymerization, obviously  $\kappa \geq \nu$ . For incomplete reaction, the size distribution problem may be visualized as one of a statistical study of degradation of the homogeneous system consisting of  $\nu$  chains which undergo  $\kappa - \nu$  cuts. Obviously here the way  $\kappa - \nu$  cuts are assigned is of importance. Both the cases in which the cuts are distributed uniformly or randomly over the subsystems will be treated as they represent two extreme possibilities of what might actually happen in practice.

*Case 1. Exactly Similar Evolution of Polymerization in Subsystems.* The polymer size distribution is governed by eq. (1) or its simplified form eq. (1a). Here the existence of thermodynamic equilibrium demands that  $\kappa$  be a multiple of  $\nu$ . The expressions for moments and averages deduced previously<sup>1</sup> apply. In particular,  $i_n$  and  $i_w$  are given by

$$i_n = n/k \quad (6)$$

$$i_w = 1 + 2[(n - k)/(k + 1)] \quad (7)$$

where  $k$  is evidently equal to  $\kappa/\nu$ .

*Case 2. Random Evolution of Polymerization in Subsystems.* In this case one defines the extent of the reaction for the overall system. Evidently  $\kappa = \nu$  corresponds to the situation when all the subsystems have achieved complete polymerization. For  $\kappa > \nu$ , the expressions for the size distribution and the averages are obtainable from our earlier work on the degradation of a homogeneous polymer system.<sup>5</sup> The number fraction is given by

$$\left. \begin{aligned} F_i &= \frac{\alpha(1 - \alpha)^{i-1}}{1 + \alpha(n - 1)} [2 + (n - i)\alpha] \\ F_n &= \frac{1}{1 + \alpha(n - 1)} (1 - \alpha)^{n-1} \end{aligned} \right\} i \leq n - 1 \quad (8)$$

where  $\alpha$  is given here by  $(\kappa - \nu)/[\gamma(n - 1)]$ . The number-average and the weight-average chain lengths now have, respectively, the form

$$i_n = \frac{n}{[1 + \alpha(n - 1)]} \quad (9)$$

$$i_w = \frac{1}{n} \left\{ n + \frac{2(1 - \alpha)}{\alpha^2} [\alpha n - 1 + (1 - \alpha)^n] \right\} \quad (10)$$

Comparing eqs. (6) and (9) we write

$$1 + \alpha(n - 1) = \bar{k}$$

where  $\bar{k}$  is interpreted as the average number of polymer chains per subsystem. It appears worth while to compare the results from the two sets of expressions. In Figure 1 we have plotted the ratio of the values of  $i_w$  using eqs. (10) and (7) for the same number-average chain length. It appears that the maximum difference between the two cases occurs for  $\bar{k} = 4$  and dwindles for higher  $\bar{k}$  values. The fact that the ratio is always greater than unity is understandable, for in case 2, in the language of degradation, the cuts are distributed randomly, whereas in case 1 each of the subsystems gets the same number of cuts. For  $\bar{k}$  large, naturally the difference whether a subsystem receives exactly  $\bar{k}$  or on the average  $\bar{k}$  cuts becomes irrelevant.

5. In this section we take account of the size distribution in the suspended particles. Let  $\phi(n)dn$  denote the fraction of suspensions containing monomers in the range  $n$  to  $n + dn$ . For complete reaction in the subsystems, obviously the polymer size distribution for the overall system would be described by the same function. For incomplete reaction it becomes difficult to treat the parallel of case 1 without introducing some subsidiary assumptions concerning the way the cuts can be assigned uniformly to subsystems of nonuniform size. We therefore consider here only the case of random evolution of polymerization in the subsystems. The corresponding results for inhomogeneity would then give higher values if the actual process were not completely random.

Here the results for various quantities of interest are obtainable from our earlier work on degradation of a polydisperse polymer system.<sup>6</sup> We have in our present notation

$$F_i = \frac{(1 - \alpha)^{i-1}}{1 + \alpha(\bar{n} - 1)} \left[ \phi(i) + \alpha \int_{t>i} \phi(t) \{2 + (t - i - 1)\alpha\} \right] \quad (11)$$

$$i_n = \frac{\bar{n}}{1 + \alpha(\bar{n} - 1)} \quad (12)$$

and

$$i_w = \frac{2 - \alpha}{\alpha} - \frac{2(1 - \alpha)}{\alpha^2 \bar{n}} \left[ 1 - \int_0^\infty \phi(t)(1 - \alpha)^t dt \right] \quad (13)$$

The degree of degradations

$$\alpha = (\kappa - \nu) / [\nu(\bar{n} - 1)]$$

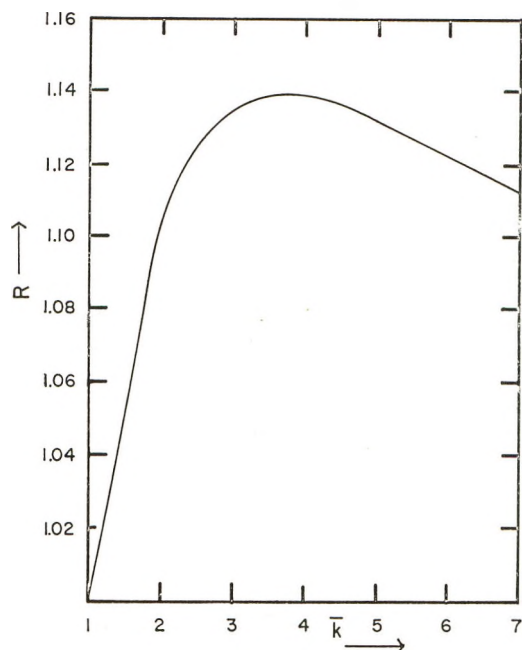


Fig. 1. Variation with  $\bar{k}$  of  $R$ , the ratio of  $i_w$  values obtained from eqs. (10) and (7) for the same number-average chain length.

while  $\bar{n}$  is the average number of monomers per subsystem. In the absence of any reasons for selecting a particular distribution we take for  $\phi$  the normal form in order to perform a few illustrative calculations. This gives

$$F_i = \frac{(1 - \alpha)^{i-1}}{1 + \alpha(\bar{n} - 1)} \left\{ \frac{e^{-(i-\bar{n})^2/(2\sigma^2)}}{\sigma(2\pi)^{1/2}} + \frac{\alpha^2\sigma}{(2\pi)^{1/2}} e^{-\gamma^2/2} \right. \\ \left. + (1 \pm I_\gamma) \left[ (2 - i\alpha) \frac{\alpha}{2} + \bar{n} \frac{\alpha^2}{4} \right] \right\} \quad (11a)$$

$$i_w = \frac{2 - \alpha}{\alpha} - \frac{2}{\alpha^2\bar{n}} \left[ 1 - \exp \left\{ \frac{\sigma^2}{2} \log^2(1 - \alpha) + \bar{n} \log(1 - \alpha) \right\} \right] \quad (13a)$$

where

$$I_\gamma = (2/\pi)^{1/2} \int_0^\gamma e^{-z^2/2} dz$$

and

$$\gamma = |(i - \bar{n})/\sigma|$$

while  $\sigma^2$  is the mean deviation. The upper sign in eq. (11a) is to be used for  $i < \bar{n}$  and the lower one for  $i > \bar{n}$ . The expression, eq. (13a), is also obtainable from Montroll's work<sup>6</sup> as a special case. However, when  $\alpha \rightarrow 0$  this form is not very convenient for numerical computations because of



occurrence of  $\alpha$  in the denominator. Under these conditions expressing eq. (13a) as a series expansion in the form

$$i_w = \bar{n} \left[ 1 + \frac{\sigma^2}{\bar{n}^2} - \alpha \bar{n} \left( \frac{1}{3} + \frac{\sigma^2}{\bar{n}^2} \right) + \dots \right] \quad (13b)$$

is helpful provided  $\alpha \bar{n} \ll 1$ .

In Figure 2 we have plotted the values of  $i_w/i_n$  against  $\bar{k}$  for different values of  $\sigma/\bar{n}$ . It appears that the departure of the statistical results for polymerization in the dispersed form, from those expected of the usual theory, should be easily observable even when the reaction in the subsystems is far from complete.

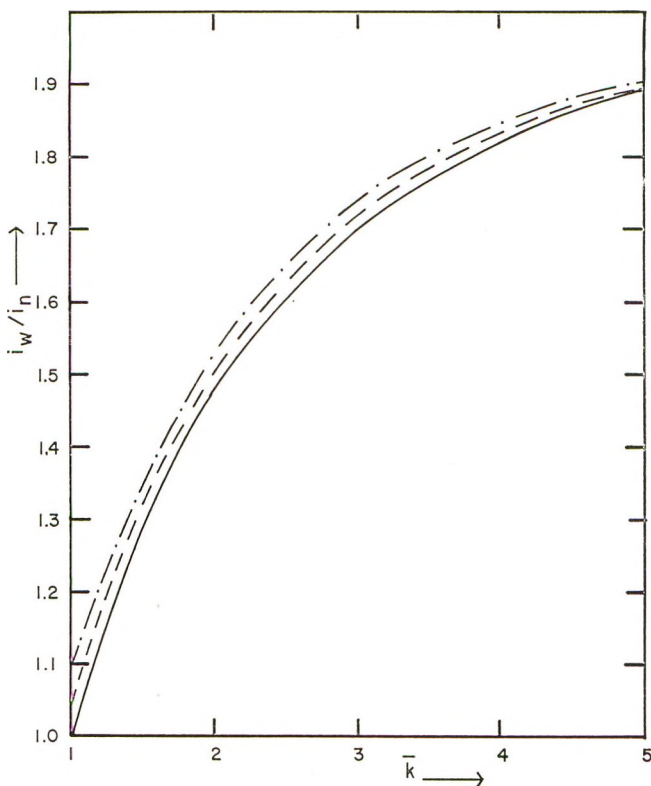


Fig. 2. Variation of  $i_w/i_n$  with  $\bar{k}$  for different values of  $\sigma/\bar{n}$ , using eqs. (12) and (13a):  
 (—)  $\sigma/\bar{n} = 0$ , (---)  $\sigma/\bar{n} = 0.2$ ; (-.-)  $\sigma/\bar{n} = 0.3$ .

6. The production of homogeneous polymers requires both a statistically narrow size distribution for the suspensions and also maximum possible polymerization in them. In this connection it is worthwhile to determine the order of size of suspensions which would be necessary so that the value of the characteristic quantity  $p$  is not unduly close to unity, but maximum possible polymerization is obtainable. Taking  $p = 1.5 \times 10^{-5}$ , which

is not very unreasonable for bulk polymerization (it corresponds to  $i_n = 2 \times 10^4$ ), one finds a radius of 10  $m\mu$  for the case of polysulfide polymers. This is much smaller than the particle size obtained in commercial suspension polymerization of this substance, but is well within the particle sizes reported in more extensively investigated addition polymerization in the dispersed phase.<sup>7</sup> Suspensions with statistically narrow size distribution could be produced by using appropriate filters. Unless conditions of high degree of homogeneity are required, the removal of particles with size greater than the maximum in the size distribution curve of suspensions should be adequate.

In this preliminary study, we have not taken account of the possibility of ring formation. These effects in the present case could become more important than in ordinary bulk polymerization because of confinement of chains over small volumes. It is also possible that the bimolecular rate constant for the condensation of the reacting units in small suspensions is affected. However, it appears prudent to wait for some experimental data before beginning to speculate in this connection as the effects might prove to be relatively unimportant.

I am thankful to Prof. M. Fixman for his interest in this investigation and for making some valuable comments.

### References

1. Nanda, V. S., and R. K. Pathria, *J. Chem. Phys.*, **30**, 27 (1959).
2. Nanda, V. S., and R. K. Pathria, *Proc. Natl. Inst. Sci. (India)*, **26**, 700 (1960).
3. Tobolsky, A., *J. Chem. Phys.*, **12**, 402 (1944).
4. Flory, P. J., *J. Chem. Phys.*, **12**, 425 (1944).
5. Pathria, R. K., and V. S. Nanda, *J. Chem. Phys.*, **30**, 31 (1959). The general formulation of this paper could take care of the situations intermediate between the cases 1 and 2. See also E. Montroll and R. Simha, *J. Chem. Phys.*, **8**, 721 (1940).
6. Nanda, V. S., and R. K. Pathria, *Proc. Roy. Soc. (London)*, **A270**, 14 (1962). See also E. Montroll, *J. Am. Chem. Soc.*, **63**, 1215 (1941).
7. D'Alelio, G. F., *Fundamental Principles of Polymerization*, Wiley, New York, 1952, Chap. VI.

### Résumé

L'analyse combinatoire du problème des polymères linéaires développée précédemment, est appliquée dans le présent article à l'étude de la nature statistique des polymères de condensation obtenus au départ d'un grand nombre de très petits systèmes. Pour les degrés de polymérisation suffisamment élevés qu'il serait possible d'atteindre expérimentalement, les données de la théorie usuelle deviennent inapplicables. La possibilité de préparer des échantillons homogènes par polymérisation directe est discutée d'un point de vue théorique.

### Zusammenfassung

In der vorliegenden Arbeit wird die früher entwickelte kombinatorische Behandlung des Problems linearer Polymerer zur Untersuchung der statistischen Natur von aus einer grossen Anzahl sehr kleiner Systeme hergestellten Kondensationspolymeren herange-

zogen. Die Ergebnisse der üblichen Theorie sind in solchen Fällen für genügend hohe Polymerisationsgrade, die experimentell erreichbar sein sollten, nicht anwendbar. Es wird die Möglichkeit, homogene Proben durch direkte Polymerisation herzustellen, von einem theoretischen Gesichtspunkt aus diskutiert.

Received April 30, 1963

## $\alpha$ - $\gamma$ Transition of Nylon 6

II. ARIMOTO, *Research Institute, Nippon Rayon Company, Ltd., Uji, Kyoto, Japan*

### Synopsis

The mechanism of the  $\alpha$ - $\gamma$  transition of nylon 6 due to iodine treatment and the structure of the  $\gamma$ -form of nylon 6 are discussed on the basis of results of x-ray diffraction and polarized micro-infrared absorption measurements on doubly oriented and iodine-treated specimens. The plane of the amide group and that of the methylene group are both parallel to the rolled plane, which is parallel to the hydrogen-bonded molecular sheet in the  $\alpha$ -form of nylon 6. The plane of the amide group is preferentially twisted to a direction roughly perpendicular to the rolled plane on coordination of iodine to the oxygen of the amide group and this preferential orientation of the amide group is retained on the removal of iodine. The preferential orientation of the amide group in the molecule supports the pleated sheet structure proposed by Kinoshita for the  $\gamma$ -form of polyamides. Infrared bands are examined, the preferential orientation of the amide group being taken into account. The structure of the  $\gamma$ -form of nylon 6 is composed of pleated sheets of similarly directed molecular chains joined by hydrogen bonds between the adjacent molecules and in such a packing of sheets the directions of molecular chains are alternately inverse along the direction of stacking of sheets.

### INTRODUCTION

The usual  $\alpha$ - and  $\beta$ -forms of ordinary nylon 6 are easily converted to a new crystal form when treated with an iodine-potassium iodide aqueous solution followed by the removal of iodine with a sodium thiosulfate aqueous solution.<sup>1,2</sup> This new crystal form was called the  $\gamma$ -form by Kinoshita<sup>3</sup> on the basis of his study of the crystal structures of a series of polyamides.

In a series of our previous papers,<sup>4-6</sup> the structural change in nylon 6 during the course of the  $\alpha$ - $\gamma$  transition caused by iodine treatment was studied by means of various measurements such as iodine-adsorption isotherms, x-ray diffraction, and ultraviolet, visible, and infrared absorptions. It becomes apparent that: (1) iodine enters into the crystalline part of nylon 6 and coordinates to the oxygen of the amide group to form a definite complex; (2) coordination occurring on the oxygen brings about dissociation of hydrogen bonds between amide groups; (3) the pseudo-hexagonal packing and configuration of polymer molecules in the complex is similar to that of polymer molecules in the  $\gamma$ -form of nylon 6; (4) there are several infrared bands closely related to that of the crystal form of nylon 6.

For the  $\gamma$ -form of polyamides made from  $\omega$ -amino acids which have even numbers of carbon atoms, Kinoshita<sup>3</sup> proposed the space group  $P2_1$  and

the structure composed of parallel pleated sheets instead of the structure composed of antiparallel extended sheets usually seen in the  $\alpha$ - and  $\beta$ -forms of polyamides. The  $\gamma$ -form of  $\omega$ -amino acid nylons, however, is not fully elucidated on account of complexities ascribed to the fact that the molecule of  $\omega$ -amino acid nylons is not symmetrical. Thus, from the view points of generality, it seems to be of interest to investigate the  $\alpha$ - $\gamma$  transition of nylon 6 caused by iodine treatment.

In the present paper a doubly oriented nylon 6 specimen was treated with iodine and studied by the methods of x-ray diffraction and of polarized micro-infrared spectroscopy. The purpose of this study is to present the results of the experiments and to obtain information on the  $\alpha$ - $\gamma$  transition and the structure of the  $\gamma$ -form of nylon 6. It is also one of the motives in this paper to examine the assignment of infrared bands of nylon 6.

## EXPERIMENTAL

### Materials

**1. Untreated Specimen.** An extruded nylon 6 bristle (diameter about 3.6 mm.) was drawn 3.5 times and hot rolled at 130°C. (the direction of rolling is the same as that of drawing). The specimen which showed good orientation and crystallinity was obtained by pressing a piece of doubly oriented bristle between two stainless steel plates and crystallizing it in a steam bath maintained at 135°C. for 1 hr. The size of the section normal to the rolling direction was about  $7.5 \times 0.35$  mm.

**2. Iodine-Adsorbed Specimen.** The untreated specimen was treated with a 1.23*N* iodine-potassium iodide aqueous solution for a week.

**3. Iodine-Desorbed Specimen.** The iodine-adsorbed specimen was treated with a sodium thiosulfate aqueous solution for the removal of iodine.

### Experimental Methods

Experimental methods used here were virtually identical with those described by Tadokoro et al.<sup>7</sup> for the measurement of the infrared pleochroism of polyvinyl alcohol. X-ray photographs were taken with nickel-filtered copper radiation, the x-ray beam being parallel to the direction of rolling.

Infrared spectra were measured with a section (about  $5\mu$  thick for the 3-7 $\mu$  region and 20 $\mu$  thick for the 7-15 $\mu$  region) cut normal to the direction of rolling by use of a Perkin-Elmer Model 13 infrared spectrophotometer with a Model 85 infrared microscope attachment, a NaCl prism, and an AgCl polarizer. The section was prepared from a specimen embedded in a mixture of two parts of solid paraffin, one part of stearic acid, and one part of ethyl cellulose by using a microtome. The section of the iodine-adsorbed specimen used here, however, was prepared by treating the section of the untreated specimen or that of the iodine-desorbed one with the iodine solu-



tion, because the iodine-adsorbed specimen suffered a loss of orientation due to its low melting point when heat was imposed upon it by embedding. The same experimental results were obtained in both cases.

The measurements were made so that the infrared beam was parallel to the direction of rolling just as in the taking of the x-ray photographs described above. The angle  $\theta$  between the rolled plane and the direction of the electric vector of the polarized beam was varied from  $0^\circ$  to  $90^\circ$  at intervals of  $10^\circ$ .

## RESULTS

### X-Ray Measurements

Figures 1a and 1b are x-ray photographs of the untreated ( $\alpha$ -form) and the iodine-desorbed ( $\gamma$ -form) specimens, respectively. Figures 2a and 2b

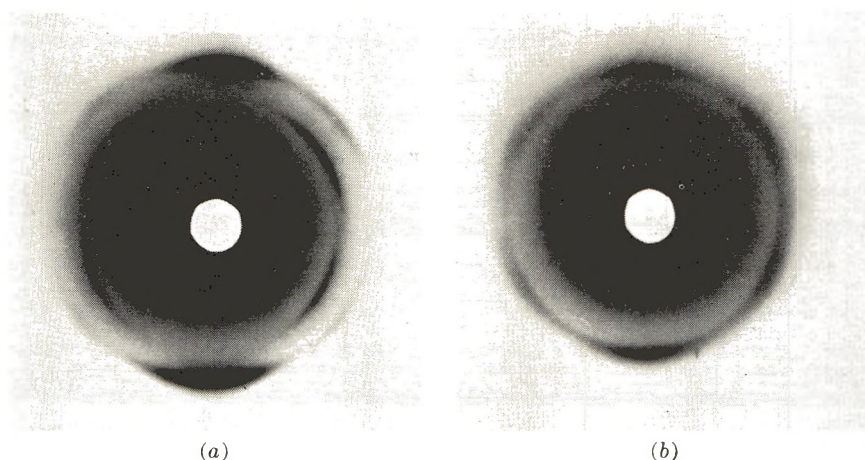


Fig. 1. X-ray photographs of (a) the untreated ( $\alpha$ -form) and (b) the iodine-desorbed ( $\gamma$ -form) specimens of doubly oriented nylon 6. The direction of the x-ray beam is parallel to that of the rolling.

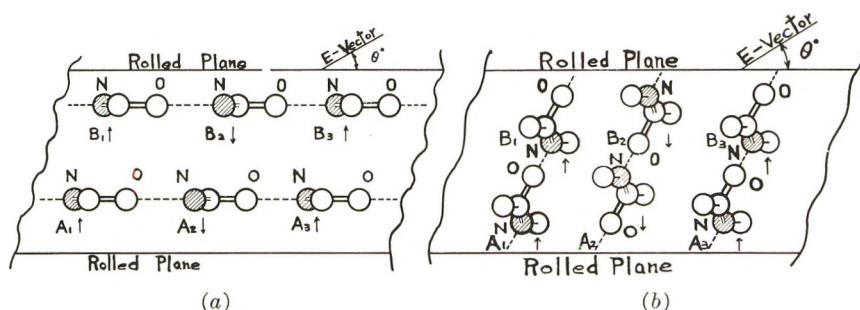


Fig. 2. Schematic diagram of sections of (a) the untreated and (b) the iodine-desorbed specimens showing the relation of the molecular sheet to the rolled plane. The arrows represent the direction of  $-\text{NH}-\text{C}-$ ; the broken line indicates the hydrogen bond.



TABLE I. Infrared Bands of Nylon 6

Untreated ( $\alpha$ -form)			Iodine-adsorbed			Iodine-desorbed ( $\gamma$ -form)			Assignment		
Wave number, $\text{cm.}^{-1}$	Character of band	Wave number, $\text{cm.}^{-1}$	Character of band	Wave number, $\text{cm.}^{-1}$	Character of band	Wave number, $\text{cm.}^{-1}$	Character of band	Wave number, $\text{cm.}^{-1}$		Character of band	
3290	vs	$\sigma \parallel$	w	$\pi \parallel$	3290	vs	$\sigma \perp$	3290	vs	$\sigma \perp$	Hydrogen-bonded NH stretching, <sup>e</sup> Unbonded NH stretching <sup>d</sup> Hydrogen-bonded NH stretching, <sup>d</sup> NH stretching in amorphous region <sup>e</sup> CH <sub>2</sub> asym. stretching CH <sub>2</sub> sym. stretching Amide I, C=O stretching Amide II, coupling of NH deformation with C—N stretching CH <sub>2</sub> deformation CH <sub>2</sub> deformation adjacent to amide group <sup>f</sup> CH deformation, <sup>e</sup> CH <sub>2</sub> twisting <sup>g</sup> Relates to amide III
3070	m	$\sigma \parallel$	w	$\sigma \perp$	3085	w	$\sigma \perp$	3090	m	$\sigma \perp$	
2930	vs	$\sigma \perp$	vs	$\sigma \perp$	2930	vs	$\sigma \perp$	2930	vs	$\sigma \perp$	
2865	s	$\sigma \parallel$	s	$\sigma \parallel$	2860	s	$\sigma \parallel$	2860	s	$\sigma \parallel$	
1642	vvs	$\sigma \parallel$	vvs	$\sigma \perp$	1635	vvs	$\sigma \perp$	1642	vvs	$\sigma \perp$	
1545	vvs	$\pi \parallel$	vvs	$\pi \perp$	1534	vvs	$\pi \perp$	1562	vvs	$\pi \perp$	
1480	m	$\pi \parallel$	m	$\sigma \parallel$	1460	m	$\sigma \parallel$	1464	m	$\sigma \parallel$	
1465	m	$\sigma \parallel$	m	$\sigma \perp$	1435	m	$\sigma \perp$	1441	m	$\sigma \parallel$	
1438	m	$\sigma \perp$	m	$\pi \parallel$	1368	w	$\pi \parallel$	1368	m	$\pi \parallel$	
1417	m	$\sigma \parallel$	m	$\pi \perp$	1340	m	$\pi \perp$	1318	w	$\pi \parallel$	

1305	sh	$\pi$		1306	m	$\pi$	CH <sub>2</sub> wagging, <sup>a</sup> CH <sub>2</sub> twisting or CH <sub>2</sub> wagging <sup>d</sup>	CH <sub>2</sub> wagging or CH <sub>2</sub> twisting
1295	wsh	$\pi$						Amide III
1271	m	$\pi$	1294	m	$\pi$ $\perp$		Amide III <sup>b</sup>	CH <sub>2</sub> wagging or CH <sub>2</sub> twisting
1247	wsh	$\pi$		1235	w	$\pi$	CH <sub>2</sub> wagging, <sup>a</sup> CH <sub>2</sub> twisting or CH <sub>2</sub> wagging <sup>d</sup>	Relates to amide III
1214	sh	$\sigma$		1214	w	$\pi$		CH <sub>2</sub> wagging or CH <sub>2</sub> twisting
1202	m	$\pi$					Amide III <sup>b</sup>	Splitting of amide I I
1171	m	$\pi$	1178	m	$\sigma$ $\perp$	$\sigma$ $\perp$		Skeletal motion involving CONH
1121	m	$\pi$	1111	w	$\pi$	1120	m	C—C stretching
1076	w	$\pi$ $\perp$	1082	w	$\pi$ $\perp$	{ 1081	m	Skeletal motion involving CONH
1074	w	$\sigma$				1074	m	C—C stretching
1041	wsh	$\pi$						Probably C—C motions <sup>d</sup>
1029	m	$\sigma$	1027	w	$\pi$	1029	w	C—C stretching <sup>a</sup>
						1000	w	C—C stretching
						977	m	CONH in-plane <sup>e</sup>
			979	m	$\sigma$ $\perp$			Appears in quenched nylon 6 <sup>a</sup>
960	m	$\sigma$						CONH in-plane
952	w	$\pi$						CONH in-plane
928	m	$\pi$						CONH in-plane
833	w	$\sigma$ $\perp$						Splitting of CH <sub>2</sub> rocking
731	s	$\sigma$ $\perp$	763	w	$\sigma$	776	w	CH <sub>2</sub> rocking
			736	s	$\sigma$ $\perp$	728	s	CH <sub>2</sub> rocking
692	s	$\sigma$ $\perp$				708	s	Amide V
								Amide V <sup>f</sup>
								Amide V <sup>f</sup>

<sup>a</sup> Intensity: vvs = very very strong, vs = very strong, s = strong, m = medium, w = weak, sh = shoulder, wsh = weak shoulder. <sup>b</sup> Polarization:  $\sigma$  = perpendicular band,  $\pi$  = parallel band,  $\perp$  = perpendicular to the rolled plane, || = parallel to the rolled plane. <sup>c</sup> Data of Asai.<sup>13</sup> <sup>d</sup> Data of Tobin and Carrano.<sup>21</sup> <sup>e</sup> Data of Nikitin and Volchek.<sup>22</sup> <sup>f</sup> Data of Miyake.<sup>14</sup> <sup>g</sup> Data of Sandeman and Keller.<sup>12</sup> <sup>h</sup> Data of Cannon.<sup>11</sup>

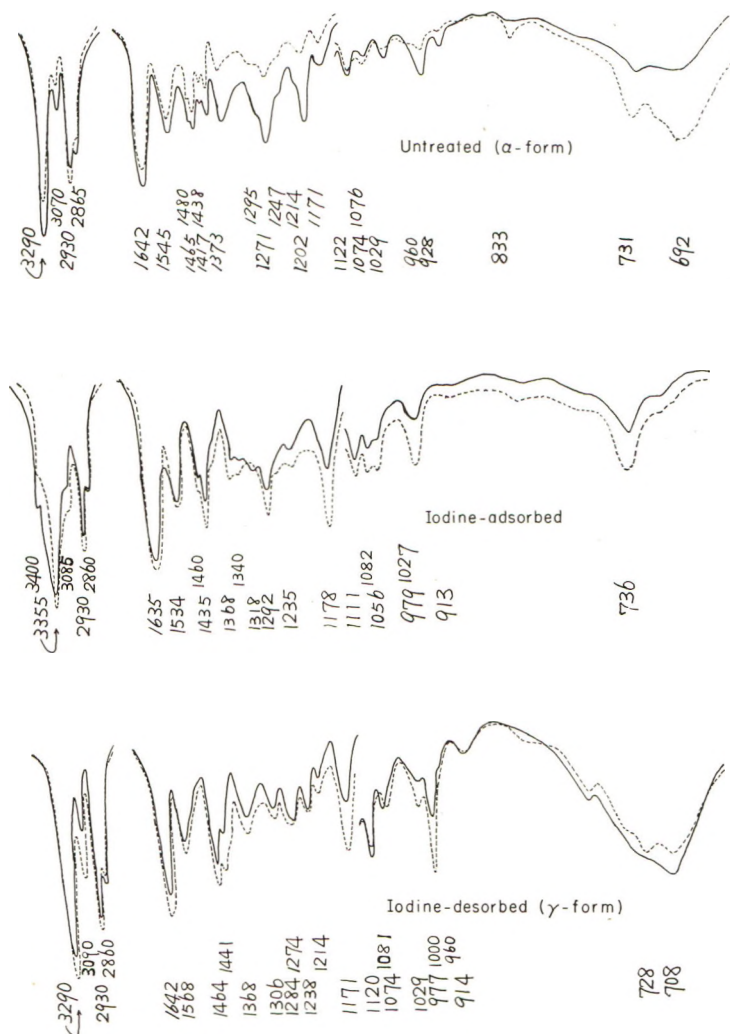


Fig. 3. Micro-infrared spectra of doubly oriented nylon 6 specimens. The direction of the infrared beam is parallel to that of the rolling: (—)  $\theta = 0^\circ$ ; (- -)  $\theta = 90^\circ$ .

are given to facilitate visualization of the relation between the molecular packing and the rolled plane.

If the specimen were oriented not doubly but uniaxially, the spots on the x-ray photographs should be uniformly spread over the circles (the Debye rings). Thus, the localization of the spots shows that the specimens were doubly oriented and that the orientation was held throughout the course of the specimen preparation. It is also found that the  $\alpha$ - $\gamma$  transition occurs without an appreciable loss of the molecular orientation.

The location of the strongest spots which are indexed (002)<sup>8</sup> in Figure 1a establishes that this crystallographic plane is oriented parallel to the rolled

plane of the specimen. Thus, the hydrogen-bonded molecular sheet of the  $\alpha$ -crystal form is parallel to the rolled plane as indicated schematically in Figure 2a, since the plane of molecules is parallel to the (002) plane in the cell. In Figure 1b spots are located at the apexes of a hexagon corresponding to the pseudo-hexagonal structure of the iodine-desorbed specimen ( $\gamma$ -form).

### Micro-Infrared Measurements

The micro-infrared spectra of microtomed sections obtained at  $\theta = 0^\circ$  (solid curve) and  $\theta = 90^\circ$  (dashed curve) are shown in Figure 3 as extreme cases. Wave number, relative intensity, and polarization are listed in Table I. In the column of polarization the notations  $\sigma$  and  $\pi$  denote the perpendicular and parallel bands, respectively, and the notations  $\perp$  and  $\parallel$  refer to the polarization with respect to the rolled plane.

The structures of the iodine-adsorbed and the iodine-desorbed nylon 6 have been discussed and it has been conjectured that they are smectic.<sup>2</sup> If the structures of these specimen were smectic, the infrared adsorption bands should show no definite polarization with respect to the rolled plane. On the other hand, almost all the absorption bands show polarization so clearly that the smectic structure for the iodine-adsorbed and the iodine-desorbed nylon 6 ( $\gamma$ -form) must be abandoned.

## DISCUSSION

### Preferential Orientation of Amide Groups due to Iodine Treatment

A polymer molecule of nylon-type polyamide alternately has amide groups and methylene groups along the molecular axis. It has been shown that the structures of the  $\alpha$ - and  $\beta$ -forms of the polyamide crystal are composed of sheets of fully extended planar chains joined by the hydrogen bonds between adjacent molecules.<sup>8,9</sup> In such a sheet of the  $\alpha$ - or  $\beta$ -form of nylon 6 all hydrogen bonds between the adjacent amide groups are possible by inverting alternate molecular chains; such an arrangement has been suggested by previous workers.<sup>8,10</sup> Thus, as illustrated in Figure 2a the successive chains named  $A_1, A_2, \dots$ , and  $B_1, B_2, \dots$ , are oppositely directed in the sheet. For convenience this molecular sheet is called the antiparallel sheet.

The infrared bands at 3290, 1642, and 1545  $\text{cm}^{-1}$  in nylon 6 (not  $\alpha$ -form) have already been assigned to the NH stretching mode, the amide I and the amide II bands, respectively.<sup>11</sup> These bands show parallel polarization with respect to the rolled plane. The planarity of the *trans*-amide group is well established, and it may be concluded that the plane of the amide group is parallel to the rolled plane. The bands at 2930 and 2865  $\text{cm}^{-1}$  have been associated with the  $\text{CH}_2$  asymmetric stretching and the  $\text{CH}_2$  symmetric stretching modes, respectively. It is expected that when the planar zig-zag hydrocarbon segment is parallel to the rolled plane the 2930  $\text{cm}^{-1}$  band shows perpendicular polarization and the 2865  $\text{cm}^{-1}$  band shows



parallel polarization with respect to the rolled plane. The observed polarizations agree with the above consideration. These results indicate that the plane of the methylene group and that of the amide group both lie nearly in the same plane which is roughly parallel to the rolled plane (Fig. 2a).

The spectral change in nylon 6 due to adsorption and desorption of iodine has been studied.<sup>5</sup> The amide characteristic bands at 3290, 1642, and 1545  $\text{cm}^{-1}$  in the untreated specimen shift to 3350, 1635, and 1534  $\text{cm}^{-1}$ , respectively, on adsorption of iodine. With the removal of iodine the former two bands revert to their original frequencies and the latter shifts to a slightly higher frequency (1562  $\text{cm}^{-1}$ ). In the iodine-adsorbed and the iodine-desorbed specimens, these amide characteristic bands show perpendicular polarization to the rolled plane (Fig. 3, Table I). The  $\text{CH}_2$  stretching bands at 2930 and 2865  $\text{cm}^{-1}$  in the untreated specimen are present at 2930 and 2860  $\text{cm}^{-1}$ , respectively, in the iodine-adsorbed and also in the iodine-desorbed specimens. The 2930  $\text{cm}^{-1}$  band shows perpendicular polarization, and the other bands show parallel polarization to the rolled plane.

From these observations it may be noticed that the directions of the transition moments of these amide characteristic bands are changed on adsorption of iodine, but the directions of the transition moments of the bands ascribed to the methylene group are unchanged. Hence, it can be concluded that on coordination of iodine to the oxygen of the amide group the plane of the amide group is preferentially twisted to a direction roughly perpendicular to the rolled plane, and this preferential orientation of the amide group is retained on desorption of iodine. The orientation of the amide group, therefore, differs from that of the methylene group in the molecule as shown in Figure 2b.

### Examination of Infrared Bands

There are three bands in the  $\text{CH}_2$  rocking band region of nylon 6. The 831  $\text{cm}^{-1}$  band in the  $\alpha$ -form of nylon 6 has been assigned by Sandeman and Keller<sup>12</sup> to the  $\text{CH}_2$  rocking mode. The polarization of this band is obviously perpendicular to the rolled plane, which is consistent with the direction of the transition moment predicted from the assignment of this band. The remaining two bands at 728 and 692  $\text{cm}^{-1}$  are attributed by Asai and his co-workers<sup>13</sup> and by Miyake<sup>14</sup> to the NH out-of-plane deformation mode (the amide V band). The polarizations of these bands are both perpendicular to the rolled plane, and it appears that the directions of the transition moments of these bands are consistent with those predicted from the above assignments.

The 728  $\text{cm}^{-1}$  band shifts to 736  $\text{cm}^{-1}$  on adsorption of iodine and to 730  $\text{cm}^{-1}$  on the removal of the adsorbed iodine. The 692  $\text{cm}^{-1}$  band shifts away from the NaCl region on adsorption of iodine and appears at 708  $\text{cm}^{-1}$  on the removal of the adsorbed iodine. Furthermore, the 692 and 708  $\text{cm}^{-1}$  bands disappear from the NaCl region on deuteration, but the 728, 736, and 730  $\text{cm}^{-1}$  bands remain almost unchanged.<sup>6</sup> On the basis

of these results, the 728, 736, and 730  $\text{cm.}^{-1}$  bands have been assigned to the  $\text{CH}_2$  rocking mode and the 692 and 708  $\text{cm.}^{-1}$  bands have been assigned to the amide V vibration. The polarizations of the former three  $\text{CH}_2$  rocking bands and one of the latter amide V bands at 692  $\text{cm.}^{-1}$  are all perpendicular to the rolled plane, but that of the 708  $\text{cm.}^{-1}$  band is parallel to the rolled plane. The directions of the transition moments of these bands agree with those predicted from the assignments<sup>5,6</sup> and the preferential orientation of the amide group discussed in the present paper.

Near 1000  $\text{cm.}^{-1}$  two bands appear at 960 and 927  $\text{cm.}^{-1}$  which have been attributed by Sandeman and Keller<sup>12</sup> to the CONH in-plane vibration. These bands show polarization parallel to the rolled plane. The corresponding bands are found at 979  $\text{cm.}^{-1}$  in the iodine-adsorbed specimen and at 977  $\text{cm.}^{-1}$  in the iodine-desorbed one. The polarizations of these bands are perpendicular to the rolled plane. These results are consistent with the directions predicted from the assignments of these bands to the CONH in-plane vibration.<sup>5</sup>

The band at 1171  $\text{cm.}^{-1}$  which is intensified by iodine treatment has not been assigned. Similar bands are found at 1147  $\text{cm.}^{-1}$  in the nylon  $5n$  and at 1181  $\text{cm.}^{-1}$  in nylon  $6n$ , where 5 and 6 represent the number of carbon atoms in the diamines and  $n$  represents the number of carbon atoms in the dibasic acid. The frequencies of these bands depend only on the number of carbon atoms in the diamines.<sup>15</sup> Sutherland et al.<sup>16</sup> have assigned the bands which are present at 1160  $\text{cm.}^{-1}$  in acetamide and at similar frequencies in other homologous monosubstituted amides to a skeletal motion involving the nitrogen atom and the carbon substituted on it. The change in polarization of the 1171  $\text{cm.}^{-1}$  band to the rolled plane due to iodine treatment suggests that the assignment of this band closely resembles that of the 1160  $\text{cm.}^{-1}$  band in monosubstituted amides.

At 1076  $\text{cm.}^{-1}$  a doublet band is observed. From the change in the polarization to the rolled plane it is likely that this band is also ascribed to a skeletal motion related to the amide group.

### Mechanism of the $\alpha$ - $\gamma$ Transition of Nylon 6

It has been reported that the  $\gamma$ -form of nylon 6 is converted into the  $\alpha$ -form by drawing followed by annealing<sup>17</sup> or by treating with a phenol aqueous solution,<sup>3</sup> and that the  $\alpha$ -form obtained by such treatments is again converted into the  $\gamma$ -form by iodine treatment.<sup>17</sup> The reversible  $\gamma$ - $\alpha$  and  $\alpha$ - $\gamma$  transition described here suggests that the arrangement of molecular chain directions in the  $\gamma$ -form is not different from that in the  $\alpha$ -form as illustrated in Figures 2*a* and 2*b*, because it is hard to believe that a sorting out or a inversion of the chain molecules leading to a special sequence of chain directions occurred during drawing, annealing, phenol treatment, or iodine treatment.

Hence, the mechanism of the  $\alpha$ - $\gamma$  transition due to iodine treatment is assumed to be as follows. Iodine enters into the crystal lattice through the space between the hydrogen-bonded molecular sheets and coordinates to

the oxygen of the amide groups to form a halogen-molecule bridge<sup>18</sup> between the amide groups lying in the adjacent sheets. Consequently, the hydrogen bond is broken, and the amide group is preferentially twisted to a direction roughly perpendicular to the molecular sheet. When iodine is removed, the amide group couples with the nearest amide group lying in the adjacent sheet instead of coupling with the original one. Thus, as illustrated in Figure 2*b*, the molecules  $A_1, B_1, \dots$ , and  $A_2, B_2, \dots$ , are joined by new hydrogen bonds between the adjacent molecules and new hydrogen-bonded molecular sheets are formed. Therefore, in such a sheet all the molecular chains are similarly directed. For convenience this molecular sheet is named the parallel sheet, corresponding to the antiparallel sheet in the  $\alpha$ -form. The structure of the  $\gamma$ -form is composed of parallel sheets, and in such a packing of the parallel sheets the direction of the chain molecules are alternately inverse along the direction of stacking of sheets.

The parallel sheet was first proposed by Kinoshita<sup>3</sup> for the  $\gamma$ -form of polyamides made from  $\omega$ -amino acids which have the odd number of methylene groups. Because of the preferential orientation of the amide group in the molecule, the parallel sheet assumes the pleated configuration. In the case of the  $\gamma$ -form, the hydrogen bond makes possible the pleated configuration; however, it may be expected that in the iodine-adsorbed nylon 6 the halogen-molecule bridge between the amide groups forces the molecules to take a similar configuration. There is no direct evidence to support the halogen-molecule bridge between the amide groups but the x-ray data on the acetone-bromine system<sup>18</sup> and the change in the frequency of the amide I band ( $C=O$  stretching mode) on adsorption of iodine<sup>5,19</sup> suggest this bridge.

The  $\alpha$ - $\gamma$  phase transition resembles that of cellulose I to II<sup>20</sup> in that a molecule of a high polymer forms a complex compound with a simple molecule and the structure of the high polymer is modified.

### Derivation of the Crystal Structure of the $\gamma$ -Form

The features of the x-ray photograph revealed that the  $\gamma$ -form has a pseudo-hexagonal cell with the plane of the polar group perpendicular to the chain axis as evidenced by the prominent meridian reflections. Hence, all the amide groups lie at about the same level in the cell, and the intermolecular distance is about 4.8 Å., a probable figure for the hexagonal close packing of the polyamide molecules.<sup>12</sup>

The chain repeat distance of the  $\gamma$ -form is shorter than that of the  $\alpha$ -form. This phenomenon has been investigated in detail by Kinoshita<sup>3</sup> for a series of polyamides, and it has been noticed that the  $\gamma$ -forms have shorter chain repeat distances by about a constant than those calculated for the fully extended forms, the difference being independent of the number of the carbon atoms involved. Kinoshita has ascribed this shortening of the repeat distance to the favorable orientation of the amide group. This orientation of the amide group is evidently confirmed in the present paper for the  $\gamma$ -form of nylon 6. Then, in the case of the  $\gamma$ -form of nylon 6, the

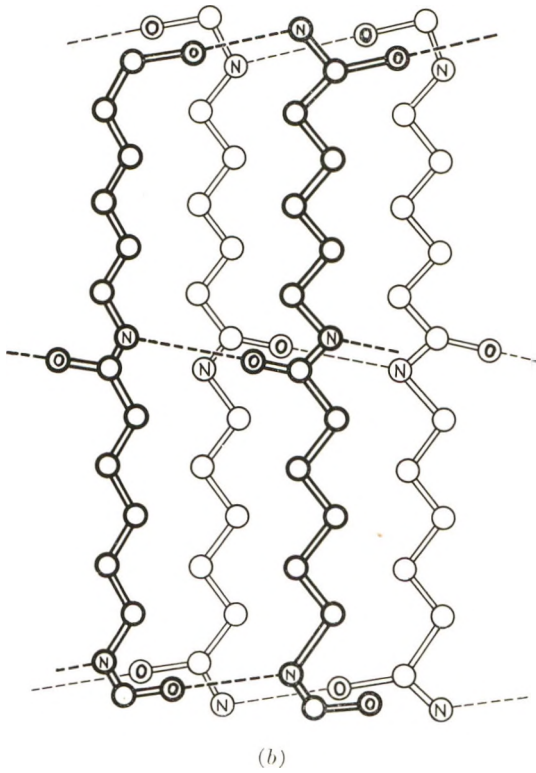
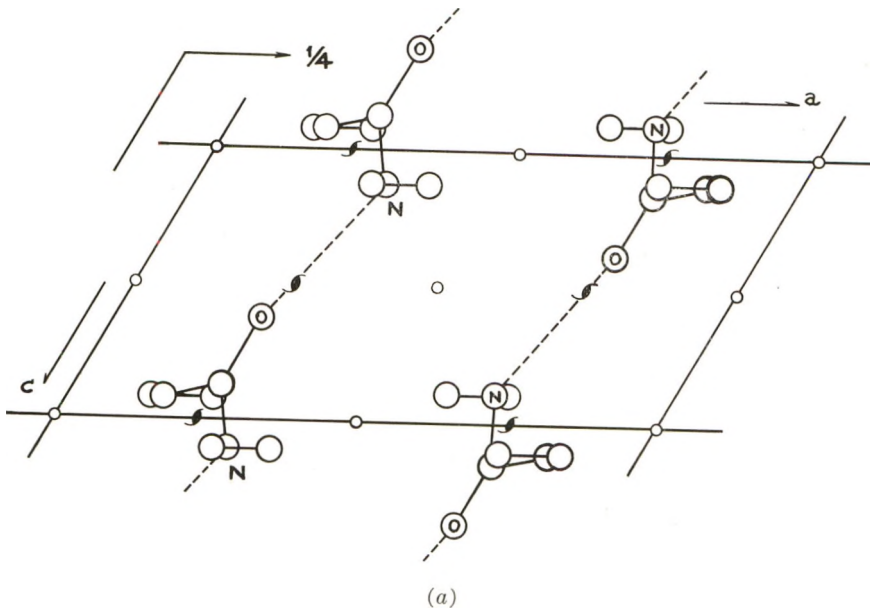
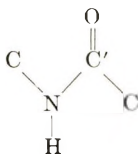


Fig. 4. Structure of the  $\gamma$ -form of nylon 6: (a) viewed along the fiber axis; (b) viewed roughly perpendicular to the  $c$  axis. The broken line indicates the hydrogen bond



difference between 17.24 Å. in the  $\alpha$ -form and 16.88 Å. in the  $\gamma$ -form results in rotation of the amide group by about  $60^\circ$  around the C—C' and C—N single bonds in



In addition to these consideration the NH  $\cdots$  O hydrogen bond length between the adjacent molecules in the parallel sheet is anticipated to be approximately 2.8 Å. by considering the frequency value of the NH stretching band.

Thus, the structure of the  $\gamma$ -form may be roughly determined; however, the height of the molecular sheet is not decided because two models, in the one model the side-by-side packing of sheets involves a  $1/2 b$  staggered shear between sheets (where  $b$  is the fiber axis) and in the other model the shear is absent, satisfy the consideration discussed here. The crystal structure is firmly established on the basis of intensity calculation. The crystal structure finally chosen has the space group  $C_{2h}^5 - P2_1/a$  and the unit cell is monoclinic with  $a = 9.33$  Å.,  $b = 16.88$  Å. (fiber axis),  $c = 4.78$  Å.,  $\beta = 121^\circ$ . The model of the crystal structure is shown in Figure 4. The detail of the structural analysis will be soon reported in a subsequent paper.

The author wishes to express his sincere thanks to Professor Shunsuke Murahashi and Professor Shuzo Seki of Osaka University for their kind encouragement in the course of this study. He is also indebted to Dr. H. Tadokoro of Osaka University for invaluable advice and criticism.

## References

1. Ueda, S., and T. Kimura, *Kobunshi Kagaku*, **15**, 243 (1958).
2. Tsuruta, M., H. Arimoto, and M. Ishibashi, *Kobunshi Kagaku*, **15**, 619 (1958).
3. Kinoshita, Y., *Makromol. Chem.*, **33**, 1 (1959).
4. Arimoto, H., *Kobunshi Kagaku*, **19**, 101 (1962).
5. Arimoto, H., *Kobunshi Kagaku*, **19**, 205 (1962).
6. Arimoto, H., *Kobunshi Kagaku*, **19**, 456 (1962).
7. Tadokoro, H., S. Seki, I. Nitta, and R. Yamadera, *J. Polymer Sci.*, **28**, 244 (1958).
8. Holmes, D. R., C. W. Bunn, and D. J. Smith, *J. Polymer Sci.*, **17**, 159 (1955).
9. Bunn, C. W., and E. V. Garner, *Proc. Roy. Soc. (London)*, **A189**, 39 (1947).
10. Brill, R., *Z. Physik. Chem.*, **B53**, 61 (1943).
11. Cannon, C. G., *Spectrochim. Acta*, **16**, 302 (1960).
12. Sandeman, I., and A. Keller, *J. Polymer Sci.*, **19**, 401 (1956).
13. Asai, A., M. Tsuboi, T. Shimanouchi, and S. Mizushima, *J. Phys. Chem.*, **59**, 322 (1955).
14. Miyake, A., *J. Polymer Sci.*, **44**, 223 (1960).
15. Arimoto, H., *Kobunshi Kagaku*, **19**, 461 (1962).
16. Beer, M., H. B. Kessler, and G. B. B. M. Sutherland, *J. Chem. Phys.*, **29**, 1097 (1958).
17. Arimoto, H., *Kobunshi Kagaku*, **19**, 212 (1962).



18. Hassel, O., and K. O. Strømme, *Acta Chem. Scand.*, **13**, 275 (1959).
19. Schmulbach, C. D., and R. S. Drago, *J. Am. Chem. Soc.*, **82**, 4484 (1960).
20. Rånby, D. G., *Acta Chem. Scand.*, **6**, 101 (1952).
21. Tobin, M. C., and M. J. Carrano, *J. Chem. Phys.*, **25**, 1044 (1956).
22. Nikitin, V. N., and B. Z. Volchek, *Vysokomol. Soedin.*, **2**, 1015 (1960).

### Résumé

Le mécanisme de la transition alpha-gamma du nylon 6 causée par un traitement à l'iode et la structure de la forme du nylon 6 sont discutés sur la base de mesures de diffraction des rayons-X et d'absorption de radiations infra-rouges polarisées, effectuées sur des échantillons doublement orientés et traités par l'iode. Le plan du groupe amide et celui du groupe méthylène sont tous deux parallèles au plan enroulé, qui est lui même parallèle à la couche moléculaire formée par les liens hydrogènes dans la forme alpha du nylon 6. Du fait de la coordination de l'iode à l'oxygène du groupement amide, le plan de ce dernier subit une torsion dans une direction approximativement perpendiculaire au plan enroulé et cette orientation préférentielle se maintient après l'élimination de l'iode. L'orientation préférentielle du groupe amide dans la molécule confirme l'hypothèse de la structure en feuilles plissées proposée par Kinoshita pour la forme gamma des polyamides. Les bandes infra-rouges ont été examinées en tenant compte de l'orientation préférentielle du groupe amide. La structure de la forme gamma du nylon 6 est constituée de feuillets plissés formés par des chaînes moléculaires semblablement dirigées et dont les molécules adjacentes sont jointes par des liaisons hydrogènes; dans cet entassement de feuillets, les directions des chaînes moléculaires sont alternativement inverses le long de la direction de l'entassement des feuillets.

### Zusammenfassung

Der Mechanismus der durch Jodbehandlung bewirkten  $\alpha$ - $\gamma$ -Umwandlung von Nylon 6 sowie die Struktur der  $\gamma$ -Form von Nylon 6 werden auf der Basis von Röntgenbeugungsmessungen und Mikroabsorptionsmessungen im polarisierten Infrarot diskutiert. Sowohl die Ebene der Amid-als auch diejenige der Methylengruppe ist der gedrehten Fläche parallel, die der die Wasserstoffbrückenbindungen enthaltenden Molekülebene in der  $\alpha$ -Form von Nylon 6 parallel ist. Die Ebene der Amidgruppe ist durch Koordination des Jods mit dem Sauerstoff der Amidgruppe bevorzugt in eine zur gedrehten Fläche senkrechte Richtung verdreht. Diese bevorzugte Orientierung der Amidgruppe wird nach der Entfernung des Jods beibehalten. Die bevorzugte Orientierung der Amidgruppe im Molekül stützt die von Kinoshita für die  $\gamma$ -Form von Polyamiden vorgeschlagene Faltblattstruktur. Es wurden die auf die bevorzugte Orientierung der Amidgruppe zurückgehenden IR-Banden untersucht. Die Struktur der  $\gamma$ -Form von Nylon 6 besteht aus "pleated sheets," die von ähnlich gerichteten, durch Wasserstoffbrückenbindungen zwischen den benachbarten Molekülen verbundenen Molekülketten gebildet werden. Die Richtungen der Molekülketten in einer solchen Faltblatt-Packung sind längs der Packungsrichtung der Ebenen abwechselnd entgegengesetzt.

Received May 1, 1963

## The Polymerizing System: Vinyl Acetate-Diphenyl

HOWARD C. HAAS and HELEN HUSEK, *Chemical Research Laboratories, Polaroid Corporation, Cambridge, Massachusetts*

### Synopsis

The polymerization of vinyl acetate in the presence of diphenyl has been studied. A chain transfer constant for diphenyl of  $6.4 \times 10^{-4}$  was obtained from conventional kinetic analysis and  $\bar{P}_n$  data. This value is in reasonable agreement with values obtained from an estimation of the combined diphenyl residues in the corresponding polyvinyl alcohols by ultraviolet spectroscopy. The conclusion, that diphenyl behaves in this system predominantly as a transfer agent and not as a comonomer, is supported by an evaluation of the data in terms of a kinetic scheme for retarded polymerization. Retardation of the rate of polymerization of vinyl acetate is observed in the presence of diphenyl and it is on this basis that abstraction of hydrogen from diphenyl as being the transfer step is discarded in favor of addition of the vinyl acetate radical chain to diphenyl. The ultraviolet dichroism of an oriented polyvinyl alcohol film containing combined diphenyl residues is presented.

The copolymerization of benzene with vinyl acetate was reported several years ago<sup>1,2</sup> but recently refuted.<sup>3,4</sup> During the interim period, we considered that if diphenyl, with its high extinction K-band, could be copolymerized with vinyl acetate, a useful film polarizer for the 250 m $\mu$  region of the ultraviolet might result. Reported polarizers for this ultraviolet range are not very efficient.<sup>5</sup> Our thought was to prepare a vinyl acetate-diphenyl copolymer, convert it to polyvinyl alcohol (PVA), prepare a film of the latter, and then stretch this film to orient the diphenyl residues in the PVA chain. This paper reports the results obtained on the polarizer and describes a brief study which concludes that vinyl acetate chain transfers with diphenyl but that the extent of copolymerization is negligible.

Pure diphenyl in alcohol solution exhibits a single absorption peak at 247 m $\mu$  with an extinction coefficient of about  $2 \times 10^4$ . The ultraviolet spectrum of an aqueous solution of PVA containing diphenyl residues (prepared from a polyvinyl acetate polymerized in the presence of diphenyl) has two absorption maxima at about 242 and 251 m $\mu$ . Since radical attack, at least by phenyl radicals, has been shown to occur at all three ring positions of diphenyl<sup>6</sup> the presence of more than one maximum is not too surprising. The ultraviolet dichroic behavior of a 1 mil oriented film of this PVA, diluted one to one with a commercial PVA (Gelvatol 2/75, Shawinigan Resins Co.), is presented in Figure 1. Dilution with normal PVA was desirable for reducing the optical density in the 250 m $\mu$  region. The

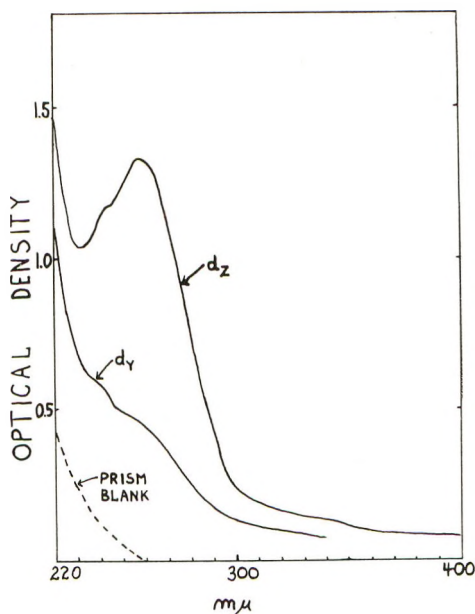


Figure 1.

best results obtained yielded dichroic ratios of 2.40 and 3.14, respectively, for the 242 and 258  $m\mu$  bands. The change from aqueous solution to PVA film resulted in a slight shift of the absorption maximum of the lower frequency band. After several polymerizations of vinyl acetate in the presence of diphenyl, it was definitely established that diphenyl residues are present in the polymer, that they can be detected and estimated by ultra-violet absorption spectra, and that several species are present, since diphenyl and mono- or dialkyl-substituted biphenyls all show a single absorption maximum in this range.

To study the polymerization of vinyl acetate in the presence of diphenyl, the polymerizations described in Table I were carried out. The catalyst,  $\alpha, \alpha'$ -azobiscyclohexanecarbonitrile was prepared according to the procedure of Thiele and Heuser<sup>7</sup> and Dox.<sup>8</sup>

TABLE I  
Polymerization of Vinyl Acetate in the Presence of Diphenyl, 59.6°C.

Tube	Vinyl acetate		Diphenyl		Catalyst, mole/l. $\times 10^2$	Polymer- ization time, min.	Polyvinyl acetate yield, g.
	g./25 cc.	mole/l.	g./25 cc.	mole/l.			
1	22.083	10.26	0	0	1.00	108	1.2198
2	19.463	9.04	3.00	0.78	0.750	397	0.8552
3	16.838	7.83	6.00	1.56	0.580	953	0.7843
4	14.225	6.61	9.00	2.33	0.415	2308	0.9950
5	11.630	5.40	12.00	3.12	0.278	5328	1.0753

Polymerizations were carried out at 59.6° in sealed glass tubes which were carefully evacuated prior to sealing. The mixtures were made up by placing the biphenyl in a 25 cc. volumetric flask, adding the catalyst, and diluting to volume at 59.6°C. with vinyl acetate monomer.

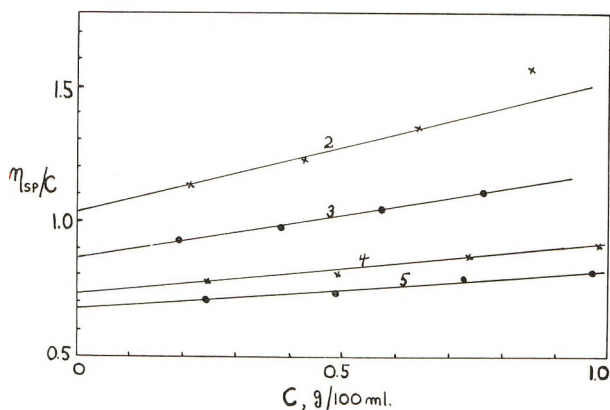


Figure 2.

Viscosity measurements were made on the polyvinyl acetates (PVAc) at 25°C. with acetone as the solvent in a Cannon-Ostwald-Fenske viscometer. The viscosity data are plotted in Figure 2 as  $\eta_{sp}/c$  versus  $c$ . In Table II, the intrinsic viscosities are recorded together with the number-average degrees of polymerization calculated from the eq. (1):<sup>2</sup>

$$\log \bar{P}_n = 3.24 + 1.40 \log [\eta] \quad (1)$$

TABLE II

Sample	$[\eta]$ , acetone, 25°C.	$\bar{P}_n$
2	1.04	1836
3	0.87	1512
4	0.73	1269
5	0.68	1182

By employing the conventional kinetic scheme,<sup>9</sup> which includes chain transfer with monomer M and solvent S, but excludes termination reactions involving solvent radicals, the chain transfer constant for diphenyl was obtained from eq. (2) by plotting  $1/\bar{P}_n$  versus  $[S]/[M]$ ,

$$\frac{1}{\bar{P}_n} = \frac{1+x}{k_2[M]} \left( \frac{fk_1[\text{Cat}]}{2} \right)^{1/2} (k_3 + k_3')^{1/2} + \frac{k_8}{k_2} + \frac{k_4[S]}{k_2[M]} \quad (2)$$

where  $x$  is the fraction of termination reactions occurring by disproportionation,  $f$  is the fraction of catalyst radicals initiating polymerization, rate constants  $k_2$ ,  $k_1$ ,  $k_3$ ,  $k_3'$ ,  $k_8$ , and  $k_4$  are, respectively, for propagation, initiation,

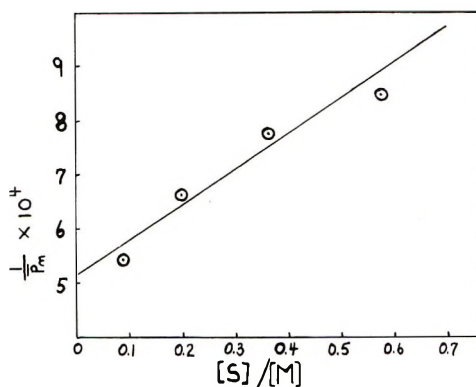


Figure 3.

termination by combination, termination by disproportionation, chain transfer to monomer, and chain transfer to solvent. The  $[\text{Cat}]^{1/2}/[\text{M}]$  ratio was maintained constant for all values of  $[\text{S}]/[\text{M}]$  (see Table I) so that the first term on the right-hand side of eq. (2) remains constant. A chain transfer constant,  $k_4/k_2$  of  $6.4 \times 10^{-4}$  was obtained from the slope of Figure 3.

The polyvinyl acetates employed in the viscosity measurements were recovered by evaporation of the acetone and converted to PVA by alkaline alcoholysis, care being taken to recover all the polymer. Quantitative ultraviolet absorption spectra were then obtained on aqueous solutions of the five samples. In Table III, the spectral data and the chain transfer constant for diphenyl as calculated from a copolymerization type treatment in which one of the  $r$ 's is zero are given.

$$\frac{d[\text{M}]}{d[\text{S}]} = 1 + \frac{k_2[\text{M}]}{k_4[\text{S}]} \cong \frac{k_2[\text{M}]}{k_4[\text{S}]} \quad (3)$$

Several comments are necessary regarding Table III. Although there are two maxima in the ultraviolet, they are so close together that the as-

TABLE III

PVA sample	PVA, g./10 cc.	Optical density at 254 $m\mu^a$	Diphenyl residues, moles/10 cc. $\times 10^6$	Diphenyl residues, mole/mole of PVAc chains	$k_4/k_2 \times 10^4$
1	0.2217	0.44 (blank)	0	0	—
2	0.1886	1.54	0.562	0.24	15.2
3	0.1590	2.22	0.914	0.38	12.7
4	0.1106	1.90	0.808	0.41	9.15
5	0.1144	2.56	1.12	0.51	7.45

<sup>a</sup> Cell path length is 1 cm.



sumption of a single maximum at 254  $m\mu$  introduces very little error. Optical density measurements for samples 2 thru 5 were corrected for absorption at 254  $m\mu$  by diphenyl free PVA (sample 1). An extinction coefficient of 20,800 was used to calculate the diphenyl content. This is a reasonable value for 2 of the 3 possible monoalkyl biphenyls and for 4 of the 6 dialkyl biphenyls in which both rings are substituted and is somewhat high for the other mono or di substituted possibilities. Therefore, we might be tending slightly to minimize the amount of biphenyl residues present. We cannot account for the variation in  $k_4/k_2$  values of Table III, but they are all certainly in reasonable agreement with the value of  $6.4 \times 10^{-4}$  obtained from  $\bar{P}_n$  measurements. The results imply that diphenyl is behaving as a chain transfer agent and not as a comonomer. This behavior and the fact that various positions on the diphenyl are involved probably explain the low efficiency of the polarizer described previously.

Although the kinetic data are limited, we have taken the liberty of interpreting it in light of Kice's<sup>10</sup> scheme for retarded polymerization. We have used the symbolism of Peebles, Clark, and Stockmayer.<sup>2</sup> The treatment leads to the equation:

$$\frac{Q_0^2}{Q_s^2} = 1 + \frac{[S]/[M]}{\alpha + \beta Q_s/[M]} \quad (4)$$

where

$$Q \equiv -d \ln[M]/dt$$

$$\alpha = k_3 k_5 / k_4 k_6$$

$$\beta = k_3 / k_2 k_4$$

$$Q_0 = k_2 (k_1[I]/k_3)^{1/2}$$

and  $Q_0$ ,  $Q_s$  are values of  $Q$  in the absence or presence of solvent, respectively. The rate constants have the same meaning as before [eq. (2)] and in addition  $k_5$  is for reinitiation by solvent radicals and  $k_6$  for termination by solvent radicals. Solvent dimerization  $k_7$ , has been neglected in the treatment.

From the data of Table I,  $Q_0$  at 59.6°C. was found to be  $0.5 \times 10^{-3}$  min.<sup>-1</sup>. This value is lower than that obtained by Peebles et al.,<sup>2</sup> so it was necessary to establish a new dependence of  $Q_0$  on initiator concentration. This is

$$Q_0 = 0.5 \times 10^{-2} [I]^{1/2} \quad (5)$$

By employing eq. (5) and the data of Table I, values of  $Q_0$  and  $Q_s$  for various initiator concentrations were calculated (Table IV) and from a plot (Fig. 4) of  $Q_s^2 [S]/[M] (Q_0^2 - Q_s^2)^{-1}$  versus  $Q_s/[M]$  a value for  $\beta$  of 267 was obtained from the slope. With  $k_1 = 2.1 \times 10^{-5}$  min.<sup>-1</sup> for azobiscyclohexanecarbonitrile at 59.6°C., it can be easily shown that  $k_4/k_2 = 0.3 \times 10^{-4}$ . Unlike the results obtained by Peebles et al.<sup>2</sup> for benzene,

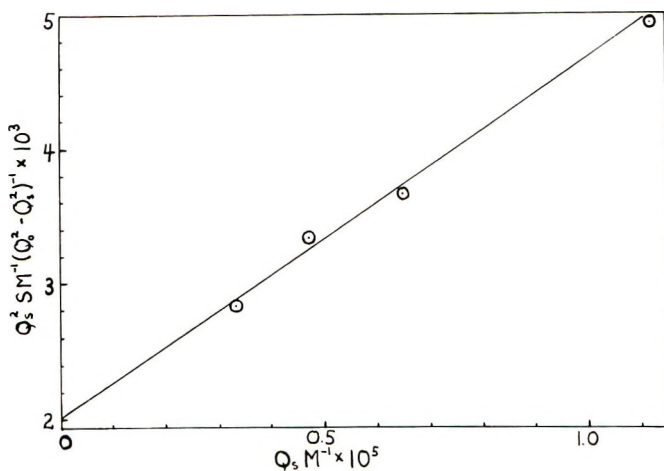


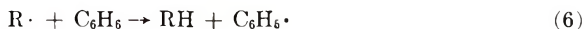
Figure 4.

TABLE IV

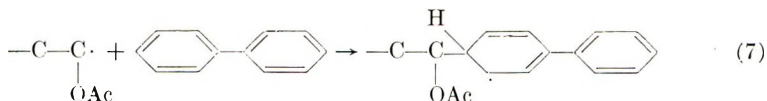
Sample	$[\text{Cat}]^{1/2} \times 10^2$ mole/liter	$Q_0 \times 10^3$	$Q_s \times 10^4$
2	8.68	0.43	1.01
3	7.64	0.38	0.51
4	6.46	0.32	0.31
5	5.29	0.26	0.18

this kinetic transfer constant is smaller than values obtained from the  $\bar{P}_n$  and analytical measurements. Although our kinetic data are admittedly crude, the result certainly lends credence to the viewpoint that diphenyl is not copolymerizing with vinyl acetate.

In their recent publication, based on the ethylene-benzene system, Mortimer and Arnold<sup>4</sup> conclude that the free radical copolymerization of benzene is impossible. They also state that benzene produces essentially no retardation in the rate of polymerization of ethylene and argue in favor for the transfer step as being



The polymerization of vinyl acetate by azonitrile catalysts should result in a rate equation involving  $[M][\text{Cat}]^{1/2}$ . The data of Table I readily demonstrate that diphenyl retards the rate of polymerization of vinyl acetate. It is therefore difficult to understand how in the vinyl acetate system, the transfer step can be of the type described by eq. (6), since  $C_6H_5 \cdot$  or  $C_6H_5C_6H_5 \cdot$ , being active radicals, should not result in much rate diminution. On the other hand, the postulate that the growing chain does add



to diphenyl to produce a radical which is resonance-stabilized, has a longer lifetime, and finally either ejects  $H\cdot$  or abstracts  $H\cdot$  from vinyl acetate, is more in accord with the facts.

### Experimental

A mixture of 7 g. of vinyl acetate, 7 g. of diphenyl, and 7 mg. of azobisisobutyronitrile were polymerized at  $80^\circ\text{C}$ . in an evacuated sealed glass tube. The polyvinyl acetate was isolated by precipitation into hexane and exhaustively purified to remove uncombined diphenyl by reprecipitations from acetone solution into hexane. PVA was obtained by dissolving the PVAc in methanol, adding a catalytic amount of sodium methoxide and refluxing for 20 min. The PVA was further purified by several reprecipitations from water into methanol. After casting a film on glass, drying, and stretching the film over a hot plate about 5 times its original length, its dichroic properties (Fig. 1) were measured with a model 14 Cary spectrophotometer equipped with a Glan-Foucault prism.

The polyvinyl acetates of Table I were isolated and purified in the same manner as described above as was also the conversion to PVA. Although only one set of spectral data is given in Table III, two sets of measurements separated by an additional reprecipitation of the PVA were made to insure that no uncombined diphenyl was contaminating the PVA samples. It is assumed and reasonably so that diphenyl is present in the polymer as the aromatic species, since one transfer mechanism (loss of  $H\cdot$ ) produces that directly, and phenylcyclohexadiene types should be readily reoxidized by air during the prolonged workup.

### References

1. Stockmayer, W. H., and L. H. Peebles, *J. Am. Chem. Soc.*, **75**, 2278 (1953).
2. Peebles, L. H., Jr., J. T. Clarke, and W. H. Stockmayer, *J. Am. Chem. Soc.*, **82**, 4780 (1960).
3. Breitenbach, J. W., G. Billek, G. Falthansl, and E. Weber, *Monatsh. Chem.*, **92**, 1100 (1961).
4. Mortimer, G. A., and L. C. Arnold, *J. Am. Chem. Soc.*, **84**, 4986 (1962).
5. McDermott, M. N., and R. Novick, *J. Opt. Soc. Am.*, **51**, 1008 (1961); A. S. Makas, *J. Opt. Soc. Am.*, **52**, 43 (1962).
6. Cadogan, J. I. G., D. H. Hey, and G. H. Williams, *J. Chem. Soc.*, **1954**, 794.
7. Thiele, J., and K. Heuser, *Ann.*, **290**, 1 (1896).
8. Dox, A. W., *J. Am. Chem. Soc.*, **47**, 1473 (1925).
9. Bamford, C. H., W. G. Barb, A. D. Jenkins, and P. F. Onyon, *Kinetics of Vinyl Polymerization by Radical Mechanisms*, Butterworths, London, 1958, p. 233.
10. Kice, J. L., *J. Am. Chem. Soc.*, **76**, 6274 (1954).

### Résumé

On a effectué l'étude de la polymérisation de l'acétate de vinyle en présence de diphenyle. A partir de l'analyse cinétique ordinaire et des valeurs de  $P_n$ , on a obtenu une constante de transfert de chaîne de  $6.4 \times 10^{-4}$  pour le diphenyle. Cette valeur s'accord assez bien avec celles que fournit la spectroscopie ultraviolette par l'estimation du nombre de groupement diphenyles incorporés dans l'alcool polyvinylique correspondant. Une

interprétation des résultats sur la base du schéma cinétique d'une polymérisation retardée renforce l'hypothèse suivant laquelle le diphényle se comporte principalement dans ce système comme un agent de transfert et non comme un comonomère. On observe un retard dans la vitesse de polymérisation de l'acétate de vinyle en présence de diphényle et c'est sur cette base que l'on écarte l'arrachement d'un hydrogène du diphényle comme étape de transfert au profit d'une addition de la chaîne radicalaire de l'acétate de vinyle au diphényle. On montre également le dichroïsme ultraviolet d'un film d'alcool polyvinylique contenant des groupes diphényles incorporés.

### Zusammenfassung

Es wurde die Polymerisation von Vinylacetat in Gegenwart von Diphenyl untersucht. Aus einer konventionellen kinetischen Analyse und  $P_n$ -Daten wurde die Übertragungskonstante von Diphenyl zu  $6,4 \times 10^{-4}$  bestimmt. Dieser Wert stimmt mit dem durch UV-spektroskopische Bestimmung der in den entsprechenden Polyvinylalkoholen eingebauten Diphenylreste ermittelten Wert gut überein. Die Annahme, dass Diphenyl in diesem System in erster Linie als Überträger und nicht als Comonomeres wirksam ist, wird durch eine Ermittlung der Daten an Hand eines kinetischen Schemas für verzögerte Polymerisation gestützt. In Gegenwart von Diphenyl wurde eine Verzögerung der Polymerisation beobachtet und man nimmt daher an, dass der Übertragungsschritt nicht in einer Wasserstoffabspaltung vom Diphenyl, sondern in der Addition einer Vinylacetatradikalkette an das Diphenyl besteht. Es wird der UV-Dichroismus eines orientierten Polyvinylalkoholfilmes mit eingebauten Diphenylresten beschrieben.

Received May 2, 1963

## Fractionation of Polymers of Higher $\alpha$ -Olefins

D. L. FLOWERS,\* W. A. HEWETT,† and R. D. MULLINEAUX, *Shell Development Company, Emeryville, California*

### Synopsis

Fractionation of 1-10 g. samples of a series of poly- $\alpha$ -olefins in a glass bead column has been studied. A thermal gradient was found to decrease fractionation efficiency relative to that obtained at constant (ambient) temperatures. A "stepwise-continuous" solvent gradient technique was developed to improve fractionation of the high molecular weight material. Fractionation efficiency decreased with increasing bead loading but was still good at polymer to bead ratios of 0.1 compared to the ratio of 0.01 usually used; efficiency is poorer in the absence of a column, even when the latter is operated at constant temperature. The Kuhn-Mark-Houwink equation was used to correlate intrinsic viscosities to light-scattering molecular weights. Values of the constants were  $K = 2.1 \times 10^{-4}$  and  $\alpha = 0.61$ . Molecular weight distribution correlations show these polymers to have very high  $\bar{M}_w/\bar{M}_n$ .

### INTRODUCTION

Fractionation of polymers, notably polyethylene, polypropylene, and polystyrene by stepwise or continuous elution techniques has been reported by a number of authors.<sup>1-9</sup> The original work of Desreux,<sup>3</sup> which provided for a number of possible solvent gradients, was modified and simplified by Francis et al.<sup>5</sup> A further modification was introduced by Kenyon and Salyer,<sup>8</sup> who reported that fractionation of certain high molecular weight polyethylenes was improved by "selective precipitation" of polymer on support. A different approach was taken by Baker and Williams,<sup>2</sup> who imposed a temperature gradient along the column and used a continuously varying exponential solvent gradient. Their success in fractionating a low conversion polystyrene by this technique led to the proposal that reprecipitation of higher molecular weight species occurred in the lower, cooler zones of the column. This method has been designated "precipitation chromatography."<sup>9</sup>

A comparison of elution fractionation and precipitation chromatography for the fractionation of polystyrene has been made by Schneider et al.<sup>10</sup> and for the fractionation of polyethylene by Guillet et al.<sup>11</sup> Precipitation chromatography was found to provide a better separation with polyethylene and with one low molecular weight sample of polystyrene, but the two methods were essentially equivalent for a majority of the polystyrenes.

\* Present address: Ampex Corporation, Redwood City, Calif.

† Present address: IBM Research Laboratory, San Jose, Calif.



It was suggested that the surprising efficiency of the elution method could be accounted for by polymer adsorption in the lower section of the column. Such adsorption has been shown to increase with increasing molecular weight on smooth surfaces with poor solvents,<sup>12</sup> which are just the conditions obtaining in elution fractionation.

A similar comparison of the two techniques was undertaken in these laboratories when inadequate separations were obtained by precipitation chromatography of the copolymers of 1-octadecene and 1-dodecene. These poly- $\alpha$ -olefins were prepared with Ziegler-type catalysts<sup>13</sup> under a wide range of conditions which led to average molecular weights between  $5 \times 10^3$  and  $1 \times 10^7$ .

The results of the investigation of the effect of fractionation variables on the fractionation of these poly- $\alpha$ -olefins and a comparison of the molecular weight distributions of the fractionated polymers are reported in this paper.

## EXPERIMENTAL AND RESULTS

### Fractionation Apparatus

Polymer fractionations were carried out using the techniques of precipitation chromatography<sup>1,2,9</sup> and modifications thereof described in the follow-

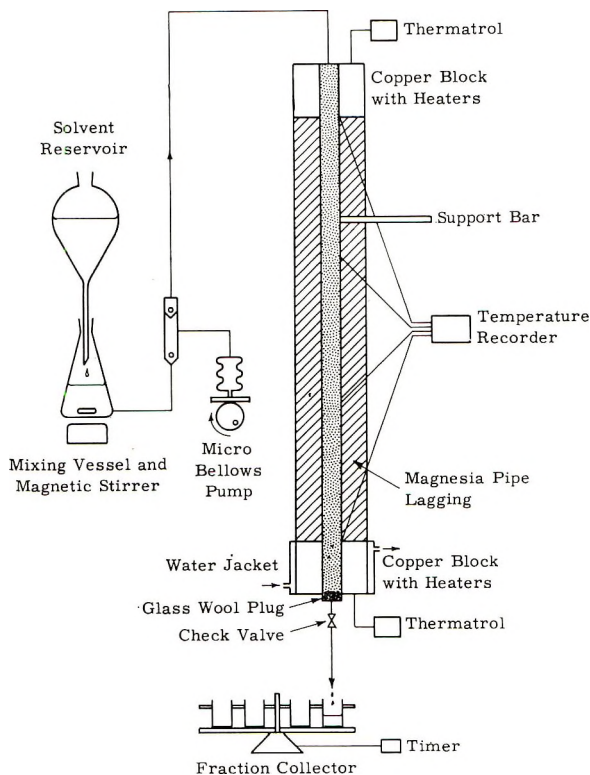


Fig. 1. Precipitation chromatography apparatus.

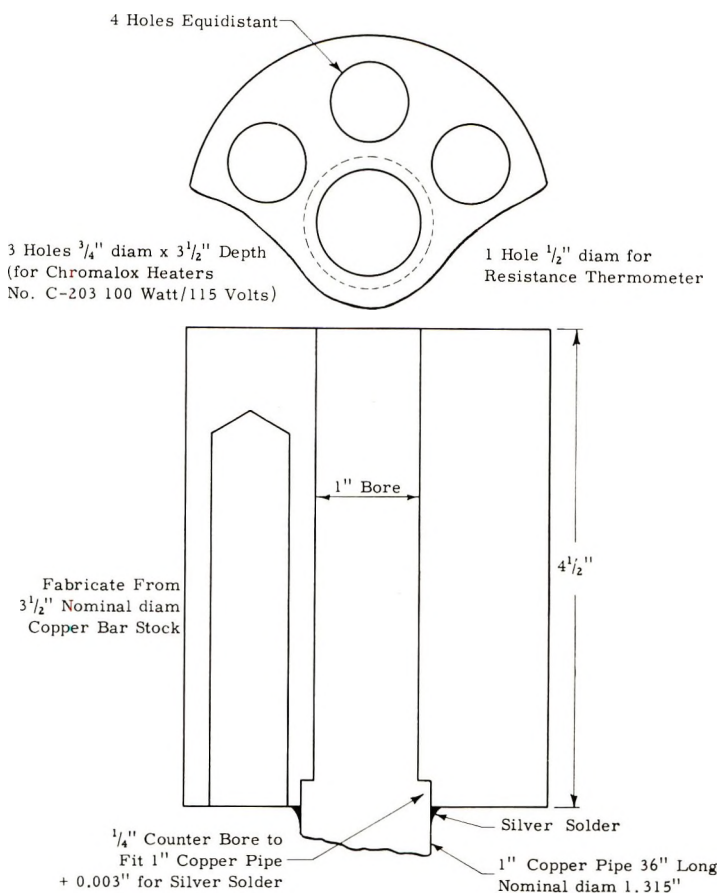


Fig. 2. Upper head.

ing section. To reduce manpower and improve reliability, numerous minor modifications of the apparatus were made. A schematic diagram of the fractionation column, which is essentially the same as that of Jungnickel and Weiss,<sup>9</sup> is shown in Figure 1. This column is both versatile and easy to operate; it has even been used to de-oil commercial polymeric additive concentrates. It consists of a 1-in. O.D. copper pipe, 36 in. long; copper is used because of its excellent heat and conductivity. Sketches of the upper and lower heads for the column are shown in Figures 2 and 3.

Chromalox, No. C-203, 100 w./115 v. heaters operated from Hallikainen Thermotrol Model 1053 electronic relays are used to thermostat the top (73°C.) and bottom (23°C.) heads of the column when a thermal gradient is used. The bottom head block also has a cooling coil machined into it. This serves to assist temperature control in the lower head at ambient temperature or below. A nearly linear temperature gradient throughout the column is obtained in this way as shown in Figure 4. The temperature gradient is continuously monitored with four evenly spaced thermocouples

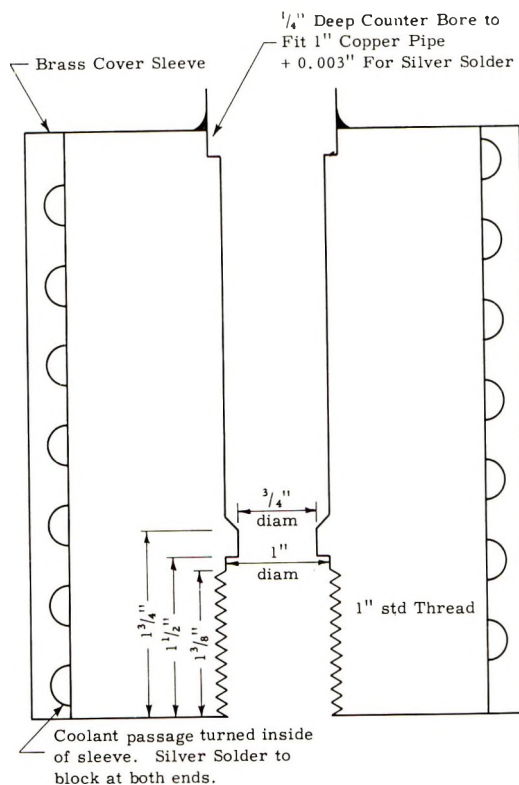


Fig. 3. Lower head. Fabricate from 4-in. nominal diameter copper bar. Counter bore for copper pipe, heater holes, and resistance thermometer hole same as shown for upper head.

attached to the column skin as shown in Figure 1. A permanent record is kept by use of a Brown recorder.

The column is wet-packed with fine glass beads, cleaned after Jungnickel's procedure.<sup>9</sup> The beads are a 200–235 mesh fraction (about 50%) of Superbrite pavement marking beads, Type 115 Regular, purchased from Minnesota Mining and Manufacturing Company. The solvent mixer, fraction collector, and micro bellows pump have been described elsewhere.<sup>9</sup> A typical precipitation chromatography curve obtained with this column at a 50°C. temperature gradient is shown in Figure 5, for one of the poly- $\alpha$ -olefins (PA 1).

### Fractionation Procedure

Before addition of the glass bead-polymer sample, the column was flushed for 24 hr. with benzene, followed by 24 hr. with ethyl alcohol. The used glass beads (75 g.) from the previous experiment were then removed to accommodate the next sample. A 1–10 g. polymer sample to be fractionated was accurately weighed and dissolved in about 50 ml. of

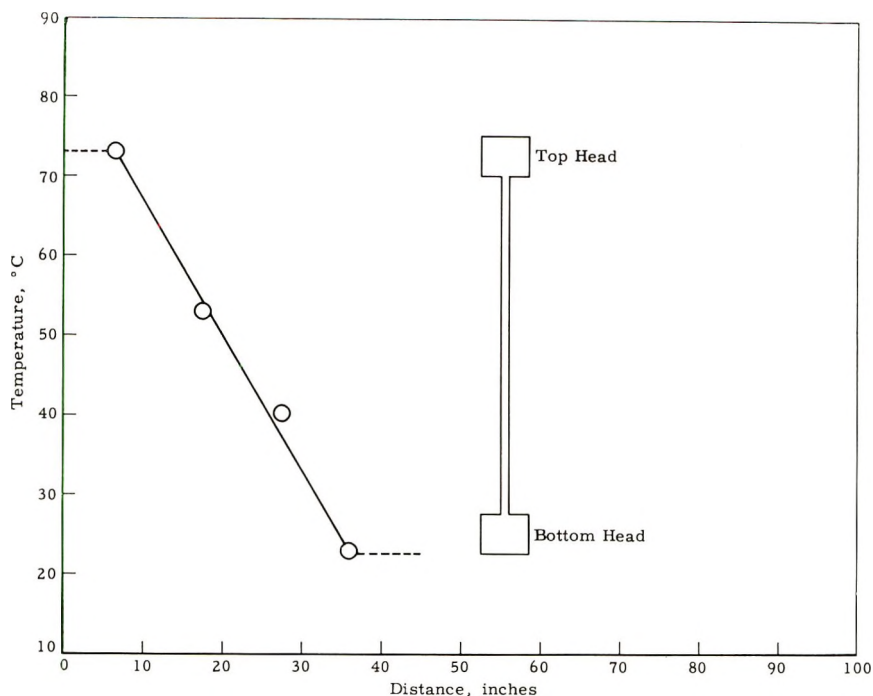


Fig. 4. Temperature profile of fractionation column.

benzene. A glass bead sample of 75–100 g. was weighed separately and added to the polymer solution. Benzene was evaporated on the steam bath with frequent stirring as the sample began to dry in order to obtain a uniformly dispersed polymer film on the beads. After drying, the sample to be fractionated was made into a slurry with 50 ml. of the nonsolvent, ethyl alcohol, and the mixture was introduced into the top of the column.

The flow rate was set by suitable adjustment of the micro bellows pump at approximately 20 ml. of eluant per hour. Ninety-minute fractions were collected in tared 1-oz. vials by a Microchemical Specialties Company fraction collector equipped with an electronic timer. Later, when the solubility and rate of solution properties of the polymer were known, 4- or 8-hr. samples were taken to save the time of recombining many small fractions. The mixing vessel contained a constant 735 ml. of an exponentially decreasing concentration of poor solvent while the dropping funnel contained the good solvent.<sup>2,9</sup>

Flow time for solvent entering the top of the column until it appeared in the eluant was approximately 4 hr. If monomer was present in the polymer, it appeared in the eluant in about 4–8 hr., but polymer fractions did not appear until about 18 hr. after the start of the fractionation. The bulk of the solvent was removed from the eluant fractions in a steam oven at 90°C. Final solvent traces were removed in a vacuum oven at 70°C., < 2 mm. Hg pressure, for 2 hr. The change in weight due to this last treat-

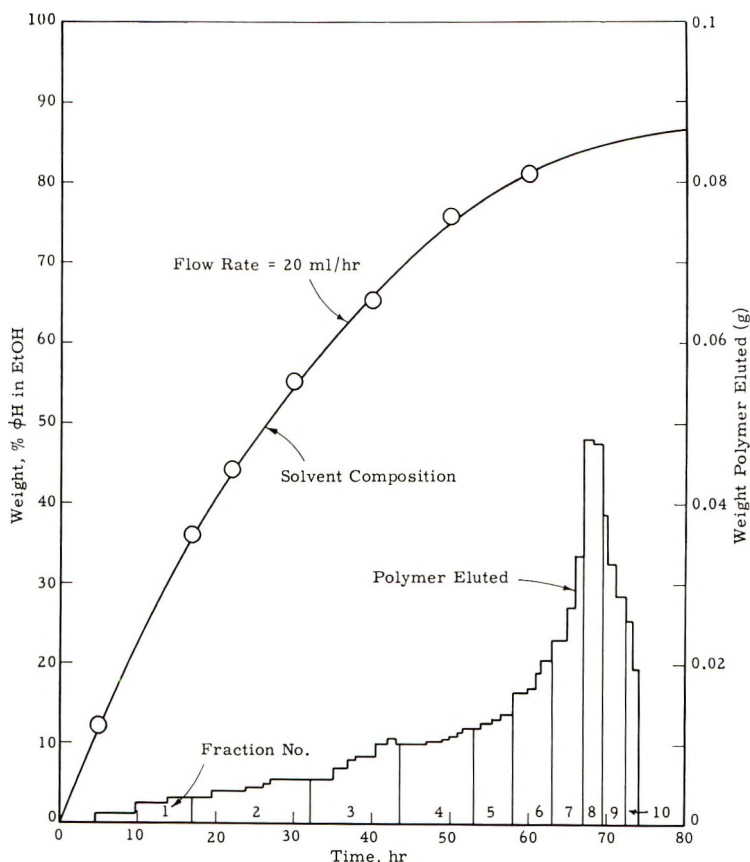


Fig. 5. Solvent gradient and polymer elution curves for PA 1.

ment was usually negligible; therefore it was assumed that all solvent had been removed.

The viscosity of polymer samples in cetane was determined both before and after a week's exposure at 90°C. in the steam oven. No resultant viscosity change was noted; thus no thermal degradation or other significant change would appear to have occurred to the polymers during fractionation and solvent removal.

In taking samples for viscosity measurement, a sufficient number of adjacent fractions were combined in the lower molecular weight ranges so that at least 0.1 g. of polymer in 10 ml. of cetane was provided. For higher molecular weight fractions, 0.04-g. samples were found to be sufficient. A total of around 10-20 fractions was ultimately obtained, each fraction being dissolved in about 5 ml. of benzene used to facilitate transfers. These were filtered through sintered glass with minimum washing into tared 10-ml. volumetric flasks and the solvent was removed as before. The flasks were reweighed to determine the weight of each combined fraction. This served as a check that all solvent had been removed and that no polymer was lost



in the combination of smaller fractions. The samples were dissolved in about 5 ml. of ASTM cetane with mild heating on the steam bath, cooled to room temperature, and the flasks were filled to mark. After thorough mixing, the solutions were filtered through millipore (SM)  $5\mu$  pore diameter filters into clean, dust-free vials for viscosity measurement. Viscosity was determined at  $100^\circ\text{F}$ . on the original sample and on samples diluted 1:1 and 1:3 with cetane. A semimicro capillary viscometer gave very satisfactory results with the 5- or 10-ml. samples available. Intrinsic viscosities,  $[\eta]$ , were obtained from these data by the conventional double plot of  $\eta_{sp}/c$  versus  $c$ . and  $\ln \eta$  versus  $c$ . From these data, the distribution curves were constructed.

### Fractionation Variables

**Thermal Gradient.** Baker and Williams<sup>2</sup> added two innovations to previous elution fractionation techniques in the development of their precipitation chromatography procedure, a solvent gradient and a temperature gradient. The difference between the log-normal distribution of our poly- $\alpha$ -olefins and the normal distribution of the polystyrenes investigated by Baker and Williams led to difficulties in the application of their method.

TABLE I  
Fractionation of PA 6 without Thermal Gradient<sup>a</sup>

Elution volume per fraction, ml. <sup>b</sup>	Solvent		Polymer	
	Benzene concn., vol.-%		Cumulative weight, %	Intrinsic viscosity, dl./g.
	Avg. column chg. per fract.	Good solvent		
3420	50 <sup>c</sup>	60	5.9	0.036
	55			
1140	64	70	15.8	0.065
1140	71	75	24.3	0.120
380	75	80	33.4	0.180
190	77	80	41.4	0.270
190	78.5	80	51.0	0.350
95	79.5	80	59.0	0.460
95	80	80	64.9	0.560
95	80	80	70.5	0.670
95	80	80	74.7	1.25
95	80	80	78.4	0.96
95	80	80	82.4	1.10
95	80	80	85.7	1.25
190	81	85	89.5	1.65
190	83	85	94.3	3.55
380	90	100	98.2	4.70

<sup>a</sup> Fractionation conditions:  $23^\circ\text{C}$ .; stepwise continuous solvent gradient; 1 g. polymer on 75 g. beads. Polymer characteristics:  $[\eta]_{\text{cetane}}^{100^\circ\text{F}}$ , 0.782;  $\bar{M}_w$ ,  $7.1 \times 10^5$ .

<sup>b</sup> Flow rate 23.8 ml./hr.

<sup>c</sup> Initial concentration in mixer.

TABLE II  
 Fractionation of PA 6 with Thermal Gradient<sup>a</sup>

Elution volume per fraction, ml. <sup>b</sup>	Solvent		Polymer	
	Benzene concn., vol.-%		Cumulative weight, %	Intrinsic viscosity, dl./g.
	Avg. column chg. per fract.	Good solvent		
1680	0 <sup>c</sup>	75	1.5	0.06
	35			
260	70	75	18.7	0.12
260	71.5	75	37.0	0.26
260	72.5	75	42.4	0.33
260	73.5	75	48.5	0.40
175	74.5	80	53.1	0.46
175	75.5	80	57.1	0.53
175	76.5	80	63.1	0.68
175	78	80	71.1	0.80
175	79.5	80	78.3	1.1
175	80	80	84.2	1.6
175	80	80	90.4	2.4
175	80	80	92.9	—
350	80	80	94.5	2.6
525	80	80	95.3	1.5
250	85	100	—	Lost

<sup>a</sup> Fractionation conditions: Top 70°C., bottom 23°C.; stepwise continuous solvent gradient; 1 g. polymer on 75 g. beads. Polymer characteristics:  $[\eta]_{\text{cetane}}^{100^\circ\text{F.}}$ , 0.782;  $\bar{M}_w$ ,  $7.1 \times 10^5$ .

<sup>b</sup> Flow rate 23 ml./hr.

<sup>c</sup> Initial concentration in mixing vessel.

Consequently, we reinvestigated the effects of temperature and solvent gradients.

PA 6 with a molecular weight of 710,000 was fractionated in the column in the presence and in the absence of a thermal gradient. From the data of Table I and II, integral distribution curves of Figure 6 were constructed.

Figure 6 clearly shows that a better fractionation was obtained in the absence of a thermal gradient with this poly- $\alpha$ -olefin. Better resolution of low-from-high molecular weight components raised the level of the curve in the low and intermediate intrinsic viscosity range and eliminated the "backlash," i.e., the return to lower intrinsic viscosity of the final fraction. Furthermore, considerably better resolution of the high molecular weight tail occurred in the absence of the thermal gradient. This resulted in spite of the fact that a lower average concentration of good solvent was used with the thermal gradient than in its absence.

**Solvent Gradient.** The exponential change in solvent concentration with total volume of solvent introduced to the column produced by the Baker-Williams mixing technique was designed to match the exponential molecular weight change characteristic of the normal molecular weight

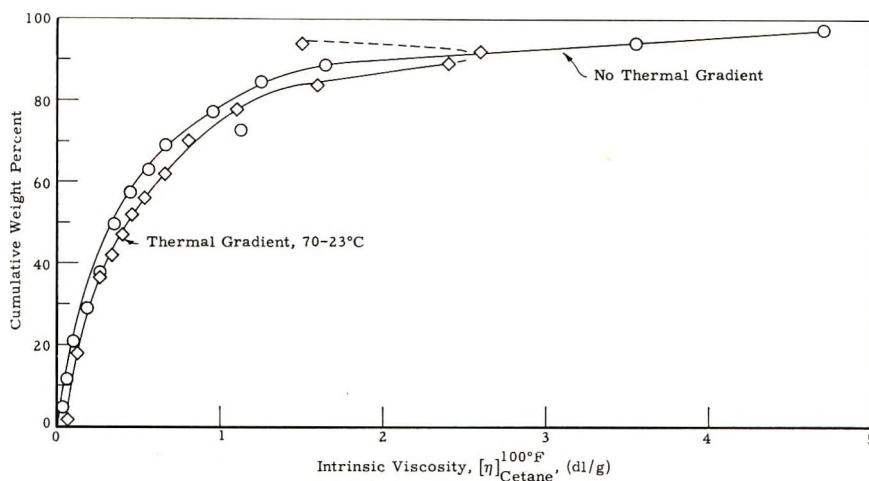


Fig. 6. Fractionation of PA 6 in presence or absence of a thermal gradient.

distribution of polystyrene. The rapid change in solvent gradient in the low molecular weight regions occurs well before the critical high molecular weight fractions are eluted for this type of distribution. Even so, both Schneider<sup>10</sup> and Jungnickel<sup>9</sup> report that the composition of the good solvent should be chosen carefully to be just capable of dissolving the least soluble portion of the sample.

The exponential solvent gradient obviously does not match the log-normal weight distribution characteristic of the Ziegler poly- $\alpha$ -olefins which has 80% of the total weight concentrated in a narrow low molecular weight band and the remaining 20% spread out over a broad high molecular weight band. Fractionation is particularly difficult in the transition between the bulk and the high molecular weight tail. For some polymers separation in this region is made even more difficult by an extreme non-linearity of the relationship between molecular weight and solubility as shown in Figure 7. The rate of change of solubility with molecular weight of octadecene/dodecene copolymers, as measured by viscosity, decreases sharply with increasing molecular weight at an intrinsic viscosity of about 0.5 dl./g. As a result, at lower molecular weights a change of 1% volume in the benzene concentration only changes the intrinsic viscosity of the eluted polymer by about 0.01 dl./g. For elution of higher molecular weight polymer, a change of 1% volume in the benzene concentration changes the intrinsic viscosity of eluted polymer by over 1.00 dl./g. Hence, a change in elution sensitivity of 100 is observed. Fractionation becomes increasingly difficult as the average molecular weight of a polymer with a log-normal distribution increases to the point where the transition between low and high molecular weight regions lies above the break point in the solubility-molecular weight curve.

As a consequence of the effects outlined above, fractionation difficulty increases with increasing molecular weight of the poly- $\alpha$ -olefins, even when

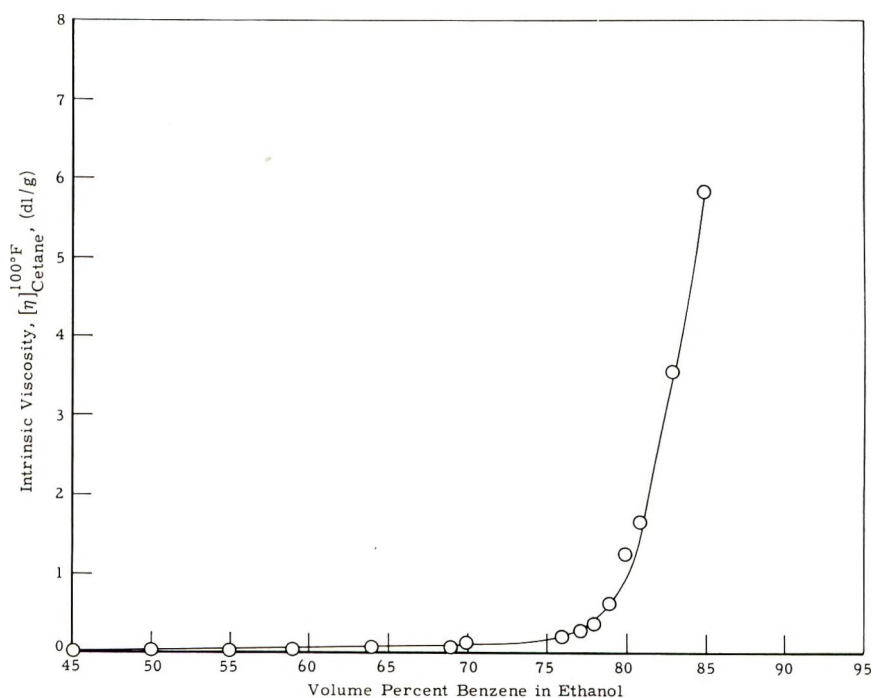


Fig. 7. Solubility-molecular weight relation of poly- $\alpha$ -olefins.

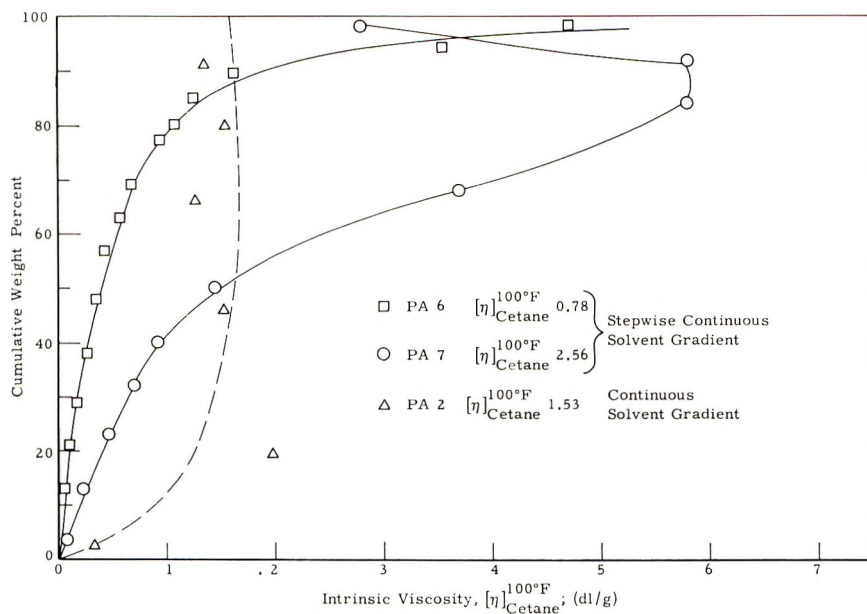


Fig. 8. Stepwise-continuous vs. continuous solvent gradient, no thermal gradient.

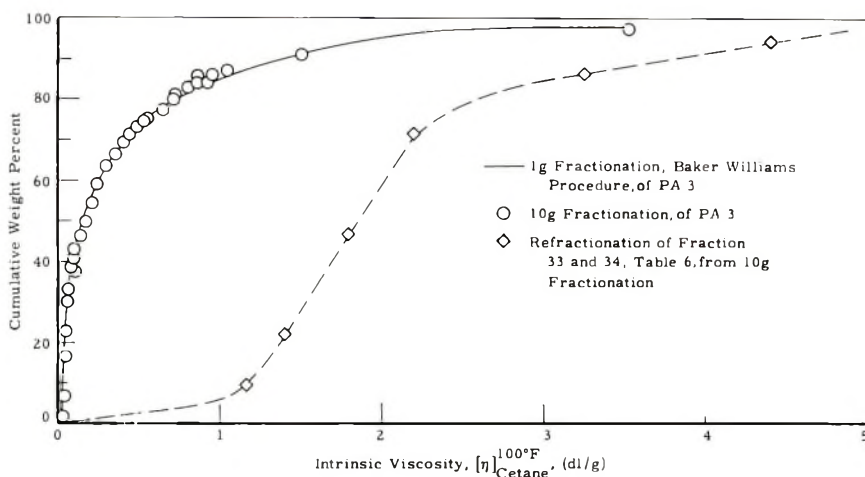


Fig. 9. Fractionation of large polymer samples.

the thermal gradient is omitted. We have overcome this difficulty by using a stepwise-continuous solvent gradient. The mixing system of Baker and Williams<sup>2</sup> is retained in this procedure. However, the good solvent used initially is a mixture of solvent and nonsolvent with insufficient solvency to dissolve any of the high molecular weight tail of the log-normal distribution. When no more polymer is eluted with this mixture, the solvent power of the good solvent is increased and further fractions are taken. In this way, the solvency change in the critical region can be controlled at a desired rate.

The improvement in fractionation efficiency obtained by this technique

TABLE III  
Fractionation of PA 2<sup>a</sup>

Elution volume per fraction, ml. <sup>b</sup>	Solvent		Polymer	
	Benzene concn., vol.-%	Good solvent	Cumulative weight, %	Intrinsic viscosity, dl./g.
	0 <sup>c</sup>			
1020	34	90		
180	70	90	2.5	0.348
240	74.2	90	19.7	1.98
210	79	90	45.9	1.53
218	82	90	66.3	1.28
120	83.4	90	78.4	1.51
1020	92	100	90.9	1.36

<sup>a</sup> Fractionation conditions: 23°C.; continuous solvent gradient; 1 g. polymer on 75 g. beads. Polymer characteristics:  $[\eta]_{\text{cetane}}^{100^\circ\text{F}}$ , 1.53;  $\bar{M}_w$ ,  $2.2 \times 10^6$ .

<sup>b</sup> Flow rate; 13 ml./hr.

<sup>c</sup> Initial concentration in mixing vessel.



is shown graphically in Figure 8. Essentially, no fractionation of a  $2 \times 10^6$  average molecular weight poly- $\alpha$ -olefin (Table III) was obtained with a continuous solvent gradient using 90% benzene in ethanol as the good solvent. Good fractionations of both higher, PA 7 (Table IV), and lower, PA 6 (Table 1), molecular weight poly- $\alpha$ -olefins were obtained by using the stepwise-continuous gradient technique starting with 60% benzene in ethanol as the good solvent.

TABLE IV  
Fractionation of PA 7<sup>a</sup>

Elution volume per fraction, ml. <sup>b</sup>	Solvent		Polymer	
	Benzene concn., vol.-%		Cumulative weight, %	Intrinsic viscosity, dl./g.
	Avg. column chg. per fract.	Good solvent		
	50 <sup>c</sup>			
1500	61	75	3.8	0.08
1500	76	80	13.1	0.22
1000	80	80	23.4	0.47
600	81.5	85	32.4	0.70
600	83.5	85	40.0	0.92
100	84	85	50.2	1.45
100	84.5	85	67.6	3.70
100	85	85	84.3	5.80
100	85	85	92.2	5.80
1600	92	100	97.2	2.80

<sup>a</sup> Fractionation conditions: 23°C.; stepwise-continuous solvent gradient; 1 g. polymer on 75 g. beads. Polymer characteristics:  $[\eta]_{\text{cetane}}^{100^\circ \text{F.}}$ , 2.56;  $\bar{M}_w$ ,  $5.5 \times 10^6$

<sup>b</sup> Flow rate 17 ml./hr.

<sup>c</sup> Initial concentration in mixing vessel.

### Large-Scale Column Fractionation

Narrow molecular weight fractions from the 1-g. analytical fractionations described above are too small to be of much use for further investigation. Fractionation of 10-g. samples by the stepwise-continuous solvent gradient, constant temperature, elution fractionation technique was investigated, therefore, as a means of preparing narrow molecular weight fractions which could be used in subsequent experiments.

The results from the fractionation of 10 g. of PA 3, a low molecular weight polymer ( $\bar{M}_w = 270,000$ ), are compared in Figure 9 (data in Table V) with the results from 1-g. precipitation fractionations. The desired solvent gradient was achieved in the 10-g. fractionation by very slowly approaching the critical concentration of 77.5% benzene in ethanol and then proceeding to the higher benzene concentrations necessary to elute the high molecular weight tail. The results indicate that the 10-g., stepwise-continuous solvent gradient elution fractionation was essentially equivalent to the 1-g. continuous solvent gradient/thermal gradient precipitation chromato-

graphic fractionation. The absence of a backlash is good evidence that the extensive elution at concentrations approaching 77.5% benzene in ethanol successfully removed the low and middle molecular weight polymer before the high molecular weight tail was eluted.

Further evidence of the efficiency of removal of low molecular weight components by this technique was obtained by combining and refractionating the last two fractions,  $[\eta] = 1.50$  and  $3.53$  dl./g., from the 10 g. fractionation. The results are tabulated in Table VI and plotted as the lower curve in Figure 9. Considerably less than 10% of the material in these fractions had intrinsic viscosities below 1.06, the intrinsic viscosity of the next lower fraction in the initial fractionation. This compares to the 50% or more low molecular weight material required to produce a backlash.

### Elution Fractionation Without Column

Even larger samples of narrow molecular weight polymers than those obtained by the technique described in the previous section are often desired. Fractions were obtained, at considerable sacrifice in fractionation efficiency, by batchwise elution of polymer from beads in ordinary Erlenmeyer flasks.

The following procedure was used. Polymer was deposited on beads in the normal fashion. The polymer-loaded beads were placed in Erlenmeyer flasks of suitable size and shaken at room temperature with the amounts and concentrations of solvents such that a slow approach to the critical concentration range was achieved. All of the resulting solutions were clear, in-

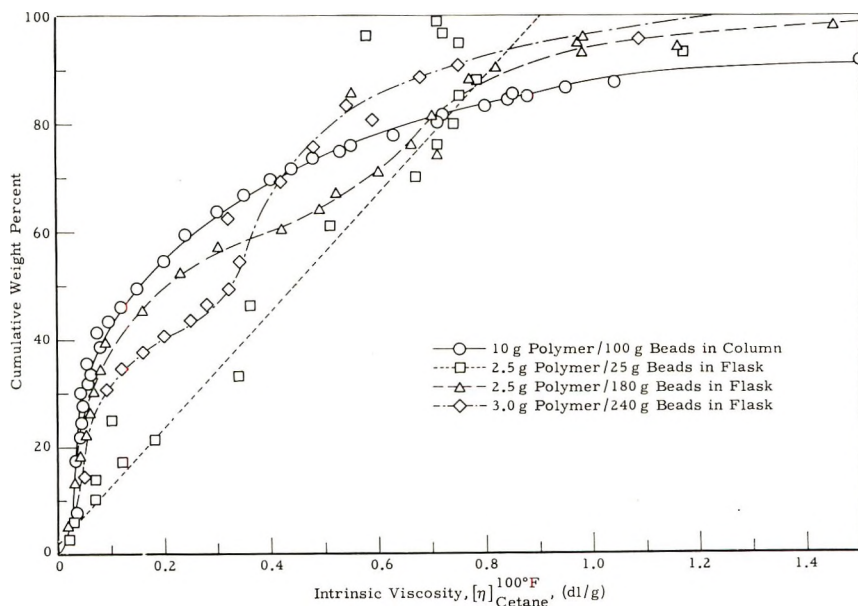


Fig. 10. Flask elution fractionation of PA 3.

TABLE V  
 Fractionation of PA 3<sup>a</sup>

Fraction	Fraction elution volume, ml. <sup>b</sup>	Benzene concn., vol.-%			Eluted polymer, g.	Cumulative weight, %	Intrinsic viscosity, dl./g.	Molecular weight $\times 10^{-3}$
		C	C <sub>1</sub>	C <sub>2</sub>				
1	527	0	25.5	50	1.3880	7.41	0.035	<10
2	217	25.5	31	50	0.4810	17.4	0.034	<10
3	300	31	41	60	0.3347	21.7	0.042	<10
4	250	55	56.5	60	0.1755	24.4	0.043	<10
5	500	56.5	58	60	0.3600	27.3	0.049	<10
6	200	58	59	60	0.1419	30.0	0.045	<10
7	395	59	64	70	0.1877	31.8	0.053	<10
8	165	64	65	70	0.1329	33.5	0.062	<10
9	215	65	66	70	0.2116	35.3	0.056	<10
10	332	66	68	70	0.3463	38.3	0.081	15
11	262	68	69	70	0.1923	41.2	0.075	13
12	280	69	71.7	77.5	0.1977	43.2	0.097	21
13	280	71.7	73.5	77.5	0.3280	46.0	0.120	35
14	280	73.5	74.8	77.5	0.3875	49.9	0.150	50
15	280	74.8	75.7	77.5	0.4397	54.3	0.200	80
16	280	75.7	76.2	77.5	0.4868	59.2	0.240	105
17	280	76.2	76.5	77.5	0.3100	63.5	0.300	150
18	280	76.5	76.8	77.5	0.2773	66.6	0.350	200
19	280	76.8	77.0	77.5	0.2630	69.5	0.400	240

20	280	77.0	77.1	77.5	0.1627	71.8	0.440	280
21	280	77.1	77.2	77.5	0.1203	73.3	0.480	330
22	280	77.2	77.30	77.5	0.1538	74.7	0.530	380
23	280	77.3	77.36	77.5	0.0677	75.9	0.550	405
24	280	77.36	77.41	77.5	0.2366	77.6	0.630	505
25	280	77.41	77.43	77.5	0.2100	80.1	0.710	610
26	280	77.43	77.5	77.5	0.0925	81.7	0.720	620
27	280	77.5	77.5	77.5	0.1328	83.1	0.800	760
28	280	77.5	77.5	77.5	0.0802	84.3	0.840	805
29	280	77.5	77.5	77.5	0.0178	84.8	0.880	880
30	280	77.5	78.3	80	0.0610	85.2	0.850	840
31	280	78.3	78.8	80	0.1308	86.3	0.950	1000
32	280	78.8	79.2	80	0.1140	87.5	1.04	1150
33	280	79.2	80.4	85	0.6237	91.5	1.50	2100
34	280	80.4	81.9	85	0.4836	97.4	3.53	8900
35	280	81.9	82.9	85	0.0008	—	—	—
36	280	82.9	89	85	~0	—	—	—

---

$\Sigma 9.3702 + 0.7549$

<sup>a</sup> Fractionation conditions: 23°C.; stepwise-continuous solvent gradient; 10 g. polymer on 100 g. beads. Polymer characteristics:  $[\eta]_{\text{cyclohexane}}^{100^\circ\text{F.}}$ , 0.435;

$\bar{M}_w$ ,  $2.8 \times 10^6$ .

<sup>b</sup> Flow rate of 35 ml./hr.

TABLE VI  
 Fractionation of Combined Fractions 33 and 34 from Fractionation of PA 3<sup>a, b</sup>

Fraction	Fraction elution volume, ml. <sup>c</sup>	Benzene concn., vol.-%		C <sub>2</sub>	Eluted polymer, g.	Cumulative weight, %	Intrinsic viscosity, dl./g.	Molecular weight × 10 <sup>-3</sup>
		C <sub>1</sub>	C					
1	600	75	76.6	80	0.0335	1.6	0.02	<10
2	870	76.6	79.0	80	0.0228	4.4	0.50	350
3	290	79.0	79.3	80	0.0735	9.0	1.16	1350
4	290	79.3	79.5	80	0.1917	22	1.40	1950
5	290	79.5	79.7	80	0.3286	47	1.80	2850
6	290	79.7	79.8	80	0.1941	72	2.20	3950
7	290	79.8	79.9	80	0.1094	87	3.26	7500
8	290	79.9	79.93	80	0.0363	95	4.40	10200
9	870	79.93	79.96	80	0.0176	99	Sample too small	—
					Σ1.0275			

<sup>a</sup> Fractionation conditions: 23°C.; continuous solvent gradient; 1 g. polymer on 75 g. beads. Polymer characteristics:  $[\eta]_{\text{cyclohexane}}^{100^\circ \text{F.}}$ , 2.43;  $\bar{M}_w$ , 4.7 × 10<sup>6</sup>.

<sup>b</sup> f 33, 0.5599 g. + f 34, 0.4676 g.; combined 1.0275 g.

<sup>c</sup> Flow rate 36.5 ml./hr.



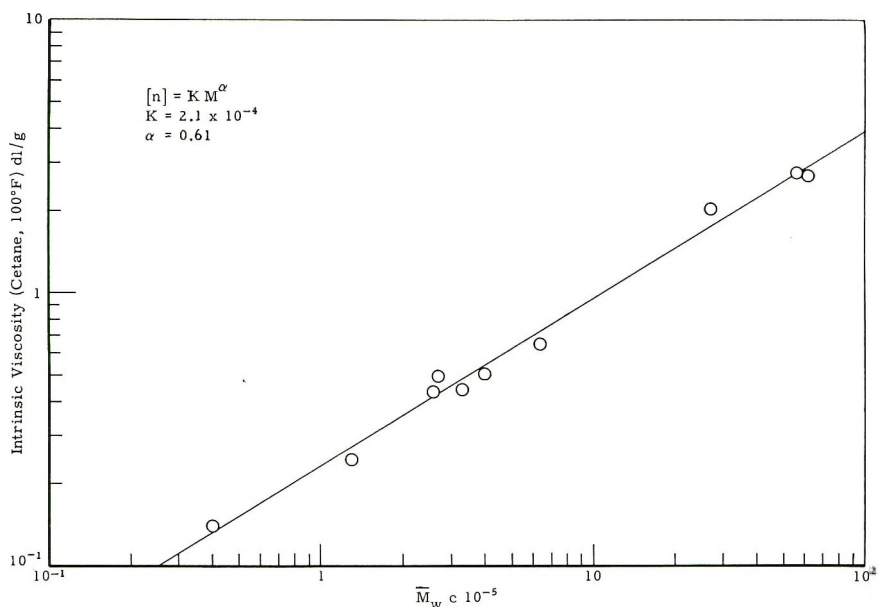


Fig. 11. Intrinsic viscosity–light scattering molecular weight correlation for poly- $\alpha$ -olefins.

dicating that polymer gel strength was sufficient to prevent removal of polymer from the beads by abrasion during the shaking.

Integral fractionation curves from several exploratory fractionations of PA 3 by this technique are compared with the 10-g. fractionation of this same polymer in Figure 10.

These results indicate that flask fractionation is not equivalent to column fractionation even when considerably lower bead loadings are used in the former. As might be expected, separation of the high molecular weight tail from the middle range material was particularly poor in the flask fractionation. Extremely poor results were obtained at higher bead loadings.

#### Molecular Weight-Intrinsic Viscosity Relation for $C_{12-18}$ Poly- $\alpha$ -olefins

The molecular weight of these Ziegler polymers was determined by light scattering, employing a Brice-Phoenix, series 1973 instrument. Zimm plots were used to correct for angular dissymmetry in these calculations. Thereafter, the Kuhn-Mark-Houwink equation

$$\eta = KM^\alpha$$

was used to correlate intrinsic viscosities to molecular weights. From the log-log plot, Figure 11, it was found that

$$K = 2.1 \times 10^{-4}$$

$$\alpha = 0.61$$

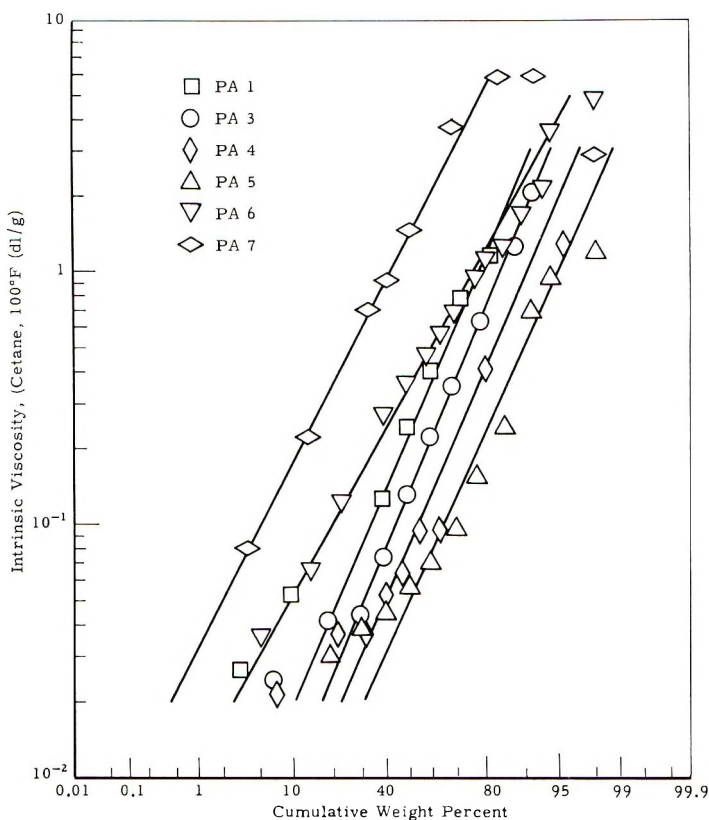


Fig. 12. Molecular weight distribution of poly- $\alpha$ -olefins.

This is somewhat in disagreement with Jungnickel's value of  $\alpha$  being 1.04.<sup>9</sup> It should be pointed out that this study was made over a much wider molecular weight range and that Jungnickel's measurements were carried out on very dilute solutions with the consequent problems of accuracy in the determination of  $\eta_{sp}$  and  $\eta_{rel}$ .

### Comparison of Molecular Weight Distribution of Polymers Obtained with Different Catalysts and Conditions

A number of poly- $\alpha$ -olefins prepared under a variety of reaction conditions with  $\text{TiCl}_4\text{-2AlEt}_3$  and modifications thereof as catalysts were fractionated so that molecular weight distributions could also be compared. Properties of these polymers are given in Table VII, and log-normal plots of the molecular weights distributions are shown in Figure 12.

Five of the six polymers shown in Figure 12 present distributions that are almost parallel to each other. Thus, it appears, in general, that all of the catalysts and conditions employed in synthesis give similar molecular weight distributions.

TABLE VII  
Molecular Weights and  $Q$  for Poly- $\alpha$ -olefins

Poly- $\alpha$ -olefin	Intrinsic viscosity, dl./g.		$\bar{M}_w \times 10^{-4}$	$\bar{M}_v \times 10^{-3}$	$\bar{M}_n \times 10^{-3}$	$Q(\bar{M}_w/\bar{M}_n)$	Notable variations in polymerization conditions
	Bulk	50%					
1	0.762	0.23	809	700	0.797	10,030	1TiCl <sub>4</sub> /2AlEt <sub>3</sub> ; 72/1 monomer/catalyst ratio
2	1.53	—	—	2450	—	—	1TiCl <sub>4</sub> /2AlEt <sub>3</sub> ; 18/1 monomer/catalyst ratio + catalyst modifier
3	0.435	0.96	345	280	0.404	8,510	Same as 1; + concentration $C$ of MW control agent
4	0.243	0.54	206	107	0.346	5,860	Same as 1; + concentration 3 <i>C</i> of MW control agent
5	0.140	0.30	37.8	44	0.149	2,520	Same as 1; + concentration 7 <i>C</i> of MW control agent
6	0.782	1.4	196	710	18.0	152	1TiCl <sub>4</sub> /2AlEt <sub>3</sub> ; 18/1 monomer to catalyst ratio + catalyst modifier
7	2.56	6.6	2,530	5,000	72.5	350	Same as 6 except 55/1 monomer to catalyst ratio

For a more quantitative comparison of these molecular weight distributions, one makes use of the observations of Weslau.<sup>14</sup> From these observations it can be shown that

$$\bar{M}_w = ([\eta]_{0.5}/K)^{1/\alpha} \exp\{\sigma_{IV}^2/2\alpha^2\}$$

where

$$\sigma_{IV} = \ln([\eta]_{0.84}/[\eta]_{0.50})$$

and

$$\bar{M}_n = ([\eta]_{0.5}/K)^{1/\alpha} \exp\{-\sigma_{IV}^2/2\alpha^2\}$$

where

$$K = 2.1 \times 10^{-4}$$

$$\alpha = 0.61$$

and  $Q$ , a conventional measure of the polydispersity of a polymer, is

$$\bar{M}_w/\bar{M}_n = \exp\{\sigma_{IV}^2/\alpha^2\}$$

These quantities as well as the viscosity-average molecular weight, as determined by viscosity-light scattering correlation, are shown in Table VII.

The large amount of low molecular weight material and the very broad high molecular weight tail characteristic of this type of distribution is well illustrated by the extremely high value of  $Q(\bar{M}_w/\bar{M}_n)$  obtained for these polymers.

## DISCUSSION

These experiments clearly show a contribution of the column to fractionation efficiency even in the absence of reprecipitation resulting from a temperature gradient. The selective adsorption proposed by Schneider et al.<sup>10</sup> could adequately account for such an effect. An alternative explanation would invoke the exchange of lower molecular weight polymer on the beads for higher molecular weight polymer in the saturated solution as it flows through lower, as yet uneluted, zones of polymer-coated beads. This explanation requires that equilibrium be established rapidly relative to the rate of flow of solvent through the column. Such is apparently the case since the results of the "flask" fractionations indicate that saturation is achieved in less than 10 min., which is the time required for the solvent to travel only approximately 1.5 in. of the 10-in. section of polymer-coated beads.

The finding by Schneider et al.<sup>10</sup> that no improvement in fractionation resulted from spreading polymer over all the beads in a column as compared to concentrating it in the center  $1/3$  of the column is evidence against the latter mechanism. However, a more thorough study is necessary to establish the mechanism by which fractionation occurs. Of particular

interest would be an examination of the effect of increasing the length of the uncoated column of beads.

The present results demonstrate that the temperature gradient inherent in precipitation chromatography does not necessarily increase fractionation efficiency. The relative efficiencies of fractionation in the presence and absence of a thermal gradient may well depend on the relative effectiveness of temperature decrease and adsorption on beads for selective removal of the high molecular weight portion of polymer from solution as it moves down the column. The stepwise-continuous solvent gradient technique offers an advantage in either system whenever difficulty is encountered in resolving the high molecular weight fractions.

The similarity of molecular weight distributions for the different reaction conditions demonstrate the importance of good fractionation to the interpretation of experimental results. Early, inadequate fractionations had indicated that both average molecular weight and molecular weight distribution were strongly affected by the reaction variables. However, the apparent variations in the latter were found to be a function of fractionation efficiency rather than reaction conditions.

The authors wish to express their thanks to J. L. Jungnickel and F. T. Weiss for aid in construction of the apparatus and interpretation of the results and to R. C. Jones for many helpful discussions.

### References

1. Allen, P. W., *Techniques of Polymer Characterization*, Butterworth, London, 1959 p. 52.
2. Baker, C. A., and R. J. P. Williams, *J. Chem. Soc.*, **1950**, 2352.
3. Desreux, V., *Rec. Trav. Chim.*, **68**, 789 (1949).
4. Desreux, V., and M. C. Speigals, *Bull. Soc. Chim., Belg.*, **59**, 476 (1950).
5. Francis, P. S., R. C. Cooke, Jr., and J. H. Elliot, *J. Polymer Sci.*, **31**, 453 (1958).
6. Fuchs, O., *Z. Elektrochem.*, **60**, 229 (1956).
7. Henry, P. M., *J. Polymer Sci.*, **36**, 3 (1959).
8. Kenyon, A. S., and I. O. Salyer, *J. Polymer Sci.*, **43**, 427 (1960).
9. Jungnickel, J. L., and F. T. Weiss, *J. Polymer Sci.*, **49**, 437 (1961).
10. Schneider, N. S., J. D. Loconti, and L. G. Holmes, *J. Appl. Polymer Sci.*, **5**, 354 (1961).
11. Guillet, J. E., R. L. Combs, D. F. Slonaker, and H. W. Coover, *J. Polymer Sci.*, **47**, 307 (1960).
12. Koral, J., R. Ullman, and R. Eirich, *J. Phys. Chem.*, **62**, 541 (1958).
13. Hewett, W. A., R. C. Jones, and L. E. Lorensen (to Shell Development Co.), U. S. Pat. 2,895,915 (1959).
14. Weslau, H., *Makromol. Chem.*, **20**, 111 (1956).

### Résumé

On a étudié le fractionnement d'échantillons de 1 à 10 grs d'une série de poly-alpha-oléfines dans une colonne de perles de verre. On a trouvé qu'un gradient thermique diminuait l'efficacité du fractionnement relativement à celle obtenue à des températures constantes (ambiantes). Une technique de gradient en solvant par étapes successives et continues a été développée pour perfectionner le fractionnement du matériel de haut poids moléculaire. L'efficacité du fractionnement décroît en augmentant la charge en



perles mais elle était encore bonne pour des rapports polymère-perles de 0.1 comparé avec le rapport 0.01 habituellement employé. L'efficacité n'est pas si bonne en absence d'une colonne même quand cette dernière est effectuée à température constante. L'équation de Kuhn-Mark-Houwink a été employée pour relier les viscosités intrinsèques aux poids moléculaires obtenus par diffusion de la lumière. Les valeurs des constantes sont  $K = 2.1 \times 10^{-4}$  et  $\alpha = 0.61$ . Des corrélations dans la distribution des poids moléculaires montrent que ces polymères ont un rapport  $M_w/M_n$ .

### Zusammenfassung

Die Fraktionierung von Proben von 1 bis 10 g einer Reihe von Poly- $\alpha$ -Olefinen mittels einer Glaskügelchenkolonne wurde untersucht. Dabei wurde gefunden, dass ein Temperaturgradient die Fraktionierungswirksamkeit gegenüber derjenigen bei konstanter Raumtemperatur herabsetzt. Zur Verbesserung der Fraktionierung von hochmolekularem Material wurde eine Technik mit "schrittweise-kontinuierlichem" Lösungsmittelgradienten entwickelt. Die Fraktionierungswirksamkeit nahm zwar mit steigender Beladung des Füllkörpers ab, war jedoch noch bei einem Verhältnis von Polymerem zu Füllkörper von 0,1 gut; vergleichsweise liegt das üblicherweise verwendete Verhältnis bei 0,01. Bei Abwesenheit einer Kolonne ist die Wirksamkeit geringer, auch wenn konstante Temperatur verwendet wird. Zur Korrelation der Viskositätszahl mit dem durch Lichtstreuung bestimmten Molekulargewicht wurde die Kuhn-Mark-Houwink-Gleichung mit den Konstanten  $K = 2,1 \times 10^{-4}$  und  $\alpha = 0,61$  verwendet. Wie aus der Molekulargewichtsverteilung hervorgeht, ist bei den untersuchten Polymeren  $M_w/M_n$  sehr gross.

Received May 3, 1963

## Investigation of the Stereoregularity of Poly(vinyl Alcohol)\*

KIYOSHI FUJII, TAKANI MOCHIZUKI, SABURO IMOTO, JUNJI UKIDA, and MASAKAZU MATSUMOTO, *Research Laboratory, Kurashiki Rayon Company, Sakazu, Kurashiki, Okayama, Japan*

### Synopsis

Studies of the steric structures of poly(vinyl alcohol), as deduced from studies of the structures of its esters, particularly poly(vinyl formate) are described. Two types of tactic poly(vinyl formate) crystallize with different structures, corresponding to their different molecular structures. Therefore, the type of molecular stereoregularity in poly(vinyl formate) samples can be deduced from an examination of the crystals produced by a given crystallization treatment. From the results of the study of the poly(vinyl formate) crystals, some conclusions can be drawn concerning the steric structure of poly(vinyl alcohol). Crystallizabilities of other tactic poly(vinyl esters) have also been investigated.

### Introduction

There has been much discussion<sup>1-4</sup> of the stereochemical structure of poly(vinyl alcohol) (PVA), based on its x-ray diffraction pattern, before Natta's work<sup>5a</sup> verifying the concept of stereospecificity in high polymers.<sup>5b</sup> Since then, there have been many attempts to prepare and characterize stereoregular PVA, with only limited success.

Except in some patents,<sup>6,7</sup> no effective catalyst yielding stereoregular poly(vinyl acetate) (PVAc) has been disclosed. Attempts in our laboratory to reproduce the results claimed in these patents, moreover, have been unsuccessful. Haas et al.<sup>8</sup> obtained a crystalline polymer from vinyl trifluoroacetate and, from this, a highly water-resisting PVA. Detailed studies on this PVA gave evidence that it has a somewhat more ordered structure than does ordinary PVA.<sup>9-11</sup> On the basis of the fiber axis repeat distance of 4.8 Å, a syndiotactic structure has been proposed for the poly(vinyl trifluoroacetate) (PVTA) and the PVA derived therefrom.<sup>10</sup> However, Chatani et al.<sup>12</sup> reported that PVTA derived from commercial PVA gave an x-ray pattern quite similar to that afforded by direct polymerization of vinyl trifluoroacetate. Moreover, a complete explanation of the fiber pattern of PVTA is rather difficult, and a repeat distance longer than 4.8 Å, is needed to account for all layers which appear.<sup>12-14</sup> So far, x-ray investigations of PVTA and of PVA derived

\* Presented at the 10th Symposium on Polymer Chemistry, Tokyo, November, 1961.

therefrom have not led to definite conclusions as to their chain configurations.

A close relationship between the water-resisting ability of PVA and the conditions of polymerization of the original PVAc was first disclosed by Ukida et al.<sup>15</sup> This work has been extended to detailed studies of the effect of the polymerization conditions of vinyl acetate on various other properties of the PVA derived therefrom. Those properties are the infrared absorption intensity of the crystallization-sensitive band at  $8.74 \mu$ .<sup>15,16</sup> crystallinity measured by x-ray and density methods,<sup>17</sup> glass temperature,<sup>18</sup> melting point,<sup>18,19</sup> rate of gelling of concentrated aqueous solutions,<sup>20</sup> dependence of the viscosity of a dilute aqueous solution on the rate of shear,<sup>21</sup> rate at which turbidity develops in dilute solution in a mixture of water and dimethyl sulfoxide,<sup>22</sup> color reaction with iodine,<sup>11</sup> and molecular dimensions of poly(vinyl acetal) in solution.<sup>23</sup> These properties all seem to be related, more or less, to the steric structure of PVA. However no conclusive results showing the steric structure—in particular, the predominant configuration—in PVA have been obtained so far.

Another approach to the problem has been taken in the preparation of closely related stereoregular (usually syndiotactic or isotactic) materials. The work first undertaken in this field was a conversion of isotactic poly(vinyl benzyl ether) to PVA by treatment with hydrogen bromide,<sup>24</sup> but a complete conversion was not attained. Recent progress in this field is remarkable.<sup>25-28</sup> Also, model materials of low molecular weight, such as stereoisomers of 2,4-pentanediol have been announced.<sup>29</sup>

As for PVAc, polymers of vinyl formate, as usually prepared, have been known to be completely amorphous.<sup>30</sup> We have, however, prepared crystallizable poly(vinyl formate) (PVF) by free radical polymerization of the monomer conducting at lower temperatures and have deduced a syndiotactic structure from the x-ray data.<sup>31</sup> Detailed studies of the crystallizability of PVI' led us to an examination of formates of PVA derived from isotactic polyvinyl ethers. These studies have led to some definite conclusions. Some of these have previously been briefly reported.<sup>23,33</sup> In the present paper, details of the preparation and the characterization of the two types of stereoregular PVF, PVA, and other polyvinyl esters will be reported.

### Preparation of Syndiotactic PVF

In the course of our studies on various vinyl esters and PVA derived therefrom, an unexpected stereoregulating effect was observed in the polymerization of vinyl formate.<sup>32</sup> PVA derived from PVF has a smaller amount of 1,2-glycol bonding and a higher water resistance than that derived from PVAc, prepared at the same polymerization temperature. All properties examined—iodine reaction, infrared absorption band at  $8.74 \mu$ , glass temperature, melting point, etc.—showed that PVA derived from the formate has a more ordered structure as compared with that

derived from the acetate as exemplified in Table I. The cause of this effect was ascribed to an interaction (hydrogen bonding) between formyl groups in the monomer. The interaction between the formyl groups also produces a marked dependence of the properties of PVI<sup>F</sup>—density, glass temperature, solubility, and gelling rate of solution—on the polymerization temperatures (see Table II). Moreover some crystallinity was shown in x-ray photographs of PVF samples prepared by polymerization at lower temperatures.

TABLE I  
Properties of PVA derived from PVF and PVAc

Monomer	Polymerization temp., °C.	D.P.	1,2 Glycol-content, mole-% <sup>a</sup>	Degree of swelling in water <sup>b</sup>	Glass temp., °C. <sup>c</sup>	Melting point, °C. <sup>d</sup>
Vinyl formate	60	4590	1.06	1.9	—	—
	-78	1090	0.23	0.95	97	265
Vinyl acetate	60	3530	1.82	3.1	90	240
	-78	1590	0.42	1.6	92	—

<sup>a</sup> Consumption of periodic acid was determined polarographically.

<sup>b</sup> Weight of water absorbed/weight of PVA at 30°C.; PVA film (0.15 mm. thickness).

<sup>c</sup> Determined dilatometrically.

<sup>d</sup> Determined from temperature-elongation curve.

TABLE II  
Properties of PVF Prepared at Different Polymerization Temperatures

Polymerization temp., °C.	Density (30°C.), g./cc.	Glass temp., °C. <sup>a</sup>	Solubility acetonitrile at room temp.
60	1.3444	—	Soluble
30	1.3445	30.5	Soluble
-30	1.3466	34.0	Insoluble
-60	1.3476	37.0	Insoluble
PVF derived from PVTA prepared at 60°C.	1.347	—	Insoluble

<sup>a</sup> Determined dilatometrically.

PVF, like PVAc,<sup>34</sup> prepared by free radical polymerization of the monomer gives two amorphous rings in its x-ray diagram in amorphous state. However, when PVI<sup>F</sup> prepared by polymerization at lower temperatures is cast from a solution in acetonitrile at room temperature a crystalline peak appears at  $2\theta = 13.5^\circ$ , with reduction in the intensity of the inner halo, as shown in Figure 1. The intensity of the peak becomes higher as the polymerization temperature is lowered. When stretched,

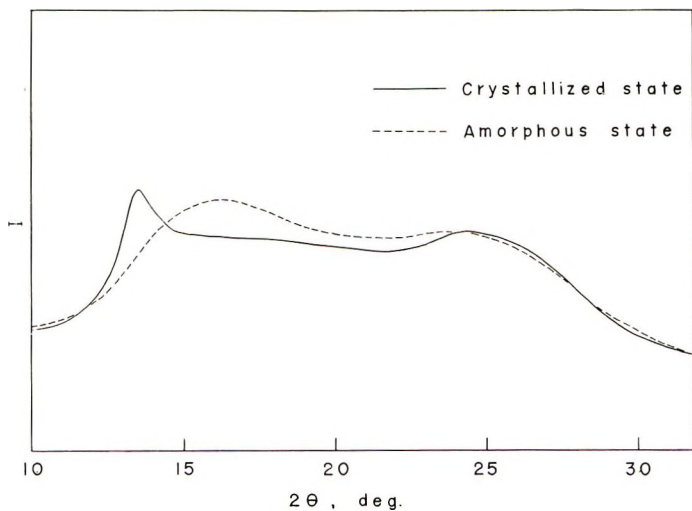


Fig. 1. Scanning curves for poly(vinyl formate) prepared by polymerization at  $-78^{\circ}\text{C}$ .

the PVF sample gives a fiber pattern, such as that shown in Figure 2. The repeat distance along the fiber axis, 5.0 Å, is consistent with that expected for an extended syndiotactic zigzag.<sup>35</sup> The result strongly suggests that the regular sequences in the polymer chain possess a syndiotactic configuration. However, the remainder of the pattern is not sufficient for a detailed analysis, hence the structure of PVF cannot be considered to be firmly established.

Although, as mentioned above, marked differences in various properties exist for PVF samples prepared at different polymerization temperatures, no difference was observed in the x-ray fiber diagrams of PVA samples derived therefrom. PVAc derived from crystallizable PVF by

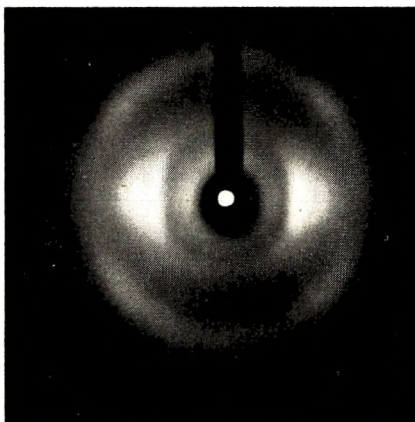


Fig. 2. Fiber pattern of poly(vinyl formate) prepared by polymerization at  $-78^{\circ}\text{C}$ . Ni-filtered  $\text{CuK}\alpha$  radiation.



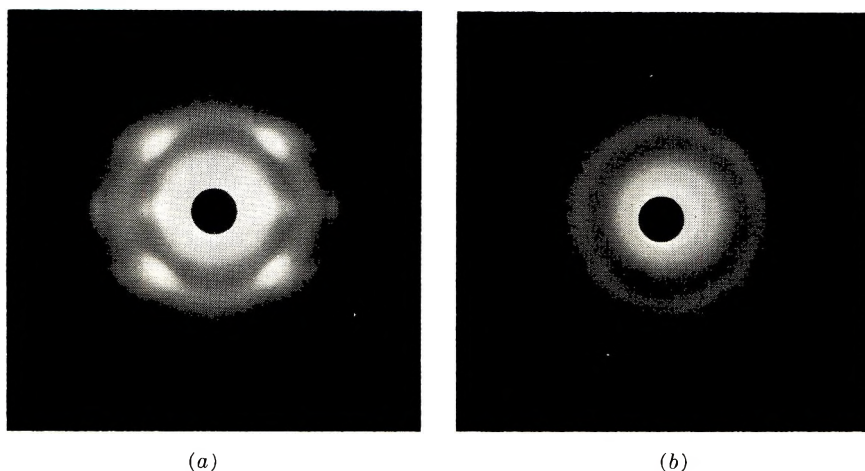


Fig. 3. Fiber patterns of poly(vinyl *tert*-butyl ether): (a) polymerized by  $\text{BF}_3 \cdot \text{O}(\text{C}_2\text{H}_5)_2$  in toluene at  $-78^\circ\text{C}$ .; (b) polymerized by  $\text{SnCl}_4$  in ethyl bromide at  $-50^\circ\text{C}$ .

hydrolysis and acetylation shows only the amorphous halos typical of PVAc prepared directly.

Next, PVTA formed by polymerization of the monomer at  $60^\circ\text{C}$ . was converted to PVF by hydrolysis, followed by formylation. The product exhibited crystallinity corresponding to that of PVF formed by polymerization of the monomer at  $-60$  to  $-40^\circ\text{C}$ ., as shown in Table II. On the other hand, PVF samples derived from PVAc formed by polymerization of the monomer at various temperature showed less crystallinity. However, in this case too, the properties of PVF improved as the polymerization temperature of the original PVAc was lowered.

Finally, crystallizable PVF was converted to PVTA by hydrolysis and esterification in trifluoroacetic acid. A stretched sample of the

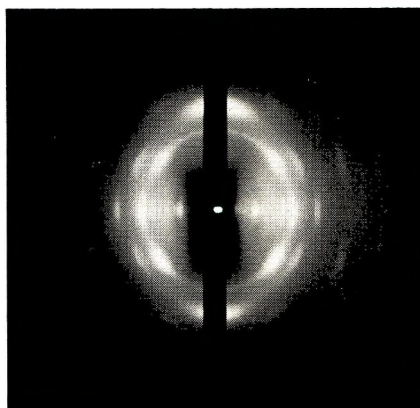


Fig. 4. Fiber pattern of isotactic polyvinyl formate derived from isotactic poly(vinyl *tert*-butyl ether).

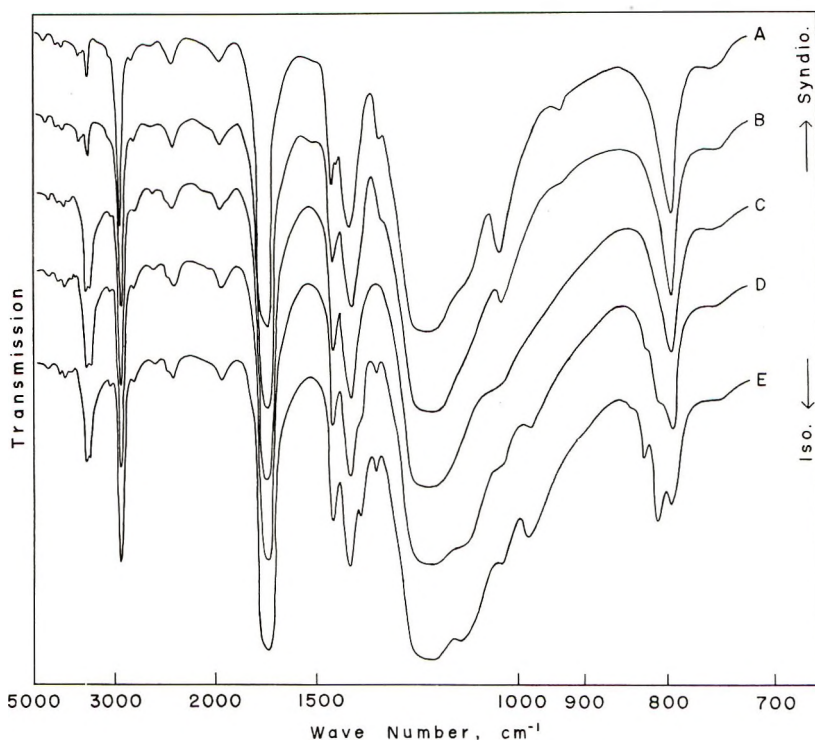


Fig. 5. Infrared spectra of poly(vinyl formate) samples having various tacticities.

resulting polymer gave a fiber pattern very similar to that of PVTA formed by polymerization of the monomer.

These data suggest that free radical polymerization of vinyl esters favors syndiotactic configurations, as predicted by Fordham.<sup>36</sup> The sensitivity of the dependence of crystallizability on structural regularity for PVF is very impressive and suggestive.

#### Synthesis of Isotactic PVF and Confirmation of Its Isotactic Structure

This close relation between crystallizability and structural regularity in PVF led us to investigate with x-rays the model PVA derived from crystallizable (presumably isotactic) polyvinyl ethers. When we decided to take up this problem, polyvinyl benzyl ether—a parent polymer of the model PVA—obtained up to that time was of low molecular weight and of poor crystallinity.<sup>24,25</sup> Therefore we tried the preparation of crystallizable polymer having higher molecular weight from vinyl *tert*-butyl ether, with subsequent conversion of this polymer to PVA. The same procedure has been developed independently at the Department of Polymer Chemistry of Kyoto University.<sup>27</sup> Vinyl *tert*-butyl ether was polymerized by a method similar to that used in the stereospecific polymerization of other vinyl alkyl ethers.<sup>37-39</sup> Fiber pattern of both crystalline and

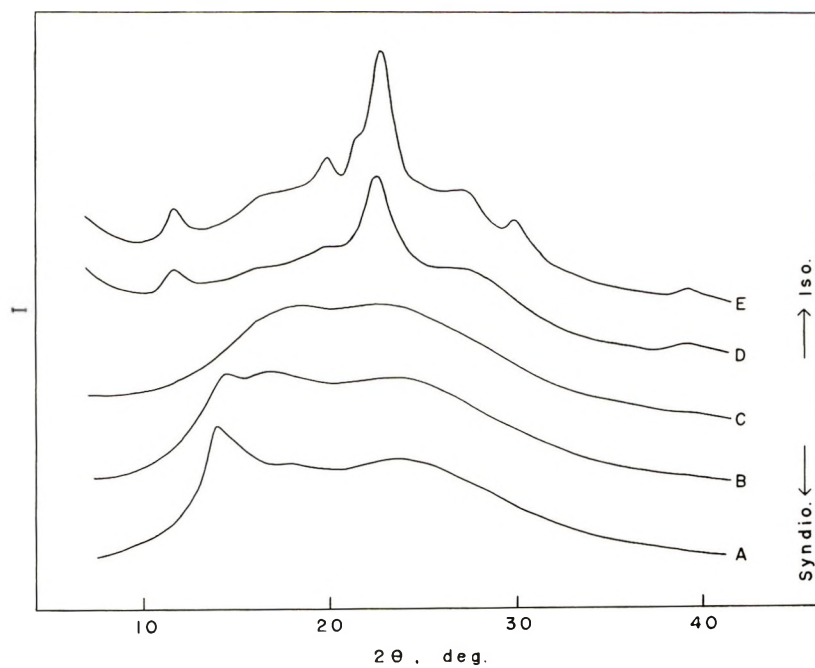


Fig. 6. Scanning curves for poly(vinyl formate) samples having various tacticities.

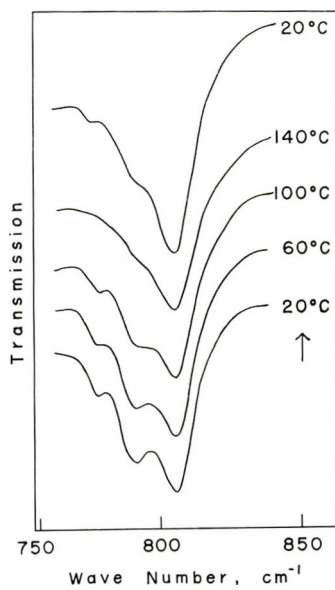


Fig. 7. Effect of temperature on the infrared spectrum of isotactic poly(vinyl formate).

amorphous (atactic) poly(vinyl *tert*-butyl ether) are shown in Figure 3. The ether bonds in polyvinyl ethers can easily be cleaved by treatment with hydrogen bromide<sup>24</sup> or acetic anhydride and a Lewis acid<sup>25</sup> to give PVA or PVAc.

The model PVA thus obtained was converted to PVF by treatment with formic acid containing a small amount of monochloroacetic acid. The product was identified as PVF by infrared and elemental analyses. It was insoluble in methyl formate or acetonitrile which dissolves PVF formed by free radical polymerization of the monomer, but was soluble in formic acid or dimethyl sulfoxide. It was cast from formic acid solution on a mercury surface and was stretched about ten times. The stretched sample gave an x-ray spectrum very rich in well oriented reflections (Fig. 4). The spectrum may be readily interpreted on the basis of a rhombohedral unit cell (only reflections with  $-h + k + l = 3n$  are present), with identity periods referred to hexagonal axis:  $a = b = 15.9$  A. and  $c = 6.55$  A. (fiber period). The calculated density of 1.49 g./cc., based on the assumption of 18 monomer units per unit cell, is somewhat higher than the value of 1.35 g./cc. observed for the unstretched sample. Indexing of the reflections shows that the space group is  $R\bar{3}c$  or  $R3c$ . The close similarity of the relative intensities of the reflections and the systematic extinctions to those reported for isotactic polystyrene<sup>40</sup> suggests that the crystal structures of these two polymers closely resemble each other.

These results lead to the definite conclusions that crystallizable PVF formed by free radical polymerization of the monomer at low temperatures has a predominantly syndiotactic structure, whereas PVA derived from crystallizable polyvinyl ethers has a predominantly isotactic structure. Predictions<sup>24</sup> that isotactic PVA could be synthesized from vinyl ethers have thus been verified.

### Infrared Spectra of Tactic PVF

Two types of tactic PVF possess different crystallization-sensitive bands, corresponding to their different steric structures. Figure 5 shows spectra of various PVF samples having different tacticities. The bands at 1420, 1272, 1026, and 924  $\text{cm.}^{-1}$  are characteristic of the syndiotactic structure, while bands at 1345, 1310, 1104, 970, 824, and 809  $\text{cm.}^{-1}$  are those for the isotactic structure.

The order of tacticities shown by the infrared data is in good agreement with that from the x-ray data, as shown in Figures 5 and 6. Preparative conditions of these PVF samples are summarized in Table III. Intensities of these bands vary with the crystallinity; therefore, the tacticity of PVF can be estimated by examination of the spectra from samples which have been subjected to a given crystallization treatment. As shown in Figure 7, these bands, measuring the crystallinity, do not disappear at a single sharp temperature, but begin to decrease at temperatures much below the temperature required to produce a completely amorphous spectrum.

TABLE III  
 Preparative Conditions of PVF Sample

Source	Monomer concn., vol.-%	Initiator	Solvent	Polymerization temp., °C.	Method of conversion to PVA
PVF	50	B(C <sub>2</sub> H <sub>5</sub> ) <sub>3</sub>	Methyl formate	-78	Methanolysis catalyzed by NaOH
PVF	100	AIBN <sup>a</sup>	—	-120	Ditto
PVtBE	33	SnCl <sub>4</sub>	Ethyl bromide	-50	Treatment by HBr
PVtBE	20	BF <sub>3</sub> ·O(C <sub>2</sub> H <sub>5</sub> ) <sub>2</sub>	<i>n</i> -Hexane	-78	Acetylation by acetic anhydride and Lewis acid and methanolysis, catalyzed by NaOH
PVtBE	5	BF <sub>3</sub> ·O(C <sub>2</sub> H <sub>5</sub> ) <sub>2</sub>	Toluene	-78	Ditto

<sup>a</sup> 2,2'-Azobisisobutyronitrile.

### Characterization of Isotactic PVA

Now we can discuss the properties of PVA on the basis of experimental facts relative to the steric structures of the corresponding formates.

As reported previously, when samples of isotactic and syndiotactic PVF were converted to PVA by heterogeneous hydrolysis they gave quite similar x-ray patterns.<sup>28,33</sup> This is in striking contrast to the difference observed in the x-ray patterns of the original two tactic PVF samples (see Fig. 8).

When cast from aqueous solution, isotactic PVA gives an x-ray spectrum similar to that of ordinary PVA. When heated, however, the former shows no crystallization, while the latter exhibits a high degree of crystallinity (see Fig. 9). A similar trend can be observed in the infrared examination of the crystallization-sensitive band at 1141 cm.<sup>-1</sup> in PVA shown in Figure 10. Thus, the crystallized state brought about by heterogeneous hydrolysis of isotactic PVF is a rather exceptional case, in that the crystallization of isotactic PVA cannot be affected by heat-treatment.

In short, isotactic PVA is less crystallizable than ordinary PVA and no new crystal structure characteristic of isotactic molecular components has been recognized. Strictly speaking, the observed spacings are somewhat expanded in isotactic PVA, as shown in Figure 9, but this is beside the point. It might result from incomplete crystallinity.

Murahashi et al.<sup>41</sup> have investigated the infrared spectrum of isotactic PVA, and found that the band at about 3.0 μ, assigned to the O-H stretch-



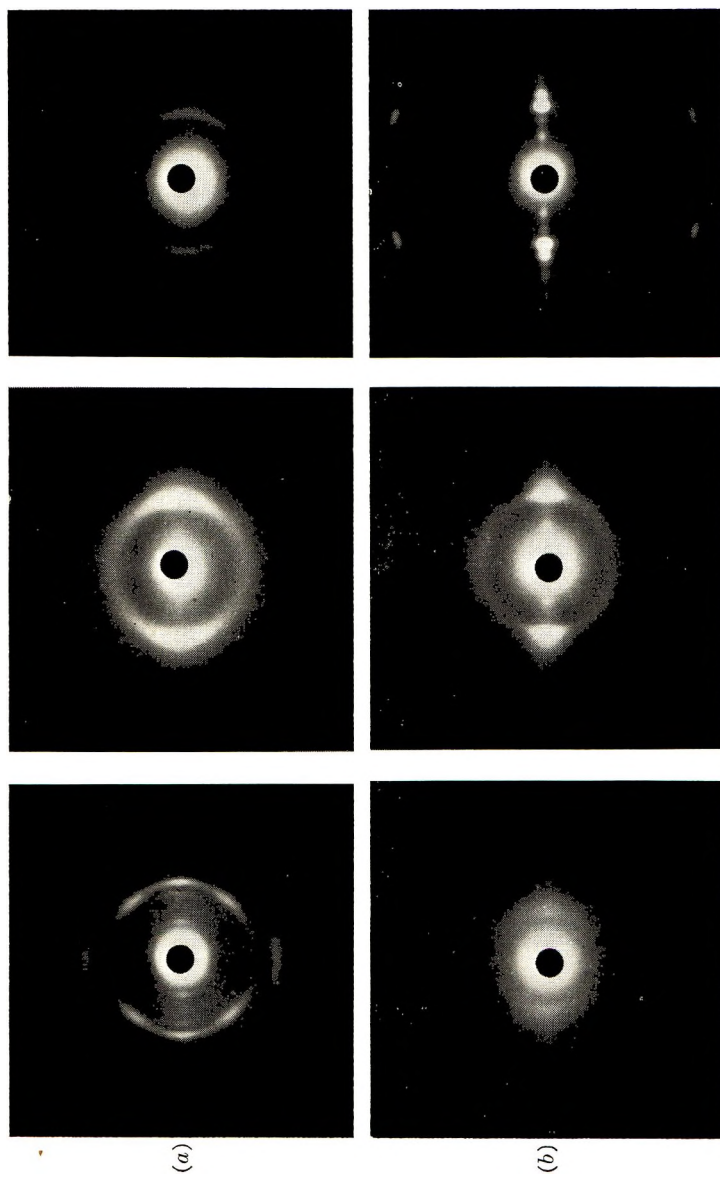


Fig. 8. Fiber patterns of poly(vinyl alcohol) samples derived from (a) isotactic and (b) syndiotactic poly(vinyl formate) by heterogeneous hydrolysis: Left figures: poly(vinyl formate); Middle figures: poly(vinyl alcohol) produced by heterogeneous hydrolysis; Right figures: poly(vinyl alcohol) after heat treatment at 200°C.

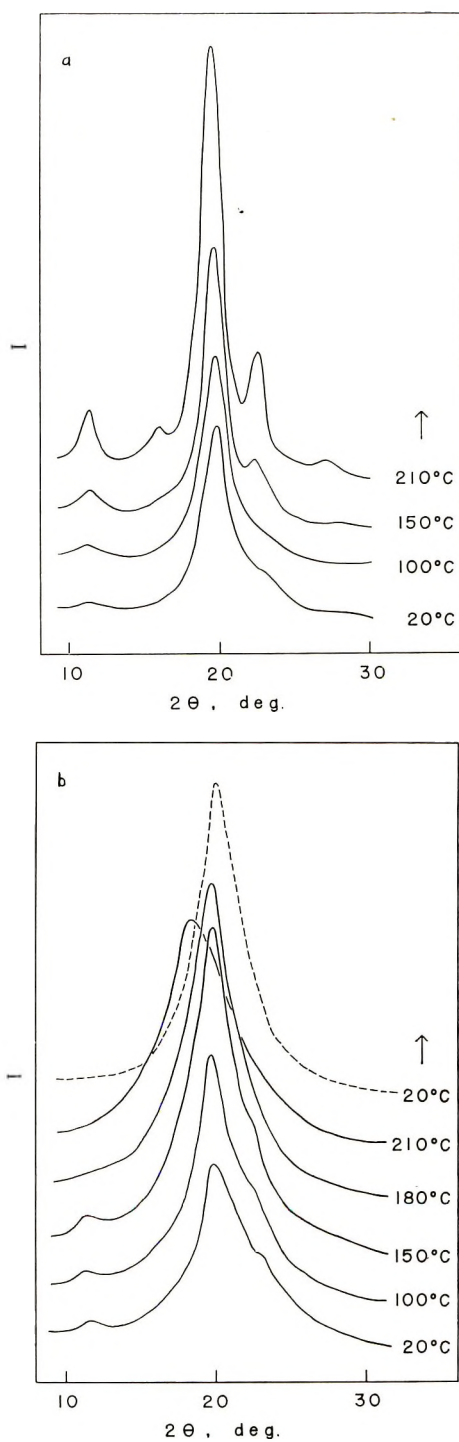


Fig. 9. Effect of temperature on the X-ray diffraction curve of poly(vinyl alcohol): (a) conventional poly(vinyl alcohol); (b) isotactic poly(vinyl alcohol).

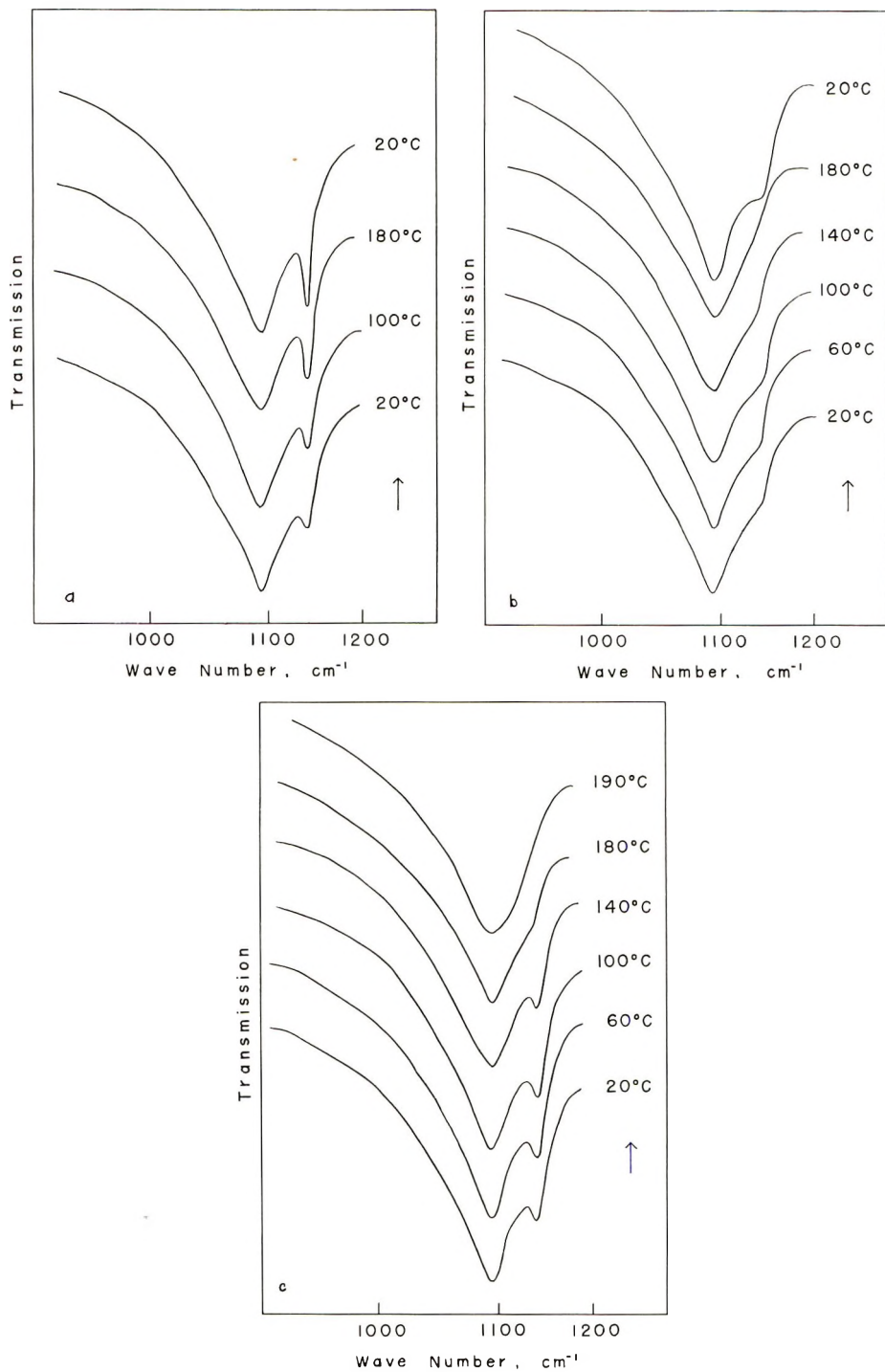


Fig. 10. Effect of temperature on the infrared absorption band at 1141 cm<sup>-1</sup> of poly(vinyl alcohol): (a) conventional poly(vinyl alcohol) cast from aqueous solution; (b) isotactic poly(vinyl alcohol) cast from aqueous solution; (c) isotactic polyvinyl alcohol made by heterogeneous hydrolysis of poly(vinyl formate).

ing vibration, shifts toward somewhat higher frequencies and shows parallel dichroism. These data strongly suggest the formation of intramolecular hydrogen bonds in isotactic PVA. In addition, the present results of x-ray and infrared examination apparently suggest that the

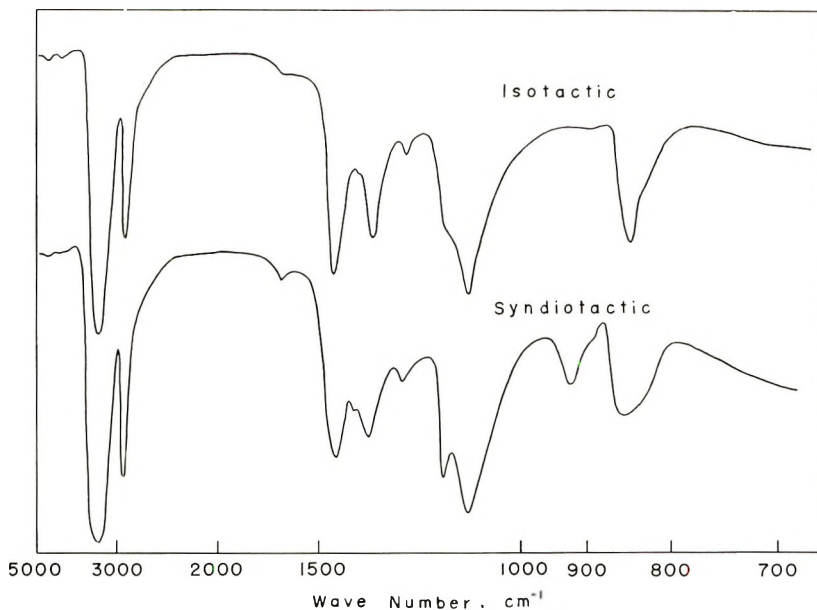


Fig. 11. Infrared spectra of isotactic and syndiotactic poly(vinyl alcohol).

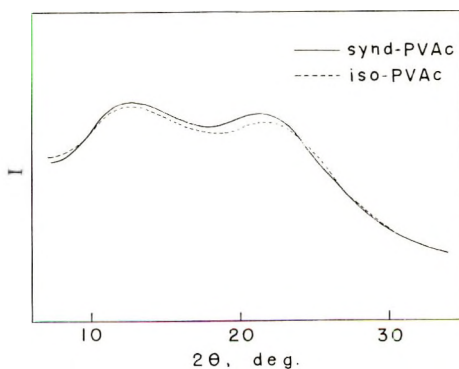


Fig. 12. X-ray diffraction curve of isotactic and syndiotactic poly(vinyl acetate).

conformation of the main chain isotactic PVA might be a planar zigzag. The cause of the lower degree of crystallizability of isotactic PVA might be ascribed to a possible preference of isotactic molecules for intramolecular, rather than intermolecular hydrogen bonding.

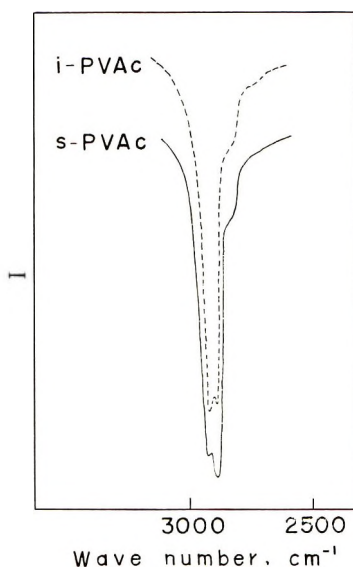


Fig. 13. A portion of the infrared spectra of isotactic and syndiotactic poly(vinyl acetate).

### Intensity of the $916\text{ cm.}^{-1}$ Band and Syndiotacticity

Another singularity observed in the spectrum of isotactic PVA is that the band at  $916\text{ cm.}^{-1}$  is practically undetectable (see Fig. 11). In the spectrum of ordinary PVA this band is observed distinctly.<sup>42,43</sup> Because of this experimental finding, intensities of the band for PVA samples of various tacticity were examined. A close relation between the band in-

TABLE IV  
 $D_{916}/D_{850}$  for Various Types of PVA

Monomer	Initiator	Solvent	Polymer- ization temp., °C.	$D_{916}/D_{850}$
Vinyl trifluoro- acetate	BPO <sup>a</sup>	None	60	0.645
Vinyl formate	$\text{B}(\text{C}_2\text{H}_5)_3$	Methyl formate	-78	0.567
Vinyl acetate	AIBN <sup>b</sup>	Methanol	0	0.437
Vinyl acetate	AIBN	Methanol	60	0.417
Vinyl benzoate	AIBN	None	60	0.305
Vinyl <i>tert</i> -butyl ether	$\text{SnCl}_4$	Ethyl bromide	-50	0.17
Vinyl <i>tert</i> -butyl ether	$\text{BF}_3 \cdot \text{O}(\text{C}_2\text{H}_5)_2$	Toluene	-78	0.02

<sup>a</sup> Benzoyl peroxide.

<sup>b</sup> 2,2'-Azobisisobutyronitrile.



tensity and the amount of syndiotactic structure was found. The ratios of the infrared absorbance at  $916\text{ cm.}^{-1}$  to that at  $850\text{ cm.}^{-1}$  for various PVA samples are given in Table IV. Some of the samples in Table IV are those that have been examined in the form of formate. The order of the  $D_{916}/D_{850}$  ratios is the same as the order of tacticities deduced from the results shown in Figures 5 and 6. It can be concluded, therefore, that this absorbance ratio can be used as a measure of syndiotacticity in PVA. Since certain problems concerning the  $916\text{ cm.}^{-1}$  band will be discussed in other reports,<sup>44</sup> further details will not be discussed here.

### Acetate and Trifluoroacetate

Isotactic PVAc prepared by acetylation of isotactic PVA gives an x-ray diagram with only amorphous halos, as does ordinary PVAc. Scanning curves for two tactic PVAc's are showing in Figure 12.

Only slight difference can be observed in their infrared spectra in the region of  $3000\text{--}650\text{ cm.}^{-1}$ . The order of the intensities of the two bands at  $2970$  and  $2930\text{ cm.}^{-1}$ , assigned to  $\text{CH}_2$  stretching, for syndiotactic PVAc is the reverse of that for isotactic PVAc, as shown in Figure 13. This relationship is apparently opposite to that observed for PVA.<sup>27,41</sup> Detailed analyses of these differences might be furthered by consideration of the conformations of the polymer molecules.

The results of these investigations have revived interest in PVTA, which had been the sole crystalline polyvinyl ester before the discovery of crystallizable PVF. (Polyvinyl esters of long chain fatty acids which show side chain crystallization<sup>45</sup> are beside the point.) Problems concerning the x-ray examination of PVTA prepared by free radical polymerization were briefly described in the introductory part of this paper. Briefly, PVTA

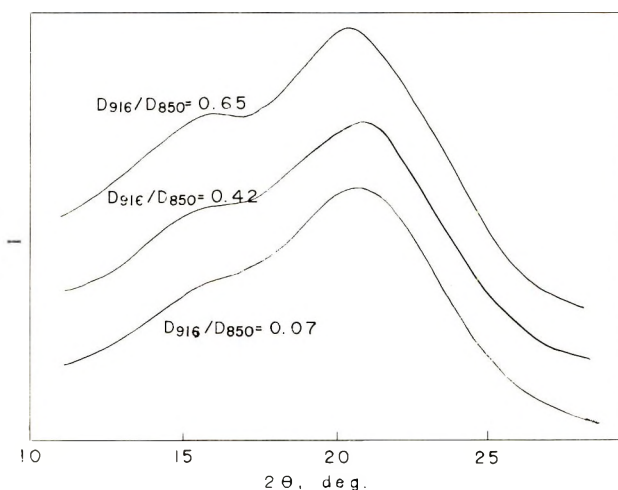


Fig. 14. X-ray diffraction curves for poly(vinyl trifluoroacetate) samples of different tacticities.

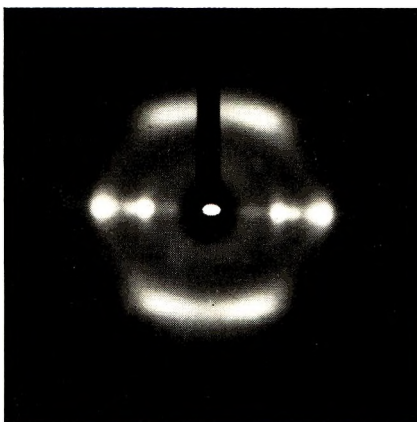


Fig. 15. Fiber pattern of syndiotactic poly(vinyl trifluoroacetate).

could not be judged to be syndiotactic from x-ray data alone. Nevertheless, the value of  $D_{916}/D_{850}$  for PVA derived from this PVTA and results of characterization of the formates show that PVTA formed by polymerization of the monomer has a predominantly syndiotactic structure.

X-ray diagrams of three PVTA samples having various tacticities are shown in Figure 14. Isotactic PVTA, when cast from solutions in acetone, gives an x-ray diagram similar to that of syndiotactic PVTA. However, the intensities of the relatively sharp inner ring increase with the syndiotactic content of the polymer. Moreover, a marked difference is observed on stretching the sample. X-ray photographs suggest that some crystallization occurs, together with orientation, in syndiotactic PVTA (see Fig. 15). Isotactic PVTA shows poor orientation on stretching, and the large number of sharp diffractions along the equator which appear in syndiotactic PVTA cannot be observed. Hence the good lateral order in PVTA might be connected with a syndiotactic structure and the fiber pattern of PVTA should be interpreted on the basis of a syndiotactic configuration. Further consideration of the fiber pattern of PVTA of the chain conformation must await more detailed analysis.

### Discussion

Definite knowledge of the steric structures of PVA has been obtained for the first time by studies of related formates. PVF is the only ester derivative which has been shown to be useful for distinguishing clearly by x-ray data between different tactic structures of the parent PVA.

High polymers of which two tactic forms have been synthesized and identified are very few. Polybutadiene,<sup>46</sup> poly(methyl methacrylate),<sup>47</sup> polybutene<sup>48</sup> have been reported to date. Now PVA is added to this group. Moreover, PVA can be converted to various ester derivatives having various crystallizabilities. Its formate takes two typical conformations corresponding to the two tactic structures—in crystalline

isotactic PVF the molecule is a  $3_1$  helix while in crystalline syndiotactic PVF the main chain is a planar zigzag. In PVAc one can investigate the effect of the steric molecular structure on various polymer properties without the influence of crystallization. The tacticities and crystallizabilities of PVA and its derivatives are summarized in Table V.

TABLE V  
Tacticities and Crystallizabilities for PVA and Its Derivatives

	Isotactic	Atactic	Syndiotactic
PVAc	Noncrystallizable	Noncrystallizable	Noncrystallizable
PVF	Crystallizable (hexagonal; $a = b = 15.9$ A., $c = 6.55$ A.)	Noncrystallizable <sup>a</sup>	Crystallizable ( $c = 5.0$ A.)
PVTA	Crystallizable <sup>b</sup>	Crystallizable ( $c = 4.8$ A.?)	Crystallizable
PVA	Crystallizable <sup>c</sup> (monoclinic; $a = 7.8$ , $b = 2.5$ , $c = 5.5$ A.)	Crystallizable	Crystallizable
PVtBE	Crystallizable ( $c = 7.58$ A.) <sup>d</sup>	Noncrystallizable	

<sup>a</sup> Shows little crystallizability.

<sup>b</sup> Very weak.

<sup>c</sup> Weak.

<sup>d</sup> Bassi et al.<sup>49</sup> have recently reported  $c = 7.65 \pm 0.05$  A.

Although a large number of investigations have been made concerning the steric structure of PVAc and of PVA, the essential facts have previously remained in doubt. The discussions were focused on the relationships between these two polymers: PVAc is very difficult to crystallize even when the molecules have a tactic structure, so that definitely crystalline products have never been observed; whereas PVA has peculiar side groups

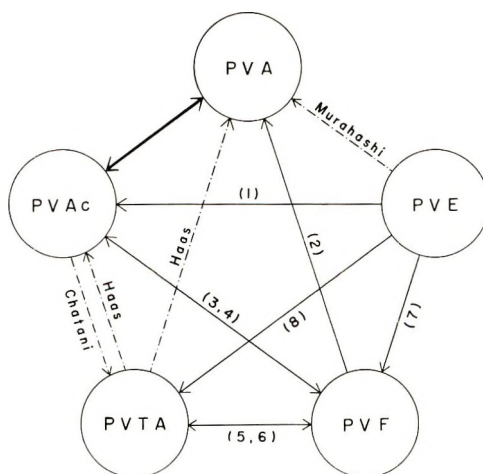


Fig. 16. Polymer transformations concerned with crystallinity and tacticity: (---) previous research; (—) present authors' research.

(OH), which are very small in size and capable of hydrogen bonding to each other.

Figure 16 relates our investigations to the previous studies, concerned with polymer transformations between these and related compounds. It has often been mentioned<sup>10,14</sup> that there is no possibility of racemization in the hydrolysis or acetylation reaction. Results of the present study are completely in accord with this.

Finally, relationships between tacticity and crystallinity in PVA remain to be discussed. At first we tried direct estimation of the amount of

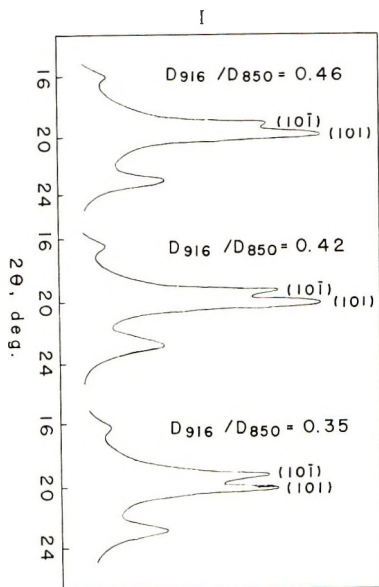


Fig. 17. Anisotropy in PVA films cast from aqueous solutions at 50°C. and heated at 215°C.

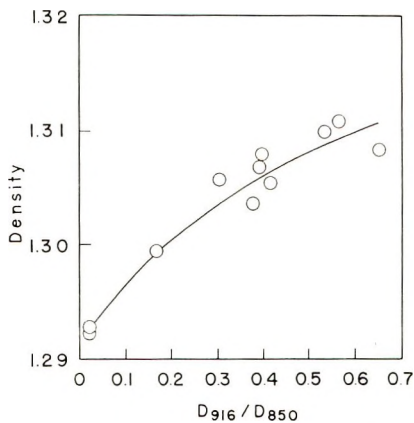


Fig. 18. Relation between density and  $D_{916}/D_{850}$  in poly(vinyl alcohol). Densities were measured by gradient tube method for PVA samples heated at 200°C.

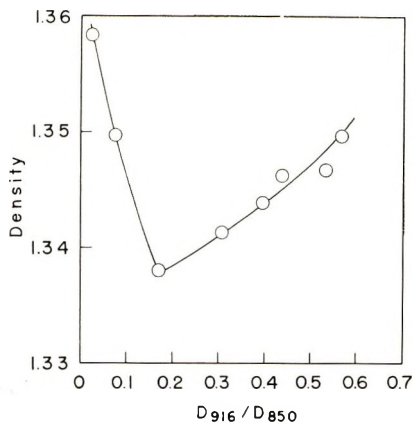


Fig. 19. Relation between density of PVF and  $D_{916}/D_{850}$  of PVA derived therefrom (gradient tube method).

the crystalline part by x-ray methods. However, strong anisotropy<sup>50</sup> was observed in PVA films cast from aqueous solution, as shown in Figure 17. This makes it very difficult to estimate the crystallinity. Therefore, densities of the samples, closely related to their crystallinity, were measured.

Densities of PVA and PVF are plotted against  $D_{916}/D_{850}$  in Figures 18 and 19, respectively. The dependence of crystallizability on the steric structure is strikingly different in these two polymers. The density of heated PVA film is slightly greater, the greater the syndiotacticity. Atactic PVF shows little crystallizability, while PVA derived therefrom exhibits a considerable degree of crystallinity. These experimental findings seem to be consistent with Bunn's<sup>51</sup> interpretation of data on atactic PVAc and PVA derived therefrom. On the other hand, tactic PVAc can also not be crystallized. Moreover, crystallinity of PVA seems to be closely related to a syndiotactic structure. Consequently, complete explanation of the crystal structure of PVA in view of the structural configuration must await more detailed analysis. We suppose that the mutual relationships between inter- and intramolecular hydrogen bonding must be considered quantitatively for elucidation of this problem.

We wish to thank Prof. I. Sakurada and Prof. S. Okamura of Kyoto University for their interest and encouragement during the work, and Dr. M. L. Huggins and Mr. Y. Sakurada of the Stanford Research Institute for their help in translating the manuscript into English.

### References

1. Mooney, R. C. L., *J. Am. Chem. Soc.*, **63**, 2828 (1941).
2. Bunn, C. W., *Nature*, **161**, 929 (1948).
3. Sakurada, I., K. Fuchino, and N. Okada, *Bull. Inst. Chem. Res., Kyoto Univ.*, **23**, 78 (1950).
4. Kakinoki, J., *Ann. Rept. Inst. Fiber Res.*, **5**, 19 (1950).



5. (a) Natta, G., P. Pino, P. Corradini, F. Danusso, E. Mantica, G. Mazzanti, and G. Moraglio, *J. Am. Chem. Soc.*, **77**, 1708 (1955); (b) M. L. Huggins, *J. Am. Chem. Soc.*, **66**, 1991 (1944).
6. Hercules Powder Co., Brit. Pat. 819,291 (Sept. 1956).
7. Hercules Powder Co., Japanese Pat. Announcement 12539 (Aug. 1962).
8. Haas, H. C., E. S. Emerson, and N. W. Schuler, *J. Polymer Sci.*, **22**, 219 (1956).
9. Ito, T., K. Noma, and I. Sakurada, *Kobunshi Kagaku*, **16**, 115 (1959).
10. Fordham, J. W. L., G. H. McCain, and L. E. Alexander, *J. Polymer Sci.*, **34**, 335 (1959).
11. Imai, K., and M. Matsumoto, *J. Polymer Sci.*, **55**, 335 (1961).
12. Chatani, Y., I. Taguchi, T. Sano, and T. Takizawa, paper presented at Symposium on Polymer Chemistry, Nagoya, October 1957 (preprint).
13. Sakurada, I., and T. Ito, private communication.
14. Bohn, C. R., J. R. Schaeffgen, and W. O. Statton, *J. Polymer Sci.*, **55**, 531 (1961).
15. Ukida, J., R. Naito, and T. Kominami, *Kogyo Kagaku Zasshi*, **58**, 128, 717 (1955).
16. Imai, K., U. Maeda, J. Ukida, and M. Matsumoto, *Kobunshi Kagaku*, **16**, 446 (1959).
17. Sakurada, I., Y. Nukushina, and T. Ito, paper presented at Symposium on Polymer Chemistry, Kyoto, November 1960 (preprint).
18. Fujii, K., and T. Inoue, unpublished work, cited by Fujii et al.<sup>31</sup>
19. Kazusa, Y., and K. Imai, paper presented at Annual Meeting of Chemical Society, Japan, Tokyo, April 1961.
20. Matsumoto, M., and Y. Ohyanagi, *J. Polymer Sci.*, **26**, 389 (1957).
21. Matsumoto, M., and Y. Ohyanagi, unpublished work; R. Naito, unpublished work.
22. Imai, K., and U. Maeda, *Kobunshi Kagaku*, **16**, 499 (1959).
23. Matsumoto, M., and Y. Ohyanagi, *J. Polymer Sci.*, **37**, 558 (1959).
24. Murahashi, S., T. Sano, and B. Ryutani, paper presented at Symposium on Polymer Chemistry, Nagoya, October 1957 (preprint); paper presented at Annual Meeting of Society of Polymer Science, Tokyo, May 1958.
25. Fujii, K., paper presented at Meeting on Polymer Research, Kobe, June 1960.
26. Murahashi, S., H. Yuki, and U. Yonemura, paper presented at Annual Meeting of Society of Polymer Science, Tokyo, May 1961.
27. Okamura, S., T. Kodama, and T. Higashimura, paper presented at Annual Meeting of Society of Polymer Science, Tokyo, May 1961; *Makromol. Chem.*, **53**, 180 (1962).
28. Fujii, K., and T. Mochizuki, paper presented at Symposium on Polymer Chemistry, Tokyo, November 1961 (preprint); *Kobunshi Kagaku*, **19**, 124 (1962).
29. Nagai, E., S. Kuribayashi, M. Shiraki, and M. Ukita, *J. Polymer Sci.*, **35**, 295 (1959).
30. Ambrose, E. J., A. Elliot, and R. B. Temple, *Proc. Roy. Soc. (London)*, **A199**, 183 (1940).
31. Fujii, K., S. Imoto, T. Mochizuki, J. Ukida, and M. Matsumoto, paper presented at Symposium on Polymer Chemistry, Kyoto, November 1960 (preprint); *Kobunshi Kagaku*, **19**, 587 (1962).
32. Fujii, K., S. Imoto, J. Ukida, and M. Matsumoto, *Kobunshi Kagaku*, **19**, 575 (1962).
33. Fujii, K., T. Mochizuki, S. Imoto, J. Ukida, and M. Matsumoto, *Makromol. Chem.*, **51**, 225 (1962).
34. Katz, J. R., *Trans. Faraday Soc.*, **32**, 77 (1936).
35. Bunn, C. W., and E. R. Howells, *J. Polymer Sci.*, **18**, 307 (1955).
36. Fordham, J. W. L., *J. Polymer Sci.*, **39**, 324 (1959).
37. Lal, J., *J. Polymer Sci.*, **31**, 179 (1958).
38. Natta, G., G. Dall'Asta, G. Mazzanti, U. Giannini, and S. Cesca, *Angew. Chem.*, **71**, 205 (1959).
39. Okamura, S., T. Higashimura, and I. Sakurada, *J. Polymer Sci.*, **39**, 507 (1959).

40. Natta, G., P. Corradini, and W. Bassi, *Nuovo Ciment, Suppl.*, **15**, 68 (1960).
41. Murahashi, S., H. Yuki, H. Tadokoro, Y. Chatani, U. Yonemura, K. Fukuda, and M. Tsutsui, paper presented at Annual Meeting of Society of Polymer Science, Tokyo, May 1961.
42. Krimm, S., C. Y. Liang, and G. B. B. M. Sutherland, *J. Polymer Sci.*, **22**, 227 (1956).
43. Tadokoro, H., *Bull. Chem. Soc. Japan*, **32**, 1334 (1959).
44. Fujii, K., and J. Ukida, *Makromol. Chem.*, **65**, 74 (1963).
45. Jordan, E. F., Jr., W. E. Palm, D. Swern, L. P. Witnauer, and W. S. Port, *J. Polymer Sci.*, **32**, 33 (1958).
46. Natta, G., *Chim. Ind. (Milan)*, **38**, 751 (1956).
47. Fox, T. G., B. S. Garrett, W. E. Goode, S. Gratch, J. F. Kincaid, A. Spell, and J. D. Stroup, *J. Am. Chem. Soc.*, **80**, 33 (1958).
48. Natta, G., *Makromol. Chem.*, **35**, 94 (1960).
49. Bassi, J. W., G. Dall'Asta, V. Campigli, and E. Strepparola, *Makromol. Chem.*, **60**, 202 (1963).
50. Mochizuki, T., *J. Chem. Soc. Japan*, **80**, 834, 1090, 1203 (1959).
51. Bunn, C. W., *J. Appl. Phys.*, **25**, 821 (1954).

### Résumé

L'étude des structures stériques de l'alcool polyvinylique est déduite des études des structures de ses esters, particulièrement le formiate de polyvinyle. Deux types de formiate de polyvinyle tactiques cristallisent avec des différences structurales correspondant à leur structures moléculaires différentes. Donc le type de stéréorégularité moléculaire des échantillons de formiate de polyvinyle peut être déduit d'un examen de cristaux produits par une cristallisation donnée. À partir des résultats de l'étude des cristaux de formiate de polyvinyle, plusieurs conclusions peuvent être tirées concernant la structure stérique de l'alcool polyvinylique. Le pouvoir de cristallisation d'autres esters polyvinyliques tactiques a également été étudié.

### Zusammenfassung

Es werden Untersuchungen über die sterische Struktur von Polyvinylalkohol auf der Basis von Strukturuntersuchungen an seinen Estern, insbesondere an Polyvinylformiat, beschrieben. Zwei Typen von taktischem Polyvinylformiat kristallisieren entsprechend ihrer verschiedenen molekularen Struktur in verschiedenen Strukturen. Daher kann die Art der Stereoregularität von Polyvinylformiatproben durch eine Prüfung der mittels einer gegebenen Kristallisationsbehandlung hergestellten Kristalle festgestellt werden. Aus den Ergebnissen der Untersuchung von Polyvinylformiatkristallen können gewisse Schlüsse auf die sterische Struktur von Polyvinylalkohol gezogen werden. Ausserdem wurde das Kristallisationsvermögen anderer taktischer Polyvinylester untersucht.

Received May 6, 1963

## Negative Spherulite of Poly- $\gamma$ -Methyl-L-Glutamate and Effect of Aging Polymer Solution on Spherulite Growth

SABURO ISHIKAWA, TOSHIO KURITA, and EIKICHI SUZUKI,  
*The Textile Research Institute of Japanese Government, Yokohama,  
Japan*

### Synopsis

Poly- $\gamma$ -methyl-L-glutamate was obtained by the NCA method in a chloroform solution using trimethylamine as initiator. After polymerization, the solution was left alone for a long time at room temperature before spherulites formed. A film was casted very slowly from this aged solution in a desiccator at room temperature. We could then obtain spherulites in these thin films. This aging treatment was one of the main factors in making the spherulites. The morphological structure, optical properties, and the molecular orientation of the spherulites were examined by infrared spectroscopy, the x-ray method, and electron microscopy. After short aging periods (1-6 months), we could obtain positive spherulites. After much longer aging periods (6-10 months), negative spherulites were obtained. The conformation of the molecules in both spherulites was the same—the so-called  $\alpha$ -helical conformation, but the orientation of the  $\alpha$ -helical axis in the spherulites was just the opposite. In the positive spherulites, the helical axes oriented along the radius, but in negative spherulites, the helical axes oriented along the tangential direction. These positive and negative spherulites were constructed with microfibriles the diameters of which were about 45-67 Å. The orientation of these microfibriles in the spherulites was just the same as the  $\alpha$ -helical axes' orientation. These microfibriles oriented by side-by-side association in making the layer structure in the spherulites so that the  $\alpha$ -helical axes were aligned parallel to these layers. Also, no evidence was observed of the presence of the so-called folding orientation of these  $\alpha$ -helical molecules or microfibriles, as was pointed out in the case of polyethylene. From these results, we know that the crystallization habits of helical molecules, such as polypeptides, were different from those of polyethylene. The helical axes of the polypeptide molecules were not oriented perpendicular to the layer surface of the spherulites, but parallel to the layer surface. The crystallization mechanism of polypeptide was not by the so-called folding mechanism, but by the side-by-side crystallization mechanism.

In a previous paper,<sup>1</sup> we reported on the fine structure of spherulites of poly- $\gamma$ -methyl-L-glutamate (PMLG). At that time, we stated that only after long aging time could we obtain a fine spherulite and that the aging time is one of the main factors in formation of spherulites.

After a much longer aging time than that used in the previous paper, we obtained another type of spherulite. Some conclusions about these phenomena were also arrived at: namely, the crystallization mechanisms of these helical molecules was apparently different from that of random coil

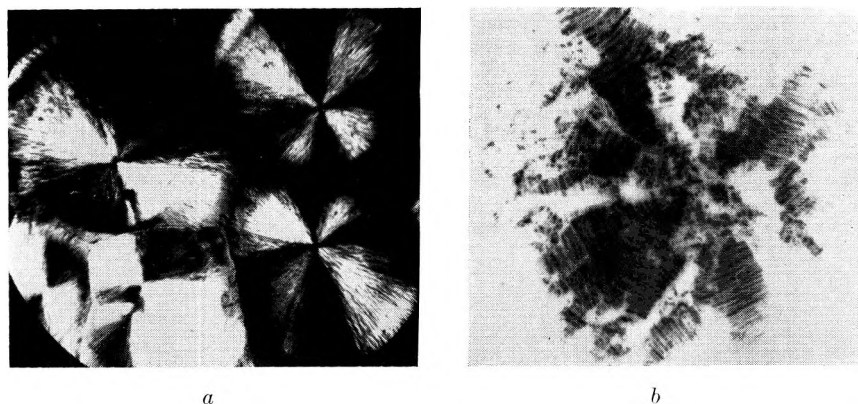


Fig. 1. Photographs of (a) positive and (b) negative spherulites of PMLG made from chloroform solution at room temperature, in polarized light. 480 $\times$ .

molecules such as polyethylene or nylon. The crystallization of these helical molecules was carried out not by a folding mechanism<sup>2</sup> but by a side-by-side orientation mechanism.

In the present paper, we wish to describe the results obtained in infrared spectra, x-ray diffraction and electron microscopy studies. The apparatus used in these studies were the same as that of previous paper, except using the electron microscope—the JEM 6A-Type.

The representative morphological structure of these positive and negative spherulites are shown in Figure 1. In the negative spherulite we observed many parallel stripes oriented to the tangential directions of the spherulites. The infrared spectrum obtained from the thinner part of the spherulite is shown in Figure 2. (For convenience in comparing with these two spectra, the spectrum of the positive spherulite is also shown.) The dichroism of these spectra is summarized in Table I. From the frequencies of these spectra and the results of Miyazawa,<sup>3</sup> it is suggested that the PMLG molecules have  $\alpha$ -helical conformations in both spherulites but the orientation of the helical molecules is just the opposite. In the positive spherulite, as was mentioned in previous paper, the helical axes are oriented almost

TABLE I  
Infrared Dichroism of the Positive and Negative Spherulites at Characteristic Frequencies

Absorption band	Wave number, cm. <sup>-1</sup>	Dichroism of the spherulite	
		Positive	Negative
N-H Stretching	3280		⊥
Amide I	1653		⊥
Amide II	1545	⊥	
Amide II	1516		⊥
Amide III	1254	⊥	
Amide V	617	—	—

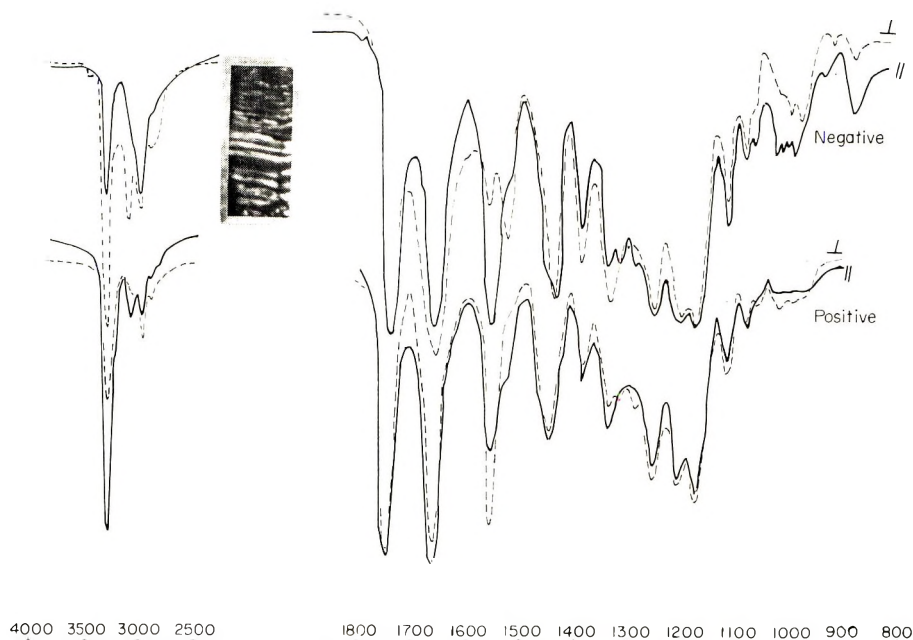


Fig. 2. Polarized infrared spectrum of the positive and negative spherulite is just the opposite at each of the characteristic frequencies. Photograph shows a part of the negative spherulite from which these spectra were obtained.

radially, but in the negative one the helical axes lie almost tangentially. Furthermore, the amide V band appears at  $617\text{ cm.}^{-1}$  in the KBr region, and this band position is characteristic of the  $\alpha$ -helical conformation.<sup>4</sup>

Further information on the conformation and the orientation of PMLG molecules in the spherulite was obtained by x-ray diffraction as shown in Figure 3. This photograph shows a typical fibrous pattern, very similar to that of Bamford et al.<sup>5</sup> The spacings obtained from the photograph agree well with Bamford's results except for some new spots. More detailed investigation of these new spots will be discussed in future. However, we know that the helical axes of PMLG molecules are oriented parallel to the stripes of the spherulite. Putting together the information from Figures 1 and 3, we know that the helical axes of PMLG molecules lie tangentially in the spherulite. These x-ray diffraction results agree very well with results of the infrared spectrum examination.

Additional evidence of the orientation of the helical axes was obtained from electron microscope observations, as shown in Figure 4. In Figure 4a, a part of the positive spherulite is shown, and in Figure 4b, a part of the negative spherulite. From these observations, we know that (1) the direction of microfibrils along the radius of the spherulite, is just the opposite of those between them; (2) the diameter of the microfibrils is just the same (about 45–67Å.) in both cases; (3) the orientation of these microfibrils is carried out by side-by-side orientation; (4) the degree of orienta-



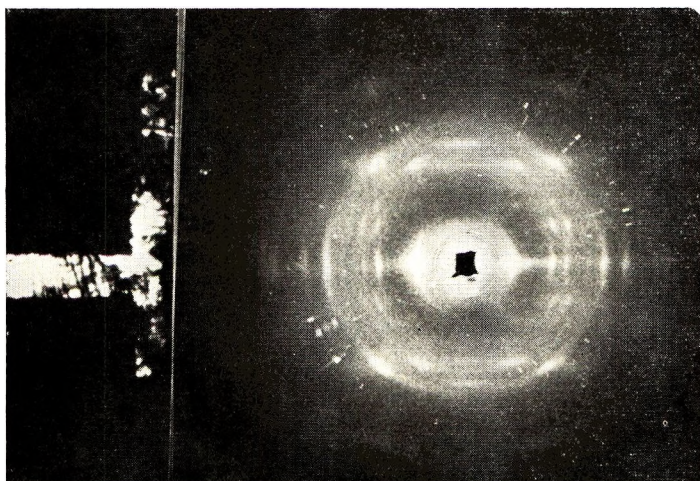


Fig. 3. X-ray diffraction photograph of (right) negative spherulite and (left) a part of the negative spherulite from which the photograph was obtained.

tion or packing of microfibrils in the negative spherulite is much higher than in the positive one; (5) the form of orientation of microfibrils in the positive spherulite is somewhat different from that of the negative one and seems like that of a Japanese *tatami* sheet. Some regular orientation pattern, about 900–1100 Å. long spacings at right angles to the microfibril direction, are found in the positive spherulite but not in negative one. Some of these results especially (1) and (4), agree very well with the results of infrared spectral and x-ray examination.

The dimensions of the diameter of the microfibrils are an average of Pauling and Corey's  $\alpha$ -helix AB6 cable model and Fraser's (9 + 2) microfibril model. However, we could not find any evidence for a coiled coil structure within these microfibrils at present. Also we could not find any evidence for U-type folding of microfibrils. It seems more reasonable to assume that there is no U-type folding of the helical molecules within these microfibrils. If this were true, we could suppose that the crystallization mechanism of these helical molecules were not like that in the case of polyethylene or nylon as proposed by Keller,<sup>2</sup> but rather that it involved side-by-side orientation.

During long aging periods, these helical molecules associate with each other in a side-by-side manner, as was suggested by Flory<sup>5</sup> and Wada.<sup>6</sup> Such aggregation becomes more marked with increasing aging time. A fairly oriented aggregation of solvated helical molecules is obtained already even in solution. This leads to formation of a highly oriented negative spherulite.

This aging effect is also apparent from the data of Table II, in which some relations between aging time, morphological appearance, birefringence of the spherulite, and composition of the solvent from which the spherulite is obtained are shown. The birefringence of the negative spherulite is

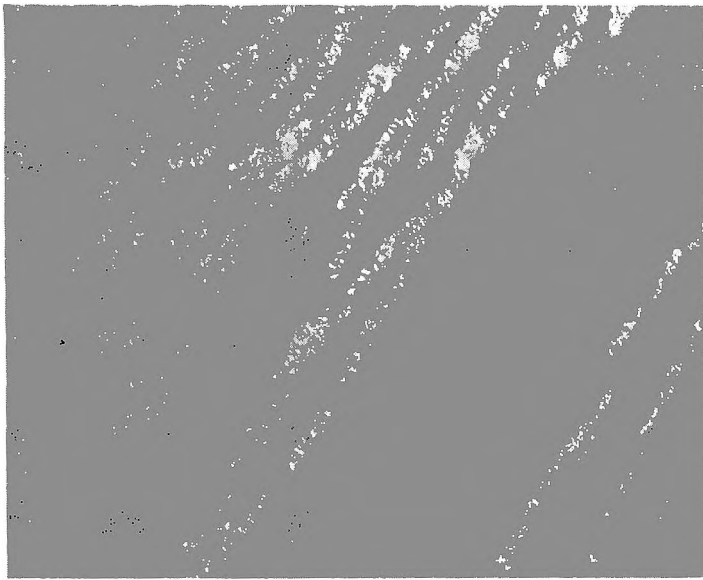
*a**b*

Fig. 4. Electron micrographs of the spherulite: (a) positive (direct); (b) negative (Pt-Pd-replica). 30,000 $\times$ .

higher than that of the positive one. This result agrees well with the x-ray diffraction pattern as shown in Figure 3 and Figure 4 of the previous paper.<sup>1</sup> If the solution contained a poor solvent such as dioxane, we could not

TABLE II  
Relation between Aging Time and Some Properties of the Spherulite

Solvent composition	Aging time, months	Optical sign	Morphological appearance of spherulite <sup>a</sup>	$\Delta n \times 10^2$
Chloroform	1	+	f	
Chloroform	2	+	f	
Chloroform	3	+	ff	
Chloroform	3.5	+ -	vf	0.3
Chloroform	4	+	vf	0.7 <sup>b</sup>
Chloroform	10	-	vf	2.4
Chloroform	0.5	+	f	
Chloroform-dioxane, 3:1	2	+	vf	
Chloroform-dioxane, 3:1	8	+	vf	
Chloroform-dioxane, 5:1	9	+	vf	
Fiber		+		1.9 <sup>c</sup>

<sup>a</sup> f denotes fine or not in morphological view point; ff denotes fairly fine; vf denotes very fine.

<sup>b</sup> Original solution (about 2% concn.) was diluted about four times before casting.

<sup>c</sup> The conformation of molecules in the fiber is almost an  $\alpha$ -helical conformation after drawing (draw ratio 2).

obtain a fine and fairly oriented spherulite. It seems that dioxane promotes poorer oriented aggregation than pure chloroform solution during aging.

We wish to express our thanks to the Ajino-moto Company for their kindness in supplying the PMLG.

### References

1. Ishikawa, S., T. Kurita, and E. Suzuki, *J. Polymer Sci.*, **B1**, 127 (1963).
2. Keller, A., *Phil. Mag.*, **2**, 1171 (1957).
3. Miyazawa, T., and E. R. Blout, *J. Am. Chem. Soc.*, **83**, 712 (1961).
4. Masuda, Y., T. Miyazawa, and J. Noguchi, paper presented at the 15th Annual Meeting of the Japanese Chemical Society, Kyoto, 1962.
5. Flory, P. J., *J. Polymer Sci.*, **49**, 105 (1961).
6. Wada, A., *J. Polymer Sci.*, **45**, 145 (1960).

### Résumé

Le poly- $\gamma$ -méthyl-L-glutamate a été obtenue par la méthode NCA en solution dans le chloroforme en employant de la triméthylamine comme initiateur. Après polymérisation, la solution est laissée à température de chambre pendant un long moment juste avant la formation de sphérulites. De cette solution on a coulé un film très lentement à température de chambre et en présence d'un dessiccateur. Ensuite nous avons pu obtenir une sphérulite dans ces minces films. Cette sorte de traitement est un des principaux facteurs pour former un sphérulite. La structure morphologique, les propriétés optiques du sphérulite et l'orientation moléculaire furent examinées en employant la spectroscopie IR, la méthode au rayons-X et le microscope électronique. Après de courtes périodes de réactions (1-6 mois), nous avons pu obtenir un sphérulite positif. Après de longues

périodes de réaction (6–10 mois) un sphérulite négatif a été obtenu. La conformation des molécules chez les deux sphérulites est la même et ils possèdent la conformation en hélice- $\alpha$ . Mais l'orientation des axes de l'hélice- $\alpha$  dans le sphérulite était exactement opposés entre eux. Dans le sphérulite positif les axes hélicoïdaux sont orientés le long du rayon du sphérulite, mais dans le sphérulite négatif les axes hélicoïdaux sont orientés dans la direction tangentielle au sphérulite. Le sphérulite positif et négatif sont construits avec des microfibrilles qui ont un diamètre d'environ 45–67 Å. L'orientation de ces microfibrilles dans le sphérulite est exactement la même que l'orientation des axes de l'hélice- $\alpha$ . C'est-à-dire que les molécules de l'hélice- $\alpha$  sont orientées dans ces microfibrilles le long de leurs axes dans les sphérulites respectifs. Ces microfibrilles sont orientées suivant une association "côte-à-côte" en formant une structure en couche dans le sphérulite. Ainsi les axes  $\alpha$ -hélicoïdaux sont alignés parallèlement à ces couches, et ainsi nous n'avons pas pu trouver l'évidence de la présence de l'orientation dirigée de ces molécules  $\alpha$ -hélicoïdales ou microfibrilles comme cela fut montré dans le cas du polyéthylène ou il en est ainsi. De ces résultats nous savons que les habitudes de cristallisation des molécules hélicoïdales telles que les polypeptides sont différentes de celles du polyéthylène. Les axes hélicoïdaux des molécules de polypeptides ne sont pas orientés perpendiculairement à la surface des couches du sphérulite, mais parallèlement à la surface de cette couche. Le mécanisme de cristallisation de polypeptides n'a pas été appelé le mécanisme dirigé mais le mécanisme de cristallisation côte-à-côte.

### Zusammenfassung

Poly- $\gamma$ -methyl-L-glutamat wurde nach der NCA-Methode in Chloroformlösung mit Trimethylamin als Starter hergestellt. Nach der Polymerisation liess man die Lösung vor der Herstellung der Sphärolithe lange Zeit bei Raumtemperatur stehen. Aus diesen gealterten Lösungen wurde im Exsikkator bei Raumtemperatur sehr langsam ein Film gegossen. In diesen dünnen Filmen bildete sich ein Sphärolith aus. Die beschriebene Alterungsbehandlung spielte bei der Herstellung der Sphärolithe eine wesentliche Rolle. Morphologische Struktur und optische Eigenschaften des Sphäroliths sowie die molekulare Orientierung im Sphärolith wurde mittels IR-Spektroskopie, Röntgenbeugung und Elektronenmikroskopie untersucht. War die Alterungszeit kurz (1–6 Monate), so entstande in positiver Sphärolith, während bei bedeutend längerer Alterungszeit (6–10 Monate) ein negativer Sphärolith erhalten wurde. In beiden Sphärolithen lagen die Moleküle in der sogenannten  $\alpha$ -Helix-Konformation vor, jedoch war die Achse der  $\alpha$ -Helix im Sphärolith in den beiden Fällen entgegengesetzt orientiert. Während im positiven Sphärolith die Helixachse in Richtung des Sphärolithradius orientiert war, war sie im negativen Sphärolithen längs der tangentialen Richtung des Sphärolithen ausgerichtet. Diese positiven und negativen Sphärolithe sind aus Mikrofibrillen mit einem Durchmesser von etwa 45–67 Å aufgebaut. Die Orientierung dieser Mikrofibrillen im Sphärolith war gleich derjenigen der Achse der  $\alpha$ -Helix, d.h. die  $\alpha$ -helixförmigen Moleküle waren innerhalb dieser Mikrofibrillen längs ihrer Achse im entsprechenden Sphärolith ausgerichtet. Diese Mikrofibrillen waren durch eine seitliche Assoziation unter Bildung von Schichtstrukturen im Sphärolithen ausgerichtet, so dass die Achsen der  $\alpha$ -Helices parallel zu diesen Schichten sind. Es konnte kein Hinweis auf das Vorliegen einer sogenannten Faltungsorientierung dieser  $\alpha$ -helixförmigen Moleküle oder Mikrofibrillen gefunden werden, wie sie etwa im Falle von Polyäthylen festgestellt wurde. Auf Grund dieser Befunde nimmt man an, dass das Kristallisationsverhalten helixförmiger Moleküle wie der Polypeptide von demjenigen von Polyäthylen verschieden ist. Die Helixachsen der Polypeptidmoleküle sind nicht senkrecht zur Schichtoberfläche des Sphärolithen, sondern parallel dazu orientiert und die Kristallisation der Polypeptide erfolgt nicht nach einem sogenannten Faltungsmechanismus, sondern nach einem Seite-an-Seite-Kristallisationsmechanismus.

Received May 6, 1963



## Temperature-Independent Viscosity Characteristics of Polymer Systems

G. V. VINOGRADOV and A. Ya. MALKIN, *Institute of Petrochemical Synthesis, Academy of Sciences of the U.S.S.R., Moscow, U.S.S.R.*

### Synopsis

The possibility of construction of temperature-independent viscosity characteristics of polymer systems by means of a "reduced variables" method similar to that of Ferry is discussed. It is stated that the viscosity as a function of temperature and shear rate can generally be regarded as the product of two functions, one of which depends only on the temperature and the other only on the shear rate. It is shown by dimension analysis and by assuming the flow of polymer systems to be viscoelastic in nature, that the ratio of apparent viscosity to initial Newtonian viscosity is a temperature-independent function of the product of the shear rate by the initial Newtonian viscosity. Hence, the latter (observed at shear rates tending to zero) appears to be a most important physical parameter governing the flow properties of polymer systems. At sufficiently low shear rates the apparent viscosity was found to be an exponential function of shear stress, so that the initial Newtonian viscosity can be determined by extrapolation. The above theoretical considerations were checked for the most reliable published data on the flow properties of condensed polymer systems over a wide range of shear rates and temperatures. Experimental results obtained for polymer systems of different nature can be represented satisfactorily by corresponding temperature-independent viscosity curves.

### Introduction

The steady viscosity of non-Newtonian polymer systems varies with the shear rate (or with the similarly dependent shear stress) and with the temperature. The relation between viscosity and temperature is most complicated and offers but little opportunity for theoretical analysis. This is why the problem of presenting viscometric data independent of temperatures deserves special attention.

The possibilities of temperature-independent presentation of the dynamical characteristics of elastomers, i.e., of the real and imaginary parts of a complex modulus of rigidity, compliance, etc., have already been investigated extensively. Ferry and his collaborators<sup>1</sup> found first, empirically, and later on the basis of the molecular theory of the high resilience of polymers, that experimental curves obtained at various temperatures can be matched by simple parallel shifting. A similar study was performed by Tobolsky et al.<sup>2</sup>

Arveson,<sup>3</sup> followed by Brunstrum et al.,<sup>4</sup> investigating the rheological properties of lubricants, proved by exclusively empirical methods, that in



the materials investigated by them, the relative viscosity versus shear rate curves match well if shifted parallel along the shear rate axis. Relative viscosity is to be understood here as the ratio of the lubricant viscosity in the experiment, to the viscosity of the dispersion media at the same temperature.

A number of papers<sup>5</sup> give results of investigations on the possibility of presenting concentration-independent viscosity characteristics of polymer solutions, as well as empirically determined reduced coordinates, in which the relation of the solution viscosities versus shear rate can be given divorced from the polymer concentration in the system.

Philippoff and Gaskins,<sup>6</sup> investigating the flow of polymer melts, concluded that experimental data cannot be confined to a single curve if a wide range of shear rates (up to 6 or 7 decimal orders) is concerned. In a narrow variation range of this factor, however (within 2 or 2.5 decimal orders), Ito<sup>7</sup> who investigated melted polyamides, as well as Schott and Kaghan<sup>8</sup> in their research on polyethylene flow, succeeded in matching their viscosity-shear rate curves obtained at different temperatures. Ito used an exclusively empirical method. Schott and Kaghan, attempting to set up a theoretical basis for their method, assumed that the effective viscosity is inversely proportional to the square shear rate (at adequately high shear rates), which, however, seems quite doubtful.

Thus, the now available data on temperature-independent characteristics of the viscosity of polymer systems appear to be rather incidental, and in some cases baseless.

A theory is suggested in this paper for establishing temperature-independent viscosity characteristics of polymer systems. The possibility of such a representation is confirmed by an analytical review of various earlier published data on the flow of high polymers. The method developed in this paper is similar to some extent to that employed by Ferry.<sup>1</sup>

### Theory

The steady viscosity of polymer systems depends on the applied stresses (or on the shear rates unambiguously related to them at a given temperature) as well as on the relaxation spectrum, characteristic of the viscoelastic materials concerned. It can be assumed that

$$\eta = \eta_{\max} f(\theta, D) \quad (1)$$

where  $\eta$  is the viscosity of the polymer system,  $D$  is the steady shear rate, and  $\theta$  is the apparent relaxation time expressed in units of time and depending on the entire set of relaxation times of the investigated polymer system, i.e.,

$$\theta = \varphi(\theta_1, \theta_2, \dots, \theta_n) \quad (2)$$

In the simplest event, a single characteristic relaxation time can be substituted for the entire spectrum. In eq. (1),  $\eta_{\max}$  denotes the initial Newtonian viscosity of the system at the given temperature, or

$$\eta_{\max} = \lim_{D \rightarrow 0} \eta$$

and

$$\lim_{D \rightarrow 0} f(\theta, D) = 1$$

The following should be pointed out regarding the functions established above.

The function  $f(\theta, D)$  is dimensionless, since it is simply the ratio of two viscosities  $\eta/\eta_{\max}$ , and its arguments have mutually inverse dimensions. This can occur if and only if  $f(\theta, D)$  is a function of a product of its arguments, i.e.,

$$\eta/\eta_{\max} = f(\theta, D) = f(\theta, D) \quad (3)$$

The function  $\varphi(\theta_i)$  is a homogeneous function of the first order. This is likewise the result of dimensional effects, since the dimensions of all arguments  $\theta_i$  are the same as that of the function  $\theta$  itself. Thus, multiplying all arguments  $\theta_i$  by some coefficient means but a change in the  $\theta_i$  scale and should give no other result than a change of the scale in which function  $\theta$  is expressed. Hence,

$$\varphi(A\theta_i) = A\varphi(\theta_i) \quad (4)$$

Let us now consider the molecular theories concerning the temperature relations of those properties of polymer systems which interest us.

As far back as 1948 and 1949, Kargin and Slonimskii<sup>9</sup> suggested a model for the mechanical behavior of polymers which most satisfactorily illustrated the main characteristic features of relaxation in the deformation of amorphous, linear polymers. Later, Rouse<sup>10</sup> studied the relationships between the internal structure of polymers, the temperature, and the characteristic relaxation spectrum. It can be concluded from these molecular theories, in particular, that the  $i$ th relaxation time can be represented by the formula

$$\theta_i = a_i \frac{\eta_{\max}(T)}{\rho(T) T} \quad (5)$$

where  $\rho$  is density.

The coefficient  $a_i$ , used in the theories of both studies,<sup>9,10</sup> is expressed in different ways. This is not the subject of the present discussion, but one fact is important, namely, that in neither of these theories does the value of  $a_i$  depend on the temperature. The relaxation spectrum appears in the said theories<sup>9,10</sup> as independent of the shear rate  $D$ ; hence,  $a_i$  does not depend on it either. Actually, however, this is not always the case. If  $\theta_i$  is a function of  $D$ , this function can be taken into account for a general consideration, assuming that the influence of the shear rate is contained in the coefficient  $a_i$ . The exact form of this factor is of no interest for the

theory presented herein, only its independence of the temperature being essential.

It can be seen from eq. (5) that the relation between the  $i$ th relaxation time at a given temperature and at an arbitrarily selected reference temperature (all values pertaining to this temperature being henceforth marked with primes), can be expressed as follows:

$$\frac{\theta_i}{\theta_i'} = \left[ \frac{\eta_{\max}(T)}{\eta'_{\max}(T)} \right] \left[ \frac{\rho'T'}{\rho T} \right] \quad (6)$$

Let us now substitute the values of  $\theta_i$  obtained from eq. (6) into eq. (4) resulting from the homogeneity of the function  $\varphi(\theta_i)$ . We obtain then a formula for reducing the relaxation spectrum at any temperature  $T$  to the reference temperature  $T'$ :

$$\varphi(\theta_i) = \varphi'(\theta_i') \left[ \frac{\eta_{\max}(T)}{\eta'_{\max}(T)} \right] \left[ \frac{\rho'T'}{\rho T} \right] \quad (7)$$

or

$$\theta = \theta' \left[ \frac{\eta_{\max}(T)}{\eta'_{\max}(T)} \right] \left[ \frac{\rho'(T)T'}{\rho(T)T} \right]$$

Introducing the expression (7) into the general viscosity formula (2) we get the following relation:

$$\frac{\eta}{\eta_{\max}} = f \left\{ D\eta_{\max}(T) \left[ \frac{\rho'T'}{\rho T} \right] \left[ \frac{\theta'}{\eta'_{\max}(T)} \right] \right\} \quad (8)$$

For a selected reference temperature the value of  $\theta'/\eta'_{\max}(T)$  in eq. (8) will be constant; hence the ratio  $\eta/\eta_{\max}$  may be regarded as a function of the type

$$\eta/\eta_{\max} = f(D\eta_{\max}\rho'T'/\rho T) \quad (9)$$

Thus, the complicated argument in the initial relation (1) can be replaced by another argument consisting only of variables subject to direct experimental measurement. If we denote the ratio  $\eta/\eta_{\max}$  by  $\eta_r$  (reduced viscosity, dimensionless), and the argument of function (9) by  $D_r$  (reduced shear rate, but in dimensions of stress), the result will be  $\eta_r = f(D_r)$ . This is a single-valued function, which should not vary with the temperature.

Thus, the theory set forth herein is based on the main assumption that the  $i$ th relaxation time can be represented as a product of two functions, one of which is independent of the temperature and the other expressed as  $\eta_{\max}/\rho T$ , as follows from some earlier publications.<sup>9,10</sup> Hence, the above basic assumption is close to that used by Ferry<sup>1</sup> in considering the temperature relation of the dynamical characteristics of the viscoelastic properties of elastomers, Ferry having supposed that any relaxation time varies with the temperature in a similar manner.

Experimental investigations of the relation between viscosity and shear rate are often conducted over a very wide range of shear rates. Logarithmic graphs are therefore usually employed to present the experimental results. It becomes evident that the relation between  $\log \eta_r$  and  $\log D_r$  may be treated as a temperature-independent characteristic. If the selected reference temperature  $T'$  is between the melting or softening temperature on the one hand and perceptible incipient polymer decomposition on the other, the value of  $\rho'T'/\rho T$  will differ but slightly from 1 (by not more than 6-8% for most commercial polymers), i.e., the value of  $\log(\rho'T'/\rho T)$  will be within  $\pm 0.03$ . When the viscosity measurements are made over a shear-rate range covering several decimal orders (usually from 3 to 7 or 8), the above correction is negligible. And, where the value of  $\rho'T'/\rho T$  can be neglected, the reduced shear rate can be calculated by the simplified formula:

$$D_r = D\eta_{\max}(T)$$

or

$$\log D_r = \log D + \log \eta_{\max}$$

This means that the choice of reference temperature is immaterial, and no temperature-density correction need be made when setting up temperature-independent viscosity characteristics.

The plotting method used for temperature-independent viscosity characteristics of condensed polymer systems may be applied to polymer solutions and gels as well. If the relation between the viscosity ( $\eta_0$ ) of a solvent (or a dispersion media) and the temperature satisfies the condition

$$\frac{\partial(\eta_0/\eta_{\max})}{\partial T} = 0$$

the temperature independence of the function

$$\eta/\eta_0 = f(Dk_T)$$

will be ensured at once. The symbol  $k_T$  denotes here the experimentally determined temperature factor<sup>3,4</sup> of parallel shift of the flow curves in logarithmic coordinates. The condition

$$\frac{\partial(\eta_0/\eta_{\max})}{\partial T} = 0$$

means also that  $k_T = \eta_0$ . As observed experimentally by Brunstrum et al.,<sup>4</sup> the shift factor  $k_T$  equals  $\eta_0$  only approximately. Consequently, the value of  $\eta_0/\eta_{\max}$  varies somewhat with the temperature. For this reason, the temperature-independent viscosity characteristics of polymer solutions or gels may be represented by a graph in logarithmic coordinates obtained by shifting the relative viscosity versus shear rate curves for various temperatures along the shear-rate axis by

$$k_T = \eta_0(\eta_{\max}/\eta_0) = \eta_{\max}$$

and along the relative viscosity axis by  $\eta_0/\eta_{\max}$ . This was not taken into consideration in previous studies.<sup>3,4</sup>

### Experimental Data on the Temperature Relation of the Viscosity of Condensed Polymers

In order to check the above theory and method of temperature-independent presentation of viscosity characteristics of polymer systems, special calculations were performed based on the most reliable experimental reports published on the flow curves of various condensed polymers.

Philippoff and Gaskins<sup>6</sup> published data on the viscosity of two polyethylenes and plasticized polyvinyl butyral. These figures deserve special attention, as the experiments were here carried out in a very wide shear-rate range and with a high degree of reliability. Flow curves were obtained within wide temperature limits, and initial Newtonian viscosities were directly measured. It should, nevertheless, be noted that the measurement results were widely scattered around the flow curves. Figure 1 illustrates the temperature-independent viscosity curve of polyethylene (sample II of the original reference<sup>6</sup>); experiments with the said material were conducted within a maximum temperature range of about 140°C.). Similar data on plasticized polyvinyl butyral are shown in Figure 2.

The temperature-independent viscosity curve of polyethylene, obtained from Dexter's experimental results<sup>11</sup> can be seen in Figure 3. A particular feature of Dexter's experiments is that the initial Newtonian viscosity region was not reached at any of the temperatures. The problem of determining  $\eta_{\max}$  will be discussed later.

The possibility of constructing the temperature-independent viscosity characteristic of a typical elastomer is a point of particular interest. To check this, the experimental data of Treloar<sup>12</sup> on the flow properties of plasticized natural rubber have been plotted in  $\log D_r$  versus  $\log \eta_r$  coordinates in Figure 4. No initial Newtonian viscosity values were given in this paper either.

The method of presenting temperature-independent viscosity characteristics may be of use in the following cases.

If experimental determinations of apparent viscosity are conducted over a wide range of shear rates and temperatures, plotting the temperature-independent viscosity curve makes it possible to check the compatibility of the experimental results.

Where experiments cover a wide temperature range but remain within a limited range of shear rates (due to limitations of the apparatus used, for instance), application of the temperature-independent presentation method enables evaluation of viscosity values at shear rates, which were not reached in the experiments.

Finally, there is no longer any need for direct viscosity measurements at all temperatures if data are required on the viscosity changes with the



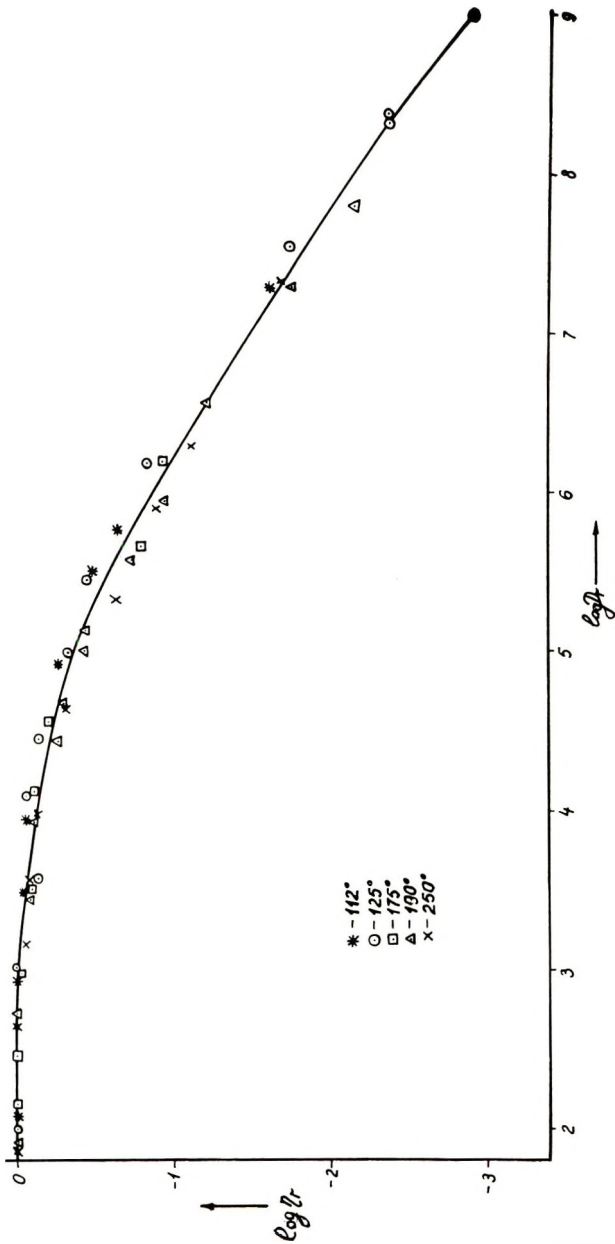


Fig. 1. Temperature-independent viscosity characteristic of polyethylene (based on data of Philippoff and Gaskins<sup>6</sup>).

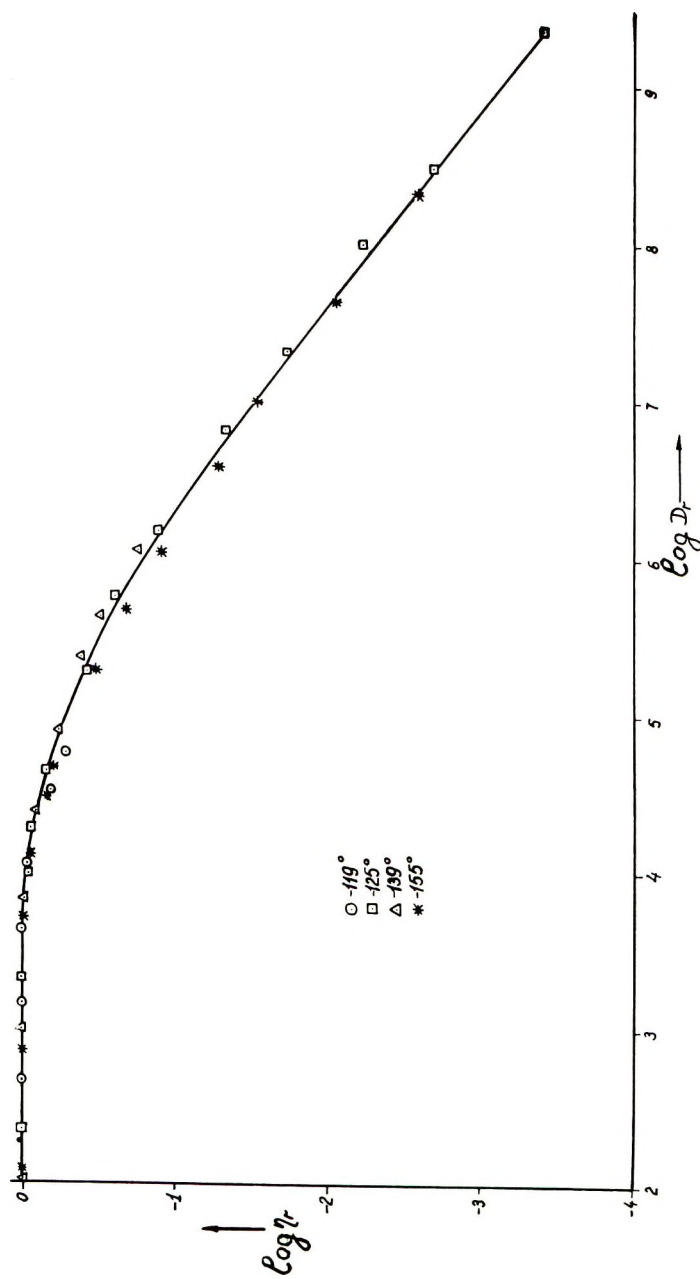


Fig. 2. Temperature-independent viscosity characteristic of plasticized polyvinyl butyral (based on data of Philippoff and Gaskins<sup>6</sup>).

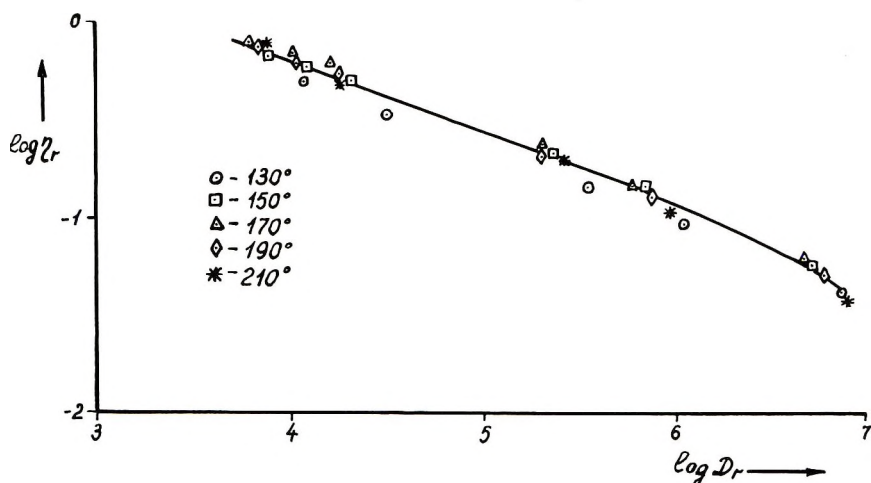


Fig. 3. Temperature-independent viscosity characteristic of polyethylene (based on data of Dexter<sup>11</sup>).

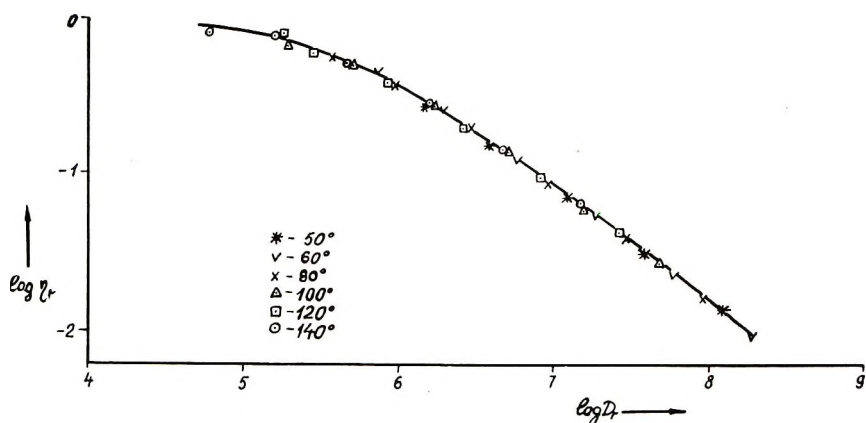


Fig. 4. Temperature-independent viscosity characteristic of plasticized natural rubber (based on data of Treloar<sup>12</sup>).

shear rate at various temperatures. For this purpose it is enough to obtain a flow curve, covering as wide a shear rate range as possible at any single temperature, preferably sufficiently remote from the melting point (for crystalline polymers), and to determine the initial Newtonian viscosities after which their variation with the temperature may be obtained with an adequate degree of reliability. The actual viscosities at various temperatures and shear rates can then be evaluated with the help of the temperature-independent viscosity characteristic.

#### Determining Initial Newtonian Viscosities

Initial Newtonian viscosities are of particular importance in the temperature-independent viscosity presentation method discussed. It is well

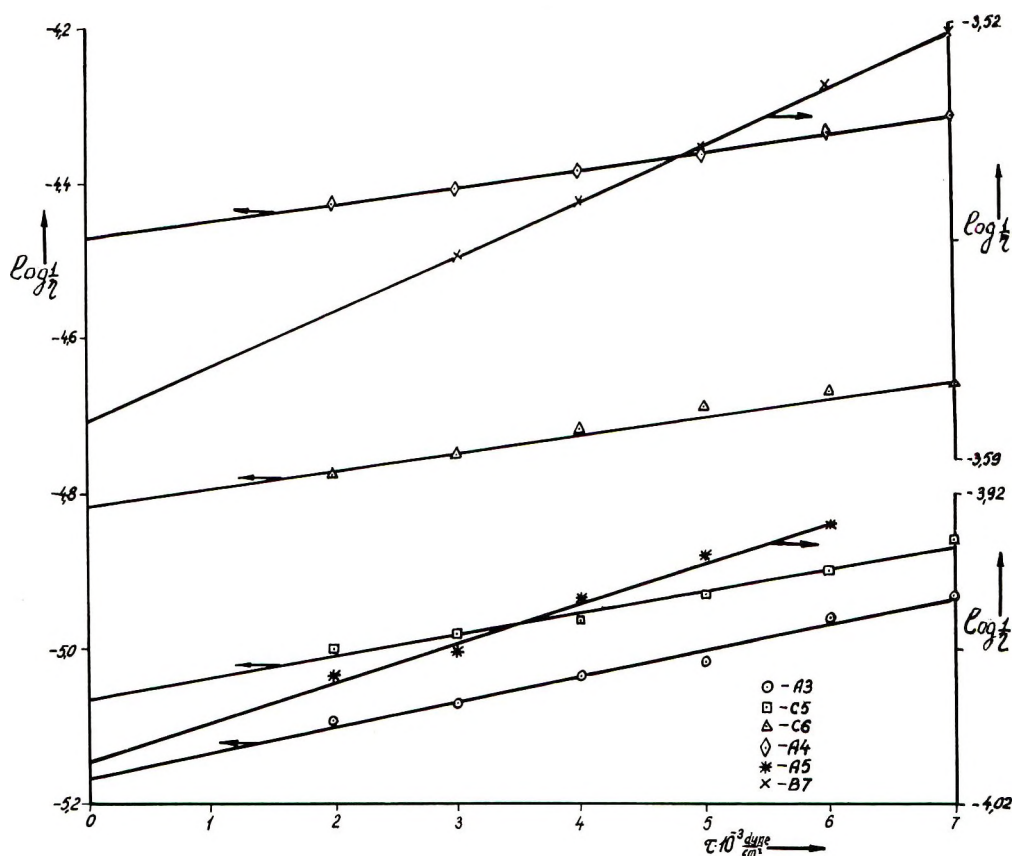


Fig. 5. Determination of initial Newtonian viscosity of polyethylenes (based on data of Tung<sup>14</sup>).

known that this parameter appears generally as a most essential physical characteristic of the material concerned, closely related to the molecular weight and the features of internal structure of high-polymer molecules. In experimental work, however, it is not always possible to reach the shear rate regions of Newtonian flow of condensed polymers. For this reason a dependable method of extrapolating experimental data on viscosity versus shear rate relations to zero shear rates (or, which is the same, to shear stress values tending to zero  $\tau \rightarrow 0$ ) should be regarded as a matter of particular importance. Spencer and Dillon<sup>13</sup> suggested plotting  $\log 1/\eta$  against  $\tau$  and extrapolating to  $\tau = 0$ . The value of  $\eta_{\max}$  can then easily be computed from the length of the intercept on the ordinate axis. Such a method was applied by the authors mentioned for the case of polystyrene; it was then observed that the relation between  $\log 1/\eta$  and  $\tau$  is linear at sufficiently low shear stresses, a feature which confirmed the feasibility of the above extrapolation.

We checked this method on the basis of the most trustworthy reports published so far. The extrapolated  $\eta_{\max}$  values were compared with

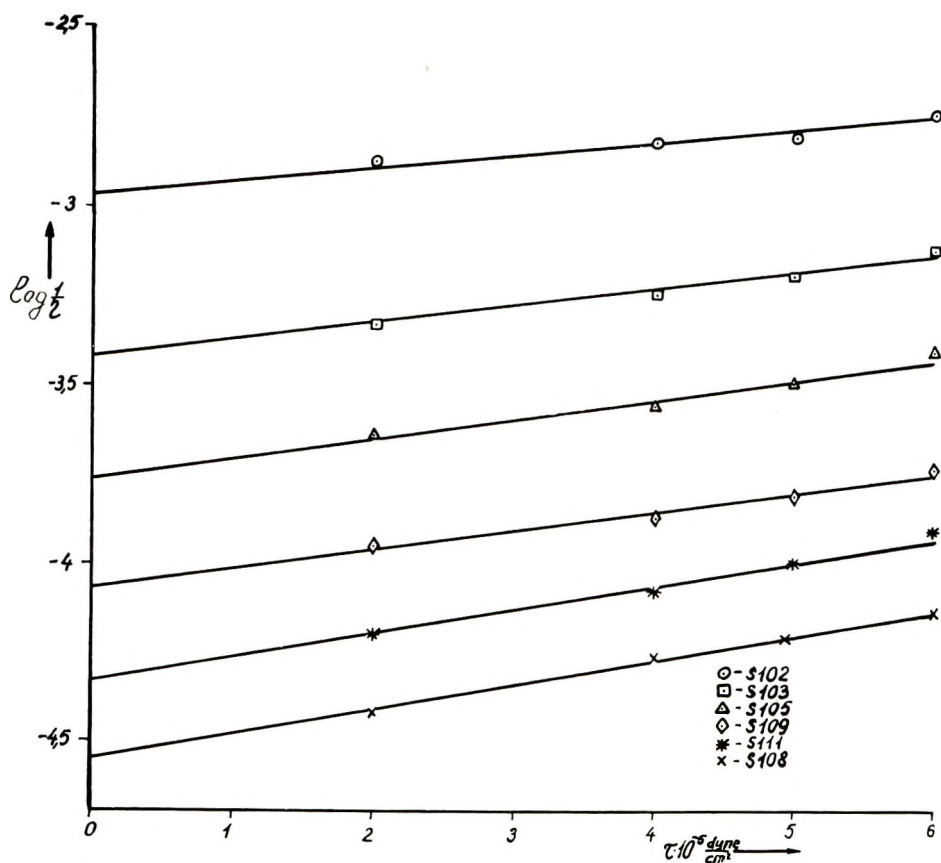


Fig. 6. Determination of initial Newtonian viscosity of polystyrenes (based on data of Rudd<sup>15</sup>).

directly observed experimental data. For this purpose a  $\log 1/\eta$  versus  $\tau$  coordinate system was used to represent Tung's<sup>14</sup> and Rudd's<sup>15</sup> results (see Figs. 5 and 6, respectively), both having conducted most exact measurements at low shear rates, and having reached the initial Newtonian viscosity regions. Tung made his investigations with narrow fractions

TABLE I  
Initial Newtonian Viscosity Values of Polyethylenes

Polyethylene sample no.	$\log \eta_{\max}$	
	Data of Tung <sup>14</sup>	From Fig. 5
A3	5.10	5.17
C5	5.01	5.06
C6	4.78	4.82
A4	4.44	4.46
A5	3.98	4.01
B7	3.58	3.58



TABLE II  
Initial Newtonian Viscosity Values of Polystyrenes

Polystyrene sample no.	$\log \eta_{\max}$	
	Data of Rudd <sup>15</sup>	From Fig. 6
S102	2.97	2.97
S103	3.40	3.42
S105	3.74	3.76
S109	4.08	4.07
S111	4.28	4.33
S108	4.52	4.55

of various polyethylenes, and Rudd with polystyrene. The sample symbols used in Figures 5 and 6, as well as in Tables I and II, are the same as in the original references.<sup>14, 15</sup>

The extrapolated  $\log \eta_{\max}$  values are compared with those found by experiment, in Tables I and II. The same method was used to determine

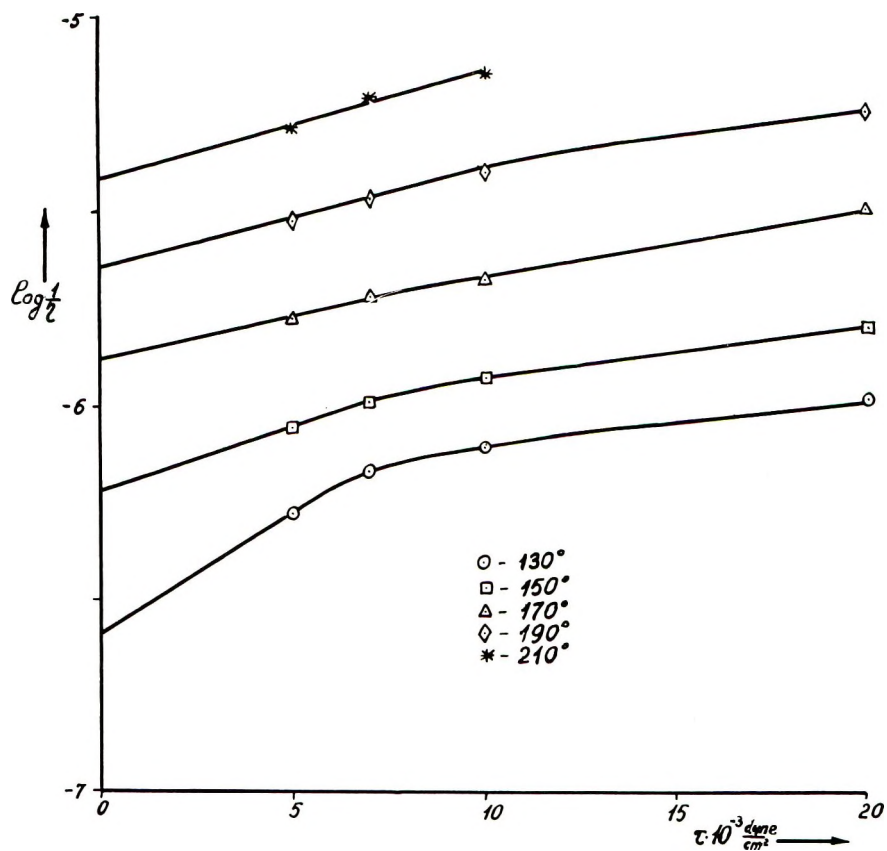


Fig. 7. Determination of initial Newtonian viscosity of polyethylene (based on data of Dexter<sup>11</sup>).

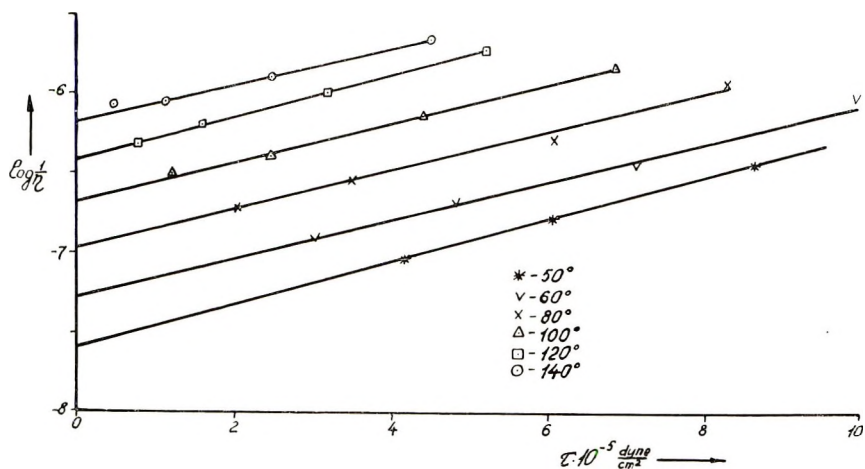


Fig. 8. Determination of initial Newtonian viscosity of plasticized natural rubber (based on data of Treloar<sup>12</sup>).

the initial Newtonian viscosities ( $\eta_{\max}$ ) required for constructing the temperature-independent viscosity characteristics of polyethylene from Dexter's experimental data (see Fig. 7) and of plasticized natural rubber from Saunders and Treloar's report<sup>12</sup> in Figure 8.

### Discussion

A detailed treatment of experimental results obtained by various investigators proved that temperature-independent viscosity characteristics can be obtained successfully even for polymer systems of widely differing chemical nature and structure. Consequently, the steady apparent viscosity can actually be represented as the product of two functions, one of which ( $\eta_{\max}$ ) depends on the temperature but not on the shear rate, and the other,  $f(D_r)$ , depends on the shear rate but not on the temperature. For polystyrene, in particular, this fact was proved by experiment.<sup>13</sup>

The temperature relation of  $\eta_{\max}$  appears similar to the temperature coefficient of shift in Ferry's investigations,<sup>1</sup> usually denoted by  $a_T$ . The widely used formula for computation of  $a_T(T)$ , known as the WLF formula, however, was found unsuitable for expressing the relation between the initial Newtonian viscosity ( $\eta_{\max}$ ) and the temperature over a sufficiently wide temperature range.

The problem of the temperature relation of  $\eta_{\max}$  is one of the most essential problems concerning the flow properties of polymers. At present, viscosity-temperature relations are usually expressed by Fraenkel-Eyring's exponential law. According to this, the relation between  $\log \eta_{\max}$  and  $1/T$  should graphically be represented by a straight line whose slope is claimed to determine the activation energy of viscous flow. Figure 9 illustrates the relation between  $\log \eta_{\max}$  and  $1/T$  for a number of polymer systems. It can be seen that only the curves plotted from Philippoff-

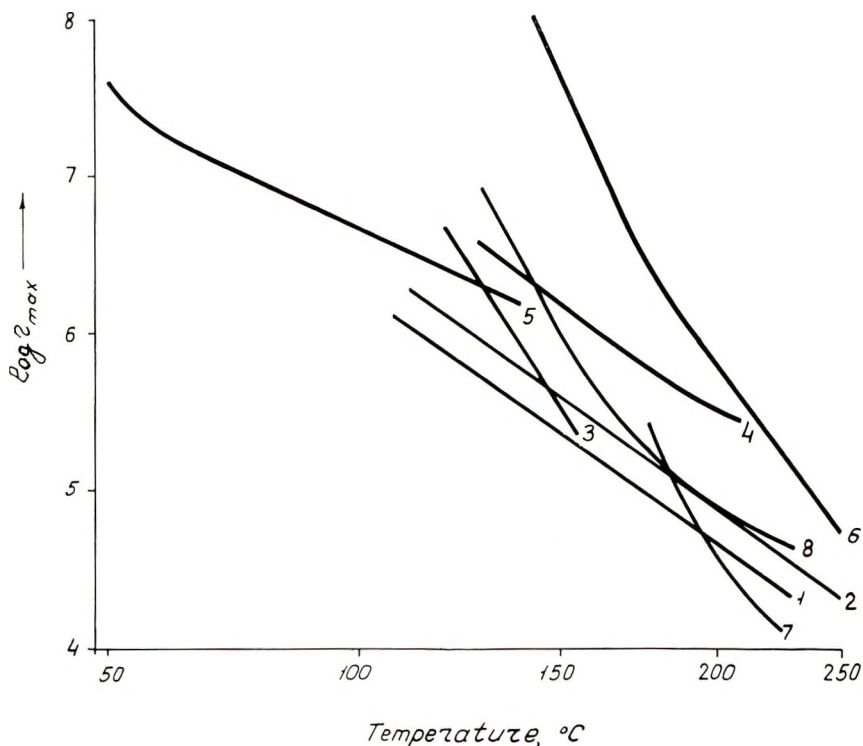


Fig. 9. Temperature relation of initial Newtonian viscosity for various polymer systems: (1) polyethylene I;<sup>6</sup> (2) polyethylene II;<sup>6</sup> (3) polyvinyl butyral;<sup>6</sup> (4) polyethylene;<sup>11</sup> (5) plasticized natural rubber;<sup>12</sup> (6) polystyrene, molecular weight 360,000;<sup>13</sup> (7) polystyrene, molecular weight 162,000;<sup>13</sup> (8) alkathene 2.

Gaskins' data<sup>6</sup> are actually straight lines. In all the other examples a noticeable curvature can be observed. Kobeko,<sup>16</sup> who examined viscosity-temperature relations for numerous products including most diverse ones, pointed out that whenever measurements covered an adequately wide temperature range, the  $\log \eta = F(1/T)$  graphs had a noticeable curvature. Hence, expressing the relation between  $\eta_{\max}$  and  $T$  in exponent form and determining the viscous flow activation energy by the slope of the  $\log \eta_{\max} = F(1/T)$  curve would not be exact. Shishkin<sup>17</sup> supposed that the activation energy itself varies exponentially with the temperature. This means that the probability of "jumps" of molecular-kinetical units increases at rising temperatures not only as a result of their own elevated energy, but also due to a lowering of potential barriers to be overcome in the elementary kinetic act. This assumption permits a satisfactory interpretation of the experimentally observed viscosity-temperature relations of various materials. The same is true for the relation between  $\eta_{\max}$  and  $T$ .

The  $\eta_{\max}$  extrapolation method suggested by Spenser and Dillon<sup>15</sup> and checked above is substantially an application of a formula proposed

earlier by Gurevich<sup>17</sup> representing the relation between apparent viscosity and shear stress:

$$\eta = \eta_{\max} e^{-a\tau} \quad (10)$$

where  $\eta_{\max}$  and  $a$  are constants.

Since the relation between  $\log \eta$  and  $\tau$  can actually be represented in rectilinear form, it may be assumed that eq. (10) will be true for sufficiently low shear stresses. Detailed calculations, which confirmed the correctness of eq. (10) at low  $\tau$  values, lead to the following important practical conclusion: experimental investigations of the relation between apparent viscosity and shear stress may be justifiably extended over low stress regions only until the test results plotted in  $\log 1/\eta-\tau$  coordinates begin to fall positively onto a straight line. Further decreasing of  $\tau$  would be impractical.

### References

1. Ferry, J. D., *J. Am. Chem. Soc.*, **72**, 3746 (1950); *Viscoelastic Properties of Polymers*, Wiley, New York, 1961, Chap. 11.
2. Tobolsky, A. V., and R. D. Andrews, *J. Chem. Phys.*, **1**, 1251 (1943); J. Bischoff, E. Catsiff, and A. V. Tobolsky, *J. Am. Chem. Soc.*, **74**, 3378 (1952); *J. Appl. Phys.*, **25**, 1092 (1954).
3. Arveson, M. H., *Ind. Eng. Chem.*, **26**, 628 (1934).
4. Brunstrum, L. C., A. C. Borg, and A. W. Sisko, *NLGI Spokesman*, **26**, No 1, 7 (1962).
5. Markovitz, H., and R. V. Williamson, *Trans. Soc. Rheol.*, **1**, 25 (1957); R. S. Porter and J. F. Johnson, *J. Appl. Phys.*, **25**, 1086 (1954).
6. Philippoff, W., and F. H. Gaskins, *J. Polymer Sci.*, **21**, 205 (1956).
7. Ito, K., *J. Appl. Phys.*, **32**, 1743 (1961).
8. Schott, H., and W. S. Kaghan, *J. Appl. Polymer Sci.*, **5**, 175 (1961).
9. Kargin, V. A., and G. L. Slonimskii, *Dokl. Akad. Nauk SSSR*, **62**, 239 (1948); *Zh. Fiz. Khim.*, **23**, 563 (1949).
10. Rouse, P. E., *J. Chem. Phys.*, **21**, 1272 (1953).
11. Dexter, F. D., *J. Appl. Phys.*, **25**, 1124 (1954).
12. Treloar, L., and D. W. Saunders, *Trans. Inst. Rubber Ind.*, **24**, 92 (1948).
13. Spenser, R. S., and R. E. Dillon, *J. Colloid Sci.*, **3**, 163 (1948); *ibid*, **4**, 241 (1949)
14. Tung, H., *J. Polymer Sci.*, **46**, 409 (1960)
15. Rudd, J. F., *J. Polymer Sci.*, **60**, 57 (1962)
16. Kobeko, P. P., *Amorfnye Veshchestva*, Academy of Sciences Press, Leningrad, U.S.S.R., 1952, Chap. 11.
17. Shishkin, N. I., *Zh. Tekh. Fiz.*, **26**, 1461 (1956).
18. Gurevich, G. I., *Zh. Tekh. Fiz.*, **17**, 1491 (1947).

### Résumé

On a étudié la possibilité de construire une courbe caractéristique de la viscosité de systèmes polymères indépendante de la température avec utilisation du procédé des "paramètres réduits" analogue à celui de Ferry. On a établi que la relation entre la viscosité en la température ainsi que la vitesse de déplacement peut être représentée dans le cas général sous la forme d'un produit de deux fonctions dont l'une ne dépend que de la température et l'autre ne dépend que de la vitesse de déplacement. En parlant des procédés de l'analyse dimensionnelle et des notions du caractère viscoélastique de la déformation des systèmes polymères on a montré que le rapport de la viscosité

apparente et de la viscosité newtonienne maximum (initiale) est une fonction indépendante de la température du produit de la vitesse de déplacement par la viscosité newtonienne maximum (initiale). Il s'ensuit que la viscosité newtonienne maximum (déterminée à la vitesse de déplacement tendant vers zéro) joue le rôle d'un paramètre physico-chimique essentiel, caractérisant les propriétés visqueuses des systèmes polymères. Dans le domaine des vitesses de déplacement suffisamment basses, la viscosité apparente est une fonction exponentielle des contraintes de cisaillement ce qui permet de trouver par extrapolation la viscosité newtonienne maximum (initiale). Cette théorie a été vérifiée sur les données publiées les plus sûres relatives à la viscosité des systèmes polymères condensés, dans de larges plages de vitesses de déplacement et des températures. Les données expérimentales sur des systèmes polymères de nature différente coïncident d'une façon satisfaisante avec les courbes caractéristiques connexes, indépendantes de la température.

### Zusammenfassung

Die untersuchte Möglichkeit, die temperatur-invariante Charakteristik der Zähigkeit von Polymersystemen unter Verwendung des Verfahrens der "reduzierten Parameter" zu konstruieren, ist analog der Methode von Ferry. Es wurde festgestellt, dass die Abhängigkeit der Viskosität von der Temperatur und der Verformungsgeschwindigkeit im allgemeinen als das Produkt von zwei Funktionen dargestellt werden kann. Hierbei hängt eine Funktion nur von der Temperatur, die andere nur von der Verformungsgeschwindigkeit ab. Anhand der Dimensionsanalysen-Methode und den Vorstellungen über den elastisch-zähen Charakter der Polymersystem-Verformungen wurde gezeigt, dass das Verhältnis der scheinbaren (effektiven) Viskosität zur maximalen Newton'schen Viskosität gleich der temperatur-invarianten Funktion des Produktes der Verformungsgeschwindigkeit und der maximalen Newton'schen Viskosität ist. Deshalb ist letztere (die bei einer sich Null nähernden Verformungsgeschwindigkeit bestimmt wurde) ein wichtiger physikalisch-chemischer Parameter, der die Viskositätseigenschaften von Polymersystemen charakterisiert. Die scheinbare Viskosität hängt im Bereich genügend kleiner Verformungsgeschwindigkeiten von der Schubspannung ab. Dadurch ist es möglich, durch Extrapolation die maximale Newton'sche Viskosität zu finden. Die Theorie wurde anhand der zuverlässigsten in der Literatur angeführten Daten in bezug auf die Viskositätseigenschaften kondensierter Polymersysteme in weiten Verformungsgeschwindigkeits- und Temperaturbereichen überprüft. Die Versuchsergebnisse ihrer Eigenart nach verschiedener Polymersystem können mit genügender Genauigkeit in Form von temperatur-invarianten Kurven dargestellt werden.

Received May 8, 1963



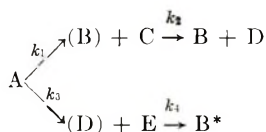
## Some Considerations of the Kinetics of the Acid Hydrolysis of Poly- and Oligosaccharides.

### II. The Trisaccharides, Isomaltotriitol, Panitol, and Isomaltotriose

ALEXANDER MELLER, *Research Laboratory, Australian Paper Manufacturers Limited, Melbourne, Australia*

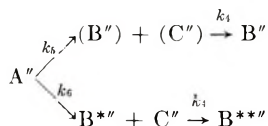
#### Synopsis

On the basis of the rate data of Jones, Dimler, and Rist on the acid-catalyzed hydrolysis of isomaltotriitol it is shown that the kinetics can be described by rate equations derived by assuming a combination of two interdependent simultaneous ("parallel") and consecutive reactions according to the scheme:



where A is isomaltotriitol; (B), B, and B\* are glucose; C is isomaltitol; D and (D) are sorbitol; and E is isomaltose present at any instant;  $k_1$  and  $k_2$  are specific rates at which the two glucosidic bonds are hydrolytically cleaved in isomaltotriitol;  $k_3$  is the specific rate of hydrolysis of isomaltitol (known); and  $k_4$  is the specific rate of hydrolysis of isomaltose (known). Values for the constants  $k_1$  and  $k_3$  have been computed from the experimental values of the composition of the hydrolysis reaction mixture and the known values for  $k_2$  and  $k_4$ . The yields of glucose and sorbitol as well as the extent of hydrolysis have then been calculated using the values for  $k_1$  and  $k_3$  (computed) and  $k_2$  and  $k_4$  (known) by means of rate equations corresponding to the above scheme. They are in very good agreement with the experimental values.

The kinetics of the acid hydrolysis of isomaltotriose can also be described by rate equations corresponding to a kinetic scheme:



where A'' is isomaltotriose; (B''), B'', B\*'', and B\*\*\* are glucose; (C'') and C'' are isomaltose at any instant;  $k_5$  and  $k_6$  are the specific rates of hydrolytic cleavage of the two glucosidic bonds in isomaltotriose, and  $k_4$  is the specific rate of hydrolysis of isomaltose (known). Assuming that  $k_5 = k_4/1.3$  and  $k_6 = k_4/1.5$ , values for the extent of hydrolysis (expressed in terms of glucosidic bond cleavage for 100 bonds) have been calculated by means of rate equations derived on the basis of the above scheme. They show good agreement with the experimental values. However, transposing the values for  $k_5$

and  $k_6$  does not alter the calculated values. Thus, only the following conclusions seem to be permissible: the glucosidic bonds in isomaltotriose most likely hydrolyze at a lower rate than isomaltose; the two bonds do not hydrolyze at the same rate; whether the rate of hydrolysis of the glucosidic link of the reducing unit is slower than that of the nonreducing unit or the reverse, remains to be established. Attention is drawn to the role of the theoretical carbohydrate structural chemist who may offer an explanation for the deductions of the kineticist in the field of both trisaccharide and disaccharide hydrolysis.

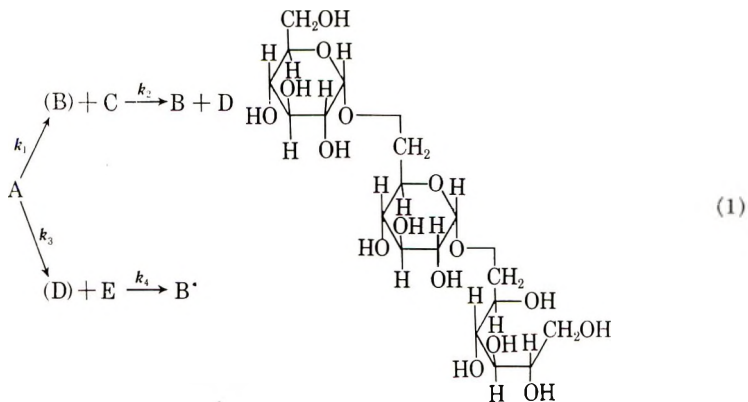
In a recent paper<sup>1</sup> the validity of the "statistical" rate equation<sup>2</sup> when applied to the rate data of the acid hydrolysis of cellotriose<sup>3</sup> was examined. It was suggested that under the experimental conditions used<sup>2</sup> (strong sulfuric acid) the measured rate may not have been entirely that of the hydrolysis of cellotriose. In support of this view it was shown that the rate constants of hydrolysis for cellobiose with dilute hydrochloric and sulfuric acid solutions at high temperatures fulfill the requirement of the Hammett acidity function, while those with strong sulfuric acid solutions are not in agreement with this requirement.

The present study is concerned with an examination of the kinetics of acid hydrolysis of isomaltotriitol, panitol, and isomaltotriose, based on published rate data.

### Isomaltotriitol

Jones, Dimler, and Rist<sup>4</sup> have determined the quantities of the hydrolysis products of the action of 0.18*N* H<sub>2</sub>SO<sub>4</sub> at 80°C. on isomaltotriitol for three periods of time. Their rate data offer a splendid opportunity for comparing the rates of hydrolysis of glucosidic bonds in a trisaccharide with those of the disaccharides constituting the structural units in the trisaccharide. Such a comparison makes it possible to establish the effect of the position of the glucosidic bond in a trisaccharide on its stability towards hydrolysing acid solutions.

The course of hydrolysis of isomaltotriitol is illustrated by the reaction scheme shown in eq. (1):



where A denotes isomaltotriitol; (B) and B are glucose (formed in the first and second steps of the "first route," respectively); B\* is glucose (formed in the second step of the "second route"); C is isomaltitol; D is sorbitol (formed in the second step of the "first route"); (D) is sorbitol (formed in the first step of the "second route"); E is isomaltose.

The above reaction scheme represents a kinetic system consisting of a combination of two interdependent simultaneous ("parallel") and consecutive reactions.

Since the hydrolysis rate constants for isomaltitol ( $k_2 = 9.1 \times 10^{-3}/\text{hr.}$ ) and isomaltose ( $k_4 = 12.3 \times 10^{-3}/\text{hr.}$ ) have separately been determined by Jones, Dimler, and Rist<sup>4</sup>, the values for  $k_1$  and  $k_3$  can be computed from the rate data on isomaltotriitol in the following way.

The rate of disappearance of A is

$$-dA/dt = (k_1 + k_3)A \quad (2)$$

from which at  $t = 0$ ,  $A = A_0$ ,

$$A = A_0 e^{-(k_1 + k_3)t} \quad (3)$$

The rates of formation and disappearance of C and E are

$$dC/dt = k_1 A - k_2 C = k_1 A_0 e^{-(k_1 + k_3)t} - k_2 C \quad (4)$$

and

$$dE/dt = k_3 A - k_4 E = k_3 A_0 e^{-(k_1 + k_3)t} - k_4 E \quad (5)$$

These two differential equations when solved by the "integrating factor" method give for  $t = 0$ ,  $C = 0$ , and  $E = 0$

$$C = \frac{A_0 k_1}{k_2 - (k_1 + k_3)} [e^{-(k_1 + k_3)t} - e^{-k_2 t}] \quad (6)$$

and

$$E = \frac{A_0 k_3}{k_4 - (k_1 + k_3)} [e^{-(k_1 + k_3)t} - e^{-k_4 t}] \quad (7)$$

Evaluation of the rate data of isomaltotriitol hydrolysis by using eqs. (6) and (7) results in  $k_1 = 9.8 \times 10^{-3}/\text{hr.}$  and  $k_3 = 5.0 \times 10^{-3}/\text{hr.}$  These values are in good agreement with those computed by Jones, Dimler, and Rist (i.e.,  $k_1 = 9.5 \times 10^{-3}/\text{hr.}$  and  $k_3 = 5.0 \times 10^{-3}/\text{hr.}$ ) using approximate equations. In a footnote of their paper it is mentioned that eqs. (6) and (7) were derived by L. F. McBurney.

Since the yields of glucose and sorbitol for three hydrolysis periods have also been determined by Jones, Dimler, and Rist, the correctness of the numerical values of  $k_1$  and  $k_3$  can be tested by using equations which express the glucose and sorbitol yields in terms of the initial isomaltotriitol concentration, time of hydrolysis and the constants  $k_1$ ,  $k_2$ ,  $k_3$ , and  $k_4$ .

Glucose yield in the first step of the first route is given by

$$d(B)/dt = k_1 A = k_1 A_0 e^{-(k_1+k_3)t} \quad (8)$$

from which for  $t = 0$ ,  $(B) = 0$

$$(B) = \frac{k_1 A_0}{-(k_1 + k_3)} [e^{-(k_1+k_3)t} - 1] \quad (9)$$

In the second step of the first route:

$$\frac{dB}{dt} = k_2 C = \frac{k_2 A_0 k_1}{k_2 - (k_1 + k_3)} [e^{-(k_1+k_3)t} - e^{-k_2 t}] \quad (10)$$

from which for  $t = 0$ ,  $B = 0$

$$B = \frac{A_0 k_1 k_2}{(k_1 + k_3) [k_2 - (k_1 + k_3)]} [1 - e^{-(k_1+k_3)t}] - \frac{A_0 k_1}{k_2 - (k_1 + k_3)} (1 - e^{-k_2 t}) \quad (11)$$

Half of the glucose yield in the second step of the second route:

$$\frac{dB^*}{dt} = k_4 E = \frac{k_4 A_0 k_3}{k_4 - (k_1 + k_3)} [e^{-(k_1+k_3)t} - e^{-k_4 t}] \quad (12)$$

from which for  $t = 0$ ,  $B^* = 0$

$$B^* = \frac{A_0 k_3 k_4}{(k_1 + k_3) [k_4 - (k_1 + k_3)]} [1 - e^{-(k_1+k_3)t}] - \frac{A_0 k_3}{k_4 - (k_1 + k_3)} (1 - e^{-k_4 t}) \quad (13)$$

Then

$$\% \text{ Glucose yield} = (B) + B + 2B^*$$

for  $A_0 = 100$ .

Sorbitol yield in the second step of the first route is:

$$D = \frac{A_0 k_1 k_2}{(k_1 + k_3) [k_2 - (k_1 + k_3)]} [1 - e^{-(k_1+k_3)t}] - \frac{A_0 k_1}{k_2 - (k_1 + k_3)} (1 - e^{-k_2 t}) \quad (14)$$

[Sorbitol yield  $D$  in the first route is the same as the glucose yield  $B$ , eq (11)].

Sorbitol yield in the first step of the second route is:

$$\frac{d(D)}{dt} = k_3 A = k_3 A_0 e^{-(k_1+k_3)t} \quad (15)$$

from which for  $t = 0$ ,  $(D) = 0$

$$(D) = \frac{k_3 A_0}{-(k_1 + k_3)} [e^{-(k_1 + k_3)t} - 1] \quad (16)$$

Then

$$\% \text{ Sorbitol yield} = D + (D)$$

for  $A_0 = 100$ .

The glucose and sorbitol yields per 100 moles of isomaltotriitol, calculated by means of eq. (11), (13), (14), and (16) using the values for the constants  $k_1$  and  $k_3$  found and  $k_2$  and  $k_4$  as provided by Jones, Dimler, and Rist, are listed in Table I.

TABLE I  
Comparison between Hydrolysis Products and Extent of Hydrolysis of Isomaltotriitol Found Experimentally and Calculated

		Hydrolysis time, hr.		
		7	24	53
Hydrolysis products, moles/100 moles isomaltotriitol				
Isomaltotriitol (unconverted)	Experimental	89.9	70.3	45.9
	Calculated	90.23	70.09	45.64
Isomaltitol	Experimental	6.14	18.2	27.1
	Calculated	6.36	17.89	28.10
Isomaltose	Experimental	3.5	8.4	13.0
	Calculated	3.02	8.64	12.96
Glucose	Experimental	7.41	24.7	54.0
	Calculated	7.39	24.68	55.03
Sorbitol	Experimental	4.12	11.5	26.4
	Calculated	3.65	12.22	26.58
% Hydrolysed (Number of glucosidic bonds split per 100 glucosidic bonds = 50 moles of isomaltotriitol)	Experimental	5.46	16.6	33.5
	Calculated	5.20	16.70	33.98

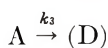
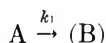
These authors have also measured the extent of hydrolysis of isomaltotriitol by determining the reducing group content of the reaction mixture after three hydrolysis periods. Using the per cent hydrolysis values they calculated the values for the overall hydrolysis constant, i.e., the simple first-order rate constant, designated as  $K_{III}$ . It should be noted that the true hydrolysis rate constant which is the specific rate of splitting the glucosidic bonds (formation of reducing ends) in isomaltotriitol, in accordance with eq. (1) is

$$k_{III} = \frac{k_1 k_2}{k_1 + k_2} + \frac{k_3 k_4}{k_3 + k_4} \quad (17)$$



The numerical value of  $k_H$  is, thus,  $8.2 \times 10^{-3}/\text{hr.}$  and the average over-all hydrolysis constant computed by Jones, Dimler, and Rist is  $7.8 \times 10^{-3}/\text{hr.}$  The simple first-order rate constant ( $K_{III}$ ) obtained from the values for the hydrolysis represents the specific rate of hydrolysis only when both linkages in isomaltotriitol are split at the same rate, i.e., when  $k_1 = k_2 = k_3 = k_4 = K_{III}$ . In this case eq. (17) degenerates to  $k_H = K_{III}$ .

The extent of hydrolysis, expressed in terms of reducing ends formed per 100 glucosidic bonds (= 50 moles of isomaltotriitol) can also be computed by using the numerical values of  $k_1, k_2, k_3$  and  $k_4$  and taking into account that hydrolytic bond splitting occurs in the reactions:



Thus,

% Hydrolysis = Number of glucosidic bonds split per

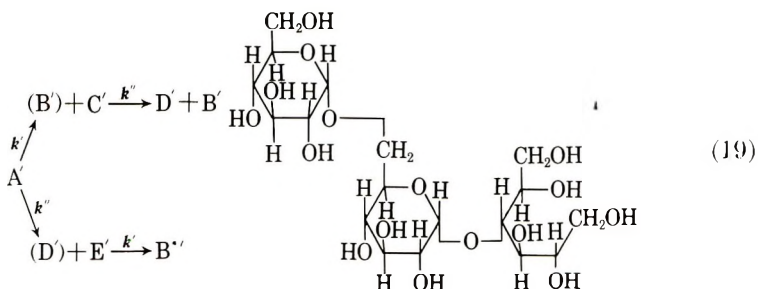
$$100 \text{ glucosidic bonds in isomaltotriitol} = \frac{(B) + (D) + B + B^*}{2} \quad (18)$$

The values for per cent hydrolysis calculated by means of eq. (18) for the experimental hydrolysis times are listed in Table I.

Inspection of the values calculated for unconverted isomaltotriitol, yields of isomaltitol, isomaltose, glucose and sorbitol as well as per cent hydrolysis shows that they are in very good agreement with the experimental values.

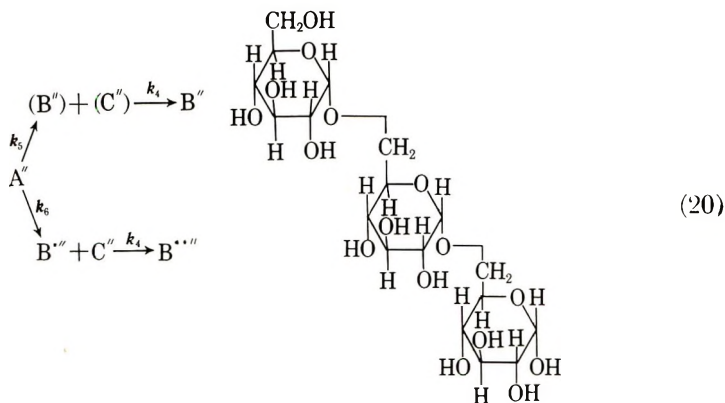
### Panitol

According to Wolfrom, Thompson, and Galkowski in the hydrolysis of panitol<sup>5</sup> the hydrolytic splitting of the glucosidic bond between the maltitol and glucose units (1,6- $\alpha$  link) occurs at the same rate as that in isomaltose; the splitting of the glucosidic bond between the sorbitol and isomaltose units (1,4- $\alpha$  link) also takes place at the same rate as that of maltose. In this hydrolysis rate study<sup>5</sup> the change in optical rotation was measured with progress of hydrolysis. The composition of the reaction mixture was not determined but calculated from the known values for the hydrolysis rate constants of isomaltose ( $k'$ ) and maltose ( $k''$ ) by means of rate equations corresponding to the scheme shown in eq. (19), where A' is panitol; (B'), B' and B\*' are glucose; C' is maltitol; D' and (D' (are sorbitol) and E' is isomaltose. Excellent agreement was found<sup>5</sup> between the optical rotation values observed for three hydrolysis periods and those computed from the calculated composition of the hydrolysis reaction mixture.



### Isomaltotriose

Jones, Dimler, and Rist<sup>4</sup> have investigated the progress of hydrolysis of isomaltotriose (conditions the same as with isomaltotriitol) after three periods of time. While separation and quantitative determination of the hydrolysis products when isomaltotriitol is hydrolyzed are instructive for establishing the source of fragment formed, the same does not apply to isomaltotriose. Breaking either of the two glucosidic bonds in isomaltotriose yields the same products, glucose and isomaltose, as shown by the reaction kinetic scheme below [eq. (20)]. Thus Jones, Dimler, and Rist suggested two methods for assessing the rate constants for the hydrolysis of the two glucosidic bonds.



Where  $A''$  is isomaltotriose;  $(B'')$ ,  $B''$ ,  $B^{*''}$  and  $B^{**''}$  denote glucose;  $(C'')$  and  $C''$  denote isomaltose.

It is assumed that: (1) both linkages hydrolyze at the same rate as isomaltose, i.e., the specific rate of bond splitting is then the simple first-order rate constant ( $K_{III}$ ); (2) reduction of isomaltotriose to isomaltotriitol may lower the hydrolysis rate constant of the glucosidic bond of the reducing unit by the same proportion as the rate constant for the hydrolysis of the glucosidic bond in isomaltose is lowered by reduction to isomaltitol, which was established in separate experiments. The hydrolysis rate constant for the nonreducing unit was calculated by the method of Kuhn and collaborators.<sup>6</sup>

As to assumption 1, it is somewhat questionable that the overall first-order rate constant represents the true rate constant of hydrolysis, as discussed above. In addition it increases even within the investigated range and the average value, as Jones, Dimler, and Rist point out, should only be considered as an approximation to the limiting rate constant.

As to assumption 2, these authors mention that changing the aglycone from an aldose (probably in the ring form) to the open chain sorbitol structure lowers the hydrolysis rate constant in the case of isomaltose  $\rightarrow$  isomaltitol, but it has the opposite effect in the case of maltose  $\rightarrow$  maltitol. These observations undoubtedly indicate that the direction and magnitude of the change in the hydrolysis rate of aldoses when reduced to alditols is dependent on the structure of the saccharide (cf. the generalization of Ivanov<sup>7</sup>). The values for the hydrolysis constants of the two glucosidic bonds computed by the second method by Jones, Dimler and Rist are:

$$k_5 = 11.6 \times 10^{-3}/\text{hr. and } k_6 = 6.8 \times 10^{-3}/\text{hr.}$$

The solutions of the rate equations, corresponding to the kinetic scheme shown in eq. (20) are:

$$A'' = A_0'' e^{-(k_5+k_6)t} \quad (21)$$

$$(C'') = \frac{A_0'' k_5}{k_4 - (k_5 + k_6)} [e^{-(k_5+k_6)t} - e^{-k_4 t}] \quad (22)$$

$$C'' = \frac{A_0'' k_6}{k_4 - (k_5 + k_6)} [e^{-(k_5+k_6)t} - e^{-k_4 t}] \quad (23)$$

$$(B'') = \frac{A_0'' k_5}{-(k_5 + k_6)} [e^{-(k_5+k_6)t} - 1] \quad (24)$$

$$B'' = \frac{A_0'' k_4 k_5}{k_4 - (k_5 + k_6)} \left[ \frac{e^{-(k_5+k_6)t} - 1}{-(k_5 + k_6)} \right] - \frac{A_0'' k_4 k_5}{k_4 - (k_5 + k_6)} \left[ \left( \frac{e^{-k_4 t} + 1}{k_4} \right) \right] \quad (25)$$

$$B^{*''} = \frac{A_0'' k_6}{-(k_5 + k_6)} [e^{-(k_5+k_6)t} - 1] \quad (26)$$

$$B^{***} = \frac{A_0'' k_4 k_6}{k_4 - (k_5 + k_6)} \left[ \frac{e^{-(k_5+k_6)t} - 1}{-(k_5 + k_6)} \right] - \frac{A_0'' k_4 k_6}{k_4 - (k_5 + k_6)} \left[ \left( \frac{e^{-k_4 t} + 1}{k_4} \right) \right] \quad (27)$$

Glucose yield per 100 moles isomaltotriose ( $A_0'' = 100$ ) is given as

$$\text{Glucose yield} = (B'') + 2B'' + B^{*''} + 2B^{***} \quad (28)$$

Using the values for  $k_4 = 12.3 \times 10^{-3}/\text{hr.}$ ,  $k_5 = 11.6 \times 10^{-3}/\text{hr.}$  and  $k_6 = 6.8 \times 10^{-3}/\text{hr.}$ <sup>5</sup> the glucose yield at  $t = \infty$  amounts to 318.3 instead of 300. This result indicates that the values for  $k_5$  and  $k_6$  computed by Method 2<sup>5</sup> are not entirely satisfactory.

Assuming that  $k_5 = k_4/1.3$  and  $k_6 = k_4/1.5$  (the basis for this assumption is discussed below) the glucose yield at  $t = \infty$  amounts to 300.4.

Using the values for  $k_5 = 9.5 \times 10^{-3}/\text{hr.}$  and  $k_6 = 8.0 \times 10^{-3}/\text{hr.}$  the per cent hydrolysis values have been calculated by an equation corresponding to eq. (18), namely,

Number of glucosidic bonds split per 100 glucosidic

$$\text{bonds in isomaltotriose} = \frac{B'' + B^{**''} + (B'') + B^{*'}}{2} \quad (29)$$

These are listed in Table II. When compared with the experimental values, the agreement is quite satisfactory.

TABLE II  
Comparison between Extent of Hydrolysis of Isomaltotriose Found Experimentally and Calculated

		Hydrolysis time, hr.		
		5	24	55
% Hydrolysis	Experimental	5	20	39
	Calculated	4.4	21.2	40.5

Although the calculated values seem to agree with the experimental values for the extents of hydrolysis of isomaltotriose a word of caution may well be in order. In the first place, the equation used contains four constants which makes it suitable to "fit" a curve with three points, i.e., the three experimental values. Furthermore, transposing the values for  $k_5$  and  $k_6$ , i.e., assuming  $k_6 = 9.5 \times 10^{-3}/\text{hr.}$  and  $k_5 = 8.0 \times 10^{-3}/\text{hr.}$ , does not alter the calculated values for per cent hydrolysis. In the light of this argument the conclusions which may safely be drawn are as follows: the glucosidic bonds in isomaltotriose most likely hydrolyze at a lower rate than that in isomaltose; the two bonds do not hydrolyze at the same rate; whether the rate of hydrolysis of the glucosidic bond of the reducing unit is lower than that of the non-reducing unit or the reverse remains to be established. It seems also evident that the interpretation of the kinetics of acid hydrolysis of oligosaccharides based on measurements of reducing group formation is somewhat uncertain. Jones, Dimler, and Rist suggested that one suitable method to establish the true ratio between the two rate constants would be to study the hydrolysis of  $C^{14}$ -labeled isomaltotriose. While the fruitfulness of such techniques has been shown by the results of enzymatic hydrolysis studies on oligo- and polysaccharides,<sup>8</sup> to the writer's best knowledge the first acid hydrolytic rate study with a labeled trisaccharide has been published only recently in a short note.<sup>9</sup> On determining the hydrolysis products from  $4\alpha,6\beta$ -bis-D-glucopyranosido-D-glucose by the isotope dilution technique and chromatographic separation it was found that at  $100^\circ\text{C.}$  with  $0.05N$   $\text{H}_2\text{SO}_4$  the  $\alpha$ -1,4 link hydrolyzes

1.5 times slower than maltose and the  $\beta$ -1,6 link hydrolyzes 1.3 times slower than gentiobiose.<sup>9</sup> These ratios when applied to isomaltose give rate constants for isomaltotriose which—as mentioned above—when substituted into eq. (29) have resulted in per cent hydrolysis values agreeing with the experimental values. It remains to be established whether this finding is coincidental or whether it may be used as a generalization.

The kinetics of acid hydrolysis of oligosaccharides is of considerable interest for both the structural carbohydrate chemist and for the industries using oligo- and polysaccharides. It is the task of the theoretical organic chemist to explain what the kineticist discloses. Here again work is still to be done in the field of disaccharides. The hydrolysis rate constants for some disaccharides are listed in Table III, and an explanation of the differences between these rate constants is probably an attractive target for the theoretical organic chemist.

TABLE III  
Hydrolysis Rate Constants for Some Disaccharides

Hydrolysis conditions	Disaccharide	Rate constant	Ref- erence
0.05N H <sub>2</sub> SO <sub>4</sub> ; 100°C.	Isomaltose	20.8 × 10 <sup>-3</sup> /hr	5
“ “ “	Maltose	84.6 “ “	“
0.18N H <sub>2</sub> SO <sub>4</sub> ; 80°C.	Maltose	51 × 10 <sup>-3</sup> /hr.	4
“ “ “	Maltitol	58 “ “	“
“ “ “	Maltobionic Acid	56 “ “	“
“ “ “	Isomaltose	12.3 “ “	“
“ “ “	Usomaltitol	9.1 “ “	“
4% H <sub>2</sub> SO <sub>4</sub> ; 45°C.	Cellobiose	0.7 × 10 <sup>-3</sup> /hr.	10
“ “ 60°C.	“	6.2 “ “	“
“ “ 75°C.	“	37.8 “ “	“
“ “ 45°C.	Cellobionic Acid	0.83 “ “	“
“ “ 60°C.	“ “	5.6 “ “	“
“ “ 75°C.	“ “	33.4 “ “	“
8% H <sub>2</sub> SO <sub>4</sub> ; 55°C.	Maltose	6.12 × 10 <sup>-6</sup> /sec.	10
“ “ 65°C.	“	23.61 “ “	“
“ “ 75°C.	“	64.0 “ “	“
“ “ 55°C.	Cellobiose	2.84 “ “	“
“ “ 65°C.	“	11.94 “ “	“
“ “ 75°C.	“	33.30 “ “	“

Thanks are due to Australian Paper Manufacturers Limited for permission to publish this paper and to Mr. D. W. Sharp for valuable assistance in the mathematical part.

### References

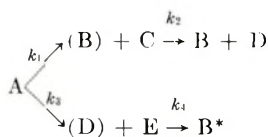
1. Meller, A., *J. Polymer Sci.*, **C2**, 97 (1963).
2. Kuhn, W., *Ber.*, **63**, 1503 (1930).
3. (a) Freudenberg, K., W. Kuhn, W. Duerr, F. Bolz, and G. Steinbrunn, *Ber.*, **63**, 1510 (1930); (b) K. Freudenberg, and G. Blomquist, *Ber.*, **68**, 2070 (1935).
4. Jones, R. W., R. J. Dimler, and C. E. Rist, *J. Am. Chem. Soc.*, **77**, 1659 (1955).
5. Wolfrom, M. L., A. Thompson, and T. T. Galkowski, *J. Am. Chem. Soc.*, **73**, 4093 (1951).



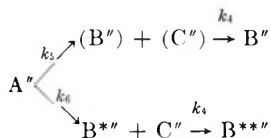
6. Kuhn, W., C. C. Molster, and K. Freudenberg, *Ber.*, **65**, 1179 (1932).
7. Ivanov, V. I., N. Ya. Lenshina, and V. S. Ivanova, *J. Polymer Sci.*, **53**, 93 (1961).
8. Whitaker, D. R., in *Marine Boring and Fouling Organisms*, Dixy Lee Ray, Ed. Friday Harbor Symposia, University of Washington Press, Seattle, 1959.
9. Klemer, A., *Tetrahedron Letters*, No. 22, 5 (1960).
10. Rogovin, Z. A., A. A. Konkin, and Yu. A. Rymashevskaya, *Chem. Abstr.*, **48**, 4449 (1954); *Khim. i Fiz. Khim. Vysokomolekule Soedin. Dokl. k Konf. po Vysokomolekul. Soedin. 7-ya, Konf.*, **1952**, 140.

### Résumé

On montre d'après les données cinétiques de Jones, Dimler et Rist sur l'hydrolyse par catalyse acide de l'isomaltotriitol que la cinétique peut être décrite par des équations de vitesses trouvées par la combinaison de deux réactions consécutives et simultanée (parallèle) et interdépendantes en accord avec le schéma suivant:



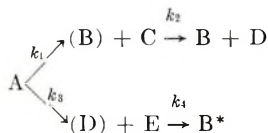
où A: isomaltotriitol; (B), B et B\*: glucose; C: isomaltitol; D et (D): sorbitol et E: isomaltose présent à chaque instant,  $k_1$  et  $k_2$ : vitesses spécifiques à laquelle les deux liaisons glucosidiques sont rompues par l'hydrolyse dans l'isomaltotriitol;  $k_3$ : vitesse spécifique d'hydrolyse de l'isomaltitol (connu);  $k_4$ : vitesse spécifique d'hydrolyse de l'isomaltose (connu). On déduit les valeurs des constantes  $k_1$  et  $k_3$  des valeurs expérimentales de la composition du mélange réactionnel d'hydrolyse et des valeurs connues de  $k_2$  et  $k_4$ . Les rendements en glucose et en sorbitol dépendant du degré d'hydrolyse ont été alors calculés au départ des valeurs de  $k_1$  et  $k_3$  (trouvés) et  $k_2$  et  $k_4$  (connus) en utilisant les équations de vitesse correspondantes du schéma ci-dessus. Elles sont en bon accord avec les valeurs expérimentales. La cinétique de l'hydrolyse acide de l'isomaltotriose peut aussi être décrite par des équations de vitesse correspondant au schéma réactionnel:



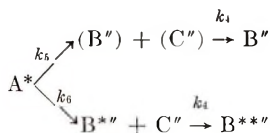
où A'': isomaltotriose; (B''), B'', B\*'' et B\*\*'': glucose; (C'') et C'': isomaltose à chaque instant;  $k_5$  et  $k_6$  sont les vitesses spécifiques de la rupture hydrolytique des deux liaisons glucosidiques dans l'isomaltotriose et  $k_4$  est la vitesse spécifique d'hydrolyse de l'isomaltose (connu). Admettons que  $k_5 = k_4/1.3$  et  $k_6 = k_4/1.5$ , on a calculé les valeurs du degré d'hydrolyse (exprimé en fonction de la rupture de la liaison glucosidique pour 100 liaisons) en utilisant les équations de vitesses provenant du schéma ci-dessus. Elles donnent un bon accord avec les valeurs expérimentales. Cependant, en transposant les valeurs pour  $k_5$  et  $k_6$  on ne modifie pas les valeurs calculées. C'est pourquoi il est seulement permis de tirer les conclusions suivantes: la liaison glucosidique de l'isomaltotriose s'hydrolyse vraisemblablement à une vitesse plus faible que l'isomaltose. De plus il reste à démontrer si la vitesse d'hydrolyse de la partie glucosidique de l'unité réductrice est plus faible que celle de l'unité non-réductrice ou l'inverse. On attire l'attention sur la structure chimique de l'hydrate de carbone théorique qui peut fournir une explication pour les déductions cinétiques dans le domaine de l'hydrolyse du trisaccharide et du bisaccharide.

### Zusammenfassung

Die Kinetik der säurekatalysierten Hydrolyse von Isomaltotriit kann unter Verwendung der Geschwindigkeitsdaten von Jones, Dimler und Rist durch Geschwindigkeitsgleichungen beschrieben werden, die unter der Annahme einer Kombination zweier voneinander abhängiger simultaner ("paralleler") Reaktionen und Folgereaktionen gemäss folgendem Schema abgeleitet wurden:



Dabei bedeuten: A: Isomaltotriit; (B), B und B\*: Glucose; C: Isomaltit; D und (D); Sorbit; E: augenblickliche Konzentration der Isomaltose;  $k_1$  und  $k_2$ : spezifische Geschwindigkeiten der hydrolytischen Spaltung der beiden glucosidischen Bindungen in Isomaltotriit;  $k_3$ : spezifische Geschwindigkeit der Hydrolyse von Isomaltit (bekannt);  $k_4$ : spezifische Geschwindigkeit der Hydrolyse von Maltose (bekannt). Die Werte der Konstanten  $k_1$  und  $k_3$  wurden aus der experimentell bestimmten Zusammensetzung des Hydrolysegemisches und den bekannten Werten von  $k_2$  und  $k_4$  berechnet. Dann wurde die Ausbeute an Glucose und Sorbit sowie das Ausmass der Hydrolyse, unter Verwendung der berechneten Werte von  $k_1$  und  $k_3$  und der Bekannten Werte von  $k_2$  und  $k_4$  mittels der obigen Schema entsprechenden Geschwindigkeitsgleichungen berechnet und in sehr guter Übereinstimmung mit den experimentellen Werten gefunden. Die Kinetik der sauren Hydrolyse von Isomaltotriose kann durch Geschwindigkeitsgleichungen beschrieben werden, die folgendem Schema entsprechen:



Dabei bedeuten: A\*: Isomaltotriose; (B''), B'', B\*'' und B\*\*'': Glucose; (C'') und C'': augenblickliche Konzentration der Isomaltose;  $k_5$  und  $k_6$ : spezifische Geschwindigkeit der hydrolytischen Spaltung der beiden glucosidischen Bindungen in Isomaltotriose;  $k_4$ : spezifische Geschwindigkeit der Hydrolyse von Isomaltose (bekannt). Unter der Annahme  $k_5 = k_4/1,3$  und  $k_6 = k_5/1,5$  wurden Werte für das Ausmass der Hydrolyse (ausgedrückt durch die Anzahl der gespaltenen glucosidischen Bindungen pro 100 Bindungen) mittels der aus obigem Schema abgeleiteten Geschwindigkeitsgleichungen berechnet und in guter Übereinstimmung mit den experimentellen Werten gefunden. Bei Vertauschung der Werte von  $k_5$  und  $k_6$  ändern sich allerdings die berechneten Werte nicht und man kann somit nur folgende Schlüsse ziehen: Die glucosidischen Bindungen in Isomaltotriose werden höchstwahrscheinlich mit einer niedrigeren Geschwindigkeit als Isomaltose hydrolysiert; die beiden Bindungen werden nicht mit gleicher Geschwindigkeit hydrolysiert. Ob die Hydrolyse der glucosidischen Bindung der reduzierenden Einheit langsamer erfolgt als diejenige der glucosidischen Bindung der nichtreduzierenden Einheit oder umgekehrt, muss erst festgestellt werden. Es wird darauf hingewiesen, dass ein Theoretiker auf dem Gebiete der Kohlehydratstruktur möglicherweise eine Erklärung für diese Ableitungen des Kinetikers bei der Hydrolyse sowohl von Tri- als auch von Disacchariden geben kann.

Received May 8, 1963

## Acrylic Anhydrides and Polymers Derived Therefrom\*

JESSE C. H. HWA,† WILLIAM A. FLEMING, and LEON MILLER,  
*Research Laboratory, Rohm and Haas Company, Philadelphia, Pennsylvania*

### Synopsis

The free-radical polymerization of four acrylic anhydrides—methacrylic anhydride, acrylic anhydride, acrylic methacrylic anhydride, and acrylic propionic anhydride—under a variety of conditions has been studied. The polymers and their polyacid and polyester derivatives were characterized by solubility, infrared spectroscopy, and x-ray diffraction. Methacrylic anhydride could be polymerized in bulk and in hydrocarbon solvents from  $-50^{\circ}\text{C.}$  to  $80^{\circ}\text{C.}$  to give soluble, linear cyclopolymers in high conversions. In a polar solvent such as dimethyl sulfoxide, gelation would result at high monomer concentrations and at high conversions. Acrylic anhydride, however, appeared to become crosslinked more readily; soluble polymers could be obtained only by polymerization in nonpolar solvents. Most of the previous and somewhat conflicting results on the cyclopolymerization of these two monomers can now be reconciled by the present findings. The physical properties of cast poly(methacrylic anhydride) suggest that it has a stiff backbone with hindered functional groups and that the monomer itself was perhaps intramolecularly associated. Some improvements in the aqueous hydrolysis of poly(methacrylic anhydride) and in the esterification of the derived polyacid by diazomethane were described. By these refinements, poly(methyl methacrylate), derived from a  $-50^{\circ}\text{C.}$  poly(methacrylic anhydride), had previously been shown to possess a novel, mixed syndiotactic and syndioduotactic (+ + - - + + - -) configuration. Acrylic methacrylic anhydride could be cyclopolymerized very much like methacrylic anhydride. The polyacid and polyester derived from this unsymmetrical anhydride are expected to have unique structures; the acrylic or methacrylic units in the derivatives do not occur more than twice in succession. Acrylic propionic anhydride, when homopolymerized, readily changed to a soluble polymer and an unidentified, immiscible liquid. Its soluble copolymer with methyl methacrylate, however, could be crosslinked by heating. An intramolecular and intermolecular disproportionation reaction was postulated to explain these two interesting observations, respectively.

### INTRODUCTION

Many 1,6-heptadienes are known to undergo what is now known as cyclopolymerization by alternating intramolecular and intermolecular propagation step.<sup>1,2</sup> Acrylic anhydride and methacrylic anhydride were early examples of such monomers.<sup>3-5</sup> The polymers obtained by free-radical polymerization were soluble in certain polar organic solvents and were believed to consist of recurring six-membered anhydride rings. Re-

\* Presented before the Polymer Division of the 144th Meeting of the American Chemical Society, Los Angeles, 1963.

† Present address: Stauffer Chemical Company, Chauncey, New York.

cently some apparently conflicting data have been reported by others. Both acrylic anhydride<sup>6</sup> and methacrylic anhydride<sup>7,8</sup> were shown to give insoluble, crosslinked polymers under certain conditions.

In 1957 we undertook a systematic study of the polymerization characteristics of acrylic anhydrides, the physical properties of the cyclopolymers, and the stereochemical configuration of the polymeric derivatives. In view of the current confusion it appears appropriate that our rather extensive experience on the preparation and behavior of the polyanhydrides be compared with those published. Hopefully some of the gaps in the current understanding of this system may be filled.

This paper therefore is concerned with: (a) a somewhat detailed description of the experimental conditions of cyclopolymerization of acrylic anhydrides so that the reasons for forming either soluble or crosslinked polyanhydrides may be more firmly established; (b) some improvements in the preparation of polyanhydride derivatives; (c) some additional physical properties of the polyanhydrides and their derivatives hitherto not reported; and (d) polymers and derivatives of unsymmetrical acrylic anhydrides.

The stereochemical configuration of poly(methyl methacrylate) derived from poly(methacrylic anhydride) has already been described elsewhere.<sup>9</sup> This paper does furnish the experimental details underlying that work.

## EXPERIMENTAL

### Materials

Unless otherwise specified, commercially available reagent-grade chemicals were used without further purification. Dimethyl sulfoxide (DMS)-was fractionated.<sup>10</sup> Azobisisobutyronitrile (AIBN) was recrystallized from methanol and dried under vacuum at room temperature, m.p. 100°C.

**Monomer Synthesis.** Symmetrical and unsymmetrical anhydride monomers were prepared by the metathesis of an acyl halide and an alkali metal carboxylate.<sup>11</sup> Table I lists the preparative conditions used and the results. As an example, the preparation of acrylic methacrylic anhydride which is apparently new is described below.

In a 1-l. three-necked flask equipped with a stirrer, separatory funnel, thermometer, and reflux condenser was placed a mixture of 108 g. (1 mole) sodium methacrylate, 0.6 g. methylene anthrone, and 500 ml. of reagent-grade benzene. While the contents were stirred, 115 g. (1.27 mole) of acrylyl chloride was added in a period of 20 min. followed by a 3-hr. reflux. Without removal of the precipitate, the benzene was stripped off under diminished pressure and the residue fractionally distilled with stirring through a 15-in. column packed with Cannon Packing (0.16 × 0.16). An oil bath was essential to avoid local superheating. Altogether 129 g. (92.3% yield) of a colorless liquid, b.p. 64°C./4 mm.,  $n_D^{20}$  1.4516, was obtained.

TABLE I  
Synthesis of Acrylic Anhydrides

Monomer	Reactants	Temp., °C.	Time, hr.	Yield, %	B.p., °C./mm.	$n_D^{20}$	Anal.				Infrared absorption, cm. <sup>-1</sup>	
							Calc.	Found	Calc.	Found	Anhydride C=O	C=C
Methacrylic anhydride	K methacrylate methacrylyl chloride	80	2	74.5 <sup>a</sup>	82/8	1.4538	62.34	62.83	6.49	6.53	1780, 1720	1630
Acrylic anhydride	K acrylate acrylyl chloride	25	20	75.5 <sup>b</sup>	26-27/0.20	1.4487	57.14	57.67	4.76	4.95	—	—
Acrylic methacrylic anhydride	Na methacrylate acrylyl chloride	80	3	92.3	64/4.0	1.4516	60.00	60.36	5.71	5.57	1780, 1720	1630
Acrylic propionic anhydride	Na acrylate propionyl chloride	15-20	2	31.0 <sup>b</sup>	31-32/0.5	1.4142	56.25	55.62	5.71	6.95	1800, 1745	1620 <sup>c</sup>

<sup>a</sup> Similar preparations with sodium methacrylate also gave the same monomer in 55-82% yield, b.p. 44-45°C./0.40-0.45 mm.,  $n_D^{20}$  1.4535,  $d_4^{25}$  1.030 g./ml.

<sup>b</sup> Salt removed by filtration before distillation.

<sup>c</sup> About half the intensity of the same absorption of other three monomers.



TABLE II  
 Polymerization of Acrylic Anhydrides

Sample No.	Monomer	Solvent	Monomer concn., %	Catalyst <sup>a</sup>	Temp., °C.	Time, hr.	Yield, %	Product solubility
1	Methacrylic anhydride	None	—	1.0% BPO	50	17.0 <sup>b</sup>	90.5	Soluble
2	"	None	—	BPO/DMA/TP	25	0.5	>50.0	Soluble
3	"	None	—	UV	-50	7.0	60.0	Soluble
4	"	Benzene	10	1.0% BPO	80	5.0	88.0	Soluble
5	"	Toluene	50	UV	-50	7.0	46.0	Soluble
6	"	DMS	15	0.5% AIBN	65	64.0	58.0	Soluble
7	"	DMS	30	0.5% AIBN	65	64.0	64.0	Soluble
8	"	DMS	50	0.5% AIBN	65	64.0	>50.0	Popcorn
9	"	DMS	75	0.5% AIBN	65	64.0	>50.0	Popcorn
10	Acrylic anhydride	None	—	0.5% AIBN	65	64.0 <sup>c</sup>	~95.0	Insoluble <sup>d</sup>
11	"	None	—	UV	-50	3.0	—	Popcorn <sup>e</sup>
12	"	Benzene	15	0.5% BPO	80	4.0	~90.0	Soluble
13	"	Toluene	50	UV	-50	5.0	95.0	Soluble
14	Acrylic methacrylic anhydride	None	—	0.5% AIBN <sup>f</sup>	65	40.0	~95.0	Soluble
15	"	DMS	50	0.5% AIBN	65	16.0	10.0	Soluble
16	"	Benzene	12	0.5% AIBN	80	18.0	99.0	Soluble

17	"g	Benzene	9	0.5% AIBN	80	16.0	98.0	Soluble
18	"g	DMS	50	0.5% AIBN	65	16.0	23.0	Soluble
19	Acrylic propionic anhydride	None	—	1.0% BPO	60-80	1.0	— <sup>b</sup>	Soluble
20	"	None	—	BPO/DMA/TP	25	16.0	— <sup>b</sup>	Soluble
21	"	None	—	UV	-50	6.0	— <sup>b</sup>	Soluble
22	"i	Toluene	50	UV	25	3.0	35.0	Soluble <sup>k</sup>
23	"j	None	—	BPO/DMA/TP	25	1.0	Good	Soluble

<sup>a</sup> AIBN = azobisisobutyronitrile; BPO = benzoyl peroxide; BPO/DMA/TP = benzoyl peroxide/dimethylamine/thiobhenol; UV = ultraviolet irradiation.

<sup>b</sup> Cured at 125°C. for 2 hr. and at 140°C. for 3 hr.

<sup>c</sup> Cured at 120°C. for 2 hr.

<sup>d</sup> Also insoluble in boiling water.

<sup>e</sup> Clear, rigid gel at -50°C., but immediately popcorn-polymerized in the sealed tube on warming to room temperature.

<sup>f</sup> Triton X-770 as mold release agent.

<sup>g</sup> Monomer consisted of equal parts of the anhydride and methacrylic anhydride.

<sup>h</sup> A clear, rigid polymer and a supernatant liquid of about equal volumes were obtained. The rigid polymer was soluble in dimethyl sulfoxide.

<sup>i</sup> Monomer consisted of 1 part of the anhydride and 4 parts of methyl methacrylate.

<sup>j</sup> Monomer consisted of 1 part of the anhydride and 2 parts of methacrylic anhydride.

<sup>k</sup> Copolymer isolated by precipitating the benzene solution from hexane. Infrared absorption spectra showed anhydride absorption at 1040 and 1815 cm.<sup>-1</sup>. The dry copolymer became crosslinked (insoluble in boiling benzene or dimethyl sulfoxide) after 30 min. heating at 145°C.

### Polymerization

**Cast Polymerization.** Polyanhydrides were prepared in a sheet form between glass molds. A commercial dough inserted between the clamped glass plates served as the confining material.<sup>12</sup> The inside walls of the plates were pretreated with G. E. Dry Film SC-87 or Triton X-100 as the mold release agent. After the acrylic monomer containing 0.5–1.0% of either azobisisobutyronitrile (AIBN) or benzoyl peroxide (BPO) was charged into the cavity of the mold by a syringe, the assembly was placed in a 50–65°C. oven for at least 16 hr. and then at elevated temperatures for several more hours. The exact heating cycle for each monomer is listed in Table II. Transparent cast sheets up to  $\frac{1}{8}$  in. in thickness could be obtained. Conventional cellophane<sup>12</sup> should be avoided as a confining material because all the anhydrides would “popcorn” polymerize.

**Precipitation Polymerization.** A mixture of monomer (20–30 g.), azobisisobutyronitrile (1.0% based on monomer), and benzene (generally 200–300 ml.) was charged to a 500-ml. three-necked flask equipped with stirrer, reflux condenser, and glass stopper. The contents were refluxed, by an oil bath, for 8 hr. or more. The polymer generally precipitated from the medium as swollen particles. The product was removed by filtration, washed with benzene, and then dried at 65°C. for 6 hr. The yield generally was 90–95%.

**Solution Polymerization in Dimethyl Sulfoxide.** Under a nitrogen atmosphere, 15–75% solutions of methacrylic anhydride in dimethyl sulfoxide containing 0.5% azobisisobutyronitrile (based on monomer) were heated, with stirring, in a suitable three-necked flask at 65°C. for 64 hr. In two experiments where viscous amber solutions were obtained, the polymer was isolated by precipitation from excess (tenfold) methanol.

**Room Temperature Polymerization.** Some polymerizations were done with benzoyl peroxide–dimethylaniline as catalyst and a trace of thiophenol as activator (BPO/DMA/TP).<sup>13</sup> At room temperature reasonably rapid polymerization rates were obtained.

**Polymerization by Ultraviolet Irradiation at –50°C.** The acrylic anhydrides have been polymerized by ultraviolet irradiation at –50°C. About 10–30 ml. of the monomer or its solution in toluene was placed in a 50-ml. glass ampule containing 5–50 mg. of benzoin as photosensitizer. The contents were degassed on a vacuum-line by conventional freeze-thaw techniques and then sealed off at  $1 \times 10^{-6}$  mm. while frozen by liquid nitrogen. The ampule was placed in a methanol bath in a transparent Dewar flask. A battery of 4 Sylvania Black Light tubes was placed about 2–3 in. from the ampules. The methanol bath was maintained at  $-50 \pm 1^\circ\text{C}$ . by means of a Dry Ice–acetone cold finger and by a combination of a Therm-O-Watch and a Jack-O-Matic (Instruments for Research and Industry, Cheltenham, Pa.) which automatically regulated the immersion of the cold finger. After 6–7 hr. of irradiation, the contents generally became a rigid, transparent plug. The tube was then opened and the plug

broken up. The swollen polymer was washed twice with 300-ml. portions of *n*-hexane. The white polymer was then dried in vacuum at 55°C. for 16 hr.

### Characterization of Polymers

**Infrared Spectroscopy.** Infrared absorption spectra of the monomers, polymers, and derivatives were obtained with a Perkin-Elmer infrared spectrophotometer model 21. The polyanhydrides and their acid derivatives were examined in the form of a Nujol mull. The polyesters were either deposited as a film on silver chloride or examined in chloroform solution with compensating chloroform cells.

**Solubility.** All the polyanhydrides were insoluble in common organic solvents, either at room or elevated temperatures within a period of several hours. Many samples, as indicated in Table II, however, were soluble in dimethylformamide or dimethyl sulfoxide at room temperature overnight,

TABLE III  
Some Characterization of Polyacids and Polyesters Derived from Poly(acrylic Anhydrides)

Parent sample	Polyanhydride and its derivatives	Notable infrared absorption bands, cm. <sup>-1</sup>	X-ray diffraction
5	Poly(methacrylic anhydride)	1750, 1815	Asymmetrical
	Poly(methacrylic acid)	Weak band at 1640	Asymmetrical
	Poly(methyl methacrylate)	1170, 1265 <sup>a</sup>	Asymmetrical
	Poly(ethyl methacrylate)	<i>J</i> value 93 <sup>b</sup> *	Asymmetrical
13	Poly(acrylic anhydride)	1735, 1800	—
	Poly(acrylic acid) <sup>d</sup>	Weak band at 1620	Asymmetrical
	Poly(methyl acrylate)	1155, 1230 <sup>a</sup>	Amorphous
	Poly(ethyl acrylate)	—	Amorphous
16	Poly(acrylic methacrylic anhydride)	1735, 1800	—
	Poly(acrylic acid-co-methacrylic acid)	Weak band at 1620	—
	Poly(methyl acrylate-co-methyl methacrylate)	3500, 1290, 955-915 <sup>e,f</sup> 955 <sup>g</sup>	—

<sup>a</sup> Infrared spectrum almost identical to that of the corresponding polyacid prepared directly from the monomer by free radical polymerization; absence of anhydride absorption.

<sup>b</sup> Described in ref. 9; gel m.p.: 40°C. (see ref. 24).

<sup>c</sup> Intermediate between the spectra of syndiotactic and isotactic poly(ethyl methacrylates) (unpublished information); absence of residual anhydride or acid bands.

<sup>d</sup> Without separating the polyanhydride from the toluene solvent, the mixture was boiled with deionized water for 1.5 hr., steam-distilled, and then freeze-dried. The polyacid reacted with diazomethane and diazoethane readily.

<sup>e</sup> These are not major absorption bands, but are bands having greater intensity than those of the random copolymer.

<sup>f</sup> Absence of a band at 1050 cm.<sup>-1</sup>.

<sup>g</sup> In chloroform solution and as film on silver chloride.

or at 110–135°C. almost instantly. On the other hand, some other samples listed in Table II as well as some known crosslinked copolymers of methacrylic anhydride and methyl methacrylate<sup>11</sup> were found to be insoluble under the same conditions, even with prolonged heating periods. The infrared absorption spectra of poly(methacrylic anhydride) (sample 5, Table III), for example, remained essentially unchanged before and after precipitating the polymer in dimethyl sulfoxide solution from methanol. Hence the dissolution is believed to be a genuine property of a linear, uncrosslinked cyclopolymer, and is not a result of severing or "reshuffling" the anhydride crosslinks of an otherwise crosslinked polyanhydride.

**Ammonolysis.** Poly(methacrylic anhydride) (sample 3, Table II) dissolved readily in excess aqueous ammonia at room temperature. On freeze-drying, the product had 7.96% N which corresponded to the composition of a 1:1 poly(methacrylic acid-*co*-methacrylamide).

**Hydrolysis.** Poly(acrylic anhydride) and poly(acrylic methacrylic anhydride) were readily hydrolyzed by boiling water, while poly(methacrylic anhydride) was not. It was found that an aqueous solution containing 15–25% dioxane was particularly effective in hydrolyzing the latter. The following examples illustrate this simple modification.

A mixture of 2.0 g. of poly(methacrylic anhydride) (sample 4, Table II) and 50 ml. deionized water was refluxed in a flask previously rinsed with dilute hydrochloric acid and excess deionized water. After 26 hr. of boiling, the powdery polymer remained unchanged! Dioxane (10 ml.) was then added. After 1 hr. of reflux, the polymer dissolved.

In a similar manner, a mixture of 10.5 g. of –50°C. poly(methacrylic anhydride) (sample 5, Tables II and III), 15 ml. of freshly distilled dioxane, and 120 ml. of deionized water was refluxed for 2.5 hr. The polymer did not dissolve. After additional 15 ml. dioxane and 45 min. reflux, complete solution resulted. The solution was refluxed for 4 hr. more, filtered, and steam-distilled. The distillate, amounting to 300 ml., was discarded. The solution was filtered and freeze-dried. After drying in vacuum at 50°C. for 16 hr., the polyacid derivative weighed 11.3 g.

**Esterification of Polyacids Derived from Polyanhydrides.** The procedure of esterifying a polyacid with diazoalkane was essentially that of Katchalsky and Eisenberg.<sup>14</sup> In preparing the methyl esters of some samples, the esterification apparently was complete in 1 hr. by mixing the polyacid and excess diazomethane<sup>15</sup> in benzene.

In many cases, however, complications were observed in this esterification step. It was found that often a substantial portion of the polyacid remained insoluble in benzene even with repeated additions of the reagent. This partial solubility, also noted by others,<sup>3</sup> was more pronounced when the polyacid was obtained by alkaline hydrolysis followed by ion-exchange.<sup>16</sup> Possibly a small fraction of alkali metal salts in the polyacid, either inadvertently formed or incompletely converted by ion exchange, could cause this solubility problem. A related undesirable effect was that in using large excess of diazomethane, for example, some polymethylene was



also formed. This polymeric impurity, if not removed, would interfere with subsequent x-ray characterization of the polyester.

An effective purification step was worked out. The following procedure is an example. To 5.8 g. (68 meq.) of poly(methacrylic acid) (derived from sample 5, see Table II and Table III) was added an estimated 160 meq. of freshly prepared and dried diazomethane in benzene.<sup>15</sup> After 1 hr. of standing at room temperature, the solution was filtered. An insoluble residue of 0.2 g. remained. The filtrate was freeze-dried, yielding 6.4 g. of polymer. Infrared absorption spectra of this product showed weak bands corresponding to water, and carboxylate salt; residual carboxylic acid groups were absent. All the polymer was now dissolved in about 200 ml. of dioxane. The solution was added to 2 l. of  $\sim 0.05N$  hydrochloric acid with stirring. After standing overnight, the polymer was isolated by filtration and allowed to stand with another charge of the dilute acid for 2 hr. Finally the polymer was washed free from acid with deionized water. The dried polymer, weighing 5.3 g., was dissolved in benzene and mixed with approximately 40 meq. of diazomethane in benzene. The yellow color remained even on warming. The resulting solution (ca. 100 ml.) was precipitated from 1 l. of hexane. After filtration and repeated washings, the dried polymer weighed 4.8 g. (some mechanical loss). Infrared spectroscopy now showed the absence of water and carboxylate groups. X-ray diffraction also showed the absence of polymethylene. The viscosity-average molecular weight of the polyester was 213,000.<sup>9</sup>

Ethyl esters of the polyacids were prepared by reacting the polyacid with diazoethane in ether-benzene mixture, followed by freeze-drying. Diazoethane was freshly prepared from ethyl *N*-nitrosoethylcarbamate by a known procedure.<sup>17,18</sup>

Table III lists the polyacids and polyesters derived from the polyanhydrides and the results of some x-ray diffraction and infrared spectroscopy.

## DISCUSSION

### Monomer Synthesis

Four monomers—acrylic anhydride, methacrylic anhydride, acrylic methacrylic anhydride, and acrylic propionic anhydride—have been synthesized by coupling the appropriate acyl halides with alkali metal acrylates (Table I). The constancy of boiling points and the correctness of elementary analysis of the first three monomers were believed sufficient to establish the purity of these monomers. Acrylic propionic anhydride was prepared under very mild conditions. From its C, H content, and refractive index this monomer probably contained some disproportionated propionic anhydride as impurity. But the authenticity of the assigned structure was based on the correct shift of 20–25  $\text{cm.}^{-1}$  in the C=O absorption and the expected intensity of the C=C absorption in the infrared spectrum of this compound.<sup>19</sup>

Synthesis of several other unsymmetrical acrylic anhydrides was attempted but not successful. These monomers—methacrylic isobutyric anhydride, dimethacrylic fumaric anhydride, methacrylic benzoic anhydride, and methacrylic cinnamic anhydride (sodium methacrylate and the corresponding acyl chlorides used in all cases)—could not be isolated in a reasonable pure state by vacuum distillation. In all cases the disproportionated, symmetrical product, or a mixture of it and the desired product, was obtained.

### Polymerization of Symmetrical Anhydrides

Both methacrylic anhydride and acrylic anhydride have been polymerized by free-radical catalysts (Table II). By bulk or solution polymerizations at  $-50^{\circ}\text{C}.$  to  $80^{\circ}\text{C}.$ , about 50–99% conversions have been achieved. Also, depending on the conditions used, the polymers obtained could be either soluble or insoluble in dimethyl sulfoxide or dimethylformamide. (Based on the evidence described in the Experimental section, solubility of the polyanhydrides in these polar solvents was a sufficient criterion to determine if the cyclopolymer was crosslinked or not.)

These findings are in reasonable agreement with those reported by most other workers. Based on the results shown in Table II, methacrylic anhydride is seen to be readily polymerized to give soluble, linear cyclopolymers either in bulk or in nonpolar solvents.<sup>5</sup> In a polar solvent such as dimethyl sulfoxide or dimethylformamide,<sup>8</sup> crosslinked “popcorn”<sup>20</sup> polymers were obtained at high monomer concentrations and at high conversions. Acrylic anhydride appears to be more readily crosslinkable;<sup>6</sup> soluble polymers were obtained only by solution polymerization.

A reasonably consistent picture of the cyclopolymerization of acrylic anhydrides can now be arrived at. There is little doubt that linear poly-(acrylic anhydrides) having recurring cyclic anhydride units can indeed be obtained by Butler’s mechanism.<sup>1</sup> The preponderance of the cyclization step, however, would depend on the nature of the monomer and its environment. Evidently occasional pendent vinyl groups may result as evidenced by weak infrared absorption bands at  $1620\text{--}1630\text{ cm.}^{-1}$  (see Table III) for the soluble polyanhydrides. The formation of pendent vinyl groups by noncyclization apparently is appreciably less severe with methacrylic than acrylic anhydride; the former is capable of surviving bulk polymerization without gelation. The difference between the behavior of methacrylic anhydride in a nonpolar and a polar solvent suggests that the monomer is intramolecularly associated in bulk or in nonpolar solvents. This point, brought up in an earlier publication,<sup>10</sup> does not seem to be unreasonable. Polar solvents very likely could break up the association to a large extent and the monomer then is more liable to undergo crosslinking. High monomer concentration and high conversions accentuate gelation.<sup>10</sup>

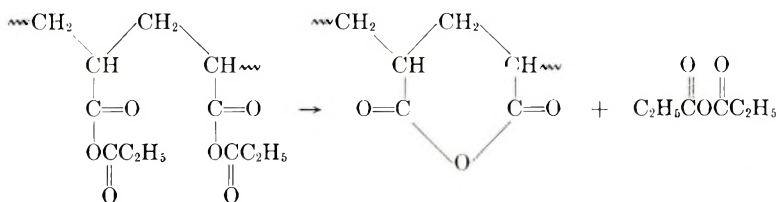
The reason why Tiers and Bovey obtained crosslinked poly(methacrylic anhydride) by bulk and solution polymerization (toluene as solvent)<sup>7</sup>

remains unclear. Since these workers did not describe the purity of the monomer used, it is not possible to resolve the discrepancy at this time.

### Polymerization of Unsymmetrical Anhydrides

Acrylic methacrylic anhydride has been homopolymerized and copolymerized with methacrylic anhydride to give soluble cyclopolymers. The behavior of this unsymmetrical divinyl monomer is similar to that of methacrylic anhydride itself. The derivatives of poly(acrylic methacrylic anhydride) are of some interest and will be described later.

Acrylic propionic anhydride has been homopolymerized in bulk at first to a linear polymer, which, at room temperature and even at  $-50^{\circ}\text{C}.$ , spontaneously changed to a rigid gel and a separate liquid phase (samples 19–21, Table II). The gel was soluble in dimethyl sulfoxide, and the liquid, though not positively identified, was believed to be propionic anhydride. This facile change may be interpreted by an intramolecular disproportionation reaction:



A sample of soluble 4:1 poly(methyl methacrylate-*co*-acrylic propionic anhydride) (sample 22, Table II) exhibited an interesting second-stage cross-linking induced by heat (see Table II, footnote k). The difference between the behavior of the homopolymer and the copolymer is that in the latter case, many anhydride units were flanked by methyl methacrylate units on both sides. Possibly because of these isolated anhydride units, an intermolecular disproportionation could now cause gelation.

### Properties of Cast Poly(methacrylic Anhydride)

After many attempts, a clear poly(methacrylic anhydride) sheet was successfully obtained by conventional techniques<sup>12</sup> and by using an appropriate mole releasing agent (sample 1, Table II). The physical properties of this bulk polymer, shown in Table IV, have several interesting aspects.

The density of the cyclopolymer points to a clue of the driving force of cyclopolymerization. From the specific gravity of its polymer, the molar shrinkage (based on each double bond) of methacrylic anhydride is very small. The value of 13.7 ml./mole of unsaturation which is one-half of 27.4 ml./mole for the divinyl monomer is very much smaller than the 22–23 ml./mole of unsaturation for many acrylic esters and glycol diacrylates.<sup>21</sup> In fact, from volume shrinkage standpoint, methacrylic anhydride is more like a monomer with one double bond than two. The density data lend

TABLE IV  
Physical Properties of Cast Poly(methacrylic Anhydride)

Test	Result
Specific gravity, 25°/25°C.	1.256 <sup>a</sup>
Refractive index, $n_D^{25}$	1.520
Vicat softening temperature (10 mils), °C.	159 <sup>b</sup>
Barcol hardness	64
Water sorption at 23°C., 4 hr., %	0.11
Water sorption at 23°C., 24 hr., %	0.41
Water sorption at 23°C., 7 days, %	2.16
Residual monomer, %	0.46
Decomposition temperature, °C.	172-175 <sup>c</sup>

<sup>a</sup> Corresponding to a molar shrinkage of 27.4 ml. (25°C.)

<sup>b</sup> Correlatable to ASTM D647 heat distortion temperature of 140°C. Vicat softening temperature of commercial cast poly(methyl methacrylate): 113-115°C.

<sup>c</sup> Evolution of an unidentified gas.

some support to the hypothesis that the two vinyl groups of methacrylic anhydride are associated. It has been postulated<sup>22</sup> and supported by others<sup>21</sup> that the volume shrinkage accompanying the polymerization of a vinyl monomer is the result of the exchange of a double bond and a van der Waals bond for two covalent bonds. The low volume contraction suggests that methacrylic anhydride does not seem to possess two independent double bonds. If the volume shrinkage hypothesis were indeed correct, it would appear that the van der Waals bond between the two vinyl groups belonging to methacrylic anhydride is not the same as that between one methacrylic anhydride molecule and another. This inferred intramolecular association could be the driving force of cyclopolymerization.<sup>10</sup>

Poly(methacrylic anhydride) is a brittle, hard polymer having a Vicat softening temperature of 159°C. which is estimated to correspond to a glass temperature of about 144°C. Direct determination of the glass temperature by conventional dilatometry was not reliable because the polymer could not be degassed at elevated temperatures without decomposition. The relative inertness of the cast poly(methacrylic anhydride) toward water is also noteworthy. These properties are consistent with those expected linear polymers having a stiff backbone and hindered functional groups.

### Stereochemical Configuration of Poly(methyl Methacrylate) Derived from -50°C. Poly(methacrylic Anhydride)

One of the aims of this work, as explained in the Introduction, was to determine the stereochemical configuration of poly(methacrylic anhydride) and its derivatives. It was thought that the formation of the cyclic anhydride rings during polymerization would improve a steric control over the configuration of the backbone different from that experienced during the free-radical polymerization of ordinary vinyl monomer. This anticipation was also arrived at independently by Butler.<sup>23</sup>



Some careful experiments designed to convert the poly(methacrylic anhydride) successively to the polyacid and then to the corresponding poly(methyl methacrylate) were carried out. A low temperature ( $-50^{\circ}\text{C}.$ ) polymer (sample 5) was selected for this study because it was felt that whatever steric control there was would be enhanced at low temperatures. Improvements in the hydrolysis and esterification steps have already been described in the Experimental section. The final polyester was characterized by a variety of methods and was compared to syndiotactic and isotactic poly(methyl methacrylates).

Based on primarily the NMR data, the stereochemical configuration of the poly(methyl methacrylate) derived from  $-50^{\circ}\text{C}.$  poly(methacrylic anhydride) was believed to be composed of a random run of syndiotactic (+ - + - + -) and syndioduotactic (+ + - - + + - -) blocks of various lengths.<sup>9</sup> The basis of this conclusion has already been described elsewhere by one of us (J. C. H. H.) and will not be repeated here.<sup>9</sup>

There is, however, one new piece of evidence with respect to the stereochemical nature of this poly(methyl methacrylate): the gel melting point of this polymer with Type II poly(methyl methacrylate) was  $40^{\circ}\text{C}.$ <sup>24</sup> (see footnote b, Table III). This gel melting point corresponds to that for an atactic poly(methyl methacrylate) prepared thermally at  $165^{\circ}\text{C}.$ <sup>25</sup> This comparison seems contradictory, since the present sample was derived from poly(methacrylic anhydride) prepared at  $-50^{\circ}\text{C}.$  One is led to conclude, therefore, that the stereochemical configuration of the poly(methyl methacrylate) derived from the anhydride is not the same as that of an ordinary atactic analog, even though the gel melting point of both polymers may be the same.

### Other Polyacid and Polyester Derivatives of the Polyanhydrides

Because of the interest in stereochemical aspect of the polyanhydrides, several polyacids and their methyl and ethyl esters have been prepared. The derivatives and their infrared and x-ray data are listed in Table III.

The parent polyanhydrides were characterized by the doublet C=O absorption and by a minor weak residual double bond absorption. Poly(acrylic acid) showed an asymmetrical x-ray diffraction but its methyl and ethyl esters had only amorphous patterns. These findings are in agreement with those by others.<sup>3,4,8</sup>

The polyacid and polyester derivatives of poly(acrylic methacrylic anhydride) are of some special interest. Since the recurring cyclic anhydride unit consisted of an acrylic and methacrylic group, the polyacid and polyester derived from the cyclopolymer must have one of the following three structures:





where A and B are, respectively, acrylic acid and methacrylic acid (or their corresponding methyl esters). The first two structures have regular structural (not to be confused with stereochemical configuration) sequences, while the third has a random one. In any event these derivatives are 1:1 copolymer of monomers A and B where no monomer unit occurs more than twice in succession. Such a structure can not be obtained directly from A and B under ordinary conditions of polymerization.

The infrared absorption spectra of poly(acrylic acid-co-methacrylic acid) and poly(methyl acrylate-co-methyl methacrylate) derived from poly(acrylic methacrylic anhydride) were compared with a random copolymer of acrylic acid and methacrylic acid and its methyl ester prepared by using diazomethane. The random copolymer (1:1 by weight) was prepared from aqueous solution using a free-radical catalyst. The spectra of the polyacid set and the polyester set were practically identical except for several bands where significant differences were observed. These differences, noted in Table III, did not appear to be due to the slightly higher methacrylic content (by weight) of the cyclopolymer derivatives. One is tempted to attribute them to the sequential difference between the regular copolymer and the random copolymer.

The NMR spectra of the same two sets of polyacids and polyesters were determined at room temperature in ca. 10% chloroform solutions with a Varian HR-60 spectrophotometer. No differences in the spectra were observed at obtainable resolution levels.

The authors wish to express their appreciation to Mr. O. H. Loeffler who encouraged the undertaking of this work, to Mr. W. Schaffer for his assistance in portions of the experiments, and to many members of the Rohm and Haas Research Laboratories for determining some of the physical data reported herein.

### References

1. Butler, G. B., *J. Polymer Sci.*, **48**, 279 (1960).
2. Marvel, C. S., *J. Polymer Sci.*, **48**, 101 (1960).
3. Crawshaw, A., and G. B. Butler, *J. Am. Chem. Soc.*, **80**, 5464 (1958).
4. Jones, J. F., *J. Polymer Sci.*, **33**, 15 (1958).
5. Miller, W. L., W. S. Brey, Jr., and G. B. Butler, *J. Polymer Sci.*, **54**, 329 (1961).
6. Mercier, J., and G. Smets, *J. Polymer Sci.*, **57**, 763 (1962).
7. Tiers, G. V. D., and F. A. Bovey, *J. Polymer Sci.*, **47**, 479 (1960).
8. Gibbs, W. E., and J. T. Murray, *J. Polymer Sci.*, **58**, 1211 (1962).
9. Hwa, J. C. H., *J. Polymer Sci.*, **60**, S12 (1962).
10. Hwa, J. C. H., and L. Miller, *J. Polymer Sci.*, **55**, 197 (1961).
11. Brotherton, T. K., J. Smith, Jr., and J. W. Lynn, *J. Org. Chem.*, **26**, 1283 (1961) and many references cited therein.
12. Schildknecht, C. E., *Polymer Processes*, Interscience, New York, 1956, p. 56.
13. Horner, L., and E. Schwenk, *Ann.*, **566**, 69 (1949).
14. Katchalsky, A., and H. Eisenberg, *J. Polymer Sci.*, **6**, 145 (1951).
15. Bachman, W. E., and W. S. Struve, *Organic Reactions*, Vol. I, Wiley, New York, 1942, Chap. 2.
16. Unpublished information.
17. *Organic Synthesis*, Coll. Vol. II, Wiley, New York, 1943, pp. 278, 464.
18. Wilds, A. L., and A. L. Meader, *J. Org. Chem.*, **13**, 763 (1948).

19. Bellamy, L. J., *The Infrared Spectra of Complex Molecules*, 2nd Ed., Wiley, New York, 1958.
20. Staudinger, H., and E. Husemann, *Ber.*, **68B**, 1618 (1935).
21. Loshak, S., and T. G. Fox, *J. Am. Chem. Soc.*, **75**, 3544 (1953).
22. Tobolsky, A. V., F. Leonard, and G. P. Roeser, *J. Polymer Sci.*, **3**, 604 (1948).
23. Butler, G. B., *Pure Appl. Chem.*, **4**, 299 (1962).
24. Watanabe, W. H., C. F. Ryan, P. C. Fleischer, Jr., and B. S. Garrett, *J. Phys. Chem.*, **65**, 896 (1961).
25. Graham, R. K., D. I. Dunkelberger, and J. R. Panchak, *J. Polymer Sci.*, **59**, S43 (1962).

### Résumé

On a étudié la polymérisation radicalaire de quatre anhydrides acryliques: l'anhydride méthacrylique, l'anhydride acrylique, l'anhydride acrylique méthacrylique et l'anhydride acrylique propionique. Sous différentes conditions on a caractérisé les polymères et leurs dérivés polyacides et polyesters par solubilité, spectroscopie infra-rouge et diffraction aux rayons-X. On peut polymériser l'anhydride méthacrylique en bloc et dans des solvants hydrocarbonés de  $-50^{\circ}\text{C}$  à  $80^{\circ}\text{C}$ , ce qui fournit des copolymères solubles, linéaires à haute conversion. Dans un solvant polaire tel que le diméthylsulfoxyde, la gélification devrait être atteinte à concentration élevée en monomère et à conversion élevée. L'anhydride acrylique, cependant, commence à former des pontages plus rapidement; on obtient seulement des polymères solubles par polymérisation dans des solvants non-polaires. On a remanié la plupart de ces résultats prévus et quelque peu contradictoires sur la copolymérisation de ces deux monomères à partir des présentes recherches. Les propriétés physiques de polyanhydrides méthacryliques précipités suggèrent la présence d'une chaîne principale rigide portant des groupes fonctionnels stériquement empêchés et le monomère lui-même peut être associé intramoléculairement. On décrit quelques améliorations dans l'hydrolyse aqueuse de polyanhydride méthacrylique et dans l'estérification des dérivés de polyacides par le diazométhane. Par ces raffinements on a montré précédemment que le polyméthacrylate de méthyle dérivé de polyanhydride méthacrylique à  $-50^{\circ}\text{C}$  possédait une nouvelle configuration, mélange de syndiotactique et syndioduotactique (+ + - - + + - -). L'anhydride acrylique méthacrylique peut facilement cyclopolymériser comme l'anhydride méthacrylique. Les polyacides et polyesters dérivés de ces anhydrides non symétriques sont tels que les unités acryliques ou méthacryliques dans les dérivés ne peuvent pas se succéder plus de deux fois. L'anhydride acrylique propionique, homopolymérisé, se transforme rapidement en un polymère soluble et en un liquide immiscible non-identifié. Son copolymère soluble avec le méthacrylate de méthyle peut cependant former des pontages par chauffage. On envisage une réaction de disproportionnement intramoléculaire et intermoléculaire respectivement pour expliquer ces deux observations intéressantes.

### Zusammenfassung

Die radikalische Polymerisation von vier Acrylanhydriden—Methacrylsäureanhydrid, Acrylsäureanhydrid, Acrylsäure-Methacrylsäureanhydrid und Acrylsäure-Propionsäureanhydrid—wurde unter verschiedenen Bedingungen untersucht. Die Polymeren und ihre Polysäure- und Polyesterderivate wurden durch Löslichkeit, Infrarotspektrum und Röntgendiagramm charakterisiert. Methacrylsäureanhydrid konnte in Substanz und in Kohlenwasserstofflösung bei  $-50^{\circ}\text{C}$  bis  $80^{\circ}\text{C}$  bei hohem Umsatz zu löslichen, linearen Cyclopolymeren polymerisiert werden. In einem polaren Lösungsmittel wie Dimethylsulfoxid erfolgt bei hoher Monomerkonzentration und hohem Umsatz Gelbildung. Acrylsäureanhydrid zeigt hingegen grössere Neigung zur Vernetzung; lösliche Polymere konnten nur durch Polymerisation in nichtpolaren Lösungsmitteln erhalten werden. Die meisten früheren, etwas widerspruchsvollen Ergebnisse über die Cyclopolymerisation

dieser beiden Monomeren können durch die jetzigen Befunde in Einklang gebracht werden. Die physikalischen Eigenschaften von gegossenem Polymethacrylsäureanhydrid sprechen dafür, dass es eine steife Hauptkette mit gehinderten funktionellen Gruppen besitzt und dass das Monomere selbst vielleicht intramolekular assoziiert ist. Einige Verbesserungen bei der wässrigen Hydrolyse von Polymethacrylsäureanhydrid und bei der Veresterung der abgeleiteten Säure mit Diazomethan wurden beschrieben. Mit Hilfe dieser Verfeinerungen wurde schon früher gezeigt, dass Polymethylmethacrylat aus einem  $-50^{\circ}\text{C}$ -Polymethacrylsäureanhydrid eine neuartige, gemischt syndiotaktische und syndioduotaktische (+ + - - + + - -)-Konfiguration besitzt. Das gemischte Acrylsäure-Methacrylsäureanhydrid verhielt sich in bezug auf die Cyclopolymerisation dem Methacrylsäureanhydrid sehr ähnlich. Die von diesem unsymmetrischen Anhydrid abgeleiteten Polysäuren und Polyester lassen eigenartige Strukturen erwarten: die Acrylsäure- oder Methacrylsäurereste folgen in den Derivaten nicht öfter als zweimal aufeinander. Acrylsäure-Propionsäureanhydrid gibt bei der Homopolymerisation leicht ein lösliches Polymeres und eine nicht identifizierte, nicht mischbare Flüssigkeit. Seine löslichen Copolymeren mit Methylmethacrylat konnten hingegen durch Erhitzen vernetzt werden. Zur Erklärung dieser beiden interessanten Befunde wurde das Auftreten einer intramolekularen bzw. intermolekularen Disproportionierungsreaktion angenommen.

Received April 24, 1963

## Electron Exchange Polymers. XX. Preparation and Polymerization of Vinylbis(1-ethoxyethyl)-hydroquinone

ROBERT E. MOSER, HIROYOSHI KAMOGAWA, HEINRICH HARTMANN, and HAROLD G. CASSIDY, *Sterling Chemistry Laboratory, Yale University, New Haven, Connecticut*

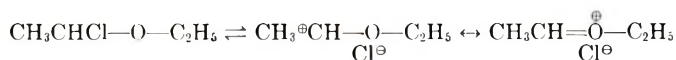
### Synopsis

The monomer vinylbis(1-ethoxyethyl)hydroquinone, [vinylhydroquinonebis(ethyl acetal)], was prepared by reacting bromohydroquinone with vinyl ethyl ether,  $\alpha$ -chloroethyl ethyl ether being used as catalyst with great care to exclude moisture. The resulting bromohydroquinonebis(ethyl acetal) was subjected to lithium-bromine exchange followed by reaction with ethylene oxide. The resulting  $\beta$ -hydroxyethylhydroquinone bis(ethyl acetal) was dehydrated to the desired monomer over potassium hydroxide at 235°. The overall yield from bromohydroquinone to purified monomer averaged 42%. The monomer polymerized under radical or anionic initiation. Polymer produced under radical initiation showed (in most instances) an intrinsic viscosity in benzene of the order of 0.32 at 29.7°C. The polymer is readily cleaved by dilute methanolic hydrochloric acid to give a polyvinylhydroquinone. A polyvinylhydroquinone prepared under anionic initiation showed an intrinsic viscosity of 0.34 in 90% methanol at 29.7°C. The polymer showed redox properties.

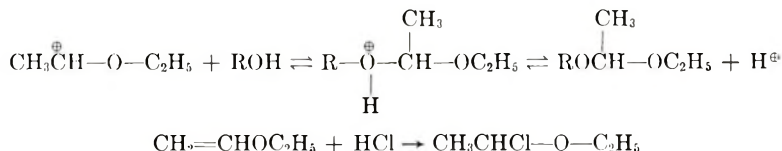
The investigation of polyvinylhydroquinone<sup>1</sup> has been hindered by lack of a completely suitable monomer. An ideal monomer would be a vinylhydroquinone, the phenolic hydrogens of which have been replaced with groups that do not retard polymerization, that can be removed easily from the polymer when it has been prepared, and that yield unreactive byproducts. Stern's vinyl bis(methoxymethyl)hydroquinone<sup>2</sup> comes close to fulfilling these requirements, but acid hydrolysis of this diacetal yields formaldehyde, which can react with the hydroquinone residues and which, in actual use, produces crosslinking.

Acetaldehyde is known to attack phenols under acid conditions,<sup>3</sup> and at the same time it undergoes self-condensation. However, the former reaction is more sluggish than that of formaldehyde, and the self-condensation polymers are water-soluble when of low molecular weight so that they are readily separated out. Thus it seemed reasonable to investigate the behavior of the acetaldehyde acetal as a protecting group for vinylhydroquinone. Acetals of this kind have been made with phenols,<sup>4</sup> and it remained to adapt the technique to a hydroquinone, using a suitable acid catalyst. The acid catalyst of choice is  $\alpha$ -chloroethyl ethyl ether, a very

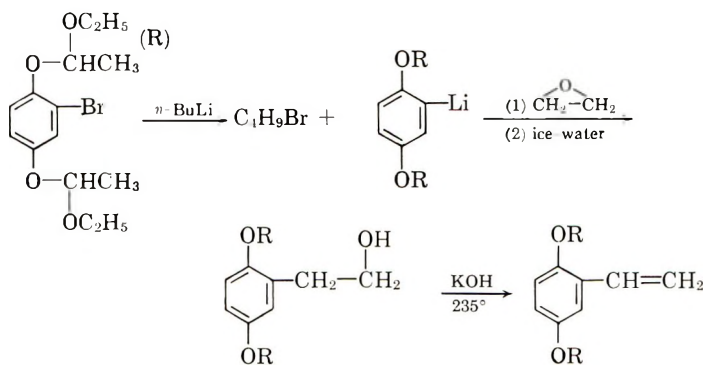
reactive substance that yields a relatively stable carbonium ion. This appears to be reactive species:



This ion, reacting with the hydroxyl group, yields an acetal and  $\text{H}^\oplus \text{Cl}^\ominus$ . The latter, in the presence of vinyl ether, continues the reaction:



When bromohydroquinone is reacted with vinyl ethyl ether, with suitable precautions, in the presence of a small ratio of  $\alpha$ -chloroethyl ethyl ether, the reaction goes essentially to completion in a short time. (Methyl vinyl ether could probably be used,<sup>5</sup> but this is a gas and may be less convenient to handle.) By halogen-lithium exchange,<sup>6</sup> followed by treatment with ethylene oxide, the  $\beta$ -hydroxyethyl derivative is prepared in good yield.<sup>7</sup> This is dehydrated with potassium hydroxide at  $235^\circ\text{C}$ ., taking advantage of the acidity of the benzylic hydrogens, to yield the desired vinyl compound:



No attempt was made to separate the optical isomers of the vinylbis(1-ethoxyethyl)hydroquinone. Acid cleavage yields the known vinylhydroquinone.<sup>8</sup>

The acetal is very easily cleaved by acid. The ready cleavage with acid explains why no polymerization ensues with boron trifluoride etherate catalyst: the mixture yields a brown color but no polymer. The monomer is polymerized by free-radical and anionic catalysts. Polymerization occurs with lithium dispersion, which is considered to act chiefly as an anionic initiator in tetrahydrofuran.<sup>9</sup> The resulting polymers behave toward oxidation as, and show the ultraviolet and infrared characteristics of, polyvinylhydroquinone prepared from other monomers.



## EXPERIMENTAL

### 1. $\alpha$ -Chloroethyl Ethyl Ether<sup>4</sup>

Vinyl ethyl ether (E.K.C. Pract.) was dried and purified by letting it stand over anhydrous calcium chloride for several days and distilling it from dried glassware. A 5-g. portion of the dried, distilled vinyl ether was placed in a small dried flask equipped with a gas inlet tube and a calcium chloride-protected outlet. The temperature was lowered to 0°C. and anhydrous hydrochloric acid gas was bubbled slowly through the liquid until no more gas was taken up by the ether. It is essential that the ether be thoroughly dry to begin with. If it is not dry, the liquid in the flask darkens, as the gas is passed in, and becomes an explosive mixture (polymerizes explosively). If this should occur, then the bulk of the vinyl ether should be redried. The flask was stoppered and kept at 0°C. until used. No further purification of the catalyst was required. Upon warming to room temperature, the chloroether becomes very unstable: it may hydrolyze explosively in the presence of moisture and it may polymerize when anhydrous. It should be made fresh just before use. Any small excess can be disposed of by pouring into running cold water.

### 2. Bis(1-ethoxyethyl)bromohydroquinone [Bromohydroquinonebis(ethyl acetal)<sup>4</sup>]

Bromohydroquinone, 15.0 g. (0.079 mole) which had been prepared from the E.K.C. (Pract.) material by recrystallizing from *n*-heptane and vacuum drying over phosphorus pentoxide, was dissolved in 50 ml. anhydrous ether in a flask equipped with a small dry addition funnel and an outlet protected with a drying tube and a nitrogen inlet. In the addition funnel was placed 19.0 ml. (15.8 g., 0.21 mole) purified vinyl ethyl ether and 1 ml. freshly prepared  $\alpha$ -chloroethyl ethyl ether. When the catalyst is added to the vinyl ether, caution should be observed for it was at this point that a violent reaction began when the reagents were not sufficiently dry. The bromohydroquinone solution was cooled to about 11°C. (tap water temperature) and the vinyl ether catalyst mixture added dropwise, with continuous stirring over a period of about 1 hr. The mixture was held at about 11°C. with stirring for 2 hr., then allowed to warm slowly to room temperature, with stirring for 6 hr. more. Throughout the reaction, moisture was excluded from the flask by maintaining a slight positive pressure of dry nitrogen. As the reaction proceeded, the initially formed brown solution gradually became yellow.

The reaction mixture was then poured into 50 ml. of 10% aqueous sodium hydroxide with vigorous stirring. The resulting layers were separated and the aqueous portion was extracted with ether. The combined ethereal solution was washed with 2% aqueous sodium hydroxide and then with water and was dried over anhydrous sodium carbonate. After filtering, the solvent was removed *in vacuo*, leaving a viscous yellow liquid. Vacuum distillation of the liquid yielded 20.30 g. (0.061 mole) of faintly yellow

liquid product, b.p. 125°C. 0.5 mm. Hg (77.1% of theory). The product, which gave a positive Beilstein test, was identified by infrared analysis (CCl<sub>4</sub> solution) showing C—H stretching peaks at 2980, 2934, and 2900, benzene in-plane vibrations at 1600, 1485, 1440, and a broad C—O band centered at 1120 cm.<sup>-1</sup>. Hydrolysis with dilute aqueous hydrochloric acid yielded bromohydroquinone quantitatively.

ANAL. Calcd. for C<sub>14</sub>H<sub>21</sub>BrO<sub>4</sub>: C, 50.50%; H, 6.35%; Br, 23.94%. Found: C, 50.36%; H, 6.41%; Br, 24.17%.

### 3. 2-Hydroxyethylbis(1-ethoxyethyl)hydroquinone<sup>6</sup>

This compound was prepared from 22.47 g. (0.068 mole) of the bromodiacetal dissolved in 75 ml. anhydrous ether under dry nitrogen. The ethereal solution was cooled to 0°C. and 4.80 g. (0.075 mole) of *n*-BuLi (16.2 g. of 29.7% *n*-BuLi in heptane, Lithium Corp. of America) was added rapidly with stirring. The resulting clear yellow mixture was stirred for 1–3 hr. at 0°C. while the lithium exchange took place. Then 4.44 g. (0.10 mole) of liquid ethylene oxide was added slowly, with constant stirring, from a dropping funnel equipped with a Dry Ice finger condenser. The resulting mixture was stirred for 5 hr. at 0°C. and overnight at room temperature until it gave a negative Michler's ketone test.<sup>10</sup> (This test is applicable to organolithiums as well as Grignard reagents.) The mixture was poured rapidly with stirring into 100 ml. of ice water and the resulting layers were separated. The aqueous layer was extracted with ether and the combined ethereal solution was washed with water and dried over anhydrous sodium carbonate. Removal of solvent *in vacuo* on the steam bath left 19.81 grams of viscous yellow oil which upon vacuum distillation yielded two fractions.

Fraction 1, b.p. 90°C. 0.5 mm. Hg, consisted of 1.81 g. of a colorless, viscous liquid which gave a negative Beilstein test, showed no hydroxyl absorption in the infrared and hydrolyzed to hydroquinone in dilute aqueous HCl. On this evidence it was identified as bis(1-ethoxyethyl)hydroquinone.

Fraction 2, b.p. 145°C. 0.2 mm. Hg, constituted 18.00 g. (0.06 mole, 89.5% of theory on bromodiacetal) of viscous yellow liquid, which gave a negative Beilstein test and showed OH absorption at 3630 cm.<sup>-1</sup> (unbonded) and 3520 cm.<sup>-1</sup> (broad bonded), C—H stretching at 2989, 2940, and 2890, benzene in-plane vibration at 1490, and a broad C—O ether band centered at 1115 cm.<sup>-1</sup> (CCl<sub>4</sub> solution) was identified as 2-hydroxyethylbis(1-ethoxyethyl)hydroquinone, which may also be named  $\beta$ -hydroxyethylhydroquinonebis(ethyl acetal).

### 4. Vinylbis(1-ethoxyethyl)hydroquinone [Vinyl hydroquinonebis(ethyl acetal)]<sup>2,11</sup>

KOH pellets (60 g.) and a few boiling chips were placed in a 300-ml. round-bottomed flask equipped with an addition funnel, Claisen head, and vacuum adapter. Dry nitrogen gas was passed through the system to rid

it of oxygen. The flask was then evacuated to 0.6 mm. and the KOH was heated on a Wood's Metal bath to 235°C. The KOH liquified and evolved water vigorously (caution). When completely dehydrated, the KOH solidified. Then 17.80 g. (0.06 mole) of  $\beta$ -hydroxyethylhydroquinonebis(ethyl acetal) was added dropwise over a period of 3 hr. to the KOH at 230–40°C. at 0.6 mm. As the addition proceeded, 9.82 g (0.035 mole) of faintly yellow liquid distilled out, b.p. 125°C./0.6 mm., and was collected, for a yield of 58.4% based on  $\beta$ -hydroxyethylhydroquinonebis(ethyl acetal), or an overall yield of 44.4% based on bromohydroquinone. On redistillation, the product had b.p. 100°C./0.2 mm.,  $[\eta]_D^{25}$  1.4971.

ANAL. Calcd. for  $C_{16}H_{24}O_4$ : C, 68.40%; H, 8.63%. Found: C, 67.70%; H, 8.70%.

The product showed vinyl absorption at 3100 and 3030, alkane C—H stretching at 2989, 2940, and 2890, benzene in-plane vibrations at 1502 and 1486, C=C stretching, phenyl conjugated at 1626, =CH<sub>2</sub> and —CH out-of-plane deformations at 905 and 990, respectively, and a broad C—O ether band centered at 1115 cm.<sup>-1</sup> (CCl<sub>4</sub> solution). It was identified as vinylbis(1-ethoxyethyl)hydroquinone. Hydrolysis at room temperature to vinyl hydroquinone, m.p. 111°C.<sup>8</sup> supported this identification.

Seven repetitions of the synthetic route yielded, on the average, 92.5% of theory for the crude product of step 2. The yield of purified product was 89.2% in one case, from 96.5% of crude, but we did not redistill the crude in other instances. Step 3 also gave good yields of the order of 89% from the bromodiactal. Step 4 is the low-yield step at present, the average of twelve runs was 66.8% of crude on the basis of the alcohol, and 51% of purified monomer. The overall yield of purified monomer was of the order of 42% on the average. The acetal is readily cleaved by dilute acid. Perhaps the method of choice is to employ the acid form of a cation exchange resin. A 7-g. portion of acetal in a mixture of 5 ml. water and 25 ml. 95% ethanol, stirred for 2 hr. at room temperature with 2 g. Dowex 50- $\times$ 8 (acid form) yielded 80% of vinylhydroquinone.

### 5. Polymerization of Monomeric Vinylbis(1-ethoxyethyl)hydroquinone

**Radical Initiation.** The freshly distilled monomer, and azobisisobutyronitrile (AIBN) initiator were weighed into small tubes, and the solvent (if employed) was added. The mixture was cooled with Dry Ice and the tubes alternately evacuated and flushed with purified nitrogen for five cycles, then evacuated and sealed at about 0.2 mm. pressure. Polymerization was carried out at 60°C. and the resulting colorless, viscous solutions were diluted with benzene, poured into a large excess of methanol, and the polymer that separated was collected as a soft solid. The polymer, dissolved in benzene and freeze-dried, yielded white, fluffy product. Table I contains examples of conditions and yields. Absence of solvent combined with long duration of heating led to crosslinking in the case of No. 8. In Table II are reported the results of viscosity measurements on one of the soluble polymers.

TABLE I  
Radical Polymerization of Vinylbis(1-ethoxyethyl)hydroquinone (VHBE) at 60°C.

No.	VHBE, g.	Solvent (benzene), ml.	AIBN, mg.	Time, hr.	Yield, %
8	1.90	0.0	20	18	Gel, insoluble
9	1.919	0.0	10	6.5	13
10	2.100	2.0	10	112	64
14	4.198	5.0	20	94	70
15	4.213	10.0	15	100	63

TABLE II  
Viscosity Measurements on Polymer from Run No. 14, of Table I<sup>a</sup>

<i>c</i> , g./100 ml. of benzene	$\bar{l}_0$ , sec.	$\bar{l}_i$ , sec.	$\bar{l}-\bar{l}_0$ , sec.	$\eta_{sp}$	$\eta_{sp}/c$ , 100 ml./g.
0.258	91.7	99.34	7.64	0.0834	0.324
0.401	91.7	104.3	12.6	0.1375	0.342
0.664	91.7	112.8	21.1	0.230	0.347
0.800	91.7	118.1	26.4	0.288	0.360
0.996	91.7	125.0	33.7	0.367	0.368

<sup>a</sup> The solvent is benzene, and the temperature, 29.7°C. The viscometer is a Cannon 75/V19.

**Anionic Initiation.** A 0.5-g. portion of freshly distilled monomer, 1 ml. of tetrahydrofuran, and 0.01 g. of lithium dispersion (30% lithium, 69% mineral oil, and 1% oleic acid, Lithium Corp. of America) were placed in a small tube. It is essential that air and moisture be completely absent from this polymerization system. The tetrahydrofuran solvent was refluxed for several hours with lithium, and distilled from lithium wire just before use. The tube was cooled with Dry Ice and evacuated to 0.1 mm. Hg and sealed. The polymerization was carried out at room temperature (ca. 20°C.) for 72 hr., during which time the color of the solution changed first to yellow, then to light green, then to yellow again. The resulting viscous yellow solution was diluted with a small amount of tetrahydrofuran and poured into a large amount of methanol to precipitate white polymer. The polymer was freeze-dried from benzene with a yield of somewhat over 50%. In one case a conversion of 80% was obtained.

The ultraviolet spectrum of this polymer in chloroform shows a strong absorption at 286  $m\mu$  as compared with that of the monomer at 310  $m\mu$ . Its infrared spectrum has CH-stretching bands due to  $-\text{CH}_3$  at 2990 and 2900  $\text{cm}^{-1}$ , while the alkane  $-\text{CH}_2-$  band is recognized at 2940  $\text{cm}^{-1}$ . A broad C—O stretching band which is attributed to the ether linkage can be seen around 1100  $\text{cm}^{-1}$ ; C = C skeletal in-plane vibrations due to the benzene ring are observed at 1600, 1570, 1480, and 1440  $\text{cm}^{-1}$ .



## 6. Acid Hydrolysis of poly[vinylbis(1-ethoxyethyl)hydroquinone]

The polymer (0.2 g.) was dispersed in 25 ml. methanol solution containing 2.5 ml. 37% hydrochloric acid. The mixture was stirred for 3 hr. at room temperature (ca. 20°C.) under nitrogen. Most of the polymer dissolved immediately after the addition and the color of the solution became gradually yellow. The yellowish solution with some insoluble residue was poured into a saturated sodium sulfate solution to precipitate polymer. The crude polymer was obtained by centrifugation. It was then reduced with aqueous sodium hydrosulfite solution, which was kept slightly alkaline with sodium bicarbonate. The polymer thus obtained was washed with water and centrifuged. This operation was repeated at least three times. It was then freeze-dried from *tert*-butyl alcohol. A white fluffy product was obtained. It gradually became pink in the air. If the polymeric acetal is brought into solution, it can be hydrolyzed, though slowly, by an acid form of a cation exchanger. Unlike the case with the monomer, this is not the method of choice.

The ultraviolet spectrum of the polymer in 90% aqueous methanol shows a characteristic absorption at 293  $m\mu$  which corresponds with that of polyvinylhydroquinone. Its infrared spectrum also corresponds with that of polyvinylhydroquinone: the  $-\text{CH}_3$  absorptions at 2990 and 2900  $\text{cm}^{-1}$  which are characteristic of the acetal are no longer present. The intrinsic viscosity  $[\eta]$  was found to be 0.34 dl./g. (90% methanol, 29.7°C.) which is of the same order as that of a polymer prepared from polyvinylhydroquinone dibenzoate, and that reported in Table II. In one case a viscosity  $[\eta]$  of 0.99 dl./g. was obtained.

ANAL. Calcd. for  $(\text{C}_8\text{H}_8\text{O}_2)_n$ : C, 70.57%; H, 5.92%. Found: C, 66.75%; H, 6.46%.

The difference between the calculated and found analytical values may be due to the presence of water which is difficult to remove. Oxidative titration of the polymer in 90% acetic acid, with 0.1*N* bromine in the same solvent as titrant, gave a typical oxidation-reduction curve, the midpoint potential of which is around +0.45 v. against the saturated calomel electrode at 29.7°C. In the titrations, the color of the solution first changes to red-brown with some precipitate and, at the end of the titration, to yellow with an increasing amount of precipitate. The stoichiometry is not satisfactory, since the partially oxidized polymer precipitates out during the titration.

We wish to thank Professor James English, Jr., for advice with respect to the protecting group. We are pleased to acknowledge that this work was supported by a grant from Research Corporation and a PHS research grant, G M 10864-10, National Institute of Arthritis and Metabolic Diseases.

## References

1. Kamogawa, H., and H. G. Cassidy, *J. Polymer Sci.*, **A1**, 1971 (1963).
2. Stern, R., J. English, Jr., and H. G. Cassidy, *J. Am. Chem. Soc.*, **79**, 5792 (1957).
3. Carswell, T. S., *Phenoplasts, their Structure, Properties, and Chemical Technology*, High Polymers Series, Vol. VII, Interscience, New York, 1947; see also E. Adler, H. v. Euler, and G. Gie, *Arkiv. Kemi. Mineral. Geol.* **16A**, No. 12 (1943).



4. von Reppe, W., *Ann.*, **601**, 81 (1956).
5. General Aniline & Film Corp., Data Bulletin TA77.
6. Gilman, H., and J. W. Morton, Jr., *Organic Reactions*, **8**, 258 (1954).
7. Barnes, R. A., *J. Am. Chem. Soc.*, **75**, 3004 (1953).
8. Updegraff, I. H., and H. G. Cassidy, *J. Am. Chem. Soc.*, **71**, 407 (1949).
9. O'Driscoll, K. F., and A. V. Tobolsky. *J. Polymer Sci.*, **31**, 123 (1958).
10. Gilman, H., and F. Schulze, *J. Am. Chem. Soc.*, **47**, 2002 (1925).
11. Marvel, C. S., and D. W. Hein, *J. Am. Chem. Soc.*, **70**, 1895 (1948).

### Résumé

La vinyl-bis-(1-éthoxyéthyle)-hydroquinone monomère, (l'acétal de bis-éthylvinyl-hydroquinone), a été préparée en faisant réagir la bromohydroquinone avec le vinyl-éthyl-éther, en présence d'éther éthyl *c*-chloroéthylé comme catalyseur en évitant toute trace d'humidité. L'acétal de la bis-éthyl-bromohydroquinone résultant est soumis à l'échange lithium-brome suivi de la réaction avec l'oxyde d'éthylène. L'acétal de la bis-éthyl-bêta-hydroxyéthylhydroquinone est transformé en monomère désiré par déshydratation au moyen d'hydroxyde de potassium à 235°. Le rendement global en monomère purifié à partir de bromohydroquinone s'élève à 42%. Le monomère polymérise par initiation radicalaire ou anionique. Le polymère produit par initiation radicalaire montre (dans la plupart des cas) une viscosité intrinsèque dans le benzène de l'ordre de 0.32 à 29.7°. Le polymère fournit rapidement sous l'action d'acide chlorhydrique dilué en solution méthanolique la polyvinylhydroquinone. La polyvinylhydroquinone préparée par initiation anionique montre une viscosité intrinsèque de 0.34 dans le méthanol à 90% et à 29.7°. Le polymère présente des propriétés redox.

### Zusammenfassung

Das Monomere Vinyl-bis-(1-äthoxyäthyl)-hydrochinon (Vinylhydrochinon-bis-äthylacetal) wurde durch Umsetzung von Bromhydrochinon mit Vinyläthyläther unter Verwendung von  $\alpha$ -Chloräthyl-äthyläther als Katalysator unter sorgfältigem Ausschluss von Feuchtigkeit hergestellt. Das so hergestellte Bromhydrochinon-bis-äthylacetal wurde einem Lithium-Brom-Austausch und anschliessend der Reaktion mit Äthylenoxyd unterworfen. Das dabei gebildete  $\beta$ -Hydroxyäthylhydrochinon-bis-äthylacetal wurde durch Wasserabspaltung mit Kaliumhydroxyd bei 235° in das gewünschte Monomere übergeführt. Die Gesamtausbeute an gereinigtem Monomeren, bezogen auf das Bromhydrochinon, betrug durchschnittlich 42%. Das Monomere polymerisierte sowohl radikalisch als auch anionisch. Das radikalisch hergestellte Polymere hatte (in den meisten Fällen) eine Viskositätszahl von 0,32 (29,7°, Benzol). Das Polymere wird durch verdünnte methanolische Salzsäure leicht zu einem Polyvinylhydrochinon gespalten. Ein anionisch hergestelltes Polyvinylhydrochinon hatte eine Viskositätszahl von 0,34 (29,7°, 90% iges Methanol). Das Polymere besass Redox-Eigenschaften.

Received February 11, 1963

Revised June 10, 1963

## Electron Exchange Polymers. XXI. Polymerization Behavior of 2,5-Dimethoxystyrene

HIROYOSHI KAMOGAWA and HAROLD G. CASSIDY,  
*Department of Chemistry, Yale University, New Haven, Connecticut*

### Synopsis

It was shown that 2,5-dimethoxystyrene polymerizes under free-radical, cationic, and anionic initiation. The less bulky character of the *ortho* substituent in the benzene ring makes the behavior of this monomer more normal than that of the previously reported vinylhydroquinone dibenzoate. Thus, a linear relationship is observed between specific extinction coefficients of copolymers in the ultraviolet absorption spectra and copolymer compositions.  $Q-e$  values are also normal ( $Q = 1.76$ ,  $e = -1.04$ ). The copolymerization behavior is well understood through these values.

2,5-Dimethoxystyrene is one of the useful monomers for the preparation of redox polymers.<sup>1</sup> It has been synthesized by Williams, Borden, and Laakso<sup>2</sup> through the pyrolysis of  $\alpha$ -(2,5-dimethoxyphenyl)-ethyl acetate, and by Zapevalova and Koton<sup>3</sup> through the reduction of 2,5-dimethoxy-1-acetylbenzene with aluminum isopropoxide followed by dehydration over potassium acid sulfate. These authors polymerized the monomer by peroxide initiation. Our purpose was to investigate the polymerization behavior of this monomer in relation to its chemical structure in order to obtain information useful in preparing various redox polymers.

### EXPERIMENTAL

#### Materials

$\beta$ -(2,5-Dimethoxyphenyl)ethanol was prepared according to the method of Barnes.<sup>4</sup> To a solution of 195 g. 1,4-dimethoxybenzene (1.41 mole) in 800 ml. dry ether was added, with stirring under nitrogen, in one portion, 417.5 g. (1.44 mole) of 3.45*N* *n*-butyllithium in heptane (Lithium Corp. of America) mixed with 500 ml. dry ether. The mixture was allowed to stand overnight at room temperature under nitrogen. The brown solution was then cooled in an ice bath for several hours, with stirring. Ethylene oxide, 70 ml. (1.41 moles) was dripped in, from a funnel equipped with a Dry-Ice finger condenser, over a period of about 1 hr. After standing for 6 hr. the solution was poured into 2 l. crushed ice and water. The yellow ether layer was separated, and the yellow aqueous layer was extracted twice with ether, removing most of the color. The ether was distilled off, and the

resulting viscous product steam distilled, to remove unreacted 1,4-dimethoxybenzene (ca. 50 g.), extracted with ether, dried with anhydrous sodium sulfate, the ether removed, and fractionated to yield 120 g. (0.658 mole, 46%) of pale yellow product, b.p. 130–142°C./0.7 mm.

2,5-Dimethoxystyrene was prepared by the method of Marvel and Hein<sup>5,1</sup> in which the acidity of the benzylic hydrogen is taken advantage of and the alcohol is dehydrated by dropping it on potassium hydroxide at 250°C. under reduced pressure. The product was distilled in the presence of a small amount of picric acid to yield ca. 50 g. (55%) of a colorless liquid boiling at 78–80°C./0.01 mm.

ANAL. Calc. for  $C_{10}H_{12}O_2$ : C, 73.17%; H, 7.32%. Found: C, 73.09%; H, 7.12%.

Styrene and methyl methacrylate were commercial products. They were purified by distillation just before use.

Lithium dispersion and *n*-butyllithium were from the Lithium Corp. of America. The former contained 30% lithium, 69% mineral oil, and 1% oleic acid; the latter, 30% lithium in heptane.

Lithium naphthalene was made in the conventional manner<sup>6</sup> from naphthalene in tetrahydrofuran and lithium dispersion, to yield a mixture containing ca. 20% lithium naphthalene.

### Polymerization Procedures

**Free-Radical Polymerization.** Monomers and  $\alpha, \alpha'$ -azobisisobutyronitrile (AIBN) as initiator, with or without the addition of a suitable solvent, were put into a pyrex tube. It was cooled in Dry Ice, evacuated, and sealed under 1 mm. Hg. A typical reaction mixture consisted of 0.5 g. of each monomer, 5 mg. AIBN, and 1 ml. solvent. Polymerization was carried out in an air bath kept at the desired temperature. After polymerization, the tube was opened up, the viscous solution diluted with a suitable amount of benzene, and the mixture poured into hexane. Precipitates thus formed were freeze-dried from benzene. In most cases white fluffy polymers were obtained.

**Ionic Polymerization.** Almost the same procedures as in the free-radical case were used, although more careful purification of solvents was done. For example, tetrahydrofuran (THF) for the solvent in the anionic polymerization was refluxed with sodium for several hours and then distilled from lithium wire just before use. In some cases polymerizations were carried out under purified dry nitrogen. Polymer solutions thus obtained were quenched with methanol, thereby precipitating white polymer. All polymers were freeze-dried from benzene.

### Characteristics of Polymers

**Viscosity Measurements.** All viscosity measurements were carried out with a Cannon-Fenske-Ostwald type viscometer in a thermostat kept at  $29.7 \pm 0.02^\circ\text{C}$ . Toluene was used as solvent.

**Measurements of Ultraviolet Spectra.** Ultraviolet absorption spectra of polymers were taken by means of a spectrophotometer, Spectronic 505 (Bausch & Lomb Co.). Chloroform was used as solvent.

## RESULTS AND DISCUSSION

### Homopolymerization of 2,5-Dimethoxystyrene (DMS)

2,5-Dimethoxystyrene undergoes polymerization not only with free-radical initiators, but also with ionic ones, such as boron trifluoride etherate, alkali metals, and organometallic compounds. The results are shown in Table I. Under some conditions, crosslinked and insoluble polymers are obtained. In the case of boron trifluoride etherate, a typical cationic initiator, a low temperature is required to obtain a soluble polymer, since the polymerization reactions are violent at higher temperatures. For the same reason lower concentrations are favorable. In the case of lithium, the functioning of which is somewhat ambiguous, the effect of solvent is marked, and the use of tetrahydrofuran may be necessary to get soluble polymers at or under room temperature. In this case, the color of the solution first changes to yellow and then to bright red with the progress of polymerization, indicating the presence of the DMS anion. This red color persists for long periods of time and disappears on quenching with methanol. The same red color is also observed in the case of typical anionic initiators, such as *n*-butyllithium and lithium naphthalene.

TABLE I  
Homopolymerization of 2,5-Dimethoxystyrene

Initiator, %/DMS	Solvent	DMS		Time, hr.	[ $\eta$ ]	Con- version, %
		Concn., %	Temp., °C.			
AIBN, 1%	Toluene	33	70	24	0.21	67
BF <sub>3</sub> ·O(C <sub>2</sub> H <sub>5</sub> ) <sub>2</sub> , 10%	CH <sub>2</sub> Cl <sub>2</sub>	20	-78	3	0.33	58
BF <sub>3</sub> ·O(C <sub>2</sub> H <sub>5</sub> ) <sub>2</sub> , 4%	CH <sub>2</sub> Cl <sub>2</sub>	20	-78	20	Gelation	—
BF <sub>3</sub> ·O(C <sub>2</sub> H <sub>5</sub> ) <sub>2</sub> , 10%	CH <sub>2</sub> Cl <sub>2</sub>	9	-78	20	Soluble polymer	—
Li, 10%	THF	33	25	18	0.08	90
Li, 10%	THF	33	-20	72	Soluble polymer	—
Li, 10%	Hexane	33	70	24	Crosslinked, insoluble	—
<i>n</i> -Butyl Li, 14%	THF	20	-78	0.5	0.20	90
Li-naphthalene, 4%	THF	20	-78	0.5	0.10	64

### Copolymerization by Free-Radical Mechanism

**Analytical Method for Copolymer Compositions.** As shown in Figure 1, DMS homopolymer and its copolymers show strong ultraviolet absorptions

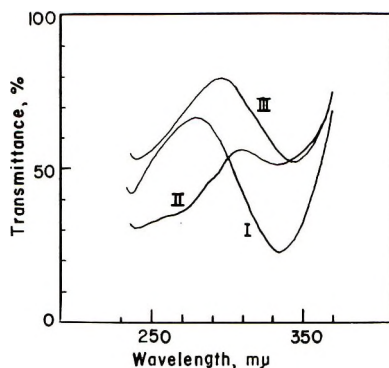


Fig. 1. Ultraviolet spectra of dimethoxystyrene copolymers: (I) homopolymer, 0.0347 g./l.; (II) DMS-St (mole fraction DMS 0.249), 0.0377 g./l.; (III) DMS-MMA (mole fraction DMS 0.0284), 0.0320 g./l. The solvent is chloroform.

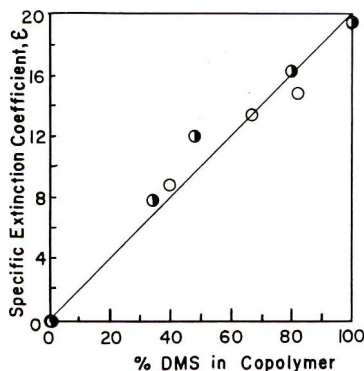


Fig. 2. Relationship between copolymer composition and specific extinction coefficient  $\epsilon$ : (—)  $\epsilon = 20.3$  (DMS); (●) DMS-St (292  $m\mu$ ); (○) DMS-MMA (maximum values at 292–297  $m\mu$ ).

between 292 and 299  $m\mu$ . In the application of ultraviolet absorption to analysis of polymer, Meehan<sup>7</sup> obtained a linear relationship between specific extinction coefficient at 262  $m\mu$  and styrene content in copolymers in the styrene-butadiene copolymer system. He reported the following equation:

$$E_{A-B} = xE_A + (1 - x)E_B \quad (1)$$

where  $E_{A-B}$  is the specific extinction coefficient of the A-B copolymer at a given wavelength;  $E_A$  and  $E_B$  are specific extinction coefficients of the A and B homopolymer; respectively, and  $x$  is the fraction of the copolymer which is the A monomer. We obtained different relations for the vinylhydroquinone-dibenzoate copolymer systems.<sup>8</sup> Specific extinction coefficients in these systems had maxima at approximately 0.5 mole per cent of copolymer compositions. We attributed this to steric effects, i.e., the bulky character of vinylhydroquinone dibenzoate groups. If this is tenable,



DMS, which carries a less bulky substituent than the benzoate group in the *ortho* position of the benzene ring, should show more tendency toward a linear curve. The values of the specific extinction coefficient at the maximum absorption were plotted against copolymer compositions calculated from the results of the elementary analysis (Fig. 2). Although the data are somewhat diffused, a linear tendency can be recognized in the diagram, supporting the above explanation. This linear relationship is indifferent of the kind of the comonomer used, since in this wavelength range specific extinction coefficients of both polystyrene and polymethyl methacrylate can be neglected as compared with that of polydimethoxystyrene.

Another interesting phenomenon in the spectrophotometric data is the shift of absorption maximum with the increased amount of the comonomer in the copolymer. In Table II are shown absorption maxima in relation to copolymer compositions. The extent of the shift is greater in the DMS-methyl methacrylate (DMS-MMA) series than in the DMS-styrene (DMS-St), showing that interactions between neighboring groups in a polymer molecule are stronger in the former. In spite of these shifts, it seems that no appreciable change of absorption coefficient accompanies the shift, as in the case of usual hydrogen bonds,<sup>9</sup> since a linear relationship holds with the values of the maximum absorption coefficient, as shown in Figure 2.

TABLE II  
Shift of Absorption Maximum with Copolymer Composition

Kind of copolymer	Composition, mole fraction DMS	Absorption maximum, $m\mu$
DMS homopolymer	1.000	292
DMS-St	0.719	292
DMS-St	0.369	293
DMS-St	0.091	295
DMS-MMA	0.733	294
DMS-MMA	0.548	296
DMS-MMA	0.284	297

**Monomer Reactivity Ratios and  $Q-e$  Values.** Relationships between monomer and initial copolymer compositions are indicated in Figure 3. Some of the values of copolymer compositions were calculated from their specific extinction coefficients using the relationship in Figure 2. Monomer reactivity ratios and  $Q-e$  values calculated from the data in Figure 3 are also shown in Table III. As regards  $Q_1$ , i.e., "resonance term," its value is rather similar to that of 2,5-dimethylstyrene (2.16) which carries electron-donating groups in the *ortho* and *meta* positions.<sup>10</sup> The "polarity term,"  $e_1$ , on the other hand, is more negative than for styrene, and also corresponds with those of 2,5-dimethylstyrene (-0.84) and *p*-methoxystyrene (-1.11). Therefore, it can be safely said that copolymerization behaviors of DMS are normal, and that the "ortho effect," which has been considered the cause

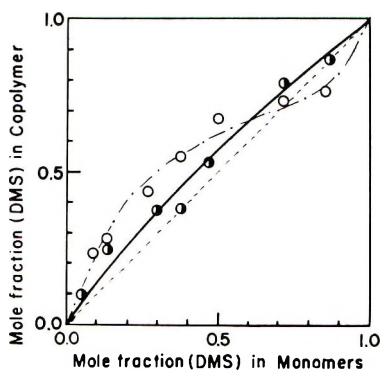


Fig. 3. Initial copolymer compositions in relation to monomer compositions: (●) DMS-St; (○) DMS-MMA.

of anomalous behavior of vinylhydroquinone dibenzoate,<sup>8</sup> is negligible. This also corresponds with the result in Figure 2. This being the case, this monomer is considered to be more reactive and more susceptible to cationic initiators than styrene, although its polymerization behavior is very similar to that of styrene in many respects. This is the reason why this monomer undergoes polymerization not only with free-radical initiators, but also with both cationic and anionic initiators, as in the case of styrene, and especially violent polymerization with cationic initiators such as boron trifluoride.

TABLE III  
Monomer Reactivity Ratios ( $r_1, r_2$ ) and  $Q-e$  Values for 2,5-Dimethoxystyrene ( $M_1$ ) at 70°C.

Comonomer $M_2$	$r_1$	$r_2$	Comonomer		DMS	
			$Q_2$	$e_2$	$Q_1$	$e_1$
Styrene	$1.13 \pm 0.13$	$0.77 \pm 0.07$	1.00	-0.80	1.76	-1.17
Methyl methacrylate	$0.72 \pm 0.04$	$0.25 \pm 0.01$	0.74	0.40	1.76	-0.91
				Mean	1.76	-1.04

### Copolymerization by Ionic Mechanisms

The results of copolymerization of DMS with boron trifluoride etherate a typical cationic initiator, as well as lithium dispersion, the character of which is somewhat ambiguous, are given in Table IV.

In the DMS-styrene system with boron trifluoride etherate as initiator, initial copolymer compositions obtained contain relatively much more DMS component than those with a free-radical initiator since, as shown above, DMS is more electronegative ( $e = -1.04$ ) than styrene ( $e = -0.80$ ). It is only natural that methyl methacrylate, which has an electropositive character ( $e = +0.40$ ) does not enter the cationic copolymerization.

TABLE IV  
 Copolymerization of DMS ( $M_1$ ) with Ionic Catalysts

Second monomer	Mole fraction DMS in monomers	Polymerization time, min.	Conversion, %	Mole fraction DMS in polymer
2% Boron trifluoride etherate/monomers, 20% monomers in ethylene dichloride, -10°C.				
Styrene	0.563	10	34.9	Homopolymer (DMS)
Styrene	0.318	5	14.2	0.824
Methyl methacrylate	0.463	1	37.8	Homopolymer (DMS)
Methyl methacrylate	0.294	1	8.7	Homopolymer (DMS)
2% Lithium dispersion/monomers, 33% monomers in tetrahydrofuran, 30°C.				
Styrene	0.503	240	26.3	0.453
Styrene	0.293	60	9.9	0.237
Methyl methacrylate	0.484	1140	2.7	0.083
Methyl methacrylate	0.298	1320	4.7	0.039

In the case of lithium dispersion, on the other hand, the data imply an anionic mechanism. O'Driscoll and Tobolsky<sup>11</sup> have proposed the "radical-ion" mechanism in the lithium-initiated copolymerization of styrene and methyl methacrylate, in which the radical-ion,  $\cdot\text{CH}_2 - \text{CXY} : ^-\text{Li}^+$ , is formed by the exchange of an electron from lithium into the unoccupied, antibonding  $\pi$ -orbital of the vinyl group. Its anionic end would add methyl methacrylate mainly, whereas the radical end would add both styrene and methyl methacrylate. According to this theory, the use of tetrahydrofuran, which solvates the carbanion very well and prevents its termination,<sup>12</sup> would be expected to favor the anionic growth. This would favor the methyl methacrylate component in the DMS-methyl methacrylate copolymer to the extent that more than 90% of initial copolymer is the methyl methacrylate component at approximately 0.5 mole per cent of monomer composition. In the DMS-styrene system, it would slightly decrease the DMS component which is more electronegative. That the anionic growth is the main mechanism of the copolymerization may be endorsed by the formation of the red DMS anion in the homopolymerization as mentioned above.

We acknowledge with pleasure that this work was supported by a research grant (GM 10864-10 from the National Institutes of Health, U. S. Public Health Service.

### References

1. For the previous paper in this series see R. E. Moser, H. Kamogawa, and H. G. Cassidy, *J. Polymer Sci.*, **A2**, 2401 (1964).
2. Williams, J. L. R., D. G. Borden, and T. M. Laakso, *J. Org. Chem.*, **21**, 1461 (1956).

3. Zapevalova, N. P., and M. M. Koton, *Zh. Obshch. Khim.*, **27**, 2142 (1957); *Chem. Abstr.*, **52**, 8089 (1958).
4. Barnes, R. A., *J. Am. Chem. Soc.*, **75**, 3004 (1953).
5. Marvel, C. S., and D. W. Hein, *J. Am. Chem. Soc.*, **70**, 1895 (1948).
6. Sorensen, W. R., and J. W. Campbell, *Preparative Methods of Polymer Chemistry*, Interscience, New York, 1961, p. 197.
7. Meehan, E. J., *J. Polymer Sci.*, **1**, 175 (1946).
8. Kamogawa, H., and H. G. Cassidy, *J. Polymer Sci.*, **A1**, 1971 (1963).
9. Pimentel, G. C., and A. L. McClellan, *The Hydrogen Bond*, Freeman, San Francisco, 1960, p. 157.
10. Young, L. J., *J. Polymer Sci.*, **54**, 411 (1961).
11. O'Driscoll, K. F., and A. V. Tobolsky, *J. Polymer Sci.*, **31**, 123 (1958).
12. Szwarc, M., *Nature*, **178**, 1168 (1956).

### Résumé

On a montré que le 2,5-diméthoxystyrène polymérise par initiation radicalaire cationique et anionique. Le caractère moins volumineux du substituant ortho sur le noyau benzénique rend le comportement de ce monomère plus normal que celui du dibenzoate de vinylhydroquinone précédemment décrit. Donc on observe une relation linéaire entre les coefficients d'extinction spécifiques des copolymères dans les spectres d'absorption ultraviolet et dans les compositions du copolymère. Les valeurs  $Q-e$  sont aussi normales ( $Q = 1.76$ ,  $e = -1.04$ ). Ces valeurs traduisent bien le comportement de la copolymérisation.

### Zusammenfassung

Die Polymerisation von 2,5-Dimethoxystyrol kann radikalisch, kationisch oder anionisch gestartet werden. Wegen der geringeren Sperrigkeit des ortho-Substituenten am Benzolring weicht dieses Monomere weniger als das früher beschriebene Vinylhydrochinondibenzoat vom normalen Verhalten ab. So wurde eine lineare Abhängigkeit der spezifischen UV-Extinktionskoeffizienten der Copolymeren von der Copolymerzusammensetzung beobachtet. Die  $Q$ - und  $e$ -Werte sind ebenfalls normal ( $Q = 1,76$ ;  $e = 1,04$ ). Das Copolymerisationsverhalten wird durch diese Werte gut wiedergegeben.

Received May 10, 1963

## Decomposition of Asymmetric Peranhydrides

G. SMETS and W. VAN RILLAER *Laboratory of Macromolecular Chemistry, University of Lowain, Belgium*

### Synopsis

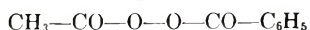
The synthesis of a peranhydride copolymer was carried out in three steps: (a) copolymerization of acrylyl chloride with methyl methacrylate, (b) reaction of the acid chloride copolymer with perbenzoic acid, (c) treatment with aqueous methanol and methylation with diazomethane, in order to avoid free carboxylic groups. The polymer contained 18.1 wt.-% peranhydride groups. The stability of this peranhydride copolymer (PerBzO<sub>2</sub>) has been compared to that of acetylbenzoic peroxide AcBzO<sub>2</sub>; the overall energies of activation of thermal decomposition in toluene solution are 24.6 and 33.2 kcal./mole, respectively. The relative importance of first-order decomposition with respect to the induced decomposition has been determined. The first-order rate constants are  $3.8 \times 10^{-4}$  sec.<sup>-1</sup> for PerBzO<sub>2</sub> at 59.7°C. and only  $5.8 \times 10^{-5}$  sec.<sup>-1</sup> for AcBzO<sub>2</sub>; consequently the peranhydride copolymer is much less stable than the low molecular weight anhydride. This unexpected result must be related to chain structural effects.

The synthesis of graft copolymers is very often based upon the presence of reactive side groups attached on the backbone polymer, which on decomposition give rise to macromolecular free radicals. As reactive group we have used peranhydride groups which were introduced on the backbone by reaction of perbenzoic acid with acid chloride functions. Their use for graft polymerization will be considered in a subsequent paper;<sup>1</sup> in the present paper, however, we will first consider the mechanism of their thermal decomposition, because it is the primary initiating step for the subsequent grafting reaction. We will compare it to that of a low molecular weight homologous anhydride.

At the same time, the synthesis of these copolymers and the determination of their composition will be described.

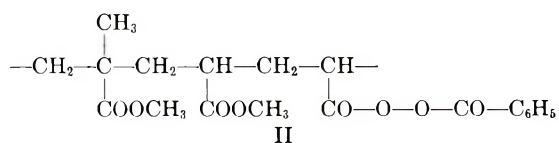
### RESULTS AND DISCUSSION

The decomposition of an asymmetric peroxide, acetylbenzoyl peroxide I (AcBzO<sub>2</sub>), has been compared to that of peranhydride groups built into an acrylyl perbenzoate copolymer II (PerBzO<sub>2</sub>), used for further grafting experiments:<sup>1</sup>



I





The decompositions were followed iodometrically by using the method of Silbert and Swern.<sup>2</sup> The reactions were carried out in toluene and in dioxane solutions for AcBzO<sub>2</sub> and in toluene only for PerBzO<sub>2</sub> at concentrations and temperatures similar to those for the graftings.

By plotting the logarithm of the residual peranhydride concentration against the time, apparent first-order rate constants and the activation energies were evaluated; the results are summarized in Table I.

TABLE I  
Rate of Decomposition of Acetylbenzoyl Peroxide and Polymeric Peranhydride

Peranhydride	Peran- hydride concn., g./100 ml.	Solvent	Temp., °C.	$k_1$ , sec. <sup>-1</sup> × 10 <sup>4</sup>	$E_a$ , kcal./ mole
AcBzO <sub>2</sub>	0.75	Toluene	70.1	0.09	33.2
			79.9	0.38	
			88	1	
AcBzO <sub>2</sub>	0.8	Dioxane	69.7	0.73	25
			79.7	2	
			85.7	3.5	
PerBzO <sub>2</sub>	3 <sup>a</sup>	Toluene	53.4	0.95	24.6
			60.8	2.2	
			66.7	4.3	

<sup>a</sup> 18.1 wt.-% peranhydride.

As can be seen from these results, the polymeric peranhydride decomposes much more rapidly than the low molecular weight asymmetric peroxide, of which the rate constants are intermediary between those of benzoyl peroxide<sup>3-10</sup> and acetyl peroxide.<sup>11-14</sup> The nature of the solvent influences strongly the rate of decomposition, being much higher in dioxane than in toluene. It was therefore assumed that asymmetric peroxides undergo a pronounced induced decomposition, as has been found previously for benzoyl peroxide,<sup>6,8,10</sup> and that the total rate of decomposition can be represented by eq. (1)

$$-d[\text{per}]/dt = k_1 [\text{per}] + k' [\text{per}]^{1.5} \quad (1)$$

where  $k'$  is equal to  $k_3 (k_1/k_4)^{0.5}$ ,  $k_1$ ,  $k_3$ , and  $k_4$  being the rate constants of the first-order decomposition, the induced decomposition, and the recombination of radicals, respectively.

By using the method of Nozaki and Bartlett<sup>6</sup> the values of the first-order rate constant  $k_1$  and  $k'$  were determined for AcBzO<sub>2</sub> and PerBzO<sub>2</sub> in toluene solutions. The following values were found: for acetylbenzoyl

peroxide at 80.7°C.,  $k_1 = 5.8 \times 10^{-3} \text{sec.}^{-1}$ ,  $k' = 3.1 \times 10^{-4} \text{sec.}^{-1} [\text{M}]^{-0.5}$ ; for peranhydride copolymer at 59.7°C.,  $k_1 = 3.8 \times 10^{-4} \text{sec.}^{-1}$ ,  $k' = 3.3 \times 10^{-3} \text{sec.}^{-1} [\text{M}]^{-0.5}$ .

The peranhydride copolymer is not only less stable than the corresponding low molecular weight asymmetric peranhydride but the relative importance of the induced decomposition over the first-order reaction is also higher. The very high rate of decomposition cannot be due to the presence of free carboxyl groups in the polymeric chain; indeed the copolymer was methylated with diazomethane before isolation (see experimental). It must therefore be related to the chain structure, (microtacticity and location of groups; and the high steric hindrance existing along it. This problem was already pointed out with copolymers containing *tert*-butyl perester groups; in that case however  $k'$  was only about twice the value of that for first-order decomposition.<sup>15</sup> These aspects will be considered in a future paper.

## EXPERIMENTAL

### 1. Preparation and Composition of Copolymers

A 33% solution in dry toluene of the two monomers, acrylyl chloride<sup>16</sup> and methyl methacrylate was polymerized at 70°C. for 1–2 hr. in the presence of 0.5% azobisisobutyronitrile as initiator. The copolymer was precipitated in petroleum ether, dissolved in dry dioxane, and treated with a dioxane solution of perbenzoic acid<sup>17,18</sup> following the method of Hahn and Fischer.<sup>19</sup> The copolymer was precipitated in petroleum ether, and twice redissolved in dioxane containing a small amount of methanol and water, and reprecipitated in a large excess of a mixture methanol/water (5/1); in this way the unreacted acid chloride units are converted to methyl ester and free carboxylic groups. Thereafter the copolymer was treated in dioxane solution with diazomethane, and isolated by freeze drying. This treatment affords an acid-free copolymer carrying peranhydride groups (18.1 wt.-%) besides methyl acrylate and methacrylate groups; the peranhydride content was determined iodometrically.

The absence of free carboxylic groups, as well as acid chloride units, was ascertained by titration in dry dimethylformamide with sodium methoxide in benzene, in the presence of thymol blue as indicator. On infrared analysis (Perkin-Elmer 112C with rock salt prisms) no H—O absorption bands could be detected. The infrared spectra of the C=O double bond region of the copolymer in chloroform solution (2.5%) show three absorption bands, one corresponding to the ester groups (1732  $\text{cm.}^{-1}$ ) and a doublet of the peranhydrides (1768 and 1802  $\text{cm.}^{-1}$ ). Similarly acetylbenzoyl peroxide absorbs at 1769 and 1808  $\text{cm.}^{-1}$ , while benzoyl peroxide absorbs at 1764 and 1787  $\text{cm.}^{-1}$ . The frequency differences of peranhydrides ( $\Delta\gamma$  23–39  $\text{cm.}^{-1}$ ) are much smaller than for usual anhydrides ( $\Delta\gamma$  60–75  $\text{cm.}^{-1}$ ); these results agree with those obtained in carbon tetrachloride solution by Davison.<sup>20</sup> The content of peranhydride units can also be

evaluated by infrared spectrometry in dioxane solution ( $700 \text{ cm.}^{-1}$ ) with  $\text{AcBzO}_2$  as reference material.

Acetylbenzoyl peroxide was prepared by air oxidation of benzaldehyde in the presence of acetic anhydride.<sup>21</sup> After crystallization from petroleum ether its degree of purity was 99.6%.

## 2. Rate Measurements

The rate of induced decomposition of  $\text{AcBzO}_2$  and of  $\text{PerBzO}_2$  was followed iodometrically. To find  $k'$ ,  $\text{AcBzO}_2$  was decomposed at  $80.7^\circ\text{C.}$  at two different concentrations (0.0179 and 0.055 mole/l.). Samples were taken at the same time intervals in the two runs; if  $[\text{per}]_1$  and  $[\text{per}]_2$  indicate the respective peranhydride concentrations at a given time, the rate equation can be used.

$$\frac{1}{[\text{per}]_1^{0.5}} = \frac{C}{[\text{per}]_2^{0.5}} + \frac{C-1}{k_1/k'} \quad (2)$$

By plotting  $[\text{per}]_1^{0.5}$  against  $[\text{per}]_2^{0.5}$ , a linear diagram is obtained whose slope and intercept on the ordinate give the values of  $C$  and  $(C-1)/(k_1/k')$ , from which  $k_1/k'$  can be calculated. The first-order rate constants of spontaneous decomposition can then be calculated by using the following integrated equation:

$$\ln \left\{ \frac{(k_1/k') + [\text{per}]^{1.5}}{[\text{per}]^{0.5}} \right\} - \ln \left\{ \frac{(k_1/k') + [\text{per}]_0^{1.5}}{[\text{per}]_0^{0.5}} \right\} = k_1 t \quad (3)$$

In the case of the peranhydride copolymer the reaction temperature was  $59.7^\circ\text{C.}$ , and the two concentrations were 0.019 and 0.0474 mole/l. The experimental data are given in Table II.

TABLE II  
Decomposition of Peranhydride

Peran- hydride	Temp., °C.	$[\text{per}]_1$ , mmoles/l.	$[\text{per}]_1^{-0.5}$	Time, min.	$[\text{per}]_2$ , mmoles/l.	$[\text{per}]_2^{-0.5}$
$\text{AcBzO}_2$	80.7	55.0	4.26	0	17.9	7.46
		46.6	4.63	25	15.5	8.17
		40.6	4.96	45	14.1	8.42
		33.5	5.46	72	12.1	9.09
		28.7	5.89	95	10.7	9.67
$\text{PerBzO}_2$	59.7	47.4	4.59	0	19.0	7.25
		37.4	5.17	10	15.5	8.03
		29.8	5.79	20	12.0	9.11
		25.4	6.27	25	10.9	9.56
		23.4	6.54	30	9.4	10.30

From these results, there was found for  $\text{AcBzO}_2$  at  $80.7^\circ\text{C.}$ ,  $C = 1.35$ ,

$$\frac{C-1}{k_1/k'} = 1.8$$

$$k_1/k' = 0.19$$

and for  $\text{PerBzO}_2$  at  $59.7^\circ\text{C}$ .,  $C = 1.55$ ,

$$\frac{C-1}{k_1/k'} = 0.12$$

$$k_1/k' = 4.77$$

The authors are indebted to the Fonds National de la Recherche Scientifique for supporting this research and to the Institut pour l'Encouragement de la recherche scientifique dans l'Industrie et l'Agriculture for a fellowship to one of them (W. V. R.).

### References

1. Van Rillaer, W., and G. Smets, *J. Polymer Sci.*, **A2**, 2423 (1964).
2. Silbert, L. S., and D. Swern, *Anal. Chem.*, **30**, 385 (1958).
3. Kamenskaya, S., and S. Medvedev, *Acta Physicochim. USSR*, **13**, 56 (1941).
4. McClure, J. H., R. E. Robertson, and A. C. Cuthbertson, *Can. J. Res.*, **20**, 103 (1942).
5. Cass, W. E., *J. Am. Chem. Soc.*, **68**, 1976 (1946).
6. Nozaki, K., and P. D. Bartlett, *J. Am. Chem. Soc.*, **68**, 1686 (1946).
7. Hartman, P. F., H. G. Sellers, and D. Turnbull, *J. Am. Chem. Soc.*, **69**, 2416 (1947).
8. Barnett, B., and W. E. Vaughan, *J. Phys. Colloid Chem.*, **51**, 926 (1947).
9. Bagdasaryan, K. S., and V. A. Milintinskiĭ, *Zh. Khim. Fiz.*, **27**, 420 (1950).
10. Conix, A., and G. Smets, *J. Polymer Sci.*, **10**, 525 (1953).
11. Walker, O. J., and G. L. Wild, *J. Chem. Soc.*, **1937**, 1132.
12. Ross, S. D., and M. A. Fineman, *J. Am. Chem. Soc.*, **73**, 2176 (1951).
13. Levy, M., M. Steinberg, and M. Szwarc, *J. Am. Chem. Soc.*, **76**, 5978 (1954).
14. Szwarc, M., *J. Polymer Sci.*, **16**, 367 (1955).
15. Smets, G., A. Poot, and G. L. Duncan, *J. Polymer Sci.*, **54**, 65 (1961).
16. Stempel, G. H., Jr., R. P. Cross, and R. P. Mariella, *J. Am. Chem. Soc.*, **72**, 2299 (1950).
17. Blatt, A. H., *Organic Synthesis*, Coll. Vol. I, Wiley, New York, 1946, p. 431.
18. D'Ans, J., J. Mattner, and W. Busse, *Angew. Chem.*, **65**, 57 (1953).
19. Hahn, W., and A. Fischer, *Makromol. Chem.*, **16**, 36 (1955).
20. Davison, W. H. T., *J. Chem. Soc.*, **1951**, 2456.
21. Jorissen, W. P., and W. E. Ringer, *J. pr.* (2), **72**, 176 (1905).

### Résumé

La synthèse d'un copolymère contenant des groupes peranhydrides a été réalisée en trois étapes: (a) copolymérisation de chlorure d'acroyle avec du méthacrylate de méthyle, (b) réaction du copolymère chlorure acide avec l'acide perbenzoïque, (c) traitement par l'alcool méthylique aqueux et méthylation au diazométhane, en vue d'éviter la présence de groupes carboxyliques libres. Le copolymère contenait 18,1% en poids de groupes peranhydrides. La stabilité de ce copolymère peranhydride ( $\text{PerBzO}_2$ ) a été comparée à celle du peroxyde d'acétylbenzoyle  $\text{AcBzO}_2$ ; les énergies globales d'activation de la décomposition thermique en solution toluénique s'élèvent à 24.6 et 33.2 kcal/mole respectivement. L'importance relative de la décomposition de premier ordre par rapport à la décomposition induite a été déterminée. Les constantes de vitesse de premier ordre s'élèvent à  $3,8 \times 10^{-4} \text{ sec}^{-1}$  pour  $\text{PerBzO}_2$  à  $59,7^\circ$  et seulement à  $5,8 \times 10^{-6} \text{ sec}^{-1}$  pour  $\text{AcBzO}_2$ ; en conséquence l'anhydride copolymère est beaucoup moins stable que l'anhydride de bas poids moléculaire. Ce résultat inattendu doit être attribué à des effets de la structure de la chaîne.

### Zusammenfassung

Es wurde ein Persäureanhydrid-Copolymeres in drei Stufen hergestellt: a) Copolymerisation von Acrylylchlorid mit Methylmethacrylat; b) Reaktion des Säurechlorid-Copolymeren mit Perbenzoesäure; c) Behandlung mit wässrigem Methanol und anschließende Methylierung mit Diazomethan zur Bindung freier Carboxylgruppen. Das Polymere enthält 18,1 Gewichtsprozent Persäureanhydridgruppen. Die Stabilität dieses Persäureanhydrid-Copolymeren ( $\text{PerBzO}_2$ ) wurde mit derjenigen von Acetylbenzoylperoxyd ( $\text{AcBzO}_2$ ) verglichen. Die entsprechenden Bruttoaktivierungsenergie der thermischen Zersetzung in Toluollösung ist 24,6 bzw. 33,2 kcal/Mol. Ausserdem wurde das Ausmass der nach erster Ordnung verlaufenden Zersetzung im Verhältnis zur induzierten Zersetzung bestimmt. Die Geschwindigkeitskonstante erster Ordnung ist bei 59,7° für  $\text{PerBzO}_2$   $3,8 \cdot 10^{-4} \text{ sec}^{-1}$ , für  $\text{AcBzO}_2$  jedoch nur  $5,8 \cdot 10^{-5} \text{ sec}^{-1}$ . Das Persäureanhydrid-Copolymere ist also viel instabiler als das Anhydrid niedrigen Molekulargewichtes. Dieses unerwartete Verhalten muss den durch die Kettenstruktur bedingten Effekten zugeschrieben werden.

Received May 13, 1963



## Graft Copolymerization with Peranhydride Side Groups

W. VAN RILLAER and G. SMETS, *Laboratory of Macromolecular Chemistry, University of Louvain, Belgium*

### Synopsis

Several copolymers of methyl acrylate, methyl methacrylate, and acrylyl perbenzoate of different peranhydride contents (5.35, 9.24, 12.6, 20.2, and 33.9 wt.-%) were prepared and used for initiating the graft polymerization of styrene. The overall rate of polymerization and the grafting rate are proportional to the square root of the peranhydride concentration, while they are practically first order with respect to the monomer concentration. The graft copolymers were separated from both homopolymers by precipitation with methanol from the chloroform solution of the copolymer; the styrene content of the graft copolymer increases with monomer concentration (e.g., 32.4 and 51.1% for monomer concentrations of 2.6 and 6.1 mole/l., respectively). The ratio of  $R_g/R_h$ , i.e., the weight of styrene bonded as graft to that as homopolystyrene has been taken as a conventional measure of the graft efficiency. At 80°C. this ratio never exceeds 0.46, independent of the composition of the initiating copolymer. It increases, however, markedly with decreasing grafting temperature; for a styrene concentration of 6.1 mole/l. it is equal to 0.64 and 1.27 at 72.1 and 55.6°C., respectively. The ratio  $R_g/R_h$  depends also strongly on steric effects: when the copolymer contains only methyl acrylate and acrylyl perbenzoate units with exclusion of methyl methacrylate,  $R_g/R_h$  is much larger than unity: at 74.9°C. it is equal to 1.68 and 2.31 for monomer concentrations of 2.6 and 4.35 mole/l., respectively, in the presence of a polymer containing 23.9 wt.-% of peranhydride. This ratio is also enhanced by the viscosity of the solution. The results are compared to those obtained with similar copolymers containing *tert*-butyl perester side groups.

The kinetics of graft copolymerization of styrene onto methyl acrylate and methyl methacrylate copolymers containing *tert*-butyl perester side groups have been described recently by one of us.<sup>1</sup> We wish now to report similar kinetic studies, in which an analogous backbone copolymer was used but carrying another reactive side group, namely a peranhydride group. Similar copolymers have already been described by Hahn and Fischer.<sup>2</sup> Although it is practically impossible to prepare two types of initiating copolymers with the same content of reactive side groups and same molecular weight, nevertheless the main difference between the two series lies in the nature of the small radicals; in the former study they were *tert*-butoxide radicals, in the present case they are benzoate radicals.

In the preceding paper the stability of the peranhydride groups was considered and their decomposition rate constants evaluated.<sup>2</sup> In the

present paper particular attention will be paid to the grafting efficiency of these copolymers with respect to styrene additions; as previously,<sup>3</sup> we will take as a conventional measure of this efficiency the ratio  $R_g/R_h$ , i.e., the weight  $R_g$  of the styrene bonded as graft taking due account of the composition of the graft copolymer, divided by the weight  $R_h$  of homopolystyrene produced simultaneously.

## EXPERIMENTAL

### 1. Preparation and Composition of Peranhydride Copolymers

The method described in the preceding paper<sup>3</sup> has been used for the preparation of the different methyl acrylate-methyl methacrylate-acrylyl perbenzoate copolymers which were used as initiator for grafting experiments. The peranhydride content is given in Table I.

TABLE I  
Peranhydride Content of Initiating Copolymers

Initiator	Peranhydride, wt.-%
P <sub>1</sub>	12.63
P <sub>2</sub>	9.24
P <sub>3</sub>	5.35
P <sub>4</sub>	9.25
P <sub>6</sub>	20.2
P <sub>6</sub>	33.9
P <sub>A7</sub> <sup>a</sup>	23.9

<sup>a</sup> Copolymer P<sub>A7</sub> contained only acrylic units.

### 2. Graft Copolymerization and Isolation of Graft Copolymers

Graft copolymerization was carried out in sealed tubes in the temperature range 70–80°C. with toluene as solvent. After reaction the copolymers were twice precipitated from toluene solution by addition of petroleum ether and dried in vacuum. The fractionation was carried out at 25°C. by progressive precipitation on addition of methanol to a 2% polymer solution in chloroform.

All fractions collected between precipitant volume fractions  $\gamma$  of 0.26 and 0.45 are practically pure polystyrene; they were redissolved in butanone and precipitated in methanol. Between  $\gamma$  0.75 and 0.8 the graft copolymer precipitated; they were isolated by freeze-drying of their dioxane solution. The remaining solution was evaporated to dryness, the polymer dissolved in dioxane, and isolated by freeze-drying; it was essentially unreacted initial copolymer.

Infrared analyses of the polymer fractions were determined by measuring the phenyl group absorption at 696  $\text{cm.}^{-1}$  in dioxane.

## RESULTS AND DISCUSSION

## 1. Rate Dependence on the Peranhydride Copolymer Concentration

The rate of polymerization of styrene (2.614 mole/l.) has been measured at five different concentrations of initiating polymer  $P_1$ . The data are given in Table II.

TABLE II  
Dependence of Rate on Peranhydride Concentration<sup>a</sup>

[Peranhydride] $\times 10^3$ , mole/l.	Polymer $P_1$ , g./100 ml.	Polystyrene, g./10 ml. solution	Degree of conversion, %	$R_p \times 10^6$ , mole/l. sec.
3.3	0.5	0.105	3.87	3.43
6.6	1.0	0.145	5.34	4.74
9.9	1.5	0.182	6.70	5.94
13.2	2.0	0.203	7.47	6.63
16.5	2.5	0.224	8.25	7.33

<sup>a</sup> Polymerization conditions: polymer  $P_1$ , 12.6 wt.-% peranhydride; styrene concentration 2.614 mole/l.; temp. 75.5°C.; time 490 min.; solvent toluene.

Plotting the square of the rates versus the peranhydride concentration yields a linear diagram, the small intercept on the ordinates being the rate of thermal polymerization. Consequently the polymerization follows the square-root law with respect to the initiator concentration, in agreement with the data of Hahn and Fischer<sup>2</sup> and of Smets and co-workers<sup>1,4,5</sup> (Fig. 1).

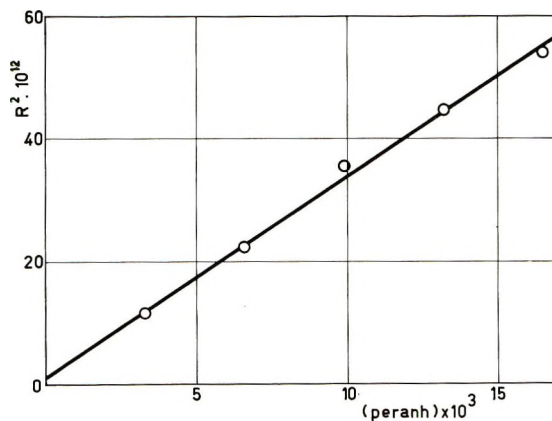


Fig. 1. Dependence of rate of styrene polymerization on peranhydride concentration (copolymer  $P_1$ ).  $[M] = 2.614$  mole/l.; temp. = 75.5°C.; solvent, toluene.

## 2. Dependence of Rate on the Monomer Concentration

The influence of the monomer concentration on the overall rate of polymerization was first examined by experiments carried out at 80°C.

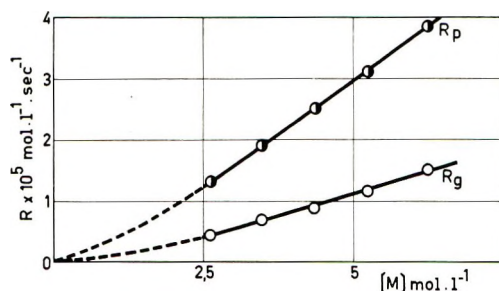


Fig. 2. Influence of monomer concentration on the total rate of polymerization  $R_p$  and the rate of grafting  $R_g$ . Copolymer P<sub>3</sub> (5.35 wt.-% peranhydride) = 5 g./100 ml.; temp. = 80°C.

in toluene solutions in the presence of a given amount of polymer P<sub>2</sub>. The results are summarized in Table III.

In all these experiments, the rate of thermal polymerization,  $R_{th}$  in the absence of peranhydride initiating polymer but in isoviscous medium (by adding inert high molecular polystyrene to the monomer-toluene mixture) is about  $1/10$  of the rate of polymerization with initiator,  $R_{per}$  (column 5). If one considers that the overall rate of polymerization  $R_{tot}$  is given by

$$R_{tot} = (k_p[M]/k_t^{1/2}) (R_{i_{per}} + R_{i_{th}})^{1/2}$$

where  $k_p$  and  $k_t$  are the propagation and termination rate constants, respectively, and  $R_{i_{per}}$  and  $R_{i_{th}}$  the rate of initiation in the presence and in the absence of peranhydride initiator, respectively, it becomes evident that

$$R_{per} = (R_{tot}^2 - R_{th}^2)^{1/2}$$

TABLE III  
Influence of the Styrene Concentration on the Rate of Polymerization<sup>a</sup>

[M], mole/l.	Time, min.	Poly- styrene content in total polymer, %	Polystyrene, g./20 ml. solution		Degree of con- version, %	Rate $R_{tot}$ $\times 10^5$ , mole/l. sec.
			Total amount	Thermal <sup>b</sup>		
1.744	540	42.2	0.444	0.050	12.4	0.66
2.614	435	52.2	0.667	0.061	12.1	1.24
3.485	375	59.4	0.880	0.103	12.1	1.88
4.356	315	63.2	1.032	0.120	11.4	2.62
5.227	260	64.5	1.093	0.124	10.0	3.36

<sup>a</sup> Polymerization conditions: polymer P<sub>2</sub>, 9.24 wt.-% peranhydride; 3% polymer solution; [peranhydride] = 0.0144 mole/l.; temp. 80°C.

<sup>b</sup> In absence of initiating polymer, but in isoviscous medium.

Consequently the rate correction for the thermal polymerization amounts only to about 1% of the total rate; therefore it was further neglected in this paper.

From the data of Table III it can be seen that the rate increases proportionally with the monomer concentration, although some curvature at low concentration indicates an order higher than unity (Fig. 2). This behavior in dilute monomer solution can be interpreted in terms of chain termination reactions between growing chains and primary radicals.<sup>6</sup>

In order to evaluate the relative importance of the graft polymerization with respect to homopolymerization and its dependence on the monomer concentration, the reaction products were fractionated and the corresponding mean rates calculated, taking due account of the styrene content of the graft copolymers.

These experiments (Table IV) show in each series that both rates of homopolymerization  $R_h$  and grafting  $R_g$  increase linearly with the styrene concentration over the whole range of concentration (Fig. 2); in a previous paper with copolymers containing *tert*-butylperacrylic units as initiator, this proportionality between the amount of grafting and the monomer concentration was only valid for low monomer concentration.<sup>1</sup>

As previously, the ratio of both rates of homopolymerization and graft polymerization was considered as a direct measurement of the efficiency of grafting; from Table IV it can be seen that this ratio  $R_g/R_h$  is always low and never exceeds a value of 0.44. It must be admitted therefore that the macroradicals not only propagate by monomer addition, but also give chain transfer with the monomer, producing both graft polymer and homopolymer (page 2430).

The relative importance of reactions b, c, and d determines the value of the ratio  $R_g/R_h$ . This ratio increases slowly with the monomer concentration; chain transfer reactions with the solvent (toluene) can easily account for it.

### 3. Influence of Polymer Concentration and Peranhydride Content

From Table IV it can be also seen that  $R_g/R_h$  ratios increase slightly with the active polymer concentration. This small increase could be attributed to the increase of viscosity of the reaction medium; indeed the experiments of series F show the influence of the addition of 1% inert polystyrene on the grafting efficiency, if they are compared to the experiments of series E.

Although small, the effect is always directed in the same sense, corroborating the influence of the viscosity. It is admitted that an increase of the viscosity of the medium diminishes the rate of diffusion of the small primary radicals, which react more easily with their polymer chain giving some new sites for grafting.

The effect of the peranhydride group content is unclear; indeed from the comparison of series C and E, and B and D an increase of  $R_g/R_h$  would



TABLE IV  
Rate of Polymerization of Styrene in Toluene at 80°C.

Series	[M], mole/l.	Time, min.	Polystyrene, g./20 ml. solution		Polystyrene content in graft polymer, %	Degree of con- version, %	Rate $\times 10^5$ , mole/l. sec.		$R_g/R_h$
			Homo- polymer	Graft polymer			$R_h$	$R_g$	
A. Polymer P <sub>3</sub> , 5.35 wt.-% peranhydride; 5% polymer solution; [peranhydride] = 0.0139 mole/l.	2.614	420	0.569	0.229	26.4	14.7	1.08	0.43	0.40
	3.485	365	0.711	0.303	32.2	13.9	1.56	0.65	0.42
	4.356	331	0.851	0.361	36.4	13.4	2.08	0.87	0.42
	5.227	300	0.938	0.438	40.2	12.6	2.51	1.15	0.46
	6.219	270	1.145	0.531	44.8	12.9	3.40	1.50	0.44
B. Polymer P <sub>4</sub> , 9.25 wt.-% peranhydride; 5% polymer solution; [peranhydride] = 0.024 mole/l.	2.614	355	0.747	0.247	32.4	18.3	1.65	0.55	0.330
	3.485	305	0.932	0.285	34.4	16.8	2.42	0.74	0.306
	4.356	275	1.014	0.378	40.5	15.3	3.08	1.15	0.373
	5.227	255	1.220	0.450	47.6	15.4	3.80	1.41	0.370
	6.099	255	1.310	0.530	51.1	14.5	4.55	1.85	0.405
C. Polymer P <sub>4</sub> , 9.25 wt.-% peranhydride; 3% polymer solution; [peranhydride] = 0.0144 mole/l.	2.614	465	0.768	0.168	35.6	17.4	1.32	0.29	0.220
	3.485	420	0.969	0.208	39.6	16.3	1.89	0.39	0.215
	4.356	360	1.114	0.245	46.8	15.0	2.46	0.54	0.220
	5.227	315	1.247	0.310	50.3	14.3	3.16	0.79	0.250
	6.099	285	1.377	0.354	54.4	13.7	3.84	0.99	0.257

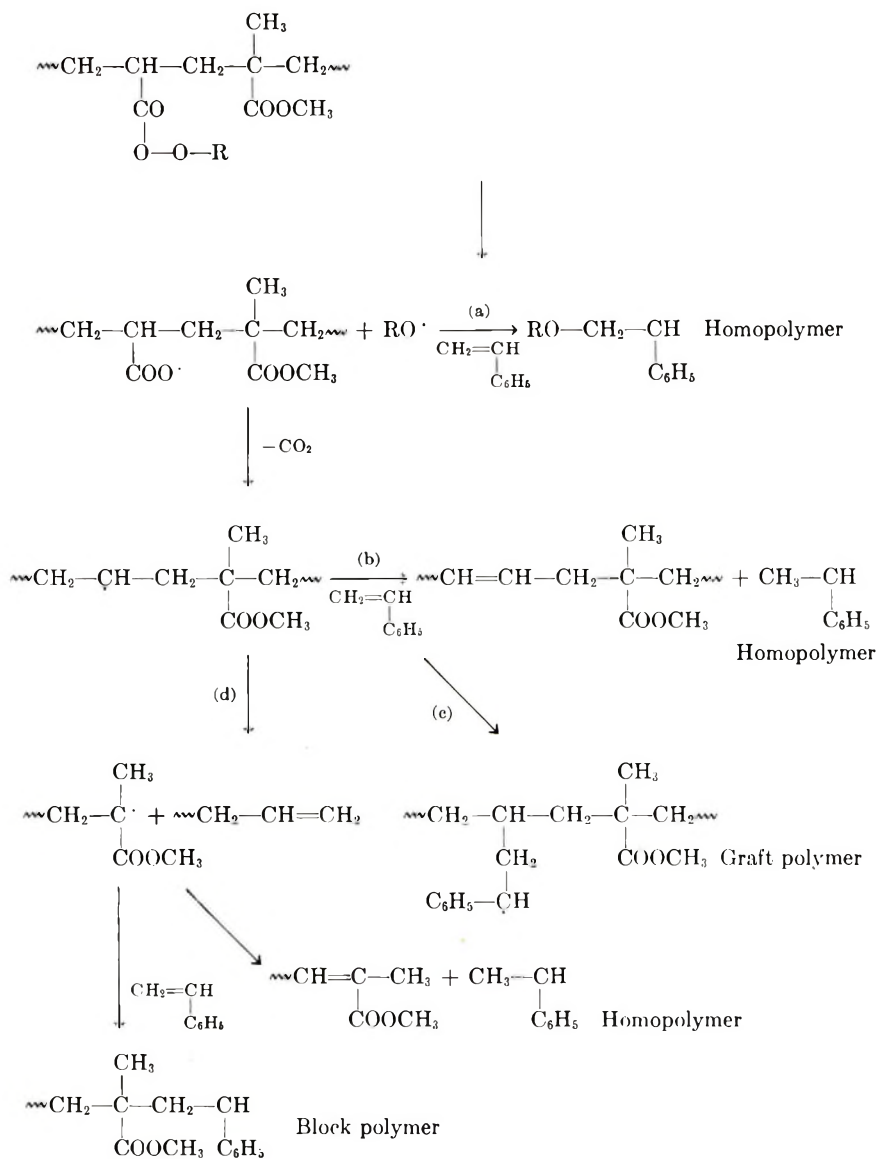
D. Polymer P <sub>6</sub> , 20.2 wt.-% 5% polymer solution; [peranhydride] = 0.0525 mole/l.	3.485	270	0.590
	4.356	220	0.647
	5.227	195	0.689
	6.099	195	0.808
E. Polymer P <sub>6</sub> , 20.2 wt.-% peranhydride; polymer solution; [peranhydride] = 0.0312 mole/l.	3.485	330	1.078
	4.356	270	1.211
	5.227	240	1.355
	6.099	210	1.503
F. Polymer P <sub>6</sub> , 20.2 wt.-% peranhydride; 3% polymer solution + 1% polystyrene; [peranhydride] = 0.0312 mole/l.	4.356	330	1.176
	6.099	210	1.457

## GRAFT COPOLYMERIZATION

2429

---

0.229	45.5	11.3	3.46	1.35	0.390
0.277	49.4	10.2	4.65	2.00	0.430
0.307	53.3	9.2	5.67	2.52	0.445
0.356	59.3	9.2	6.63	2.92	0.440
0.366	50.3	19.9	2.62	0.89	0.340
0.466	57.5	18.5	3.58	1.38	0.385
0.551	61.9	17.5	4.46	1.83	0.410
0.618	64.5	16.7	5.73	2.35	0.410
0.486	59.8	18.3	3.52	1.44	0.410
0.625	64.6	16.4	5.50	2.37	0.430



be related with an increase of the peranhydride content. This statement is however contradicted by the results of series A. This disagreement must be related to differences of inherent viscosities of the initiating polymer as well as to the viscosity of the solution.

Concerning the possibility of a degradation of the initiating polymer in the course of grafting polymer,  $P_5$  has been used as initiator for the polymerization of styrene (6.099 mole/l.) at  $72^\circ\text{C}$ . The initial intrinsic viscosity was 0.6; after reaction and fractionation it was only 0.2, while that of the graft polymer was 0.95.

This experiment shows that degradation reactions occur even in the

TABLE V  
Influence of Temperature on Rate of Polymerization of Styrene in Toluene

Series	Temp., °C.	[M], mole/l.	Time, min.	Polystyrene, g./10 ml. solution		Poly- styrene content in graft polymer, %	Degree of con- version, %	Rate $\times 10^4$ , mole/l. sec.		$R_g/R_h$
				Homo- polymer	Graft polymer			$R_h$	$R_g$	
A. Polymer P <sub>5</sub> , 20.2 wt.-% peranhydride; 5% polymer solution; [peranhydride] = 0.0525 mole/l.	72.1	3.485	365	0.454	0.233	45.0	18.9	1.98	1.02	0.515
	72.1	4.356	295	0.491	0.265	49.0	16.8	2.67	1.44	0.540
	72.1	5.227	250	0.526	0.338	55.8	15.9	3.36	2.16	0.640
	72.1	6.099	220	0.559	0.357	56.4	14.4	4.08	2.60	0.640
B. Polymer P <sub>5</sub> , 20.2 wt.-% peranhydride; 3% polymer solution; [peranhydride] = 0.034 mole/l.	69.9	4.356	495	0.953	0.510 <sup>a</sup>	54.9	16.2	1.54	0.82	0.530
	75.0	4.356	465	1.188	0.501 <sup>a</sup>	54.4	18.6	2.04	0.86	0.420
	79.7	4.356	390	1.442	0.569 <sup>a</sup>	58.8	22.2	2.97	1.17	0.400
	84.8	4.356	330	1.679	0.526 <sup>a</sup>	56.4	24.4	4.07	1.27	0.310
C. Polymer P <sub>6</sub> , 33.9 wt.-% peranhydride; 3% polymer solution; [peranhydride] = 0.0529 mole/l.	55.6	6.099	420	0.277	0.353	70.4	9.9	1.05	1.34	1.270

<sup>a</sup> Polystyrene, g./20 ml. solution.



presence of high monomer concentration, which is a rather unexpected result.

#### 4. Influence of Temperature on Grafting Efficiency

The influence of the temperature on the efficiency of grafting can be shown by comparison of series D of Table IV with series A of Table V, as well as from the results of series C, Table V.

The ratio  $R_g/R_h$  increases markedly with a decrease of grafting temperature; this can be interpreted as due to a decrease of chain transfer with the solvent, of which the activation energy is higher than that of the propagation reaction. The increase of viscosity of the medium may also reduce the rate of diffusion of the small benzoate radicals away from the chain and favor the abstraction of an hydrogen atom of the main chain, with formation of a new site of grafting. Experiment C of Table V is particularly noteworthy, with its  $R_g/R_h$  value equal to 1.27.

#### 5. Influence of Polymer Composition

With respect to the  $R_g/R_h$  values a double comparison can be made with experiments described previously.

Figure 3 shows the dependence on the monomer concentration for two copolymers of methyl acrylate and methyl methacrylate, of which one contained *tert*-butyl peracrylate ester groups<sup>1</sup> (formula A, Table VI), while the other one contained acrylyl perbenzoate groups (formula B).

On decomposition both copolymers give the same macroradical; they differ only by the nature of the small radicals which are produced simultaneously of which one is a *tert*-butyloxy, the other one a benzoate (or phenyl) radical.

While the ratio  $R_g/R_h$  increases slowly with the monomer concentration in the case of the peranhydride copolymer, it decreases appreciably for the perester copolymer (Fig. 3). This effect may be due to an increased efficiency of the *tert*-butyloxy radical in concentrated monomer solutions and has been discussed previously.

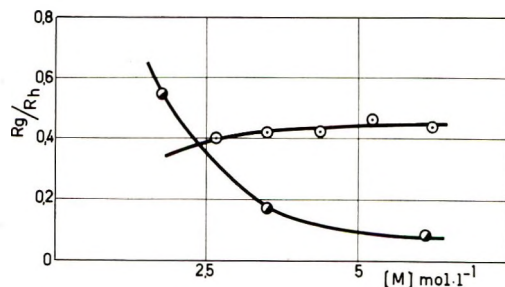


Fig. 3. Influence of the monomer concentration on the  $R_g/R_h$  ratio: (●) methyl acrylate-methyl methacrylate-*tert*-butyl peracrylate copolymer, 56.4-38-5.6 (85°C.); (○) methyl acrylate-methyl methacrylate-acrylyl perbenzoate copolymer, 57.2-40-2.8 (80°C.).

TABLE VI

Copolymer type	Structure	Molar composition
A	$  \begin{array}{ccccccc}  & & & & & & \text{CH}_3 \\  & & & & & &   \\  -\text{CH}_2- & \text{CH}- & \text{CH}_2- & \text{CH}- & \text{CH}_2- & \text{C}- & \\  &   & &   & &   & \\  & \text{C}=\text{O} & & \text{C}=\text{O} & & \text{C}=\text{O} & \\  &   & &   & &   & \\  & \text{OCH}_3 & & \text{O}-\text{OC}_4\text{H}_9 & & \text{OCH}_3 &   \end{array}  $	56.4/5.6/38
B	$  \begin{array}{ccccccc}  & & & & & & \text{CH}_3 \\  & & & & & &   \\  -\text{CH}_2- & \text{CH}- & \text{CH}_2- & \text{CH}- & \text{CH}_2- & \text{C}- & \\  &   & &   & &   & \\  & \text{C}=\text{O} & & \text{C}=\text{O} & & \text{C}=\text{O} & \\  &   & &   & &   & \\  & \text{OCH}_3 & & \text{O}-\text{O}-\text{C}=\text{O} & & \text{OCH}_3 & \\  & & &   & & & \\  & & & \text{C}_6\text{H}_5 & & &   \end{array}  $	57.2/2.8/40
C	$  \begin{array}{ccccccc}  & & & & & & \\  -\text{CH}_2- & \text{CH}- & \text{CH}_2- & \text{CH}- & \text{CH}_2- & \text{CH}- & \\  &   & &   & &   & \\  & \text{C}=\text{O} & & \text{C}=\text{O} & & \text{C}=\text{O} & \\  &   & &   & &   & \\  & \text{OCH}_3 & & \text{O}-\text{O}-\text{C}_6\text{H}_5 & & \text{OCH}_3 &   \end{array}  $	47.7/12.3/40
D	$  \begin{array}{ccccccc}  & & & & & & \\  -\text{CH}_2- & \text{CH}- & \text{CH}_2- & \text{CH}- & \text{CH}_2- & \text{CH}- & \\  &   & &   & &   & \\  & \text{C}=\text{O} & & \text{C}=\text{O} & & \text{C}=\text{O} & \\  &   & &   & &   & \\  & \text{OCH}_3 & & \text{O}-\text{O}-\text{C}=\text{O} & & \text{OCH}_3 & \\  & & &   & & & \\  & & & \text{C}_6\text{H}_5 & & &   \end{array}  $	47.6/12.4/40

If these systems are compared to copolymers of type C (Table VI), in which methyl methacrylate units are absent, much higher  $R_g/R_h$  ratios have been obtained, even up to 5<sup>(1)</sup>. From this comparison it must be concluded that steric hindrance plays an important role in the graft initiation, not only by a decrease of accessibility of the sites of grafting, but likely also by a lack of space for grafting side chains. Conversely, if this interpretation is correct, a decrease of steric hindrance must increase the ratio of grafting. This has been borne out with grafting experiments in which an initiating methyl acrylate-acrylyl-perbenzoate anhydride copolymer (formula D) was used instead of a copolymer containing methacrylic units (formula B). The results are summarized in Table VII.

As can be seen from these data, the  $R_g/R_h$  ratios are much higher than in the preceding case; they increase with increasing monomer concentration, and with increasing viscosity of the reaction medium.

The last experiment listed in Table VII is especially interesting, because it was carried out in the presence of methanol instead of toluene. Because of the insolubility of polystyrene in the reaction medium, a change of the  $R_g/R_h$  could be expected. In fact, only a minor change has been stated, although the rates of homopolymerization and graft polymerization both decrease. The results of Table VII confirm completely the importance of steric hindrance with respect to grafting and agree with the interpreta-

TABLE VII  
Rate of Polymerization of Styrene in Toluene at 74.9°C.

	[M], mole/l.	Time, min.	Polystyrene, g./20 ml. solution		Polystyrene content in graft polymer, %	Degree of conversion, %	Rate $\times 10^6$ , mole/sec.		$R_g/R_h$
			Homo-polymer	Graft polymer			$R_h$	$R_g$	
Polymer P <sub>57</sub> , 23.9 wt.-% peranhydride	2.614	185	0.257	0.435	42.2	12.55	1.12	1.88	1.68
	2.614 <sup>a</sup>	185	0.213	0.433	43.0	11.9	0.92	1.87	2.02
	4.356	120	0.289	0.672	50.5	10.6	1.93	4.48	2.31
	4.356 <sup>b</sup>	120	0.212	0.466	44.8	7.5	1.41	3.10	2.19

<sup>a</sup> In the presence of 2% polystyrene.

<sup>b</sup> In the presence of methanol instead of toluene.

tion given above.  $R_g/R_h$  values higher than 2 (instead of about 0.5) are easily obtained.

## CONCLUSIONS

The overall kinetics of polymerizations of styrene initiated by the thermal decomposition of polymeric peranhydrides are the same as for low molecular weight peroxides; the rate is practically first order with respect to the monomer concentration and proportional to the square root of the peranhydride concentration, the thermal polymerization being unimportant. The low  $R_g/R_h$  ratios (0.4–0.6) are mainly due to the steric hindrance existing along the polymeric chain, which contains appreciable amounts of methyl methacrylate; indeed in the absence of these units, the  $R_g/R_h$  exceeds unity considerably and may attain values of 2.2–2.3.  $R_g/R_h$  increases weakly with increasing monomer concentration, but appreciably with a decrease of grafting temperature; chain transfer reaction with solvent can easily account for it. The small increase of  $R_g/R_h$  with increasing viscosity of the reaction medium may be due to a transfer reaction of the low molecular primary radical with the polymeric chain, giving new sites of grafting.

The authors are indebted to the Centre des Hauts Polymères I.R.S.I.A. Belgium for supporting the research and for a fellowship to one of them (W. V. R.).

## References

1. Smets, G., A. Poot, and G. L. Duncan, *J. Polymer Sci.*, **54**, 65 (1961).
2. Hahn, W., and A. Fischer, *Makromol. Chem.*, **16**, 36 (1955).
3. Smets, G., and W. Van Rillaer, *J. Polymer Sci.*, **A2**, 2417 (1964).
4. Smets, G., *Pure Appl. Chem.*, **4**, 287 (1962).
5. Smets, G., A. Poot, M. Mullier, and J. P. Bex, *J. Polymer Sci.*, **34**, 287 (1959).
6. Bamford, C. H., A. D. Jenkins, and P. Johnston, *Trans. Faraday Soc.*, **55**, 1481 (1955).

## Résumé

Plusieurs copolymères d'acrylate de méthyle, de méthacrylate de méthyle et de péroxyde d'acrylate ont été préparés à différents teneurs en peranhydride (5,35; 9,24; 12,6; 20,2; et 33,9% en poids) et utilisés pour l'initiation de la polymérisation greffée du styrène. La vitesse globale de polymérisation, de même que la vitesse de greffage sont proportionnelles à la racine carrée de la concentration en peranhydride, et pratiquement de premier ordre par rapport à la concentration en monomère. Les copolymères greffés ont été séparés des deux homopolymères par précipitation progressive en ajoutant du méthanol à la solution chloroformique du copolymère. La teneur en styrène du copolymère greffé augmente avec la concentration en monomère, par exemple 32,4 et 51,1 à des concentrations de 2,6 et 6,1 moles/l, respectivement. Le rapport  $R_g/R_h$ , c.à.d. du poids du styrène lié comme greffon au homopolystyrène formé simultanément, est pris comme mesure conventionnelle de l'efficacité de greffage. A 80°C ce rapport ne dépasse jamais 0,46, indépendamment de la composition du copolymère initiateur. Il croît toutefois notablement en diminuant la température de greffage; à une concentration en styrène de 6,1 moles/l il est égal à 0,64 et 1,27 à 72,1 et 55,6°C respectivement. Ce rapport  $R_g/R_h$  dépend également fortement des effets stériques: lorsque le copoly-

mère ne contient que des unités acryliques (acrylate de méthyle, perbenzoate d'acryloyle) à l'exclusion de méthacrylate de méthyle,  $R_g/R_h$  dépasse considérablement l'unité: à 74,9°C il est égal à 1,68 et 2,31 pour des concentrations en monomères égales de 2,6 et 4,35 moles/l respectivement en présence d'un copolymère contenant 23,9% en poids de peranhydride. Ce rapport croît aussi par augmentation de la viscosité de la solution. Les résultats sont comparés à ceux obtenus avec des copolymères semblables porteurs de groupes latéraux peresters.

### Zusammenfassung

Es wurden mehrere Copolymere aus Methylacrylat, Methylmethacrylat und Acrylylperbenzoat mit verschiedenem Peranhydridgehalt (5,35; 9,24; 12,6; 20,2 und 33,9 Gewichtsprozent) hergestellt und zum Start der Pfropfpolymerisation von Styrol verwendet. Sowohl die Bruttopolymerisationsgeschwindigkeit als auch die Pfropfgeschwindigkeit sind der Quadratwurzel der Peranhydridkonzentration proportional und bezüglich der Monomerkonzentration praktisch von erster Ordnung. Die Pfropfcopolymeren wurden durch Fällung, u.zw. durch Zusatz von Methanol zur Chloroformlösung des Copolymeren, von den beiden homopolymeren getrennt. Die Styrolkonstante des Pfropfcopolymeren nimmt mit steigender Monomerkonzentration zu (z.B. 32,4 und 51,1 für Monomerkonzentrationen von 2,6 bzw. 6,1 Mol/l). Als konventionelles Mass für die Pfropfungswirksamkeit diente das Verhältnis  $R_o/R_h$ , d.h. das Gewichtsverhältnis von aufgepfropftem Styrol zu Homopolystyrol. Dieses Verhältnis überschritt bei 80°C, unabhängig von der Zusammensetzung des als Starter verwendeten Copolymeren, nie den Wert 0,46, stieg jedoch mit abnehmender Pfropfungstemperatur deutlich an und hatte bei einer Styrolkonzentration von 6,1 M bei 72,1° bzw. 55,6° die Werte 0,64 bzw. 1,27. Das Verhältnis  $R_o/R_h$  ist auerdem stark von sterischen Effekten abhängig: Wenn das Copolymere nur Methacrylat-Acrylylperbenzoat-Einheiten enthält, ist  $R_o/R_h$  bedeutend grösser als eins. Z.B. war  $R_o/R_h$  bei 74,9°C in Gegenwart eines Polymeren mit 23,9 Gewichtsprozent Peranhydrid bei Monomerkonzentrationen von 2,6 bzw. 4,35 Mol/l gleich 1,68 bzw. 2,31. Dieses Verhältnis nimmt ausserdem mit steigender Viskosität der Lösung zu. Die experimentellen Ergebnisse werden mit denjenigen verglichen, die bei Verwendung ähnlicher Copolymerer mit tert.-Butylperester-Gruppen erhalten wurden.

Received May 13, 1963



## Sorption and Diffusion of Water Vapor by Nylon 6

KOJI KAWASAKI and YOSHIYASU SEKITA, *Electrotechnical Laboratory, Nagata-cho, Chiyoda-ku, Tokyo, Japan*

### Synopsis

The interaction between nylon 6 and water has been studied from water vapor sorption isotherms, diffusion of water vapor in the polymer, and nuclear magnetic resonance (NMR) properties. The variations in water sorption properties of various heat treated specimens seem to result from the difference in the degree of loose packing in the amorphous regions. From the effect of water vapor on NMR narrow line intensity, it has been found that there are two characteristic sorption types of water vapor in nylon 6, that is, water molecule is comparatively immobile at the lower water content, and considerably mobile at water contents above 4 wt.-%. Furthermore, it may be supposed that there is in addition another sorption state of water vapor below 2 wt.-% that corresponds to the monolayer capacity of water vapor in the polymer.

### 1. Introduction

The sorption of water vapor by polyamides has been studied by several investigators.<sup>1-5</sup> While the effects of water on the dynamic mechanical, dielectric, and nuclear magnetic resonance (NMR) properties of polyamides<sup>6-12</sup> has been attributed to the disruption of interchain bonding in the amorphous regions, the mechanism of water sorption in polyamides is not incompletely understood.

In order to obtain further information on the interaction, we consider the water vapor sorption isotherms, diffusion of water vapor in the polymer, and NMR properties.

### 2. Experimental

The specimens used were polycapraamide (nylon 6) in the form of a uniaxially oriented film (300% elongation) with a film thickness of 40  $\mu$ .

A dry-heat-treated specimen was obtained by heating the oriented film at 150°C. for 3 hr. under vacuum, and an aqueous-heat-treated specimen was obtained by heating the dry-heat-treated specimen in boiling distilled water for 1.5 hr.

The water vapor sorption equilibria and kinetics were determined by weighing with a sensitive quartz spring (36.7  $\mu$ g./div.) in an evacuated glass chamber and measuring the spring's elongation with a cathetometer.

For sorption measurement, water vapor was admitted into the chamber at the desired pressure, controlled by saturated salt solution, and the temperature of the chamber was maintained to within  $\pm 0.2^\circ\text{C}$ .

The density of the specimen was determined by the flotation method, using  $\text{CCl}_4$  and  $\text{C}_6\text{H}_5\text{CH}_3$ .

Proton magnetic resonance absorption measurements were made at 40 Mcycles/sec. with a Japan Electron Optics J.N.M.S. broadline spectrometer of a bridge arrangement and a 12 in. J.N.M.S. electromagnet for high resolution use. The specimen was placed in a thin-walled glass tube fixed to a sample coil in a center of the magnet. The sample tube was evacuated and water vapor admitted into this tube. The dry specimen was maintained in vacuum at  $25^\circ\text{C}$ . for 5 days and the water-containing specimen was in equilibrium with various partial pressures of water vapor for 3 days; NMR spectra for these samples were determined with constant weak radiofrequency field at constant modulation amplitude about 1 gauss.

### 3. Results

The sorption isotherms of water vapor for nylon 6 treated under various conditions are shown in Figure 1.

Sorption isotherms of polymers have usually been treated by the Bru-

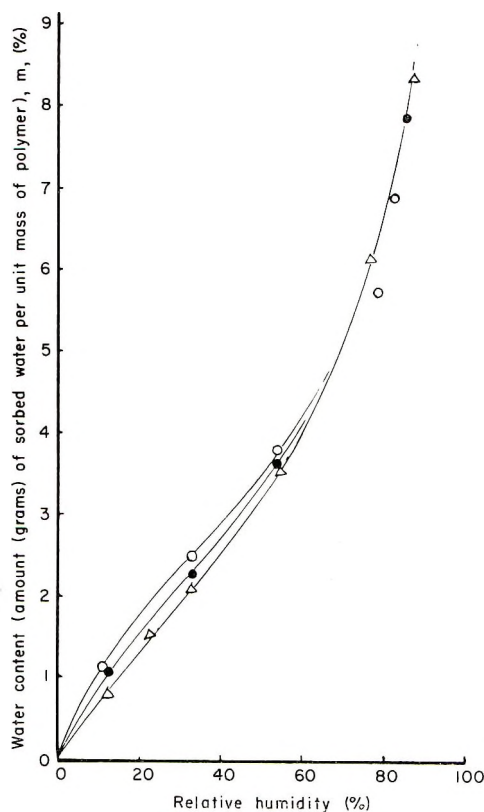


Fig. 1. Sorption isotherms of water vapor by nylon 6 at  $25^\circ\text{C}$ .: (O) untreated; ( $\Delta$ ) dry-heat-treated; ( $\bullet$ ) aqueous-heat-treated.

nauer-Emmett-Teller (BET) equation.<sup>13</sup> From this equation, the monolayer capacity  $m_0$  and the constant  $C$  related to the heat of sorption were determined.

The graphs of the BET equation yield rather good straight lines in the region of 10–60% R.H.<sup>1,4,12</sup>

From these isotherms,  $m_0$  and  $C$  are 1.98% and 5, respectively, for the untreated specimen, 1.86% and 7 for the dry-heat-treated specimen, and 1.77% and 8 for the aqueous-heat-treated specimen.

The densities for the specimens used are shown in Table I. From the density scale, the per cent crystallinity is calculated by well known methods,<sup>14,15</sup> the crystalline and amorphous density being taken as 1.212 and 1.115, respectively.<sup>16</sup>

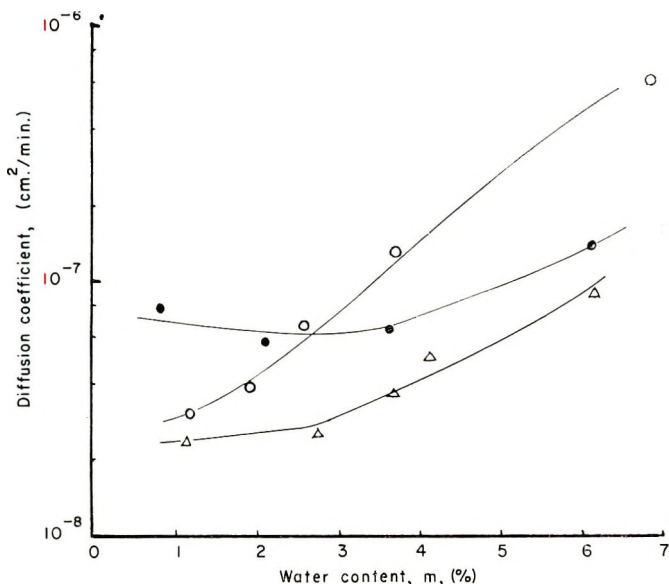


Fig. 2. Variation of diffusion coefficient with water content in nylon 6 at 25°C.: (O) untreated; ( $\Delta$ ) dry-heat-treated; ( $\bullet$ ) aqueous-heat-treated.

According to the Clausius-Clapeyron equation, the differential heat of sorption is about 11 kcal./mole for nylon 6 with 0.5 wt.-% water.

Even when the diffusion coefficient  $D$  is dependent on the concentration of the  $\text{H}_2\text{O}$  penetrant in the film, it has been obtained from a slope in the initial linear portion of a plot of  $Q/Q_e$  versus  $\sqrt{t}/L$  for the sorption or desorption,<sup>17</sup> where  $Q$  is the weight of  $\text{H}_2\text{O}$  gained or lost by sorption or desorption by time  $t$ ,  $Q_e$  is that weight of  $\text{H}_2\text{O}$  when equilibrium is attained, and  $L$  is the film thickness.

In our case,  $D$  was only calculated from the initial slope for sorption.

Figure 2 shows  $D$  for water in the oriented nylon 6 of Figure 1 with the water content at 25°C. In Figure 2, the concentration of water is the

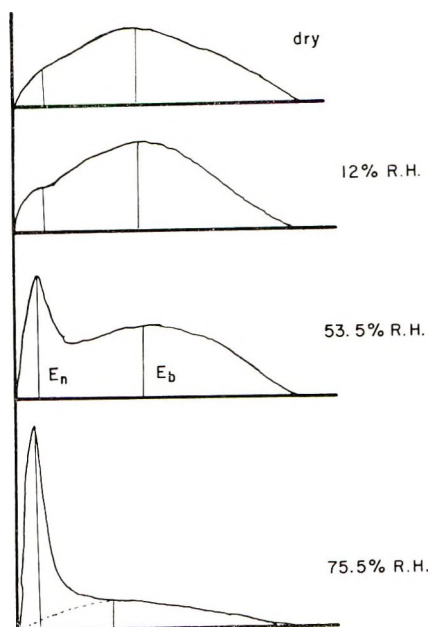


Fig. 3. Nuclear magnetic resonance spectra of nylon 6 at 25°C. at various relative humidities.

mean value of initial and equilibrium water content of the specimen for each range in progressing sorption process.

Figure 3 illustrates the NMR line-shapes for dry and water-containing nylon 6 at 25°C. In the present case, let us consider the variation of peak intensity with water content, since the NMR line-width measurements of the narrow component are biased by modulation broadening.

The ratio,  $R$ , of the maximum meter reading of the narrow line,  $E_n$ , to that of the broad line,  $E_b$ , as shown in Figure 3, is expressed as follows:

$$R = \frac{E_n}{E_b} = \frac{\zeta_n (\partial \chi''_n / \partial \nu)}{\zeta_b (\partial \chi''_b / \partial \nu)} = \frac{\zeta_n N_{0n} [\partial g_n(\nu) / \partial \nu]_{\max}}{\zeta_b N_{0b} [\partial g_b(\nu) / \partial \nu]_{\max}} \quad (1)$$

where the subscripts  $n$  and  $b$  denote the narrow components and the broad ones, respectively,  $\zeta$  is a filling factor,  $\chi = \chi' - i\chi''$  is the nuclear magnetic susceptibility,  $\nu$  is the frequency,  $g(\nu)$  is the shape function, and  $N_0$  is the number of magnetic nuclei in the specimen under observation per cubic centimeter of the substance.<sup>18,19</sup>

If water vapor is not sorbed in the crystalline portion of polymer, eq. (1) becomes:

$$R = \alpha \zeta_n N_{0n} \left[ \frac{\partial}{\partial \nu} g_n(\nu) \right]_{\max} \quad (2)$$

where  $\alpha$  is a constant.

If the spin-spin relaxation time  $T_2$  is a constant, it is expected that the intensity ratio  $R$  increases linearly with the water content  $m$  of polymer.

The plot of  $R$  against water content is shown in Figure 4. This graph indicates a marked variation in the region above 3–4%. This increase of the peak intensity ratio seems to result from the change of  $g(\nu)$  which is a function of  $T_2$ .

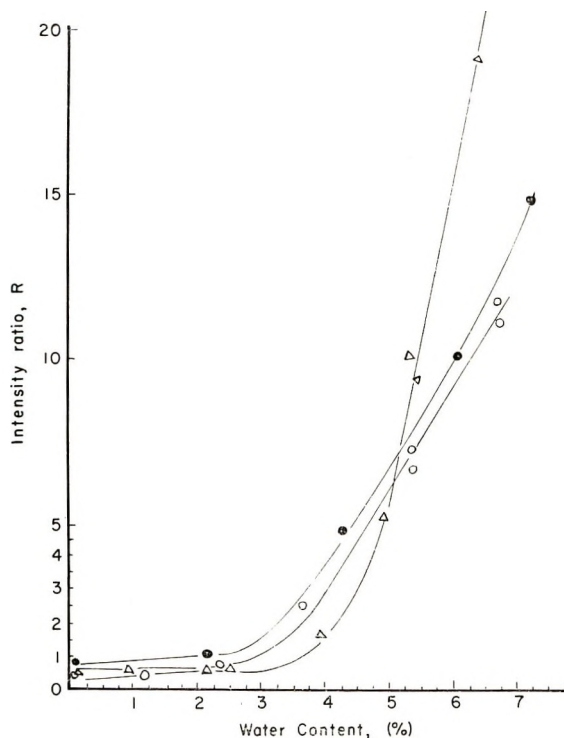


Fig. 4. Variation of intensity ratio  $R$  with water content for nylon 6 at 25°C.: (O) untreated; ( $\Delta$ ) dry-heat-treated; ( $\bullet$ ) aqueous-heat-treated.

From the line-width measurement, it has been observed that at low water content the NMR width for sorbed water is broad, and this width decreases with increasing water content.<sup>20</sup> The patterns for these widths are not clear, however, because of the uncertainty of splitting to narrow and broad lines.

#### 4. Discussion

The water sorption isotherm for the untreated nylon 6 of Figure 1 is in agreement with the results obtained by several authors.<sup>3,4</sup>

In general, it has been considered that water vapor is sorbed in the amorphous regions of a polymer, but the sorption properties for nylon 6 treated with various conditions are somewhat different (Table I and Fig. 1).



TABLE I  
Crystallinity of Nylon 6 with Various Heat Treatments

Specimen	Film thickness, $\mu$	Treatment	Density, g./cm. <sup>3</sup>	Crystallinity, %
Oriented	40	Untreated	1.141	30
Oriented	40	Dry-heat-treated	1.146	36
Oriented	40	Aqueous-heat-treated	1.151	39

These properties are also found in the diffusion characteristics of water in nylon 6. Figure 2 shows that  $D$  for water is dependent on concentration of water in the film and increases rapidly in the region above 4%.

It is of interest that water content and diffusion coefficient for the aqueous-heat-treated nylon 6 are larger than those of the dry-heat-treated nylon 6, contrary to the results for per cent crystallinity. This seems to result from the difference in the degree of "loose packing" in the amorphous regions.

$R$ , as shown in Figure 4, has an inflection in the slope at 3-4 wt.-%. This result indicates that there are two characteristic sorption types of water in nylon 6, i.e., the nuclei are comparatively immobile at the lower water content and considerably mobile at water contents above 4%.

It has been considered that the water in the region below 4% is principally sorbed as a consequence of the breaking up of an interaction of amide groups between chains in the amorphous regions of the polymer.

From the effects of sorbed water on the density<sup>16,5</sup> and the Young's modulus<sup>21</sup> of polyamides, however, it may be supposed that there is further another sorption state of water vapor below 2% that corresponds to the monolayer capacity of water vapor in nylon 6.

In this region, free amide groups either weakly or not bonded to neighboring chains, may be included in the sorption mechanism.

This also was suggested from the extension of nylon 6 as a function of the extent and nature of sorbed water that was already reported in our previous work.<sup>12</sup>

We would like to thank Mr. Oka for his measurements of the sorption isotherms.

## References

1. Bull, H. B., *J. Am. Chem. Soc.*, **66**, 1499 (1944).
2. Rouse, P. E., Jr., *J. Am. Chem. Soc.*, **69**, 1069 (1947).
3. Furuya, H., *Kobunshi Kagaku*, **15**, 389 (1958).
4. Koshimo, A., T. Tagawa, and M. Tsuruta, *Kobunshi Kagaku*, **17**, 417 (1960).
5. Starkweather, H. W., Jr., *J. Appl. Polymer Sci.*, **2**, 129 (1959).
6. Woodward, A. E., J. M. Crissman, and J. A. Sauer, *J. Polymer Sci.*, **44**, 23 (1960).
7. Curtis, A. J., *J. Res. Natl. Bur. Std.*, **65A**, 185 (1961).
8. Boyd, R. H., *J. Chem. Phys.*, **30**, 1276 (1959).
9. Woodward, A. E., R. E. Glick, J. A. Sauer, and R. Gupta, *J. Polymer Sci.*, **45**, 367 (1960).

10. Illers, K. H., and R. Kosfeld, *Makromol. Chem.*, **42**, 44 (1960).
11. Shaw, D. J., and B. A. Dunell, *Can. J. Chem.*, **39**, 1154 (1961).
12. Kawasaki, K., Y. Sekita, and K. Kanou, *J. Colloid Sci.*, **17**, 865 (1962).
13. Brunauer, S., P. H. Emmett, and E. Teller, *J. Am. Chem. Soc.*, **60**, 309 (1938).
14. Hunter, E. A., and W. G. Oakes, *Trans. Faraday Soc.*, **41**, 49 (1945).
15. Price, F. P., *J. Chem. Phys.*, **19**, 973 (1951).
16. Kinoshita, Y., *Sci. Repts. Toyo Rayon Co.*, **9**, 1 (1954).
17. Long, F. A., and L. G. Thompson, *J. Polymer Sci.*, **15**, 413 (1955).
18. Bloembergen, N., E. M. Purcell, and R. V. Pound, *Phys. Rev.*, **73**, 679 (1948).
19. Andrew, E. R., *Nuclear Magnetic Resonance*, Cambridge Univ. Press, London and New York, 1955, p. 108.
20. Sekita, Y., and K. Kawasaki, unpublished data.
21. Kishimoto, A., and H. Fujita, *Kolloid Z.*, **150**, 24 (1957).

### Résumé

On a étudié l'interaction entre le nylon 6 et l'eau à partir des propriétés des isothermes de sorption de la vapeur d'eau, de la diffusion de vapeur d'eau dans le polymère et de la résonance magnétique nucléaire (NMR). Les variations dans les propriétés de sorption d'eau de différents échantillons traités à la chaleur résultent de différence dans le degré de tassement libre dans les régions amorphes. A partir de l'effet de la vapeur d'eau sur l'intensité de la bande étroite du spectre NMR, on trouve qu'il y a deux types caractéristiques de sorption de vapeur d'eau dans le nylon 6; cela signifie que la molécule d'eau est comparativement immobile à de faibles teneurs en eau, et considérablement mobile à une teneur en eau au-dessus de 4% en poids. De plus, on peut supposer qu'il y a un autre état de sorption de vapeur d'eau en-dessous de 2% en poids, qui correspond à la capacité de la couche monomoléculaire en vapeur d'eau du polymère.

### Zusammenfassung

Die Wechselwirkung zwischen Nylon 6 und Wasser wurde an Wasserdampfsorptionsisothermen, an der Diffusion von Wasserdampf im Polymeren sowie durch magnetische Kernresonanzmessungen (NMR) untersucht. Die Unterschiede der Wassersorptionseigenschaften verschiedener hitzebehandelter Proben gehen anscheinend auf Unterschiede im Ausmass der lockeren Packung in den amorphen Bereichen zurück. Wie der Einfluss von Wasserdampf auf die Intensität der schmalen NMR-Linien zeigt, gibt es zwei charakteristische Type der Wasserdampfsorption in Nylon 6: Während im Falle niedrigen Wassergehaltes das Wassermolekül relativ unbeweglich ist, zeigt es bei Wassergehalten von über 4 Gew.% eine beträchtliche Beweglichkeit. Ferner kann angenommen werden, dass bei einem Wassergehalt von weniger als 2 Gew.% ein weiterer Sorptionszustand des Wasserdampfes entsprechend der Kapazität einer monomolekularen Schicht von Wasserdampf im Polymeren vorliegt.

Received May 13, 1963

## Copolymerization of Tetrafluoroethylene with Isobutene Induced by Ionizing Radiation

YONEHO TABATA, KENKICHI ISHIGURE, KEICHI OSHIMA, and  
HIROSHI SOBUE, *Department of Nuclear Engineering and Industrial  
Chemistry, Faculty of Engineering, University of Tokyo, Tokyo, Japan*

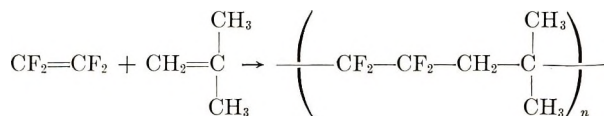
### Synopsis

Radiation-induced copolymerization of tetrafluoroethylene with isobutene was carried out in the liquid state of the monomers at low temperature. The composition curve of the tetrafluoroethylene-isobutene copolymer was obtained. Infrared spectra, x-ray diffraction, and melting points of the copolymers obtained were also measured. It was concluded from these experimental results that an alternating crystalline isobutene tetrafluoroethylene copolymer can be obtained by a radical process induced by ionizing radiation. This seems to be the first case in which an alternating crystalline copolymer was obtained by a radical mechanism over an extremely wide range of molar concentration of the components in the monomer mixture.

### INTRODUCTION

Radiation-induced copolymerizations of tetrafluoroethylene with ethylene and propylene were reported in previous papers.<sup>1,2</sup> In this paper, the copolymerization of tetrafluoroethylene with isobutene by ionizing radiation is reported.

It was found from this investigation that the copolymerization could take place in a wide range of monomer ratios to yield crystalline copolymers with an alternating structure:



### EXPERIMENTAL

The tetrafluoroethylene used was a Nitto Kagaku product. Purified commercial product of isobutene was used as the other monomer. These monomers were condensed into an ampule at liquid nitrogen temperature. The ampule containing solid monomers was evacuated to  $10^{-3}$ – $10^{-4}$  mm. Hg. Irradiation was carried out by  $\gamma$ -rays from a  $\text{Co}^{60}$  source at low temperature.

Melting points, infrared spectra, and x-ray diffraction of the copolymers were determined.

## RESULTS AND DISCUSSION

## 1. Copolymerization Rate

The relation between per cent conversion and irradiation time at various dose rates is shown in Figure 1. The copolymerization is preceded by an induction period. The conversion increases linearly with the irradiation time. The rate of copolymerization is proportional to the square root of the dose rate. This suggests, that termination may be a bimolecular reaction. These results also indicate that the copolymerization proceeds by a radical mechanism.

The relation between the conversion and the mole fraction of tetrafluoroethylene in the monomer mixture is shown in Figure 2.

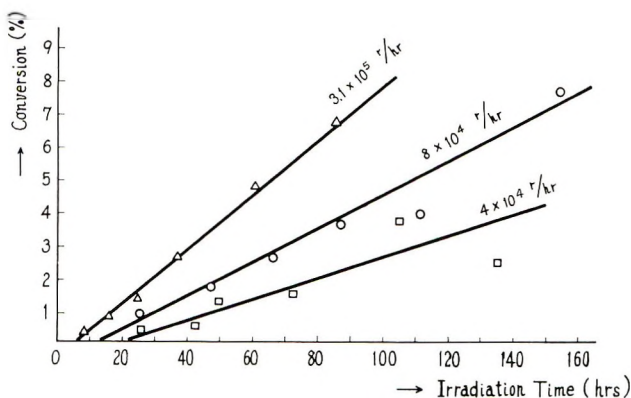


Fig. 1. The relation between the copolymerization yield (weight per cent for total monomer mixture) and irradiation time at various dose rates at  $-78^{\circ}\text{C}$ . Tetrafluoroethylene content of the monomer mixture was 71 mole-%.

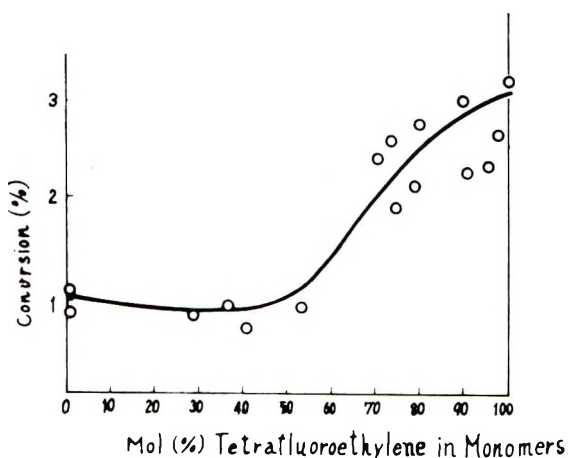


Fig. 2. The relation between the copolymerization yield and the molar concentration of tetrafluoroethylene in monomer mixture. Irradiation dose was  $9.3 \times 10^6$  r and the dose rate  $1.9 \times 10^6$  r/hr.

It is apparent from the figure that the rate of copolymerization is constant below an equimolar concentration of tetrafluoroethylene and increases rapidly with the molar concentration of tetrafluoroethylene in the monomer mixture. The acceleration phenomenon appears to be due to a gel effect.

## 2. Effects of Radical Inhibitors on the Copolymerization

It is well known that the polymerization of isobutene proceeds by a cationic and not by a radical mechanism in the liquid state of the monomer at low temperature.<sup>3</sup> On the contrary, as reported in previous papers,<sup>4</sup> the polymerization of tetrafluoroethylene proceeds by a radical mechanism in the liquid state of monomer at low temperature.

In this experiment, it was observed that the copolymerization of tetrafluoroethylene with isobutene was inhibited by several radical scavengers.

*p*-Benzoquinone and pyrogallol are only slightly soluble in the monomer mixture but *p*-benzoquinone is soluble in an acetone solution of the monomer mixture at low temperature.

The effects of the radical scavengers on the copolymerization examined both in the homogeneous and heterogeneous systems at  $-78^{\circ}\text{C}$ . are shown in Table I.

TABLE I  
Effects of Inhibitors on the Copolymerization<sup>a</sup>

Molar concentration of tetrafluoroethylene in the monomer mixture, %	Compounds added	Amounts of the compounds added to the monomer mixture, %	Irradiation time, hr.	Relative yield
77.2	Acetone	40	182	0
	<i>p</i> -Benzoquinone	3.4		
90.6	<i>p</i> -Benzoquinone	2.0	120	0.08
91.6	Pyrogallol	0.88	120	0.44

<sup>a</sup> Dose rates:  $2 \times 10^5$  r/hr.

It is apparent from these results that *p*-benzoquinone inhibits completely the copolymerization in the homogeneous system, and that both pyrogallol and *p*-benzoquinone inhibit markedly the copolymerization in the heterogeneous system, in spite of the fact that the solubility of the inhibitors in the monomer mixture is extremely small. It is obvious from both these results and the dependence of the copolymerization rate on the dose rate as described above that the copolymerization proceeds by a radical mechanism.



### 3. Monomer Reactivity Ratio

No isobutene homopolymer could be extracted by any solvent extraction technique; it was thus concluded that the homopolymerization did not take place in a wide range of monomer ratios.

The composition curve of tetrafluoroethylene–isobutene copolymer is shown in Figure 3.

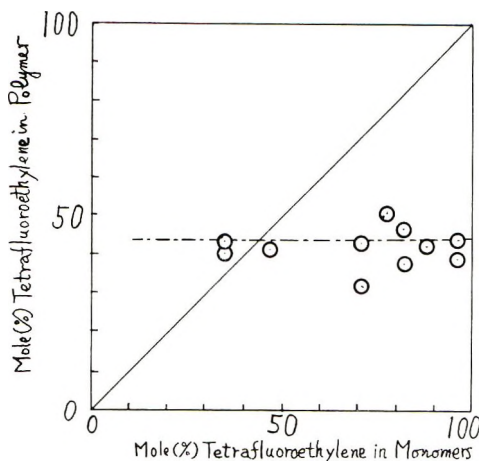
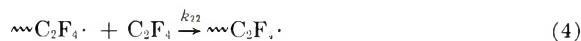
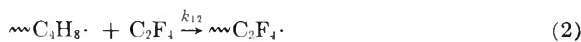


Fig. 3. Composition curve of tetrafluoroethylene–isobutene copolymers at  $-78^{\circ}\text{C}$ .

Fluorine content in the copolymers was determined by elementary analysis. It is evident from the results that the composition of the copolymer is always constant over the entire monomer composition range in the monomer mixtures, within experimental errors.

The copolymerization processes are described by eqs. (1)–(5):



where

$$r_1 = k_{11}/k_{12} \quad (5)$$

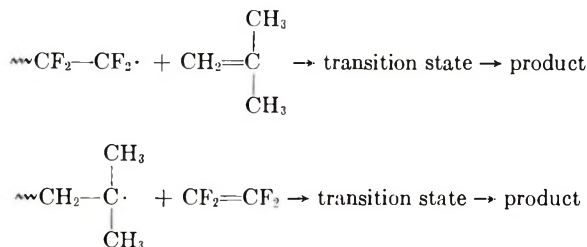
$$r_2 = k_{22}/k_{21}$$

and where  $k$  is the rate constant and  $r$  represents the monomer reactivity ratio.

From the composition curve of tetrafluoroethylene–isobutene copolymer, the reactivity ratios can be determined to be  $r_1 \cong 0$  and  $r_2 \cong 0$ . It is evident from the results that the rate constant of the propagation,  $k_{12}$ ,

is much greater than  $k_{11}$ , and also  $k_{21}$  is greater than  $k_{22}$ , namely  $k_{12} \gg k_{11}$ ,  $k_{21} \gg k_{22}$ .

This indicates that the copolymerization could take place in an "alternating" fashion. Let us consider the transition states for the reactions:<sup>5</sup>



It is well known that the fluorine atom is a strong electron-withdrawing substituent, while, methyl group is an electron-donating substituent. Therefore, it will be easily understood in this copolymerization system that strong interactions exist between the positively polarized tetrafluoroethylene radical and the negatively polarized isobutene double bond as well as between the negatively polarized isobutene radical and the positively polarized tetrafluoroethylene double bond.

The transition states for the reactions (2) and (3) are more stable than the transition states for the reactions (1) and (4).

The authors believe that the effect of polarity would play the most important role for the complete alternating propagation in this copolymerization system.

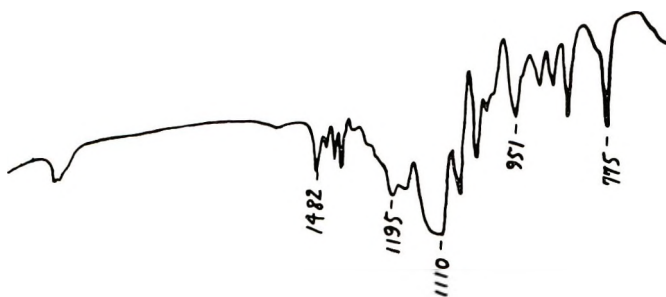


Fig. 4. Infrared spectrum of one of the copolymers in wave number  $\text{cm}^{-1}$  (NaCl prism).

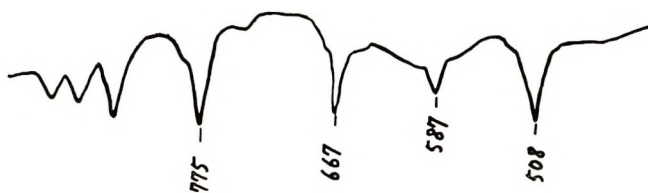


Fig. 5. Infrared spectrum of one of the copolymers in wave number  $\text{cm}^{-1}$  (KBr prism).

#### 4. Infrared Spectra of the Copolymers

The infrared spectra of one of the copolymers in the regions of NaCl and KBr prisms are shown in Figures 4 and 5, respectively.

It is evident from the figures that the spectra of the copolymer are quite different from those of the two homopolymers, and are not to be obtained by superposition of the spectra of the two homopolymers. It was reported in previous papers<sup>1,2</sup> that in the case of copolymerizations of the ethylene-tetrafluoroethylene and propylene-tetrafluoroethylene systems, almost

TABLE II  
Tentative Assignment of Isobutene-Tetrafluoroethylene Copolymer

Wavelength, cm. <sup>-1</sup>	Intensity	Assignment
2973	m	$\nu_a(\text{CH}_3)$
2945	m	$\nu_u(\text{CH}_2)$
2890	vw	$\nu_s(\text{CH}_3)$
1482	m	$\delta(\text{CH}_2)$
1460	vw	$\delta_u(\text{CH}_3)$
1440	w	$\delta_u(\text{CH}_3)$
1411	m	
1384	m	$\delta_s(\text{CH}_3)$
1329	w	$\delta(\text{CH}_2)$
1274	w (shoulder)	$\omega(\text{CH}_2)$ or $\nu(\text{CH}_2)$
1232	w (shoulder)	$\omega(\text{CH}_2)$
1195	s	$\nu_a(\text{CF}_2)$
1166	s	$\nu_s(\text{CF}_2)$
1110	vs	$\nu(\text{CF}_2)$
1062	s	$\delta(\text{CH}_2)$
1028	m	
1011	m	
993	w	
951	m	$\delta(\text{CH}_3)$
899	m	
875	m	
849	m	
786	vw (shoulder)	
775	s	$\gamma(\text{CH}_2)$
667	s	$\delta(\text{CF}_2)$
587	s	$(\text{CF}_2)$
570	w (shoulder)	$\delta(\text{CF}_2)$
522	w (shoulder)	$\gamma(\text{CF}_2)$
508	s	$\delta(\text{CF}_2)$

all the absorption bands of the copolymers obtained increases or decrease continuously with the molar concentration of one component in the monomer mixture. However, in the case of the isobutene-tetrafluoroethylene system, the absorption bands of the copolymer obtained remained always constant over an extremely wide range of molar concentration of the components in the monomer mixture.

These experimental facts suggest that the alternative possibilities of the production of a mixture of homopolymers or a block copolymer can be definitely excluded and that the copolymer has always a highly definite regular structure, independent of the concentration of the components in the monomer mixture.

A tentative assignment of the absorption bands of the copolymer is shown in Table II.

### 5. X-Ray Diffraction of the Copolymer

The x-ray diffraction curve of one of the copolymers is given in Figure 6.

It is obvious from the figure that the copolymer is highly crystalline and that the diffraction curve is quite different from those of polytetrafluoroethylene and polyisobutene (only crystallizable under stretching at room temperature). It was also reported in a previous paper<sup>1</sup> that the copolymer of ethylene-tetrafluoroethylene was crystalline, and that the crystalline structure varied continuously with the molar concentration of one component in the monomer mixture. In the case of the copolymer of isobutene-tetrafluoroethylene, the crystalline structure of the copolymer remained constant in an extremely wide range of molar concentration, as well as the infrared spectra of the copolymer.

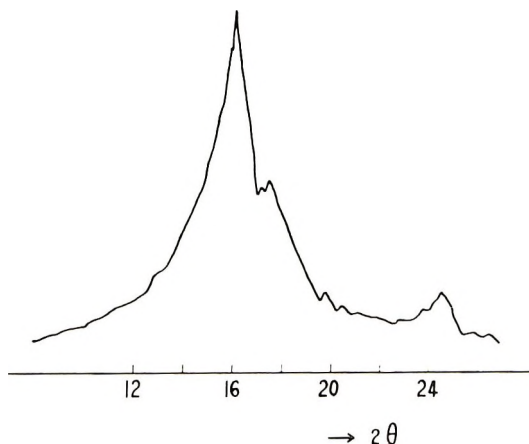


Fig. 6. X-ray diffraction intensity curves of one of the copolymers.

These facts indicate that the copolymer has a definite alternating crystalline structure.

### 6. Melting Point of the Copolymer

The melting point of the copolymer which was obtained by polymerization at  $-78^{\circ}\text{C}$ . was about  $200^{\circ}\text{C}$ ., and the copolymer decomposed at a temperature very near the melting point, while the melting point of the

copolymer polymerized at  $-43^{\circ}\text{C}$ . was appreciably higher ( $210\text{--}220^{\circ}\text{C}$ .) The latter copolymer was decomposed by heating in a temperature region of  $300\text{--}305^{\circ}\text{C}$ . The decomposition temperature (probably depending on the degree of polymerization) is much higher than that of the former copolymer.

The determination of the crystalline structure and the physical properties of the copolymer are now progressing in our laboratory by measurements of x-ray diffraction, infrared spectra, and nuclear magnetic resonance.

### SUMMARY

It was concluded from these experimental results that an alternating crystalline isobutene-tetrafluoroethylene copolymer can be obtained by a radical process induced by ionizing radiation. This seems to be the first case in which an alternating crystalline copolymer was obtained by a radical mechanism in an extremely wide range of molar concentration of the components in monomer mixture.

### References

1. Tabata, Y., H. Shibano, and H. Sobue, *Kogyo Kagaku Zasshi*, **65**, 737 (1962); Y. Tabata, H. Shibano, and H. Sobue, *J. Polymer Sci.*, **A2**, 1977 (1964).
2. Tabata, Y., K. Ishigure, and H. Sobue, *Kogyo Kagaku Zasshi*, **65**, 1626 (1962); *J. Polymer Sci.*, **A2**, 2235 (1964).
3. Davison, W. H. T., S. H. Pinner, and R. Worrall, *Chem. Ind. (London)*, **1957**, 1274, R. L. Rogers, *Nucleonics*, **15**, No. 11, 180 (1957); R. Worrall and A. Charlesby, *Intern. J. Appl. Radiation Isotopes*, **4**, 84 (1958); R. Worrall and S. H. Pinner, *J. Polymer Sci.*, **34**, 229 (1959); W. H. T. Davison, S. H. Pinner, and R. Worrall, *Proc. Roy. Soc. (London)*, **A252**, 187 (1959); A. S. Hoffman, *J. Polymer Sci.*, **34**, 241 (1959).
4. Tabata, Y., H. Shibano, and H. Sobue, paper presented at 4th Japanese Conference on Radioisotopes, Kyoto, Oct. 1961.
5. Alfrey, T., Jr., J. J. Bohrer, and H. Mark, Eds., *Copolymerization*, Interscience, New York, 1952.

### Résumé

On a effectué la copolymérisation induite par radiation du tétrafluoroéthylène avec l'isobutène, les monomères étant à l'état liquide et à basse température. On a obtenu la courbe de composition du copolymère du tétrafluoroéthylène-isobutène à partir des résultats expérimentaux. D'autre part, on a mesuré les spectres infra-rouges, la diffraction aux rayons-X et le point de fusion des copolymères obtenus. On conclut de ces résultats expérimentaux et des discussions qu'un copolymère cristallin alterné di'sobutène et de tétrafluoroéthylène peut être obtenu par un processus radicalaire induit par radiation ionisante. Ceci semble être le premier cas d'un copolymère cristallin alterné obtenu par mécanisme radicalaire dans un domaine extrêmement large de concentration molaire des constituants du mélange des monomères.

### Zusammenfassung

Die Strahlungs-copolymerisation von Tetrafluoräthylen mit Isobuten wurde bei tiefer Temperatur mit den flüssigen Monomeren durchgeführt. Die Zusammensetzungskurve der Tetrafluoräthylen-Isobuten-Copolymeren wurde experimentell ermittelt. Ausserdem wurden die IR-Spektren und Röntgenbeugungsdiagramme der Copolymeren auf-



genommen und der Schmelzpunkt bestimmt. Wie aus den experimentellen Befunden hervorgeht, kann in einem durch ionisierende Strahlung gestarteten radikalischen Prozess ein alternierendes kristallines Isobuten-Tetrafluoräthylen-Copolymeres gebildet werden. Dies ist anscheinend der erste Fall, in welchem ein alternierendes kristallines Copolymeres über einen extrem weiten Bereich der molaren Konzentration der Komponenten im Monomergemisch nach einem radikalischen Mechanismus gebildet wurde.

Received May 13, 1963

## $\gamma$ -Radiation-Induced Changes in the Structure of Polyethylenes

W. C. SEARS, *Department of Physics and Astronomy, University of Georgia, Athens, Georgia*

### Synopsis

The concentrations of *trans*-vinylene groups in Marlex 50 and DYNH polyethylenes were determined from infrared spectra before and after irradiation of polyethylene films with gamma rays. Values of  $G$  for *trans*-vinylene growth were found to be 2.2 and 1.7 for Marlex 50 and DYNH polyethylenes, respectively. *trans*-Vinylene decay constants and concentrations at infinite dose were evaluated. The growth and decay of vinyl unsaturation and growth of vinylidene unsaturation in Marlex 50 are discussed. Assignment was made of polyethylene bands at 889 and 894  $\text{cm}^{-1}$  to vinylidene unsaturation and to ethyl groups in saturated paraffins, respectively, on the basis of different means of saturating the double bond. The frequencies of new bands produced in Marlex 50 and DYNH by irradiation were correlated with those of substituted cyclopentanes and cyclohexanes. It was concluded that a complex mixture of these cyclic compounds was formed in Marlex 50 and DYNH. There appeared to be no correlation between the frequencies of these irradiation-induced bands and frequencies known to be characteristic of conjugated double bonds.

### INTRODUCTION

The kinetics of unsaturation growth and decay in polyethylene irradiated with  $\gamma$ -rays have been studied by Dole et al.<sup>1</sup> They postulated a zero-order growth of *trans*-vinylene groups followed by first-order elimination of these groups. Dole et al.<sup>1</sup> and Lawton et al.<sup>2</sup> reported different  $G$  values for *trans*-vinylene production in linear and branched polyethylene. Lawton et al.<sup>2</sup> incorrectly assumed that the rate of *trans*-vinylene production was linear up to 50 MR(megaröntgen). Dole et al.<sup>1</sup> concluded that as the *trans*-vinylene concentration increases, the initial first-order elimination of vinyl and vinylidene groups becomes less than first-order. Formation of ring link compounds in irradiated polyethylene were reported by Dole et al.<sup>1</sup> Slovokhotova and Karpov<sup>3</sup> attributed a very weak 938  $\text{cm}^{-1}$  band in irradiated polyethylene to crosslinking.

One might expect growth of conjugated *trans*-vinylene groups during irradiation of polyethylene, especially at high doses. The objectives in the present work have been to: (a) resolve the differences in the rates of *trans*-vinylene formation reported by Dole et al.<sup>1</sup> and Miller et al.<sup>4</sup> for Marlex 50 and DYNH polyethylenes; (b) determine the evidence for and against the formation of conjugated double bonds and ring links in irradiated polyethylenes.

## EXPERIMENTAL

### A. Spectroscopic and Irradiation Procedures

Infrared absorption spectra of pressed polyethylene film, roughly 0.188 mm. thick, were measured with a Beckman IR-4 infrared spectrophotometer before and after irradiation. Each film specimen, 4.03 cm. long and 1.43 cm. wide, was weighed and cemented along two sides to a rectangular aluminum wire frame, which was mounted inside a cylindrical absorption cell equipped with KBr windows for spectroscopic measurements. After initial measurement of the infrared spectrum, each mounted specimen was placed inside a Pyrex test tube and the open end of the tube was joined to a constricted tube. Following pumping on the sample at a minimum pressure of less than  $1 \mu$  of mercury for two or three days, the evacuated sample tube was sealed off at the constriction. Evacuation of the sample tube prevented oxidation during irradiation at the Oak Ridge National Laboratory with  $\gamma$ -rays from a  $\text{Co}^{60}$  source. To prevent oxidation after irradiation, the sample tubes were opened in an atmosphere of helium in an evacuable housing fitted with a Plexiglas top, arm ports, and Neoprene gloves. The irradiated specimen was transferred in this housing to the helium-filled absorption cell for another measurement of its infrared spectrum, with the light passing through the same portion of the specimen as in the original spectrum.

Polyethylene films of uniform thickness were found to give undesirable interference bands between 1 and  $16 \mu$ . Interference bands tend to distort true polymer bands far more at long wavelengths, because the intensity of interference bands increases with increasing wavelength. Useful spectroscopic film specimens, which were prepared by pressing the polymer between unpolished platens, exhibited no interference bands because of their rough surfaces.

### B. Polymers

Marlex 50 polyethylene, which was obtained from the Phillips Petroleum Company, initially had a very low *trans*-vinylene concentration and a relatively high concentration of vinyl groups. Highly branched DYNH polyethylene from the Union Carbide Plastics Company had vinylidene and *trans*-vinylene unsaturation but little vinyl unsaturation initially.

### C. Dosimetry

The dose rates for the Marlex 50 and DYNH irradiations were  $1.3 \times 10^6$  and  $5.4 \times 10^6$  roentgen/hr., respectively.  $\text{Ce}(\text{SO}_4)_2$  in  $0.4M$   $\text{H}_2\text{SO}_4$  solution was used as a relative dosimeter, and its radiation yield was established by irradiation in a  $\text{Co}^{60}$  source which had been carefully measured with  $\text{FeSO}_4$ . The radiation yield for the  $\text{FeSO}_4$  was accepted as  $G(\text{Fe}^{+++}) = 15.6 \pm 0.3$  ions/100 e.v.<sup>5</sup>

Correction in dose was made for the difference in gamma ray absorption

coefficient in air and polyethylene. Since absorption of gamma rays is due mainly to Compton scattering, the doses in air were corrected by multiplying by the ratio of the electron density per gram of polymer,  $3.44 \times 10^{23}$  electrons/g., to the electron density per gram of air,  $3.01 \times 10^{23}$  electrons/g. The sample tubes were immersed in water at roughly  $20^\circ\text{C}$ . during irradiation. The uncertainty in dose of  $\pm 10\%$  is due largely to non-uniformity of flux over the whole film.

#### D. Analytical Method for Determining Unsaturation

The concentration of *trans*-vinylene groups in polyethylene films was determined on the basis of the measured absorptivity at  $966\text{ cm.}^{-1}$  of a polybutadiene polymer from Phillips Petroleum Company having 90% *trans*-vinylene unsaturation. The absorptivity,  $\alpha$ , in liters per mole per centimeter was determined on the basis of the equation

$$\alpha = A_s/ct = A_s M_s / 1000 P_s Q_s \quad (1)$$

where  $A_s = \log (T_0/T)$  is the absorbance of the polybutadiene standard at  $966\text{ cm.}^{-1}$ ,  $c$  is the concentration of *trans*-vinylene groups in moles per liter,  $t$  is the film thickness in centimeters,  $M_s$  is the gram-molecular weight of polybutadiene monomer,  $P_s$  is the number of *trans*-vinylene groups per monomer unit of polybutadiene, and  $Q_s$  is the surface density in grams per square centimeter, which was determined by weighing a portion of film of known area. Since surface density is polymer density times thickness, values for the polymer density and film thickness were not required in determining absorptivity from eq. (1). Using base line technique<sup>6</sup> for measuring absorbance, the absorptivity of the *trans*-vinylene group was found to be 111 l./mole-cm. on the spectrophotometer used in this work. Binder<sup>7</sup> reported a *trans*-vinylene absorptivity of 109 l./mole-cm. on another IR-4 spectrophotometer. Hampton<sup>8</sup> reported an absorptivity of 139 l./mole-cm. for the *trans*-vinylene group. However, infrared absorptivities generally are not transferrable from one instrument to another<sup>9</sup> without sacrificing accuracy. Therefore, the *trans*-vinylene concentration reported by Dole et al.,<sup>1</sup> using Hampton's absorptivity, and those by Miller et al.,<sup>4</sup> using Anderson and Seyfried's<sup>10</sup> absorptivity of  $K_{0.1} = 35.6$ , may be in error.

The number of *trans*-vinylene groups per ethylene unit,  $P_x$ , can be determined from the equation

$$P_x = (A_x M_x) / (1000 \alpha Q_x) \quad (2)$$

where  $A_x$  is the observed absorbance of polyethylene at  $966\text{ cm.}^{-1}$  and  $M_x$  is the gram-molecular weight of ethylene.

The *trans*-vinylene concentration  $C$ , in moles per gram of polyethylene, is given by the equation

$$C = [P_x / (d - f P_x) m N] \quad (3)$$

where  $d$  is number of atomic mass units (amu) per ethylene group,  $f$  is the number of amu per hydrogen molecule,  $m$  is the mass of one amu, and  $N$  is Avogadro's number.

## RESULTS AND DISCUSSION

### A. *trans*-Vinylene Unsaturation

Infrared spectra of Marlex 50 polyethylene before and after a dose of  $2.5 \times 10^{22}$  e.v./g. are shown in Figure 1. Base line *A*, which was used by Dole et al.,<sup>1</sup> was rejected because it did not compensate for absorption at  $966 \text{ cm.}^{-1}$  by the  $940$  and  $983 \text{ cm.}^{-1}$  bands. Base line *B* may not compensate enough for the  $983 \text{ cm.}^{-1}$  band, whereas base line *C* appears to compensate too much. Base lines *A* and *B* nearly merged together in both spectra of DYNH polyethylene in Figure 2 and also in Marlex 50 after a dose of  $2.7 \times 10^{21}$  e.v./g. Therefore, the *trans*-vinylene concentrations, which were determined in this investigation in Table I, were based on absorbances from Figures 1 and 2 using base line *B*. Table I also gives the *trans*-vinylene concentrations reported by Dole et al.<sup>1</sup> for Marlex 50 and B-3125.

A concentration of  $0.009 \times 10^{-4}$  mole/g. was observed in this work on Marlex 50 specimens prior to irradiation. Initial *trans*-vinylene concentrations were determined by the Phillips Petroleum Company<sup>11,12</sup> to be about  $0.014 \times 10^{-4}$  and  $0.053 \times 10^{-4}$  mole/g. for Marlex 50 sample No. OSS 21,154 used in this investigation and a commercial production sample, respectively. The initial concentration in Marlex 50 was so low that its effect on determining the decay constant, concentration at infinite dose, and initial growth rate was almost negligible.

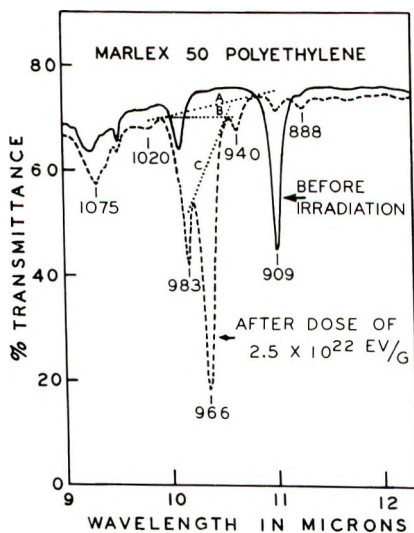


Fig. 1. Infrared spectra of Marlex 50 polyethylene before and after  $\gamma$ -irradiation.



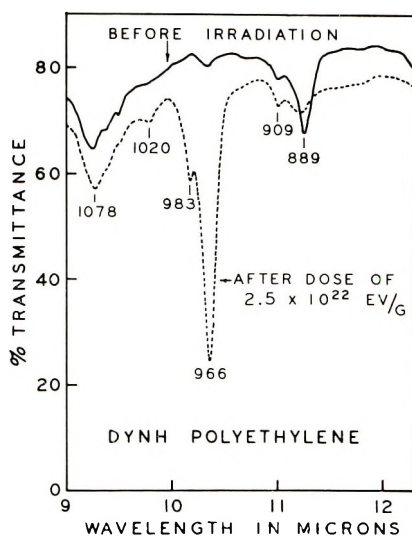


Fig. 2. Infrared spectra of DYNH polyethylene before and after  $\gamma$ -irradiation.

Using base line *C* the apparent *trans*-vinylene concentrations<sup>13</sup> were 6% and 10% lower than the concentrations determined with base line *B* in Marlex 50 after doses of  $2.7 \times 10^{21}$  and  $2.5 \times 10^{22}$  e.v./g., respectively. The apparent concentration using base line *A* instead of *B* would have been the same after  $2.7 \times 10^{21}$  e.v./g. for Marlex 50 and DYNH, the same for DYNH after  $2.5 \times 10^{22}$  e.v./g. and 2.0% higher for Marlex 50 after  $2.5 \times 10^{22}$  e.v./g. Obviously, the difference in concentrations in this work and those reported by Dole et al.<sup>1</sup> were not the result of differing base lines. The uncertainty in dose in the present work was  $\pm 10\%$ , which would correspond to an uncertainty in concentration of roughly  $\pm 8\%$ .

The *trans*-vinylene decay constant, concentration at infinite dose, and the initial growth rate were evaluated by using the equations formulated by Dole et al.,<sup>1</sup> but in a different manner. The decay constant,  $k_2$ , was

TABLE I  
Comparison of *trans*-Vinylene Concentrations in Marlex 50, DYNH, and B-3125 Polyethylenes

Dose, e.v./g. $\times 10^{-21}$	Observed concentrations, mole/g. $\times 10^{-4}$				
	This work		Dole et al. <sup>1</sup>		Miller et al. <sup>4</sup>
	Marlex 50	DYNH	Marlex 50	B-3125	DYNH
0	0.009	0.056	0.058	0.061	0.11
2.7	0.84	0.70	0.53 <sup>a</sup>	—	—
2.9	—	—	—	—	1.08
25	2.9	2.5	—	—	—
Infinite	3.1	2.7	0.707	0.42	—

<sup>a</sup> Value interpolated from Figure 5, reference 1.

determined as follows: at two different doses,  $D_1$  and  $D_2$ , and corresponding concentrations,  $(Vl)_1$  and  $(Vl)_2$ , respectively, eq. (10) from their<sup>1</sup> work gives

$$(Vl)_1 - (Vl)_0 = [(Vl)_\infty - (Vl)_0](1 - e^{-k_2 D_1}) \quad (4)$$

$$(Vl)_2 - (Vl)_0 = [(Vl)_\infty - (Vl)_0](1 - e^{-k_2 D_2}) \quad (5)$$

where  $(Vl)_0$  and  $(Vl)_\infty$  are the *trans*-vinylene concentrations after zero and infinite dose, respectively. Dividing eq. (4) by eq. (5) gives

$$\frac{(Vl)_1 - (Vl)_0}{(Vl)_2 - (Vl)_0} = \frac{1 - e^{-k_2 D_1}}{1 - e^{-k_2 D_2}} \quad (6)$$

TABLE II  
Comparison of Growth and Decay Constants for *trans*-Vinylene Unsaturation in Different Polyethylene Types

Polyethylene type	Decay constant $k_2$ , g./e.v. $\times 10^{+21}$		Initial growth rate $G_0$		
	This work	Dole et al. <sup>1</sup>	This work	Dole et al. <sup>1</sup>	Lawton et al. <sup>2</sup>
Marlex 50	0.119	0.52	2.2	2.4	2.2
DYNH	0.105	—	1.7	—	2.2
B-3125	—	0.58	—	1.7	—

The decay constants shown in Table II were determined from eq. (6) by an iteration method using the concentrations and doses in Table I. The decay constants determined in this investigation for each polymer were less than one-fifth of the corresponding values reported by Dole et al.<sup>1</sup> A smaller decay constant allows the concentration to rise more rapidly and to a higher concentration than those given earlier.<sup>1</sup>

Dole et al.<sup>1</sup> used a graphical method in evaluating their *trans*-vinylene decay constants, concentrations at infinite dose, and initial growth rates. The accuracy of their method is limited by inaccuracies inherent in measuring small concentrations. Evaluation of the concentration at infinite dose in this investigation was accomplished by eq. (10) in the work by Dole et al.<sup>1</sup> in the form

$$(Vl)_\infty = (Vl)_0 + [Vl - (Vl)_0]/(1 - e^{-k_2 D}) \quad (7)$$

Table I gives the values of concentrations at infinite dose as determined in this work and by Dole et al.<sup>1</sup>

The  $G_0$  value for *trans*-vinylene growth is defined as the number of groups formed per 100 e.v. at zero dose. By this definition

$$G_0 = 100N\Phi' \quad (8)$$

where  $\Phi'$  is the initial growth rate in moles per electron-volt. Combining eq. (8) with eq. (9) from the work of Dole et al.<sup>1</sup> gives

$$G_0 = 100N(Vl)_\infty k_2 \quad (9)$$

The values of  $G_0$  calculated from eq. (9) in this work are listed in Table II together with corresponding values reported by Dole et al.<sup>1</sup> and Lawton et al.<sup>2</sup>

Dole et al.<sup>1</sup> determined their  $G_0$  value from the equation

$$G_0 = 100N[d(Vl)/dD]_0 + 100Nk_2(Vl)_0 \quad (10)$$

taking the value of  $[d(Vl)/dD]_0$  from the slope of the broken curve in their Figure 5.<sup>1</sup> The  $G_0$  value for Marlex 50 reported by Dole et al.<sup>1</sup> was 2.4, 0.2 of which was the last term on the right in eq. (10). However, when  $G_0$  was calculated by eq. (9) with the use of the values given by Dole et al.<sup>1</sup> for  $(Vl)_\infty$  and  $k_2$ , the same value, 2.2, was obtained for Marlex 50 as in this work. The present method of determining  $G_0$  appears to be more trustworthy than the slope method, because it is based on the whole curve rather than on low concentrations.

The kinetic constants for DYNH and B-3125 polyethylenes in Tables I and II indicate the same initial *trans*-vinylene concentrations and  $G_0$  values. However, calculating  $G_0$  by eq. (9) by using the  $(Vl)_\infty$  and  $k_2$  values reported by Dole et al.<sup>1</sup> yields the value 1.5 instead of 1.7 as reported for B-3125.

Lawton et al.<sup>2</sup> reported that Marlex 50 and DYNH each had  $G$  values of 2.2 for *trans*-vinylene on the basis of total unsaturation determinations by bromination. These values were based on incorrect assumptions that: (a) *trans*-vinylene formation was linear with dose up to 50 MR; (b) the initial vinyl and vinylidene concentrations decreased to zero at 50 MR. Therefore, their *trans*-vinylene concentration of  $1.08 \times 10^{-4}$  mole/g. after a dose of 50 MR should be about  $1.0 \times 10^{-4}$  mole/g. Their initial *trans*-vinylene concentration for DYNH polymer was  $0.11 \times 10^{-4}$  mole/g., which is higher than the concentrations  $0.056 \times 10^{-4}$  and  $0.073 \times 10^{-4}$  mole/g. determined in this investigation and by Smith,<sup>12</sup> respectively. Calculating the *trans*-vinylene concentration in DYNH at a dose of 50 MR ( $2.9 \times 10^{21}$  e.v./g.) from eq. (4) by using the constants determined in this work yielded the value  $0.74 \times 10^{-4}$  mole/g., which is significantly lower than  $1.08 \times 10^{-4}$  mole/g. reported by Miller et al.<sup>4</sup> After using the bromination method of Miller et al.,<sup>4</sup> Dole et al.<sup>1</sup> concluded that the infrared method was more reliable than the chemical method for several reasons. Although Miller et al.<sup>4</sup> favored bromination over infrared technique, because of uncertainty over the contribution of crystallinity, the same investigators<sup>2</sup> in a later publication cited absorbance measurements on films as proof that DYNH and Marlex 50 had the same  $G$  values for *trans*-vinylene formation. Nevertheless, it is shown clearly in their<sup>2</sup> Figure 4 that DYNH required a higher dose than Marlex 50 to give the same *trans*-vinylene absorbance. The effect of crystallinity merits further study. Eliminating crystallinity might lower the *trans*-vinylene concentrations by Dole et al.<sup>1</sup> and this investigation, making them farther below those obtained by Lawton et al.<sup>2</sup> Slovokhotova and Karpov<sup>3</sup>

have shown that high electron beam doses almost completely eliminated crystallinity in polyethylene.

### B. Vinyl Unsaturation

Dole et al.<sup>1</sup> postulated that the vinyl concentration during decay of these groups should depend on the *trans*-vinylene constants according to their eq. (14). Since the concentration of vinyl groups is directly proportional to the absorbance of the 909  $\text{cm}^{-1}$  band, this equation can be written

$$\ln \left( \frac{A_0}{A} \right)_{909} = \frac{k_1}{k_2} \left[ 1 - \frac{(VL)_0}{(VL)_\infty} \right] (1 - e^{-k_2 D}) \quad (11)$$

where  $A_0$  and  $A$  are the absorbances at 909  $\text{cm}^{-1}$  at zero dose and dose  $D$ , respectively, and  $k_1$  is the vinyl decay constant. Since the vinyl absorbance at doses of  $2.7 \times 10^{21}$  and  $2.5 \times 10^{22}$  e.v./g. in Marlex 50 was the same, namely 0.0212, it is apparent that eq. (11) will yield a different value of  $k_1$  for each finite dose. For our low and high dose Marlex 50 samples the apparent  $k_1$  values were  $1.0 \times 10^{-21}$  and  $0.30 \times 10^{-21}$  g./e.v., respectively, as compared with Dole's value of  $1.61 \times 10^{-21}$  g./e.v. over the range of doses up to  $3 \times 10^{21}$  e.v./g. These data apparently indicate, by lack of constancy of  $k_1$  with dose, that the theory does not hold at high doses. Nevertheless, a nearly constant limiting vinyl concentration was reached at the highest dose. On the basis of Dole's data in their eq. (14) the vinyl concentration at infinite dose should be 0.058 times the initial concentration. From the vinyl absorbance observed in this investigation for Marlex 50 this ratio for both low and high dose samples was found to be 0.094. This higher limiting concentration ratio indicates that vinyl groups were being formed probably by  $\gamma$ -irradiation directly, as suggested by Dole et al.<sup>1</sup> Growth of vinyl groups is indicated, also, by increasing intensity of the 909  $\text{cm}^{-1}$  vinyl band during irradiation of polyethylenes containing little or no vinyl unsaturation initially. This growth was reported by Dole et al.<sup>14</sup> for pile irradiation of du Pont polyethylene PM-1, and it is observed also in Figure 2 for  $\gamma$ -irradiated DYNH. There appears to be little difference in the equilibrium vinyl concentration in linear and branched polyethylenes. The rate of forming vinyl groups during  $\gamma$ -irradiation probably is related to scission of the polymer chain. Although Miller et al.<sup>4</sup> incorrectly assumed that the vinyl concentration declined rapidly to zero during irradiation, they suggested two mechanisms of vinyl production, namely, disproportionation of radical chain ends and cleavage of the polymer radical.

### C. *trans*-Vinylene and Crosslinking Correlations

The infrared spectra of irradiated Marlex 50 in Figure 1 clearly shows new bands at 940, 983, 1020, and 1075  $\text{cm}^{-1}$ . These bands might be associated with *trans*-vinylene unsaturation, crosslinking, branching, conju-

gation, or ring link formation. Substantially weaker new bands at these same frequencies are indicated in Figure 2 for DYNH. Efforts to correlate these bands with those of molecules having *trans*-vinylene unsaturation in A.P.I. spectra<sup>15</sup> were negative. Although a few olefins had very weak bands near 1020 and 1075  $\text{cm}^{-1}$ , they also had stronger bands at other frequencies, which were not observed in irradiated polyethylenes.

The band observed by Slovokhotova and Karpov<sup>3</sup> in irradiated polyethylene at 938  $\text{cm}^{-1}$  appears to be the band observed in this work at 940  $\text{cm}^{-1}$ . This difference agrees with their<sup>3</sup> *trans*-vinylene band at 964  $\text{cm}^{-1}$  and in this work at 966  $\text{cm}^{-1}$ . Their<sup>3</sup> assignment of the 940  $\text{cm}^{-1}$  band to  $\text{R}_1\text{CH}_2\text{C}(\text{CH}_3)_2\text{CH}_2\text{R}_2$  and  $\text{R}_1\text{R}_2\text{CHC}(\text{CH}_3)_2\text{CHR}_3\text{R}_4$  groups was made on the basis of correlations by McMurry and Thornton,<sup>16</sup> who gave the range 932–934  $\text{cm}^{-1}$  for these structures. Clearly both 938 and 940  $\text{cm}^{-1}$  are outside this specified range. If these structures were formed during irradiation, the methyl group doublet at 1367 and 1382  $\text{cm}^{-1}$  of nearly equal intensities should have been observed in Marlex 50 and DYNH. Slovokhotova and Karpov<sup>3</sup> demonstrated that melting polyethylene increased the intensity of the methyl band and shifted its maximum intensity to 1367  $\text{cm}^{-1}$ . They also found that irradiation decreased the polymer crystallinity. Hence, the radiation-induced increase in intensity of the methyl bending band in Marlex 50 and DYNH observed in this work has been attributed to decreased crystallinity instead of branch formation.

#### D. Conjugated Double Bonds

With so many *trans*-vinylene groups being formed at the highest dose, it would be surprising if some of them were not conjugated. The out-of-plane hydrogen deformation vibration in *trans*-vinylene groups was reported by O'Connor<sup>17</sup> to be shifted by conjugation from 967  $\text{cm}^{-1}$  to 983, 988, 989, 991, and 994  $\text{cm}^{-1}$  in (a) *cis*, *trans*, (b) *trans*, *trans*, (c) *cis*, *cis*, *trans*, (d) *cis*, *trans*, *trans*, and (e) *trans*, *trans*, *trans*, conjugated groups, respectively. Jackson et al.<sup>18</sup> showed that the *cis*, *trans*-conjugated 983  $\text{cm}^{-1}$  band is accompanied also by a weaker band at 948  $\text{cm}^{-1}$ . The observed 940  $\text{cm}^{-1}$  band appears to be too low in frequency and too weak in intensity to correspond to the 948  $\text{cm}^{-1}$  correlation band for the *cis*-*trans* conjugation.

Chapman and Taylor<sup>19</sup> observed that in  $\beta$ -carotene, having eight repeating units of the form  $-\text{CH}=\text{CH}-\text{C}(\text{CH}_3)=\text{CH}-$  in head-to-tail arrangement, the *trans*-vinylene band was observed at 968  $\text{cm}^{-1}$  and the only effect of conjugation was to make the 825  $\text{cm}^{-1}$   $\text{R}_1\text{R}_2\text{C}=\text{CHR}_3$  band unusually weak.

Blout et al.<sup>20</sup> found that conjugation in polymers shifted the C=C stretching band to lower frequencies, splitting it into more weak components as the number of conjugated groups increased. Allan et al.<sup>21</sup> found that for isomers of  $\text{CH}_3\text{CH}=\text{CH}-\text{CH}=\text{CHOOCH}_3$ , the *trans*, *trans*-



TABLE III  
Wave Numbers of Infrared Bands and Relative Intensities of Substituted Cyclopentanes from A. P. I. Spectra<sup>15</sup>

Molecule	Observed bands nearest wave numbers indicated <sup>a</sup>					
	7.5-16 $\mu$	888 cm. <sup>-1</sup>	940 cm. <sup>-1</sup>	983 cm. <sup>-1</sup>	1020 cm. <sup>-1</sup>	1075 cm. <sup>-1</sup>
Methylcyclopentane	979m	890m		979m	1010w	
<i>n</i> -Propylcyclopentane	1072m	891s	938m			1072m
Isopropylcyclopentane	1321s	877m	938m	980m		1062w
		895m				
<i>n</i> -Butylcyclopentane	894vs	894vs	938s	980vw	1020vw	1073m
<i>sec</i> -Butylcyclopentane	938s	898m	938s		1020m	1085vw
<i>tert</i> -Butylcyclopentane	940s	899m	940s		1020sh	
<i>n</i> -Decylcyclopentane	721vs	892s	936s	976m	1025m	1078m
1- <i>trans</i> -2-Dimethylcyclopentane	983vs	897vw	946msh	983vs		1081w
1- <i>trans</i> -3-Dimethylcyclopentane	981s	882vw		981s	1020m	1080vw
1-Methyl- <i>cis</i> -2-ethylcyclopentane	935m	884w	935m	986w	1010vw	1080w
1,1,3-Trimethylcyclopentane	1309m	888vw	939vw			1083vw
						sh
1,trans-2- <i>cis</i> -4-Trimethylcyclopentane	1305m	879vw	937w		1024w	1080vw
1,1,3,3-Tetramethylcyclopentane	1312s	891vw	939w			1085m
		sh				
Average		891.1	938.5	980.7	1019.0	1078.1

<sup>a</sup> Intensities: vs = very strong, s = strong, m = medium, w = weak, vw = very weak, sh = shoulder.

compound absorbed at 1642 and 1614  $\text{cm}^{-1}$  and the *cis,cis*-compound at 1623 and 1587  $\text{cm}^{-1}$ . Chapman and Taylor<sup>19</sup> observed weak bands at 1623 and 1565  $\text{cm}^{-1}$  in vitamin A palmitate for the conjugated double bonds.

The C=C stretching bands observed in Marlex 50 and DYNH polyethylenes before irradiation were at 1643  $\text{cm}^{-1}$  (vinyl) and 1648  $\text{cm}^{-1}$  (vinylidene), respectively. After irradiation these bands had nearly vanished and no new bands close to the frequencies for conjugated groups were observed. Likewise, there appeared to be no correlation suggesting conjugation of acetylenic groups or olefins with acetylenic groups.<sup>22</sup> Therefore, it was concluded that infrared spectra lend no support to formation of conjugated double bonds in polyethylene during irradiation.

### E. Ring Link Formation

It may be assumed that some or all of the new or intensified bands observed in irradiated polyethylene in Figures 1 and 2 at 888, 940, 983, 1020, and 1075  $\text{cm}^{-1}$  are due to *trans*-vinylene unsaturation or ring links. The band reported by Dole et al.<sup>1</sup> at 990  $\text{cm}^{-1}$ , which they attributed to *trans*-1,2-disubstituted cyclopentanes or cyclohexanes, apparently is the band at 983  $\text{cm}^{-1}$ .

The observed infrared wave numbers and relative intensities of substituted cyclopentanes and cyclohexanes from A.P.I. spectra<sup>15</sup> are shown in Tables III and IV, respectively. The strongest band between 7.5 and 16  $\mu$  is frequently one of the correlation bands. Possibly the best correlations for the 983  $\text{cm}^{-1}$  band are for 1-*trans*-2-dimethylcyclopentane and isobutylcyclohexane. Monosubstituted cyclopentanes give the best correlation for the 940 and 1020  $\text{cm}^{-1}$  bands, whereas the monosubstituted cyclohexanes appear to contribute mainly to the 983  $\text{cm}^{-1}$  band. Significantly, 1-*trans*-2-dimethylcyclohexane has a strong band at 991  $\text{cm}^{-1}$ , no band at 983  $\text{cm}^{-1}$ , a weak band at 945  $\text{cm}^{-1}$ , and bands of medium intensity at 1003 and 966  $\text{cm}^{-1}$ . Although the bands in Tables III and IV do not all correlate precisely with the observed frequencies, several of the bands in Figures 1 and 2 are sufficiently broad to make a mixture of them plausible. On the basis of the average of the correlation frequencies in Tables III and IV, it is concluded that a mixture of these compounds was formed in irradiated polyethylenes. Whereas Dole et al.<sup>1</sup> postulated only 1,2-disubstituted cyclopentanes and cyclohexanes, it appears that the substituent positions are more varied.

Ring link formation is cyclization or a kind of crosslinking in which loss of a hydrogen atom from each of two carbon atoms in the same molecule results in establishing a bond between the two carbon atoms. If the terminal carbon atom in the polymer chain bonds with the fifth or sixth carbon atom, a monosubstituted cyclopentane or cyclohexane would be formed. Curling of a polymer chain back on itself farther from the end of the chain could result in linking the chain to itself by a C—C bond, forming 1,2-

TABLE IV  
Wave Numbers of Infrared Bands and Relative Intensities of Cyclohexanes from A.P.I. Spectra<sup>15</sup>

Molecule	Strongest band <sup>a</sup> 7.5-16 $\mu$	Observed bands nearest wave numbers indicated <sup>a</sup>					
		888 cm. <sup>-1</sup>	940 cm. <sup>-1</sup>	983 cm. <sup>-1</sup>	1020 cm. <sup>-1</sup>	1075 cm. <sup>-1</sup>	
Ethylcyclohexane	888vs		987s	1014w	1062vw		
Isobutylcyclohexane	890s	941w	981s	1035m	1060w		
<i>sec</i> -Butylcyclohexane	890vs		989m	1015m	1075w		
	963m		sh		1065w		
1- <i>trans</i> -4-Dimethylcyclohexane	991vs	946m		1029s	1073vw		
1- <i>trans</i> -2-Dimethylcyclohexane	966m	945m			1062w		
1-Methyl- <i>trans</i> -4-isopropylcyclohexane	890s	942m	987m		1070vw		
1-Methyl-1- <i>n</i> -propylcyclohexane	934m	934m	982w	1017vw	1083vw		
Average	889.8	940.7	985.2	1022.0	1070.0		
Average of Tables I and II combined	889.9	939.5	982.6	1020.1	1074.5		

<sup>a</sup> Intensities: vs = very strong, s = strong, m = medium, w = weak, vw = very weak, sh = shoulder.

disubstituted cyclopentanes or cyclohexanes. *cis*-1,2-Substituents cannot be ruled out, as indicated by the frequencies of 1-methyl-*cis*-2-ethylcyclopentane. If the end of a branched polymer chain curls back on itself and bonds by  $\gamma$ -activation it could form 1,3- or 1,4-disubstituted ring link compounds similar to 1-*trans*-3-dimethylcyclopentane. Formation of 1,1,3-trisubstituted ring link compounds appear improbable as compared with previous types. In all of these cases, except for branched chains, the substituents are almost certainly higher in molecular weight than those in Table I.

Comparison of absorbances per unit surface density at  $983\text{ cm}^{-1}$  in irradiated Marlex 50 and DYNH indicates that the concentration of ring links in Marlex 50 is nearly four times that in DYNH. One reason for more rapid growth of ring links in Marlex 50 could be that in the crystallites the polymer lies in a plane folded back and forth along itself. Therefore, the proximity of these segments of the same chain greatly enhances the probability of ring link formation. Since linear Marlex 50 is more crystalline than branched DYNH, the former polymer would be expected to form more ring links than DYNH for the same dose.

### F. Vinylidene Unsaturation

The origin of the  $888\text{ cm}^{-1}$  band is of importance because of its bearing on the structure of polyethylene before and after irradiation. Nielsen and Holland<sup>23</sup> assigned a very weak  $888\text{ cm}^{-1}$  band in Marlex 50 to rocking of methyl endgroups, but they indicated some uncertainty in this assignment because of vinylidene groups absorbing also at  $888\text{ cm}^{-1}$ . It is possible to resolve this uncertainty on the basis of different treatments used to remove unsaturation in polyethylene.  $\gamma$ -Irradiation decreased the intensity of the initial  $889\text{ cm}^{-1}$  band in DYNH, as indicated in Figure 2, revealing a band at  $894\text{ cm}^{-1}$ . Dole et al.<sup>14</sup> had observed this phenomenon earlier after pile irradiation. Using bromination to remove unsaturation, Dole et al.<sup>14</sup> showed that the initial vinylidene band at  $890\text{ cm}^{-1}$  was destroyed, leaving an  $894\text{ cm}^{-1}$  band, which they attributed to ethyl groups. Likewise, Bryant and Voter<sup>24</sup> found that the initial vinylidene band at  $889\text{ cm}^{-1}$  was removed completely by hydrogenation, leaving a band at  $894\text{ cm}^{-1}$ .

The average out-of-plane hydrogen deformation frequency for 12 pure vinylidene compounds in current A.P.I. spectra<sup>15</sup> was found to be  $889.0 \pm 3\text{ cm}^{-1}$ , whereas the rocking methyl or ethyl vibration in fifteen liquid *n*-paraffins was found to have an average value of  $890.7 \pm 4\text{ cm}^{-1}$ . The average value of all solid paraffins in A.P.I. spectra was found to be  $890.6 \pm 3.6\text{ cm}^{-1}$ . The methyl or ethyl band was very weak in all cases except 2,2-dimethylhexane, but in six solid state paraffins no band was observed near  $891\text{ cm}^{-1}$ . This band became more constant in intensity and frequency as the molecular weight of the liquid *n*-paraffins increased. Comparing the spectrum of *n*-hexadecane with 2,6,11,15-tetramethylhexadecane, it was found that the  $891\text{ cm}^{-1}$  band intensity was lowered by in-

creasing the number of methyl groups. Bryant and Voter<sup>24</sup> found that the ethyl group band at 891  $\text{cm}^{-1}$  in low molecular weight hydrocarbons was shifted to 894  $\text{cm}^{-1}$  in high molecular weight polyethylenes. Therefore, the conclusions from this frequency shift and the various treatments used to remove vinylidene groups in polyethylene is that the  $889 \pm 1$  and 894  $\text{cm}^{-1}$  bands had their origins in vinylidene unsaturation and ethyl groups in saturated hydrocarbons, respectively.

Marlex 50 polyethylene, having almost no initial vinylidene unsaturation, formed vinylidene groups during irradiation as shown in Figure 1. Whereas highly branched DYNH had a moderately intense ethyl band at 894  $\text{cm}^{-1}$ , highly linear Marlex 50 exhibited no ethyl band before or after irradiation.

This work was supported jointly by the United States Atomic Energy Commission and the University of Georgia. The author is grateful to Dr. W. W. Parkinson, Jr. at the Oak Ridge National Laboratory for irradiation of all samples, measurement of doses, and helpful discussions during this investigation. Appreciation also is extended to the Phillips Petroleum Company and to the Union Carbide Plastics Company for providing samples of polyethylene.

### References

1. Dole, M., D. C. Milner, and T. F. Williams, *J. Am. Chem. Soc.*, **80**, 1580 (1958).
2. Lawton, E. J., J. S. Balwit, and R. S. Powell, *J. Polymer Sci.*, **32**, 257 (1958).
3. Slovokhotova, N. A., and V. L. Karpov, *Symposium on Radiation Chemistry*, N. A. Bakh, Ed., Akademii Nauk, SSSR, Moscow, 1955 (translation by Consultant's Bureau, New York), p. 165, 175.
4. Miller, A. A., E. J. Lawton, and J. S. Balwit, *J. Phys. Chem.*, **60**, 599 (1956).
5. Hochanadel, C. J., and J. A. Ghormley, *J. Chem. Phys.*, **21**, 880 (1953).
6. Wright, N., *Ind. Eng. Chem., Anal. Ed.*, **13**, 1 (1941); J. J. Heigl, M. F. Bell, and J. U. White, *Anal. Chem.*, **19**, 293 (1947); G. Pirlot, *Bull. Soc. Chim. Belg.*, **58**, 28 (1949).
7. Binder, J. L., *Anal. Chem.*, **26**, 1877 (1954).
8. Hampton, R. R., *Anal. Chem.*, **21**, 923 (1949).
9. Williams, V. Z., *Perkin-Elmer Instr. News*, **10**, 2 (1958).
10. Anderson, J. A., and W. D. Seyfried, *Anal. Chem.*, **20**, 998 (1948).
11. Smith, D. C., private communication.
12. Smith, D. C., *Ind. Eng. Chem.*, **48**, 1161 (1956).
13. Sears, W. C., Research Report for 1963 on U. S. Atomic Energy Commission Contract No. AT-(40-1)-2418, p. 4.
14. Dole, M., C. D. Keeling, and D. G. Rose, *J. Am. Chem. Soc.*, **76**, 4304 (1954).
15. American Petroleum Institute Research Project 44, *Catalog of Infrared Spectral Data*, Carnegie Institute of Technology, Pittsburgh.
16. McMurry, H. L., and V. Thornton, *Anal. Chem.*, **24**, 318 (1952).
17. O'Connor, R. T., *J. Am. Oil Chemists Soc.*, **33**, 1 (1956).
18. Jackson, J. E., R. F. Paschke, W. Tolberg, H. M. Boyd, and D. H. Wheeler, *J. Am. Oil Chemists Soc.*, **29**, 232 (1952).
19. Chapman, D., and R. J. Taylor, *Nature*, **174**, 1011 (1954).
20. Blout, E. R., M. Fields, and R. Karplus, *J. Am. Chem. Soc.*, **70**, 194 (1948).
21. Allan, J. L. H., G. D. Meakins, and M. C. Whiting, *J. Chem. Soc.*, **1955**, 1874.
22. Bellamy, L. J., *The Infrared Spectra of Complex Molecules*, 2nd Ed., Methuen and Co., Ltd., London, 1958, Chap. 4, p. 59.
23. Nielsen, J. R., and R. F. Holland, *J. Mol. Spectroscopy*, **6**, 403 (1961).
24. Bryant, W. M. D., and R. C. Voter, *J. Am. Chem. Soc.*, **75**, 6113 (1953).



### Résumé

Les concentrations en groupement vinyène-*trans* dans les polyéthylènes du type Marlex 50 et DYNH ont été déterminées au moyen des spectres de rayons gamma. Les valeurs de  $G$  pour la croissance du vinyène-*trans* sont trouvées égales à 2,2 et 1,7 pour les polyéthylènes du type Marlex 50 et DYNH, respectivement. Les constantes de dégradation du vinyène-*trans* et les concentrations à dose infinie ont été évaluées. La croissance et la dégradation de l'insaturation vinylique et la croissance de l'insaturation du vinylidène dans le Marlex 50 ont été discutées. L'insaturation du type vinylidène a été mise en évidence chez le polyéthylène par des bandes à 889 et 894  $\text{cm}^{-1}$  ainsi que des groupes éthyle chez les paraffines saturées, sur la base de moyens différents de saturation de la liaison double. Les fréquences de nouvelles bandes produites hors de l'irradiation du Marlex 50 et du DYNH ont été mis en relation avec les bandes des cyclopentanes et cyclohexanes substitués. On peut conclure qu'un mélange complexe de ces composés cycliques était formé chez le Marlex 50 et le DYNH. Il est apparu également qu'il n'y avait pas de corrélation entre les fréquences de ces bandes induites par irradiation et les fréquences connues comme étant caractéristiques des doubles liaisons conjuguées.

### Zusammenfassung

In Polyäthylen Marlex 50 und DYNH wurde die Konzentration der *trans*-Vinylengruppen vor und nach der Bestrahlung der Polyäthylenfilme mit Gammastrahlen IR-spektroskopisch bestimmt. Die  $G$ -Werte für die Bildung von *trans*-Vinylengruppen in Polyäthylen Marlex 50 und DYNH waren 2,2 bzw. 1,7. Die Zerfallskonstante der *trans*-Vinylengruppen sowie deren Konzentration bei unendlicher Dosis wurden bestimmt. Bildung und Zerfall von Vinylidoppelbindungen und Bildung von Vinylidendoppelbindungen in Marlex 50 werden diskutiert. Unter Verwendung verschiedener Methoden zur Absättigung der Doppelbindung konnten die Polyäthylenbanden bei 889 und 894  $\text{cm}^{-1}$  der Vinylidendoppelbindung bzw. den Äthylgruppen in gesättigten Paraffinen zugeordnet werden. Die in Marlex 50 und DYNH als Folge der Bestrahlung auftretenden neuen Banden stimmten in ihrer Frequenz mit denjenigen substituierter Cyclopentane und Cyclohexane überein. Das lässt auf die Bildung eines komplizierten Gemisches dieser cyclischen Verbindungen in Marlex 50 und DYNH schließen. Dagegen wurde keine Übereinstimmung der Frequenzen dieser strahlungsinduzierten Banden mit denjenigen der bekannten, für konjugierte Doppelbindungen charakteristischen Banden festgestellt.

Received May 13, 1963

## Synthetic Polysaccharides. I. Methyl Mono- and Methyl Di-*O*-allyl- $\alpha$ -D-Glucosides and Their Polymerization\*

RICHARD G. SCHWEIGER, *Research Laboratory, Kelco Company, San Diego, California*

### Synopsis

Methyl mono- and methyl di-*O*-allyl- $\alpha$ -D-glucosides are prepared by the reaction of methyl  $\alpha$ -D-glucoside with allyl chloride in alkali in a two-phase system. The mono-allyl ether consists mainly of a mixture of methyl 2-, 4-, and 6-*O*-allyl- $\alpha$ -D-glucosides, the diallyl compound of 2,6- and 4,6-di-*O*-allyl- $\alpha$ -D-glucosides in approximately a 1:1 ratio. Both compounds are homopolymerized with oxygen as the catalyst. The poly-(monoallyl glucoside) is a water-soluble, brittle, clear resin with a softening point of 100–110°C. The poly(diallyl glucoside) is a brittle, clear, but completely insoluble resin with no softening point. Copolymerization with acrylamide under certain conditions yields water-soluble polymers, aqueous solutions of which exhibit high viscosities and have the typical appearance and consistencies of those of polysaccharides.

### INTRODUCTION

In previous years increasing efforts have been made to synthesize polysaccharides or similar polymers. Different sugar derivatives with unsaturated groups attached have been prepared in order to polymerize them subsequently. Vinyl ethers of glucose<sup>1</sup> and galactose derivatives<sup>2</sup> have been obtained by the reaction of acetylene with the corresponding sugars with only one free hydroxyl group. Recently *N*-substituted acryl- and methacrylamides were synthesized and polymerized by Whistler et al.<sup>3</sup> They obtained both derivatives by the reaction of glucamine with acrylic and methacrylic anhydrides. Black et al. reported the esterification of hydroxyl groups of suitable sugar derivatives by using the same reagents.<sup>4</sup>

All of these monomers could be polymerized to high molecular weight products. However, usually the starting materials and reagents are not commercially available and difficult to synthesize. Besides, most of the polymers have to be partially hydrolyzed to exhibit the typical properties of polysaccharides.

Other types of potential monomers are the allyl sugars. In the previous literature fully substituted sugars or polyalcohols such as methyl tetra-*O*-

\* Presented before the Division of Carbohydrate Chemistry, 144th National Meeting of the American Chemical Society, Los Angeles, Calif., April, 1963.

allyl- $\alpha$ -D-glucoside, hexaallyl mannitol, etc. have been described. These, of course, are water insoluble and, on polymerization, yield insoluble, brittle resins. As to allyl sugars with a lower degree of substitution (D.S.) only mixtures of various compounds which were not separated are reported.<sup>5</sup>

## RESULTS AND DISCUSSION

### Methyl Mono- and Methyl Di-*O*-allyl- $\alpha$ -D-glucosides

This paper gives information on the preparation of water-soluble allyl ethers with uniform D.S. which may be suitable for homo- and copolymerizations. Methyl- $\alpha$ -D-glucoside was used as the starting material. If the reaction was carried out by the standard procedure with the use of allyl bromide in aqueous alkali, similar mixtures as described previously were obtained. However, if carried out in a two-phase system, for example, water-toluene, only methyl mono- and methyl di-*O*-allyl- $\alpha$ -D-glucosides were formed. Apparently the reaction occurs in the aqueous phase and most of the diallyl ether, as soon as formed, is removed into the organic phase thus being protected from further substitution. By this procedure allyl bromide could be substituted by allyl chloride and the reaction be performed under normal pressure. The separation of both products was based on the difference of their solubility in ether and water. The crude diallyl compound was obtained by repeated ether extractions in a separatory funnel, the monoallyl ether by a subsequent continuous ether extraction of the aqueous layer. The crude products then were purified by distillation. The yields and analytical data are given in Table I. The D.S. was calculated from the degree of unsaturation obtained by the addition of bromine. The ratio of the yields could be changed by varying the amount of allyl chloride. Usually the ratio became more in favor of extract II when the amount of allyl chloride was decreased.

Paper chromatographic examinations with two different irrigants indicated one major compound for each fraction. Other spots were very faint due to impurities in small amounts. The quantities of these impurities were less

TABLE I

	Boiling point (0.15 mm.), °C.	Yield, g.	D.S.	$R_f$ values	
				A	B
Extract I	148-152	23.5	1.98	0.757 <sup>b</sup>	0.015 <sup>b</sup>
				0.919 <sup>a</sup>	0.577 <sup>a,c</sup>
				0.966 <sup>b</sup>	0.955 <sup>b</sup>
Extract II	166-170	42.5	0.96	0.757 <sup>a</sup>	0.015 <sup>a</sup>
				0.919 <sup>b</sup>	0.577 <sup>b</sup>

<sup>a</sup> Major spot.

<sup>b</sup> Very faint spot.

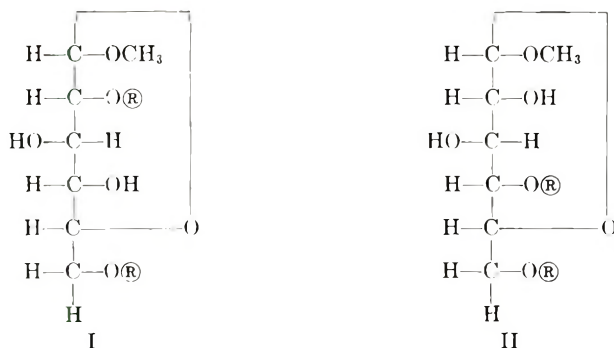
<sup>c</sup> Showing as a streak on the chromatogram; the  $R_f$  value corresponds to the center of this streak.

TABLE II  
 Consumption of Periodate and Formation of Formic Acid

Monoallyl glucoside			Diallyl glucoside		
Substance	NaIO <sub>4</sub> consumption, mole/mole	HCOOH formation, mole/mole	Substance	NaIO <sub>4</sub> consumption, mole/mole	HCOOH formation, mole/mole
Sample	1.4	0.34	Sample	0.9	0.02
6- <i>O</i> -	2.0	1.0	2,4- <i>O</i> -	0	0
4- <i>O</i> -	1.0	0	2,6- <i>O</i> -	1.0	0
3- <i>O</i> -	0	0	3,6- <i>O</i> -	0	0
2- <i>O</i> -	1.0	0	4,6- <i>O</i> -	1.0	0

than 1%, since removal of one trace compound ( $R_f$  0.757 in A) from the diallyl fraction changed the degree of unsaturation only slightly.

In order to locate the position of the allyl groups both products were oxidized with periodate and the consumption of periodate as well as the formation of formic acid determined. The experimental values in comparison to theoretical values for all possible isomers are shown in Table II. The results suggest that of the monoallyl glucoside fraction only about one-third consists of the 6-*O*-allyl ether. As to the diallyl glucoside, the 2,6-, (I), and 4,6-di-*O*-allyl glucosides, (II), are to be considered. Major portions of the other isomers can be excluded.



After periodate oxidation and subsequent hydrolysis only I would produce glyoxal. Glyoxal was isolated as its 2,4-dinitrophenylosazone in a 40% yield indicating that the diallyl fraction consists of both I and II in an approximate ratio of 1:1.

Since the monoallyl ether can be considered as the intermediate for the formation of the diallyl ether, the portion of the monoallyl fraction which is not substituted in the 6-position may be assumed to be a mixture of 2- and 4-*O*-allyl glucosides in approximately a 1:1 ratio. Similarly, the presence of an essential amount of 3-*O*-allyl glucoside is unlikely and, accordingly, the monoallyl fraction consists of 2-, 4-, and 6-*O*-allyl glucosides in similar quantities.

### Homopolymerization

Both allyl sugars were homopolymerized at 110–115°C. with the use of oxygen as the catalyst. The degree of unsaturation determined by the addition of bromine decreased as expected, leveling off after several hours (Fig. 1). The polymer from the monoallyl glucoside is a water-soluble, brittle, and clear resin with a softening point of 100–110°C. It appears

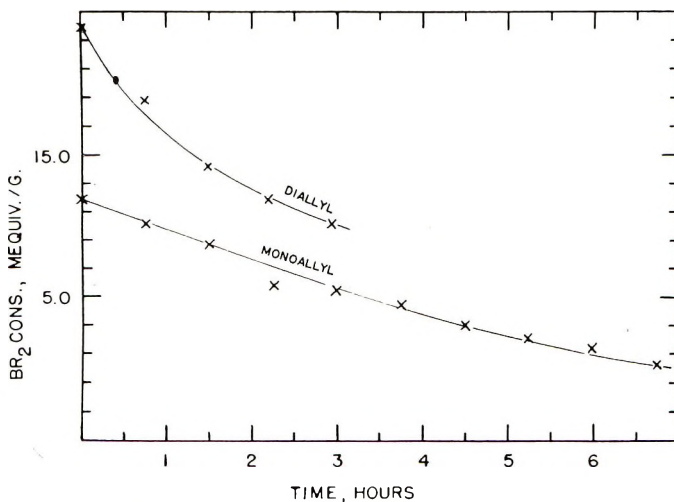


Fig. 1. Homopolymerization of methyl mono- and methyl di-*O*-allyl- $\alpha$ -*D*-glucosides.

to be hygroscopic. A 10% aqueous solution has a low viscosity, probably indicating a low molecular weight. The poly(diallyl glucoside) is a brittle, glassy resin with no softening point. Although the monomer is soluble in water and alcohol, the polymer is completely insoluble in any solvent due to, assumingly, its matrix structure. The product starts darkening at temperatures of above 250°C.

### Copolymerization with Acrylamide

In order to test the possibility of copolymerizing with other monomers, mixtures of allyl sugar and acrylamide in methanol were initiated at elevated temperatures with methyl ethyl ketone peroxide. The amount of sugar in the polymer was calculated from the nitrogen content. Table III shows that copolymers are definitely obtained but that the amount of sugar in the polymer is comparatively low.

This amount apparently can be increased by increasing the concentration of allyl sugar in the monomer mixture. All copolymers of monoallyl ether and acrylamide are insoluble but highly swollen in water; the copolymers with diallyl glucoside neither dissolve nor do they swell appreciably in water.

In order to improve the method and especially to obtain a higher proportion of sugar in the polymer two major changes were made in the pro-



TABLE III  
 Copolymerization with the Use of a Peroxide Catalyst

Sugar	Weight ratio, allyl sugar:acrylamide	N, %	Sugar, %
Monoallyl	2:1	11.06	42
	1:1	13.30	30
	1:2	14.56	23
	2:1 <sup>a</sup>	12.88	32
Diallyl	2:1	11.35	40
	1:1	12.65	33
	1:2	14.15	25

<sup>a</sup> Acetylated allyl glucoside having a D.S. of 1.07 (with respect to allyl) was used.

cedure. The acrylamide (as a solution in ethanol-water) was added dropwise to the polymerizing allyl ether over an extended period of time. Thus, the concentration of allyl sugar was always kept as high as possible. Furthermore, oxygen instead of a peroxide was used as the catalyst. Oxygen is known to initiate allyl but not acrylic or vinyl polymerizations. The polymerization or copolymerization of acrylamide, however, may be initiated secondarily by the allyl radicals. Table IV shows that the percentage of sugar was indeed, highly increased, usually being the higher, the longer the time required for the addition of the acrylamide. However, the viscosity of an aqueous solution of the pure monoallyl glucoside-acrylamide copolymer was low indicating a low molecular weight. In the subsequent experiments increasing percentages of diallyl glucoside were added to the monomer mixture, the assumption being that this initiates branching and thus increases the molecular size. This happened, indeed, as indicated by the drastic increase of the viscosity. The drop of the viscosity of the fourth sample was due to partial insolubility while the last sample was essentially insoluble.

Figure 2 shows a plot of the viscosity (logarithmic scale) against the concentration of aqueous solutions. Each sample is marked by the percentage of diallyl glucoside in the initial monomer mixture (Table IV). Although the viscosity of the 4.4% sample was relatively low, it is remarkable that, especially at high concentrations, the solutions exhibited a high

 TABLE IV  
 Copolymerization with the Use of Oxygen as the Catalyst

Monoallyl, wt.-%	Diallyl, wt.-%	Acrylamide, wt.-%	N, %	Sugar, %	Viscosity (3%), cpoise
66.7	0	33.3	7.65	60	5
63.4	3.3	33.3	9.55	50	10
62.3	4.4	33.3	9.35	51	104
51.9	5.3	42.8	8.65	55	920
60.0	6.7	33.3	7.90	58	234
50.0	16.7	33.3	9.25	51	Insoluble

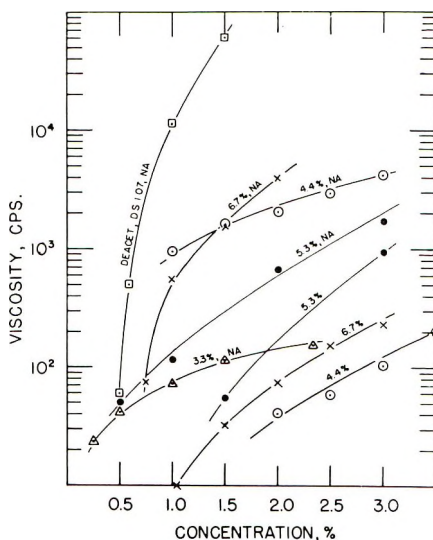


Fig. 2. Viscosities of aqueous solutions of copolymers at varying concentrations.

viscoelasticity, showing consistencies similar to those of psyllium or quince seed gums. In contrast, the 5.3% sample had a high viscosity, but its flow was shorter and without this distinct elasticity.

All of these polymers were saponified to split off the amide groups and form the corresponding sodium salts. These modified products are denoted in Figure 2 by Na. Surprisingly, all samples showed a tremendous increase of their viscosity. Also, the solubility of the partially insoluble polymers was highly improved. Solutions of sodium salts of the 3.3 and 5.3% samples exhibited a high elasticity, the latter showing stringy flow characteristics, somewhat similar to fucoidan. The 4.5% sample had a smooth flow, showed little elasticity, and no stringiness at high viscosities. The remaining two products were starchlike, clear pastes with extremely high viscosities. The sodium salt of one polymer obtained through poly-

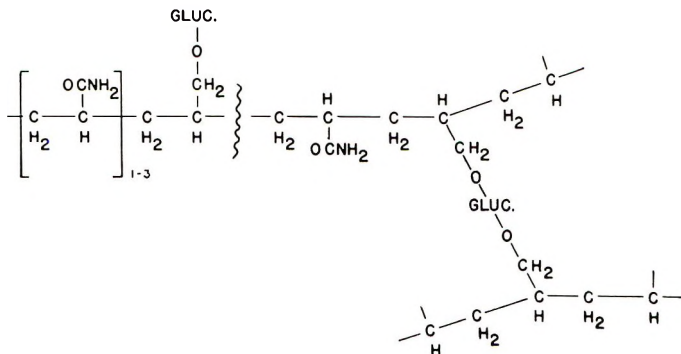


Fig. 3. Presumed structure of copolymers.

merization of acetylated allyl sugar with a D.S. of 1.07 (Table III; actually a mixture of mono- and diallyl ethers with 7-8% of the latter) had a viscosity of over 60,000 cpoise at a 1.5% concentration. Solutions of both products thinned out and formed tiny, gelatinous particles when diluted to 0.5-0.8%. However, if passed through a colloid mill, even at these low levels, smooth solutions were obtained.

The appearance and consistency of these solutions were characteristic for those of natural polysaccharides. However, unlike all natural polysaccharides and most synthetic ones produced up to now, these copolymers exhibited a tremendous stability and very likely a great resistance to enzymatic attack. As shown in Figure 3, the presumed structure of these copolymers consists of carbon backbones to which the glucoside units are attached through ether bondings. The diallyl glucoside unit initiates two branches and, similarly, ether bondings form the bridge from the principal to the side chains. Both types of bondings are known to be chemically extremely stable; so, all of these polymers should resist treatments under most pH conditions, heat treatment, etc. Of course, under certain conditions the amide groups may be split off or the glucoside units may be demethylated to produce semiacetal groups. Such reactions, however, are not degradations but rather desirable modifications of these polymers.

## EXPERIMENTAL

### Preparation of Allyl Ethers

A 100-g. portion of methyl  $\alpha$ -D-glucoside was mixed thoroughly with a solution of 31 g. of sodium hydroxide in 35 ml. of water. A round-bottomed flask with three necks and equipped with mechanical stirrer, reflux condenser, and dropping funnel was used as the reaction vessel. After adjusting the temperature to 85-90°C., a mixture of 68 ml. of allyl chloride (1.6 mole/mole of glucoside) and the same volume of toluene were added slowly within about 4 hr. Heating with stirring was continued for 3 hr. more. Then the mixture was neutralized with acetic acid, steam-distilled, and extracted five times with ether in a separatory funnel. The ether layer was dried over sodium sulfate and concentrated to a syrup. The water layer was extracted continuously with ether for 48 hr., and the extract concentrated to a syrup also. Both products were distilled under reduced pressure. The first few grams of each distillate was discarded. The data are shown in Table I.

The determination of the D.S. was carried out by the addition of bromine to the double bonds. An excess of 0.1*N* bromine solution was added to an aqueous solution of an aliquot of the sample to be determined. After keeping the mixture for 5 min., potassium iodide was added and the free iodine titrated with a 0.1*N* sodium thiosulfate solution. The consumption of bromine per gram of product with a D.S. of 1 and of 2 (mono- and di-

allyl ethers) was calculated and plotted on a curve against the D.S. The D.S. of the samples to be determined was taken from this curve.

### Chromatographic Examinations

Chromatographic examinations were carried out on Whatman #4 filter paper using (A), ethyl acetate-acetic acid-formic acid-water (18:3:1:4, v/v), and (B), benzene-methyl ethyl ketone-2% aqueous formic acid (9:1:1 v/v),<sup>6</sup> as the irrigants, and permanganate-periodate<sup>7</sup> as the spray reagent. The results,  $R_f$  values included, are given in Table I.

Part of the diallyl ether fraction was separated on a cellulose column with B as the solvent. All fractions containing the two fastest moving ethers were combined, concentrated to a syrup, and the syrup distilled under reduced pressure. When reacted with bromine as described above, 14.4 meq.  $\text{Br}_2/\text{g.}$  was consumed; the starting material consumed 14.3 meq.  $\text{Br}_2/\text{g.}$

### Oxidation with Periodate

For the oxidation with periodate 0.5-g. portions were diluted with 15 ml. of water to which 10 ml. of a 1*N* sodium periodate solution was added. Both the periodate consumption and the formic acid formation were determined every 10-20 min. on 1 ml.-aliquots. The periodate consumption was determined by reducing the residual periodate with 0.1*N* arsenite solution and titrating the excess arsenite with 0.1*N* iodine, and the formic acid formation by direct titration with 0.1*N* sodium hydroxide after decomposition of excess periodate with propylene glycol. The values reported in Table II were obtained by extrapolation to zero time.

A 1.015-g. portion of the diallyl ether was oxidized in 10 ml. of a 0.772*N* sodium periodate solution, and the solution then was extracted continuously with ether. The extract was concentrated to a syrup, the syrup diluted with water, then a hot solution of 2 g. of 2,4-dinitrophenylhydrazine in 400 ml. of 1*N* hydrochloric acid was added, and the mixture heated for 2 hr. on a steam bath. The precipitate was collected on a fritted glass funnel, washed with water, and dried; yield 1.65 g., m.p. 230-235°C.; after extracting and washing with hot ethanol (about 150 ml.) and drying; 0.67 g., m.p. 290-310°C. (dec.). This product was recrystallized from 24 ml. of nitrobenzene, the precipitate filtered off, washed with 5 ml. of nitrobenzene and then with ethanol, and dried; yield 0.406 g., m.p. 324-327°C. (dec.), undepressed when admixed with authentic glyoxal-2,4-dinitrophenylosazone.

### Homopolymerization

Ten-gram portions of the mono- and diallyl ethers were placed separately in test tubes, heated in an oil bath to 110-115°C., and a stream of oxygen was passed through them. At this temperature both substances were thin oils initially. The monoallyl ether started to thicken considerably after

about 3–4 hr. The temperature was raised to 130–140°C. and heating and treatment with oxygen were continued for another 3 hr. The polymer retained its solubility in water. The diallyl compound was water- and methanol-soluble initially but lost its solubility in water after about 1 hr. After 2 hr. and 50 min. it dissolved only in boiling methanol and about 10 min. later it solidified to a completely insoluble resin. The temperature was raised to 140°C. after about 2 hr. in order to be able to maintain the stream of oxygen.

The degree of unsaturation of both products was determined during the polymerization and plotted on a curve against the time (Fig. 1). The method used, addition of bromine to the double bonds, is described above.

### Copolymerization with Acrylamide

(a) Varying portions (0.5 to 1.0 g.) of the monoallyl ether and acrylamide and, in another experimental series, diallyl ether and acrylamide were dissolved in about 5 ml. of methanol, a few drops of methyl ethyl ketone peroxide (60% in dimethyl phthalate) were added, and the mixture was kept at 50–55°C. for 48 hr. The precipitate was filtered off, washed with methanol, dried, and analyzed for nitrogen. Results including the amount of sugar in the polymers calculated from the nitrogen analysis are given in Table III.

(b) Mixtures of mono- and diallyl glucosides (3 g. total), the ratios of which are given in Table IV, were placed in test tubes, the temperature adjusted to 115–120°C., and a stream of oxygen was passed through them. Then a solution of 1.5 g. (in one sample somewhat more) of acrylamide in ethanol–water (7:3, v/v) was added dropwise over a period of 30–60 min. As the solvent evaporated it was replaced by water. The mixture was stirred frequently. After 2–3 hr. it started to thicken considerably. Some more water was added in order to be able to maintain the stream of oxygen. The polymerization was discontinued after 4–5 hr., an aqueous solution of 0.1 g. of ammonium persulfate was added, and the mixture was kept at 50°C. for 15 hr. The polymer then was precipitated and washed thoroughly with methanol and dried. The yield usually was 3.5–4.0 g.

### References

1. Reppe, W., and co-workers, *Ann.*, **601**, 84 (1956); B. I. Mikhant'ev and V. L. Lapenko, *J. Gen. Chem., USSR (Eng. Transl.)*, **27**, 2810 (1957); W. A. P. Black, E. T. Dewar, and D. Rutherford, *Chem. Ind. (London)*, **1962**, 1624.
2. Whistler, R. L., H. P. Panzer, and J. L. Goatley, *J. Org. Chem.*, **27**, 2961 (1962).
3. Whistler, R. L., H. P. Panzer, and H. J. Roberts, *J. Org. Chem.*, **26**, 1583 (1961).
4. Bird, T. P., W. A. P. Black, E. T. Dewar, and D. Rutherford, *Chem. Ind. (London)*, **1960**, 1331.
5. Tomecko, C. G., and R. Adams, *J. Am. Chem. Soc.*, **45**, 2698 (1923); P. L. Nichols and E. Yanovsky, *J. Am. Chem. Soc.*, **66**, 1625 (1944); *ibid.*, **67**, 46 (1945); A. N. Wrigley and E. Yanovsky, *J. Am. Chem. Soc.*, **70**, 2194 (1948).
6. Lederer, M., *Chromatographic Reviews*, Vol. I, Elsevier, Amsterdam-London-New York-Princeton, 1959, p. 50.
7. Lemieux, R. U., and H. F. Bauer, *Anal. Chem.*, **20**, 920 (1954).



### Résumé

On a préparé des méthyl-mono- et méthyl-di-*O*-allyl- $\alpha$ -D glucosides par la réaction du méthyle  $\alpha$ -D-glucoside avec le chlorure d'allyle en solution alcaline dans un système à deux phases. L'éther monoallylique est constitué principalement d'un mélange des méthyl, 2-, 4- et 6-*O*-allyl- $\alpha$ -D-glucosides, l'éther diallylique contient des méthyl, 2,6- et 4,6-di-*O*-allyl glucosides en quantités semblables. Les deux substances sont homopolymérisées avec l'oxygène comme catalyseur. Le poly(monoallyl glucoside) est une résine cassante, pure, soluble dans l'eau avec un point d'amollissement de 100-110°; le poly(diallyl glucoside) est une résine cassante et pure aussi, mais elle est complètement insoluble et ne possède pas de point de ramollissement. La copolymérisation avec de l'acrylamide sous certaines conditions produit des polymères solubles dans l'eau dont les solutions aqueuses sont très visqueuses et sont semblables à celles des polysaccharides.

### Zusammenfassung

Methyl-mono- und Methyl-di-*O*-allyl- $\alpha$ -D-glukoside werden durch Reaktion von Methyl- $\alpha$ -D-glukosid mit Allylchlorid in Alkali in einem Zwei-Phasen-System hergestellt. Der Monoallyläther besteht hauptsächlich aus einem Gemisch von Methyl-2,4- und -6-*O*-allyl- $\alpha$ -D-glukosiden, der Diallyläther enthält Methyl-2,6- und -4,6-di-*O*-allyl glukoside im Verhältnis von etwa 1:1. Beide Substanzen werden mit Sauerstoff als Katalysator homopolymerisiert. Poly(monoallyl-glukosid) ist eine wasserlösliche, spröde, klare Masse mit einem Erweichungspunkt von 100-110°. Poly(diallyl-glukosid) ist ebenfalls eine spröde, klare, aber vollkommen unlösliche Masse, die keinen Erweichungspunkt hat. Copolymerisation mit Acrylamid ergibt unter gewissen Bedingungen wasserlösliche Polymere, deren wässrige Lösungen z.T. hoch viskos sind und wie typische Lösungen von Polysacchariden erscheinen.

Received May 6, 1963

## Polymerization Behavior of Aziridines with 1,2-Epoxydes\*

C. G. OVERBERGER and MARTIN TOBKES, *Department of Chemistry, Polytechnic Institute of Brooklyn, Brooklyn, New York*

### Synopsis

A number of Lewis acid catalysts have been investigated for the copolymerization of 1,2-butylenimine with 1,2-epoxydes. The most active catalyst, boron trifluoride etherate, has been shown to give polymers containing a polyimine backbone in which the residual NH groups in the polymer chain are  $\beta$ -hydroxyalkylated by the epoxide. It has been demonstrated that the imine is far more reactive than the epoxide under these conditions, regardless of the chain length of the epoxide monomer. The polyimine chain appears to grow to an appreciable extent before any epoxide enters the polymer. These results are interpreted as being due to the preferential complexing of the catalyst by the basic imine residues in the polymer, which renders the catalyst unavailable for polymerization of the epoxide. The homo- and copolymerization behavior of 1-(*p*-toluenesulfonyl)-aziridine, *N,N*-diphenyl-1-aziridinecarboxamide and *N,N*-diethyl-1-aziridinecarboxamide with 1,2-epoxydes has been investigated under conditions of catalysis by boron trifluoride etherate and by triethylamine. In no instance could copolymers be obtained.

### INTRODUCTION

Although homopolymers of epoxydes and aziridines are well documented in the literature, copolymers of these compounds with each other have not been characterized and have been mentioned only in the patent literature.<sup>1,2</sup> The nature of these polymeric products as well as the effects of variables such as substituents and catalyst systems thereon form the subject of the present paper.

### RESULTS AND DISCUSSION

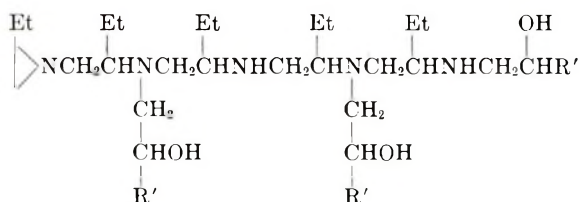
#### Polymers Derived from 2-Ethylaziridine and 1,2-Epoxydes

An initial evaluation of several catalysts for the copolymerization of 2-ethylaziridine (butylenimine) with 1,2-epoxydodecane gave the following results. Active:  $\text{BF}_3 \cdot \text{Et}_2\text{O}$ ,  $\text{AlCl}_3$ ,  $\text{AlBr}_3$ ,  $\text{SnCl}_4$ ; weak activity:  $\text{SnCl}_4 \cdot 5\text{H}_2\text{O}$ ,  $\text{TiCl}_4$ ,  $\text{SbCl}_5$ ,  $\text{Et}_2\text{Zn}$ -alumina;<sup>3</sup> inactive:  $\text{HCl}$  (g),  $\text{FeCl}_3$ ,  $\text{ZnCl}_2$ ,  $\text{FeCl}_3 \cdot 6\text{H}_2\text{O}$ ,  $\text{Al}(i\text{-PrO})_3\text{-ZnCl}_2$ .<sup>4</sup>

\* Taken from the dissertation submitted by Martin Tobkes to the Faculty of the Polytechnic Institute of Brooklyn in partial fulfillment of the requirements for the degree of Doctor of Philosophy (Chemistry), 1963.

From the aluminum isopropoxide-zinc chloride catalyzed reaction there was isolated 17% of 1-(2-hydroxydodecyl)-2-ethylaziridine. The formation of analogous products upon reaction of aziridines with epoxides under neutral conditions has been previously reported.<sup>5,6</sup>

Because of its activity, ease of handling, and solubility in the polymerization systems, boron trifluoride etherate was selected as the catalyst for most intensive study. A typical polymer prepared from butylenimine (59 mole-% monomer feed) and epoxydodecane, using this catalyst (2 wt.-%), was found to contain 67 mole-% of imine and had a molecular weight of 957, which corresponds to a product composed of 5-6 imine and 3 epoxide residues. However, analysis of the phenylthiourea derivative of the polymer indicated that 89% of the polymeric nitrogens were tertiary, implying a significant degree of branching. A polymer prepared under the same conditions from butylenimine and epoxyoctane was found to contain 80% tertiary amine residues. It is, therefore, believed that these polymers are not true copolymers, but exist as structures similar to



in which a polyimine backbone is  $\beta$ -hydroxyalkylated by the epoxide. This contention was further substantiated by the results of an attempt to prepare a copolymer of 1-ethylaziridine (which cannot form branches) with epoxydodecane. From a 59 mole-% feed of the aziridine there was obtained a polymer of molecular weight 788 containing 86 mole-% of imine residues. This corresponds to a product consisting of 8 imine residues and only 1 epoxide residue. It is possible that the epoxide in the chain (which is probably terminal) acts as a chain-stopper.

The effect of monomer feed upon polymer composition was studied in

TABLE I  
Effect of Butylenimine Feed on Polymer Composition (2 wt.-%  $\text{BF}_3 \cdot \text{Et}_2\text{O}$ , 70°C.)

Comonomer	Imine feed, mole-%	Reaction time, hr.	Polymer yield, %		Imine in polymer, mole-%
			Crude	Pure	
Epoxydodecane	20	16	24	5.0	61
"	40	3	18	5.1	77.2
"	59	3	29	2.1	76.6
"	80	1	28	2.5	82
Epoxyhexane	20	10	25	3.1	64.6
"	40	2.5	36	11.4	73.4
"	60	3	44	11.9	75.4
"	80	1	30	12.1	85.8

the polymerization of butylenimine with epoxydodecane and with epoxyhexane. The results of these experiments are shown in Table I.

These results show the greater reactivity of the imine, regardless of the chain length of the epoxide comonomer. The apparent inhibitory effect of epoxide is demonstrated by the slower polymerization rates observed at higher epoxide concentrations. When these experiments were carried out to higher conversions, more epoxide appeared in the polymer, indicating that the polyimine backbone is formed first, with epoxide entering the polymer after the main chain has grown.

These results are interpreted as being due to preferential complexing of the boron trifluoride by the more basic polymeric and monomeric imine, which renders the catalyst unavailable for epoxide chain growth. A similar phenomenon has been observed by Jones<sup>7</sup> and Barb,<sup>8</sup> who observed that the rate of acid-catalyzed polymerization of ethylenimine falls off with increasing conversion. This was interpreted as being due to competition for catalyst by monomeric and polymeric imine. The same observation and interpretation was made by Eastham<sup>9</sup> for the case of the polymerization of ethylene oxide by boron trifluoride catalysis.

If the suggestion of preferential complexing of catalyst by monomeric and polymeric imine is valid, one would expect that increasing catalyst concentration in an imine-epoxide system would lead to polymer containing more epoxide. Indeed, it was found that raising the boron trifluoride etherate concentration from 1 to 4 wt.-% in a system containing 59 mole-% of butylenimine and 41 mole-% of epoxydodecane resulted in the lowering of the imine content in the polymers obtained from 73.3 mole-% to 67.2 mole-%.

### **Polymers Derived from *N*-Substituted Aziridines and 1,2-Epoxydes**

Since the high basicity of the aziridines discussed so far relative to the epoxydes appears to prevent true copolymerization from taking place, it was decided to investigate less basic aziridine derivatives, namely those having electron-withdrawing groups attached to the ring nitrogen. This substitution would also preclude branch formation in the polymers derived therefrom.

Initial studies involved attempts to prepare copolymers of 1-(*p*-toluenesulfonyl)aziridine (tosylaziridine) with 1,2-epoxydes. This monomer is the only aziridine derivative reported to be polymerizable by basic catalysts;<sup>10</sup> traces of acids are, in fact, claimed to inhibit polymerization. In the present studies all attempts to copolymerize tosylaziridine with high levels of epoxydodecane or propylene oxide by means of triethylamine catalysis gave as the only polymeric products, tosylaziridine homopolymers. Under the same conditions homopolymerization of the epoxydes was successful. Copolymerizations attempted in benzene as a solvent (from which polymer precipitated) led to polymers of higher intrinsic viscosity (0.14–0.21 in *m*-cresol at 30°C.) than those obtained under homogeneous con-

ditions in dimethylsulfoxide (0.06–0.07). Mixtures of benzene and dimethylsulfoxide as solvent afforded polymers intermediate in intrinsic viscosity (0.11) between values obtained in the pure solvents, but within the range of experimental error of the other determinations. In *m*-cresol no polymerizations occurred. The reasons for these viscosity phenomena remain unclear. However, in the case of *m*-cresol, at least, the solvent probably is an acidic polymerization inhibitor.

Since tosylaziridine appeared to be considerably more reactive than epoxides towards polymerization by basic catalysis, it was decided to attempt its copolymerization by means of acid catalysis, viz., boron trifluoride etherate. No copolymers were obtained when the copolymerization of tosylaziridine with propylene oxide was attempted. The results of these experiments are shown in Table II.

TABLE II  
Copolymerization of Tosylaziridine with Propylene Oxide at 75°C.

Tosylaziridine feed, mole-%	Yield of Polytosylaziridine, %
20	6 <sup>a</sup>
40	8
60	20
80	69
100	97 <sup>b</sup>

<sup>a</sup> Polypropylene oxide of molecular weight 373 also isolated.

<sup>b</sup>  $[\eta] = 0.27$  in *m*-cresol at 30°C.

The failure to isolate copolymers from tosylaziridine led to the investigation of other *N*-substituted aziridines, viz., *N,N*-diphenyl-1-aziridine-carboxamide and *N,N*-diethyl-1-aziridinecarboxamide. Attempts to copolymerize these compounds with propylene oxide by means of triethylamine or boron trifluoride etherate catalysis led only to oligomers ( $DP = 4-8$ ) of the aziridine derivatives.

## EXPERIMENTAL

### Materials

Solvents were distilled from molecular sieves prior to use. Propylene oxide, ethylenimine, and epoxydodecane were purchased from Matheson, Coleman and Bell. The preparations of 2-ethylaziridine (b.p. 89–90°C.,  $n_D^{25}$  1.4172; reported<sup>7</sup> b.p. 88–89°C.,  $n_D^{25}$  1.4165) and 1-ethylaziridine (b.p. 51°C.,  $n_D^{25}$  1.3927; reported<sup>11</sup> b.p. 51.2–52.3°C.,  $n_D^{25}$  1.3938) were carried out in 68% and 55% yield, respectively, by the Wenker procedure<sup>12</sup> as modified by Campbell et al.<sup>13</sup> Reaction of hexene-1 with peroxytrifluoroacetic acid<sup>14</sup> yielded 1,2-epoxyhexane (b.p. 120–121°C.,  $n_D^{25}$  1.4040; reported<sup>14</sup> b.p. 117–119°/750 mm.,  $n_D^{20}$  1.4060) in 87% yield. The preparation of 1-(*p*-toluenesulfonyl)-aziridine was carried out by the method of Berchet<sup>10</sup> in 76% yield, m.p. 64.5–65°C. (64–65°C.<sup>10</sup>) The procedure



of Bestian<sup>15</sup> was employed to prepare *N,N*-diphenyl-1-aziridinecarboxamide, m.p. 77–78°C. (79°C.) and *N,N*-diethyl-1-aziridinecarboxamide, b.p. 98–100°C./43 mm.,  $n_D^{22}$  1.4625 (b.p. 79°C./11 mm.) in 68% and 84% yields, respectively.

### Preparation of Alkylaziridine-Epoxyde Polymers

A mixture of monomers and catalyst was heated in a sealed polymerization tube. At the end of the reaction period the contents of the tube were washed with alkaline-saturated sodium chloride, dried, and volatile material removed at 180°C./0.1 mm. in a rotary evaporator. The crude residue was taken up in hot acetone and chilled, causing the polymer to precipitate out as a pale yellow gum. This process was repeated two more times to afford the pure polymer.

#### 1-(2-Hydroxydodecyl)-2-ethylaziridine

A mixture of 18.4 g. (0.100 mole) of epoxydodecane, 7.11 g. (0.100 mole) of butylenimine, 225 mg. of aluminum isopropoxide, and 225 mg. of zinc chloride was shaken in a sealed tube at 68°C. for a period of 14 days. Workup as above afforded 4.30 g. (16.9%) of a product melting at 37–41°C. Recrystallization from acetone gave the pure material as white needles, m.p. 42.7–43.3°C.

ANAL. Calcd. for  $C_{16}H_{33}NO$ : C, 75.23%; H, 13.02%; N, 5.48%; neut. equiv., 255; mol. wt., 255. Found: C, 74.88%; H, 12.75%; N, 5.51%; neut. equiv., 248; mol. wt. (vapor phase osmometry), 264.

#### Phenylthiourea Derivatives of Imine-Epoxyde "Copolymers"

A solution of "copolymer" in toluene was reacted with excess phenyl isothiocyanate (1.10 mole per mole of nitrogen in the polymer) overnight at room temperature. Solvent and excess reagent were then removed under high vacuum at moderate temperature in a rotary evaporator. The residue was thrice precipitated from chloroform into hexane and then freeze-dried from benzene.

#### Triethylamine-Catalyzed Polymerizations of Tosylaziridine

A mixture of 0.01 mole of tosylaziridine (plus 0.04 mole of epoxide) and 88.4 mg. of triethylamine in benzene (dimethylsulfoxide, *m*-cresol) was heated at 75–80°C. for 20 hr. If the polymer precipitated from solution (or alternatively, solvent was removed *in vacuo* and the residue suspended in benzene), it was filtered and washed with benzene. The products obtained were powdery materials, melting with decomposition from 213 to 295°C.

#### $Bf_3 \cdot Et_2O$ -Catalyzed Polymerizations of Tosylaziridine

To a polymerization tube containing a solution of tosylaziridine (and propylene oxide) in a minimum amount of benzene at 0°C. there was added

catalyst and the tube sealed. After permitting the contents of the tube to slowly come to room temperature, the tube was inserted in a bath at 75°C. for 48 hr. Filtration afforded the polymer.

### Polymerizations of *N,N*-Disubstituted 1-Aziridinecarboxamides

To an ice-cooled polymerization tube containing a solution of 5 mmoles of the aziridinecarboxamide (plus 20 mmoles of propylene oxide) in 3 ml. of benzene there was added 64 mg. of catalyst ( $\text{Et}_3\text{N}$  or  $\text{BF}_3 \cdot \text{Et}_2\text{O}$ ). The tube was sealed and heated for 1 wk. at 75°C.

Polymers derived from the diphenyl derivative were purified by precipitation from benzene solutions into hexane. The corresponding diethyl derivatives were purified by successively washing with saturated sodium chloride, drying, removing volatile material in a rotary evaporator at 100°C./0.3 mm. and precipitating an ethyl acetate solution of the residue into hexane.

The authors wish to acknowledge partial support of this research by the Sugar Research Foundation, Inc.

### References

1. I. G. Farbenindustrie A.-G., Brit. Pat. 466,344 (1937).
2. Ulrich, H., Ger. Pat. 651,797 (1937).
3. Furukawa, J., T. Tsuruta, T. Saegusa, and G. Kakogawa, *J. Polymer Sci.*, **36**, 542 (1959).
4. Osgan, M., and C. C. Price, *J. Polymer Sci.*, **34**, 153 (1959).
5. Wilson, A. L., U. S. Pat. 2,475,068 (1949).
6. Funke, A., and E. Benoit, *Bull. Soc. Chim. France*, **1953**, 1021.
7. Jones, G. D., *J. Org. Chem.*, **9**, 125, 484 (1944).
8. Barb, W. G., *J. Chem. Soc.*, **1955**, 2564.
9. Eastham, A. M., *Adv. Polymer Sci.*, **2**, 18 (1960).
10. Berchet, G. J., U. S. Pat. 2,269,997 (1942).
11. Epstein, J., R. W. Rosenthal and R. J. Ess, *Anal. Chem.*, **27**, 1435 (1955).
12. Wenker, H., *J. Am. Chem. Soc.*, **57**, 2328 (1935).
13. Campbell, K. N., A. H. Sommers, and B. K. Campbell, *Organic Syntheses*, Coll. Vol. III, Wiley, New York, 1955, p. 148.
14. Emmons, W. D., and A. S. Pagano, *J. Am. Chem. Soc.*, **77**, 89 (1955).
15. Bestian, H., *Ann.*, **566**, 210 (1950).

### Résumé

On a étudié un certain nombre de catalyseurs acides de Lewis pour la copolymérisation de la 1,2-butylèneimine avec les 1,2-époxydes. On a montré que le catalyseur le plus actif, l'éthérate de trifluorure de bore, fournit des polymères contenant une chaîne principale polyimine dans laquelle les groupements résiduels NH dans la chaîne polymérique sont hydroxylalcoylés en bêta par l'époxide. On a démontré que l'imine est beaucoup plus réactive que l'époxide dans ces conditions, sans tenir compte de la longueur de chaîne de l'époxide monomère. La chaîne de polymère semble croître appréciablement avant que l'époxide ne vienne s'attacher sur le polymère. On interprète ces résultats comme étant dus à la complexation préférentielle du catalyseur par les résidus imine basiques dans le polymère, ce qui rend le catalyseur inefficace pour la polymérisation de l'époxide. On a étudié l'homopolymérisation et la copolymérisation de la 1-(*p*-toluènesulfonyl)-aziridine de la *N,N*-diphényl-1-aziridine-carboxamide et de la *N,N*-

diéthyl-1-aziridinecarboxamide avec les 1,2-époxydes avec l'éthérate de trifluorure de bore et la triéthylamine comme catalyseurs. Dans aucun cas on n'a pu obtenir de copolymères.

### Zusammenfassung

Eine Anzahl von Lewis-Säure-Katalysatoren wurde hinsichtlich ihrer Wirksamkeit bei der Copolymerisation von 1,2-Butylenimin mit 1,2-Epoxyden untersucht. Der wirksamste Katalysator ist Bortrifluoridätherat. Seine Verwendung führt zur Bildung von Polymeren mit einer Polyiminhauptkette, in welchen die NH-Gruppen in der Polymerkette durch das Epoxyd  $\beta$ -hydroxyalkyliert wurden. Das Imin ist unter den gegebenen Bedingungen unabhängig von der Kettenlänge des Epoxydmonomeren viel reaktionsfähiger als das Epoxyd. Die Polyiminkette wächst offenbar schon zu einem beträchtlichen Ausmass, bevor noch ein Einbau von Epoxyd stattfindet. Das wird einer bevorzugten Komplexierung des Katalysators durch die basischen Iminreste zugeschrieben, so dass der Katalysator für die Polymerisation des Epoxydes nicht verfügbar ist. Das Homo- und Copolymerisationsverhalten von 1-(*p*-Toluolsulfonyl)aziridin, *N,N*-Diphenyl-1-aziridinecarboxamid und *N,N*-Diäthyl-1-aziridinecarboxamid mit 1,2-Epoxyden wurde unter Verwendung von Bortrifluoridätherat und von Triäthylamin als Katalysator untersucht. In keinem der Versuche wurden Copolymere gebildet.

Received May 15, 1963

## A Series of Poly(methylene Acetals) Derived from Aliphatic Aldehydes

EDWARD SCHONFELD, *Industrial Research and Development Laboratory,  
Nopco Chemical Company, Harrison, New Jersey*

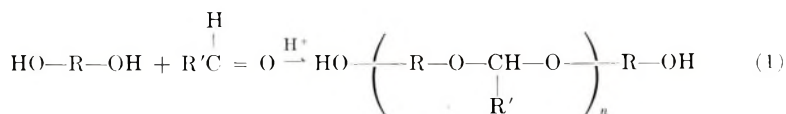
### Synopsis

A series of poly(methylene acetals) were prepared from 1,5-pentanediol by systematically varying the aldehyde. The viscosity of each polymer was measured, and, for the first four members of the series, shown to vary inversely with the length of the pendant chain of the aldehyde. A comparison of the viscosity of a polyether (a polyoxypropylene glycol) in which the ratio of carbon to oxygen in the chain is 2/1 with that of a poly(methylene acetal) in which the carbon to oxygen ratio is 3/1 indicated a significant decrease in viscosity with increasing concentration of ethereal oxygen.

### Introduction

One of the structural features which differentiate polyethers from many other types of condensation polymers is the absence of polarizable groups at successive intervals along the polymer chain. The presence of urethane groups in polyurethanes, for example, or amide groups in polyamides, both of which are capable of exerting secondary valence forces through hydrogen bonding results in polymers having high values for their melting points, viscosities, and second-order transition points.

Poly(methylene acetals), formed by the reaction of an aldehyde with a glycol,<sup>1</sup>



are a particular type of polyether, and in common with other types of polyethers, have the relatively nonpolar C—O—C bonds recurring periodically as connective links in the polymer chain. Consequently, such polymers have a minimum of intermolecular association because of the absence of potentially polarizable groups (such as ester, amide, urethane, urea, or carbonyl) on the polymer molecule. Increased flexibility of the polymer molecule and a low second-order transition point can be anticipated because of the presence of recurring ethereal oxygen linkages which activate the rotation of the neighboring carbon linkages.<sup>2</sup> Rotation about the C—C bond in ethane, for example, is restricted because of mutual

repulsion of the hydrogen atoms of one methyl group for those of the other. With the insertion of an oxygen atom between the two methyl groups, as in dimethyl ether, a physical separation of the methyl groups occurs with a resulting increase in the ease of bond rotation. The fact that the melting points of aliphatic polyesters lie below that of polyethylene despite the polar nature of the carbonyl group and the accompanying secondary valence forces resulting from dipole-dipole interaction is attributed to the flexibility imparted to the polymer chain by the ethereal oxygen of the ester linkage.<sup>3</sup>

Poly(methylene acetals) which do not have polarizable groups along the polymer chain and which do have recurring ethereal oxygen linkages might be expected to be low melting solids or even liquids at room temperature. A systematic variation of the aldehyde was undertaken in order to verify this assumption. Through a stepwise increase in the molecular weight of the aldehyde, it should be possible to observe the effect upon the viscosity of the polymer resulting from an homologous series of pendant groups occurring at regular intervals. Such an effect would presumably be caused by interference in the symmetry and orientation of the polymer chain. The diol chosen for this study was 1,5-pentanediol because, as has been previously reported,<sup>4</sup> it is the lowest molecular weight  $\alpha,\omega$ -glycol which polymerized rather than cyclized when reacted with paraformaldehyde. The advantage of using the lowest molecular weight diol capable of forming a polymer is that the ratio of chain-atom carbon to ethereal oxygen is kept at a minimum. The structure of the resulting polymer will diverge from that of a hydrocarbon, such as polyethylene, and the effect of the oxygen will be more apparent.

### Experimental

Poly(methylene acetals) were prepared by the method previously described.<sup>1</sup> The aldehydes used were: paraformaldehyde; paraldehyde; *n*-propionaldehyde; para-*n*-butyraldehyde; and *n*-valeraldehyde.

At the completion of the condensation step between the aldehyde and glycol, the solution was filtered and the solvent removed by gentle heating at 20 mm. of pressure. In order to remove the last traces of solvent, the temperature was increased to 125°C. and the pressure reduced to 2 mm. The only polymer stable under these conditions was the poly(methylene acetal) derived from paraformaldehyde. The other poly(methylene acetals) decomposed as the temperature approached 125°C.

The viscosities of the poly(methylene acetals) were determined by measurements made at 25°C. in a Brookfield viscometer.

Molecular weights of the polymers were determined by endgroup analysis for hydroxyl.<sup>5</sup> Since the polymer is linear and is terminated at each end by hydroxyl,<sup>4</sup> the number-average molecular weight can be calculated from the following equation:

$$\bar{M}_n = \frac{2 \times 56.1 \times 1000}{\text{hydroxyl number}}$$



where the hydroxyl number is defined as the number of milligrams of KOH equivalent to the hydroxyl content of one gram of the polyol.

### Results

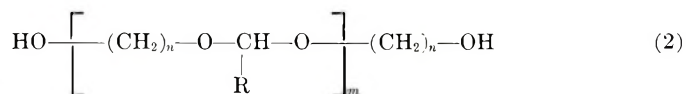
The molecular weights and viscosities of the poly(methylene acetals) are listed in Table I.

TABLE I  
Properties of Polyacetals Derived From 1,5-Pentanediol With Various Aldehydes

Aldehyde	Hydroxyl number	$\bar{M}_n$	Viscosity, cpoise
Paraformaldehyde	112, 112	1000	—
Paraldehyde	119, 122	930	880
<i>n</i> -Propionaldehyde	134, 139	825	715
Para- <i>n</i> -butyraldehyde	76, 78	1460	470
<i>n</i> -Valeraldehyde	90, 91	1245	630

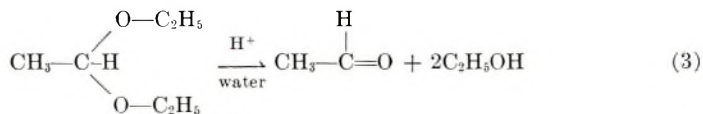
The polyacetal formed by the reaction of paraformaldehyde and 1,5-pentanediol was a low melting (32–36°C.), waxy solid. Its viscosity at 25°C. was, therefore, not measured. From the data in Table I, it is apparent that the polymer with the lowest viscosity was obtained by condensing para-*n*-butyraldehyde with 1,5-pentanediol. The viscosity of the polymers decreases as the number of carbon atoms in the aldehyde increases. The presence of a bulky group, pendant to the polymer, interferes with the symmetry and orientation of the polymer chain. In the example using valeraldehyde, the side chain is sufficiently large to overcome the anticipated decrease in viscosity.

The poly(methylene acetals) are considered to be the linear condensation product of a glycol with an aldehyde. Accordingly, the structure of the polymer can be written as follows:



where  $m$  is the degree of polymerization of the polymer,  $n$  is the number of methylene groups in the starting glycol ( $n = 5$  in the examples discussed in this paper) and R is H, CH<sub>3</sub>, C<sub>2</sub>H<sub>5</sub>, etc.

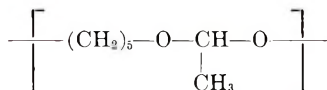
The condensation of an alcohol with an aldehyde results in the formation of an acetal accompanied by the elimination of one mole of water for each acetal linkage formed. Acetals are known to be unstable to aqueous mineral acid and to decompose into the original alcohol and aldehyde as shown by eq. (3).



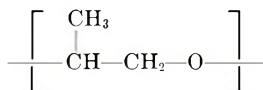
If the polyacetal of 1,5-pentanediol and formaldehyde has the structure indicated by eq. (2), then decomposition of the polymer would yield the starting materials. Accordingly, 25 g. of poly(pentamethylene formal) was dissolved at room temperature in 350 ml. of acetone and 100 ml. of 3% HCl added. The solution was refluxed for 1 hr. Acetone was distilled at 57–58°C. A strong smell of formaldehyde was noted in the acetone. A positive formaldehyde test, indicated by a deep red color, was obtained upon addition of phenylhydrazine hydrochloride, potassium ferricyanide, and concentrated HCl to the acetone.<sup>6</sup> Pure acetone does not give a red color under these conditions. Benzene (150 ml.) was added, the solution azeotroped to remove the water, and the benzene distilled. The residue was a liquid boiling at 240°C. and with a  $n_D^{20}$  of 1.4493. The literature values for 1,5-pentanediol are: b.p. = 239.4°C. and  $n_D^{20} = 1.4499$ .

The decomposition of the polymer under conditions of acetal hydrolysis, and the characterization of the hydrolyzate as the starting glycol and aldehyde have been demonstrated. Therefore, the structure of the poly(methylene acetal) can be represented by eq. (2).

A comparison of the viscosity of a commercial sample of a polyether, a polyoxypropylene glycol having a number-average molecular weight of 1025, with the viscosity of the polyacetal derived from paraldehyde and 1,5-pentanediol indicated a substantially lower viscosity (130 cpoises) for the polyoxypropylene glycol. Examination of the structure of the repeating unit of the poly(methylene acetal)



indicates that there are six chain carbon atoms for every two oxygen atoms, a 3/1 ratio of C/O, whereas in the polyoxypropylene glycol repeating unit



the C/O ratio of chain atoms is 2/1. The effect of ethereal oxygen upon the melting point has previously been mentioned. An inversely proportional relationship exists between the ethereal oxygen concentration and the viscosity of a polyether insofar as the structure of a polyether and a poly(methylene acetal) may be judged to be comparable.

### References

1. Schonfeld, E., *J. Polymer Sci.*, **49**, 277 (1961).
2. Guth, E., H. M. James, and H. Mark, *Advances in Colloid Science*, Vol. II, Interscience, New York, 1946, p. 262.
3. Hill, R., and E. E. Walker, *J. Polymer Sci.*, **3**, 609 (1948).
4. Schonfeld, E., *J. Polymer Sci.*, **59**, 87 (1962).
5. Critchfield, F. E., *Organic Functional Group Analysis*, Macmillan, New York, 1963, pp. 81–86.
6. Allport, N. L., *Colorimetric Analysis*, Chapman & Hall, London, 1947, pp. 237–238.

### Résumé

On a préparé une série d'acétals polyméthyléniques à partir du 1,5-pentanediol en changeant systématiquement l'aldéhyde. La viscosité de chaque polymère a été mesurée et, pour les quatre premiers membres des séries, on a démontré qu'elle varie inversement avec la longueur de la chaîne latérale de l'aldéhyde. Une comparaison de la viscosité d'un polyéther (un polyoxypropylène glycol) dans lequel la proportion carbone-oxygène de la chaîne est 2/1, avec celle d'un poly(méthylène acétal) dans lequel la proportion carbone-oxygène est 3/1, indique une diminution importante de la viscosité avec l'augmentation de la concentration en oxygène éther.

### Zusammenfassung

Eine Reihe von Poly(methylenacetalen) wurde aus 1,5-Pentandiol unter systematischer Variation des Aldehyds dargestellt. Die Viskosität jedes Polymeren wurde gemessen und zeigte bei den ersten vier Gliedern der Reihe eine Änderung im umgekehrten Sinne mit der Länge der Aldehydseitenkette. Ein Vergleich der Viskosität eines Polyäthers (ein Polyoxypropylenglykol), bei welchem das Verhältnis Kohlenstoff zu Sauerstoff in der Kette 2:1 ist, mit der eines Poly(methylenacetals), bei welchem das Kohlenstoff-Sauerstoff-Verhältnis 3:1 ist, spricht für einen charakteristischen Viskositätsabfall mit steigendem Gehalt an Äthersauerstoff.

Received January 21, 1963

Revised June 21, 1963

## BOOK REVIEW

N. G. GAYLORD, Editor

**Quantum Mechanics, Vols. I and II**, A. MESSIAH, Ed., Interscience, New York, North-Holland, Amsterdam, 1961. Vol. I, 576 pp., \$8.00; vol. II, 560 pp., \$8.50.

The textbook literature in quantum mechanics contains many outstanding "classics" treating this important field from every conceivable point of view. In addition, there has been, within the past few years, a veritable flood of new textbooks in quantum mechanics, many of them excellent.

It is therefore with some surprise that this reviewer finds himself able to welcome, enthusiastically and almost without reservations, this new book as not only outstanding in itself, but as actually filling a real gap.

By using roughly twice the number of pages of the average textbook while at the same time rigorously restricting the number of main topics treated, the author manages to present with extraordinary thoroughness all the fundamental aspects of the field in a way which is at once comprehensible to the serious beginner and illuminating and useful to the expert. Mathematical and conceptual difficulties, in which the subject abounds, are not glossed over nor treated with excessive, and forbidding, conciseness.

The exposition, though elegant and precise is leisurely and expansive; this is a boon to the less advanced student. At the same time it is never verbose or circumlocutory.

The author introduces almost every chapter or major subdivision with a brief survey of what is to be covered, often giving an explanation of the relation of the material to the general development; this is an excellent device for orienting the reader.

The general approach to the subject is a mixture of the historical, heuristic, and formal ones; the coordination of the different approaches is good and confusion is minimized.

The first part, consisting of the first eight chapters of Vol. I, entitled "The Formalism and Its Interpretation" begins with a brief historical survey of the origin of quantum theory and then develops very thoroughly the Schrödinger approach and its formalism including the associated statistical interpretation. As examples, one-dimensional systems are carefully and exhaustively discussed. One chapter is devoted to a very welcome and thorough exposition of the classical approximation and the WKB method.

Part One ends with an extensive discussion of the general formalism of quantum theory mainly based on Dirac's approach (and using his notation); the mathematical framework and physical interpretation are discussed separately.

Part Two, "Simple Systems," consists of four chapters and includes, besides the topics universally treated, a valuable chapter on scattering problems.

Volume II is divided into three parts: "Symmetries and Invariance," "Methods of Approximation," and "Elements of Relativistic Quantum Mechanics."

The first of these (Part Three) brings together in highly useful form, and treats from a unified viewpoint, topics that are often scattered or slighted. The chapter "Invariance and Conservation Theorems; Time Reversal" is especially welcome.

Part Four discusses time-independent and dependent perturbation theory including modern and powerful formulations of it, variational methods (this includes discussion of the usual molecular methods and a lucid and precise treatment of their very basis, the Born-Oppenheimer approximation), and collision theory.

Part Five also includes an introductory discussion of field quantization and radiation theory.

Each chapter contains an extensive set of problems which complement the presentation of the textual material. Four mathematical appendices complete the book. The index

is adequate. The printing is very clear and legible though the margins are somewhat narrow.

The only criticisms this reviewer feels he can make are relatively minor: He would have liked a more profound and extensive discussion of some basic conceptual and philosophical aspects, including those that, like the "hidden variables" problem, still excite some controversy. The translation, especially in the first volume, though very adequate and unambiguous, falls short of the ideal; too often the very elegance of a phrase in the French original becomes clumsy in the translation. There are quite a number of misprints, especially in names, which are repeated again and again ("Condon and Shortly," "Clebsch-Gordon," "Eckhart"). These, though in themselves unimportant, make one wonder about the thoroughness of the proofreading.

But these are minor matters, the book is to be strongly recommended to every serious student of this subject whatever his primary interest and prior knowledge.

*Ernest M. Loeb*

Polytechnic Institute of Brooklyn  
Brooklyn, New York